SWIM

June 23-27, 2008

Naples, Florida USA

Program and Proceedings Book

Welcome to the 20th Saltwater Intrusion Meeting (SWIM), affectionately referred to as "SWIM", that has been held on a biennial basis since 1968. SWIMs deal with the ever interesting topic of saline ground water in coastal and inland aquifers and are attended by a multi-disciplinary group of people with a wide variety of expertise including chemistry, engineering, geology, geophysics, mathematics, physics, and management. Traditional topics that are covered include the characterization of saline ground water with chemical and geophysical methods, development and application of mathematical models, and design of effective management strategies for aquifers containing saline ground water. New topics were added in later years, such as the impact of global climate change and sea level rise on freshwater resources, and submarine ground water discharge. The meetings are very successful in bringing together people who are interested in saline groundwater issues: well-known specialists, water managers and students.

The SWIM was first convened in 1968 by the late Professor Dr. W. Richter, who invited several German, Dutch and Danish colleagues to his institute in Hanover, Germany. Dr. Richter felt that these three countries had similar problems with saline ground water and that an informal dialogue would be mutually beneficial. The first SWIM concluded with a consensus to meet again. The next five meetings were organized by countries surrounding the North Sea (1970, Vogelenzang, The Netherlands; 1972, Copenhagen, Denmark; 1974, Ghent, Belgium; 1977, Medmenham, UK; and 1979, Hanover, Germany). The number of meeting participants has steadily grown over the years. Also the countries of interested participants expanded away from the North Sea. Subsequent meetings were organized in Sweden (Uppsala, 1981) and then Italy (Bari, 1983). After a short return to countries of its originating members (1986, Delft, The Netherlands and 1988, Ghent, Belgium) SWIMs were held in a variety of locations across Europe (1990, Danzig, Poland; 1992, Barcelona, Spain; 1994, Cagliari, Italy; 1996, Malmö, Sweden; 1998, Ghent, Belgium; 2000, Miedziezdroje, Poland; 2002, Delft, The Netherlands; 2004, Cartagena, Spain). The last SWIM was held in 2006 in Cagliari, Italy

While the SWIMs were being held in Europe, a separate group was formed around 2000 by Professors Alex Cheng (USA) and Driss Ouazar (Morocco) to meet the growing worldwide needs for a global conference on salt water intrusion. This group, called Salt Water Intrusion in Coastal Aquifers (SWICA), held its first conference in 2001 in Essaouira, Morocco and a second meeting in 2003 in Merida, Mexico. The third SWICA meeting was held together with the 19th SWIM. This joint SWIM-SWICA conference was held in 2006 in Cagliari, Italy. At this joint meeting, participants decided to combine the best features of both meeting series and to merge under the SWIM name. The meeting style would remain informal and collegial as in SWIM, but the venue would become worldwide as in SWICA. The group decided that subsequent meetings will be alternately held outside and within Europe on a biannual basis. The 2008 meeting is being held here, in Florida, USA. The 2010 meeting will return to Europe.

This proceedings book serves as a permanent reminder of the 20th SWIM. It contains nearly 100 papers submitted by participants and reviewed by the scientific committee. We are grateful to all those that helped with this process. Digital copies of the proceedings book will be made available from the website after the meeting.

This meeting would not be possible without the efforts of numerous individuals. We are particularly indebted to our sponsors for their generous contributions. With their support, we were able to offer an affordable registration fee and help fund travel for students in need of assistance. We thank Rene Price and Gregory Allard for arranging the Everglades field trip and John Doherty and Alyssa Dausman for hosting the PEST Fest. We thank The Naples Beach Hotel & Golf Club for providing exceptional facilities and staffing. We also thank the meeting coordinator, Sharon Borneman, for helping to make the 20th SWIM a huge success.

On behalf of the Organizing Committee, we sincerely hope that you enjoy the 20th SWIM. Without your participation, the SWIM would not be possible.

Conference Co-Organizers,

Christian Langevin, *Luc Lebbe*, *Mark Bakker*, and *Clifford Voss*

Table of Contents

A Special Thank You to Our Sponsors

Platinum Level

US Geological Survey

UF/IFAS Tropical Research and Education Center

Gold Level

Schlumberger Water Services

Silver Level

USGS – Greater Everglades Priority Ecosystems Science (PES)

GeoTrans, Inc.

In-Situ, Inc.

Miami-Dade County

Additional Contributions

ESI - Environmental Simulations, Incorporated

McLane Environmental, LLC

National Ground Water Association

Saltwater Separation, LLC

St. Johns River Water Management District

Organizing Committee

Christian Langevin
U.S. Geological Survey
Fort Lauderdale, Florida

Luc Lebbe
Ghent University
Ghent, Belgium

Mark Bakker
Delft University of Technology and KIWA
Delft, the Netherlands

Cliff Voss
U.S. Geological Survey
Washington, D.C.

Scientific Committee

Program Agenda

Abstract/Paper page numbers are indicated at the end of listings
when applicable [example: " ...(p. 2)"]

Sunday, June 22, 2008

6:00pm-8:00pm	**Early Bird Social & Poster setup, Registration Open** [CONFERENCE CENTER]

Monday, June 23, 2008

7:00am-5:00pm	**Conference Registration Open** [CONFERENCE CENTER ATRIUM]
7:30am-8:30am	**Morning Refreshments** [POSTER SESSION ROOM]
8:30am-9:00am	**Welcome & Announcements - Christian Langevin, Meeting Organizer, and Others** [RIVER OF GRASS BALLROOM]
General Session I: Case Studies in Salt Water Intrusion	
9:00am-9:25am	**Assessing Well Field Impacts on Water Quality in the Upper Floridan Aquifer in Southwest Florida** - *Terry Bengtsson* (Featured Speaker) .....(p. 22)
9:25am-9:40am	**Modeling of Historical Evolution of Salt Water Distribution in the Phreatic Aquifer in and around the silted up Zwin Estuary Mouth (Flanders, Belgium)** - *Luc Lebbe* .....(p. 141)
9:40am-9:55am	**Assessment of Groundwater Resources in Rmel Coastal Aquifer (Morocco) by SEAWAT** - *Abdelkader Larabi* .....(p. 136)
9:55am-10:10am	**Dynamic Groundwater Equilibrium during a Base Level Drop: The Dead Sea Case** - *Yael Kiro* .....(p. 121)
10:10am-10:40am	**Refreshment Break** [POSTER SESSION ROOM]
General Session II: Case Studies in Salt Water Intrusion, continued	
10:40am-10:55am	**Simulation of Processes Controlling Migration of Saline Water and Brine above a Flooded Salt Mine in Western New York, USA** - *Richard Yager* ..... (p. 321)
10:55am-11:10am	**A Case Study of Finite-Element Numerical Modeling on Salt Water Intrusion for the Ping-Tung Plain** - *Jing-Yea Yang* ..... (p. 325)
11:10am-11:25am	**Salt Water Intrusion in the Shallow Aquifers of Venice** - *Eloisa Di Sipio* ..... (p. 59)
11:25am-11:40am	**Study of Saltwater Intrusion into the Coastal Aquifer of Tavabe-e Arsanjan, Iran** - *Gholmareza Rakhshandehroo* ..... (p. 217)
11:40am-11:55am	**Vulnerability Assessment of Groundwater Aquifer due to the Construction of the City Tunnel in Malmö, Sweden** - *Kenneth M Persson*..... (p. 194)
11:55am-12:10pm	**Combined Groundwater Quality and Groundwater Model Approach as Main Tool of an Aquifer Management for Sustainable Water Supply in the Santo Domingo Valley, Baja California Sur, Mexico** - *Jobst Wurl* ..... (p. 317)
12:10pm-1:25pm	**Lunch in Sunset Terrace**

Monday, June 23, 2008 (continued)

General Session III: Management of Coastal Aquifers	
1:25pm-1:50pm	**An Assessment of the Impact of Geologic Heterogeneity on Predictions of Seawater Intrusion in Coastal Aquifers** - *Whitney Trainor* (Featured Speaker) (p. 270)
1:50pm-2:05pm	**Artificial Recharge of Fresh Water in the Belgian Coastal Dunes** - *Alexander Vandenbohede* (p. 282)
2:05pm-2:20pm	**Management of the Iao and Waihee Aquifer Areas With the Aid of a 3-D Numerical SUTRA Model, Maui, Hawaii** - *Stephen Gingerich* (p. 84)
2:20pm-2:35pm	**Pumping of Brackish and Saline Water in Coastal Aquifers: An Effective Tool for Alleviation of Seawater Intrusion** - *Mohsen Sherif* (p. 254)
2:35pm-2:50pm	**Managing Seawater Intrusion Using Multiple-depth Monitoring Wells** - *Wes Danskin* (p. 49)
2:50pm-3:05pm	**Field Validation of Simulation-Optimization Model for Protecting Excessive Pumping Wells** - *Namsik Park* (p. 186)
3:05pm-3:35pm	**Refreshment Break** [POSTER SESSION ROOM]
General Session IV: Variable Density Flow and Transport Modeling	
3:35pm-3:50pm	**Benchmarks for Two- and Three-Dimensional Variable-Density Ground-Water Flow Simulators: Analytical Expressions for Unstable Convection** - *Clifford Voss* (p. 294)
3:50pm-4:05pm	**Solute Extraction in Variable Density Flow: Shock Wave Driven Transport Compared to Pumping** - *Shaul Sorek* (p. 258)
4:05pm-4:20pm	**Use of Image Analysis to Develop New Benchmarking Datasets for Variable Density Flow Scenarios** - *Rohit Goswami* (p. 87)
4:20pm-4:35pm	**Modeling of the Potential for Vertically Downward Saltwater Migration from a Dredge Pond** - *Peter Andersen* (p. 8)
4:35pm-4:50pm	**Freshwater-Saltwater Mixing Zone in Coastal Aquifers: Biased vs. Reliable Monitoring** - *Eyal Shalev* (p. 248)
4:50pm-5:05pm	**Simulation of Coastal Wastewater Injection in Hawaii using SUTRA, and the Value of Compelling Visualizations in Conveying Results to the Non-Specialist Public** - *Charles D Hunt, Jr.* (p. 97)
5:30pm-7:30pm	**Welcome Reception on Ocean Lawn**

Tuesday, June 24, 2008

7:00am-5:00pm	**Conference Registration Open** [CONFERENCE CENTER ATRIUM]
7:30am-8:30am	**Morning Refreshments** [POSTER SESSION ROOM]
General Session V: Submarine Groundwater Discharge & Field Studies	
8:30am-8:55am	**Analytical Benthic Flux Model Forced by Surface-Water Waves: Application to the South Atlantic Bight, USA** - *Jeffrey King* (Featured Speaker) ..... (p. 117)
8:55am-9:10am	**Mechanisms Driving Submarine Groundwater Discharge and Associated Radium Flux: Implications for Use of Radium as a Tracer** - *Holly Michael* ..... (p. 149)
9:10am-9:25am	**The Role of Fresh and Saline Submarine Groundwater Discharge in Nutrient Contribution to Coastal Seawater, Dor Bay (Israel)** - *Yishai Weinstein* ..... (p. 310)
9:25am-9:40am	**Global Land-Ocean Linkage: Direct Inputs of Water and Associated Nutrients to Coastal Zones via Submarine Groundwater Discharge (SGD)** - *Hans H. Dürr* ..... (p. 72)
9:40am-9:55am	**Causes of Borehole Flow and Effects on Vertical Salinity Profiles in Coastal Aquifers** - *Delwyn Oki* ..... (p. 170)
9:55am-10:10am	**Characterization of Local Rainwater Lenses in Agricultural Areas with Upward Saline Seepage: Monitoring Results** - *Perry de Louw* ..... (p. 54)
10:10am-10:40am	**Refreshment Break** [POSTER SESSION ROOM]
General Session VI: Field Studies of Salt Water Intrusion	
10:40am-10:55am	**Altered Hydroperiod and Saltwater Intrusion in the Bald Cypress Swamps of the Loxahatchee River** - *David Kaplan* ..... (p. 109)
10:55am-11:10am	**Global Warming and Salt Water Intrusion: Bangladesh Perspective** - *Md. Abu Noman* ..... (p. 167)
11:10am-11:25am	**An Investigation of Groundwater Flow on a Coastal Barrier using Multi Electrode Profiling** - *Søren Erbs Poulsen* ..... (p. 209)
11:25am-11:40am	**Pumping Test Analyses in an Aquifer with Fresh Water/Salt Water Interface** - *Liliana Cecan* ..... (p. 37)
11:40am-11:55am	**Assessing the Extent of Saltwater Intrusion in the Aquifer System of Southern Baldwin County, Alabama** - *Dorina Murgulet* ..... (p. 159)
11:55am-12:10pm	**Freshwater Lens Development on Padre Island, Texas** - *Egon Weber* ..... (p. 306)
12:10pm-1:25pm	**Lunch in Sunset Terrace**

Tuesday, June 24, 2008 (continued)

General Session VII: Parameter Estimation	
1:25pm-1:50pm	**Incorporating Initial Conditions in the Model Calibration Process** - *John Doherty* (Featured Speaker) ..... (p. 64)
1:50pm-2:05pm	**Saltwater Intrusion and Hydraulic Conductivity Estimation in East Baton Rouge Parish, Louisiana** - *Frank Tsai* ..... (p. 274)
2:05pm-2:20pm	**General Guidance Concerning Inverse Modeling Techniques and Value of Field Data Types for Seawater Intrusion Simulation** - *Clifford Voss* .. (p. 296)
2:20pm-2:35pm	**Efficient Calibration of Seawater Intrusion Models** - *Juan José Hidalgo* ..... (p. 95)
2:35pm-2:50pm	**Calibration of a Density-Dependent Groundwater Flow Model of the Lower West Coast Floridan Aquifer System** - *Jorge Restrepo* ..... (p. 229)
2:50pm-3:05pm	**Saltwater/Freshwater Interface Movement in Response to Deep-Well Injection in a Coastal Aquifer** - *Alyssa Dausman* ..... (p. 50)
3:05pm-3:35pm	**Refreshment Break** [POSTER SESSION ROOM]
General Session VIII: Geochemistry	
3:35pm-4:00pm	**Chemical and Isotopic Evidence for Seawater Intrusion – Examples from the Coastal Aquifers of the Mediterranean and the Dead Sea** - *Yoseph Yechieli* (Featured Speaker) ..... (p. 328)
4:00pm-4:15pm	**Base Exchange Indices as Indicators of Salinization or Freshening of (Coastal) Aquifers** - *Pieter Jan Stuyfzand* ..... (p. 262)
4:15pm-4:30pm	**Use of Geochemical Tools to Study Groundwater Salinization in Volcanic Islands: a Case Study in the Porto Santo (Portugal) and Santiago (Cape Verde) Islands** - *Maria Teresa Condesso de Melo* ..... (p. 41)
4:30pm-4:45pm	**Geochemistry of Phosphorus in a Carbonate Aquifer Affected by Seawater Intrusion** - *Rene Price* ..... (p. 213)
4:45pm-5:00pm	**Time Scale of Water-Rock Interaction Processes in the Fresh-Saline Water Interface of Coastal Aquifers** - *Amos Russak* ..... (p. 233)
5:00pm-5:15pm	**Utilizing Stable Isotopes (^{2}H, ^{18}O) to Better Identify Different Water Types of the Floridan Aquifer System in Southwest Florida** - *Ed Rectenwald* ..... (p. 225)
5:15pm-5:30pm	**Geochemical and Isotopic Study of the Origin of Salinization in an Unconfined Coastal Aquifer of Cap Bon (Tunisia)** - *Mohamed Fethi Ben Hamouda* ..... (p. 18)
5:30pm-7:00pm	**Poster Presentations & Social** [POSTER SESSION ROOM]

Wednesday, June 25, 2008

8:00am-5:00pm	**Optional Field Trip**

Thursday, June 26, 2008

7:00am-5:00pm	**Conference Registration Open** [CONFERENCE CENTER ATRIUM]
7:30am-8:30am	**Morning Refreshments** [POSTER SESSION ROOM]
General Session IX: Variable Density Flow & Transport Modeling	
8:30am-8:55am	**Variable Density Flow and Transport in Tsunami Impacted Coastal Aquifers: Laboratory Investigations in Homogeneous Saturated Porous Media** - *Meththika Vithanage* (Featured Speaker) ..... (p. 290)
8:55am-9:10am	**The Delayed Effects of Variable Density Flow on Flow and Heads in Fresh Groundwater** - *Frans Schaars* ..... (p. 240)
9:10am-9:25am	**Experimental Mapping of the Saltwater/Freshwater Mixing Zone** - *Elena Abarca* ..... (p. 3)
9:25am-9:40am	**Virginia Ground Water Withdrawal Permitting Program – Modeling for Resource Management** - *Roberta Patton* ..... (p. 190)
9:40am-9:55am	**A Saltwater Upconing Model to Evaluate Wellfield Feasibility** - *Gregory Council* ..... (p. 45)
9:55am-10:10am	**Dispersive Behavior of the Mixing Zone between a Shallow Freshwater Lens and Upward Seeping Saline Groundwater** - *Sara Eeman* ..... (p. 76)
10:10am-10:40am	**Refreshment Break** [POSTER SESSION ROOM]
General Session X: Impacts of Increased Water Demand, Optimization Modeling, & Case Studies	
10:40am-10:55am	**Brackish Groundwater as a New Resource for Drinking Water, Specific Consequences of Density Dependent Flow, and Positive Environmental Consequences** - *Theo Olsthoorn* ..... (p. 174)
10:55am-11:10am	**Analytical Method for Preliminary Management of Pumping and Injection in Coastal Areas** - *Namsik Park* ..... (p. 182)
11:10am-11:25am	**Compositional Change of Groundwater Chemistry in the Shallow Aquifer of Small Tropical Island Due to Seawater Intrusion** - *Ahmad Zaharin Aris* ..... (p. 9)
11:25am-11:40am	**TBD**
11:40am-11:55am	**The Use of Mapping the Salinity Distribution Using Geophysics on the Island of Terschelling for Groundwater Model Calibration** - *Arjen Kok* ..... (p. 124)
11:55am-12:10pm	**Verifying the Use of Specific Conductance as a Surrogate for Chloride in Seawater Matrices** - *Robert Mooney* ..... (p. 155)
12:10pm-1:25pm	**Lunch in Sunset Terrace**

Thursday, June 26, 2008 (continued)

General Session XI: Management of Coastal Aquifers	
1:25pm-1:40pm	**Salt Water Intrusion Modeling in the Flemish Coastal Plain based on a Hydrogeological Database** - *Dieter Vandevelde* ..... (p. 286)
1:40pm-1:55pm	**Management of Coastal Aquifers -- The Case of a Peninsula -- State of Qatar** - *Nauman Rashid* ..... (p. 221)
1:55pm-2:10pm	**Evaluating Safe Yield for Supply Wells in an Aquifer with Fresh Water / Salt Water Interface** - *Gregory Nelson* ..... (p. 163)
2:10pm-2:25pm	**Saltwater Intrusion Monitoring in the Biscayne Aquifer near Florida City, Miami-Dade County, Florida: 1996-2007** - *Christopher Peters* ..... (p. 195)
2:25pm-2:40pm	**Dynamics of Negative Hydraulic Barriers to Prevent Seawater Intrusion** - *María Pool* ..... (p. 203)
2:40pm-2:55pm	**Alternative Approaches for Water Extraction in Areas Subject to Saltwater Upconing** - *David Tarbox* ..... (p. 266)
3:05pm-3:35pm	**Refreshment Break** [POSTER SESSION ROOM]
3:35pm-4:00pm	**Seawater Intrusion in Australia - A National Perspective of Future Challenges** - *Adrian Werner* (Featured Speaker) ..... (p. 311)
4:05pm-6:00pm	**Planning for 2010 & 2012 SWIMs**
6:00pm-7:00pm	Dinner on Own
7:00pm-9:00pm	**PEST Fest*** [RIVER OF GRASS BALLROOM]

***PEST FEST: A Festive Primer on the PEST Software for Parameter Estimation and Uncertainty Analysis**

The FEST will be a relaxed and happy occasion, hosted by John Doherty, author of PEST. The other entertainer will be Alyssa Daussman from the Fort Lauderdale office of USGS, who has lots of PEST and SEAWAT experience.

All are welcome to attend. **Admission is free.**

Friday, June 27, 2008

7:00am-12Noon	**Conference Registration Open** [CONFERENCE CENTER ATRIUM]
7:30am-8:30am	**Morning Refreshments** [POSTER SESSION ROOM]
General Session XII: Variable Density Flow & Transport Modeling	
8:30am-8:55am	**Salinization by Free Convection in Heterogeneous Aquifers: Results from a Numerical Modeling Study** - *Vincent Post* (Featured Speaker) .....(p. 205)
8:55am-9:10am	**An Assessment Tool for Aquifer Storage and Recovery in Stratified Coastal Aquifers** - *Mark Bakker* .....(p. 13)
9:10am-9:25am	**Tidal Effects on Transient Dispersion of Simulated Contaminant Concentrations in Coastal Aquifers** - *Ivana La Licata* .....(p. 132)
9:25am-9:40am	**The Influence of Three-Dimensional Dune Topography on Salt Water Intrusion in Marina Romea, Italy: A Numerical Modeling Study Using LIDAR data** - *Pauline Mollema* .....(p. 151)
9:40am-9:55am	**Simulations of the Dynamics of Surface Water-Groundwater Interactions in a Coastal Environment During a 25-Year/72-Hour Storm** - *William Hutchings* .....(p. 101)
9:55am-10:10am	**Modeling Brine Discharge into the Soil** - *Mohamed J Safi* .....(p. 236)
10:10am-10:40am	**Refreshment Break** [POSTER SESSION ROOM]
General Session XIII: Effects of Sea Level Rise & Climate Change & Geophysics	
10:40am-10:55am	**Impacts of Climate Change on the Coastal Groundwater Systems in The Netherlands** - *Gualbert Oude Essink* .....(p. 178)
10:55am-11:10am	**Climate Change Impact in a Shallow Coastal Mediterranean Aquifer, at Saïdia, Morocco** - *Júlio Carneiro* .....(p. 30)
11:10am-11:25am	**An Investigation into Control of Saltwater Intrusion Considering the Effects of Climate Change and Sea Level Rise** - *Hany Abd-Elhamid* .....(p. 4)
11:25am-11:40am	**Time Domain Electromagnetic Induction and High Resolution Electric Resistivity Soundings to Map Salt Water Intrusion in Coastal Sandy Aquifers, Los Angeles County, California** - *Ted Johnson* .....(p. 105)
11:40am-11:55am	**Large-scale Geoelectrical Measurements to Investigate a Buried Valley and its Interaction to Deep Saltwater Intrusion** - *Joern Schuenemann* .....(p. 244)
11:55am-12:10pm	**Evolution of the Marine Intrusion Using Geophysical Methods after 25 Years in the Motril-Salobreña Aquifer (Southern Spain)** - *Carlos Duque* .....(p. 68)
12:10pm	**Wrap up Conference - Meeting Organizer**
12:10pm-1:25pm	**Lunch in Sunset Terrace**

Optional Field Trip – Everglades National Park

Organized by: Southwest Florida EcoTours, Inc.

Field Trip Schedule - Wednesday, June 25, 2008

7:30am	Board Buses at The Naples Beach Hotel & Golf Club
8:00am	Depart for Big Cypress National Preserve
9:00am	Arrive at Big Cypress National Preserve
9:15am-11:30am	Group Airboat Rides & View Native Florida Wildlife
11:30am	Board Buses to Rookery Bay National Estuarine Reserve
12:00pm-1:00pm	Rookery Bay Educational Presentation & Boxed Lunch
12:45pm-1:15pm	Self-Guided tour of Learning Center & Rookery Bay Store
1:15pm	Board Buses for Picayune Strand State Forest
2:15pm-3:45pm	Tour Picayune Strand State Forest
4:00pm-5:00pm	Board Buses & Return to Naples Beach Hotel

An airboat ride will be given to all field trip attendees, on airboats that seat a maximum of 18 guests. The airboats will leave approximately every 8 minutes to insure everyone a seat into the backwaters of the Big Cypress National Preserve which borders the northern edge of Everglades National Park. The airboat ride will last approximately 35 minutes. Attendees will also be allowed to view native Florida wildlife in an animal sanctuary and have the opportunity to safely hold a small alligator while a colleague takes a photo of them.

Following the airboat ride, the field trip attendees will re-board the buses for a trip to Rookery Bay National Estuarine Research Reserve for a 45 minute presentation by the educational staff of the facility. Rookery Bay will also allow the attendees to eat their boxed lunches during the presentation. They do recycle at the Rookery Bay so items will need to be put in the proper receptacles following lunch. Upon conclusion of the presentation, attendees will enjoy, at no charge, to view their educational learning facility which includes their aquarium and interactive displays. Attendees will also have the opportunity to purchase items in their store. Rookery Bay will have educational pamphlets and brochures available for the attendees.

We will then re-board the buses at Rookery Bay with staff from the South Florida Water Management District for a tour of the Picayune Strand State Forest, which is currently undergoing hydrologic restoration. We will include a couple of stops for the group for a first-hand look at the project.

Following the tour of Picayune Strand State Forest, the buses will return to the Naples Beach Hotel and Golf Club by 5:00pm.

Poster Directory

Abstract/Paper page numbers are indicated at the end of listings when applicable [example: "…(p. 2)"]

Poster #

Conference Papers

Listed alphabetically by presenting author.
Presenting author names appear in **bold**.

Experimental Mapping of the Saltwater/Freshwater Mixing Zone

Elena Abarca and *T. Prabhakar Clement*
Department of Civil Engineering, Auburn University, Auburn, AL, USA

ABSTRACT

The mixing zone between freshwater and seawater is of extreme importance for reactive transport processes and seawater recirculation. The amplitude of this mixing zone is proportional to the dispersion coefficients. Therefore, actual detailed measurements of the mixing zone would help to evaluate the dispersion coefficients. Experiments have been widely used to map the seawater intrusion wedge. However, none effort has been devoted to actually map the mixing zone. Here, we proposed a methodology based on the visualization of the mixing between an alkaline freshwater solution and acidic seawater by means of a pH indicator. Depending on the pH of the ending solutions, different portions of the mixing zone can be mapped. The experiments carried out in a 2D tank at a lab scale (50 x 20 x 2.2 cm) show a thin but measurable mixing zone. The experimental results have been used to calibrate a numerical model of the experiment and allowed us to quantify the dispersivity values of the system. In particular, we evaluated the transverse dispersion coefficient since mixing occurs basically perpendicular to the flow direction.

Contact Information: Elena Abarca, Auburn University, Department of Civil Engineering, 238 Harbert Engineering Center, Auburn, Al 36849 USA, Phone: 334-844-6273, Fax: 334-844-6290,
Email: ema0004@auburn.edu

An Investigation into Control of Saltwater Intrusion Considering the Effects of Climate Change and Sea Level Rise

H. F. Abd-Elhamid and *A.A. Javadi*
School of Engineering, Computing and Mathematics, University of Exeter, Exeter, UK

ABSTRACT
A large number of coastal aquifers are threatened by saltwater intrusion. Saltwater intrusion may occure due to human activities and by natural events such as climate change and sea leael rise. In coastal aquifers, overabstraction due to high demands for domestic water supply is the main cause of saltwater intruson. Also the rise in sea level due to the climate change accelerates the saltwater intrusion into the aquifers which reduces the fresh groundwater resources. With the impact of sea level rise and overpumping combined together the problem becomes even more serious and requires fast solutions. Coastal aquifers are affected by the rise in the sea level due to climate change and global warming. It is estimated that the mean sea level will rise in a range between 20 to 88 cm during the current century. The rise in sea level will shift the saltwater interface further inland. As a result, the extraction wells that were originally in fresh groundwater, may then be located in brackish water or saline water and upconing may occur. Consequently, the abstraction rates of these wells may have to be reduced or the wells abandoned. This is considered one of the most serious impacts of sea level rise. Therefore, saltwater intrusion due to sea level rise should be predicted and prevented (or at least controlled) to protect groundwater resources. This paper presents a review of the mathematical models developed to study the impacts of climate change and sea level rise on saltwater intrusion in coastal aquifers and the measures that caould be taken to reduce the impact. The impact of climate change and sea level rise on saltwater intrusion is discussed and analyzed. A new method is proposed to control saltwater intrusion considering the impact of climate change and sea level rise. The main benefits of the proposed methodology are discussed. It is shown that the proposed method is economical, has less environmental impact and could be used for sustainable development of water resources in coastal areas.

Keywords: climate change, sea level rise, saltwater intrusion, groundwater protection.

INTRODUCTION
Throughout the world, the areas with arid and semi-arid climate are suffering from water shortage problem. Population growth and continuous development require larger quantities of water, especially in the coastal regions where about 70% of the world population dowel. It is a great challenge to supply the required water, while the available water resources are nearly constant. This requires practical measures to protect the available resources from pollution, saltwater intrusion and other contaminants that deplete the current resources. Saltwater intrusion is a major problem in coastal regions all over the world. In coastal areas the aquifers are in hydraulic contact with the sea. Under normal conditions the freshwater flows into the sea. However, over-pumping may result in inversion of the groundwater flow from the sea towards the inland causing saltwater intrusion. Also the rise in sea level will accelerate the saltwater intrusion. Salinization of groundwater is considered a special category of pollution that threatens groundwater resources, because mixing a small quantity (2 percent) of saltwater with groundwater makes freshwater unsuitable and can result in abandonment of freshwater supply.

Therefore, saltwater intrusion should be prevented or at least controlled to protect groundwater resources. Recently, considerable attention has been focused on models to study the control of

saltwater intrusion in order to protect local groundwater. Various models have been developed to investigate saltwater intrusion. However, only few models have been developed to study the control of saltwater intrusion in coastal aquifers. This paper will discuss and analyze the models that have been developed to study the control of saltwater intrusion to highlight their benefits and limitations and will suggest a new methodology to control saltwater intrusion. Also the study will be used to analyze the position and movement of the fresh water/salt water interface to determine the response of the interface to the rise in sea level.

THE IMPACTS OF CLIMATE CHANGE AND SEA LEVEL RISE

Climate change is a result of natural and/or man-made activities. Due to climate changes the sea water level will rise for several reasons including oceans and seas thermal expansion, glaciers and ice caps melting and Greenland and Antarctic ice sheets melting. Sea level rise has many effects on coastal regions on the long term such as increase in coastal erosion and sea water intrusion. Climatic change has already caused changes in the sea level during the last decade. Global mean sea-level rise has been ranged from (10-20 mm/yr) during the last century IPCC (1996). Future sea-level rise due to climate change is expected to occur at a rate greatly exceeding that of the recent past; for example during the next 100 years, sea-levels are expected to rise at a rate between 20–88 mm/yr (IPCC 2001). In recent years a numbers of models have been developed to investigate the effect of climate change and sea level rise on saltwater intrusion in coastal aquifers (e.g. Sherif, and Singh 1999).

MEASURES TO CONTROL SALTWATER INTRUSION

A number of different measures have been used to control seawater intrusion and to protect the groundwater resources. The main principle of protection is to increase the volume of fresh groundwater and reduce the volume of saltwater. Todd (1974) discussed various means of preventing saltwater from contaminating groundwater sources including: (1) reduction of the abstraction rates, (2) relocation of abstraction wells, (3) subsurface barriers, (4) natural recharge, (5) artificial recharge, (6) abstraction of saline water, and (7) combination of injection and abstraction systems. Extensive research has been carried out to investigate saltwater intrusion in coastal aquifers. However, only few models have been developed to study the control of saltwater intrusion. These models use one or more of the previous measures to study the control of saltwater intrusion. The reduction of abstraction rates aims to reduce the pumping rates and use other water resources (Scholze et al. 2002). The relocation of abstraction well aims to move the wells further inland (Sherif and Al-Rashed 2001). Subsurface barriers aim to prevent the inflow of seawater into the basin (Harne et al. 2006). Natural recharge aims to recharge aquifers with additional surface water (Ru et al. 2001). Artificial recharge aims to increase the groundwater levels, using surface spread for unconfined aquifers and recharge wells for confined aquifers. The sources of water for injection may be surface water, groundwater, treated wastewater or desalinated water (Papadopoulou et al. 2005). The abstraction of saline water aims to reduce the volume of saltwater by extracting brackish water from the aquifer (Sherif and Hamza 2001). The combination of injection of freshwater and extraction of saline water can reduce the volume of saltwater and increase the volume of freshwater (Rastogi et al. 2004).

THE LIMITATIONS OF THE PREVIOUS MODELS TO CONTROL SALTWATER INTRUSION

The previous methods for controlling saltwater intrusion have many limitations. Most of these methods are costly and some of them might not be applicable in certain cases. Furthermore, they are generally temporary solutions and with the population growth and increasing demand the intrusion will be increased. The source and the cost of fresh water for injection, especially in

areas that suffer from scarcity of water and the fact that the disposal of the brine into the sea can cause many problems, have usually been ignored. One of the future challenges is the sea level rise due to climatic change and its effects on saltwater intrusion. Climate change has caused changes in the sea level because rising temperature makes the seawater expand and glaciers and ice caps to melt. The effects of climate change and sea level rise on saltwater intrusion in the long term should be considered in the control models. The majority of the previous control models did not consider this point, while few centimetres rise in sea level could have a great effect on saltwater intrusion. This study considers the effect of increase in sea level due to climate change on the fresh water/salt water interface with the focus on determining changes in the position of the interface with time and identifying measures to control such movements.

THE PROPOSED METHODOLOGY TO CONTROL SALTWATER INTRUSION CONSIDERING SEA LEVEL RISE

In this study a new methodology is proposed to study the control of saltwater intrusion. This methodology aims to overcome the limitations of the previous methods. The proposed methodology, Abstraction, Desalination and Recharge (ADR), consists of three steps; abstraction of brackish water from the saltwater zone, desalination of the abstracted brackish water using RO treatment process, and recharge of the treated water into the aquifer. The main benefits of the (ADR) methodology are to return the mixing zone into the original status and to reach a dynamic balance between fresh and saline groundwater through two processes; (1) Abstraction of brackish groundwater to reduce the volume of saline water, and (2) Recharge of treated brackish water to increase the volume of fresh groundwater. The Abstraction-Recharge process helps to move fresh water/salt water interface toward the sea and is considered an efficient method to control saltwater intrusion. This process will continue until a state of dynamic equilibrium is reached with respect to the salinity distribution. Then a suitable quantity of treated brackish water is injected to the aquifer to maintain the balance between fresh and saline groundwater and the excess of the treated brackish water may be used for different purposes or stored in the aquifer. The second step of this methodology, desalination of brackish water using the RO treatment process aims to produce fresh water from the brackish water and use it for recharging the aquifer to overcome the scarcity of water in these areas. It is generally less expensive than other sources of freshwater for injection. For example, desalination of seawater has a lot of problems such as; high cost, high pollution (mainly carbon emission), and disposal of the brine. Desalinating brackish water is an efficient alternative to seawater desalination, because the salinity of brackish water is less than one-third of that of seawater. Therefore, brackish water can be desalinated at a significantly lower cost than sea water. A simulation model is developed for the investigation of saltwater intrusion to analyze the position and movement of the fresh water/salt water interface. The predicted sea-level rise data will be incorporated into the simulation model by specifying an annual increase of 8.8 mm/year as predicted by IPCC (2001) for the current century. Finally the model will study different scenarios to control saltwater intrusion considering the expected rise in sea level for the purpose of determining the optimum locations, depths and rates of abstraction and recharge for the system.

CONCLUSIONS

Over-pumping is considered the main cause of saltwater intrusion into coastal aquifers in many areas of the world and sea level rise accelerates the intrusion. Saltwater intrusion poses a major limitation to utilization of groundwater resources. Groundwater provides about one-third of the total freshwater consumption in the world so saltwater intrusion should be prevented or at least controlled. A number of methods have been used to control saltwater intrusion but they have many limitations. The proposed methodology (ADR) is an attempt to overcome the limitations of

the previous methods. It is considered an economical solution and has less environmental impact because desalinating brackish water using RO treatment process involves lower energy consumption, lower cost and lower pollution and carbon emission as compared with conventional methods of sea water desalination and waste water treatment. It also provides fresh water for recharge using the treated brackish water. The (ADR) technique is considered an efficient method to control saltwater intrusion. It is capable of preventing saltwater intrusion because it increases the volume of fresh groundwater and decreases the volume of saltwater, while considering economical aspects, environmental impact and sustainable development of water resources. Also the effect of sea level rise due to climate change can be considered by varying the seawater level in the numerical model according to the estimated sea levels over the current century as predicted by IPCC (2001).

REFERENCES

Harne, S, Chaube, UC, Sharma, S, Sharma, P, Parkhya, S, (2006). "Mathematical modelling of salt water transport and its control in groundwater." *Natural and science*, 4(4): 32-39.

Papadopoulou, MP, Karatzas, GP, Koukadaki, MA, Trichakis, Y, (2005). "Modelling the saltwater intrusion phenomenon in coastal aquifers – A case study in the industrial zone of

Herakleio in Crete." Global NEST journal, Vol. 7 (2): 197-203.

Rastogi, AK, Choi, GW, Ukarande SK, (2004). "Diffused interface model to prevent ingress of seawater in multi-layer coastal aquifers." J. special hydrology, 4(2): 1-31.

Ru, Y, Jinno, K, Hosokawa, T, Nakagawa, K, (2001). "Study on effect of subsurface dam in coastal seawater intrusion." 1st Int. Conf. Saltwater Intrusion and Coastal Aquifers, Monitoring, Modelling, and Management (Morocco).

Scholze, O, Hillmer G, Schneider, W, (2002). "Protection of the groundwater resources of Metropolis CEBU (Philippines) in consideration of saltwater intrusion into the coastal aquifer." 17th Salt Water Intrusion Meeting, Delft, the Netherlands.

Sherif, MM, Singh, VP, (1999). "Effect of climate change on sea water intrusion in coastal aquifers." J. Hydrological processes, 13: 1277-1287.

Sherif, MM, Al-Rashed, MF, (2001). "Vertical and horizontal simulation of seawater intrusion in the Nile Delta Aquifer." 1st Int. Conf. Saltwater Intrusion and Coastal Aquifers, Monitoring, Modelling, and Management (Morocco).

Sherif, MM, Hamza KI, (2001). "Mitigation of seawater intrusion by pumping brackish water." J. Transport in Porous Media, 43 (1): 29-44.

Todd, DK, (1974). "Salt-water intrusion and its control." Water Technology/Resources. Journal of American Water Works Association, 66(3): 180-187.

Contact Information: H. Abd-Elhamid, Department of Engineering, University of Exeter, Exeter, EX4 4QF, UK, Phone: +44 1392 263909, Fax: +44 1392 217965, Email: hfa201@ex.ac.uk

Modeling of the Potential for Vertically Downward Saltwater Migration from a Dredge Pond

Peter F. Andersen[1], *Lisa M. Grogin*[1] and *Ronald L. Bartel*[2]
[1]GeoTrans, Inc., Roswell, GA, USA
[2]Northwest Florida Water Management District, Havana, FL, USA

ABSTRACT

Modeling was conducted to assess the potential for migration of saltwater deposited in a dredge pond into a freshwater aquifer. A local-scale SEAWAT model was constructed to evaluate the significance of head differences between the dredge pond, the aquifer system, and an adjacent creek on loss of containment of the saltwater deposited in the pond. Results from this model were used to provide guidance on how to operate the dredge pond and to develop hydraulic metrics for when it would be safe to initiate deposition of the saltwater and dredge materials into the pond. The results of this model compared favorably to those of another variable density groundwater flow and transport model. Dredging operations are currently underway and field data are being collected. Comparison of the field data to model results will be possible once the data have been processed. A second, more general model, was used to investigate the problem of an unstable saltwater interface (saltwater overlying freshwater) and to evaluate the interplay between hydraulic and density gradients on downward saltwater migration.

Contact Information: Peter F. Andersen, GeoTrans, Inc., 1080 Holcomb Bridge Road, Building 100, Suite 190, Roswell, GA 30076 USA, Phone: 770-642-1000, Fax: 770-642-8808, Email: pandersen@geotransinc.com

Compositional Change of Groundwater Chemistry in the Shallow Aquifer of Small Tropical Island Due to Seawater Intrusion

A. Zaharin Aris [1], *Abdullah M. Harun*[2], *Kim K. Woong*[3] and *Praveena S. Mangala*[2]
[1]Department of Environmental Sciences, Universiti Putra Malaysia, Malaysia
[2]School of Science and Technology, Universiti Malaysia Sabah, Malaysia
[3]Department of Environmental Science and Engineering, Gwangju Institute of Science and Technology, Republic of Korea

ABSTRACT
A detailed groundwater chemistry study were undertaken to examine the evolution of groundwater in the shallow aquifer of Manukan Island, Sabah, Malaysia since fresh groundwater aquifers especially for small islands are often exposed to heavy pumping and consequently to risks of seawater intrusion. Geochemical data on dissolved major constituents in analyzed groundwater samples revealed the main processes responsible for their geochemical evolution. The results of analysis showed that the groundwater was chemical highly enriched with Na^+ and Cl^- an indication of seawater intrusion into the aquifer as also supported from the Na-Cl signature on the Piper diagram. Compositional change from Ca-rich to Na-rich water types can be explained mostly by simple mixing process. From the PHREEQC calculation, calcite and aragonite solubility showed positive values of the saturation indices (SI) indicating supersaturation which lead to mineral precipitation condition of water by these minerals.

INTRODUCTION
Groundwater usage for daily supply in the small island of Manukan, Sabah, well known as diver's paradise, has drastically increased over the last decade due to the rapid increase in visitors to the island. Increased groundwater demand leads to a decline of water levels and deterioration of water quality. With the current increased groundwater pumping, incursion of seawater into the island's aquifers is a natural and expected significance consequence, especially in the low lying area of the island. In general, small carbonate islands are highly susceptible to seawater intrusion due to the high permeability of the aquifers.

Increased knowledge of the geochemical processes that control groundwater chemical composition in small islands of tropical regions could lead to improved understanding of the hydrochemical systems in such areas, and lead to development of a sustainable scheme for groundwater management. In this paper, we report on the geochemical processes that changed the groundwater chemistry observed in Manukan, Sabah.

MATERIALS AND METHODS

Study site
Located about 7.45 km from Kota Kinabalu, capital city of Sabah, Malaysia (Figure 1), Manukan (5°57'-5°58' N and 115°59'-116°01' E) is one of the islands of the Tunku Abdul Rahman Park. Covering an area of 206 000 m^2, the island is a crescent shaped, one and half kilometer long and three kilometer wide in the middle. Almost 80% of the area of the island is high relief and covered by forest (western side of the island), while remaining 20% of the area is developed for tourism activities which are located on the low lying are of the island (eastern part of the island). Geologically, Manukan Island was isolated from the mainland about one million years ago (Basir *et al.*, 1991). The island is underlay by interbedded sandstone and shales of the Middle Miocene Crocker Range Formation. The main aquifer of Manukan Island comprises Quaternary

carbonates and coarse sandy alluvium, which overlie the older rocks. Overall the limited extent of the aquifer and low elevation of the island lead to very limited water storage, which is primarily dependent on the aquifer thickness, and distribution of the sands, which are often found at sites near the coast.

The groundwater recharge for Manukan Island aquifer depends entirely on infiltration. Sabah has a warm and humid climate with annual rainfall between 2000-2500 mm, humidity between 80-90% all year round and temperatures from 21 to 32°C. The climate is affected by the northeast and southwest monsoons, which are dominant during November to March and May to September respectively. The periods between the monsoons are marked by heavy rainfall.

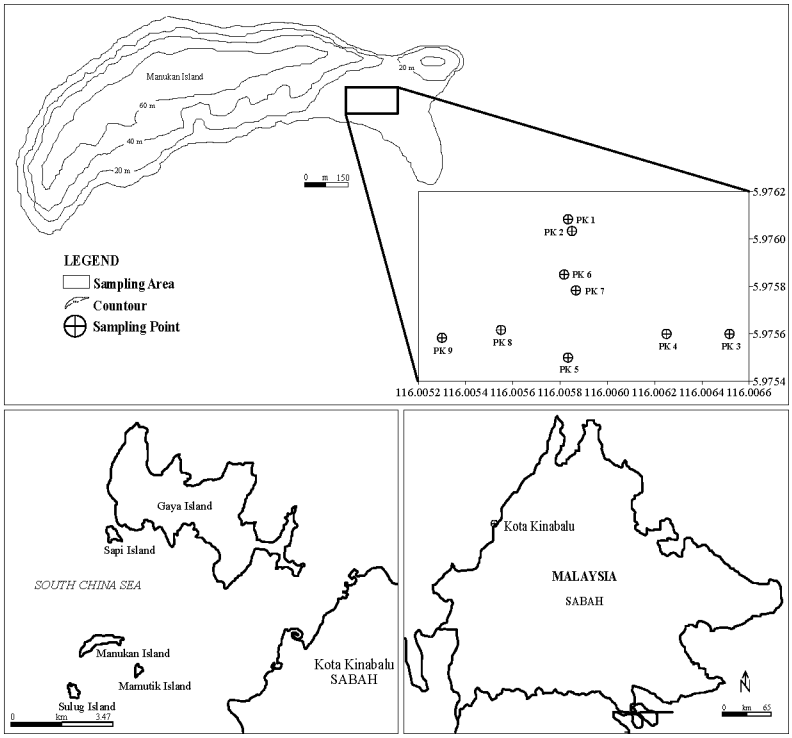

Figure 1. Schematic map showing the geographical locality of Manukan Island.

Sampling and analysis

In order to assess the groundwater quality of the surficial aquifer on Manukan Island, water samples were collected from the existing wells every two month between March 2006 and January 2007. A total of 162 samples were collected during the sampling period from 9 wells located on the low lying area of the island (Figure 1). Sampling, preservation and water analyses were performed in accordance with the standard procedures devised by APHA (1995).

GENERAL HYDROCHEMISTRY

In the cationic triangle of Piper diagram, most samples were plotted on Na-dominant area. In the anionic triangle, the values are almost plotted near the seawater signature because of predominance of Cl^-. The simple mixing process between seawater and fresh groundwater are clearly evidence in the cation triangle where most of water samples were plotted near Na-Cl water type area and some samples were plotted near Ca-Cl dominant water type area (Figure 2).

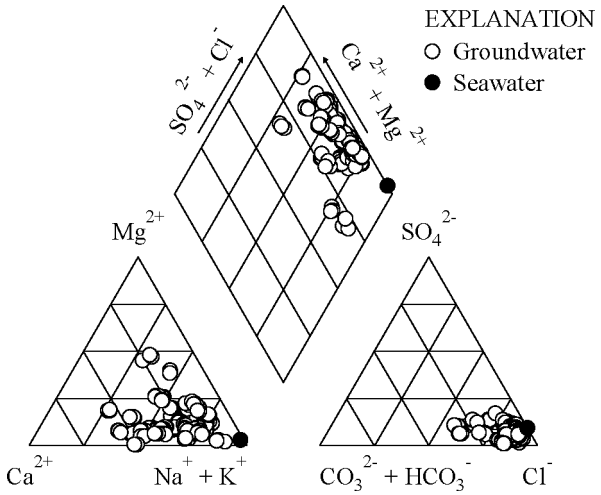

Figure 2. Piper diagram representing the groundwater chemistry of the study area.

The dominant hydrochemical process on Manukan Island is seawater-freshwater mixing as supported by the increased of its groundwater salinity and electrical conductivity (EC) values compared with Abdullah *et al.* (1996) data. The correlations (between major ions such as Na^+, Cl^-, SO_4^{2-} with EC and salinity) clearly identified the main elements that contributed to the groundwater salinity and their tendency to exhibit a similar trend of salinization pattern.

The lower concentration of Ca^{2+} compared to Na^+ found in the study period is a result from the cation exchange process that occurs naturally when seawater intrudes into aquifer system. Presuming that Ca^{2+} is the dominant ion for the aquifer matrix of the study area, the following Equation 1 can describe the above-mentioned process (Appelo & Postma, 2005):

$$Na^+ + \frac{1}{2}Ca\text{-}X_2 \rightarrow Na\text{-}X + \frac{1}{2}Ca\text{-}X_2 \quad (1)$$

When Ca^{2+} exchanged with Na^+, the water becomes saturated for calcite and precipitation resulted (Chappelle, 1983). At high pH, Ca^{2+} and Mg^{2+} are usually transferred to a solid phase; therefore their concentrations are controlled by mineral precipitation. With regards to the above condition, in this study the hydrochemical modelling of the water samples was performed using the aqueous speciation program PHREEQC. The results of the calculation for the degree of saturation index (SI) of the groundwater with respect to selected specified minerals are shown in Figure 3. From the plot, it shows that SI of calcite and dolomite are positive values higher than 1, indication supersaturation which lead to mineral precipitation condition of water by this mineral due to an extend effect from seawater intrusion.

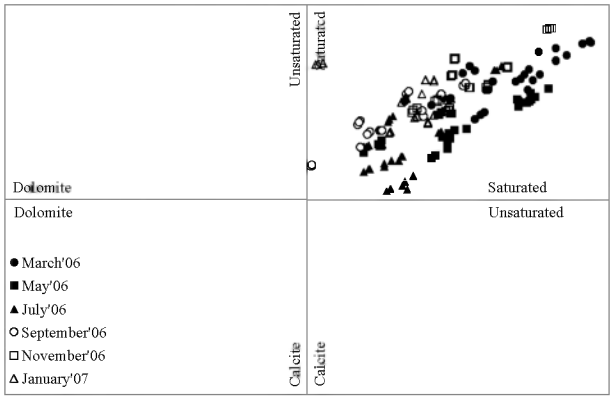

Figure 3. Saturation indices plot for calcite and dolomite.

CONCLUSIONS

A diversity of geochemical processes is taking place in the mixing zone of fresh groundwater-seawater is rather complicated; it represents an over exploitation of an aquifer. The salinization of the groundwater occurred as a result of increasing ionic concentrations attributed to seawater intrusion into the aquifer system. The increase in concentrations of major elements in groundwater with salinity (Cl^-) leads to cation exchange processes and subsequently leads to carbonate minerals precipitation.

ACKNOWLEDGEMENTS

This work has been supported by the Ministry of Science, Technology and Innovation (MOSTI), Malaysia through the ScienceFund research project of SCF0039-SEA-1/2007.

REFERENCES

Abdullah, M.H., Musta, B. & Ramli, M.Z. 1996. Groundwater quality as freshwater resource in Manukan island-a preliminary finding. In: Proceedings of geology and environmental seminar, pp 33–37. Bangi, Selangor. [in Malay]

APHA. 1995. Standard Methods for the Examination of Water and Wastewater. 19th Ed. American Water Works Association, Water Environment Federation, Washington.

Appelo, C.A.J. & Postma, D. 2005. Geochemistry, Groundwater and Pollution. 2nd Ed. Rotterdam: A.A. Balkema.

Basir, J.; Sanudin, T. & Tating, F.F. 1991. Late Eocene planktonic foraminifera from the Crocker Formation, Pun Batu, Sabah. Warta Geologi 14(4): 1-15.

Chappelle, F.H. 1983. Groundwater geochemistry and calcite cementation of the Aquia aquifer in Southern Maryland. Water Resour. Res. 19: 545-558.

Contact Information: A. Zaharin Aris, Department of Environmental Sciences, Universiti Putra Malaysia, 43400 UPM Serdang, Selangor, Malaysia Phone: (+603) 8946 7461; Fax: (+603) 8943 8109, Email: zaharin@env.upm.edu.my

An Assessment Tool for Aquifer Storage and Recovery in Stratified Coastal Aquifers

Mark Bakker
Water Resources Section, Faculty of Civil Engineering and Geosciences, Delft University of Technology, Delft, The Netherlands

ABSTRACT

The major benefit of aquifer storage and recovery in a coastal, saline aquifer is well known: it may be an efficient approach to store available freshwater so that it can be used when needed. There are two possible problems with the storage of freshwater in saline aquifers. First, the freshwater tends to float up and form a thin pancake at the top of the aquifer that cannot be recovered; additional recovery problems may be caused by horizontal head gradients that may transport the stored freshwater bell away from the recovery well. Second, the quality of the freshwater may change, either through mixing with the salt water or through chemical reactions. In this paper, we present a simple approach to assess the significance of the first problem for the storage and recovery of freshwater in stratified aquifers containing salt or brackish water and no significant horizontal gradients.

The main purpose of the approach is to perform a quick assessment of the feasibility of aquifer storage and recovery of freshwater in a saline aquifer given the following information:

- The thickness, hydraulic conductivity and porosity of the strata of the stratified aquifer,
- The density difference between the freshwater and the saline water,
- The recharge rate during freshwater storage,
- The expected time periods for injection, storage, and recovery,
- The position of the well screen in the aquifer.

Application of the approach answers the question whether it is possible to store and recover freshwater under the given circumstances and whether further investigations into the effects of horizontal gradients, mixing and chemical reactions are justified.

Contact Information: Mark Bakker, Water Resources Section, Faculty of Civil Engineering and Geosciences, Delft University of Technology, Stevinweg 1, 2628 CN Delft, The Netherlands, and KWR, Groningenhaven 7, 3433 PE Nieuwegein, The Netherlands. Phone: +31 152783714, Email: mark.bakker@tudelft.nl

Simulating Density-Dependent Flows Using the Lattice Boltzmann Method

Kathleen J. Bardsley and *Michael C. Sukop*
Department of Earth Sciences, Florida International University, Miami, FL, USA

ABSTRACT
Seawater intrusion is a continuing concern in south Florida and in many other coastal areas. Although there is extensive research on this topic, more tools are required to fully understand and predict the location and behavior of the freshwater/seawater boundary. The lattice Boltzmann method is a radically different numerical tool because it is not based on discretization of a series of differential equations. It has been used to simulate fluid flow in various disciplines. Recent advances in lattice Boltzmann modeling permit simulation of large-scale density-dependent ground water flow and heat/solute transport. These simulations can be accomplished while retaining the advantages of 'regular' lattice Boltzmann methods, such as solute/heat transport at high Reynolds numbers (characteristic of flow inside a conduit). We show how this method can be applied to density-dependent flows, including a Henry-like problem.

INTRODUCTION
Seawater intrusion is a classic density-dependent problem in hydrogeology. It must be fully understood in order to be able to predict and prevent groundwater deterioration in coastal areas. Various software programs have been developed and are being used to model coupled fluid flow and solute transport for density-dependent applications: SUTRA, SEAWAT, and HST3D are popular examples. All of the current programs are either finite difference or finite element methods. Density-dependent flow problems are exceptionally challenging for conventional numerical methods due to inherent non-linearity; definitive solutions are often elusive and a completely different modeling approach may be advantageous. The lattice Boltzmann method (LBM) represents such a numerical tool because it is not based on discretization of a series of differential equations. Instead, its foundation lies in the kinetic theory of gasses as proposed by Boltzmann. A key advantage of lattice Boltzmann method is that it has the ability to solve the Navier-Stokes equations in larger conduits and pores. Hence it allows for eddy diffusion brought on by inertial components of flow at higher Reynolds numbers, which may occur in some coastal aquifers. Simulation of these phenomena is not possible with traditional Darcy's law-based groundwater models. Some geologists and engineers have been able to successfully apply LBM to fluid flow and contaminant transport problems (Ginzburg and d'Humieres, 2003; Anwar et al., 2008). There are only a handful of scientists attempting to apply LBM to density-dependent flows in general (e.g., Shan, 1997; Dixit and Babu, 2006); even fewer have considered seawater intrusion (Servan Camas, 2007).

LATTICE BOLTZMANN METHOD BASICS
Most numerical modeling tools are based on discretization of differential equations. LBMs are based on discretization of the movement and interaction of hypothetical particles using a particle distribution function, f (Sukop and Thorne, 2006). The moments of the particle distribution function provide the macroscopic fluid properties, e.g., density and velocity. In LBMs, time, space, and velocity directions are all discretized. On each point in space, called a lattice node, a discrete set of f_a corresponding to a choice of velocity directions $\mathbf{e}_a$ are stored. Directions in two dimensions are (0,0), (±1,0), (0, ±1), (±1, ±1), and the lattice based on these nine directions is referred to as the D2Q9 grid (Figure 1).

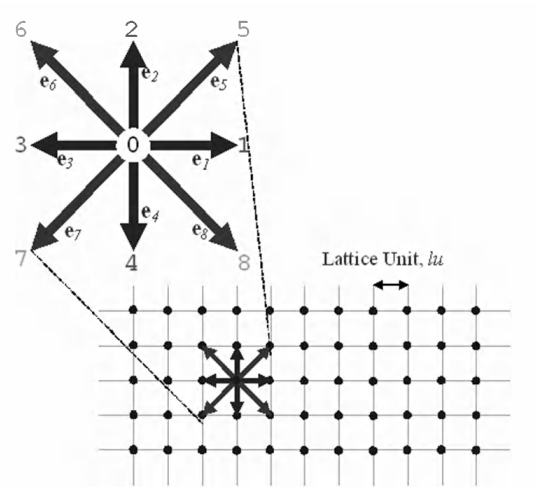

Figure 1. D2Q9 grid (Sukop and Thorne, 2006), $\mathbf{e}_{1\text{-}8}$ are unit velocity vectors

At each time step, the f_a are updated according to a *collision* step $f_a^*(\mathbf{x},t) = f_a(\mathbf{x},t) - \frac{1}{\tau}\left(f_a^{eq}(\mathbf{x},t) - f_a(\mathbf{x},t)\right)$ and a *streaming* step $f_a(\mathbf{x}+\mathbf{e}_a, t+1) = f_a^*(\mathbf{x},t)$ (Sukop and Thorne, 2006). The assumptions of unit time step $\Delta t = 1$ time step (*ts*) and unit node spacing $\Delta x = \Delta y = 1$ lattice unit (*lu*) have been incorporated. The key to the collision step is the equilibrium distribution function f^{eq}, which is defined per direction as $f_a^{eq} = w_a \rho\left(1 + 3\mathbf{e}_a \cdot \mathbf{u}^{eq} + \frac{9}{2}\left(\mathbf{e}_a \cdot \mathbf{u}^{eq}\right)^2 + \frac{3}{2}\mathbf{u}^{eq} \cdot \mathbf{u}^{eq}\right)$ where $w_0 = \frac{4}{9}$, $w_1 = w_2 = w_3 = w_4 = \frac{1}{9}$, $w_5 = w_6 = w_7 = w_8 = \frac{1}{36}$, $\rho = \sum_a f_a$ and $\mathbf{u}^{eq} = \frac{1}{\rho}\sum_a f_a \mathbf{e}_a$.

The superscript on $\mathbf{u}^{eq}$ is to distinguish it from the actual macroscopic velocity that is computed after the collision step. Additional details of LBMs including incorporation of buoyant forces can be found in Sukop and Thorne (2006).

BUOYANCY

We present two density-dependent flow problem examples here. The first example is an initial value problem with half of the domain filled with saltwater.

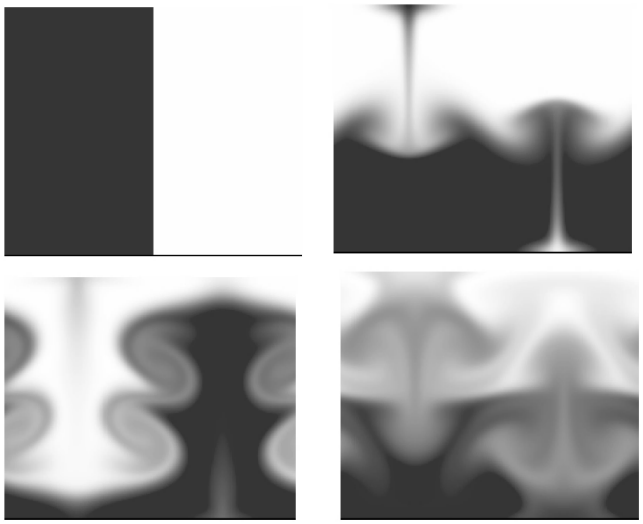

Figure 2. Initial time at upper left to approaching equilibrium at bottom right.

The second example involves fluid flow through a narrow opening between two plates at different temperatures. We have compared our results with the analytic equation:

$$v = \frac{\Delta T g \beta \rho B^2}{12\mu}\left[\left(\frac{y}{B}\right)^3 - \left(\frac{y}{B}\right)\right]$$ where: v = velocity, ΔT = temperature difference between plates, g = gravity, β = coefficient of volume expansion, ρ = fluid density, B = half width of opening, y = position in opening. Figure 3 is the result of the comparison.

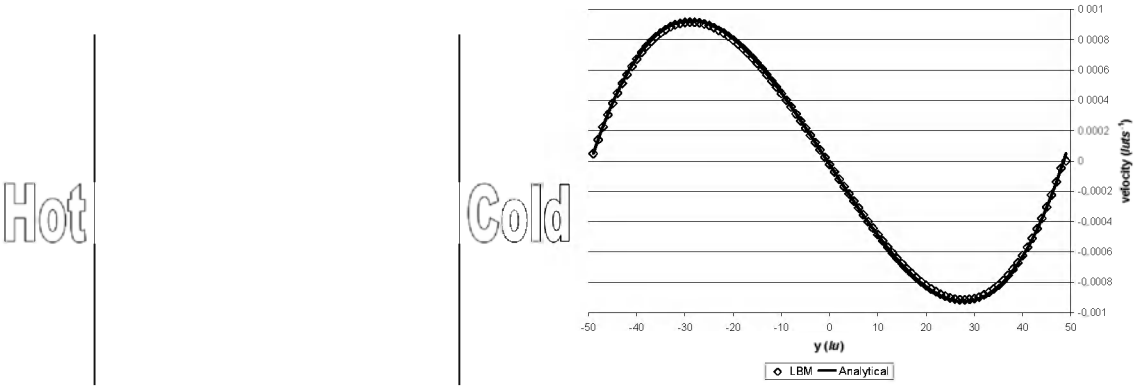

Figure 3. Left: Simulation domain, Right: Solid line analytical, dashed line LBM solution. This grid resolution results in two percent error.

HENRY-LIKE PROBLEM

The next step is to model the classic Henry problem. The Henry problem consists of a rectangular domain representing a confined aquifer with a freshwater inflow boundary condition on the right and a saltwater inflow boundary along the left. The top and bottom boundaries are closed (Henry, 1964). We were able to simulate a problem similar to the Henry problem. However we have yet to simulate the classic Henry problem with LBM using the physical parameters.

CONCLUSION

We used LBM to simulate three density-dependent flow problems. One available analytical solution was closely matched by LBM. Further work is needed to translate the physical Henry problem parameters into LBM inputs.

REFERENCES

Anwar S.A., Cortis, A.C. and Sukop, M.C. 2008. Lattice Boltzmann simulation of solute transport in heterogeneous porous media with conduits to estimate macroscopic Continuous Time Random Walk model parameters. Progress in Computational Fluid Dynamics, In press.

Servan Camas, B., 2007. Saltwater intrusion simulation heterogeneous aquifer using lattice Boltzmann method. M.S. thesis, Louisiana State University, Baton Rouge, LA, USA, 77p.

Dixit, H.N. and Babu V. 2006. Simulation of high Rayleigh number natural convection in a square cavity using the lattice Boltzmann method. International Journal of Heat and Mass Transfer, v. 49:727-739.

Ginnzburg, I. and d'Humieres, D. 2003. Multi-reflection boundary conditions for the lattice Boltzmann models. Physical Review E, v. 68:066614-1-30.

Guo, W. and Langevin, C.D. 2002. *User's guide to SEAWAT: A computer program for simulation of three-dimensional variable-density ground-water flow*. U.S. Geological Survey, Techniques of Water-Resources Investigations 6-A7, Tallahassee, Florida.

Henry H.R. 1964. Effects of dispersion on salt encroachment in coastal aquifers. U.S. Geological Survey Water Supply Paper 1613-C, C71-C84.

Shan, X. 1997. Simulation of Rayleigh-Benard convection using a lattice Boltzmann method. Phys. Rev. E, v. 55:2780-2788.

Simpson, M.J. and Clement, T.P. 2003. Theoretical analysis of the worthiness of Henry and Elder problems as benchmarks of density-dependent groundwater flow models. Advances in Water Resources, v. 26:17-31.

Sukop, M.C., Thorne, Jr. D.T., 2006. *Lattice Boltzmann Modeling: An introduction for geoscientists and engineers.* Springer, Heidelberg, Berlin, New York 172 p.

Contact Information: Kathleen J. Bardsley, Florida International University, Department of Earth Sciences, PC 323 – University Park, Miami, FL 33199 USA, Phone: 305-348-7203, Fax: 305-348-3877, Email: Katie.bardsley@fiu.edu

Geochemical and Isotopic Study of the Origin of Salinization in an Unconfined Coastal Aquifer of Cap Bon (Tunisia)

M. F. Ben Hamouda[1], *J. Tarhouni*[2], *K. Zouari*[3] and *C. Leduc*[4]
[1]Geochemistry and Isotope Hydrology Unit, CNSTN, Tunisia
[2]Rural Engineering Water and Forest Department, INAT, Tunisia,
[3]Environnement and Radioanalyse Laboratory, ENIS, Tunisia
[4]UMR G-EAU, Institut de Recherche pour le Développement, Montpellier, France

ABSTRACT
In the Plio-quaternary aquifer of the eastern coast of Cap Bon (Tunisia), the groundwater quality is deteriorating. Different methods using geochemistry (ions Na^+, Cl^-, Ca^{2+}, Mg^{2+}, Br^-) and isotopes (^{18}O ,^{2}H) are compared with the hydrodynamic information for identifying the main processes involved in the increase in salinization. Along the coast, the seawater intrusion resulting from the groundwater overexploitation is identified but is not the only cause of the qualitative degradation: the irrigation development that induces the soil leaching and the fertilizers transfer to groundwater over the whole aquifer extent is another major reason of the salinization increase.

INTRODUCTION
As many other semi-arid regions, the Cap Bon peninsula (N.E. Tunisia) shows a parallel increase in overexploitation and mineralization of groundwater resources. Because of the regional situation along the seashore, the seawater intrusion in the unconfined Plio-quaternary aquifer is an obvious explanation for the rising salinity but other processes may also intervenene. Surveys including level measurements, hydrochemical and isotopic samplings were performed in 2001, 2002 and 2003 and results were compared with previous information. The study area is 45 km long and 17 km wide at the most, with a mean annual rainfall of about 500 mm and potential evapotranspiration of about 1100 mm. The landscape is a coastal plain slightly sloping (3%) towards the sea. The Plio-quaternary aquifer extends over 475 km^2 and its thickness varies between 30 and 150 m. Groundwater flows from NW, at the foot of a mountain range, to SE in the coastal plain. Two deeper aquifers exist but they are separated from the Plio-quaternary aquifer by an impervious clayey layer.

METHODS AND RESULTS
Piezometric and salinity maps of the Plio-quaternary aquifer were established. The continuous increase in pumping has created several depressions in the water table, up to 12 m below msl and induced a deterioration of the water quality. The temporal changes in water-table level and salinity are often similar which suggests a strong link between them. Several geochemical approaches were performed to identify the importance of the marine intrusion in the increase in mineralization.

The chloride is strongly correlated to the sodium for the majority of the samples (Fig. 1). The predominance of sodium and chloride is explained by the proximity of the sea, via the spray and/or a progress of seawater intrusion. Even for points far from the sea, the Na^+/Cl^- molar ratio (meq/l) does not significantly differ from the Mediterranean ratio (0.86). This indicator is then of a limited interest for distinguishing the origins of the mineralization. The contents of Ca^{2+} and Mg^{2+} in meq/l are very variable. In most cases, Ca^{2+} is higher than Mg^{2+} but for 4 samples (11635, 11637, 11281,11828) where the Ca^{2+}/Mg^{2+} ratio lower than 1 (Fig. 2) indicates a mixing with the seawater (marine ratio 0.2). These points are close to the sea in the region where the mineralization is the highest.

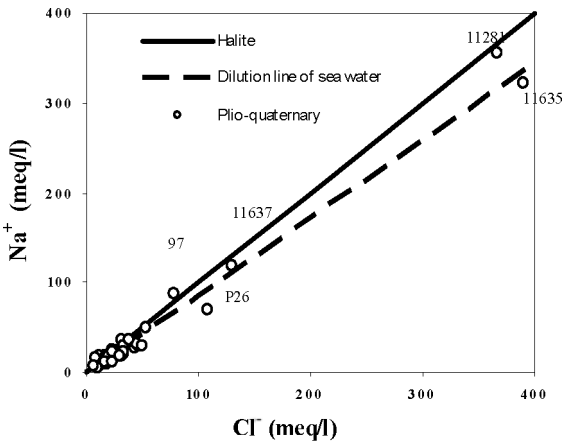

Figure 1. $[Na^+]/[Cl^-]$ correlation

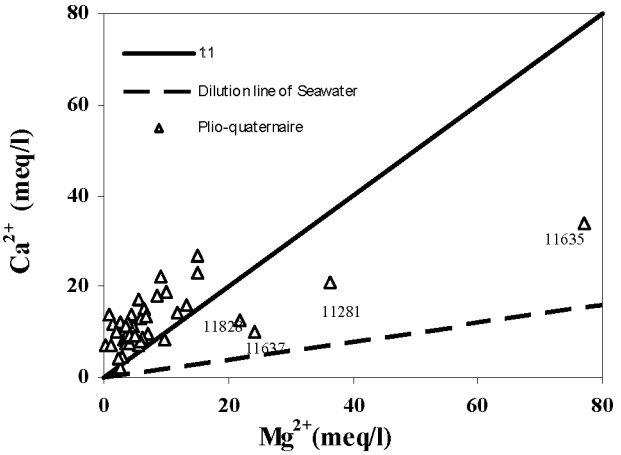

Figure 2. $[Ca^{2+}]/[Mg^{2+}]$ correlation

The Br^-/Cl^- ratio is often used for identifying a possible seawater intrusion because of its relatively constant value ($1{,}5.10^{-3}$) in the present sea water. In the Plio-quaternary aquifer, the Br^-/Cl^- ratio is in general lower than the marine ratio (Fig. 3). The few points close to the dilution line of seawater may trace a mixing with the recent seawater intrusion.

Other samples, with a lower Br^-/Cl^- ratio, suggest the existence of other pole of water with a different mineralization. This suggests a contribution of superficial water and possibly returns of water irrigation into the aquifer and an evaporation of water during the infiltration within the aquifer formation. The points which the ratio Br^-/Cl^- are located over to the line of dilution of sea water are outside of the seawater intrusion.

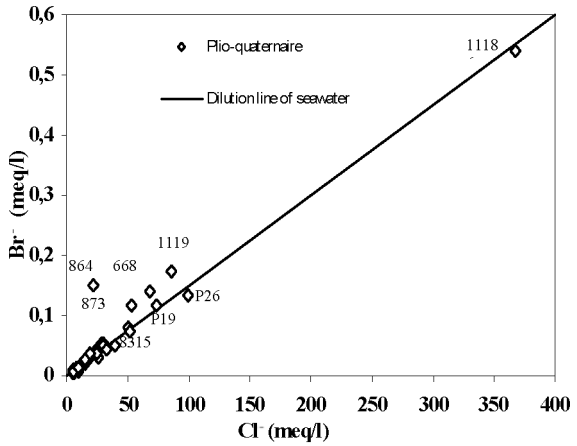

Figure 3. Content in Br^- and Cl^-

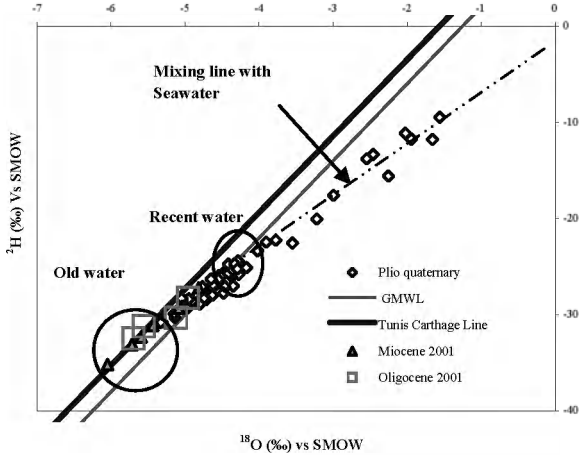

Figure 4. Isotopic content (^{18}O, ^2H)

The Br^-/Cl^- ratio identifies also points which seem contaminated by seawater. These points differ sometimes from those distinguished by the Ca^{2+}/Mg^{2+} ratio. These two approaches are complementary but imperfectly discriminating.

The graph ^{18}O vs. ^2H shows three groups (Fig.4). The first one (^{18}O between -4.3 and -5.5 ‰) is between the global meteoric water line (GMWL) and the local meteoric line of Tunis-Carthage (LMWL). This reveals the important contribution of the present rain to the groundwater recharge. These points are situated all over the plain and especially close to the temporary rivers.

The second group, along the mixing line with the seawater, corresponds to wells in the piezometric depression (P19, 11281, 11635, 8684, P3, 5729, 6077, 5610), but two exceptions (3002, 5994). The recent seawater contamination is then clearly identified. The third group with isotopic values lower than the mean present rainfall (^{18}O between -4.82 and -6.05 ‰) is made of wells in Miocene and Oligocene aquifers with a probable mixing between present and old waters.

DISCUSSION AND CONCLUSIONS

In the old measurements, typical of the natural state, the upstream part of the Plio-quaternary aquifer was more mineralized than downstream. This implies that the rainfall infiltration in aquifer outcrops is significantly complemented by the infiltration from temporary rivers floods when they reach the plain. Recent observations confirm the importance of the present recharge: after rainy years, as 2003 and 2004, the decrease in mineralization is clear. In this region, the $^{18}O/^{2}H$ study is the most efficient geochemical tool for characterizing the seawater intrusion. As the most depressed areas are not systematically the most mineralized or contaminated by the seawater, other processes modifying the Plio-quaternary chemistry are to be searched for. An upward leakage from the Miocene aquifer is very weak or even nil: its mineralization is lower (less than 1 $g.l^{-1}$ for 90 % of the samples), even in the depressed area. The return of irrigation water to the Plio-quaternary water-table affects the whole region, whatever the thickness of the unsaturated zone (1 to 31 m), as shown by the NO_3^- content (median value of 90 $mg.l^{-1}$ in 2001). The absence of correlation between content of nitrate and thickness of the unsaturated zone indicates that all the area can be contaminated by this pollution. This a fundamental driver of the geochemsitry changes for the coming decades.

The determination the contribution of seawater in the plio-quaternary aquifer has been based on the calculation of the mass balance of the chloride. The contribution of seawater in the plio-quaternary aquifer has been estimated to be between 4 and 10% and may reach a maximum of 70 % depending on location translating the heterogeneity of the process of salinization in this region.

The table summarizes the various approaches applied for the distinction of the origin of salinity. With for the rows all the water samples and for the columns all the geochemical methods and the hydrodynamic information, this table highlights in each cell, if the method gave in this point information on the origin of the salinization and also the degree of certainty of the information (no doubt yes, no doubt not, possible yes, possible not, no idea). Confrontation between the various approaches permits to highlight the efficient methods, the methods requiring a confrontation with other methods and the methods insufficient for the determination of the origin of salinity. All around the Mediterranean sea, the human modifications of the natural water cycle are now superimposed over the large natural hydrological variability, following asynchronous dynamics. Even in apparently simple cases as this present study, a cautious and critical approach is necessary. Only the comparison of different methods at different spatial and temporal scales can lead to the pertinent identification of main processes at work. However, the variability of the results obtained according to the methods underlines the difficulty of interpretations. The overlap of different processes, the limitations related on the data and interpretations make particularly delicate the quantification of the evolutions of the next decades.

Sample No	Piez.Lev (m)	Salinity (mg/l)	$\delta^{18}O$ ‰	$\delta^{2}H$‰	Na/Cl meq/l	Ca/Mg meq/l	Br/Cl Meq/l	Hydro	Salinity	Isotopes	Na/Cl	Ca/Mg	Br/Cl	**Origin of salinization**
P1	33	2144	-4,84	-28	0,83	3,06	1,14E-03	NDN	PN	NDN	PY	NDN	PN	No Seawater intrusion
P 3	1,2	2035	-1,95	-11,8	1,11	2,60	1,41E-03	PY	PY	PY	PN	PN	PY	Possible mixing with seawater
P19	3,5	3520	-3,55	-22,6	0,75	2,32	1,58E-03	PY	PY	NDY	NDY	PN	PY	Possible mixing with seawater
P26	8,3	8371	-1,56	-9,5	0,63	1,79	1,36E-03	PN	PY	PY	NDY	PN	NDY	Evaporation + dissolution
97	3,7	7296	-4,46	-27,1	1,11	1,54	1,63E-03	PN	PY	PN	PN	PN	PN	Evaporation + dissolution
892	-7,7	3469	-4,39	-26,9	0,61	1,88	1,85E-03	NDY	PY	PN	NDY	PN	PY	Possible mixing with seawater
996	13,6	2650	-4,9	-28,6	0,82	2,35	1,76E-03	PN	PN	PN	PY	PN	PN	No Seawater intrusion
1129	27,3	2067	-5,05	-29,1	0,93	2,15	1,78E-03	NDN	NDN	NDN	NDN	NDN	PN	No Seawater intrusion
3093	40,9	1265	-4,7	-27,5	0,77	4,12	1,85E-03	NDN	NDN	NDN	PY	NDN	PY	Fresh water-No Seawater intrusion
3113	5,6	1153	-5,31	-30,8	0,86	36,08	1,44E-03	PN	NDN	NDN	PY	NDN	PN	Fresh water-No intrusion
3190	52,9	2451	-4,71	-28,4	0,84	3,13		NDN	NI	NDN	NDN	NDN		Dissolution by irrigation return flow
3202	47	1920	-1,66	-11,8	1,62	1,36	1,58E-03	NDN	NDY	NDY	NDN	NDN	PN	Evaporation
4814	102	3417	-4,48	-25,6	1,10	2,22	1,46E-03	NDN	NDN	NDN	NDN	NDN	PN	Evaporation
5610	-1,6	1293	-3,78	-22,3	0,90	1,83	8,30E-04	NDY	PY	NDY	PN	PN	PN	very weak mixing with sea water
5729	10,9	1510	-2,03	-11,2	0,66	0,87		NDN	NDN	NDY	NDY	NDY		very weak mixing with sea water
5743	28,8	2400	-4,42	-24,8	1,06	1,37		NDN	PN	NDN	NDN	NDN		Dissolution by irrigation return flow
5972	40,2	1485	-4,55	-26	0,60	8,21	1,63E-03	NDN	NDN	NDN	PY	NDN	NDN	Fresh water-No Seawater intrusion
5994	25,8	1862	-2,55	-13,8	0,92	3,96		NDN	NDN	PY	PN	PN		Evaporation
6077	15,6	1613	-3	-17,6	0,84	4,53		PN	PN	PY	PY	NDN		Possible mixing with seawater
6686	38,1	1702	-4,77	-27,1	0,87	4,36		NDN	NDN	NDN	PY	NDN		Fresh water
8088	50,4	1958	-4,68	-27,6	0,82	4,57		NDN	NDN	NDN	PY	NDN		Fresh water-No Seawater intrusion
8315	4,8	4762	-4,65	-27,3	0,93	1,22	1,41E-03	PY	PY	PN	PN	PN	PY	Possible mixing with seawater
8346	0,4	2323	-5,14	-30,3	0,92	3,28		PY	PY	NDN	PN	NDN		No Seawater intrusion
8377	72,4	2010	-4,95	-28,4	0,92	3,28		NDN	PN	NDN	PN	PN		No Seawater intrusion
8400	4,7	1971	-5,04	-28,5	0,88	2,42	1,65E-03	PN	NDN	NDN	NDN	NDN	NDN	Fresh water-No Seawater intrusion
8403	10,4	3648	-4,28	-25,8	0,85	2,42	1,71E-03	NDN	PY	PN	PY	PN	PY	Possible mixing with seawater
8420	-0,4	2413	-4,5	-26	0,81	2,65	1,58E-03	NDY	PY	PN	NDY	PN	PY	Seawater intrusion
8647	2	1696	-5,15	-29,9	0,48	3,13	7,04E-03	NDN	NDN	NDN	PY	NDN	NDN	Fresh water-No Seawater intrusion
8684	4	3232	-2,46	-13,4	0,92	1,27	2,04E-03	PY	PY	NDY	PN	PN	PN	Seawater intrusion
8737	0,8	3578	-4,42	-25,7	0,63	2,12	2,19E-03	PY	NDY	PY	PY	PN	PN	Possible mixing with seawater
8774	1,6	2995	-4,76	-28,2	0,60	1,23	1,37E-03	PY	PY	PN	PY	PN	NDY	Possible mixing with seawater
8820	40,6	1453	-5,05	-28,3	1,94	1,70	1,39E-03	NDN	NDN	NDN	NDN	NDN	PN	Fresh water-No Seawater intrusion
8894	-2,8	2848	-4,6	-26,6	0,58	3,12		NDY	PY	PN	PY	PN		Possible mixing with seawater
10959	-2	1162	-4,44	-26,6	0,73	0,76		NDY	PN	PN	PY	PY		Possible mixing with seawater
10995	-0,2	3226	-4,02	-23,4	0,71	13,80		PY	PY	PY	PY	NDN		Possible mixing with seawater
10996	1,6	1023	-5,33	-30,8	0,52	5,48	1,30E-03	PY	NDN	NDN	PY	NDN	PN	Fresh water-No Seawater intrusion
11186	3,7	3802	-4,55	-26,4	0,92	2,21	1,47E-03	PY	PY	PN	PN	NDN	PY	Possible mixing with seawater
11191	6,4	2355	-4,35	-27	0,64	1,33	2,03E-03	PN	PY	PY	PY	PN	PN	Possible mixing with seawater
11635	0,4	27160	-2,26	-15,6	0,82	0,44		NDY	NDY	NDY	NDY	NDY		Seawater intrusion
11637	0,8	10430	-4,36	-25,4	0,90	0,42		NDY	NDY	PY	PY	NDY		Seawater intrusion
11650	4,3	2331	-4,65	-26,3	0,93	4,95		PN	PN	PN	PY	PN		Dissolution, irrigation return flow
11829	6,8	2432	-4,33	-24,7	0,63	2,01	1,58E-03	PN	PN	PN	PY	PN	PY	Possible mixing with seawater
11269	-8,7	1702	-4,47	-27,1	0,68	1,82		NDY	PY	PN	PY	PN		Possible mixing with seawater
11281	1	36315	-3,22	-20,1	0,97	0,58		PY	NDY	NDY	PY	NDY		Seawater intrusion
11828	4,3	4090	-4,48	-27,8	0,58	0,57	1,68E-03	PN	NDY	PN	NDY	NDY	PY	Possible mixing with seawater
11869	3,2	858	-4,8	-28,9	0,99	1,89		NDN	NDN	NDN	NDN	NDN		Fresh water, No Seawater intrusion
13143	-1,05	21050			0,5675	0,6667		NDY	NDY		NDY	NDY		Seawater intrusion
13207	-0,66	9960			0,6475	0,875		NDY	NDY		NDY	NDY		Seawater intrusion
		No doubt yes : NDY	**No doubt non: NDN**	**Possible yes: PY**	**Possible non: PN**	**No idea : NI**		require confrontation with other methods	efficient method for samples near the sea	adequate method	insufficient method	require confrontation with other methods	require confrontation with other methods	

Contact Information: Mohamed Fethi Ben Hamouda, Geochemistry and Isotope Hydrology Unit, CNSTN, Techno park of Sidi Thabet, 2020 Tunisia, Phone: 00 216 98 628 648, Fax: 00 216 71 537 555,
Email: f.benhamouda@cnstn.rnrt.tn

Assessing Well Field Impacts on Water Quality in the Upper Floridan Aquifer in Southwest Florida

Terry Bengtsson
South Florida Water Management District, Fort Myers, FL, USA

ABSTRACT
The Upper Floridan Aquifer is the principal freshwater source in Florida for public water supply, and consists of multiple geologic formations within a broad, thick carbonate platform that forms the Floridan Peninsula. Each formation may have variable lithology, intrinsic permeability and porosity due to changing depositional environments and diagenetic history. Additionally, structural and tectonic movement may have induced fractures and dissolution zones that affect distribution of ground water flow within these formations. Horizontal and vertical hydraulic conductivity of these units, and the aquifer as a whole, are variable by orders of magnitude, and are scale and location dependent.

In South Florida, water within the Upper Floridan Aquifer is brackish, as fresh ground water flow from central Florida mixes with relic seawater, connate water and seawater. A broad transition zone generally extends south beneath Lake Okeechobee, east to just offshore in the Atlantic Ocean, and west to far offshore in the Gulf of Mexico. The vertical transition of brackish to seawater salinity at depth occurs more abruptly.

Within the past decade water supply plans for southwest Florida have targeted the Upper Floridan Aquifer as a source to meet future water supply demands. Since the late 1990s, five Upper Floridan well fields have been constructed to produce potable drinking water using reverse osmosis treatment. However, unanticipated water quality deterioration in the raw water has been experienced at three of the five locations.

This paper examines available data and uses a density-dependent solute transport model to evaluate potential responses to varying pumping stress. Two-dimensional, axisymmetric SUTRA models and a Monte Carlo statistical approach are used to evaluate upconing potential.

INTRODUCTION
The need for sustainable drinking water sources has driven southwest Florida utilities to develop brackish water supply from the Upper Florida Aquifer (UFA). Regional water supply plans (South Florida Water Management District [SFWMD] 2000; 2006) list regulatory constraints, environmental and water resources protection, and a projected increase of 88 percent in public water demand from 2005 to 2025 as reasons to look for alternative water sources. Traditional freshwater supply from surface water and shallow ground water sources may have reached sustainable limits, at least for larger users. Since the late 1990s, five public-water well fields have been constructed that use the UFA, and expansion of these and other existing facilities are planned, under design or are being constructed. Three of the five public-water well fields have encountered unanticipated water quality deterioration with these changes occurring much sooner than predicted. Possible explanations for these changes include anomalies in geologic structure and lithology, fractures and influences from improperly constructed or abandoned wells.

The UFA is a multilayered sequence of carbonate units that has two to several thin flow zones of high permeability interlayered with thick zones of lower permeability (Reese 2000). The aquifer is bounded by overlying clay layers within the Hawthorn Group and by underlying gypsiferous

dolomite in the Avon Park Formation or other low permeable materials within the Ocala Formation. The SFWMD defines a Middle Confining Unit (MCU) within the Ocala Formation and upper portion of the Avon Park Formation (SFWMD 2004). However, within this confining unit flow zones and secondary permeability may be locally present. Reported hydraulic properties of UFA demonstrate a heterogeneous distribution that reflect variations in lithology, post-depositional alternations, lateral continuity of units and structural features. The salinity of water in the UFA generally increases with depth and toward the coast, though anomalies may exist and greater change may be found within the MCU.

The premise of this paper is that the problems encountered at recently constructed well fields are associated with upconing of poor quality water from below and that future facilities should evaluate this potential and adjust the design and operation of the well field accordingly. This paper uses available hydrogeologic information, probability analysis and a density-dependent solute transport simulator to assess upconing potential.

METHODS

The SUTRA (Voss 1984) code is used to examine an upconing response to a pumping stress in a brackish water aquifer. Considering the challenges of calculating adjective and dispersive solute transport and the uncertainty of associated aquifer properties, some assumptions are made to assist in the analysis of this problem. A two-dimensional, axisymmetric finite-element grid is used to represent a vertical section of the UFA, and to approximate an assumed radial flow of a conservative solute to a well. Horizontal isotropic aquifer properties and saturated flow through porous media are assumed. Temperature is assumed to be constant and fluid density is dependent on only the one solute concentration. A numerical grid employs 9,315 elements of varying dimensions to cover 5,280 radial and 1,520 vertical feet of aquifer, and has 9,520 nodal points for calculating pressure and concentration. Perimeter boundary conditions are: specified constant pressure and concentration along the upper and lower limits of the modeled area, assumed constant hydrostatic pressure along the vertical seaward boundary, and a combination of a specified flux and no-flow conditions to represent the well and flow divide on the landward boundary.

The hydraulic properties, total hydraulic head and chloride concentrations used in the model are a composite of published values in reports and water use permit applications (Table 1 and Figure 1). The model conceptualization is representative of the southwest Florida area and not tied to a specific location, as the model is use for demonstration purposes.

Once a quasi-steady state simulation of estimated initial conditions and hydraulic properties is established, a Monte Carlo approach (Niederreiter and Spanier, 1998) is used to examine the probability of response to pumping stress. Due to the large range of uncertainty in hydraulic properties and computational times of sample runs, Latin hypercube sampling (McKay 1979) is used, and focus is given to four variables: vertical hydraulic conductivity, transverse dispersivity, porosity and pumping stress. Random values within ranges posted in Table 1 are used to represent probability distributions of these properties that are likely to affect vertical upconing. Pumping stress is varied in categories of four rates, increments of 500 gallons per minute, and with one to four pumping wells spaced 500 to 2,000 feet apart in 500-foot increments. Wells are assumed to tap the Upper Floridan with 500 and 700 feet of casing and total depths, respectively. The wells are pumped for one year.

Table 1. Initial and Range in Hydraulic Properties

Unit	K_x ft/d	K_y ft/d	S_s	n_e	m ft	d_l ft	d_t ft
Lower Hawthorn	50	50	1e-6	0.15	220	3.0	0.3
Suwannee	20	20	1e-6	0.15	250	3.0	0.3
Ocala	10	10	1e-6	0.15	350	3.0	0.3
Avon Park	250	250	1e-6	0.15	600	3.0	0.3

Unit	K_x	K_y	S_s	n_e	d_l	d_t
Lower Hawthorn	1.0-1000	0.1-100	1e-5-1e-7	0.01-0.2	0.3-30.0	0.1-30.0
Suwannee	0.1-100	0.001-100	1e-5-1e-7	0.01-0.2	0.3-30.0	0.1-30.0
Ocala	0.1-100	0.001-100	1e-5-1e-7	0.01-0.2	0.3-30.0	0.1-30.0
Avon Park	1.0-1000	0.1-100	1e-5-1e-7	0.01-0.2	0.3-30.0	0.1-30.0

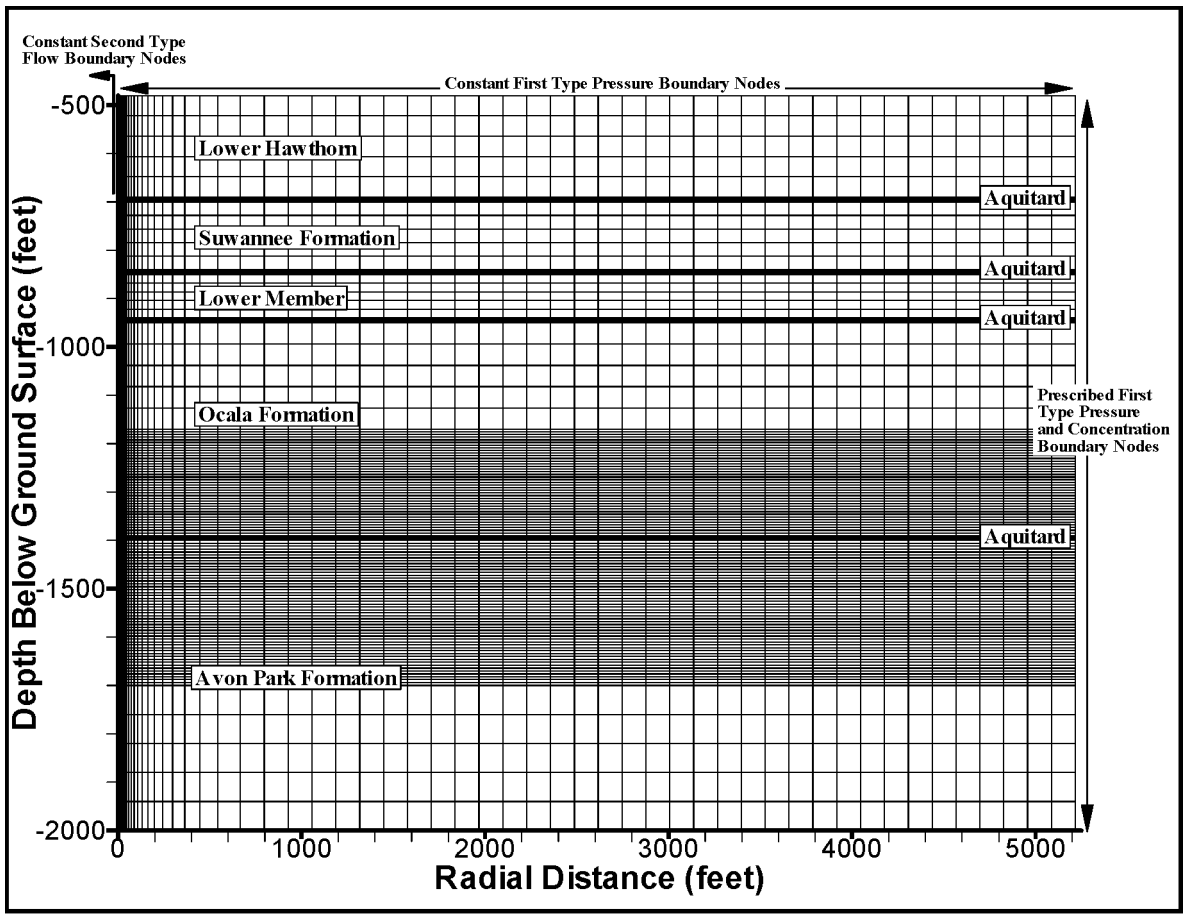

Figure 1. Model Grid (axisymmetric) and Boundary Conditions

RESULTS

This approach provides a framework to assess risk of meeting expectations of a planned well field. More rigorous statistical treatment may be used to define reliability or explore nonrandom distributions of the hydraulic properties. Greater complexities may be added to the numerical model if field data can support them. This modeling approach is useful in guiding a field investigation program to reduce uncertainty in the hydraulic properties.

REFERENCES

McKay, M.D. Conover, W.J. and Beckman, R.J. 1979. A Comparison of Three Methods for Selecting Values Input Variables in the Analysis of Output from a Computer Code. Technometrics 21: 239-245

Niederreiter, H and Spanier, J. 1998. Monte Carlo and Quasi-Monte Carlo Methods, 1998, Proceedings of a Conference held at the Claremont Graduate University, Claremont, California, USA, June 22-26, 1998

Reese, R.S., 2000. Hydrogeology and Distribution of Salinity in the Floridan Aquifer System. USGS. Water Resources Investigations Report 98-4253. Tallahassee, Florida

SFWMD, 2000. Lower West Coast Water Supply Plan, April 2000. SFWMD. West Palm Beach, Florida, Volumes 1, 2 & 3

SFWMD, 2006. Lower West Coast Water Supply Plan, 2005-2006 Update. SFWMD. West Palm Beach, Florida, Volumes 1 & 2

SFWMD, 2004. Hydrogeologic Investigation of the Floridan Aquifer System, Big Cypress Preserve, Collier County, Florida. Florida Technical Publication WS-18. SFWMD. West Palm Beach, Florida

Voss, C.I., 1984,. A finite-element simulation model for saturated-unsaturated, fluid density-dependent ground–water flow with energy transport or chemically reactive single species solute transport. USGS. Water Resources Investigations Report 84-4369

Contact Information: Terry Bengtsson, Water Supply Department, South Florida Water Management District, 2301 McGregor Boulevard, Fort Myers, Fl 33901, 239-338-2929-7740, 239-229-1822, Email: tbengts@sfwmd.gov

Physical and Numerical Modeling of Buoyant Groundwater Plumes

Linzy K. Brakefield[1,2], *Elena Abarca*[1], *Christian D. Langevin*[2] and *T. Prabhakar Clement*[1]
[1]Department of Civil Engineering, Auburn University, Auburn, AL, USA
[2]U.S. Geological Survey, Florida Integrated Science Center, Fort Lauderdale, FL, USA

ABSTRACT
In coastal states, the injection of treated wastewater into deep saline aquifers offers a disposal alternative to ocean outfalls and discharge directly into local waterways. The density of treated wastewater is similar to that of freshwater, but is often much lower than the ambient density of deep aquifers. This density contrast can cause upward buoyant movement of the wastewater plume during and after injection. Because of large injection volumes at some wastewater treatment plants (WWTP), it is important to be able to determine the fate and transport rates of the plume. In this study, both physical and numerical modeling were undertaken to investigate and understand buoyant plume behavior and transport.

INTRODUCTION
Because more than 98 percent of the Earth's potable water supply comes from groundwater (Fetter 1988), underground sources of drinking water (USDW) need protection from possible contamination, especially in urban areas where wastewater production is high. In southeastern Florida, the sizeable population produces large amounts of wastewater, which must be properly disposed of. A viable option for disposal of this treated wastewater is deep-well injection. As part of the U.S. Environmental Protection Agency's Underground Injection Control Program (UIC), injection wells have been classified into five major types. The first type (Class I) is used for injection of municipal wastewater beneath the lowermost USDW. In southeastern Florida, the total daily injection rate for all wells is ~265 Mgal/d (Muniz et al. 2005). The high injection rate has led to concerns over the safety of the local USDW; therefore, it is important to determine the fate and transport of the resulting waste plumes.

Because injected water undergoes primary and secondary treatment at a WWTP, the density of the water is close to that of freshwater (~1.000 g/cc). In contrast, an ambient density of about 1.025 g/cc is typical for saline aquifers used for waste disposal in Florida. This density difference causes buoyant upward movement of the plume during and after injection. The objective of the current study is to investigate the fate and transport of freshwater buoyant plumes in saline aquifers under hydrostatic conditions. This objective was accomplished using both physical and numerical modeling.

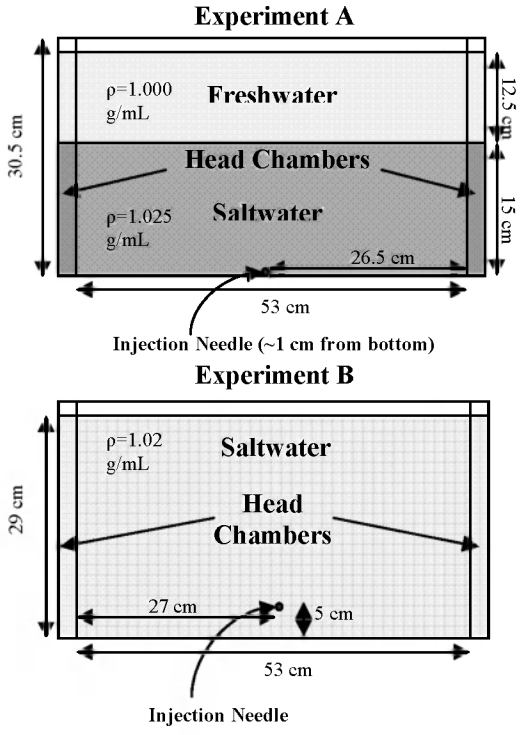

Figure 1 (A and B). Physical model set-up for experiments A and B

METHODOLOGY

Physical Modeling

A 2-D transparent flow tank (53 cm × 30.5 cm × 2.7 cm) was used as the physical model (Figure 1). The tank consists of two lateral head chambers and a central porous media chamber that was carefully packed with glass beads (~1 mm) under saturated conditions to avoid air entrapment and layering. Syringes fastened to two holes (~1 cm diameter), drilled at different heights, were used for injection. The saltwater was prepared using sodium chloride and de-ionized water. The density was measured using an ASTM 111H hydrometer. Three food coloring dyes were used for plume visualization. Digital images of the experiments were captured using time-lapse photography.

Physical models were designed to replicate real-world buoyant groundwater plume problems and allow for easy visualization under controlled laboratory conditions. Furthermore, the experimental results were used later for comparison to numerical modeling results for code validation. In this study, two physical experiments (A and B) were carried out using the same tank. Experiment A was conducted to mimic a scenario in which the saline aquifers used for disposal are overlain by freshwater layers representing the USDW. In this exercise, a 24-mL freshwater slug was injected over a 14-second period into a static, density-stratified system of saline water overlain by freshwater (Figure 1A). Experiment B was designed to investigate plume behavior in a confined system. The zero-pressure upper air boundary was used to conceptually model a non-leaky, impermeable confining unit. In this exercise, 60 mL of freshwater was injected over a 41-second period into the static, fully saline, confined system (Figure 1B). Experiment B utilized an injection point 5 cm from the bottom of the tank, which allowed for better plume visualization than the injection point used in Experiment A.

Numerical Modeling

Experiment B was modeled numerically using SEAWAT Version 4 and compared to laboratory data. SEAWAT couples a modified version of the MODFLOW code with the MT3DMS transport code through the density term in order to solve the variable density flow and transport equations (Langevin et al. 2008). The grid resolution was 0.1 cm × 0.1 cm × 2.7 cm. The MOC (Method of Characteristics) was used to solve the advective part of the transport equation. Time stepping was determined using a Courant number of 0.25. A hydraulic conductivity value of 1.0995 cm/sec was shown to give the best matching qualitative results when compared to Experiment B. Longitudinal dispersivity was calibrated to a value of 0.01 cm, with a transverse to longitudinal dispersivity ratio of 1:10. The low dispersivity values were required to replicate the fingering patterns in the physical experiment (Liu and Dane 1997). Initial heads in the model were 29 cm. Only two zero-pressure boundary conditions were added, at the left and right top corners, to allow fluid and salt to exit the domain while maintaining a hydrostatic system (Voss and Souza 1987). The injection point was modeled using a well boundary condition. Two species were simulated in the model, allowing use of both molecular diffusivities; species 1 was used to represent total dissolved solids of sodium chloride in the water, and species 2 was a tracer representing the dye injected in the well.

RESULTS

Results from Experiment A show a freshwater plume that develops fingers as it migrates upwards (Figure 2). These fingers are presumably caused by small-scale porous media heterogeneities and by dense fluid sinking into the rising relatively lighter fluid. The fingers appear to rise at similar rates until they reach the overlying freshwater layer. However, the

middle finger advection is slightly faster than that of the outer two fingers. As the plume rises, hydrodynamic dispersion causes mixing between the plume and the ambient saltwater along the boundary of the two fluids. As fingering becomes more complex, the surface area of the plume in contact with the ambient water increases, thereby increasing mixing and salt entrainment into the plume. Saltwater entrainment can be visualized by a dilute concentration of the tracer being left behind in a "tail" as the plume rises (Figure 2). As mixing increases, the density contrast between the plume and the ambient water decreases, which lessens the uplifting buoyant force. With decreasing buoyancy, vertical velocities diminish. This cycle continues as the vertical velocity decreases, declining rapidly when the plume makes contact with the freshwater layer. When the boundary is reached, the average plume density is greater than the freshwater, resulting in only some of the injectate entering the bottom of the freshwater layer while the rest spreads out laterally along the boundary. Thus, the freshwater layer behaves similar to a confining unit in that vertical transport is considerably reduced.

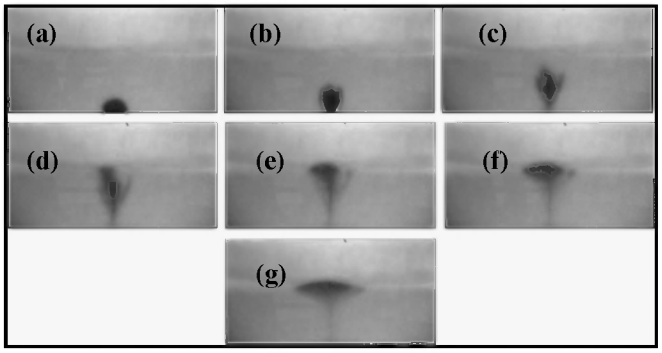

Figure 2. Experiment A results: [times are from end of injection (sec)] (a) 0, (b) 90, (c) 210, (d) 330, (e) 510, (f) 750, (g) 1410

The results from experiment B are shown in Figure 3 (left-hand column). As with the results from Experiment A, the plume also rises vertically and fingers until it reaches the boundary. In this case, the boundary is the top of the tank open to the atmosphere, which simulates a confining unit. The fingering between plumes in Figures 2 and 3 is similar early in the experiments as slight instabilities form due to small-scale heterogeneities and the density difference between the injected and ambient water. In addition, the initial instabilities later develop into distinct fingers, or pathways for flow. Upon reaching the upper boundary, both plumes exhibit similar behavior in that vertical advection decreases and the plume begins to spread laterally along the boundary. The complex fingering pattern also evolves into a cone-shaped formation at the upper boundary.

One main difference between results from these two physical experiments is the variation in plume behavior that occurs when the plumes reach their respective overlying boundaries, due to the inherent differences between the boundaries themselves. Even though both plumes begin an outward lateral migration after reaching the boundary, the plume underneath the confining unit (Figure 3) laterally expands faster than the plume underneath the freshwater layer (Figure 2). In Experiment A, when the freshwater plume makes contact with the boundary, the plume pushes up into the freshwater layer, displacing some of the overlying water and mixing with it. In Experiment B, however, the

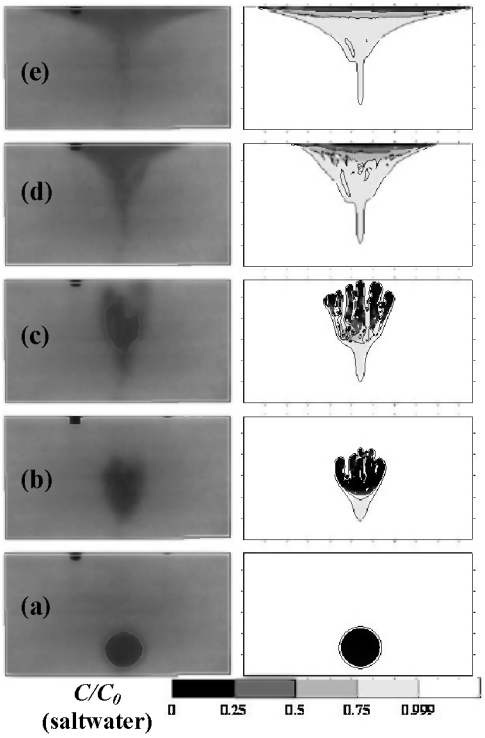

Figure 3. Experiment B and SEAWAT results: [times are from end of injection (sec)] (a) 27, (b) 369, (c) 685, (d) 1385, (e) 2631

freshwater plume cannot continue its vertical path once in contact with the confining layer, resulting in immediate outward expansion.

Because Figure 3 displays results from the numerical modeling effort in the right-hand column, the results of Experiment B and the SEAWAT simulation can be compared at specific times. The shape of the experimental plume appears to be matched well by the SEAWAT simulation results. As with the physical model, the plume in the SEAWAT simulation contains initial instabilities that develop into preferential pathways and elongated fingers. The fingers reach the confining unit at slightly different times and join to form a conical shape beneath the boundary, leaving a tail created by saltwater entrainment. The experimental and simulated plumes have a similar bulk vertical velocity as well as similar lateral spreading once the boundary is reached. Fingering in the simulated plume was more complex than in the experimental results. Because concentration contours were not obtained from the experiment, the numerical model reveals more quantitative information in regards to concentration stratification and the degree of mixing occurring between the plume and the ambient water. Results from the numerical model show that freshwater begins mixing with the saline water at injection. This mixing appears to increase as the plume moves vertically upward, causing saltwater entrainment and creating a tail of brackish water behind the plume. However, relatively freshwater does appear to have reached the confining layer. Although it cannot be determined how fresh this water is, Figure 3 indicates that the relative concentration of salt is between 0 to 0.25, which represents "relatively fresh" water.

DISCUSSION AND CONCLUSIONS

Experiments A and B show that a buoyant plume will experience more lateral spreading once it makes contact with a confining unit than when it makes contact with an overlying freshwater layer of the same permeability. Overall, the buoyant plumes in both scenarios exhibited similar behavior in terms of fingering and transport dynamics. The numerical simulation results show that SEAWAT (with MOC as the advection solver) is capable of modeling these types of scenarios, and that mixing of the plume with the ambient water increased with vertical transport. Further experiment and numerical details can be found in Brakefield (2008).

REFERENCES

Brakefield, L.K. 2008. Physical and Numerical Modeling of Buoyant Groundwater Plumes. M.S. Thesis. Auburn University, Auburn, AL.

Fetter, C.W. 1988. Applied Hydrogeology, 2nd Ed., Merrill Publishing Co., Columbus, OH.

Langevin, C.D., D. Thorne, A.M. Dausman, M.C. Sukop, and W. Guo. 2008. SEAWAT Version 4: A Computer Program for Simulation of Multi-Species Solute and Heat Transport. U.S. Geological Survey Techniques and Methods Book 6, Chapter A22, 39 p.

Liu, H. H., and J.H. Dane. 1997. A numerical study on gravitational instabilities of dense aqueous phase plumes in three-dimensional porous media, Journal of Hydrology, 194, 126-142.

Muniz, A., et al. 2005. Why current regulations protect Florida's subsurface environment, in Underground Injection: Science and Technology, edited by C.-F. Tsang and J. A. Apps, Elsevier, Amsterdam, The Netherlands.

Voss, C.I., and W.R. Souza. 1987. Variable Density Flow and Solute Transport Simulation of Regional Aquifers Containing a Narrow Fresh-Water-Saltwater Transition Zone, Water Resources Research, 23, 1851-1866.

Contact Information: Linzy K. Brakefield, U.S. Geological Survey, 3110 SW 9th Ave., Ft. Lauderdale, FL 33315 USA, Phone: 954-377-5924, Fax: 954-377-5901, Email: lbrake@usgs.gov

Climate Change Impact in a Shallow Coastal Mediterranean Aquifer, at Saïdia, Morocco

Júlio F. Carneiro[1], *M. Boughriba*[2], *A. Correia*[1], *Y. Zarhloule*[2], *A. Rimi*[3] and *B. EL Houadi*[4]
[1]Geophysical Centre of Évora, Department of Geosciences, University of Évora, Évora, Portugal
[2]Laboratory of Hydrogeology-Environment, Faculty of Sciences, Oujda, Morocco
[3]Scientific Institute, Department of Physics of the Globe, Rabat, Morocco
[4]Hydraulic Basin Agency of Moulouya, Oujda, Morocco

ABSTRACT
A density dependent numerical flow model was applied to study the climate change impact in an unconfined shallow aquifer in the Mediterranean coast of Morocco. The stresses imposed to the model were derived from the IPCC emission scenarios and included recharge variations, rising sea level and advancing seashore. The simulations show that there will be a significant decline in the renewable freshwater resources and that salinity increases can be quite large but are limited to a restricted area.

INTRODUCTION
The IPCC fourth assessment report (IPCC 2007) reinforces that consistent climate changes are underway. Changes in the temperature, precipitation and sea level may deeply impact the groundwater quality and quantity of coastal aquifers, notably due to changes in the recharge patterns and to encroachment due to the rising seawater level. Therefore, it is of relevance to study the climate change impacts on the groundwater quality and quantity in coastal aquifers.

This paper presents one such study, focusing in a shallow unconfined aquifer, the Saïdia coastal aquifer, located in the Mediterranean coast of Morocco. The climate change impacts were addressed using a numerical groundwater flow and transport model for several of the IPCC climate change scenarios.

STUDY AREA
The coastal aquifer of Saïdia (figure 1), located in northeast Morocco, occupies an area of around 30 km^2. It is limited to the west by the river Kiss and to the east by the river Moulouya. In the south, the Ouled Mansour hills bound the coastal plain, while the northern boundary is the Mediterranean Sea. The aquifer is made up of a sequence of alluvial and beach deposits, composed of fine to medium sands with remains of shells. Its thickness varies from 10 m to 25 m, with maximums at the two sand dunes that align parallel to the seashore. Between those dunes, the sand layers are covered by a clay layer up to 4 m thick (figure 1). The alluvial and beach deposits overlay marls from the Miocene outcropping at the Ouled Mansour hills.

The aquifer is of local relevance, its waters being used mainly for irrigation, since its high salinity does not allow for other uses. The main pumping zones are located in the fertile areas close to the Kiss and Moulouya rivers. Several sources of salinity contribute to the low quality of the groundwater, apart from the influence of the sea. At the SW edge of aquifer (figure 1), two springs (Ain Zebda and Ain Chebbak) of high salinity groundwater from the adjacent Triffa aquifer discharge into the Saïdia aquifer. Additionally, agriculture relies abundantly on pesticides and resulting in irrigation returns enriched in dissolved substances (Melloul et al. 2006).

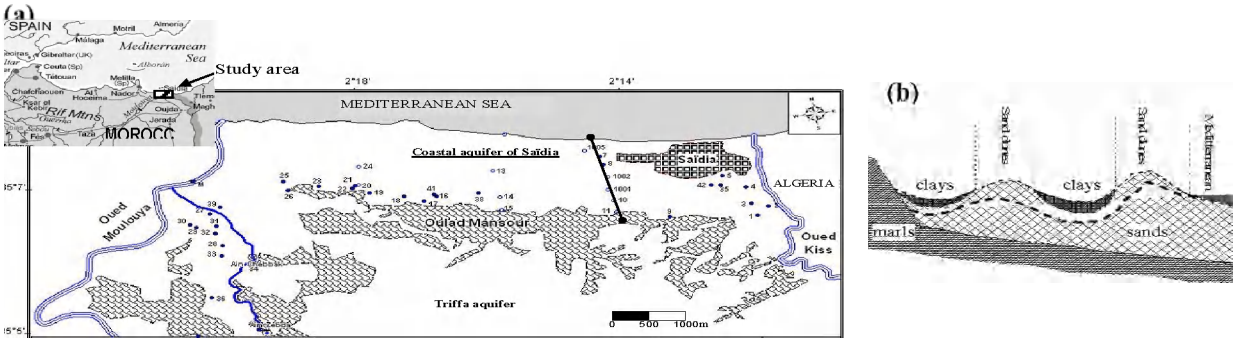

Figure 1. a) map of the study area; b) schematic N-S cross section

The large Mouluoya river is an influent source, but the role of the seasonal Kiss river is less clear, varying along the year. Recharge to the aquifer occurs mainly in the dunes strips and is about 23% of precipitation (Melloul et al. 2006). Recharge from runoff coming from the Ouled Mansour hills also plays a significant role.

NUMERICAL MODEL AND SIMULATED CLIMATE CHANGE SCENARIOS

A density dependent numerical model was built to simulate the flow and transport behavior of the aquifer. A finite element model was built using the code FEMWATER (Liu et al 2001) where flow and transport are coupled though the dependence of the density and dynamic viscosity on the salinity of the groundwater. The finite element mesh was refined along the seashore (figure 2) and although the geologic complexity is small, the numerical model considers five vertical layers to represent accurately the density variation with depth. The model was extended three to four kilometers into the Mediterranean, where a constant head-constant salinity boundary was imposed. Along the top layer, within the Mediterranean, a constant head boundary was considered. Calibration of the model was done against measurements collected in 45 piezometers and wells scattered around the modeled area.

It was decided to study the climate change impact in the Saïdia aquifer for three IPCC (IPCC 2007) emission scenarios: a) **A1B scenario** (the IPCC reference one); b) **B1 scenario**, which shows the smallest variations in temperature and sea level rise; and c) **A1FI** scenario, which is the worst case scenario. The stresses considered were (table 1): a) **sea level rise** – the effect of which is incorporated by changing the constant head value in the Mediterranean boundary; b) **advance of the seashore line** – the new location of which is found from a digital terrain model; c) **variation of recharge** – since runoff in the plain is negligible, recharge variation was computed considering the changes in precipitation (P) and real evapotranspiration (ETR), where the ETR is computed resorting to Turc's equation, as a function of precipitation (P) and temperature (T):

$$ETR = -P\left[0.9 + P^2\left(300 + 25T + 0.05T^3\right)^{-2}\right]^{-1/2} \qquad (1)$$

Table 1. Stresses imposed by climate change

IPPC scenario	*Temperature change (ºC)*	*Sea level rise (m)*	*Precipitation decrease*	*Recharge decrease*	Observations
B1	1.1	0.18	6%	9%	*B1 lower values*
A1B	2.8	0.35	12%	19%	*A1B mean values*
A1FI	6.4	0.59	38%	47%	*A1FI higher values*

RESULTS

Scenario A1FI, the worst case scenario, shows that by 2099 decrease in hydraulic heads due to reduced recharge will not be substantial, reaching maximum values around 0.9 m at the southern limit of the aquifer (figure 2). Particularly at the main pumping area close to the Moulouya river, drawdown will increase by 0.7 m, which is not significant. However, there is a considerable decline in the hydraulic gradient and in the freshwater flowing volume, that decrease on certain areas up to 50% to 60% of the present day values. That is, the renewable freshwater resources decrease considerably. Even in the zones near the Moulouya, and despite the stabilizing influence of the river, flow volumes decrease by as much as 20% to 30%.

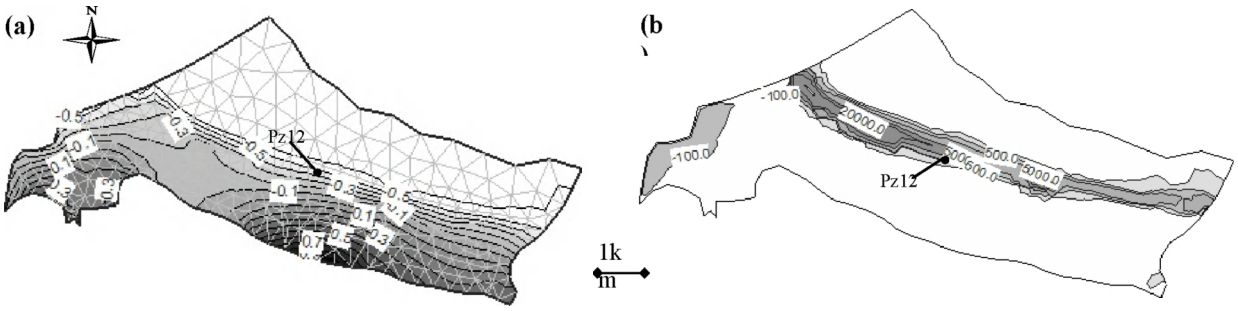

Figure 2. A1FI simulations at 35000 days: a) Decrease in hydraulic head (m). Also shown the finite element mesh; b) Variation of salinity (mg/l)

Scenario A1FI also shows that the salinity will increase sharply in the area closer to the advancing shoreline. For instance, the salinity at piezometer Pz12 is expected to rise as much as 3000 mg/l. Such an increase is restricted to a very narrow area near the freshwater/saltwater interface, with the remainder of the aquifer maintaining its mean salinity (figure 2). At the upstream Moulouya river it is expected that salinity will decrease, due to added contribution of leakage from the river of the aquifer and diminished discharge from the Triffa aquifer. Scenarios A1B and B1, which consider smaller climate change variations, show smaller impacts in the renewable resources and in the water quality of the Saïdia aquifer. This can be envisaged by the behavior of hydraulic heads in the area closer to the Moulouya and in the evolution of salinity in piezometer Pz12 (figure 3).

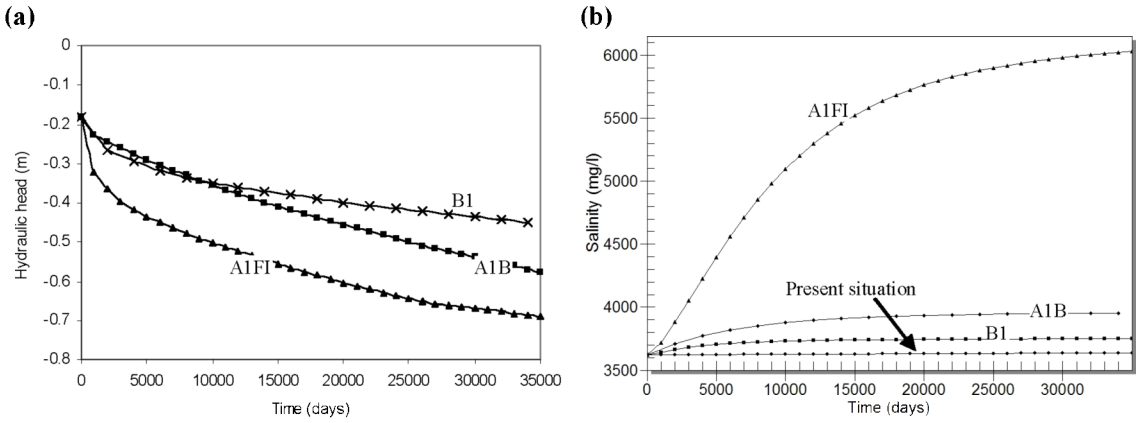

Figure 3. a) Decrease in hydraulic head near the Moulouya (m); b) Increase in salinity expected at piezometer Pz12.

CONCLUSIONS

A numerical model of the shallow unconfined Saïdia aquifer in the Mediterranean coast of Morocco was implemented with the aim of studying the impacts due to rising temperatures and sea level during the 21st century. Regional predictions of the IPCC scenarios B1, A1B and A1FI were used. The variation in recharge was determined by taking into account the anticipated variations in precipitation and in temperature.

The simulations were conducted for a period of approximately 100 years. The main effect of the climate change in the Saïdia aquifer will be the decrease in renewable resources, which in the worst case scenario may be reduced by to 50% to 60% of present day values, due to the decline in recharge and the diminished contributions from the adjacent Triffa aquifer. The water quality will be affected mostly in the area immediately adjacent to the advancing seashore. Localised areas may see a small decrease in salinity due to the added inflow freshwater from the Moulouya and diminished inflow from high salinity springs.

REFERENCES

IPCC, 2007: Climate Change 2007: Impacts, Adaptation and Vulnerability. Contribution of Working Group II to the 4th Assessment Report of the IPCC, M.L. Parry, O.F. Canziani, J.P. Palutikof, P.J. van der Linden and C.E. Hanson, Eds., Cambridge, Cambridge University Press.

Lin, H., D. Richards, C. Talbot, G. Yeh, J. Cheng, H. Cheng and N. Jones, 2001: FEMWATER: A Three-Dimensional Finite Element Computer Model for Simulating Density-Dependent Flow and Transport in Variably Saturated Media, Version 3.0 users manual., U.S. Army Engineer Waterways Experiment Station.

Melloul, A, M. Bourhriba, Y. Zarhloule, J.L. Probst, M. Boufiada, A. El Mandour and M. Snoussi, 2006. Vulnerability assessment of groundwater resources: evaluation of seawater intrusion and effect of climatic change. Coastal plain of Saïdia Morocco. IGME. Hidrogeologia y aguas Subterraneas, 17, Madrid.

Contact Information: Júlio F. Carneiro, Geosciences Department, Rua Romão Ramalho 59, 7000 Évora, Portugal, Phone: +351 266745301, Email: jcarneiro@uevora.pt

Brine Formation and Entrapment in the Eastern Mediterranean Coastal Plain Aquifer

M. Caspi[1], *E. Shalev*[2] and *H. Gvirtzman*[1]
[1]Inst. of Earth Sciences, the Hebrew University of Jerusalem, Jerusalem, Israel
[2]Geological Survey of Israel, Jerusalem, Israel

ABSTRACT

The coastal plain aquifer of Israel, Gaza strip and Sinai Peninsula is located along the Mediterranean coast and includes a transition zone between fresh groundwater originated inland and Mediterranean seawater. The geometry of this interface depends on the specific density of both water bodies.

Throughout geological history, ocean sea level fluctuates many times due to glacial-interglacial cycles. At glacial periods the sea retreats, the coastal shelf is exposed, rain permeates the land and creates a freshwater aquifer in an area that previously was saturated with seawater. During interglacial periods, the sea floods the land and seawater penetrates the fresh-water aquifer. In both cases, during glacial or interglacial periods, the fresh-saline water interface moves inland or seaward.

This theory predicts that salinity of groundwater in the coastal plain aquifer would range from freshwater to seawater. Yet, the saline water pumped through some wells in the Gaza strip aquifer deviates from the expected saltwater-freshwater mixture. The most noticeable deviation is found in Cl concentrations, reaching up to 67,000 mg/l, i.e. 3 times the Cl content of sea water. These high levels of Cl concentrations are also found in the waters of the Bardawill lagoon and sabkhas in northern Sinai.

In view of the geochemical composition of the Gaza aquifer with the water encountered in the Bardawill region, we suggest that brine formed in an ancient lagoon or beach sabkha in the Gaza region had immersed into the aquifer, and efficiently trapped at the sediments beneath. This efficient entrapment was possible due to layers of clay that are interbedded in the aquifer and due to the impermeable Saqiye group which restrict the aquifer at its bottom.

This study aims to examine the physical and chemical feasibility of the suggested mechanism using a numerical simulation. The simulation reconstructs the aquifer migration inland or seaward, the submergence of lagoon water and their entrapment between clay layers in the aquifer as a result of sea level changes. The simulation uses the Bardawill lagoon as a current model which represents an actual process of brine formation and submergence, and uses the coastal plain aquifer of Gaza as a model for brine entrapment.

So far, the model has revealed the formation of two interfaces, one facing land and the other facing the sea, and the lagoon brine situated in-between (Figure 1a). Figures 1b, 1c and 1d display the diminish of the lagoon due to sea level rising and the dilution of the aquifer brine by seawater. We are currently repeating the same simulations using an anisotropic heterogeneous aquifer with clay layers to simulate the brine entrapment. Further analysis of this model will reveal rates and locations of brine formation and migration as well as the latent salinization potential of the entrapped brine.

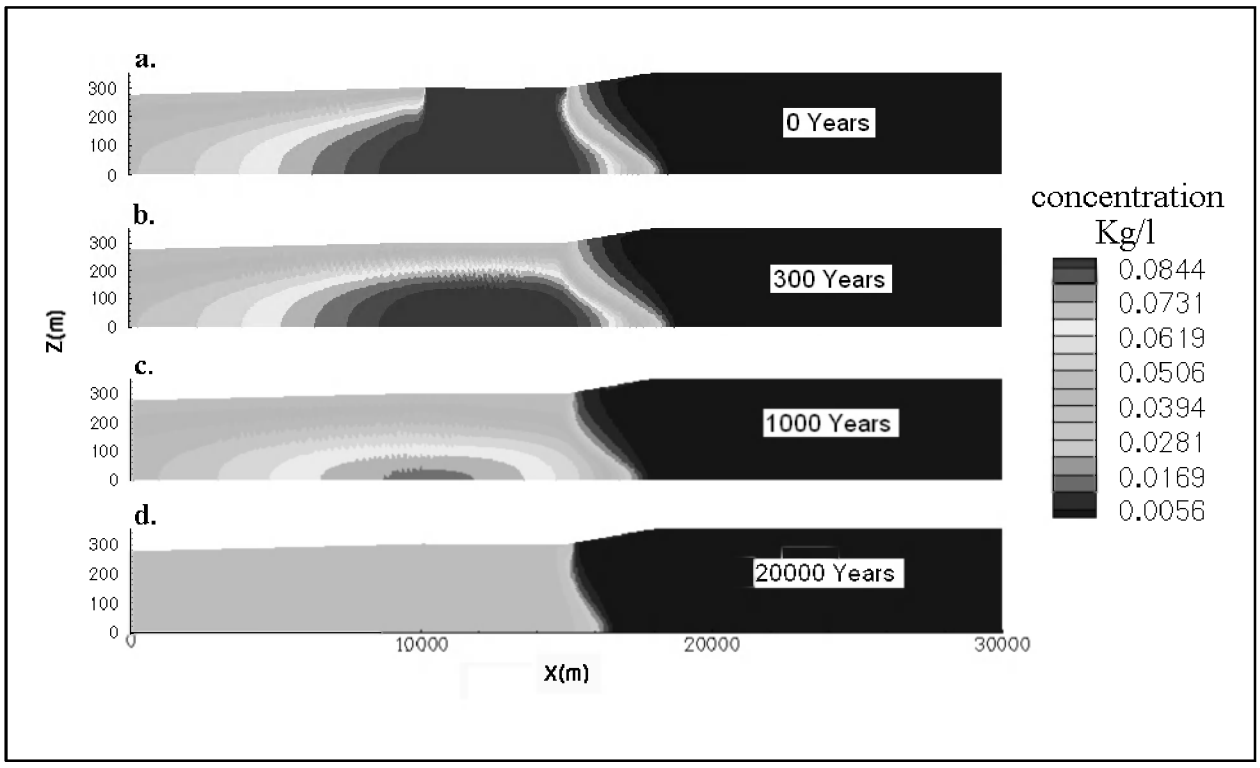

Figure 1. Four stages of lagoon diminish and infiltration of seawater into the aquifer.
a - The lagoon recharges the aquifer with brine. One interface is between seawater (Green) and brine (Red) and the other separate brine from freshwater (Blue).
b and **c** – When the sea level rises the lagoon disappears and seawater submerges into the aquifer and dilutes the brine.
d - New steady state. One interface between seawater and freshwater.

Contact Information: Mati Caspi, Inst. of Earth Sciences, The Hebrew University of Jerusalem, Jerusalem 91904, ISRAEL, Phone: 972-2-6584839, Mobile: 972-54-5366134, Fax: 972-2-5668581, Email: mataniash@gmail.com

The Interplay between Tidal Fluctuations and Physical Heterogeneity on Seawater Intrusion

Eduardo Castro[1], *Daniel Fernadez*[1] *and Jesus Carrera*[2]

[1]Department of Geotechical Engieneering and Geosciencies, School of civil Engineering, Technical University of Catalonia, Barcelona, Spain

[2]Institute of Earth Sciences "Jaume Almera", Spanish Research Council (CSIC), Barcelona, Spain

The interaction between temporal fluctuations (i.e., tidal fluctuations), physical heterogeneity and local dispersion processes mainly controls the width of the mixing zone in seawater intrusion problems. Heterogeneity causes the toe of the salt-water interface to recede while increasing both the width and slope of the mixing zone. Yet, the role of temporal fluctuations, inducing an increase of the longitudinal as well as the transverse effective dispersion processes in complex geological formations, is still largely unknown. Here, we used a combined numerical and experimental approach to investigate the impact of the joint effects of tidal fluctuations and heterogeneity in coastal aquifer. Seawater intrusion experiments were conducted in an intermediate-scale sand box filled whit three different mixtures of quartz sands. The spatial distribution of the sand is well-known and follows a complex heterogeneous structure model. The TRANSDENS seawater intrusion code was used to simulate the experimental observations. Results demonstrate that neglecting the joint effect of the tidal fluctuation and heterogeneity produces an inaccurate evaluation of the saltwater intrusion process.

Contact Information: Eduardo Castro, Department of geotechnical Engineering and Geo-Sciences, Technical University of Catalonia (UPC), C/ Jordi Girona 1-3, Building D-2,08034, Barcelona, Spain. Phone: +34 934016852; Fax +34 934017251, Email: eduardo.castro@upc.edu

Pumping Test Analyses in an Aquifer with Fresh Water/Salt Water Interface

Liliana Cecan, *Gregory Nelson, Charles McLane* and *Maura Metheny*
McLane Environmental, LLC, Princeton, NJ, USA

ABSTRACT
In order to analyze pumping test data in a fresh water aquifer with a laterally encroaching or underlying salt water zone, methods typically employed for fresh water aquifers may not produce accurate estimates of aquifer parameters because they fail to account for the change in aquifer geometry and distribution of heads caused by movement of the salt water interface in response to pumping. This paper presents a methodology to analyze pumping test data in coastal aquifers using the SEAWAT density-dependent flow and transport numerical code. Comparisons of the hydraulic conductivity and vertical anisotropy estimates obtained from pumping test data using a classical method (Hantush-Jacob) and a numerical groundwater flow model which does not account for changes in salt water density (MODFLOW) with values obtained using the more sophisticated SEAWAT model suggest that standard methods may overestimate horizontal hydraulic conductivity and underestimate vertical anisotropy of the aquifer.

ACKNOWLEDGMENTS
The authors wish to thank Mark White of Environmental Partners Group and Andrew Miller of Head First for many hours of discussions that have helped to improve this paper.

INTRODUCTION
Obtaining accurate estimates of aquifer parameters is of paramount importance for proper management of groundwater resources. A single well pumping test is one of the standard procedures for estimating hydraulic properties of aquifer systems, such as transmissivity and storativity. Commonly, hydraulic conductivity and vertical anisotropy are estimated from measured pumping test drawdowns. Pumping test analysis in a coastal aquifer with an adjacent or underlying salt water zone should be evaluated as a flow problem in which not only movement of the water table but also of the salt water interface may change the thickness of the aquifer in the vicinity of the pumping well, and thus the results of the test. In addition, it is often necessary to make corrections to measured groundwater elevations to account for salt water density fluctuations with depth and time. Thus, in a coastal aquifer setting it may be necessary to apply techniques beyond the standard groundwater modeling methods to produce more accurate estimates of the hydraulic conductivity and vertical anisotropy using salt water transport modeling as described in the sections below.

STUDY AREA
We consider for our analysis data from an aquifer test in the Pamet Flow Cell, a fresh water lens aquifer on Cape Cod, Massachusetts (Figure 1). The glacial sediments of Lower Cape Cod were deposited in a lacustrine deltaic system by meltwaters from the Cape Cod Bay and South Channel glacial lobes that occupied the area 15,000 years ago. These glacial sediments consist predominantly of sand with some gravel and few silt or clay deposits (Masterson 2004; Andrew Miller personal communication 2007), and extend to depths of up to 900 ft below sea level, where they contact the underlying crystalline bedrock (Masterson 2004). There is sufficient contrast in the hydrostratigraphy of these deposits that they generally should not be characterized as homogeneous for the purpose of modeling movement of the salt water interface (e.g. upconing beneath a pumping well).

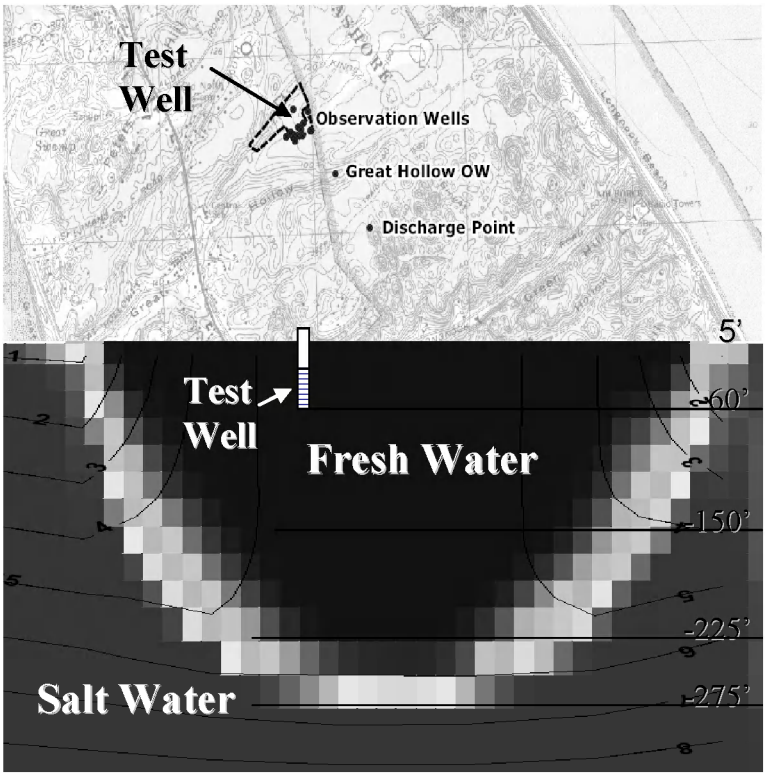

Figure 1 Site Map

A ten-day aquifer test was performed using a set of monitoring wells, installed in the shallow (at about -60 feet amsl), intermediate (at about -150 feet amsl) and deep (at about -250 feet amsl) zones. The water level elevation at the proposed supply well location is at about 5 feet amsl, which implies that the thickness of the fresh water lens in the area is about 200 feet. During the ten-day pumping test the pumping rate was maintained at 500 gpm (0.72 MGD), producing drawdown of about 20 feet at the pumping well which is screened from -30 to -60 feet amsl; up to 4.5 feet at the monitoring wells in the shallow zone; about 1 feet at the intermediate wells; and about 0.2 feet at the deep wells after a fresh water head correction was applied.

HYDRAULIC CONDUCTIVITY ESTIMATES

Hydraulic conductivity and anisotropy estimates for the well cluster data set using classical analytical methods for leaky confined aquifers (Hantush-Jacob) and simple numerical models (MODFLOW) estimated horizontal hydraulic conductivities of 150 to 300 feet/day for the area, and a horizontal to vertical hydraulic conductivity anisotropy range of 2:1 to 10:1. MODFLOW simulations also performed for the same area, using a box model that accounted for recharge and heterogeneity, estimated horizontal hydraulic conductivities of about 100 ft/day and a horizontal to vertical hydraulic conductivity anisotropy range of 10:1 to 30:1. This model does not account for the upconing of the salt water interface caused by pumping. Further improvements on the estimated horizontal and vertical hydraulic conductivities can be made by accounting for the moving interface.

The USGS SEAWAT calibrated numerical transient groundwater flow model (Masterson 2004) prepared for Lower Cape Cod, Massachusetts (LCape) was used to assist in the analysis of the pumping test data at the site. The model can account for the moving interface caused by pumping. The model offers the advantage of being readily available from the USGS, but carries a penalty of extended computational time as it contains three other flow cells in addition to the Pamet Lens (PametL) flow cell of interest. From the USGS SEAWAT LCape regional model, telescopic mesh refinement (TMR) was applied to extract a smaller computational grid that covers only the extent of the Pamet flow lens in order to significantly decrease model execution time. The resulting model grid was refined to increase modeling accuracy. The refined, SEAWAT PametL model uses the same coastal boundaries and initial conditions as the original USGS LCape SEAWAT regional model. Boundaries on the north and south ends of the flow cell along which the LCape model was cut to create the PametL model have been set as constant head and constant concentration boundaries using values taken from corresponding locations in the USGS LCape SEAWAT regional model.

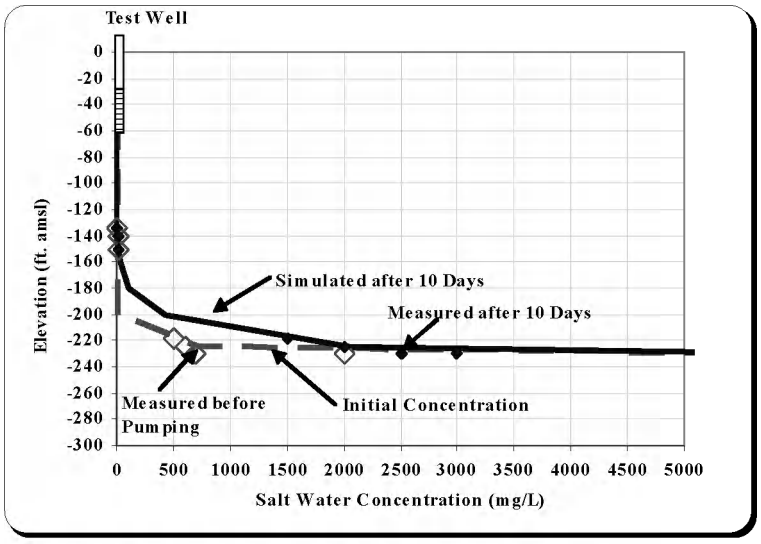

Figure 2 Measured and Simulated Results

Figure 2 shows the observed and the simulated salt water concentration vs. elevation curves obtained using the SEAWAT PametL numerical model simulations. The ten-day aquifer pumping test data was used to calibrate the SEAWAT PametL proposed numerical model, and will be used to estimate the safe yield pumping rate. The horizontal and vertical hydraulic conductivities estimated through the calibration of the PametL model yielded reasonable matches between the observed and simulated transient drawdown and salt water concentration distributions. The calibrated PametL model exhibited a lower horizontal hydraulic conductivity (ranging from 200 feet/day in the shallow layers to 10 feet/day in the deeper layers of the model) and a higher vertical anisotropy (ranging from 30:1 in the shallow layers to 1000:1 in the deeper layers of the model) than the preliminary hydraulic conductivity estimates determined using the classical analyses of pumping test data.

Using a salt water numerical model well calibrated to both, measured drawdown and salt water concentrations, improves the horizontal and vertical hydraulic conductivities estimates. Accurate estimates of these parameters are of paramount importance in determining safe yield, and maximum upconing caused by pumping (Ma et al., 1997; van Dam, 1999). Nelson et al. (*this conference*) shows that, by accounting for vertical anisotropy in the aquifer zone between the well and the interface, the predicted impacts to the pumping well from upconing may be greatly reduced, and wellfield safety yield estimates maybe increased.

DISCUSSION AND CONCLUSIONS

For a site situated in a coastal aquifer, application of a classical analytical technique, a standard numerical flow model, and a salt water flow and transport numerical model produced different estimates of hydraulic conductivity and vertical anisotropy. The differences are attributed to the salt water model's capability to account for changes in heads caused by pumping, changes in groundwater density and groundwater density distribution, and changing boundary conditions (moving salt water interface) during pumping. The classical analytical and numerical models do not account for the above mentioned changes in fitting the aquifer test data, and therefore overestimate horizontal hydraulic conductivity and underestimate vertical anisotropy.

A ten-day pumping test in which drawdown and specific conductance is measured at multiple cluster wells is beneficial for calibrating the salt water numerical models needed to be used to evaluate safe yield pumping rates. Thus, when conducting pumping tests in coastal aquifer studies, it is important to measure not only the drawdown at cluster wells, but also the changes in the salt water interface induced by pumping. If, in addition to calibrating to heads, the model is calibrated to concentration and to changing boundaries (upconing) a better estimate of horizontal and vertical hydraulic conductivities can be obtained.

REFERENCES

Guo, Weixing and Christian D. Langevin. 2002. User's Guide to SEAWAT: A Computer Program for Simulation of Three-Dimensional Variable-Density Ground-Water Flow. U.S. Geol. Survey, Techniques of Water-Resources Investigations 6-A7. Tallahassee, Florida, 77 p.

Ma, Tain Shing, Marios Sophocleous, Yun-Sheng Yu, and R. W. Buddemeier. 1997. Modeling saltwater upconing in a freshwater aquifer in south-central Kansas. *J. Hydrol*. v 201:120-137.

Masterson, John. 2004. Simulated Interaction between Freshwater and Saltwater and Effects of Ground-Water Pumping and Sea-Level Change, Lower Cape Cod Aquifer System, Massachusetts. Scientific Investigations Report 2004-5014. Reston, Virginia, 72 p.

Nelson,Gregory, Liliana Cecan, Charles McLane, Maura Metheny, *in prep.* Evaluating Safe Yield for Supply Wells in an Aquifer with Fresh Water / Salt Water Interface, *This Meeting*.

van Dam, J.C. 1999. "Exploitation, Restoration and Management". In. Bear, Jacob, and others, Eds., Seawater Intrusion in Coastal Aquifers - Concepts, Methods and Practices, Dordrecht, The Netherlands, Kluwer Academic Publishers, pp. 73-125.

Contact Information: Liliana Cecan, McLane Environmental, LLC, 707 Alexander Road, Suite 206, Princeton, NJ 08540 USA. Phone: 609-987-1400, Fax: 609-987-8488, Email: lcecan@mclaneenv.com

Use of Geochemical Tools to Study Groundwater Salinization in Volcanic Islands: a Case Study in the Porto Santo (Portugal) and Santiago (Cape Verde) Islands

M. T. Condesso de Melo[1], *J. Silva*[2], *A. Lobo de Pina*[2,3], *A. Mota Gomes*[2,3], *F. Almeida*[2], *R. Moura*[4] and *M A. Marques da Silva*[2]

[1]CVRM - Geo-Systems Centre, Instituto Superior Técnico, Lisboa, Portugal
[2]GeoBioTec, Geosciences Department, University of Aveiro, Aveiro, Portugal
[3]Geosciences Department, Institute for Higher Education, Praia, Cape Verde
[4]Department of Geology, Faculty of Sciences, University of Porto, Porto, Portugal

ABSTRACT

Porto Santo (Portugal) and Santiago (Cape Verde) are two volcanic islands of the Macaronesia region with scarce freshwater resources that rely on groundwater and seawater desalination plants to guarantee public water supply and irrigation needs. Rainfall is less than 400 mm/year and unreliable, as it usually occurs as short heavy events that may produce flash floods and strong landscape erosion (locally called 'badlands').

Volcanism in the studied regions occurred intermittently since at least Palaeogene (in Santiago) and Lower Miocene (Porto Santo) in an environment characterized by dramatic eustatic and isostatic sea-level fluctuations and active tectonics. Periods of prolonged volcanic activity under submarine or subaerial conditions alternated with phases of volcanic quiescence dominated by intensive erosion and deposition of sedimentary formations. The islands are mainly composed of basaltic-trachytic-rhyolitic lava flows and some alkaline rocks, with a subordinate amount of pyroclastic and sedimentary rocks.

Studied volcanic formations are often very heterogeneous from the hydrogeological point of view. The principal hydrogeological formations are formed by the modern unconsolidated sedimentary formations (alluvium, conglomerates and eolianites) that outcrop downstream the principal spring-fed creeks or by volcanic formations with interstratified high permeability levels of pillow lavas, breccia and hyaloclastites. Groundwater recharge is by rainfall infiltration in the higher part of the islands. The water infiltrates and moves downward in the interior of the islands with preferential flow occurring along zones with faults, fractures and dykes. The aquifers discharge to several springs, wells, boreholes and along the shoreline where increasing salinities are becoming a major constraint on groundwater utilization.

Detailed hydrogeochemical investigations have been carried out in both islands to characterize groundwater quality, to determine the origin of groundwater salinization processes and to identify the principal areas in risk of seawater intrusion in order to develop mitigating measures to reduce contaminating risk. The geochemical results obtained point to two different sources of groundwater salinization, one due to prolonged water-rock interaction in aquifer formations which have high natural background salinities; and, the other one due to seawater intrusion along low-lying alluvial valley aquifers and other shallow coastal aquifers. Seawater intrusion is aggravated in these aquifers by overpumping for tourism (in Porto Santo) and agriculture (in Santiago) and also by illegal removal of alluvium materials for construction.

Keywords: volcanic islands, salinization, groundwater quality, natural background

INTRODUCTION

Fresh water resources in volcanic islands located in semiarid regions are limited and extremely vulnerable to climate changes and management practices. Surface water circulation is often confined to the highest parts of the islands and/ or to short periods after the heavy rainfall events, which occasionally occur during the wet season. Groundwater resources are usually the principal source of fresh water for local populations and agriculture. However, due to the common water shortage problems that affect these regions, the emphasis is placed on groundwater availability rather than quality and groundwater resources face an increasing risk of contamination.

The main risk of groundwater contamination in volcanic islands is salinization, which may result from natural rock-water interaction processes (cation exchange, dissolution, precipitation, surface complexation) between circulating groundwaters and volcanic materials that are enriched in several geochemical elements (Cl, Na, Si, As, F); or, from seawater intrusion due to non sustainable groundwater abstraction. Strong evaporation may also contribute for salt reconcentration in areas with shallow water levels.

STUDY AREAS

The present study was carried out in two volcanic islands located in the Atlantic Ocean along the west coast of Africa – Porto Santo (Portugal) and Santiago (Cape Verde), which have very limited natural resources, including serious water shortages, and where groundwater is the principal source of freshwater. Both islands have a semi-arid to sub-tropical climate with unreliable and erratic rainfall leading in some years to prolonged droughts.

Porto Santo is a small volcanic island (42.26 km^2) located in the northeast part of the Madeira archipelago between 32° 59' and 33° 07' N parallels of latitude and 16° 16' and 16° 24' W meridians of longitude. The island has a relatively steep relief in its northeast and southwest extremes, which are over 450 m above sea level, and a low lying flattened area in its central part, which is approximately 150 m high.

Santiago is a mountainous volcanic island located in the south part of the Cape Verde archipelago between 15° 20' and 14° 50' N parallels of latitude and 23° 50' and 23° 20' W meridians of longitude. It is the largest island, both in size (991 km^2) and population (236 627 inhabitants), and where the capital, Praia, is located. Water resources in the island of Santiago are limited and due to its characteristically steep relief and eroded soils, most surface water drains into the ocean immediately after the occasional rains. Less than one-third of the Santiago population is connected to any type of water supply system and safe drinking water is, therefore, in short supply.

HYDROGEOLOGICAL SETTING

The two studied volcanic islands are very heterogeneous from the geological and hydrogeological point of view. In Porto Santo groundwater resources are limited in general to the principal sedimentary formations - the calcoarenites from the eolinite formation and the old and modern beach sand deposits. Most of the volcanic formations have low permeability but in some parts of the island interstratified levels of hyaloclastites and submarine volcaniclastic deposits increase locally the permeability and create conditions for spring occurrence.

In Santiago the principal hydrogeological formations are the submarine pillow lava formations and the modern alluvium and conglomerate formations located along the principal creeks. Groundwater recharge is by rainfall infiltration in the higher part of the island. The water

infiltrates and moves downward in the interior of the island with preferential flow occurring along zones with faults, fractures and dykes. The aquifer discharges to several springs, wells, boreholes and along the shoreline where increasing salinities are becoming a major constraint on groundwater utilization.

METHODS

Groundwater samples were collected from springs, wells and boreholes located within the two studied islands. A multiport flow-through cell connected in-line to the sampling points was used to obtain reliable geochemical field. Groundwater samples were taken from the discharge during pumping conditions and once stabilisation of the principal field parameters (pH, T, Eh, DO) was observed for subsequent major, minor, trace element and stable isotopic analysis. On-site measurements included the determination of alkalinity by acid colorimetric titration.

RESULTS AND CONCLUSION

Groundwater samples collected in Porto Santo are all very mineralized (EC>1.6 mS/cm) and with characteristic pH values above 7.5. Groundwater along the coastline and near the saline intrusion interface is characterized by higher electrical conductivity (>4.78 mS/cm), lower Na/Cl ratios and slightly higher Ca/Mg ratios compared to the groundwater sampled in areas further away from coastline (Figure 1). It suggests that Na in these samples is being partially removed from the groundwater and replaced by Ca, which is confirmed by the higher Ca/Na ratios. The samples collected in a short distance from the coastline present Br/Cl very close to seawater mixing line (0.0016) but samples collected inland show enrichment in Br and Si over Cl and Br, respectively, which may be attributed to rock-water interactions.

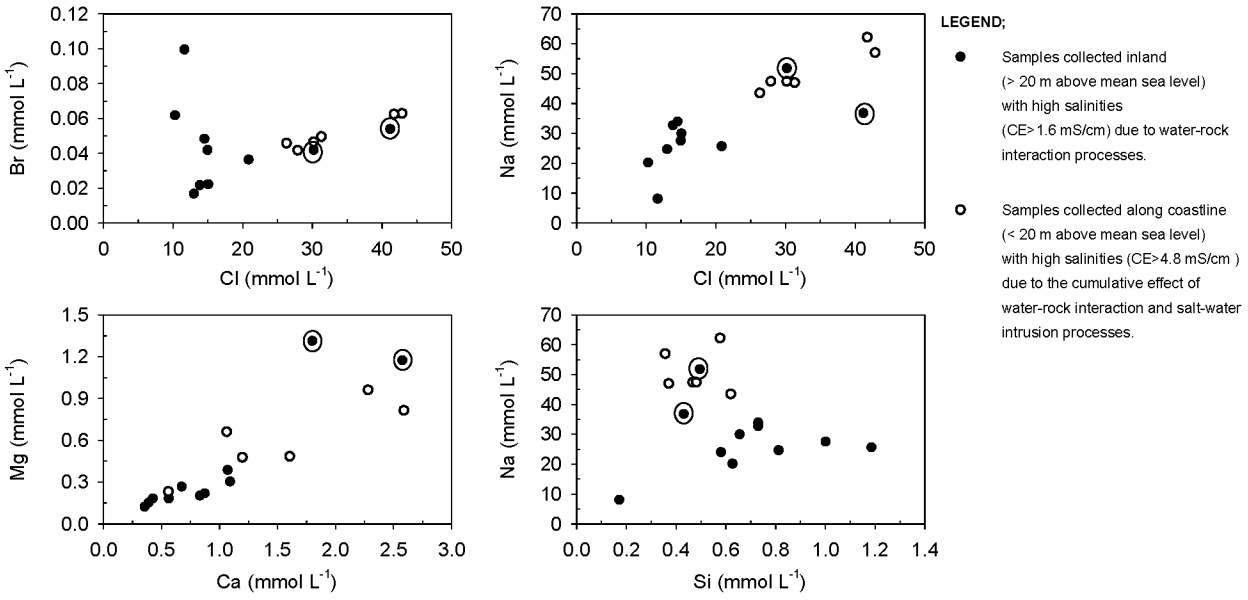

Figure 1. Chemical molar ratios determined in groundwater samples collected in Porto Santo island showing differentiated values depending on the origin of salinity.

Groundwaters in Santiago display a great variability in their chemical and physical features. They range from dilute waters (EC=362 µS/cm) with an average temperature of 26ºC to groundwaters that are generally more saline (CE~1 000–12 000 µS/cm). Groundwater samples collected along the coast have often Cl concentrations exceeding 500 mg/l as a result of saline

intrusion. Stable isotopic data shows a slight enrichment in shallow high salinity groundwater samples which may indicate a contribution of evaporation for increasing salinities.

Thus the geochemical results obtained show that different processes – evaporation, water-rock interaction and sea water intrusion are contributing for groundwater salinization and limiting its use for public supply.

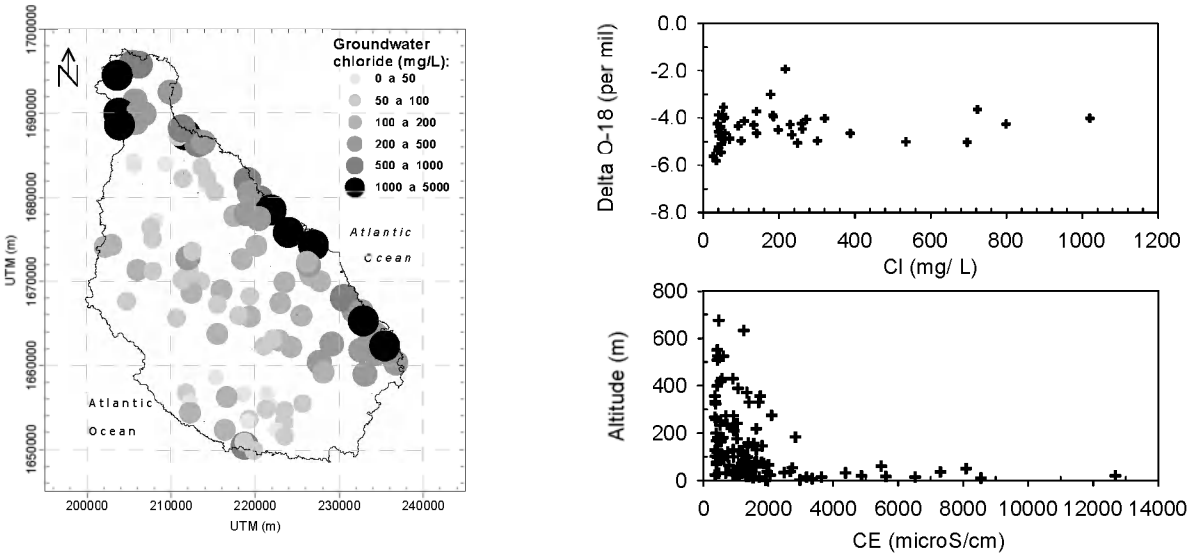

Figure 2. Groundwater chloride distribution and evolution of stable isotopic content as a function of groundwater salinity in Santiago.

REFERENCES

Carvalho, M. G. & Brandão, J. M. 1991. Geologia do Arquipélago da Madeira, Museu Nacional de História Natural, Lisboa, 169 pp.

Duarte, R. S. 1995. Recursos hídricos e subterrâneos da Região Autónoma da Madeira. Notícia Explicativa VII.3, Ministério do Ambiente, Direcção Geral do Ambiente, Lisboa, 31 pp.

ACKNOWLEDGEMENTS

The authors would like to thank the financial support received from FCT (Lisbon, Portugal) and the European Social Fund through the EU III Community Support Framework (SFRH/BPD/30775/2006; SFRH/BD/9790-1/2003), and express their gratitude to Dr. Sílvio Santos, Eng. João Manso and Arquitect Pedro Araújo for permitting the access to historical documents and the use of the collected chemical data.

Contact Information: M. Teresa Condesso de Melo, CVRM - Geo-Systems Centre, IST, Av. Rovisco Pais, 1049-001 Lisboa, Portugal. Phone: +3512184172; Fax: +351218417442; Email: tmelo@ist.utl.pt

A Saltwater Upconing Model to Evaluate Wellfield Feasibility

Gregory W. Council[1] *and Christopher J. Richards*[2]
[1]GeoTrans, Inc., Roswell, GA, USA
[2]Northwest Florida Water Management District, Havana, FL, USA

ABSTRACT
A SEAWAT modeling analysis was conducted to evaluate potential saltwater upconing at a proposed wellfield in northwest Florida, USA. A practical approach was developed for setting and adjusting the model-edge head and salinity boundary conditions in the three-dimensional model. Simulations of 1,000 yr duration provided appropriate equilibrium pre-pumping conditions. Simulations of well withdrawal resulted in upconing of the 250 mg/L chloride concentration surface by 35 m in 50 years, which is still below the production zone of the wells. The modeling results are being used to plan a future water-supply source and to develop a supplemental field study.

INTRODUCTION
The Northwest Florida Water Management District has identified an area in northeast Franklin County as a potential location for a new 7,600 m^3/d wellfield. The wellfield, located approximately 10 km inland (northwest) of the Gulf of Mexico, would help meet projected future water demand in this growing rural county. The wellfield area is largely covered by planted pines and by wetlands that have been altered by past silvicultural practices.

A field investigation program and groundwater modeling analysis were conducted to help assess the feasibility of this groundwater supply. Density-dependent groundwater modeling was used to estimate saltwater upconing that would potentially result from the groundwater withdrawal.

The general hydrogeology of the region consists of two aquifers – the Surficial Aquifer System (SAS) and the Floridan Aquifer System (FAS) – separated by an aquitard called the Intermediate System (Pratt et al. 1996). The proposed water supply wells would be screened in the FAS, which is a regional limestone aquifer with significant zones of secondary porosity formed by mineral dissolution.

METHODS
A SEAWAT (Langevin et al. 2003) model was constructed to assess potential effects of the proposed groundwater withdrawals. A three-dimensional model grid was designed with 328 rows, 263 columns, a minimum horizontal spacing of 30 m near the proposed wellfield, and a maximum horizontal spacing of 300 m. Vertically, the model consisted of 16 layers (Figure 1), with layers 1 and 2 representing the SAS and Intermediate System, respectively. Test simulations with different levels of discretization were used to assess appropriate domain size and grid spacing for this analysis.

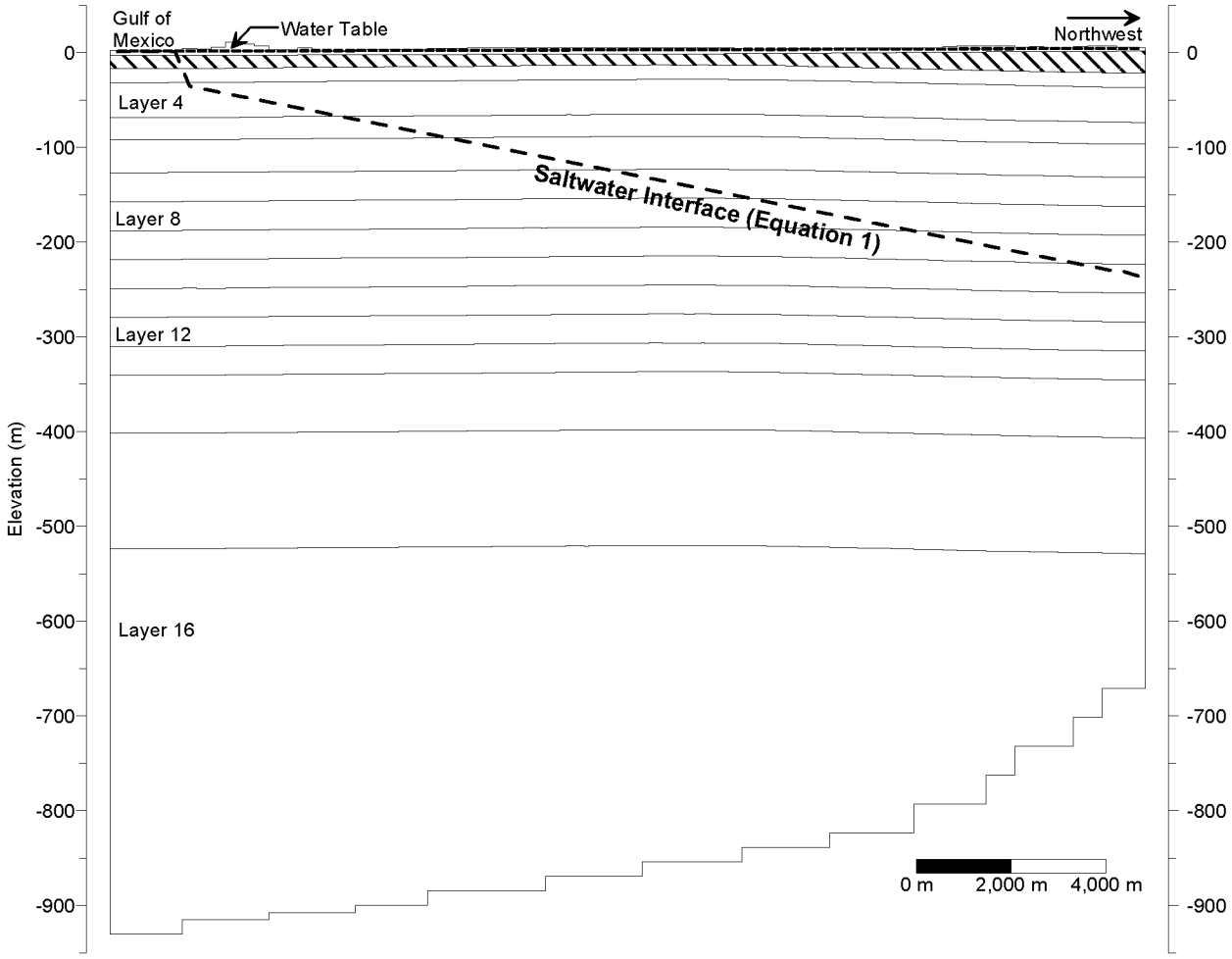

Figure 1. Model layers and specification of boundary conditions along the southwestern model edge (column 1).

Along the lateral model edges, head and salinity were specified using a sharp saltwater interface assumption (Figure 1). However, the interface was not assumed to be sharp in the model interior, but rather a brackish zone was allowed to develop through dispersion. The freshwater head (h_f) on the boundary above the interface was defined based on interpretation of regional monitoring data. Subsequently, the elevation of the saltwater interface (z_s, relative to mean sea level) was specified according to:

$$z_s = -\alpha h_f \qquad (1)$$

The parameter α was used to adjust the interface location to approximately match field conditions. For ideal steady conditions, the Ghyben-Herzberg relationship would apply and α would be 40. However, based on interpretation of borehole geophysical logs and depth-discrete concentration data, a value of 70 appeared to be a more reasonable estimate of α for this study. Boundary nodes below the assumed saltwater interface were assigned a salinity of 35 g/L, corresponding to a specific gravity of 1.025. The head below the interface (h_s) was specified such that no vertical flow occurred across the interface on the boundary.

A 1,000-year pre-pumping equilibrium simulation was used to set initial conditions for predictive simulations. The 1,000 year time frame was shown to be appropriate based on stability of solute mass in the model and stability of the simulated salinity field. Each time boundary conditions or hydrogeologic properties were modified (e.g., during sensitivity simulations), a new pre-pumping equilibrium simulation was conducted to set initial conditions.

Model parameter values and reasonable ranges were initially estimated from analytical analyses of FAS aquifer performance tests (APTs) and SAS slug tests. Parameters were subsequently adjusted to optimize the fit between model-simulated and measured drawdown data for one of the APTs. Additionally, the boundary conditions in the model were adjusted so that the pre-pumping simulation reasonably matched observed heads at wells within the study area. A calibration sensitivity analysis was conducted to refine the reasonable ranges of model parameters.

A 1,000-year base-case predictive simulation was executed with two wells withdrawing 3,800 m^3/d each and with best-estimate values for model parameters and boundary conditions based on the calibration analysis. Subsequently, a predictive sensitivity analysis was conducted wherein model parameters were adjusted within their reasonable ranges to examine the effect of such changes on model results. Alternative withdrawal scenarios were also simulated by assuming different well locations and/or withdrawal rates.

RESULTS AND CONCLUSIONS

Figure 2 shows the simulated upconing of the 250 mg/L chloride concentration (0.46 g/L salinity) surface for the base case. This concentration represents the Secondary Maximum Contaminant Level (SMCL). The maximum amount of upconing is 35 m after 50 years of pumping, and 85 m after 1,000 years of pumping (steady-state). Figure 2 also shows that the pumping has minimal effect on the deeper saline water, represented by the 15,000 mg/L chloride (28 g/L salinity) surface.

Results from sensitivity simulations indicated that the degree of upconing was insensitive to most model parameters; a notable exception was that higher vertical conductivity of the FAS resulted in greater upconing and vice versa. Importantly, some reasonable parameter changes (e.g., lower values of α, higher dispersivity) resulted in a higher initial elevation of the SMCL surface which then allowed withdrawals to pull this surface further into the production zone.

The feasibility of the proposed wellfield can be judged partially on these model results. The amount of upconing would not likely result in withdrawal of water exceeding the chloride SMCL within 50 years. A field program is currently being planned that will better define the current (pre-pumping) elevation of this surface. The model will be updated based on data from the additional field investigation and then used for a revised assessment of withdrawal effects.

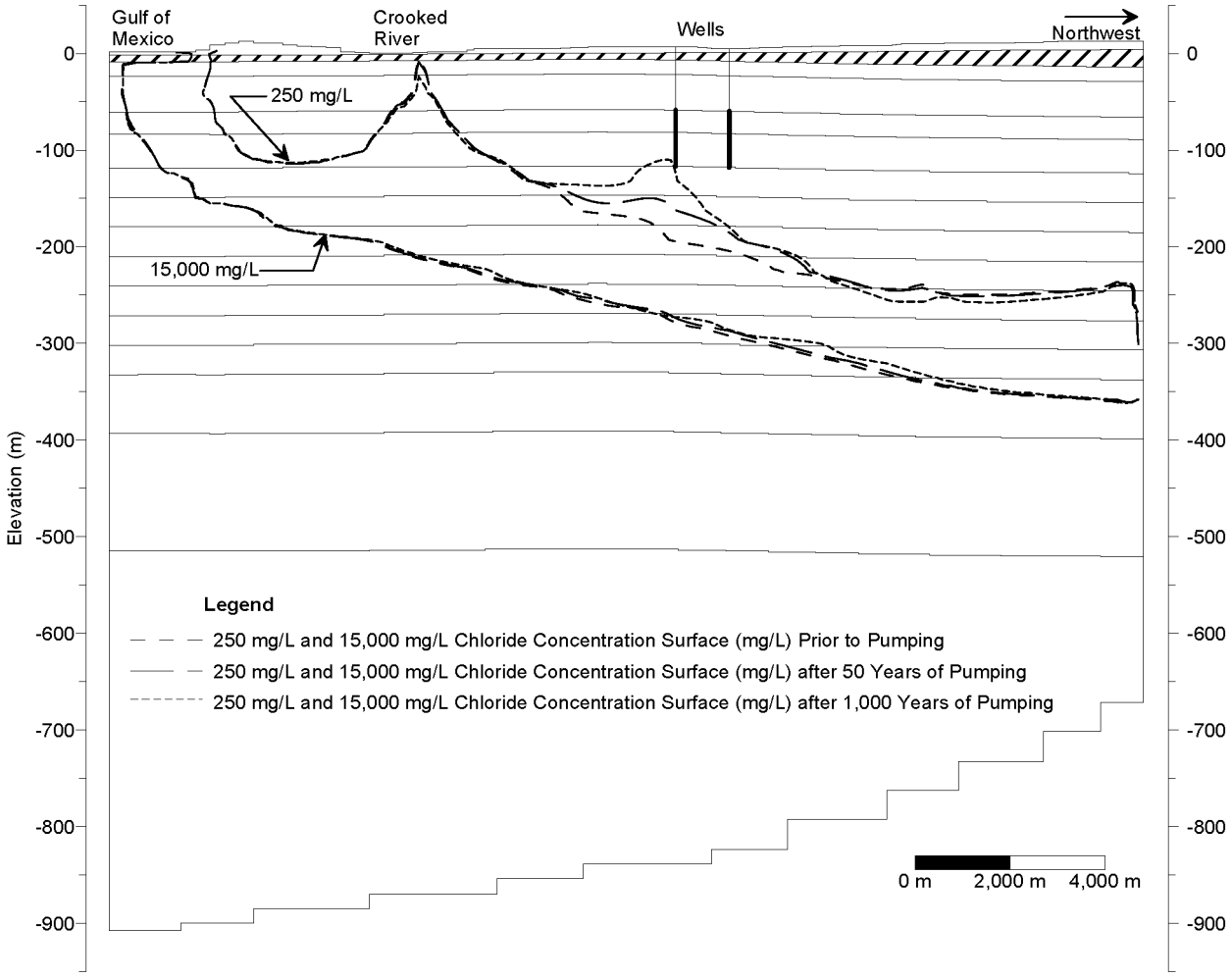

Figure 2. Simulated upconing for the base case predictive simulation (column 153).

REFERENCES

Langevin, Christian D., W. Barclay Shoemaker, and Weixing Guo, 2003. MODFLOW-2000, the U.S. Geological Survey Modular Ground-Water Model—Documentation of the SEAWAT-2000 Version with the Variable-Density Flow Process (VDF) and the Integrated MT3DMS Transport Process (IMT): USGS Open-File Report 03-426, 43p.

Pratt, Thomas R., Christopher J. Richards, Katherine A. Milla, Jeffry R. Wagner, Jay L. Johnson and Ross J. Curry, 1996. *Hydrogeology of the Northwest Florida Water Management District*. Northwest Florida Water Management District Water Resources Special Report 96-4. October.

Contact Information: Gregory W. Council, GeoTrans, Inc., 1080 Holcomb Bridge Road, Building 100, Suite 190, Roswell, GA 30076 USA, Phone: 770-642-1000, Fax: 770-642-8808, Email: gcounci1@geotransinc.com

Managing Seawater Intrusion using Multiple-depth Monitoring Wells

Wesley R. Danskin[1] and *Steven M. Crawford*[2]
[1]U.S. Geological Survey, San Diego, CA, USA
[2]U.S. Geological Survey, Henderson, NV, USA

ABSTRACT

Local water resources are scarce in the San Diego area, California. Nearly all water used along this semiarid coast is imported from hundreds of miles away. As the local population increases and externally supplied water decreases, governmental agencies are looking to expand use of scant ground-water resources. Water managers, however, are concerned that additional pumpage near the coast will induce seawater intrusion. To help managers detect any intrusion, the U.S. Geological Survey constructed several deep monitoring sites between the production wells and the ocean. Each site includes five piezometers, installed to different depths between the water table and about 1,500 feet. Ground-water levels in each piezometer are monitored continuously via transducers and the data are transmitted via satellite to the Internet. Levels are used to determine if a hydraulic gradient has been established from the coast to the pumping wells, indicating possible seawater intrusion. Water samples are collected from the piezometers to determine if seawater is present at any of the five depths. To detect possible intrusion between the sampled depths, the deepest piezometer is logged with an electromagnetic induction geophysical tool, which measures changes in salinity throughout the entire 1500-foot thickness. Managers are using the ground-water-level, water-quality, and salinity data from the multiple-depth wells to detect seawater intrusion and then to adjust pumpage in order to minimize adverse effects. More information is available on the project website http://ca.water.usgs.gov/sandiego.

Contact Information: Wesley R. Danskin, U.S. Geological Survey, 4165 Spruance Road, Suite 200, San Diego, CA 92101 USA, Phone: 619-255-6132, Fax: 619-255-6101, Email: wdanskin@usgs.gov

Saltwater/Freshwater Interface Movement in Response to Deep-Well Injection in a Coastal Aquifer

Alyssa M. Dausman[1], *Christian Langevin*[1], *Michael C. Sukop*[2], and *Virginia Walsh*[3]
[1]U.S. Geological Survey, Florida Integrated Science Center, Ft. Lauderdale, FL, USA
[2]Florida International University, Department of Earth Sciences, Miami, FL, USA
[3]Miami-Dade Water and Sewer Department, Miami, FL, USA

ABSTRACT
Southeastern Florida has disposed of secondarily treated, low total dissolved solids (TDS), wastewater by injecting it into a saltwater aquifer more than 2500 ft below land surface (BLS) since the 1950s. In theory, a confining unit above the zone of injection prevents less dense effluent from migrating vertically upward toward protected drinking water (< 10,000 mg/L TDS) sources at depths of about 1200 ft BLS. However, ammonia concentrations indicative of effluent have been observed in monitoring wells open in and above the confining unit. Water levels, in the protected drinking water aquifer above the zone of injection at a wastewater treatment plant, have increased over 20 ft in the last 30 years. The increased water levels and ammonia concentrations, from vertical migration of effluent, could potentially affect the location of the saltwater interface (the transition from freshwater to saltwater in the aquifer). A variable-density groundwater flow and solute transport model was created and calibrated to better understand the system. Future injection scenarios were simulated to observe the long-term effects of deep-well injection, including the migration of effluent and prediction of interface movement. Results show that long-standing increased water levels at the site with freshwater injected into the ground could affect movement of the interface downward and seaward in southeastern Florida. Based on the Ghyben-Herzberg principle, the interface transition zone could move from about 1700 ft below sea level (BSL) to over 2500 ft BSL at the injection site.

INTRODUCTION
The Florida peninsula is the emergent part of the Florida Platform, containing the Floridan aquifer system (FAS). The FAS consists of the Upper, middle, and Lower Floridan aquifers (UFA, MFA, LFA; Figure 1; Reese and Richardson, 2008). In southeastern Florida, the UFA is an artesian aquifer about 1000 ft BSL and is about 100-200 ft thick. Background water levels in the UFA range from about 30 ft above sea level (ASL) at the coast to about 55 ft ASL inland (Meyer, 1989). The UFA contains mostly brackish groundwater, defined by a TDS concentration of less than 10,000 mg/L. The brackish-water zone is about 1200 ft thick near the coast and thickens toward the center of the platform. The depth to the base of brackish water generally follows the Ghyben-Herzberg principle (Herzberg, 1901; Reese, 1994). The transition zone (referred to herein as the interface) from brackish water (defined above) to seawater (35,000 mg/L TDS) is about 150 ft thick in southeastern Florida. Just below the UFA lies the middle confining unit 1 (MCU1) and the MFA, which has properties similar to those of the UFA. The MFA, however, is slightly more brackish than the UFA. The native

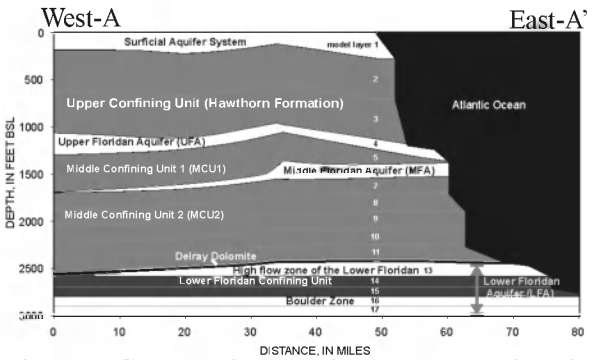

Figure 1: Cross section showing hydrogeologic units along the eastern margin of the Florida Platform in southeastern Florida (Reese and Richardson, 2008; McNeill, 2002), geologic units and layering scheme used for numerical modeling. Location shown in Figure 2.

waters of the LFA have TDS concentrations equal to seawater. The LFA is not artesian and has water levels near sea level.

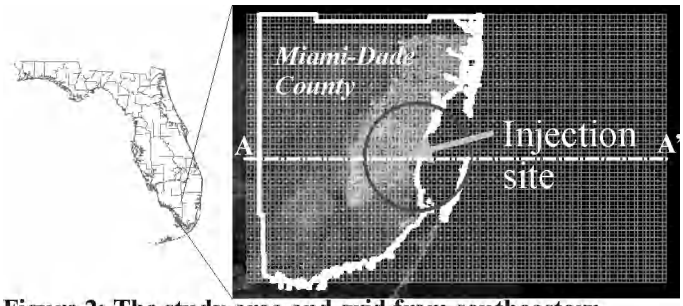

Figure 2: The study area and grid from southeastern Florida. A-A' cross section line shown for Figure 1.

The largest capacity deep-well injection plant in the United States, constructed in southeastern Florida during the 1970s, injects about 100 Mgal/d of secondarily-treated effluent into the saline and highly-transmissive parts of the LFA (Figures 1 and 2). The Delray Dolomite and middle confining unit 2 (MCU2) separate the zone of injection from the overlying UFA and MFA, which are protected under the U.S. Environmental Protection Agency's (USEPA) Safe Drinking Water Act (SDWA). The SDWA stipulates that aquifers containing groundwater with TDS less than 10,000 mg/L are "protected by law" (contamination by effluent is illegal). However, ammonia concentrations exceeding ambient conditions have been observed in monitoring wells open in and above the MCU2 and MFA (Figure 1), suggesting effluent has migrated upward (Maliva et al., 2007). Vertical migration is probably due to salinity-induced buoyancy effects created by injection of the low-TDS effluent into the saline native waters of the LFA.

Historical site records indicate injection of effluent into the LFA has caused more than a 20-ft increase in UFA groundwater levels; pre-injection water levels average about 42 ft ASL, whereas current water levels are about 65 ft ASL. Although the increase in heads is pervasive at the site, no nearby offsite monitoring wells are available to determine the aerial extent of the water-level increase. Some onsite monitoring wells show an increase in effluent concentration, indicated by anomalously high ammonia concentrations, or a decrease in TDS, caused by freshening of the well from effluent migration. An increase in effluent concentration, however, is not observed in all onsite monitoring wells. At present, the decrease in TDS in some of the wells with the increased water levels may indicate localized upward vertical migration of effluent.

The State permit for deep-well injection requires facility upgrades to be completed by 2010; effluent will be treated to drinking water standards prior to injection. This decreases the potential for contamination and allows deep-well injection to continue. The purpose of this study is to use groundwater modeling to address the following questions concerning deep-well injection. First, has the water injected over the past 25 years (~ 700 billion gallons) migrated (1) horizontally within the LFA towards the Atlantic Ocean, or (2) vertically towards the MFA/UFA? Second, if the majority of low-TDS injectate is migrating vertically upward, could it affect the overall location of the interface in the MFA/UFA? Finally, if the injectate is treated to drinking water standards, could it be considered future "recharge" to the UFA as a result of vertical migration?

MODELING APPROACH

The U.S. Geological Survey is developing a variable-density groundwater flow and solute transport model of southeastern Florida using SEAWAT (Version 4; Langevin et al., 2008). The numerical model is designed to assess (1) the fate and transport of injectate in the UFA and LFA, and (2) the movement of the brackish-water/freshwater interface in response to injection. The domain of a three-dimensional model spans the boundaries of Miami-Dade County (Figure 2). The top boundary is at sea level and the bottom is 3000 ft BSL. The model grid consists of 17 layers (Figure 1), 66 rows, and 104 columns (covering an area of about 57 by 89 miles, Figure

2). The interface depth was estimated using salinity data from Reese (1994) in combination with an automated parameter estimation program (PEST; Doherty, 2004). PEST is also used to calibrate model parameters, including hydraulic conductivity, porosity, and storage, by matching model output to water levels measured in the field. All estimated parameters are within realistic ranges of reported values. The injection rate into the LFA was obtained from historical records; current injection rates were used to estimate future injection rates. The model simulation period begins in January of 1983 and extends 148 years. Three "solute" species are simulated by the model: TDS (species 1), the relative concentration of injectate prior to 2010 (species 2), and the relative concentration of injectate after 2010 (species 3). A high level disinfectant (HLD) upgrade to the treatment facility is estimated to be complete by 2011.

MODEL RESULTS

The model predicts that after 148 years of injection, heads in the MFA and UFA will reach over 70 ft ASL at the site (Figure 3). Over the 148-year simulation, species 1, 2, and 3 continue to migrate upward at the site toward the UFA, as well as horizontally towards the coast in the LFA. Although effluent will migrate both horizontally and vertically upward in the FAS; the UFA is not contaminated with species 2 at the end of the simulation. Results also suggest that the injectate never reaches the Atlantic Ocean (Figures 3 and 4). By the year 2131, 120 years after the injectate is treated to drinking water standards, the secondarily-treated effluent represented by species 2 is well mixed and diluted. Low concentrations of species 2 (less than 5% of the original) still remain in some of the area (Figure 3). After 120 years, the injectate treated to drinking water standards (species 3) extends outward about 13 miles from the site in the MFA, just beneath the UFA (Figures 1, 3, and 4). The overall interface location in the MFA around the site shifts landward a few miles, with the brackish-water zone being "recharged" with injectate by 2031 (Figure 3). Model results suggest that injection has a local effect on the interface position within the MFA near the site (the interface moves in several miles by 2031). Injection does not appear to have had a regional effect on the interface position.

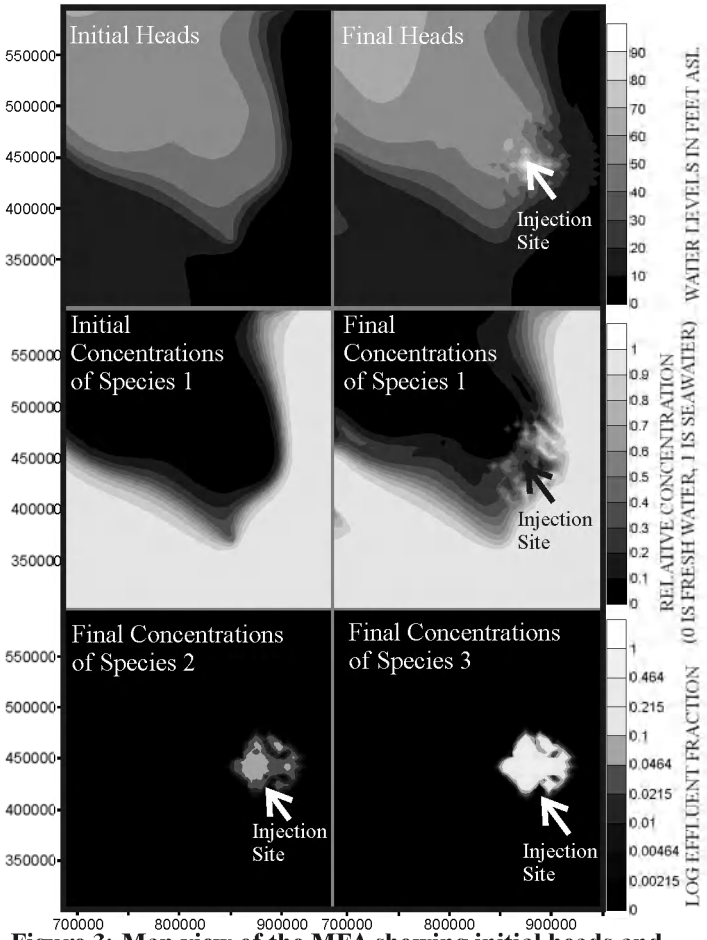

Figure 3: Map view of the MFA showing initial heads and concentrations, and final heads and concentrations of species 1, 2, and 3 after 148 years of injection. Coordinates are in feet, State Plane 83.

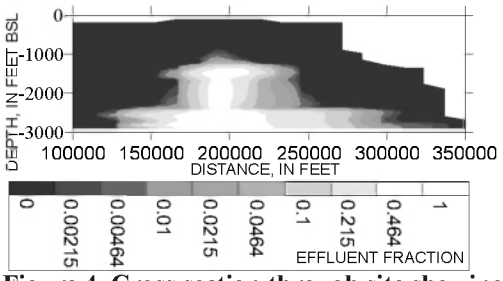

Figure 4. Cross section through site showing species 3 after 120 years of injection.

DISCUSSION AND CONCLUSIONS

The observed local freshening of certain monitoring wells at the site coincides with an increase in ammonia, although this is probably caused by the vertical upward migration of effluent over the last 25 years, rather than overall seaward movement of the interface. Over a longer, 148-year time period, however, the predicted increase in water levels at the site may affect the interface location in Miami-Dade County, depending on the areal extent of the increased water levels in the MFA and UFA. Based on the Ghyben-Herzberg principle, the interface transition zone could move from about 1700 ft BSL to over 2500 ft BSL at the injection site. The model results suggest that residual secondarily-treated effluent remains in the aquifer system as a result of 28 years of injection. This residual effluent, however, appears to be diluted over time due to the injection of higher quality water and mixing with native groundwaters.

The model presented here is a first step in understanding the long-term effects of a deep-well injection facility; a higher resolution model of the same area is being developed. This more refined model could provide additional insight in the localized vertical migration of effluent, as well as the long-term movement of the interface and injectate in the Floridan aquifer system.

REFERENCES

Doherty, J. 2004. Model-Independent Parameter Estimation User Manual: 5th Edition. Watermark Numerical Computing.

Herzberg, A. 1901. Die Wasserversorgung einiger Nordseebader. J. Gasbeleucht. Wasserversorg., 44, pp. 815-819.

Langevin, C.D., Thorne, D., Dausman, A.M., Sukop, M.C., and Guo, W. 2008. SEAWAT Version 4: A Computer Program for Simulation of Multi-Species Solute and Heat Transport. U.S. Geological Survey Techniques and Methods: Book 6, Chapter A22, 39 p.

Maliva, R.G., Guo, W., and Missimer, T. 2007. Vertical migration of municipal wastewater in deep injection well systems, South Florida, USA. Hydrogeology Journal.

McNeill, D.F. 2002. A Geological Review of the Confining Capability of a Regional Dolomite Unit: Application to the MDWAS South District WWTP. McNeill Geological Services Inc. Prepared for the Miami-Dade County Attorney.

Meyer, F.W. 1989. Hydrogeology, ground-water movement, and subsurface storage in the Florida aquifer system in southern Florida. U.S. Geological Survey Professional Paper 1403-G, 59 p.

Reese, R.S. 1994. Hydrogeology and the Distribution and Origin of Salinity n the Floridan Aquifer System, Southeastern Florida. U.S. Geological Survey WRIR 94-4010, 56 p.

Reese, R.S. and Richardson. E. 2008 (in press). Synthesis of the hydrogeologic framework of the Floridan Aquifer System and delineation of a major Avon Park permeable zone in central and southern Florida. U.S. Geological Survey Scientific Investigations Report 2007-5207.

Contact Information: Alyssa M. Dausman, U.S. Geological Survey, 3110 SW 9th Avenue, Fort Lauderdale, Florida 33315 USA. Phone: 954-377-5972, Fax: 954-377-5900, Email: adausman@usgs.gov

Characterization of Local Rainwater Lenses in Agricultural Areas with Upward Saline Seepage: Monitoring Results

Perry G.B. de Louw[1], *Gualbert H.P. Oude Essink*[1], *Bart J.M.Goes*[1] and *Francesco Sergi*[2]
[1]Geological Survey of the Netherlands-Deltares
[2]University of Rome

INTRODUCTION

Saline groundwater with chloride concentration exceeding 5000 mg/l is found within five metres below surface level in the southwest of the Netherlands in the province of Zeeland. Upward flowing of this saline groundwater leads to salinization of the surface water and in some cases salinization of the root zone. Infiltrating rainwater forms fresh to brackish water lenses which facilitates agriculture in these areas. Shape, thickness and dynamics of these lenses are determined by seepage velocities, water management (e.g. surface water levels and drainage system) and precipitation surplus. To designate potential risk areas for future salinization with respect to change of water management, climate change and sea level rise, a monitoring campaign and numerical variable density modeling were carried out. Some of the monitoring results are presented in this paper.

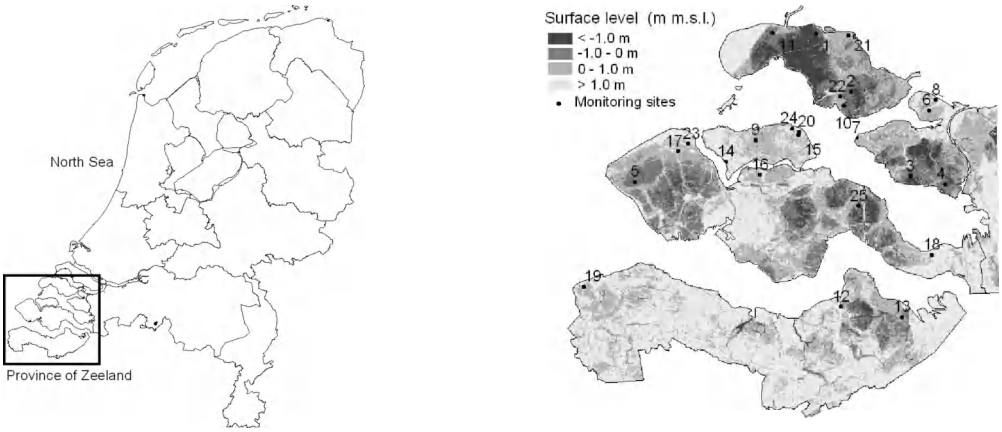

Figure 1. The surface level of the province of Zeeland relative to mean sea level and the location of the 25 monitoring sites

SITE DESCRIPTION

Several transgressions occurred during the Holocene in the province of Zeeland. During these events, seawater could infiltrate and salinize the underlying aquifers. The province of Zeeland can roughly be divided in two different areas, the so-called 'old' and 'new' land, which relate to the period of reclamation. The 'old' land has experienced land subsidence during a longer period and is therefore situated down to two metres below sea level, whereas the 'new' land is situated mainly above sea level (Figure 1). Surface water levels are maintained at about 0.5 to 3.0 m below sea level. Groundwater seepage from the first aquifer takes place into almost all ditches and in the 'old' land also in the parcels between the ditches. In about 70% of the province the brackish-salt interface is found within five metres depth.

METHODS

The monitoring campaign was carried out using a T-EC probe and CVES to measure the salt distribution in the shallow subsoil at 25 different agricultural parcels (Figure 1). A typical agricultural parcel in Zeeland is drained by ditches (ditch distance of 50 to 200 m) and drain

tubes at about 1 m below the surface. The field measurements were carried out from ditch to ditch between the drain tubes.

T-EC probe

The T-EC probe is constructed for the 1D in-situ measurement of temperature and electrical conductivity of soft soils like peat and clayey soils. In the ditch and at different distances from the ditch the T-EC probe was used to measure the temperature and the bulk (soil and water) electrical conductivity (EC) below the groundwater level at 10 cm interval down to a depth of 4.0 m. Detailed soil descriptions were carried out for estimation of the Formation Factor which is needed to convert the bulk-EC into the EC of the groundwater. Chemical analyses on local groundwater samples showed that chloride is the dominant anion and that EC-values could be converted into Cl-concentration using an established empirical EC-Cl relation.

CVES

2D geo-electrical measurements, or Continuous Vertical Electrical Soundings (CVES), have been carried along several profiles at eight agricultural sites to map the spatial variation of thin fresh/brackish water lenses within a parcel. The CVES measurements have been done with an AbemSAS4000 connected to four multi-electrode cables with an electrode spacing of 1 m. The measured electrical resistivity data have been recalculated (inverted) into real soil resistivities with a computer program (SensInv2D). Based on an empirical relation it is estimated that a water resistivity of 1.2 Ohm-m corresponds with a chloride concentration of ~3000 mg/l. Given a dominant soil type of clayey sand (Formation Factor 2.5), a water saturated soil resistivity of ~2.5 Ohm-m represents a chloride concentration of ~3000 mg/l.

RESULTS

T-EC probe measurements

Eeman et. al. (2008) characterized the shape of modeled rainwater lenses using spatial moments of chloride concentration change with depth, where the centre of mass (1^{st} moment) indicates the centre, the variance (2^{th} moment) the width and the skewness (3^{th} moment) the symmetry of the transition zone. However, the measured chloride profiles show a S-shaped curve (figure 2) and the measurements show too much variation to apply the statistical moments method. Therefore comparable characteristics are used which are determined graphically as shown in figure 2. Parameter *b* represents the depth of the centre of the transition zone where salt change with depth is at its maximum and *c* is the corresponding chloride concentration. The distance from this point to the depth where the chloride concentration (*e*) becomes more or less constant is characterized by parameter *d* and it represents the width of the lower half transition zone. At almost all surveyed sites chloride concentrations of the groundwater at phreatic level (parameter *a*) has significantly higher values than fresh rainwater. This implies that the top of the transition zone is located in the unsaturated zone and could not be determined with the T-EC probe that can only be applied in the saturated zone.

For 15 of the 25 sites an S-shaped chloride profile (figure 2) was found and the characteristics of the rainwater lens could be determined (table 1). In general, the measurements at relatively saline sites show a wider transition zone with its centre at shallower depth. These sites are situated in the lowest parts of Zeeland, in the 'old land' with highest seepage rates. At the other sites not mentioned in table 1, no salt groundwater was found and showed a relatively fresh profile (average Cl of 400 mg/l) with only slightly increasing salt content with depth. These sites are all located in the higher parts of Zeeland where no seepage or little seepage into the parcel takes

place. However, seepage of saline groundwater into ditches happens almost everywhere (figure 2) because surface water levels are maintained at 0.5m below sea level or lower.

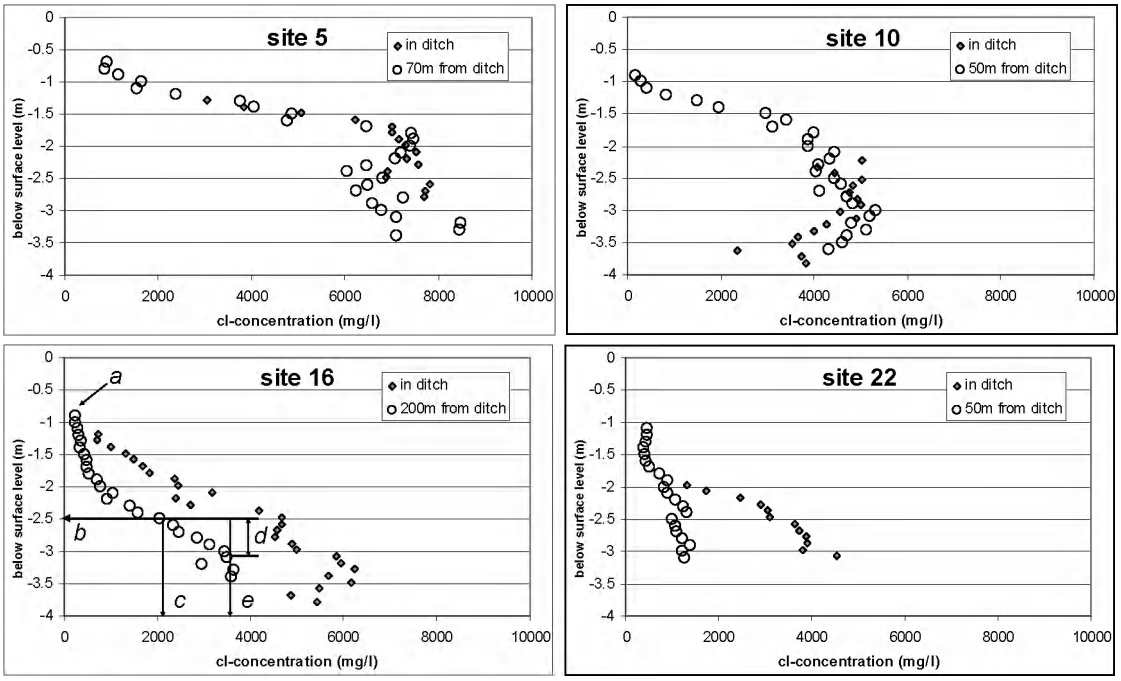

Figure 2. Cl-profiles based on T-EC probe measurements in ditch and parcel

	a	*b*	*c*	*d*	*e*		*a*	*b*	*c*	*d*	*e*
	cl-conc	depth	cl-conc	width	cl-conc		cl-conc	depth	cl-conc	width	cl-conc
site nr.	*mg/l*	*m*	*mg/l*	*m*	*mg/l*	site nr.	*mg/l*	*m*	*mg/l*	*m*	*mg/l*
2	500	2.0	1900	1.5	3000	12	400	2.1	1000	0.4	1700
3	960	0.7	5000	1.1	9000	13	500	2.4	2000	0.9	3800
4	600	0.9	3300	1.1	6200	16	250	2.5	2100	0.6	3600
5	900	1.3	3800	0.9	7000	21	370	1.3	1500	0.7	2800
7	470	1.5	1600	1.0	2400	22	470	2.1	900	0.6	1300
9	300	2.0	750	0.5	1000	24	1400	1.3	3000	0.4	4000
10	170	1.4	2200	1.2	4500	25	380	0.9	2500	0.8	5000
11	550	1.6	4000	1.8	7000						

Figure 3. Rainwater lens parameters *a,b,c,d* and *e* based on T-EC measurements for different monitoring sites (see figure 2 for explanation parameters)

CVES measurements

In the figure 3 an example CVES profile is shown. At the left side of the profile (x-position: 40 to 100 m) there is a relatively thick saturated zone (2 to 8 m thick) with an estimated chloride concentration of less than 3000 mg/l. At the right side of the profile (x-position: 120 to 240 m) the zone with a lower chloride concentration is much thinner (~2 m). Below these brackish zones the soil resistivity is very low (<2.5 Ohm-m) which indicates saline groundwater and/or clay. No major lithological differences have been observed along the profile. The relatively thick brackish water lens at the left side of the profile can be explained by the fact that the agricultural drainage pipes are situated at a higher level than at the other side of the profile causing higher groundwater levels and therefore lower seepage rates and probably even infiltration for most part of the year.

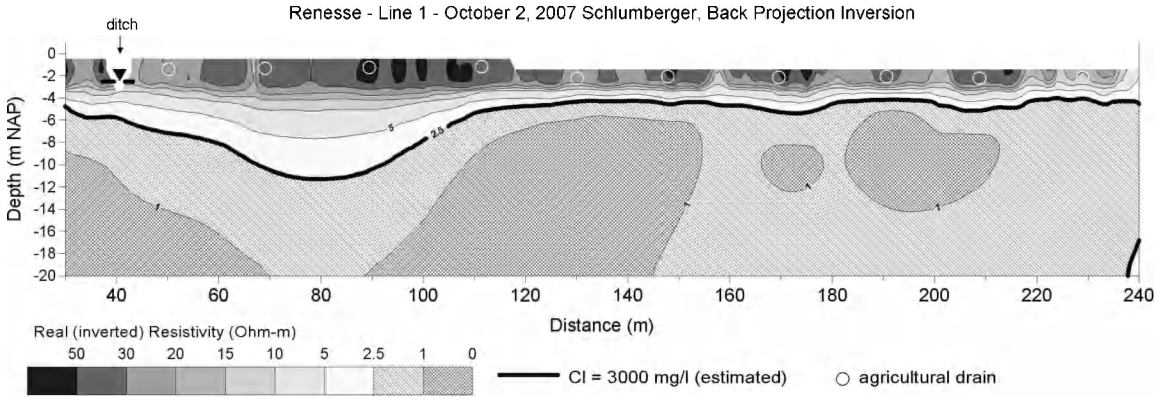

Figure 3. CVES profile for site 11

DISCUSSION AND CONCLUSIONS

The combination of T-EC probe (up to 4m depth) and 2D geo-electrical measurements (up to 20m depth) have proven to be a useful tool to visualize and characterize lateral variations of local rainwater lenses floating on saline groundwater. The monitoring results showed there is no sharp boundary between infiltrating fresh rainwater en saline seepage groundwater but there is a gradual transition zone with an average width of 2.0 m. At sites with high seepage rates no fresh groundwater was found and the transition zone already begins in the unsaturated zone with its centre at shallow depth (0.5-1.5m).

Little is known about the dynamics of these local rainwater lens caused by changes of precipitation surplus and seepage rates. Therefore an intensive monitoring network will be installed at two parcels this coming year where salt distribution of groundwater, soil moisture, drainage and surface water will be measured every hour for at least two years.

REFERENCES

Eeman, S. A. Leijnse, S.E.A.T.M. van der Zee. (2008). Modeling fresh water lenses on saline groundwater (in prep).

Contact Information: Perry G.B. de Louw, Geol. Survey of the Netherlands-Deltares, PO Box 80015, 3508 TA, Utrecht, The Netherlands. Phone: +31 2564806: Email: Perry.delouw@tno.nl

Submarine Groundwater Discharge at an Open Ocean Marine Beach in California

A. B. Boehm and ***N. R. de Sieyes***
Department of Civil and Environmental Engineering, Stanford University, Stanford, CA, USA

ABSTRACT

Experiments were conducted in July 2006 to investigate the role of the neap-spring tidal cycle on variability of submarine groundwater discharge at Stinson Beach, California. Submarine groundwater discharge is the flow of water, regardless of fluid composition or driving force, from the seabed to the sea. Stinson Beach is a Central California community of approximately 650 residences where onsite wastewater treatment systems (septic systems) are used exclusively for wastewater disposal. Shallow groundwater at the site has high concentrations of dissolved inorganic nitrogen, soluble reactive phosphate, and human fecal bacteria. Monitoring across a fortnight showed a groundwater-derived freshening and nutrification of the surf zone at neap tide. Saline and fresh groundwater discharge to the surf zone was estimated using a combination of analytical models and a surf zone mass balance using a single rip cell, or the zone of circulation between two adjacent rip currents, as a control volume. Total discharge, the sum of the fresh and saline components, was maximal at spring tide, and was approximately 140% of total discharge at neap tide. However, discharge of the fresh component was maximal at neap tide, approximately an order of magnitude above the spring tide counterpart. Changes to discharge estimates across the fortnight were closely linked to changes in seaward hydraulic gradient across the fresh part of the aquifer. Gradients in this region appear to be controlled to a large degree by aquifer overheight, or hydraulic mounding, near the beach face. Dupuit estimates of seaward fresh groundwater flow in the fresh part of the aquifer agreed well with the results of the mass balance, i.e. fresh seaward flow was markedly increased at neap tide. Interestingly, the nutrification and freshening of the surf zone was not associated with a similar increase in fecal indicator bacteria concentrations in the surf zone, indicating that the surficial aquifer may be attenuating these septic effluent constituents to a high degree. However, the freshening and nutrification of the surf zone at neap tide was followed by a 4-day increase in chlorophyll *a* concentrations in the surf zone. The role of nutrient-enrichment by SGD in causing increases of chlorophyll *a* in the coastal ocean at the site was explored using a controlled mesocosm experiment. A full year of dense hydraulic head monitoring at the field site helped elucidate the importance not only of fortnightly tides but also swell events and seasonal precipitation in driving water table fluctuations at the site.

Contact Information: Nick R. de Sieyes, Department of Civil and Environmental Engineering, Stanford University, Y2E2 Environment & Energy Building, 473 Via Ortega, M-17, Stanford, CA 94305-4020 USA,
Phone: 805-403-6820, Fax: 650-725-3164, Email: desieyes@stanford.edu

Salt Water Intrusion in The Shallow Aquifers of Venice

Fulvio Zezza and ***Eloisa Di Sipio***
Department of Architectural Construction, University IUAV of Venice, Venice, VE, Italy

ABSTRACT
This paper presents the results concerning the water circulation of the first 50 m depth of the Venice subsoil, till now not interested by hydrogeological evaluation.
This research describes the aquifers, characterized by a significant thickness and constance, recognized in the Venetian geological context and the different hydrochemical facies of perched and confined aquifers, interested by salt water intrusion and influenced by tide variations, whose effects are diminishing with depth.

INTRODUCTION
A recent research on the geological settings of the Venice city centre subsoil (Zezza 2007), focused on the lithostratigraphic reconstruction of the first 50 m from the ground level, shed new light on the circulation of shallow groundwater.

The historical centre of Venice is located on the southern threshold of the Veneto Platform. The particular depositional events (marine transgression and regression), which have affected this region over the last 2 M years (Brambati et al. 2003), creates a typical stratigraphical sequence characterized by a great deal of variability in both the horizontal and vertical directions (McLennen et al. 1997; Carbognin et al. 2004). The analysis of the upper part of the sedimentary sequence by means of the lithostratigraphic method has allowed to distinguish the *cyclothemic organization* of Late Pleistocene, typical of lagoonal area, from the *multistorey sandbody,* the sedimentary structure typical of the city centre subsoil (Zezza 2007). The *cyclothemic organization* is constituted by a rhythmical alternation of sand, silt, clay and peat deposits, while the *multistorey sandbody* is formed by a vertical recurrence of sand body, created by alluvial channel and bank and overflowing deposits, whose complexity is influenced by climatic variations of the last glaciation (Wurm) and by the fluvial condition changes over time. If we consider the distribution of permeability characteristics in the subsoil, it is easily recognizable the influence of the *multistorey sandbody* sedimentary structure: the levels with a medium permeability correspond to sand, while the sediments characterized by low permeability or practically impermeable are clayey-sandy silt and clay deposits (Fig.1). From an hydrogeological point of view, the succession of these levels in the Late Pleistocene deposits identify a multilayered aquifer systems, constituted by four confined aquifers, located respectively at depth of 12-14 m, 18.5-21.5 m, 26-30 m and >30 m from the mean sea level, while the sandy silt typical of tidal Holocene channel and the landfill deposits are able to store perched aquifers (Fig.1).

METHODS
Sixty one piezometers, disposed at different depths all over the city and realized mainly during restoration intervention to control water level variations, have been used as references for the present work (Fig.2a). The great part of these (> 50) reaches a maximum depth of 6-8 m, while the remaining are able to involve the permeable deposits located under 12 m depth. Conductivity logs, together with temperature, pH and piezometry values, have been collected in each well in different periods, and the measured data allows to verify whether significant variations take place over the time. Moreover, the influence of tidal variations, registered at Punta della Salute marigraph, on the water level have been considered. The area of San Basilio (SB) has been

selected as sampling areas, due to the existence of some still open piezometers tapping aquifers at different depth: cation and anion contents have been determined, respectively, by ICP-MS and ion chromatography, together with isotope analyses in order to determine the hydrogeochemical facies of water.

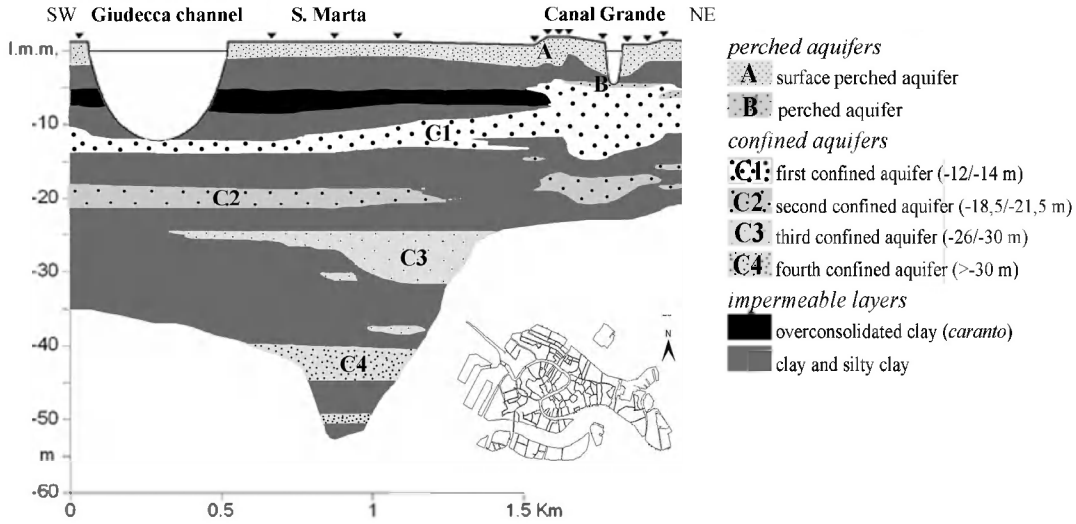

Figure 1. Groundwater circulation in the Late Pleistocene – Holocene deposits of Venice historical centre (from Zezza 2007, modified)

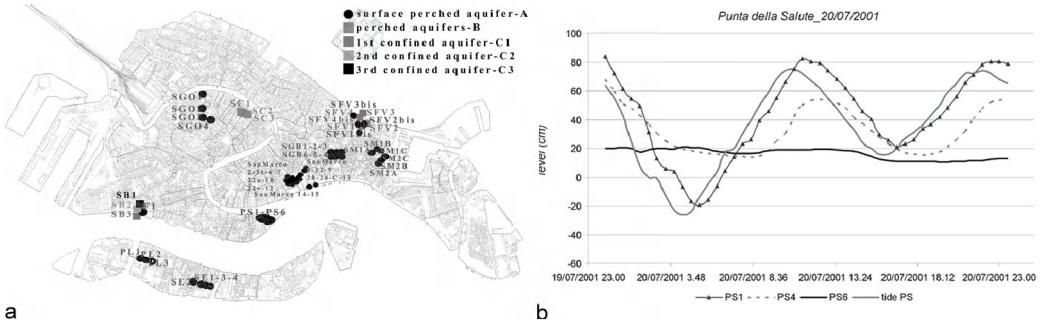

Figure 2. Relationship between water level and tide variations. a) Location of piezometers interesting different aquifers; b) in the perched aquifer of Punta della Salute, the piezometer more distant from the bank channel (PS6) shows the lower influence of tide

RESULTS

The first perched aquifer (A, Fig.1), located in the landfill deposits, has a thickness of 3.5-4 m, is characterized by high permeability values ($k=10^{-1}$-10^{-3} cm/s) and it is limited by clay and silty clay sediments of lagoonal origin. It is widespread all over the urban settlement and shows an homogeneous behaviour: the water level is included between 0.70 and 0.05 m on m.s.l. Due to its high hydraulic conductivity, this landfill soil is directly connected with the lagoon and therefore, the perched aquifer is immediately affected by the hydrostatic pressure variation driven by tides. The tide fluctuations determines water level variations that diminish gradually from 10-15 cm near the channel bank (PS1) to 2-3 cm at a distance of 8-9 m (PS6, Fig.2b). Other perched aquifers (B) are stored in semipermeable sediments (silty sand or sandy silt), located at a depth

of 6-8 m from the ground level. These aquifers are irregularly distributed, have a limited extension and thickness (about 2 m) and locally their behaviour is typical of an aquiclude; the water table trend (between 0.70 and -0.80 m from the ground level) is influenced by tide variations only during low tide. The confined aquifers recognized at different depth in the alluvial sequence of the Late Pleistocene are related to the sand bodies identified by the lithostratigraphic correlation method (Zezza 2007, Fig.1). The data collected all over the piezometers interesting the Pleistocene sediments show that these three aquifers (C1-C2-C3) are not influenced by rainfall and that the piezometric levels variation due to tide fluctuations diminishes progressively with depth.

From the physical chemical analyses, the water of the first perched aquifer is slightly basic ($7.1<pH<8$) and T values range from 21.9 to 15.6 ° C. The electrical conductivity (EC) measurements reveals the presence of saline water all over the year ($2.9<EC<28.9$ mS/cm), while the Cl content is close to that of salt water ($Cl \geq 10{,}000$ mg/l). Moreover, all the three confined aquifers are characterized by slightly basic water ($7.1<pH<7.8$), with T means values of 17.8, increasing with depth. The EC ($3.8<EC<21.2$ mS/cm) and the Cl contents, typical of brackish water (300- 10000 mg/l), highlight the existence of the salt water intrusion phenomena. Therefore, following the Piper classification, the Venice shallow waters, both of perched and confined aquifers, can be defined as chloride-sulphate-alkaline waters (Fig.3a). Moreover, the anion ternary diagram focuses the existence of a mixing process between fresh and salt water related to the increasing of Cl content.

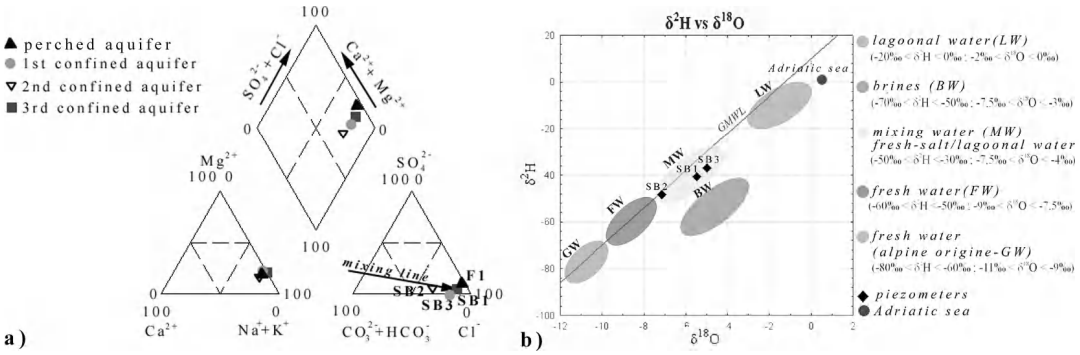

Figure 3. a) Geochemical classification of Venice water samples with Piper diagram (meq/l). b) Isotopic analyses of the confined aquifers

DISCUSSION AND CONCLUSIONS

The perched and confined aquifers waters have the same hydrochemical characterization, present typical salt water values (Cl) and can be considered as recent waters. The sea water presence in the shallow groundwater is confirmed by the (Ca+Mg)/(Na+K) ratio, ranging between 0.27 (sea water value) and 0.31, and by the Na/Cl and K/Na ratios, that exceed the sea water value (respectively of 0.86 and 0.02) only in the C2 aquifer. Moreover, in this aquifer, the negative chloride-alkaline ratio (Cl-Na+K)/Cl registered can be explained by the local presence of semipermeable layer that slow down the salinization process. The relationship between SO_4 and Cl ions confirms the presence of brackhish water within both the perched and confined aquifers, and reveals a redox environment in the first aquifer (C1), due to the presence of organic matter and peat.

The mixing phenomena is confirmed also by the isotopic analyses conducted on samples collected in the San Basilio area (Fig.3b). In particular, for the confined aquifers, the salinization

process is decreasing with the distance from the lagoonal margins (from C1 to C3) or it is conditioned by the permeability variations within the subsoil: the first and the third aquifers presents a similar behaviour, while the second seems more protected by the semipermeable lithofacies bordering it.

To conclude, the hydrogeological characterization of the first 50 m of the Venice subsoil highlights the existence of different aquifers, perched or confined, all interested by salt water intrusion, characterized by the same geochemical water facies and whose behaviour is strictly connected with the sedimentation processes, that is the interbedding of permeable and impermeable deposits. Moreover, the evolution process of the fresh water towards the composition of seawater has been identified.

REFERENCES

Brambati A., Carbognin L., Quaia T., Teatini P., Tosi L. 2003. The Lagoon of Venice: geological setting, evolution and land subsidence. Episodes, vol. 26 (3): 264-268

Carbognin L., Teatini P., Tosi L. 2004. Eustacy and land subsidence in the Venice Lagoon at the beginning of the new millennium. Journal of Marine System , vol.51: 345-353

McClennen C.E., Ammerman A.J., Shock S.G. 1997. Framework stratigraphy for the Lagoon of Venice, Italy: revealed in new seismic- reflection profiles and cores. Journal of Coastal Research, vol. 13 (3): 745-760

Zezza F. 2007. Geologia, proprietà e deformazione dei terreni del centro storico di Venezia. Estratto Quaderni IUAV, Secondo Convegno "La Riqualificazione delle città e dei territori - Geologia e Progettazione nel centro storico di Venezia", Venezia 7 dicembre 2007, Ed. Il Poligrafo

Contact Information: Eloisa Di Sipio, University IUAV of Venice, Architectural Construction Department, Terese – Dorsoduro 2206, I-30123 Venice, Italy, Phone: ++39-041-257-1291 or ++39-349-1942566,
Fax: ++39-041-522-3627, Email: disipio@iuav.it

Stochastic Study on Impact of Heterogeneity of Coastal Aquifers on Movement of Transition Zone (TZ) between Freshwater and Saltwater Induced by Pumping

Guoping Ding, *Eungyu Park, Huali Chen, Jinuk Cho* and *Jinhee Kang*
Department of Geology, Kyungpook National University, Daegu, South Korea

ABSTRACT

Extensive extraction of fresh groundwater in coastal areas is not uncommon and the resultant effect is serious seawater intrusion. Recovery of head and Total Dissolved Solids (TDS) starts as soon as the pumping wells are shut off. In the paper, TZ is treated as a mixing zone, and the first spatial moment is borrowed to express the centroid of the zone. The characteristics of movement of centroids with time in a synthetic heterogeneous aquifer are studied. The heterogeneity of the aquifer is presented by 12 random realizations, which are controlled by the stochastic parameters such as spatial structure, variance, and correlation length of the hydraulic conductivity field of the aquifer in the SGSIM model. 12 cases corresponding to these realizations are designed and a 2D density-dependent flow and solute transport model is setup to derive the distributions of head and TDS for each case. A base-case considering homogeneous aquifer is designed as the benchmark case. The displacements of the centroids between the base-case and the other 12 cases are computed. The accumulated distances of centroids at different percentage of recovery of head for each case are computed as well. Results suggest the movement of TZ is largely delayed compared with the recovery of head. The sensitivity of TZ to variance and correlation length is mainly dependent on the spatial structure of the hydraulic conductivity field of the aquifer. If the hydraulic conductivity field owns an isotropic spatial structure, TZ is more sensitive to correlation length than variance. However, when the hydraulic conductivity field has an anisotropic spatial structure, TZ is more sensitive to variance than correlation length throughout the recovery process. When both the variance and correlation length are large, TZ can move landward further. The landward intrusion of TZ compared with that in homogeneous base-case implies a simplified homogeneous model may underestimate the location and movement of TZ.

Contact Information: Guoping DING, Department of Geology, Kyungpook National University, 1370 Sankyuk-dong, Buk-gu Daegu 702-701, Korea, Phone: 82-53-9515356, Email: gpding@gmail.com

Incorporating Initial Conditions in the Model Calibration Process

John Doherty
Watermark Numerical Computing, Brisbane, Australia.

ABSTRACT
Means by which estimation of initial heads and concentrations over the entirety of a model domain is incorporated into the model calibration process are discussed. This brings the benefits of reduced potential error in parameters employed by the model, and of predictions made by it. It also allows better quantification of the possible extent of these errors. A two step process is briefly described. First the location of a notional freshwater-saltwater interface is parametrically defined. Second, these parameters are estimated simultaneously with aquifer hydraulic properties using regularised inversion techniques which can accommodate the estimation of large numbers of parameters. A maximum likelihood solution to the combined inverse problem is sought through use of appropriate Tikhonov regularisation constraints which collectively attempt to enforce a set of initial conditions which are as hydraulically realistic as possible.

INTRODUCTION
One of the most difficult tasks involved in construction of a saltwater intrusion model is the assignment of initial conditions. Realistic heads and concentrations must be assigned to every cell in the model domain. To make matters more difficult, these are often the outcome of unknown stresses over unknown amounts of time. Furthermore, spatial sampling of these quantities is often very poor.

If initial conditions are wrongly assigned, the model will move water and salt in order to correct this misassignment, at the same time as it moves them in response to stresses represented in the model. The problem is exacerbated when a model is run for calibration purposes. Parameter estimates may be compromised if initial conditions are wrongly assigned, and if hydraulic property estimates are the only quantities that are allowed to vary through the parameter estimation process in order to minimise misfit between model outputs and historical field measurements. This problem is compounded by the fact that spatial variation of initial heads and concentrations is often strongly dependent on spatial variation of subsurface hydraulic properties. Assignment of the former independently of a calibration process which seeks to estimate the latter is unlikely to result in initial head and concentration fields that are physically plausible on the one hand, and acceptable to the model on the other hand.

If initial conditions are uncertain, then (like any other uncertain model input) their estimation should be included in the model calibration process. Reasons for this include the following.

1. Field data that is directly or indirectly informative of the initial disposition of groundwater heads and salt concentrations can be included in the calibration dataset, and the information content of this data with respect to these dispositions thereby "tapped"; this will hopefully result in better assignment of initial conditions than would otherwise be the case.
2. With better assignment of initial conditions, parameter estimates will be better, because their need to play a compensatory role for misassignment of initial conditions is thereby mitigated.
3. With uncertainty of initial conditions recognised by their inclusion in the calibration process, this uncertainty (together with that of correlated hydraulic properties) can be quantified as a by-product of the parameter estimation process.

4. Quantification of parameter uncertainty then leads to quantification of predictive uncertainty. Removal of initial conditions from the purview of the calibration and predictive uncertainty analysis processes may result in serious underestimate of potential predictive error as it depends directly on initial conditions, and/or on parameters whose estimates may be compromised through misassignment of initial conditions.

Two problems must be addressed, however, if initial conditions are to be included in the parameter estimation process. The first is that of how to represent these conditions parametrically so that the parameter estimation process is provided with "handles" through which it can alter them. The second is that of accommodating the large number of parameters that parametric representation of initial conditions may entail.

PARAMETRIC REPRESENTATION OF INITIAL CONDITIONS

Where a simulated groundwater system is comprised of one or a number of aquifers separated from each other by aquitards of lower hydraulic conductivity, the disposition of salt and fresh water in each aquifer is often described, qualitatively at least, using the freshwater-saltwater interface concept. In truth, fresh and salt water are not separated by a sharp interface, as there is a significant mixing zone between the two which is the site of complex flow processes. Furthermore, even to the extent that an "interface" can be identified, its landward extension can vary along the coast in response to local pumping and aquifer heterogeneity.

Nevertheless, because it is easier to describe a surface parametrically than a three-dimensional body, the interface concept is useful. The diffuse nature of salt concentrations in the vicinity of the "interface" can then be described using parameters which govern the degree of "concentration spread" about it. Above the interface, salt concentrations can be described as asymptotically approaching some (possibly location-dependent) freshwater background concentration with increasing elevation, while below the interface concentrations asymptotically approach a (possibly location-dependent) background saltwater concentration with decreasing elevation. The width of the interface (this being determined by the rate of approach to asymptotic concentrations both above and below it) then becomes a parameter that is adjustable through the parameter estimation process. This too can be location-dependent if desired.

In numerical experiments conducted to date, pilot points have been employed for parametric description of the freshwater-saltwater interface. Pilot points have often been used as parametric descriptors of two-dimensional hydraulic property variability. They were introduced by Certes and de Marsily (1991) and have been employed by many others since then. Doherty (2003) first combined their use with regularised inversion (see below), allowing the estimation of many more pilot point parameters than had hitherto been possible. Tonkin and Doherty (2005) illustrate the use of hundreds of pilot points in a complex multi-layer setting.

In work undertaken so far, pilot points used for parametric description of the freshwater-saltwater interface have been placed in two rows within each aquifer represented in the model – one row being in front of the toe of the freshwater-saltwater interface and the other being behind its head. The latter position is often well defined in a model as it coincides with the aquifer's maximum seaward extent. The location of the interface toe is often only poorly known. However this does not matter, for it is part of the role of the parameter estimation process to assess where this may be; it is only necessary that pilot points be placed somewhere near this toe, preferably on its landward side.

Elevations are then assigned to all pilot points. The elevation of the freshwater-saltwater interface in every pertinent model cell is then computed through spatial interpolation between the rows of pilot points. If interpolation leads to an interface elevation that is locally above or below the top or bottom of the aquifer this does not matter; fresh and saltwater are dispersed about the interface in the usual manner, but concentrations are only assigned to cells that lie within the hydrostratigraphic unit to which the pilot points (and hence the interface) are assigned. Note that this unit can be comprised of many model layers.

Elevations assigned to pilot points are adjusted through the calibration process. So too are the "spreading parameters" that govern the sharpness (or otherwise) of the freshwater-saltwater interface.

If using the SEAWAT (Langevin et al, 2003) model, computation of a head field that is complimentary to an interface-derived concentration field can be accomplished through running the model for a single steady-state stress period in which an approximation to historical time-averaged stresses is supplied. Computation time for this stress period is normally minimal; if necessary, the MODFLOW component of SEAWAT can be de-coupled from its MT3DMS component for this stress period to lower the burden of initial head computation even further.

PARAMETER ESTIMATION

Hunt et al (2007) describe the advantages of highly parameterised inversion as a vehicle for automatic parameter estimation, and briefly discuss the means through which this can be achieved in a manner that results in estimated parameter fields that are as realistic as possible. In contrast to classical approaches to parameter estimation which rely on the "principle of parsimony", the regularised inversion approach allows inclusion in the parameter estimation process of as many parameters as are needed to extract all information worth extracting from a calibration dataset. Those parameters, or parameter combinations, for which information is lacking, are simply left unaltered, and/or are assigned values that are enlightened by "plausibility constraints" built into the parameter estimation process.

The hybrid inversion methodology described by Tonkin and Doherty (2005) and available through PEST (Doherty, 2007) implements highly parameterised inversion through combining two different, but complimentary, regularisation techniques, namely the subspace and Tikhonov methods. The former allows subdivision of parameter space into orthogonal estimable and inestimable components. The latter allows re-formulation of the inverse problem as one of minimisation of misfit between model outputs and field measurements subject to constraints of maximum parameter plausibility. Through use of "super parameters" which collectively span estimable parameter space, the number of model runs required per iteration of the parameter estimation process is then reduced to a number which is far smaller than the number of parameters that are actually defined (which can number in the hundreds, or even thousands). Use of this methodology in the saltwater intrusion modelling context allows simultaneous estimation of interface parameters, together with (pilot-point-based) aquifer/aquitard hydraulic property parameters to take place with a numerical burden that is little greater than that of classical parameter estimation, but is far more stable, and infinitely more flexible, thus allowing the benefits outlined above of including initial conditions in the parameter estimation process to be realised.

Tikhonov constraints on initial condition parameters that have been employed successfully to date include the following:

1. maximum adherence of initial concentration fields to "training fields" computed using model runs undertaken on the basis of likely hydraulic property distributions;
2. (where appropriate) minimal changes in concentrations within all active cells of the model domain over an initial model stress period in which model inputs approximate pre-run, long-term stresses.

UNCERTAINTY ANALYSIS

The matter of uncertainty analysis was cited above as one of the benefits of including initial conditions in the calibration process. In contrast to traditional parameter estimation and uncertainty analysis, inestimability of certain parameters (or parameter combinations) does not require that such parameters (or parameter combinations) be omitted from this process. Nor does it compromise computation of values for estimable parameters. In fact if inestimable (and hence uncertain) parameters are *not* represented in these processes, achievement of maximum likelihood solutions to the inverse problem of model calibration becomes less likely, while uncertainty analysis becomes impossible. Once included however it then becomes a simple matter to quantify (with integrity) parameter and predictive uncertainty, the contribution to this uncertainty by different parameter types (which now include initial conditions), and the potential benefits of different data acquisition strategies in reducing predictive uncertainty.

REFERENCES

Certes, C., and de Marsily, G., 1991. Application of the pilot point method to the identification of aquifer transmissivities, *Advances in Water Resources*, 14(5), 284-300.

Doherty, J., 2003. Ground water model calibration using pilot points and regularization, *Ground Water*, 41(2), 170-177.

Doherty, J., 2007. PEST: Model Independent Parameter Estimation. Watermark Numerical Computing, Brisbane, Australia.

Hunt, R.J., Doherty, J, and Tonkin, M.J., 2007. Are models too simple? Arguments for increased parameterisation. *Ground Water* 45 (3), 254–262

Langevin, C.D., Shoemaker, W.B., and Guo, Weixing, 2003, MODFLOW-2000, the U.S. Geological Survey Modular Ground-Water Model–Documentation of the SEAWAT-2000 Version with the Variable-Density Flow Process (VDF) and the Integrated MT3DMS Transport Process (IMT): U.S. Geological Survey Open-File Report 03-426, 43 p.

Tonkin, M. and Doherty, J., 2005. A hybrid regularised inversion methodology for highly parameterised models. *Water Resources Research*. Vol. 41, W10412, doi:10.1029/2005WR003995.

Contact Information: John Doherty, Watermark Numerical Computing, 336 Cliveden Avenue, Corinda, 4075, Australia. Phone: +61 7 3379 1664. Email: johndoherty@ozemail.com.au

Evolution of the Marine Intrusion Using Geophysical Methods after 25 Years in the Motril-Salobreña Aquifer (Southern Spain)

Carlos Duque[1], *María Luisa Calvache*[1], *Antonio Pulido-Bosch*[3], *Antonio González Ramón*[2], *Juan Carlos Rubio*[2], *José Antonio Navarro*[2], *Manuel López-Chicano*[1] and *Wenceslao Martín-Rosales*[1]

[1]Universidad de Granada. Departamento de Geodinámica. Granada. Spain
[2]Instituto Geológico y Minero de España. Oficina de Proyectos de Granada. Spain
[3]Universidad de Almería. Departamento de Hidrogeología y Química Analítica. Almería. Spain

ABSTRACT

Two Geophysical surveys have been compared to determine possible changes in marine intrusion in the Motril-Salobreña aquifer in Southern Spain. The first one was carried out with Vertical Electric Soundings (VES) before 1981. The second one was finished in 2006 and it was made using Time Domain Electromagnetic (TDEM) soundings. The zone selected for this study was a coastal aquifer with a lot of human alterations to the surface water and ground water. The changes happened in the area are not affecting, at least for the moment, to the saltwater encroachment. The analysis of the water table trend shows a similar situation between 25 years ago and now.

INTRODUCTION

Southern-Spain is one of the places of Europe with a higher potential risk of desertification due to the special climate properties and the human activity developed in this area. The absence of water is the main cause of the increasing hazards day by day, so the pumpings and hydraulic actions (as dams and transfers) are frequent. This kind of problems result in a decrease of the quality and quantity of the water resources, and the coastal areas are especially sensible because it is necessary to add the marine intrusion as another risk for the groundwater quality.

The groundwater in the Motril-Salobreña coastal aquifer (in the South of Spain) is suffering a lot of changes during the last twenty-five years related with some human actions. They are affecting directly or indirectly to the groundwater dynamics, and due to the contact with the Mediterranean Sea in the south boundary of the aquifer, could change the location of the saline wedge. It is remarkable the construction of a dam in one of the main recharge inputs, the river Guadalfeo; also the agriculture activity is suffering important changes from traditional cropping (such as sugar cane) with high infiltration rates of the irrigation water to greenhouses with increasing occupied surface. The population of the main cities in the area is growing continuously and in summer time, it reaches important maximums due to the tourism. Also, it is planned housing development with golf courses associated. The storage of the aquifer is about 250 Mm^3 (Castillo, 1975; Duque et al., 2007) with annual resources of 35 Mm^3, so for the moment, no water supply problem has been resulted. Anyway it is essential to know if all these changes are impacting the groundwater of the Motril-Salobreña aquifer, especially those related with the seawater intrusion before the effects start to affect the population.

GEOLOGICAL SETTING

The Motril-Salobreña aquifer, with a surface of 42 km^2, is composed of detrital material (gravels, sands and clays) resulting from the erosion of the nearby mountains like Sierra Nevada. Along the aquifer boundaries, metamorphic-rocks outcrop with different hydrogeologic properties (Fig. 1), mostly impermeable schist and permeable carbonates, the geological structure of these materials is very complex. The south boundary is marked by the Mediterranean Sea.

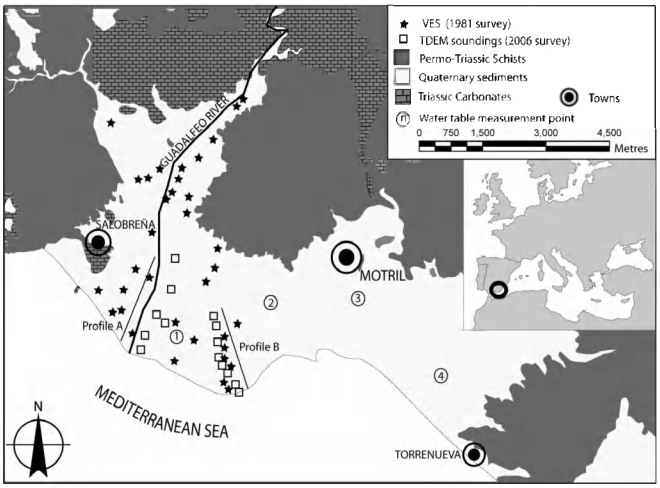

Figure 1. Location, geological map and situation of the geophysical and water table measurements

METHODOLOGY AND RESULTS

The best way for detecting the marine intrusion in this aquifer is the geophysical methods due to the great depth and the absence of deep boreholes. Nowadays we are able to compare the results obtained with electrical methods in 1981 (Geirnaert et al., 1981) with those acquired in a very recent electromagnetic survey in 2006 (Duque et al., 2008). The aim will be to establish if there are any changes.

The surveys developed until 1981 by different projects used Vertical Electric Soundings with different lengths in the Western zone of the aquifer (Fig. 1). It is, probably, the most interesting zone of the aquifer due to the presence of the Guadalfeo River and the size heterogeneity of the aquifer sediments because of the affection to the resistivity measurements. Thirty-four VES were organized in two profiles perpendicular to the coast and another two parallel to the coast. The results explained by Geirnaert et al. (1981) indicated an incipient marine intrusion in the VES nearest to the sea (Fig. 2). In 2006, Duque et al. designed a TDEM survey with 28 measurement points distributed in 4 profiles. Only 2 of the profiles were situated in the west zone (Fig. 1), so they were selected to compare the results with those of 1981 perpendicular to the coast. The comparison, after 25 years, shows almost the same marine intrusion. It is necessary to take into account some differences in the interpretation of the data, but both authors identify as saltwater saturated materials the lowest resistivities detected. In the profile A, the 1981 results did not reach big depths in the points nearest to the coast, so they interpreted a small decrease in the resistivities as marine intrusion (Fig. 2). In the 2006 survey, it was possible to reach 200 meters in depth, so lower values were detected that can be really related with seawater.

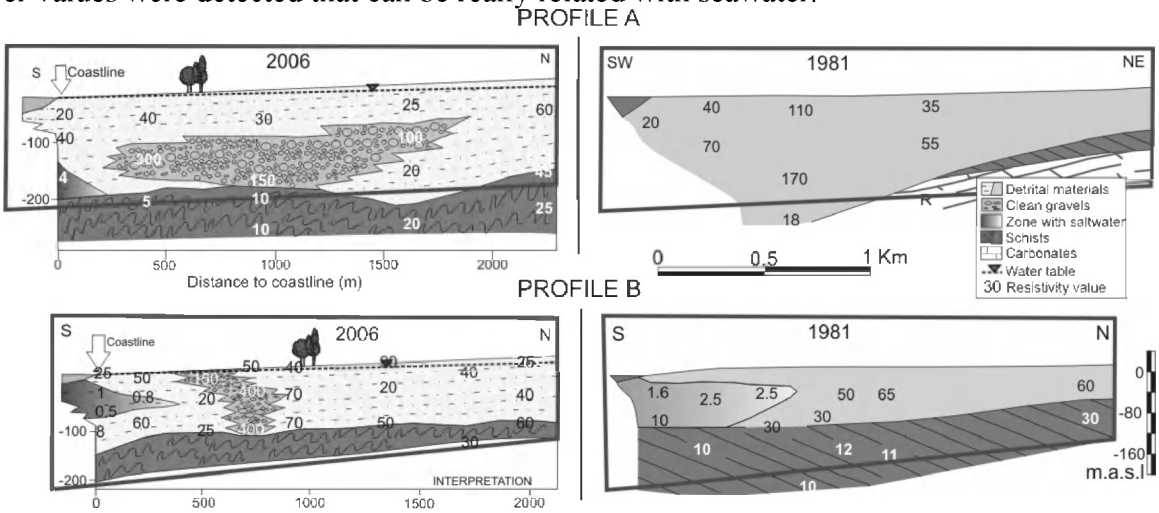

Figure 2. Geological interpretations of the VES in 1981 (right) and the TDEM soundings in 2006(left). The section in the frame remarks the coincident zones.

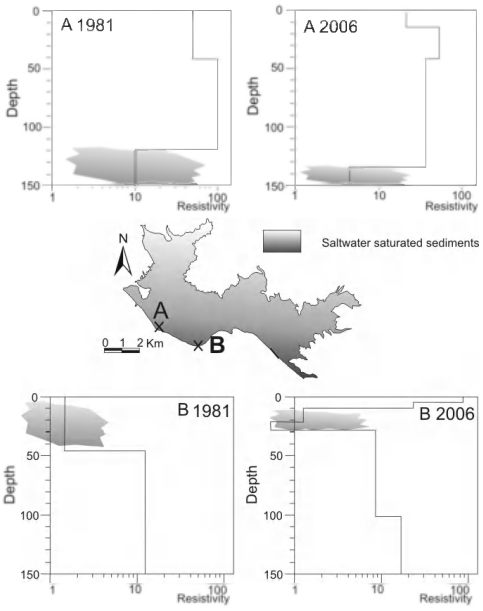

Figure 3. Resistivity versus depth curves in the points with coincident location of VES and TDEM soundings measurements points

The profile B is located along the former Guadalfeo mouth as demonstrated the delta morphology of the coastline. The whole interpretation of 1981 shows marine intrusion with an unusual shape, it is not a wedge. The detailed analysis of the depth-resistivity diagram (Fig. 3) allows a better interpretation. The area under the minimum resistivity zone can be related with detrital sediments saturated with freshwater. It is an anomalous situation due to the presence of an inversion of the ordinary situation or hydrological reversals (Goldman et al., 2003). A gravimetry survey (Duque et al., 2008) allows us to determine where the basement of the aquifer is located and so, it is possible to know that the change in resistivities is not related with the presence of the basement. During the 2006 survey it was possible to detect a very similar situation with more details, probably related with the improvements of the geophysical techniques (Fig. 3). The location of the low resistivity zone and the small change after 25 years sustains the possibility of a clay layer with high salinity content where the fresh groundwater can not penetrate to wash the contaminated sediments (Custodio, 2004). The origin of the salinity is maybe related with old marine intrusion events or with the depositional environment during the sedimentation process (it is remarkable the recent aquifer formation in the last centuries). The detail comparison of the VES and TDEM soundings in the profile A (figure 3) shows a very similar situation. Taking into account the differences in the techniques and in the location of the measurement points, we can assume a stable marine intrusion situation in the western area of the Motril-Salobreña aquifer. The marine intrusion is directly related with the water table; therefore the water table evolution will be related with the geophysical results obtained. The 25-year water table record in four points is analyzed (Fig. 4). The studied period coincides with the time length of measurements of the electrical and electromagnetic methods. The differences between the current and the 25-years ago water table are reduced, and the main changes during this time happened in the dry period of 1990-1995. In the last 2 years an incipient decrease of the water table was happening but it looks like that it is not affecting to the marine intrusion, at least for the moment. The cause of the drop is not clear for the time being because we are in a dry period, but maybe some of the human actions in the last few years are starting to affect.

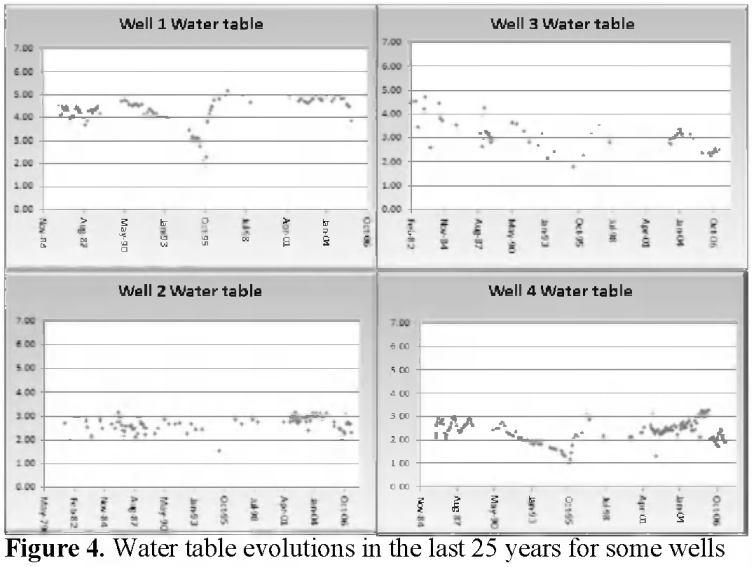

Figure 4. Water table evolutions in the last 25 years for some wells

CONCLUSIONS

The marine intrusion in the Motril-Salobreña aquifer is stable from 1981 or, at least the situation 25 years ago and now is very similar as it has been presented with the use of geophysical

techniques. The water table analysis shows small changes between 1981 and now. The low resistivities measured in the former mouth of the Guadalfeo River were detected 25 years ago and now in a near topographic surface location. The origin could be related with some low permeability materials that can not be washed by the fresh groundwater flow. The marine intrusion is not growing in a dangerous way, but it is starting a dry period with an associated drop in the water table. It is complicated to differentiate human activity and climate effects, however if the recovering capability of the aquifer during the wet periods is affected by the changes in the zone, it could be the starting point for the saltwater encroachment. An adequate monitoring activity will be possible to quantify and to advise for a sustainable resources management of one of the best preserved aquifers in the south of Spain.

REFERENCES

Castillo E., 1975. Hidrogeología de la Vega de Motril y sus bordes. Master Thesis. 184 p.

Custodio E., 2004. Myths about seawater intrusion in coastal aquifers. Proceedings of 18th SWIM, Cartagena. 599-608.

Duque, C.,Calvache, M.L., Pedrera, A., Martín-Rosales, W., López-Chicano, M., 2008. Combined time domain electromagnetic soundings and gravimetry to determine marine intrusion in a detrital coastal aquifer (Southern Spain). Journal of Hydrology, 349,536-547.

Duque C., Calvache M.L., Pedrera A., López-Chicano M., 2007. Cálculo de las reservas de un acuífero detrítico costero mediante gravimetría. Proceedings of TIAC, Almería.

Geirnaert W., Pulido-Bosch A., Castillo E. and Fernández-Rubio R., 1981. Estudio de la geometría del acuífero detrítico de la vega de Motril-Salobreña mediante SEV. In: Proceedings of 1st simposio del Agua en Andalucía, 291-302.

Goldman, M., Kafri, U., Yechieli, Y., 2003. Application of the TDEM method for studying groundwater salinity in different coastal aquifers in Israel. Proccedings of TIAC pp. 45-56.

ACKNOWLEDGMENTS

This study was made possible by funding approved for projects CGL2007-63450/HID financed by the MEC of Spain and the Spanish program of FPI.

Contact Information: Carlos Duque, Departamento de Geodinámica, Universidad de Granada. 18071, Granada, Spain. Phone 0034958243351; Email: cduque@ugr.es

Global Land-Ocean Linkage: Direct Inputs of Water and Associated Nutrients to Coastal Zones via Submarine Groundwater Discharge (SGD)

Hans H. Dürr[1], *Rens van Beek*[1], *Caroline P. Slomp*[2], *Hans Middelkoop*[1] and *Marc Bierkens*[1]
[1]Department of Physical Geography, Faculty of Geosciences, Utrecht University, Utrecht, The Netherlands
[2]Department of Earth Sciences – Geochemistry, Faculty of Geosciences, Utrecht University, Utrecht, The Netherlands

ABSTRACT
Direct discharge of freshwater and associated dissolved nutrients via Submarine Groundwater Discharge (SGD) may have potentially important impacts on coastal water bodies, such as increased eutrophication or hypoxia. Yet, at the global scale, SGD has received little attention compared to efforts made to estimate other pathways of nutrients to the ocean such as riverine inputs. Most studies on the nutrient flux to the coastal zone by SGD have focused on local to regional scales, with the major part of the research being carried out in the Northern hemisphere (U.S. and Europe), and concentrating on areas of high total SGD including recycled fluxes from the saltwater / freshwater mixing zone. While at local scales, the effects of this recycling in the 'subterranean estuary' are important to understand short-term changes in nutrient availability, at the global scale, quantification of the yet poorly constrained net fluxes of freshwater and nutrients discharged via this transport path to the oceans is crucial. Here, we present the first steps towards spatially-explicit estimates of nutrient inputs to the coastal zone via freshwater SGD at the global scale, using baseflow estimates from a global hydrological model, combined with assessments of nutrient concentrations in coastal groundwater bodies.

INTRODUCTION / BACKGROUND
In many areas of the world, continental groundwater flow contributes significantly to freshwater and nutrient fluxes, not only as baseflow to rivers, but also as submarine groundwater discharge (SGD) directly to the coastal zone (Church 1996; Moore 1996). SGD can be an important freshwater source, e.g. in dry areas of the Mediterranean, and clustered assessment based on coastal attributes has been proposed for large-scale estimates of its contribution (Bokuniewicz et al. 2003). At the global scale, near-shore coastal water bodies are generally said to be nitrogen (N)-limited (Howarth and Marino 2006). Inputs from river water are mainly at or slightly below Redfield ratio (N/P~14) (Seitzinger et al. 2005). As phosphorus (P) is mostly efficiently retained in groundwater systems (Spiteri et al. 2008), continental groundwater directly discharging into the sea (SGD) mainly shows N/P ratios >> 16, especially in agricultural areas. Delayed discharge (on the order of several to tens of years) of contaminated groundwater is possible, and box modelling has shown that nutrient inputs via SGD have the potential to significantly affect coastal zone nutrient cycling at the global scale (Slomp and van Cappellen 2004). In most nutrient SGD studies, typically groundwater concentrations of nutrients are multiplied with the total SGD water flux, i.e. including the recycled seawater flux, to estimate nutrient fluxes. Separation of the seawater and freshwater components of SGD is essential, however, since only the freshwater component represents a net input to the marine environment. In this study, we quantify hydrological processes on land, taking into account local variations in topography and lithology, to identify where fresh SGD of nutrients may be important on a global scale.

METHODS
Global hydrological models are typically constructed as a set of cascading reservoirs. They generally include a highly simplified representation of groundwater bodies, and are either tuned or calibrated to a set of known total annual discharge values at the last gauging station.

Here, a new global hydrological model at 0.5° spatial resolution is used (van Beek et al. in preparation), where the parameterization of the shallow/active groundwater reservoir is based on the equation of Kraaijenhof-van de Leur (1958), formulated on the basis of Boussinesq – Dupuit assumptions, for the reservoir coefficient k_r (t^{-1}):

$$k_r = \frac{\pi^2 kD}{4fB^2} \quad (1)$$

where: *k is the hydraulic conductivity (L t^{-1} e.g., m/day), D is the aquifer thickness (L, 50m assumed), f is the drainable porosity (dimensionless, obtained from global lithology data, together with climate data from the Holdridge life zones classification) and B is the aquifer width (L). Permeability was obtained from a global lithology map, drainage distance from the Hydro1K dataset.*

The model is calibrated on periods of low flows from 290 rivers that could be used for this procedure, drawing on the 8% of the time series with the lowest discharges, i.e. flows that are exceeded 92% of the time. As such, groundwater discharge is available for each terrestrial 0.5° grid cell, including coastal cells.

However, in order to estimate actual freshwater SGD fluxes, total baseflow per cell can only serve as a maximum number. Following the first steps taken here, some important amendments will be necessary to distinguish: i) the coastal water divide where baseflow will become SGD in contrast to groundwater discharging into coastal, but still well-defined, streams, ii) human groundwater extraction, and iii) low-lying areas where salt-water intrusion is the more pressing problem.

A range of coastal groundwater nutrient concentrations will be provided based on groundwater nutrient concentrations for nitrogen (DIN – dissolved inorganic nitrogen), obtained from a large collection of coastal and other groundwater nutrient data, and coupled to information on lithology, landuse, and population.

RESULTS AND DISCUSSION

We test various approaches for DIN transport in groundwater, by (i) assuming shallow, oxic systems with rapidly flowing groundwater to be most common, i.e. with conservative flow of DIN (Spiteri et al. 2008), versus (ii) DIN attenuation scenarios based, for example, on half-life approaches. Thus, we provide a range of coastal water and nutrient fluxes, based on the size of the coastal ribbon, and show coastal areas that are potential hotspots for elevated direct groundwater inputs of DIN. This is based on conditions of high baseflow, combined with extensive agricultural land use and a high population density.

SGD nutrient fluxes in coastal zones show a contrasting picture (Figure 1). Compared to global estimates of riverine inputs of N and P via surface water discharge (Seitzinger et al. 2005), nutrient SGD fluxes show certain similarities in many areas, but fluxes may greatly differ locally. Similarities of elevated flow can be found, for example, in highly populated areas of the US (e.g. NE coast) or SE Asia. Fluxes may be very different locally (e.g. parts of Indonesia, Indian catchments), and especially in areas where surface flow is near zero, as for example in the karstic areas of Yucatan.

Freshwater SGD is an important net pathway for nutrients to the ocean. This fresh SGD has the potential to perturb local and regional nutrient cycling at numerous coastal sites but only a very

limited number of field studies have been performed in many potentially important regions, such as the (sub-) tropical areas of Africa, South America and SE Asia.

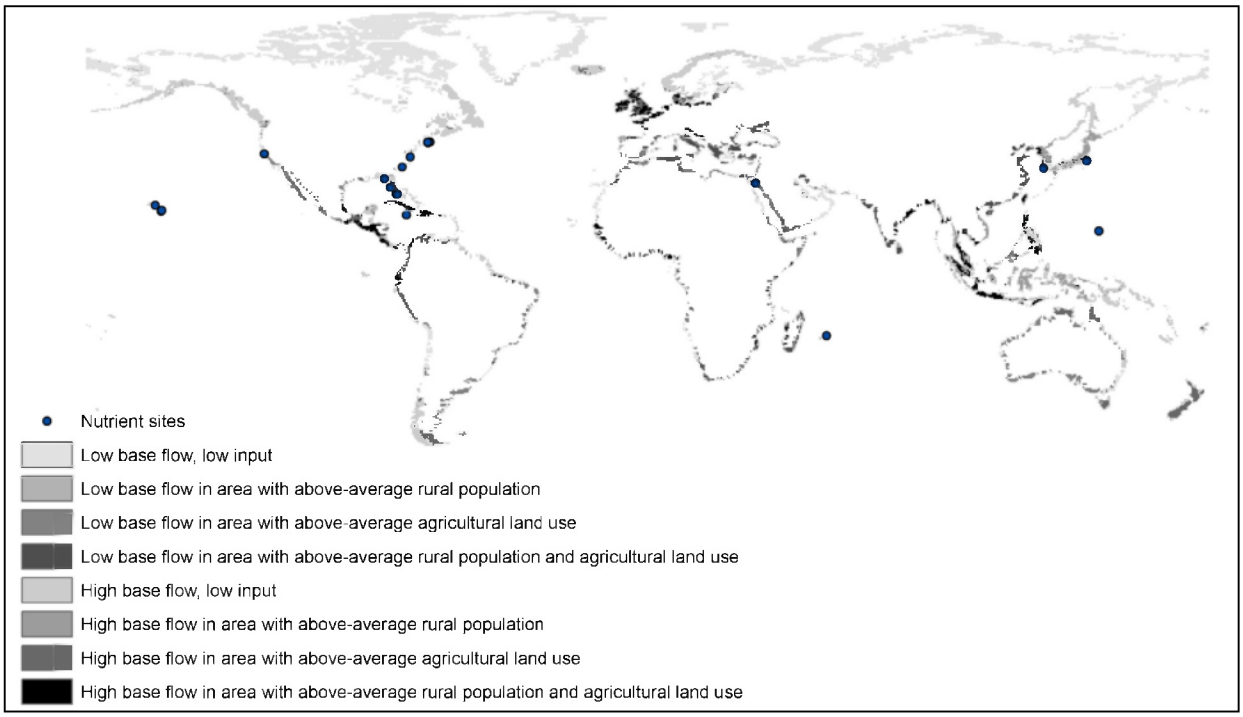

Figure 1. Potential hotspots with elevated N input. NB: Very local phenomena are not detected; the figure represents total groundwater flow in coastal cells, not SGD; groundwater abstraction, saltwater intrusion and groundwater residence time are not yet considered here.

CONCLUSIONS

First steps have been taken towards 1) obtaining spatially explicit estimates of SGD at the global scale, using baseflow estimates from a new global hydrological model and 2) identifying potential hot spots of freshwater nutrient SGD. Our results show that SE Asia, especially Indonesia, and Central America are hot spots for both river and groundwater fluxes, since they show high baseflow, high runoff and high levels of anthropogenic activity, while the exact locations and time scales of groundwater and surface water flows may be different.
As a source of 'new' nutrients, especially nitrogen (less P), freshwater SGD is potentially important for coastal nutrient cycling at the global scale, given the N-limitation of most coastal waters, and shows a strong response to human impact.

We emphasize the need to carry out field studies in (sub-) tropical areas of Africa, South America and South-East Asia. Recent publications show that efforts are now being made to study nutrient fluxes at sites where seawater recycling is relatively minor (e.g. Hawaii, Ubatuba Bay in Brazil – Special Issue of Estuarine, Coastal and Shelf Science, and others), this will facilitate actual calibration of direct SGD in the future. Further coordinated experimental and modeling efforts by biogeochemists, hydrogeologists and coastal oceanographers are needed in high 'risk' areas. Ultimately, this will allow direct groundwater inputs to be included in spatially explicit models for nutrient export to coastal waters.

REFERENCES

Bokuniewicz, H., Buddemeier, R., Maxwell, B. and C. Smith. 2003. The typological approach to submarine groundwater discharge (SGD). Biogeochemistry, 66(1-2), 145-158.

Church, T.M. 1996. An underground route for the water cycle. Nature, 380(6575), 579-580.

Howarth, R.W. and R. Marino. 2006. Nitrogen as the limiting nutrient for eutrophication in coastal marine ecosystems: Evolving views over three decades. Limnol. Oceanogr., 51(1, part 2), 362-376.

Kraaijenhof-van de Leur, D.A. 1958. A study of non-steady groundwater flow with special reference to a reservoir-coefficient. De Ingenieur 70, 87-94.

Moore, W.S. 1996. Large groundwater inputs to coastal waters revealed by Ra-226 enrichments. Nature, 380(6575), 612-614.

Seitzinger, S.P., Harrison, J.A., Dumont, E., Beusen, A.H.W. and A.F. Bouwman. 2005. Sources and delivery of carbon, nitrogen, and phosphorus to the coastal zone: an overview of Global Nutrient Export from Watersheds (NEWS) models and their application. Global Biogeochemical Cycles, 19, GB4S01, doi:10.1029/2005GB002606.

Slomp, C.P. and P. van Cappellen. 2004. Groundwater inputs of nutrients to the coastal ocean: controls and potential impact. Journal of Hydrology, 295, 64-86.

Spiteri, C., Slomp, C.P., Tuncay, K. and C. Meile. 2008. Modeling biogeochemical processes in subterranean estuaries: The effect of flow dynamics and redox conditions on submarine groundwater discharge of nutrients. Water Resources Research, 44, W02430, doi:10.1029/2007WR006071.

Van Beek, L.P.H, Dürr, H.H., Karssenberg, D., de Vries, L.M. and M. Bierkens. in preparation. Baseflow calibration in a global hydrological model. To be submitted to Water Resources Research.

Contact Information: Hans H. Dürr, Department of Physical Geography, Faculty of Geosciences, Heidelberglaan 2, P.O. box 80.115, Utrecht University, NL-3508 TC Utrecht, The Netherlands, Phone: 0031 (0)30 253 2754, Fax: 0031 (0)30 253 1145, Email: h.durr@geo.uu.nl

Dispersive Behavior of the Mixing Zone between a Shallow Freshwater Lens and Upward Seeping Saline Groundwater

S. Eeman, *A. Leijnse* and *S.E.A.T.M. van der Zee*
Department of Soil Physics, Ecohydrology and Groundwater Management, Wageningen University, The Netherlands

ABSTRACT
This study focuses on the mixing zone between thin, shallow freshwater lenses and underlying, upward seeping saline groundwater, under homogeneous isotropic conditions. The role of longitudinal and transverse dispersivities is analyzed at different phases of lens formation, increasing insight into the mixing processes. Spatial moments are used to characterize the mixing zone in time and spatially.

INTRODUCTION
Salt water intrusion and upward seepage of saline groundwater is a widespread problem in low-lying areas of coastal zones that are important for agriculture or ecologically, such as in the North and West regions of the Netherlands, Southwest Florida, and many other deltaic areas such as the Camargue in France and the Nile delta in Egypt. Where soil surface is situated below sea level, the pressure of this sea level moves saline groundwater upward into superficial water networks. On the other hand, infiltrating rainwater forms fresh water lenses. Phreatic rise is limited by the surface elevation, which in its turn limits the maximum possible depth of the fresh water lens (Ghijben Herzberg).

Changing climate and sea level rise may change the delicate balance between fresh and saline water flows. Climate change may increase drought due to reduced differences between rainfall and evapotranspiration, an increase of dry periods, and a decreased availability of irrigation water from rivers in such periods (Beersma *et al.*, 2004). Sea level rise also directly increases the driving force of the seepage flux of saline groundwater up to tens of kilometers from the coast (Oude Essink, 2001). Change in this balance between fresh and saline water fluxes may influence the availability of fresh water in the root zone. Hence, the thickness of both the fresh water lens and of the mixing zone is important for crop yield and natural vegetation diversity.

So far, studies have mainly focused on large-scale seawater intrusion. Here the transition zone is assumed negligible, as it is commonly relatively thin compared to the lens thickness (Oude Essink, 2001). This assumption is valid for cases with either a small dispersion to convection ratio or a large seepage factor (flux to conductivity ratio) (Sakr, 1999). For small (single field) scales, neither are the case.

Our primary aim is to quantify the shape of fresh water lenses, taking into account the transition zone between fresh and saline water, which we define as the second central moment of concentration change with depth. The set of dimensionless parameters that we analyzed is valid on all scales. However, we expect our results to be most interesting on the field scale, defined as the distance between two parallel ditches or other forms of drainage such as pipe drainage. This scale is most relevant for assessing damage to crops or natural vegetation due to saline water entering the root zone.

THEORY

Physical description of the system

The situation we are interested in is a vertical cross section through a long, narrow field between 2 ditches (see Figure 1). The width of a half field, which is sufficient for symmetry-reasons, is set at 25 meters. The ground water level is high, generally around one meter below surface, which is a common situation in Dutch polders and similar areas. Dispersivities are estimated at 0.25 m (longitudinal) and 0.025 m (transverse). In the given system, the development of rainwater lenses on saline groundwater is influenced by different factors, such as water fluxes and properties, soil properties and geometry. The upper boundary is a flux boundary, where net precipitation causes infiltrating fresh water. The side boundaries are no-flow boundaries, both are hydrological divides. The lower boundary is a flux boundary where saline groundwater seeps upward into the system, caused by the position of the field below sea level.

Numerical modeling approach

We used SUTRA for our numerical modeling (Voss and Provost, 2003*)*, which is a physically based numerical code, that is able to model density dependent saturated and unsaturated flow in two or three dimensions. It solves the classical equations for flow and transport. The model has been verified for density dependent flow situations. We chose our time steps and mesh density such that numerical dispersion remained smaller then mechanical dispersion.

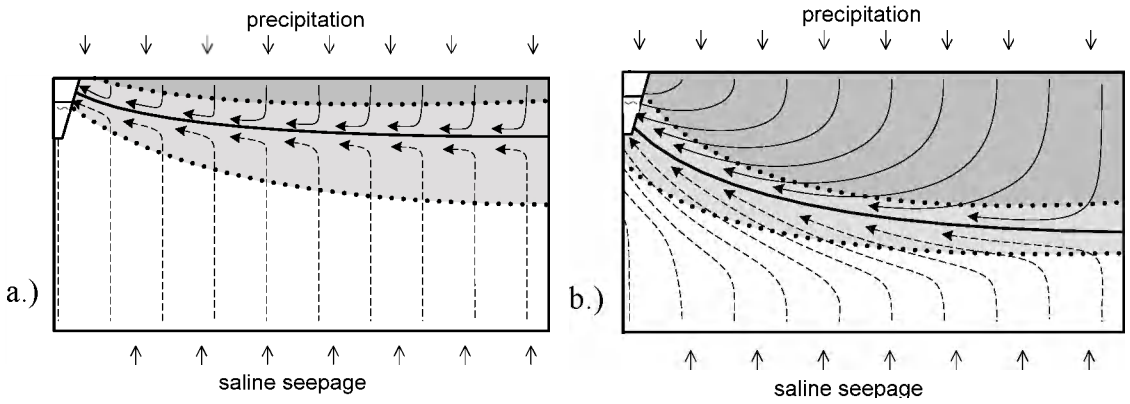

Figure 1. Flow lines of infiltrating fresh water (grey) and upward seeping saline water (white), from the ditch to the middle of a field. a.) during initial lens formation and b.) at steady state (right). Solid lines: imaginary sharp interface. Dotted lines: observed mixing zone

RESULTS

Dispersive behavior

Together with molecular diffusion, which is assumed to be of minor importance, dispersivity is the main parameter determining the width and development of the mixing zone. Therefore, we investigated the effect of dispersion on the development of the mixing zone. To quantify these processes, we defined the interface as the line that connects the vertical first moments of concentration change. From the numerical results, we determined the velocity components in parallel and perpendicular directions with respect to the interface.

Using the dispersion-velocity relations as formulated by (Bear, 1979) we determined the relative contributions of longitudinal and transverse dispersion to the total dispersion flux perpendicular to the interface. These relative contributions are given by

$$\frac{\alpha_l v_t^2}{\alpha_l v_t^2 + \alpha_t v_l^2} \quad \text{(longitudinal contribution)} \qquad (1)$$

$$\frac{\alpha_t v_l^2}{\alpha_l v_t^2 + \alpha_t v_l^2} \quad \text{(transverse contribution)} \qquad (2)$$

Here v_l, v_t, α_l and α_t are the longitudinal and transverse components of the velocity and dispersivity, respectively. The contribution of longitudinal and transverse dispersion to mixing was determined for a fresh water lens that develops in an initially saline domain. Longitudinal dispersivity was assumed to be an order of magnitude larger than transverse dispersivity. The relative contributions of longitudinal and transverse dispersion are shown while the lens develops, and at steady state conditions in Figure 2.

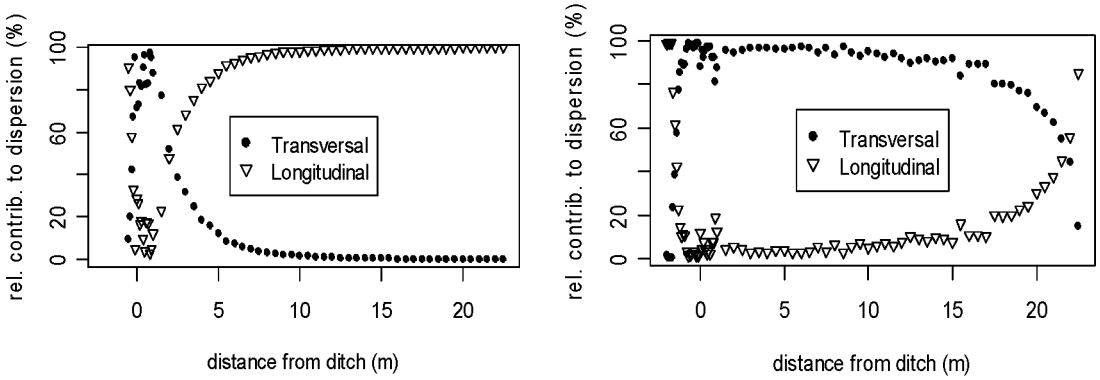

Figure 2: dispersion during lens development (after 1 year; left) and at steady state (right).

Close to the hydrological divide in the middle of the field, dispersivity is highly influenced by boundary effects. Transverse dispersion is always dominant near the ditch boundary, due to the high, velocities, which are nearly parallel to the mixing zone. The curvature in the mixing zone in this area complicates determination of parallel and perpendicular velocity in this zone: in equations (1) and (2), longitudinal ad transverse velocity components are needed. These components (respectively parallel and perpendicular to the interface) can only be calculated well if the interface is almost horizontal, due to the rectangular grid. Near the ditch the interface is significantly tilted and the different velocity components are not well estimated.

Disregarding the boundary regions, near the ditch and near the water divide, we observed that longitudinal dispersion is significant during lens development (Figure 2), and increases towards the centre of the field. When the lens has reached its steady state shape, the influence of longitudinal dispersion disappears almost entirely (Figure 2). The mixing zone now shifted towards an equilibrium situation, more or less parallel to the flow direction (Figure 1). The dominance of longitudinal dispersion during lens development leads to a significantly larger mixing zone at this stage, due to the larger value of longitudinal dispersivity.

DISCUSSION AND CONCLUSIONS

The phase of lens formation determines the importance of longitudinal and transverse dispersion, respectively. This observation can be understood from the different flow directions and velocities of the precipitation and seepage fluxes in different phases.

Since the dynamics of lens formation for small and large scale situations are characterized by different characteristic times, also the importance of longitudinal and transverse dispersion may be expected to be scale dependent.

REFERENCES

Bear, J. 1979. Hydraulics of Groundwater, McGraw-Hill, New York.

Beersma, J.J., A.T. Buishand, H. Buiteveld. 2004. Droog, droger,droogst. (in Dutch) KNMI199-II, De Bilt.

Oude Essink, G.H.P. 2001. Salt water intrusion in a three-dimensional groundwater system in the Netherlands: a numerical study. Transport in Porous Media 43, 137-158.

Sakr, S.A. 1999. Validity of a sharp-interface model in a confined coastal aquifer. Hydrogeology Journal 7, 155-160.

Voss, C.I., A.M. Provost. 2003. SUTRA, a model for saturated-unsaturated variable-density groundwater flow with solute or energy transport. USGS, Manual No. 02-4231, Reston, Virginia.

Contact Information: Sara Eeman, Wageningen University, Center for water and Climate. Droevendaalsesteeg 4, P.O. Box 47, 6700AA Wageningen, The Netherlands, Phone: (+31) (0)317 48 2532, Email: sara.eeman@wur.nl

Groundwater Quality Monitoring on Northeast Yucatan Peninsula, Mexico

Oscar Frausto[1], *Lars Mattes*[2], *Thomas J. Ihl*[3] , *Adrian Cervantes*[1] and *Steffen Giese*[4]
[1]Sustainable Development Division, University of Quintana Roo, Mexico
[2]Geohidrology Department, Technical University of Berlin, Germany
[3]Urban Observatory of the Riviera Maya, University of Quintana Roo, Mexico
[4]Environmental and Geology Secretary of Thüringen, Germany

ABSTRACT
The aims of the study are to determine groundwater flow direction, to detect ground and surface water quality and to identify contaminations in the aquifer of the Northeast Yucatan Peninsula, Mexico. As a synthesis of this investigation potential zones for drinking water supply in future have to be determined.

INTRODUCTION
The easterly part of the Yucatan Peninsula is formed a by Tertiary - Pleistocene limestone plain that is underlying by porous and fissured limestone. Along the coastline Pleistocene reef limestone are exposed in quarries from the Northern Cape to Tulum. An important geomorphologic characteristic at the westerly border of the investigation area is the Holbox Fracture System. It consists of a series of fractures running NNE-SSW from Cabo Catoche to Playa del Carmen. The length of the system is about 100 km and about 50 km wide running parallel to the coast.

The karstic aquifer is unconfined where a fresh water lens floats above denser saline water. The aquifer transmissivity is very high combined with a very low hydraulic gradient ranging from 7-10 mm/km through most of the northern part of the peninsula (Marin, 1990; Gonzalez-Herrera *et al.*, 2002). Beddows *et al.* (2007) determined the hydraulic gradient in the range of $5 - 10 \times 10^{-5}$ in the centre of Yucatan peninsula and along the Caribbean coast and Gonzalez-Herrera (1984) reported the porosity in the range of 7 – 41 %. The average porosity of Pleistocene deposits along the Caribbean is determined by Harris in the range of 14 -23 % (Harris, 1984).

METHODS
The following representation of the hydrochemical results is focussed on the most important parameters for characterizing the water quality due to potential contamination sources (Fetter, 2001) in the investigation area. One of the most important impacts on ground water related to the increase of salinity is seawater. Electrical conductance of seawater at the Mexican Caribbean coast is represented by a value greater than 54,400 µS/cm (Matthes *et al.*, 2006, Wurl & Giese, 2005).

Physicochemical parameters
The dominant ions of seawater and of freshwater affected by seawater are chloride and sodium. The values of EC range between 102 - 53,300 µS/cm. The highest value is detected in Cenote Chemuyil in a depth of 29 m and is close to seawater conductance. Increased values of 10,000 - 30,000 µS/cm were detected on the island Isla Mujeres and in a sinkhole in Cancun. Groundwater samples with EC values up to 5000 µS/cm are located nearby the coastline in the southerly part of Solidaridad The bulk of ground and surface water, like e.g. samples of the capture zones for drinking water supply of Cancun and Playa del Carmen, shows EC values in the range of 1,000 - 1,500 µS/cm .

The concentration of nitrate shows a range from not detectable to 111 mg/l. The amount of samples represents values less than 5 mg/l. These very low concentrations are dominant in the capture zones of Playa del Carmen and Cancun. Increased values were found in the urban areas of Cancun, Playa del Carmen, Tulum and Cobá.

Ammonia concentrations range from not detectable to 72 mg/l. Very high ammonia concentrations ranging between 30 to 72 mg/l were detected in the Cenote Chemuyil and in Tulum.

Iron and manganese were analyzed in very low concentrations. The range of concentrations of iron is 0.018 – 0.736 mg/l and of manganese 0.001 – 0.185 mg/l. The dominant concentration of iron is in the range of 0.08 – 0.16 mg/l and of manganese less than 0.04 mg/l.

PH was measured in the range of 6.8 – 9. The bulk of samples shows a pH value in the range of 7 – 7.5 that is due to the buffer of limestone. Zinc was measured in 47 samples in the range from not detectable to 0.130 mg/l. Twelve samples show values above the detectable value of 0.001 mg/l.

Groundwater flow direction

Groundwater levels related to ground surface were measured during the field campaign between March 2007 and September 2007. Contour lines of equal groundwater levels were constructed by the use of groundwater elevation. The calculation of groundwater levels in the northerly part of Isla Mujeres was done by the assumption that groundwater levels at the coastline are equal to the sea level. The highest water level of more than 3 m above the mean sea level was found in the westerly part of Solidaridad. The general flow direction is from west - east directed to the coastline. A variation of this direction is identified in the area northwesterly of Cancun, where the flow direction turns to north showing a parallel orientation to the coastline. Along the coast between Tulum and Playa del Carmen the water level of 1 m contour line was detected near to the coast indicating a high gradient to the sea. Northerly of Playa del Carmen the 1 m contour line tends more in direction to the inland.

Contaminations and sources of pollution

The groundwater in the investigation area is high vulnerable caused by structural fractures and high solubility of the limestone aquifer represented by caves and conduit systems with high hydraulic conductivity (INEGI 2005). Because of the absence of rivers the runoff of surface water will infiltrate rapidly into the aquifer along sinkholes, fissures and fractures. Hence, contaminated surface runoff from urban area represents an extremely hazard of groundwater contamination. Typical urban sources of pollution are leakages from landfills (industrial and household waste) producing an impact of organic material. By the lowering of pH and redoxpotential heavy metals become mobile and will be dissolved and transported in groundwater. Gas stations and scrap yards are locations for potential oil, grease and gas pollution.

Water quality related to Mexican drinking water supply standard

The assessment of water quality is evaluated by the comparison of the collected samples to the Mexican drinking water standard (Tab. 1).

Potential areas of inundation and seawater intrusion

The northern part of Yucatan peninsula is plain and shallow related to the distance of surface to groundwater. It contains solution depressions locally known as sabanas (Ihl, et al. 2007). This geomorphologic setting is due to temporary floods represented by polje-like depressions that seasonally filled with water creating swamps. Along the coastline a stripe of increased electrical conductance was detected, representing the influence of seawater. It was discussed before that the thickness of the freshwater lens will grow related to increasing distance to the coastline. Hence, the locations of potential wellfields in future should be located far away from the coastline.

Table 1. Percentages of exceeding values of dominant Mexican drinking water standards

Dominant Parameters of exceeding values of Mexican drinking water standard	Samples [%]
TDS	23 %
Cl	19 %
NO3-N	16 %
NH3-N	73 %
SO4	3 %
Total hardness	23 %
Na	22 %

DISCUSSION AND CONCLUSIONS

In the inland at the westerly border of the investigation area the results show low salinity at shallow water depth represented by electrical conductance (EC) of 102 µS/cm. Increasing salinity with a maximum EC value of about 4900 µS/cm was found at shallow water depth near to the coastline building up a sequence of stripes parallel to the coastline. The comparison of EC to chloride and sodium concentration shows that the increase of salinity is due to the rise of the fresh-saltwater interface at the shoreline following the general build up of a freshwater lens that is floating on denser saline groundwater.

The comparison of the chemical results to the Mexican standard of drinking water shows exceeding values of total dissolved solids (TDS), chloride and sodium. Ammonia concentrations exceeding the Mexican standard of drinking water were found in 137 samples showing a widespread distribution.

Anthropogenic sources of nitrogen compounds were established by the distribution of maximum concentrations of nitrate combined with very low oxygen contents in shallow water depth. A second source of ammonia impact to groundwater was identified at the urban waste disposal site in Cancun, where increased ammonia concentrations were identified in direct vicinity to the landfill site indicating most likely a leakage. Another source of pollution was identified in the urban area of Cancun by the detection of gasoline. An oil film combined with the smell of gasoline was found in a household well in the quarter Bonfil. The location of the contamination source could not be detected. In the investigation area the general groundwater flow is determined to the east in direction to the coastline. A variation of this direction is identified in the district Isla Mujeres, where the flow direction tends to north.

ACKNOWLEDGMENTS

This study is funded by the FOMIX CONACYT-QROO, Project *"Estudio geohidrológico y evaluación de fuentes contaminantes del acuífero Norte de Quintana Roo, México"*, clave: QROO-2005-C01-19177.

REFERENCES

Beddows, P., Smart, P.L. Whitaker, F.F. & Smith, S. 2007: Decoupled fresh-sanline groundwater circulation of a coastal carbonate aquifer: Spatial patterns of temperature and specific electrical conductance.- Journal of Hydrology 345, 18-32, Springer, New Cork.

Fetter, C.W., 2001: Applied hydrogeology.- 691 p., 5th Ed., MacMillan publishing house, New York.

Gonzales-Herrera, R. A., 1984: Correlación de muestras de roca en pozos de la ciudad de Merida.- Civil Engineering Thesis, Universidad Autónoma de Yucatán, 129 p., Mérida, México.

Gonzales-Herrera, R. & Sanchez-Y-Pinto, I, Gamboa-Vargas, J., 2002: Groundwater-flow modeling in the Yucatan karstic aquifer, Mexico.- Hydrogeology Journal 10: 539-552, Springer, New York.

Harris, N.J., 1994: Diagenesis of upper pleistocene strandplain limestones, northeastern Yucatan Peninsula, Mexico. - MSc Thesis, 133 p. Universtiy of New Orleans, USA.

Ihl, T., Frausto, O., Rojas, J., Giese, S., Goldacker, S., Bautista, F., & Bocco, G. (2007): Identification of geodisasters in the state of Yucatan, Mexico. N. Jb. Geol. Palanont. Abh. 2007, vol. 246/3, p. 299-311, Stuttgart.

INEGI, 2005: Estudio Hidrologico del Estado de Quintana Roo.- 79 p., Gobierno del Estado de Quintana Roo, Mexico.

Marin, L.E., 1990: Field investigations and numerical simulation of groundwater flow in the karstic aquifer of Northwestern Yucatan, Mexico.- PhD. Thesis, Northern Illinois University, 183 p, DeKalb, USA.

Matthes, L., Tröger, U. & Frausto, O., 2006: Dynamik der Salz-Süßwasser-Grenzschicht durch Übernutzung des Grundwasserleiters von Cozumel, Mexiko.- in: Inidikatoren im Grundwasser, Conference of Hydrogeology Section, SDGG 2006, Vol.43, p.92, DGG, Hannover, Germany.

Wurl, S. & Giese, S., 2005. Ground Water Quality Research on Cozumel island, State of Quintana Roo, México. In. Frausto, O. (ed.). Desarrollo Sustentable: turismo, costas y educación. Universidad de Quintana Roo. México. Pp. 171 – 176.

Contact Information: Oscar Frausto, University of Quintana Roo / Sustainable Development Division, Hans-Berger Str. 13, Jena, 07477 Germany, Phone: 03641332642, Fax: 052(987)8729112, Email: ofrausto@uqroo.mx

Management of the Iao and Waihee Aquifer Areas with the Aid of a 3-D Numerical SUTRA Model, Maui, Hawaii

Stephen B. Gingerich
U.S. Geological Survey, Pacific Islands Water Science Center, Honolulu, Hawaii, USA

ABSTRACT

A ground-water flow model of central and west Maui, including the heavily utilized Iao and Waihee aquifers in central Maui, has been developed using the US Geological Survey's recently enhanced three-dimensional solute transport (3-D SUTRA) computer code. The code is capable of simulating variable-density ground-water flow and solute transport in heterogeneous, anisotropic aquifers. The ground-water model for Maui simulates freshwater and the underlying brackish-water transition zone and incorporates hydrogeologic features such as valley-fill barriers and the sediments that form a caprock and a barrier between the lavas of West Maui and Haleakala Volcanoes (figure 1). New estimates of recharge during 1926–2004, historical distributions of monthly pumpage, and the position of mean sea level at monthly intervals were used as input to the model.

The resulting freshwater-lens size and position were simulated for the period 1926–2006. Estimated recharge for central and west Maui declined 44 percent between 1979 and 2004 because of decreased agricultural land use, more efficient irrigation, and recent periods of low rainfall. In some parts of the Iao and Waihee areas, simulations show that water levels declined as much as 20 feet and the transition zone moved upward about 200 feet, as withdrawal from these areas began in 1948 and increased to as much as 22 million gallons per day by 2006. These results matched historic water-level and salinity data for these areas. Figure 2 shows the simulated water-table contours in 2006, at the end of the simulation period.

The ground-water flow model is useful as a tool to forecast the effects of future ground-water withdrawal and changes in recharge distributions. The relative benefits of redistributing ground-water withdrawal using existing infrastructure or adding more wells to spread pumping out are compared using different model scenarios. The effects of changes in recharge caused by drought conditions, changing land use, or increased streamflow above the aquifers are also simulated. The results of these scenarios are available to water-system managers so that they can most effectively manage the ground-water resource.

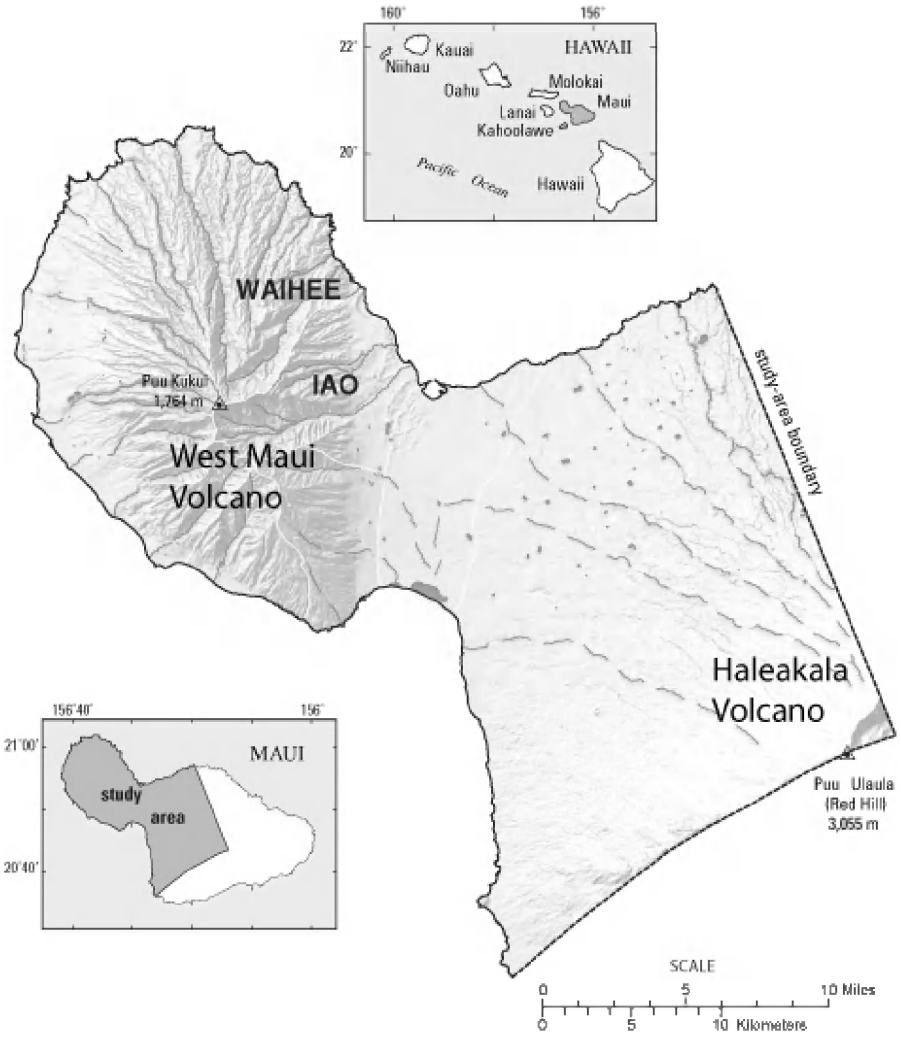

Figure 1. Study area and location of Iao and Waihee aquifer areas, Maui Hawaii, USA.

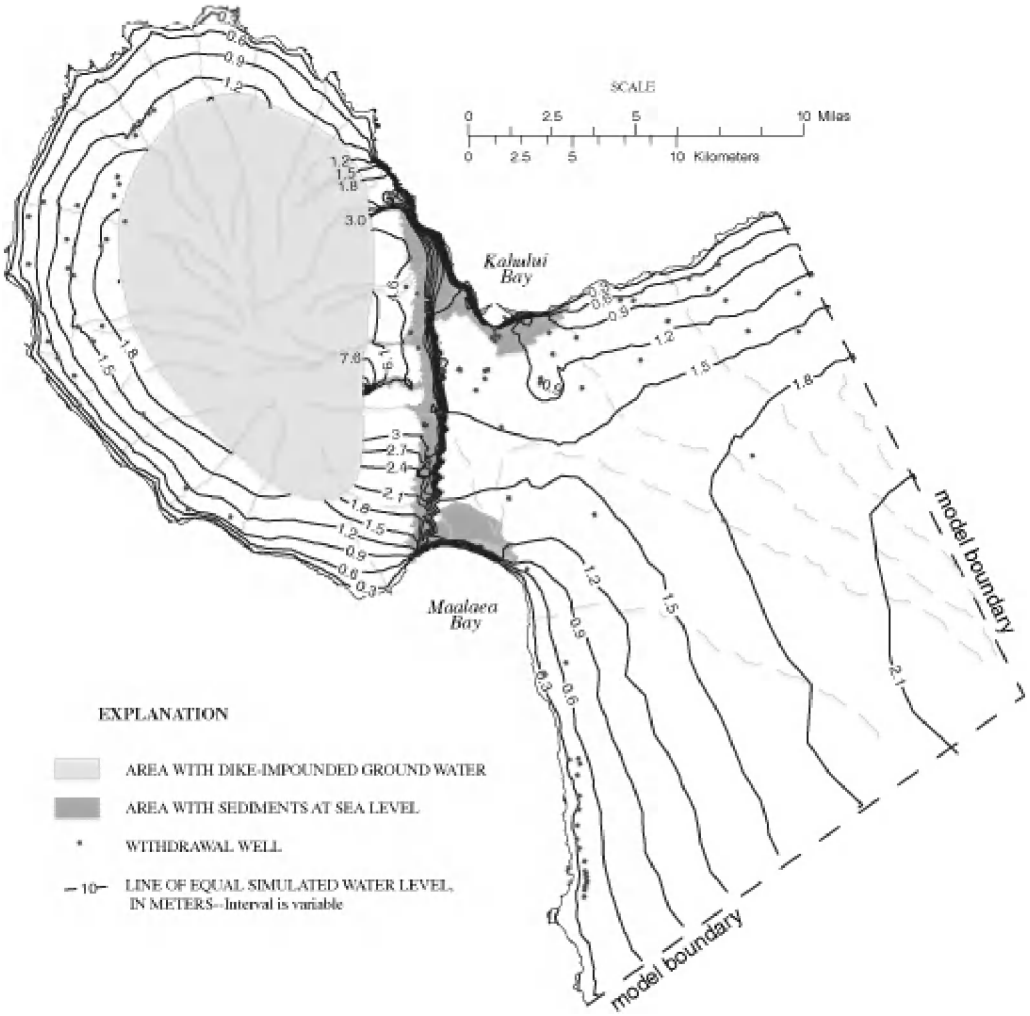

Figure 2. Simulated water-table contours in 2005, Maui Hawaii, USA.

Contact Information: Stephen B. Gingerich, U.S. Geological Survey, Pacific Islands Water Science Center, 677 Ala Moana Blvd., #415, Honolulu, Hawaii, 96813, USA, Phone: 808-587-2411, Fax: 808-587-2401, Email: sbginger@usgs.gov

Use of Image Analysis to Develop New Benchmarking Datasets for Variable Density Flow Scenarios

R. R. Goswami[1,2] and *T. P. Clement*[1]
[1]Department of Civil Engineering, Auburn University, Auburn, AL, USA
[2]Geosyntec Consultants, Boca Raton, FL, USA

ABSTRACT
Image analysis (IA) techniques are used to measure properties such as concentration and water content in porous media experiments. Measurements made by IA techniques provide extensive spatial information on a temporal scale. However, a robust analysis of the accuracy of IA techniques has not been presented in previous publications. Therefore, results from experiments using IA techniques are not widely accepted as benchmarking datasets. The conventional method for testing the accuracy of IA techniques is the computation of global mass balance error. We demonstrate the limitations of quantifying IA errors based on this conventional method. We also introduce an alternate statistics-based method for estimating errors. The entire discussion is presented using a theoretical test problem. We also present the results of a physical laboratory experiment processed using the IA technique. The dataset is from a sinking plume experiment simulated by injecting saltwater into a freshwater aquifer. The experimental results are also compared with numerical modeling results generated using SEAWAT.

INTRODUCTION
Experimental studies have been conducted by using both qualitative (Goswami and Clement 2007) and quantitative (MRI, Gamma-radiation) methods to analyze porous media systems. One of the rapidly evolving non-invasive quantitative techniques is image analysis (IA). IA records an optical image property (such as pixel intensity, hue, color, etc.) and relates it to a system property such as concentration or water content. All IA techniques have the following two major parts: (i) acquiring and processing the digital images, and (ii) selecting a calibration-relationship between the intended system property and the image property (e.g., concentration-intensity relationship). A variety of errors may be introduced while acquiring and processing digital images. The most common source of error is non-uniform lighting. There may also be errors in image acquisition and processing due to hardware and software problems (Hansen et al. 2006). Since the calibration-relationship is not known, selection of the best-fit function for correlating the image property with the system property would also involve errors. We propose to categorize all possible errors into the following two categories:

1. Calibration-Relationship Error (CRE): error in the approximate calibration-relationship
2. Experimental Error (EE): error in the image property (e.g., intensity) due to various experimental factors such as non-uniform lighting, hardware problems, etc.

In the published literature, researchers have primarily used comparison of global mass balance errors and dispersion coefficients to test the accuracy of the results. Calculation of mass balance requires use of the entire range of measured values; therefore, they cannot be used to quantify local errors.

The main body of this paper is organized into three major sections. In the first section, we generate a theoretical test problem and use it to demonstrate the limitations of the commonly used mass-balance method to measure errors. In the second section, a statistics-based error

estimation method is proposed. In the third section, we provide and compare results from our physical experiment and the application of IA technique and numerical modeling.

THEORETICAL TEST PROBLEM

The theoretical test problem was generated by considering diffusion of a point source in a two-dimensional domain. The following analytical solution was used to simulate the concentration profiles (Fischer et al. 1979):

$$C(x,z) = \frac{M}{4\pi t\sqrt{D_x D_z}} \exp\left(-\frac{x^2}{4D_x t} - \frac{z^2}{4D_z t}\right) \quad (1)$$

where $C(x,z)$ is the concentration at a given point (x,z) in the domain, t is the time from the start of the point-injection, M is the mass injected in the domain, and D_x and D_z are the diffusion coefficients in x and z directions respectively. The predicted plume concentration distribution is given in Figure 1. The analytical concentrations obtained were converted into pixel intensity values using the following concentration-intensity relationship:

$$I_i = A\left(1 - \exp\left(-BC_i\right)\right) \quad (2)$$

where I_i is the pixel intensity corresponding to a given concentration value C_i, The values of parameters A and B were selected based on empirical criterion (Goswami et al. 2008).

Introducing Experimental Error

Experimental error (EE) is associated with randomly distributed errors in the acquired image property which can be simulated by using the MATLAB® function *randn* (Hansen et al. 2006). The simulated noise was added to the intensity profile corresponding to the theoretical concentration data, thereby generating a '*noisy intensity*' profile. We then used the true concentration-intensity relationship (Equation 2) to estimate concentrations that will have some experimental error (EE). The concentrations obtained from this noisy dataset will be identified as $C_{estimate,\,EE}$.

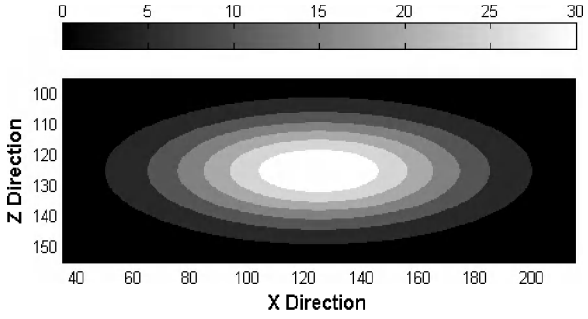

Figure 1. Concentration contours for the true solution (theoretical problem)

Limitations of Using Mass Balance Method

The estimated concentration dataset obtained after introducing experimental errors ($C_{estimate,EE}$) was processed to calculate the values of mass balance error. The total mass, calculated by determining the zeroth spatial moment of the concentration distribution, was found to be very low (<1%). As is commonly done in literature, we assumed the percentage error in mass balance as a quantitative estimate of error in the computed concentration values. Values of two concentration contours [5 mg/l (low) and 20 mg/l (high)] obtained from $C_{estimate,EE}$ were compared with the C_{true} values (obtained using Equation 1). The mass balance error was used to compute the error bounds using the relationship:

$$C_{error\,bound} = C_{true}\left(1 \pm \%\,Mass\ Balance\ Error \times C_{true}\right) \quad (3)$$

Figure 2a presents the 5 mg/L and 20 mg/L concentration contours obtained from the noisy dataset. It can be seen that the $C_{estimate,EE}$ values have speckle-type noise distributed around C_{true} values. The figure also has error bounds estimated using Equation 3. Since the error bounds do not predict the true contours, it can be deduced that mass balance error is not a good indicator of

error in $C_{estimate,EE}$. We also employed a trial-and-error approach to generate two contours that will bound the observed spread around the predicted 5 mg/L and 20 mg/L contours. We estimated that a value of ±10% error will bound the 20 mg/l contour (22 mg/l and 18 mg/l) and ±15% error will bound the 5 mg/l contour (4.25 mg/l and 5.75 mg/l). These 'trial and error' bounds are shown in Figure 2b along with $C_{estimate, EE}$ and C_{true}. It can be observed that these trial-and-error contours closely bound C_{true}. Therefore it can be concluded that the error associated with 5 mg/L and 20 mg/L contours are approximately ±15% and ±10%, respectively. These values are considerably higher than the mass balance error, which was less than 1%. These results indicate that the mass-balance method fails to predict the local errors associated with a contour level.

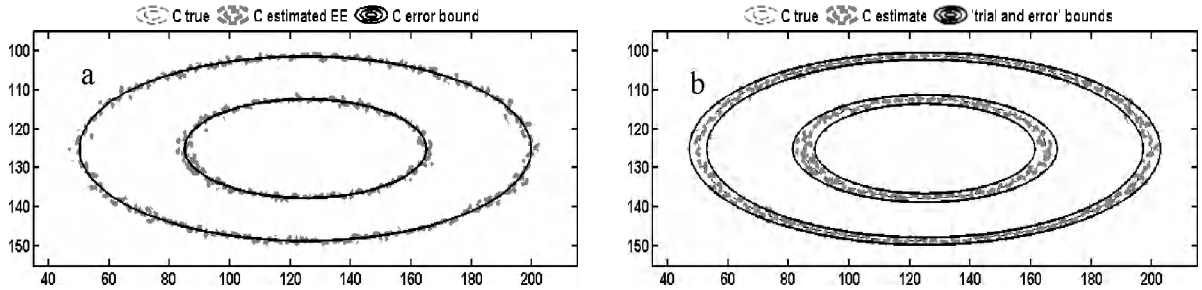

Figure 2. 5 g/l and 20 g/l contours for C_{true} and $C_{estimate, EE}$. 2a shows the $C_{estimate, EE}$ and C_{true} with corresponding mass balance error bound and 2b presents $C_{estimate, EE}$ with 'trial and error' bounds of 10% and 15% for 20 mg/l and 5 mg/l contours, respectively

STATISTICS BASED ERROR ESTIMATION METHOD

Typical IA datasets involve a large number of measurements. Therefore, standard statistical methods can be used to quantify error (Taylor 1997). The two errors listed earlier in the paper can be calculated as follows:

1) *Calibration-Relationship Error (CRE)*

$$\sigma_{c,relationship} = \sqrt{\frac{\sum_{i=1}^{N} \left(C_{i,measured} - C_{i,estimated}\right)^2}{df}} \qquad (4)$$

where $\sigma_{c,relationship}$ is an estimate for CRE computed directly from regression statistics, N is the number of measurements in the calibration dataset, p is the number of parameters used in the relationship, df is the degrees of freedom of the relationship given by N-p;

2) *Experimental Error (EE)*

$$\sigma_{c,experiment} = \left|\frac{dC}{dI}\sigma_I\right| \qquad (5)$$

where $\sigma_{c,experiment}$ is the error in concentration due to noise in pixel intensity values (or image property), dC/dI is the slope of the concentration-intensity relationship, and σ_i is the randomly distributed error in the recorded pixel intensity field.

BENCHMARKING DATASETS

We conducted a variable-density experiment by injecting a saltwater pulse source into a freshwater aquifer under ambient flow conditions. Detailed information about the methodology and the experiment are available in Goswami et al. (2008). Figure 3a shows the dense-plume pictorial dataset obtained from the experiment. The IA technique we developed was used to extract concentration values from the pictorial dataset and the results are shown in Figure 3b.

Numerical modeling of the experiment was completed using SEAWAT (Langevin and Guo 2006) and the modeled contours are shown in Figure 3c. Comparing Figures 3a, b and c, we can conclude that the IA technique and the numerical results are in good agreement. Using the new statistics-based error estimation technique, we calculated the percentage errors in the concentration values measured by the IA technique. We found approximately 15% error in the concentration values determined by the IA technique.

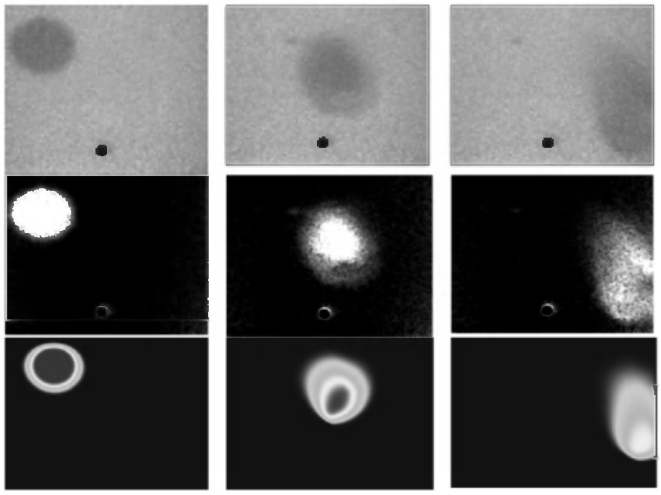

Figure 3. (top) digital images from the experiment, (center) concentrations from the IA technique, (bottom) concentrations from numerical model (SEAWAT)

CONCLUSIONS

This study demonstrates the inability of global mass balance errors to estimate local errors in IA concentration measurements. A new statistics-based approach was proposed to evaluate errors in IA techniques. The new error estimation method was used to quantify IA estimation errors in a sinking plume experiment. The error was found to be approximately 15%.

This study is not intended to represent the state-of-the-art in the application of IA, but to provide a simple method to calculate errors inherent in the application of an IA technique.

REFERENCES

Fischer, H.B., E.J. List, R.C.Y. Koh, J. Imberger, and N.H. Brooks. 1979. Mixing in inland and coastal waters Academic Press, Inc.

Goswami R. R., T. P. Clement. 2007. Laboratory-scale investigation of saltwater intrusion dynamics. Water Resources Research 43, doi:10.1029/2006WR005151.

Goswami R. R., B. Ambale, and T. P. Clement. 2008. Error estimation of concentration measurements obtained from image analysis, under review

Hansen, P.C., J.G. Nagy, and D.P. O'Leary. 2006. Deblurring Images: Matrices, Spectra and Filtering. Society for Industrial and Applied Mathematics.

Langevin, C.D. and W.X. Guo. 2006. MODFLOW/MT3DMS-based simulation of variable-density ground water flow and transport. Ground Water 44: 339-351

Taylor, J.R. 1997. An introduction to error analysis. Second Edition. University Science Books.

Contact Information: Rohit R. Goswami, Geosyntec Consultants, 5901 Broken Sound Pkwy NW, Suite 300, Boca Raton, FL 33487; Phone:561-995-0900, Email:rgoswami@geosyntec.com

Feasibility Study for Raw Water Supply to a Proposed Reverse Osmosis Plant on New Providence Island, Bahamas

Weixing Guo, *Wm. Scott Manahan* and *Thomas M. Missimer*
Missimer Groundwater Science, A Schlumberger Company, Fort Myers, FL, USA

ABSTRACT
A hydrogeological investigation was conducted to study the feasibility of raw water supply to a proposed reverse osmosis (RO) plant on New Providence Island, Bahamas. The study included field investigation and development of a SEAWAT model. After calibration, the model was used to evaluate the long-term water quality changes due to different withdrawal scenarios. Both wellfield and lake withdrawals were considered. The results indicate the raw water total dissolved solids (TDS) concentration would increase quickly due to vertical migration of salt from below. There is no significant difference to the simulated water quality changes between well or lake withdrawals.

INTRODUCTION
Reverse osmosis (RO) water treatment facilities in the Bahamas typically use wells tapping seawater as the raw water supply. To reduce treatment costs for a site on New Providence Island, a hydrogeological investigation was conducted on a man-made lake containing brackish water and on the surrounding shallow groundwater system. The investigation included test drilling, aquifer testing, water sampling and analysis, and groundwater modeling. A 3-D SEAWAT model was developed. The model was calibrated and used to evaluate various scenarios of withdrawals from wells and a man-made lake as an alternate source of raw water.

SITE HYDROGEOLOGY AND FIELD INVESTIGATION
The project site is located at the western portion of New Providence Island (Figure 1). Five boreholes were drilled to depths up to 30 m below land surface near the 0.05 km^2 man-made lake to obtain groundwater quality data and for hydraulic testing purposes. Field data indicate that the Lucayan Formation of Pleistocene age underlies a thin veneer of sandy soil at the site. The upper 5 m of sediments consists primarily of white to light gray limestone. The limestone from 5 to 10 m is harder, more porous, and more permeable than the shallower unit. The limestone from 10 to 30 m is hard, well indurated, and generally, has a high apparent porosity and permeability. However, dense limestone layers with low apparent porosity and permeability are also present and provide a degree of separation between the zones with high permeability.

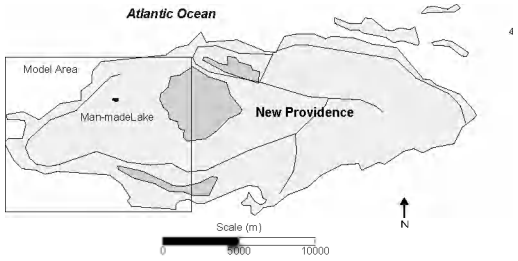

Figure 1. Location of Study Area

The lake was reportedly excavated between 1994 and 1997. The depth of the lake varies from approximately 3 to 5 m and averages about 4 m. Water quality within the lake is relatively uniform. The average dissolved chloride and TDS concentrations of two samples obtained from the lake during January 2007 were 2,040 mg/l and 4,150 mg/l, respectively. Wells with depths of greater than 30 m on the island are known to produce water with TDS concentrations of approximately 34,000 mg/l or greater (seawater quality). Less saline groundwater exists at shallower depths. In the site area, the shallow groundwater was density-stratified with TDS values ranging from less than 1,000 mg/l near the land surface to about 30,000 mg/l at a depth of 30 m. Slug tests and constant rate pump tests were conducted at various depth intervals. The hydraulic conductivity calculated from these tests ranged from 3.54 to 597 m/day. The ratio of horizontal to vertical hydraulic conductivity was estimated to vary from 10:1 to 100:1.

DEVELOPMENT OF SEAWAT MODEL

SEAWAT is a computer program that couples two popular groundwater modeling codes MODFLOW (McDonald and Harbaugh, 1988) and MT3DMS (Zheng and Wang, 1998) for simulation of flow with variable density (Guo and Langevin, 2002). For this project, SEAWAT-2000 (Langevin et al., 2004) was used. Only a portion of the island was modeled. The model consisted of 110 rows and 160 columns with a uniform grid spacing of 80 m. The model had eight flat layers. Information on these layers including the layer thickness and hydraulic parameters, is shown in Table 1. A constant head (zero m) and concentration boundary (35,000 mg/l) was specified along the coastline in the model in all layers. Along the northern and eastern edges of the model, constant concentration boundaries were specified to simulate the potential mass flux entering the model through dispersion. The values specified for these constant concentration boundaries were consistent with the values of initial concentrations for each layer (Table 1). The inland area of layer 8 was specified as a constant concentration with a value of 32,000 mg/l based on measured data. No-flow boundary conditions were specified along the northern and eastern edges of the model in layers 1 through 7 since they are located approximately along the hydrologic divides on the island.

Table 1: Model Layers and Hydraulic Parameters

Layer	Thickness (m)	Initial TDS (mg/l)	Kh (m/day)	Sy
1	3.66	2300	3.66	0.1
2	0.91	2300	3.66	0.1
3	1.52	2650	0.61	0.2
4	1.52	2800	60.96	0.2
5	1.52	2800	152.40	0.25
6	10.67	8000	152.40	0.25
7	6.10	15000	304.80	0.3
8	4.57	32000	304.80	0.3

The model was calibrated to the TDS concentration of the lake. The current TDS concentration in the lake is approximately 4,150 mg/l. It was assumed that the aquifer has the same water quality as it was 10 years ago, and the initial TDS concentration in the lake was the same as the surrounding aquifer, 2,300 mg/l, when the lake was excavated. It was also assumed that the salt in the lake was only coming from the surrounding aquifer and that increases in salinity were due to evaporative concentration of solutes in the lake.

Net recharge was applied to the inland area in the model. For the lake, it was assumed that the lake loses water by net evaporation. A series of model simulations were made using different combinations of recharge/ET rates. Figure 2 shows the results of model simulation with different net recharge/net evaporation rates. The results indicate 12.7 cm/yr recharge over the land area and a 12.7 cm/yr net ET rate at the lake would give the closest TDS concentration to the values actually measured in the lake.

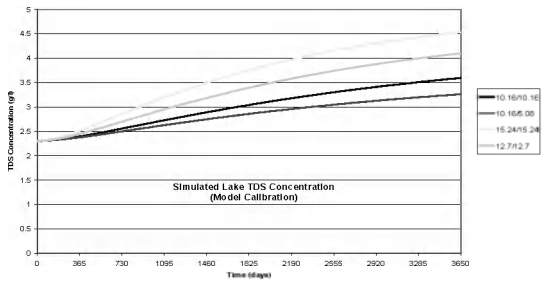

Figure 2. Model Calibration (Values are Recharge/ET Rates in cm/yr)

EVALUATION OF WITHDRAWAL SCENARIOS

A total of seven scenarios were evaluated. All of the scenarios were run for 10 years from the base conditions. Three options were evaluated: (a) withdrawals from the lake; (b) withdrawals from four wells; and (c) withdrawals from seven wells. The results of the groundwater modeling indicate that continuous raw water pumpage at a rate of 3,785 m^3/day (1.0 MGD) from the lake would result in a TDS increase from approximately 4,200 mg/l to 13,200 mg/l over a 10-year period (Figure 3). Continuous pumpage at the same rate from a series of shallow wells constructed near the lake resulted in a predicted TDS change from approximately 2,000 mg/l to 12,400 mg/l during the same stress period. The simulated increase in raw water salinity is relatively rapid with the majority of the TDS changes occurring within the first year of pumpage and then leveling off. It seems that withdrawal from wells is slightly better than lake withdrawal in terms of water quality. This is likely due to the fact that some of the wells would capture some fresher water from the up-gradient direction.

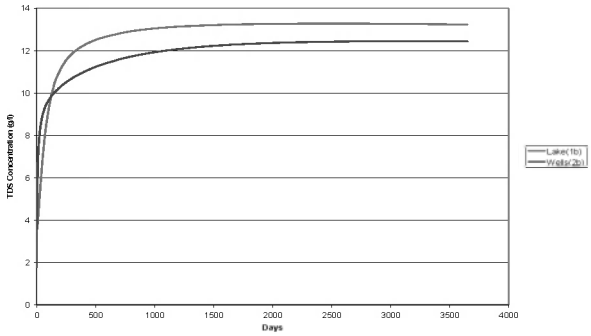

Figure 3. Simulated TDS Concentration of Raw Water

SUMMARY

A hydrogeological investigation, including field testing and modeling, was conducted for a site on New Providence Island, Bahamas to study the feasibility of raw water supply development from a man-made lake and/or wells for a proposed RO plant. Use of brackish raw water will economically allow the recovery efficiencies to be higher and cause the permeate water quality to be better than that obtained using seawater throughout the life-cycle of the plant. The brackish

source of water would produce the most energy efficient RO plant design based on the raw water available for use. Use of wells, rather than the lake water, would result in lower pre-treatment costs for the facility. Since the water will be used for irrigation, there may be some seasonal blending opportunities to further reduce the overall water production cost.

A SEAWAT model was developed as a tool to assess the water quality changes under different withdrawal scenarios. The projected 10-year brackish raw water TDS concentration between 12,400 and 13,200 mg/l is roughly one-third of normal seawater.
The predicted increase in raw water salinity is relatively rapid and then levels off. It seems that withdrawal from wells is slightly better than lake withdrawal in terms of water quality. This is likely due to the fact that the wells would capture some fresher water from the up-gradient direction.

REFERENCES

Guo, W. and C.D. Langevin. 2002. User's guide to SEAWAT: A computer program for simulation of three-dimensional variable-density ground-water flow, *U.S. Geological Survey TWRI Book 6, Chapter 7*, 79 p.

Harbaugh A.W, E.R. Banta, M.C. Hill, and M.G. McDonald. 2000. MODFLOW-2000, the U.S. Geological Survey modular ground-water model-User guide to modularization concepts and the groundwater flow process. *U.S Geological Survey Open-File Report* 00–92.

Langevin, C.D., W. B. Shoemaker, and W. Guo. 2003. MODLFOW-2000, the U. S. Geological Survey Modular Ground-water Model- Documentation of the SEAWAT-2000 Version with the Variable-Density Flow Process (VDF) and the Integrated MT3DMS Transport Process (IMT), *U.S. Geological Survey Open-File Report 03-426*, Tallahassee, Florida.43 p.

McDonald M.G., and A.W. Harbaugh. 1988. A Modular Three-Dimensional Finite-Difference Ground-Water flow Model. *U.S. Geological Survey Open-File Report* 83-875.

Zheng, C., and P.P. Wang. 1999. MT3DMS-A modular three-dimensional multispecies transport model for simulation of advection, dispersion and chemical reactions of contaminants in ground-water systems: Documentation and user's guide: U.S. Army Corps of Engineers Contract Report SERDP-99-1.

Contact Information: Weixing Guo, MGS, 1567 Hayley Lane, Suite 202, Fort Myers, FL 33907, USA.
Phone: 1-239-481-6494, Fax: 1-239-481-6393, Email: wguo1@slb.com

Efficient Calibration of Seawater Intrusion Models

Juan J. Hidalgo[1], *Jesús Carrera*[2] and *Agustín Medina*[3]

[1]Department of Geotechnical Engineering and Geosciences, School of Civil Engineering, Technical University of Catalonia, Barcelona, Spain

[2]Institute of Earth Sciences "Jaume Almera", Spanish Research Council (CSIC), Barcelona, Spain

[3]Department of Applied Mathematics III, School of Civil Engineering, Technical University of Catalonia, Barcelona, Spain

ABSTRACT

The calibration of groundwater models is a complex and time-consuming task. In seawater intrusion models the computational burden of the calibration process is increased by the high computational cost of solving the coupled non-linear equations that describe density-dependent flow and transport. The automatic calibration of seawater intrusion models with analytical evaluation of the sensitivities (variations of the state variables with respect to the parameters) is a feasible alternative to the more common parameter perturbation approach. The efficiency of this method lies in the fact that the matrices required for solving the inverse and the forward problems are equal if the Newton-Raphson method is used for solving the latter one. The extra cost of the Newton-Raphson method is compensated with a more efficient computation of the sensitivities. The computational performance of the proposed method is tested by calibrating a synthetic seawater intrusion problem and comparing the results with the ones obtained with the parameter perturbation technique. The comparison is made for variable problem dimensions such as number of nodes, matrix bandwidth and number of estimated parameters.

Contact Information: Juan J. Hidalgo, Department of Geotechnical Engineering and Geo-Sciences, Technical University of Catalonia (UPC), C/ Jordi Girona 1-3, Building D-2, 08034 Barcelona, Spain, Phone: +34 934017244; Fax: +34 934017251, Email: juan.hidalgo@upc.edu

The Role of Salt Sources in Density-Dependent Flow

Juan J. Hidalgo[1], *Jesús Carrera*[2] and *Agustín Medina*[3]

[1]Department of Geotechnical Engineering and Geosciences, School of Civil Engineering, Technical University of Catalonia, Barcelona, Spain

[2]Institute of Earth Sciences "Jaume Almera", Spanish Research Council (CSIC), Barcelona, Spain

[3]Department of Applied Mathematics III, School of Civil Engineering, Technical University of Catalonia, Barcelona, Spain

ABSTRACT

In groundwater variable density problems, the fluid can be viewed as consisting of two components: water and salt. Fluid mass balance is given by the flow equation, which, consequently, must account for both salt and water sources. However, most of the density-dependent flow simulation codes neglect the salt sources that do not come dissolved in water when establishing fluid mass balance. Here such salt sources will be called pure salt sources to distinguish them from the mixed salt and water sources and as an analogy with pure water. Pure salt sources can have their origin either in internal processes such as chemical reactions, dissolution or precipitation, or in the boundary conditions. Pure salt boundary sources occur when water flux is prescribed to be zero and either the salt flux (Neumann boundary conditions) or the concentration (Dirichlet boundary conditions) is prescribed at the boundary. Consistency between flow and transport boundary conditions is required, which is not always accomplished. In this work, pure salt sources are considered in fluid mass balance and the effects on the resulting flow regime and concentration distribution are explored. Two test cases are used to illustrate the role of pure salt sources. The first one is the saltwater bucket problem, which deals with the addition of salt to a close domain. It shows that neglecting pure salt sources in the flow equation causes heads to fall, which is physically inconsistent with an increase of mass. The second one is the Elder problem, which shows that acknowledging the presence of pure salt sources reduces fingering but increases substantially overall salt transport and causes the fluid to flow out through the prescribed head boundaries. It also gives an insight into the use of analogies between heat and salt transport problems.

Contact Information: Juan J. Hidalgo, Department of Geotechnical Engineering and Geo-Sciences, Technical University of Catalonia (UPC), C/ Jordi Girona 1-3, Building D-2, 08034 Barcelona, Spain, Phone: +34 934017244; Fax: +34 934017251, Email: juan.hidalgo@upc.edu

Simulation of Coastal Wastewater Injection in Hawaii using SUTRA, and the Value of Compelling Visualizations in Conveying Results to the Non-Specialist Public

Charles D. Hunt, Jr.
U.S. Geological Survey, Pacific Islands Water Science Center, Honolulu, HI, USA

ABSTRACT

Treated wastewater is injected into a permeable basaltic aquifer 1.2 km from the shore at Kihei, on the island of Maui (Figure 1). Excessive macroalgae smother corals and wash up on beaches in the area, creating odor and removal problems. Nutrients are a potential contributor to algal growth, so the fate of injected wastewater nutrients is of interest.

The USGS code SUTRA was used to model 3-D variable-density flow and solute transport in the injection plume and surrounding regional ground water. Objectives were to demonstrate plume behavior and estimate where it discharges to coastal waters. Salt was the sole solute because the plume is driven by salinity-density contrasts. Nutrient transport was not modeled, and nutrient fluxes were estimated separately. The finite-element mesh had variable spacing (finest near the water table, injection well, and coast) and contained 74,592 elements in 37 vertical layers. Simulations were transient, but stresses were held steady, and equilibrium was reached during model runs.

The plume is buoyant because effluent salinity is 1 percent seawater, whereas receiving water in the aquifer is 20-100 percent. Although effluent is injected 14-58 m below sea level, it rises to the water table and spreads out laterally (Figure 2). At an injection rate of 11,400 m^3/d, the modeled plume was 1.5 km wide at the shore (Figure 3), equaling a coastal flux of 7,600 m^3/d per km of coast. Regional ground-water flux is 6,600 m^3/d per km and mostly diverts around the plume, with some mixing at the margin. Essentially, the plume grows wide enough to displace a nearly-equal volume of regional flow. Stated another way, plume width is largely a ratio of injection rate to regional flow rate, a principle that can be deduced from analytical equations for injection in a uniform flow field. The plume was 20 percent wider when horizontal-to-vertical permeability ratio was reduced by an order of magnitude (from 200:1 to 20:1 by raising vertical permeability), but aside from that one test, long execution times made thorough parameter-sensitivity analysis impractical given other, non-modeling objectives of the study. Discharge from the plume core is about 60 percent effluent and 2-3 years old, according to the model. Calibration data were sparse, and the model can be considered only semi-quantitative.

Model results were processed with the USGS program Model Viewer, and the resulting visualizations were critically important in conveying findings to stakeholders, regulators, and the public. Effluent fate had been largely unknown, with little certainty of where effluent would discharge and skepticism among some that it would even reach the shore. Compelling pictures of the plume convey the required understanding to non-specialists.

[Figures 1-3, references, and contact information follow on subsequent pages.]

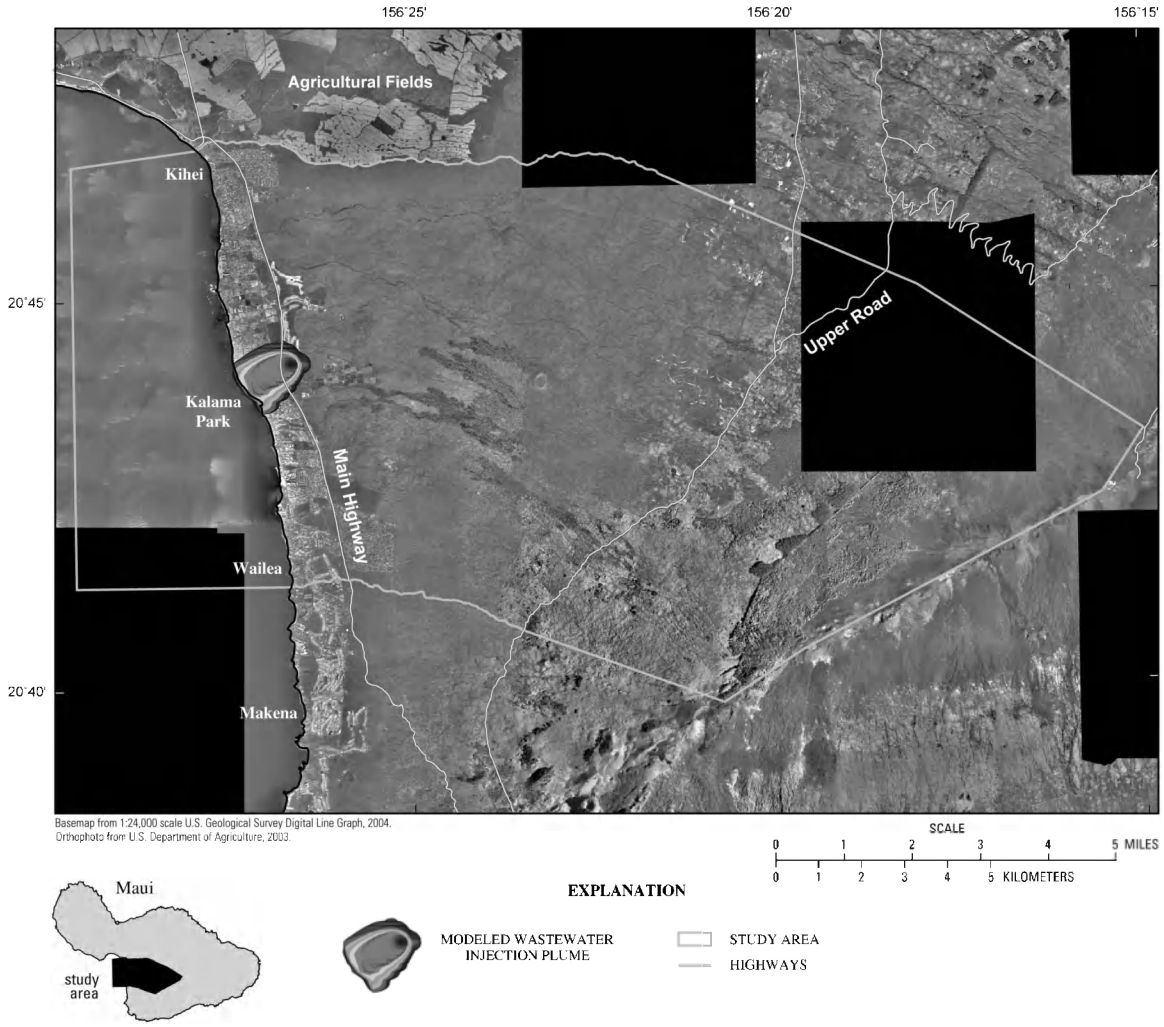

Figure 1. Simulated wastewater injection plume overlaid on aerial photo of the Kihei area, Maui, Hawaii. [Grayscale version of color original in Hunt, 2007.]

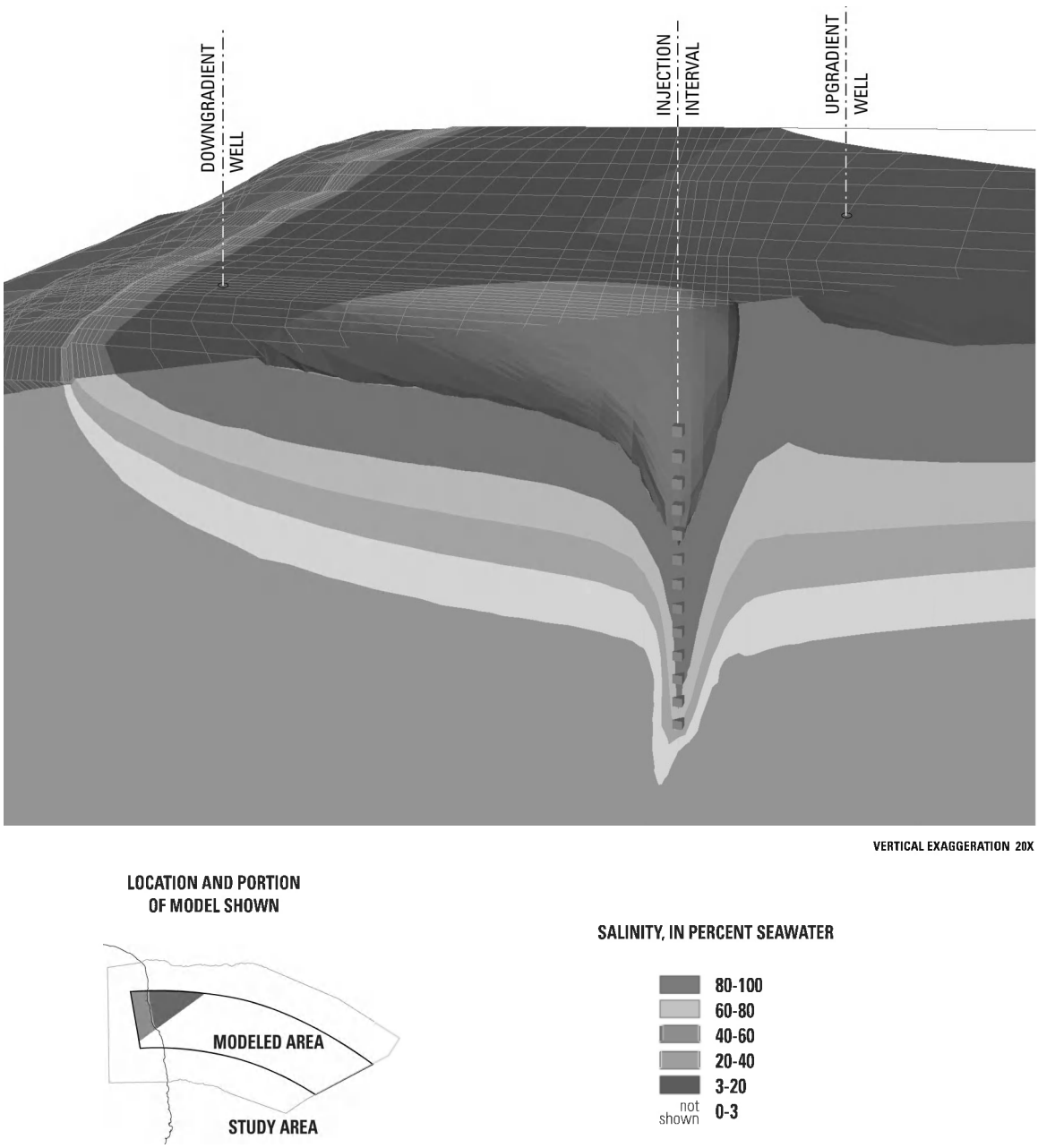

Figure 2. Cutaway block diagram showing simulated wastewater injection plume at Kihei, Maui, Hawaii. Effluent of 1 percent salinity is injected deep into brackish saline water but rises buoyantly, spreads laterally, and flows toward the coast at left. [Grayscale version of color original in Hunt, 2007.]

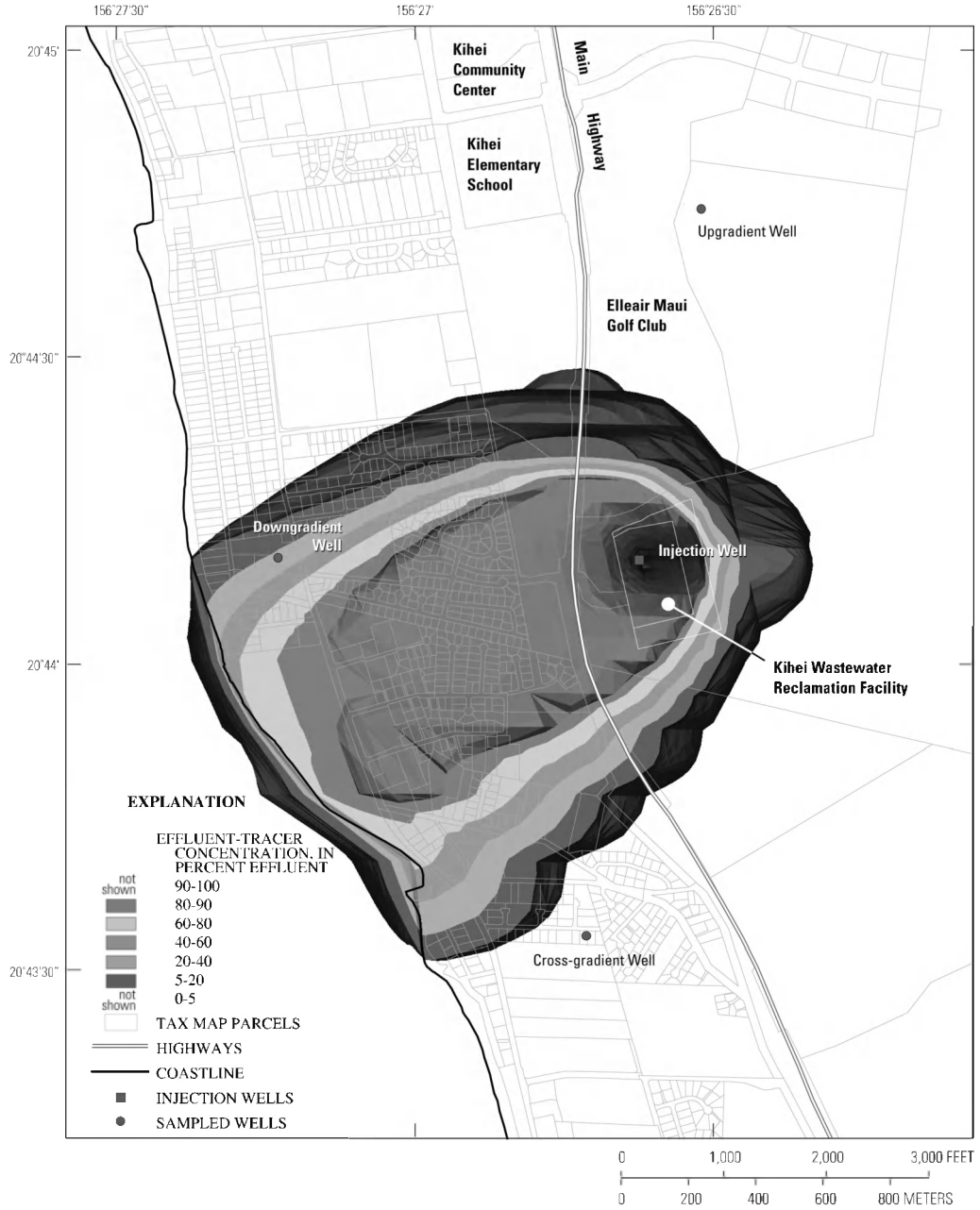

Figure 3. Simulated wastewater injection plume, and tax map for reference at Kihei, Maui, Hawaii. [Grayscale version of color original in Hunt, 2007.]

REFERENCES

Hunt, C.D., Jr., 2007, Ground-water nutrient flux to coastal waters and numerical simulation of wastewater injection at Kihei, Maui, Hawaii: U.S. Geological Survey Scientific Investigations Report 2006–5283, 69 p. http://pubs.usgs.gov/sir/2006/5283/

Contact Information: Charles Hunt, U.S. Geological Survey, 677 Ala Moana Blvd, Suite 415, Honolulu, HI, 96813, USA. Phone: 808-587-2414, Email: cdhunt@usgs.gov

Simulations of the Dynamics of Surface Water-Groundwater Interactions in a Coastal Environment During a 25-Year/72-Hour Storm

William C. Hutchings and *David L. Tarbox*
HSA Engineers & Scientists, Tampa, Fl, USA

ABSTRACT

The effects of the 25-year/72-hour storm were simulated with a numerical, variable-density model for a site located in Southeast Florida. The modeling was conducted to evaluate the effects of the storm on surface water-groundwater interactions and general groundwater flow throughout this coastal Biscayne aquifer environment. The modeled storm event is expected to generate 0.32 meters of precipitation within 72 hours. Storm water discharge to surface water and drainage wells was simulated with a surface water model and the results were included in a flow/solute transport model.

Lake stages significantly increase to approximately 1.35 m; however, these levels are designed to be less than the adjacent groundwater levels resulting in the creation of hydraulic sinks and strong vertical upward flow. Salinities within the lakes generally increase due to the convergent flow from approximately 500 to 2500 milligrams per Liter (mg/L). The water table rapidly drops following the storm event and, after approximately one week, the groundwater elevations across the site are within approximately 0.3 meters of static conditions. The normal shallow groundwater flow pattern is also generally resumed one week after the storm event. Deep groundwater flow is generally upward and seaward, from the western part of the site following the storm event; which appears to be due to the increased recharge to the aquifer throughout the area and the discharge to the drainage wells. The deep drainage wells accommodate the design discharge and, at the peak of the discharge, decrease the salinity concentration from approximately 35,000 parts per million (ppm) to an average of 15 ppm in the vicinity of the wells resulting in vertical flow.

INTRODUCTION

This numerical model was constructed to evaluate the effects of the 25-yr/72-hour storm on surface water-groundwater interactions in this coastal environment. The site is located in the vicinity of North Miami, Dade County, Florida. Due to the proximity of the Site to Biscayne Bay and the historical lowering of the water table, seawater intrusion has occurred and the underlying Biscayne aquifer is occupied by both fresh and saline water separated by a transition zone. As a result of these conditions, the variable-density model, SEAWAT-2000 (Langevin et al., 2003), was used to simulate groundwater flow in this environment.

The setting is a large-scale, modern, residential community, with a catchment area of 193.54 acres that includes two artificial lakes approximately 7.6 m deep. Pervious areas represent 84.9 acres or 43.9% with storm water designed to discharge to retention ponds, lakes, and to drainage wells. Storm water management was designed with a surface water model and the results are included in the SEAWAT-2000 model. The surface water-groundwater interactions are potentially affected by the amount of rainfall, surface water elevations, depth of the surface water bodies, and aquifer characteristics. The effects of the event on the steady state flow field throughout the surficial aquifer are also evaluated.

METHODOLOGY

The model includes various natural hydrologic boundaries in order to create the natural groundwater and surface water system. The 17-layer model consists of 81 columns (6,785 m) that range from 200 m near the western and eastern model boundaries to 13.5 m within the site and 76 rows (5,270 m) that range from 100 m near the northern and southern boundaries to 17 m within the site.

Biscayne Bay and Arch Creek (located south of the site) are modeled as constant heads with an average elevation of 0.22 meters and a salinity or total dissolved solids (TDS) concentration of 35,000 parts per million (ppm). The Oleta River is simulated with the river package with a decreasing linear hydraulic gradient and increasing TDS concentrations downgradient towards Biscayne Bay. The Mangrove Preserve is in direct hydraulic connection with Biscayne Bay and is modeled with a constant head; however, the depth of the saline water in the preserve is less than the depth associated with Biscayne Bay and Arch Creek Canal. In contrast the altered mangrove preserve is a fairly static water body that appears to be isolated from the tidal effects of Biscayne Bay; therefore, the drain package was used to simulate this environment.

For the steady state simulation the lakes on-site were simulated with cells whose hydraulic conductivities are set at 10,000 m/day in order to represent the natural steady state stage. The steady state salinity-flow vector distribution across the calibrated model is depicted on **Figure 1**. For the post-development simulations, the lake stages were modeled with both the constant head and river packages and the lake stages were input every 6 hours for 84 hours. The surfaces of Ibis and Southeast lakes were set to the design elevations (1.37 m and 1.33 m, respectively) determined from the HydroCAD 8.0 model (HydroCAD Software Solutions LLC, 2006) provided by ES Consultants, Inc. An additional simulation was conducted with the lake stages set at maximum elevations of approximately 2.75 m. The surfaces of the lakes are set to the design elevations by the constant heads and the high-K cells allow mixing to occur. Since the constant heads cannot be turned off during a simulation, the lakes were also modeled with the river package. Use of the river package allows the lake stages to be set at the elevations determined by the HydroCAD model and the package to be turned off after the peak stage, thereby, allowing the lakes to respond naturally to the cessation of the storm event.

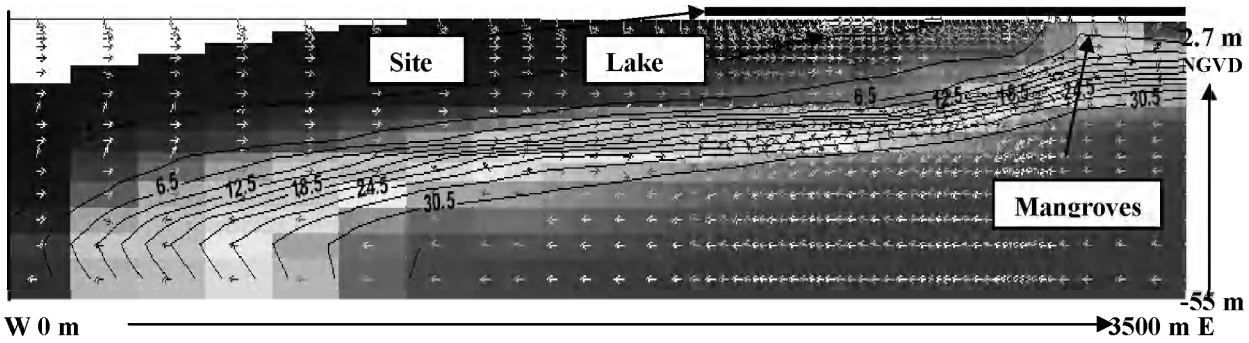

Figure 1. Steady state salinity-flow vector cross-sectional diagram (CI =3 g/l from 0.5 g/l)

The western boundary of the model determines the groundwater flux to Biscayne Bay and was set to a specified head of (1.0 m) with the constant head package (Lietz et al., 2002). In addition, a simulation was conducted with the western boundary modeled as a general head boundary with a constant head in the Everglades to confirm the elevation of the specified head. When simulating the 25-year/72-hour storm, the constant head along the western boundary of the

model was switched to a general head boundary located 3,500 meters west of the general head boundary cells with a head elevation of 1.7 meters, in order to allow groundwater within the model to fluctuate.

The post-development model is constructed with land-use categories to represent current and predicted conditions. Areas occupied by roads and buildings are assigned recharge rates consistent with urban development runoff coefficients and retention basins are assigned recharge rates based on wetland runoff coefficients. In addition, the system of 28 drainage wells is simulated with all wells screened in the lower layer of the model. The discharge rates to the wells are generally consistent with the time-varying rates determined from the HydroCAD model. HydroCAD rates vary every two hours and the SEAWAT-2000 model rates represent rates that take place every six hours. These differences should not significantly affect the results. The discharge rates and total volumetric discharge to each well vary. For example, the discharge rates for a high volume well cluster range from 905 to 47,456 m^3/day. Considering 11 basins, the maximum rates per basin (over a six-hour period) range from 7,975 in basin 3 to 119,449 cubic meters per day (m^3/day) in Phase 1A, with an average of 31,354 m^3/day.

RESULTS & CONCLUSIONS

Results of the post-development simulation with the design lake elevations of 1.37 and 1.33 m are depicted in the salinity-flow vector cross section diagram after 72-hours (**Figure 2**). This figure depicts the three dimensional convergent flow to Ibis Lake resulting in the increased TDS. The effects of the drainage wells are evident by the decreased TDS near the base of the aquifer and the upward and seaward flow. Seaward flow is due to the regional recharge and discharge to the drainage wells. The water table elevation in the vicinity of the site is also generally lower in the post-development simulation because of the reduced infiltration and discharge of storm water primarily by drainage wells to the lower Biscayne aquifer. Northwest of the site, a hydraulic mound is created in both the pre and post-development simulations due to the additional recharge and the regional boundary configurations. Results of the post-development simulation with the design lake elevations of approximately 2.75 m are depicted in the salinity-flow cross-section diagram (**Figure 3**) after 72-hours. In contrast to the previous simulations, the lakes create downward vertical flow increasing discharge through the bottom of the lakes and seaward flow.

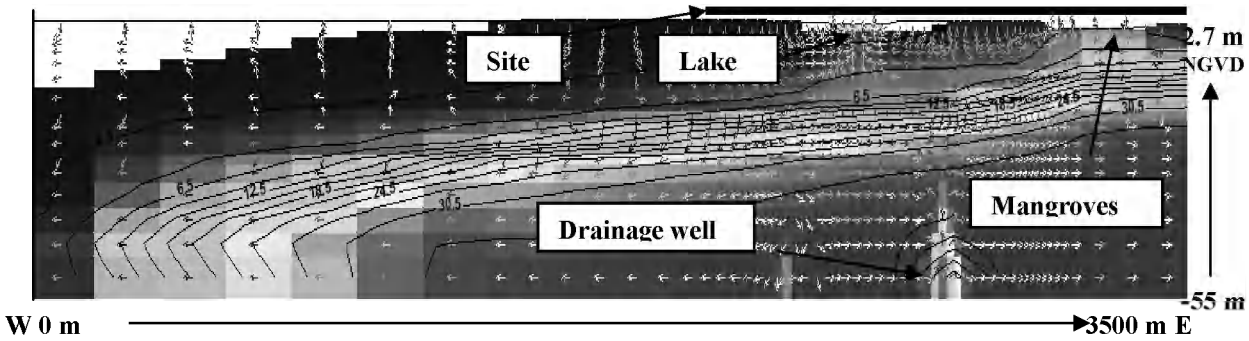

Figure 2. Salinity-flow vector cross-sectional diagram at 72 hrs (CI =3 g/l from 0.5 g/l)

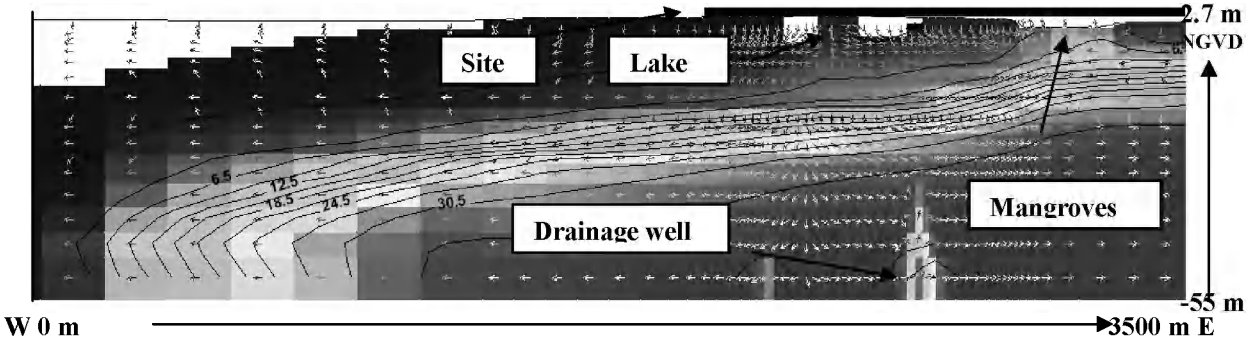

Figure 3. Salinity-flow vector cross-sectional diagram at 72 hrs and lake stages of 2.75 m (CI =3 g/l from 0.5 g/l)

From near the western end of the site, the deep groundwater flow is generally seaward, in contrast to steady state flow in which deep groundwater flows landward. This change in flow direction is due to the regional effects of the storm event and discharge to the drainage wells, and persists for approximately seven weeks following the event. A significant density difference between the injected storm water and the deep formation water exists for approximately two weeks following the storm event, creating upward groundwater flow. Normal groundwater elevations and flow patterns in the shallower parts of the aquifer are generally resumed approximately one week after the storm event. The groundwater elevations at this time are approximately 0.3 meters greater than the average steady state elevations. Deep groundwater flows eastward for more than four weeks and gradually this deep saline groundwater reverses and flows westward, establishing the average shallow freshwater, transition zone, and deep saline water configuration and characteristic flow. The drainage wells appear to accommodate the design discharge and, at the peak of the discharge, decrease the background salinity concentration from 35,000 ppm to the approximate range of 8,000 to 31,000 ppm, with an average of 15 ppm in the vicinity of the wells. During the storm event, the average horizontal groundwater flow direction is perturbed by vertical groundwater flow created as a result of the salinity and density differences between the TDS of the saline formation water and the injected freshwater. As a result of the brevity of the storm event and discharge, these differences range between 20 and 30 ppm one week following the storm event and become relatively minor after approximately four weeks, regardless a small upward flow of deep groundwater persists for several weeks or more.

REFERENCES

Langevin, C.D., 2003, MODFLOW-2000, the U.S. Geological Survey Modular Ground-Water Model-documentation of the SEAWAT-2000 with VDF and IMT: U.S. Geological Survey Open-File Report 03-426, 43 p. Tallahassee, Florida.

Lietz, A.C., Dixon, J., and Byrne, M., 2002, Average altitude of the water table (1990-99) in the Biscayne Aquifer, Miami-Dade County, Fl: U.S.G.S. OFR 02-91, map, Tallahassee, Florida.

Contact Information: William C. Hutchings, P.G., HSA Engineers & Scientists, 4019 East Fowler Avenue, Tampa, FL 33617 USA, Phone 813-971-3882; Fax 813-971-1862; Email: bhutchings@hsa-env.com

Time Domain Electromagnetic Induction and High Resolution Electric Resistivity Soundings to Map Salt Water Intrusion in Coastal Sandy Aquifers, Los Angeles County, California

Theodore A. Johnson[1], *Nancy Matsumoto*[1] and *John R. Jansen*[2]
[1]Water Replenishment District of Southern California, Lakewood, CA, USA
[2]Aquifer Science & Technology, Waukesha, WI, USA

ABSTRACT
Due to severe groundwater overdraft in the first half of the 20th century, salt water intruded into the coastal aquifers of the West Coast Basin in southern Los Angeles County, California. The intrusion contaminated fresh groundwater supplies resulting in the shutdown of wells or necessitating expensive reverse osmosis treatment. The extent of the intrusion is generally known, but the details are complicated due to concentration and density differences of the saline water, the gradients and hydraulic properties of the multi-layered sandy aquifers, and the shape of the fresh water/salt water interface.

A geophysical pilot test was performed in the basin using Time Domain Electromagnetic Induction (TDEM) and High Resolution Electric Resistivity (ER) to determine which method might be most suitable for full-scale intrusion mapping of the basin. Project challenges included the depth of the intrusion (200 to 800 feet), varying salinities (chloride concentrations ranging 100 mg/L to over 6,000 mg/L), multiple aquifers with different horizontal extents of intrusion, and a heavily urbanized area with abundant potential electrical interference. The ER soundings provided high resolution images of the upper 250 to 300 feet, but could not reach the greater depths due to the lack of an open corridor long enough for the survey. The TDEM using a 20m x 20m loop with four turns of the wire proved the most effective at measuring the brackish and salty water at depth with the smallest footprint and minimal noise. The results compared favorably to nearby monitoring wells. Due to the success, a full scale TDEM survey at 35 sites was performed in early 2008 and the results will be available at the conference proceedings.

INTRODUCTION
Severe overdraft of the West Coast Groundwater Basin in southwestern Los Angeles County, California from the early 1900s to the late 1950s caused over 600,000 acre-feet of salt water to intrude into the coastal sandy aquifers that are used for potable, agricultural, and industrial supply (California Department of Water Resources, 1962). Groundwater provides a third of the water supply to the region, with the remainder being imported via aqueducts from the Colorado River and Northern California located hundreds of miles away from the Los Angeles region. Thus, the intrusion was a serious threat to the future usability of the local groundwater resource. The intrusion caused impacted wells to be shut off or necessitated the construction and operation of expensive reverse osmosis brackish groundwater desalination plants to make the water potable.

In 1950s, the Los Angeles County Flood Control District undertook testing to evaluate the use of injection wells for seawater intrusion control. The tests were successful, so the West Coast Basin Barrier Project (WCBBP) was constructed consisting of a nine-mile stretch of 153 injection wells and 302 observation wells that currently inject approximately 13,600 acre feet per year of potable and advanced-treated recycled waste water into the multiple aquifers. Lipshie and Larson (1995), CDWR (1957), and Johnson and Whitaker (2004) describe the barrier systems in detail.

Although the WCBBP currently protects the aquifers from further intrusion, approximately 250,000 acre feet of brackish groundwater was stranded on the landward side of the barrier after it was completed. This stranded brackish groundwater is known as the "saline plume", and it is a continued threat to the groundwater resources in the West Coast Basin. Two desalination facilities have been constructed to remove relatively small amounts of this brackish groundwater (approximately 4,000 acre feet per year), but additional studies are being performed to evaluate the full extent of the plume so that an overall salt water management policy can be developed by local water managers. The overall shape of the intrusion is generally well known, but the details are complicated due to the concentration and density differences of the saline water, the gradients and hydraulic properties of the multi-layered sandy aquifers, and the shape of the fresh water/salt water interface. Therefore, mapping of the intrusion using geophysical methods was pilot-tested to determine its three-dimensional extent.

METHODS

Under ideal conditions, several geophysical methods can easily detect zones of saline groundwater as highly conductive (low resistivity) volumes in the sub surface. This survey area was much less than ideal due to the dense residential and industrial land use and limited open space. These factors created severe restrictions on the survey area and types of geophysical methods that could be used.

Given the site conditions, the objectives of this study could be best accomplished through the use of two electrical methods; a high resolution electrical resistivity survey to map the lateral and vertical resistivity distribution of the upper 300 to 400 feet, and a time domain electromagnetic induction (TDEM) survey to map the electrical resistivity to depths of over 500 feet. The specific electrical property measured by these methods is electrical resistivity. Electrical resistivity is measured in units of ohm-meters (ohmm), and is the mathematical inverse of the more familiar property of electrical conductivity. Resistivity is a material property that can be used to determine the characteristics of the subsurface. Sandy zones filled with air or fresh water generally have resistivity values of 30 to 50 Ohmm or higher depending on the silt content of the sand. Clay rich soils have resistivity values of about 20 to 30 Ohmm or less. Sandy zones filled with brackish or saline water have low resistivity values, typically 1 to 10 Ohmm or less, depending on the degree of salinity in the groundwater.

Electrical resistivity measurements are made by passing weak electrical currents through the ground using a pair of electrodes (current electrodes) while measuring the resultant voltage field in the ground at another pair of electrodes (potential electrodes). The measured voltage is a function of the electrical resistivity of the soils beneath the electrodes. The subsurface penetration of the electrical current is a function of the current electrode separation. By making measurements with electrodes at different spacings, a resistivity survey can delineate vertical variations in resistivity with depth in the subsurface material. By making a series of soundings at different positions along a profile line, lateral changes in resistivity can also be measured. Multi-node resistivity systems use a cable system with multiple conductors to connect many electrodes to a switching box. The switching box selects pairs of current and potential electrodes to make resistivity measurements. The spacing between current and potential electrodes, the spacing between the electrode pairs, and the position of the center of the electrode arrays are changed to provide resistivity measurements to different depths and different positions along a profile line. These systems can make hundreds of measurements in a matter of a few hours. The

data can be interpreted to produce a relatively high resolution two dimensional section that shows the lateral and vertical changes in resistivity along the profile line.

The TDEM method uses a heavy gauge wire laid out as a square or rectangle to form a transmitter loop. A current of several amps is passed through the transmitter loop and switched off to create a broad band electromagnetic (EM) pulse of radio waves. The EM pulse measures the change in resistivity of the subsurface with depth as it propagates deeper into the ground.

RESULTS

Resistivity profiles were conducted at two sites in the West Coast Basin on October 24th, 2006. The profiles at both sites detected high resistivity material (over 50 Ohmm) in the upper 50 to 100 feet. This layer represents sandy soils filled with air or fresh water. Beneath this layer lies a zone of lower resistivity material (40 Ohmm) that consists of silty sand. Resistivity values are generally above 10 to 20 Ohmm where the sand is saturated with relatively fresh water. Several pockets of very low resistivity below 10 Ohmm are also present. These zones indicate portions of the aquifer saturated with brackish or saline water with the more saline zones indicated by lower resistivity values of a few Ohmm. The distribution of low resistivity material suggests that the saline water is concentrated in pockets similar to coarser grained channel deposits that may have been preferential flow paths for sea water intrusion. The presence of the conductive zone prevented the current from penetrating deeper and the resistivity survey did not detect the bottom of this layer.

Four TDEM soundings were conducted at three locations in the survey area. Soundings 2 and 3 were conducted in the same location using two different transmitter loop configurations to optimize the depth of penetration while reducing noise from cultural features. A single turn 40m x 40m loop and a smaller 20m x 20m loop with four turns of the wire were used. The smaller loop using multiple turns was found to produce the best data at depth. The TDEM soundings detected three to four electrical layers. The upper layer has intermediate resistivity (41 to 121 ohmm) and is between 150 feet to over 300 feet thick. This layer appears to represent a combined average of the upper two layers seen on the resistivity data. The two middle layers are much more conductive (0.9 to 15 ohmm), with the lowest resistivity material present in the deeper portion of the two layers. The combined thickness of the two middle layers varies from 150 feet thick to about 200 feet thick. These layers represent sand filled with brackish to saline water. Soundings 2 and 4 detected a higher resistivity unit (50 to 100 ohmm) below the conductive unit that represents the base of the saline zone. Sounding 1 did not detect the lower unit, possibly due to the higher noise level in the larger transmitter loop.

DISCUSSION AND CONCLUSIONS

The geophysical survey appears to have detected a brackish to saline water in the aquifer at a depth of between 200 to 500 feet in the study area. An apparent fresh water sand zone may be present below the saline zone. The TDEM method achieved greater penetration given the limited space available and seems to have provided the most useful data. The resistivity method produced higher resolution data to depths of between 200 to 350 feet below the surface. It is likely that the depth of investigation of the resistivity method could be increased to about 400 to 500 feet if a longer electrode spread could be deployed. The geophysical results were compared to driller's logs and water quality data from adjacent wells. The well data confirmed the presence of saline to brackish aquifers at the depths mapped by the geophysical data. Due to the success of the pilot study, an additional 35 TDEM soundings were conducted in early 2008 to

provide better resolution of the salt water intrusion. This information will be used to site additional monitoring wells and plan a water quality management program for the aquifer.

REFERENCES

California Department of Water Resources, 1957. Seawater Intrusion in California. Bulletin 63, Appendix B.

California Department of Water Resources, 1962. Planned Utilization of the Ground Water Basins of the Coastal Plain of Los Angeles County. Bulletin 104, Appendix B – Safe Yield Determinations.

Johnson, T.A., and R. Whitaker, 2004. Salt Water Intrusion in the Coastal Aquifers of Los Angeles County, California: Coastal Aquifer Management, edited by Cheng, A.H., and Ouazar, D., Lewis Publishers, Chapter 2, pgs. 24-48.

Lipshie, S.R., and R.A. Larson, 1995. The West Coast Basin, Dominguez Gap, and Alamitos Seawater-Intrusion Barrier System, Los Angeles and Orange Counties, California. In Association of Engineering Geologists News, Vol 38, No. 4, pgs 25-29.

Contact Information: Ted Johnson, Water Replenishment District of Southern California, 4040 Paramount Blvd, Lakewood, CA 90712 USA, Phone & Fax: 562-275-4240; Email: tjohnson@wrd.org

Altered Hydroperiod and Saltwater Intrusion in the Bald Cypress Swamps of the Loxahatchee River

David Kaplan[1], *Rafael Muñoz-Carpena*[1], *Yuncong Li*[2], *Yongshan Wan*[3], *Marion Hedgepeth*[3] and *Dick Roberts*[4]

[1]Agricultural and Biological Engineering Dept., University of Florida, Gainesville, FL, USA
[2]Soil and Water Science Dept., University of Florida, Homestead, FL, USA
[3]Coastal Ecosystems Dept., South Florida Water Mgmt. District, West Palm Beach, FL, USA
[4]Florida Park Service, Dept. of Environmental Protection, Hobe Sound, FL, USA

ABSTRACT

The Loxahatchee River is located in southeastern Florida, USA, and contains one of the last remnants of bald cypress (*Taxodium distichum*) river-swamp in the region. Hydrological modifications in the river channel and watershed have resulted in reduced freshwater flow and saltwater intrusion into this historically freshwater ecosystem, which has caused the retreat of bald cypress upriver. The loss of bald cypress as salinity in the floodplain increases has been accompanied by a transition to mangrove-dominated communities, which are more salt-tolerant. Previous watershed modeling efforts have focused on predicting river salinity under various management scenarios, with the goal of keeping river salinity below identified threshold levels for bald cypress health, but have not addressed hydrological conditions in the floodplain, which are a key control on floodplain vegetation. The aim of this study is to characterize soil moisture and soil porewater salinity dynamics in the floodplain at several depths and distances from the river during both wet and dry seasons. Twenty-four combined dielectric probes measuring soil moisture, salinity, and temperature were installed at four locations and three depths along two transects perpendicular to the river. Analysis of data collected over a three-year period has shown that soil moisture can be functionally tied to distance, topographical elevation, and river stage. These relationships are useful in evaluating the effects of proposed river management scenarios on floodplain hydrology. Additionally, increases in soil porewater salinity in floodplain during the dry season were shown to be related to the magnitude and duration of river salinity, with an apparent time lag between river and porewater salinity peaks (22-64 days), which increases with elevation and distance from river.

INTRODUCTION

The upper watershed of the Northwest Fork of the Loxahatchee River is home to one of the last remnants of bald cypress (*Taxodium distichum*) swamp in southeast Florida. However, a changing salinity regime in the river and its floodplain has been linked to vegetative changes in the floodplain (SFMWD 2005). Of primary concern is the loss of bald cypress and transition to mangrove-dominated communities as salinity in the floodplain increases. A Minimum Flow and Level (MFL) for the Northwest Fork was adopted in April 2003. However, due to reduced freshwater flow in the Northwest Fork, it was recognized that low dry-season flows would immediately trigger exceedances of the MFL, requiring the development of a Recovery Plan. The proposed Recovery Plan initiated an intensive watershed and hydrodynamic modeling effort focused on predicting river salinity under various management scenarios, with the goal of keeping river salinity below identified threshold levels for bald cypress health (2 parts per thousand, equivalent to an electrical conductivity [EC] of 0.3125 siemens per meter [S/m] at 25° C). As these models have not addressed hydrological conditions in the river floodplain (soil moisture and soil porewater salinity), the aim of this study is to characterize soil moisture and salinity dynamics at several depths and distances from the river in the floodplain during both wet and dry seasons. An additional objective is to derive relationships between river hydrology (stage

and salinity) and floodplain soil conditions to better predict the effects of management scenarios proposed by the South Florida Water Management District (SFWMD).

METHODS

Twenty-four combined dielectric probes (Stevens Hydra Water, Beaverton, OR) were installed at four locations and three depths along two previously-established vegetation survey transects perpendicular to the Northwest Fork of the Loxahatchee River. Transect 1 is in an upriver location not impacted by daily tides and is dominated by upland forest and hydric hammock at higher elevations and mature bald cypress swamp in the floodplain. Transect 7 is in a transitional area that receives daily tidal flooding and contains both upper tidal and riverine forest types. At each transect, twelve probes were installed at four distances from the river and three depths below ground surface (bgs) to capture the spatial and temporal variation of hydrological parameters over wet and dry seasons. Each cluster of three probes was wired to a field data logger (CR-10, Campbell Scientific, Logan, UT), which recorded soil moisture, soil bulk EC, and temperature every 30 minutes. Data collection began in September 2004 and has been ongoing since.

Soil moisture time series developed for each probe are reported as measured soil moisture. However, Mortl (2006) found three major soil categories in the Loxahatchee River floodplain to have widely varying hydraulic characteristics, and thus, when comparing moisture values across soil categories it is helpful to scale the measured values using effective soil moisture (Θ), which ranges from a value of zero at residual moisture (θ_r) to 1 at saturation (θ_s). Effective soil moisture was then fit to a common three-parameter sigmoid model at Transect 1 (eqn. 1):

$$\Theta = \frac{\theta - \theta_r}{\theta_s - \theta_r} = \frac{A}{1 + e^{-\frac{h-b}{c}}} \qquad (1)$$

where h is river stage, and A, b, and c are fitting parameters. Model selection was made by minimizing combined r^2 values for all measurement locations. Porewater EC values were calculated from bulk EC and soil moisture based on calibrations by Mortl (2006) and compared to river salinity values at each transect and with known bald cypress thresholds. Piezometers, slotted at probe installation depths, were also installed in several locations in 2007 to verify probe EC measurements and fill data gaps due to equipment failure.

RESULTS

Experimental results for several locations on Transects 1 and 7 are given in Figure 1. Effective soil moisture was plotted against river stage, and fit to a common sigmoid model (not shown). The Nash-Sutcliffe coefficient of efficiency (*ceff*) was used as a measure of goodness of fit. For soils which exhibited a wide range of θ values, the sigmoid model does a good job of predicting soil moisture based on river stage ($0.72 < ceff < 0.89$). For deeper sandy soils which are below the water table for long periods and surface soils of the lower floodplain, which only rarely dry out, the sigmoid model performed fairly ($0.32 < ceff < 0.66$). At Transect 7, daily tidal flooding resulted in near-constant soil saturation for all probes (Fig. 1), however responses to brief periods of drawdown in the shallowest (i.e., highest elevation) probes were evaluated using a Fourier smoothing technique. When mean tide elevation is above probe elevation, smoothing collected Data from 15-and 30-minute readings to a 6-hour time series revealed a close correlation between measured soil moisture and tidal stage data (not shown).

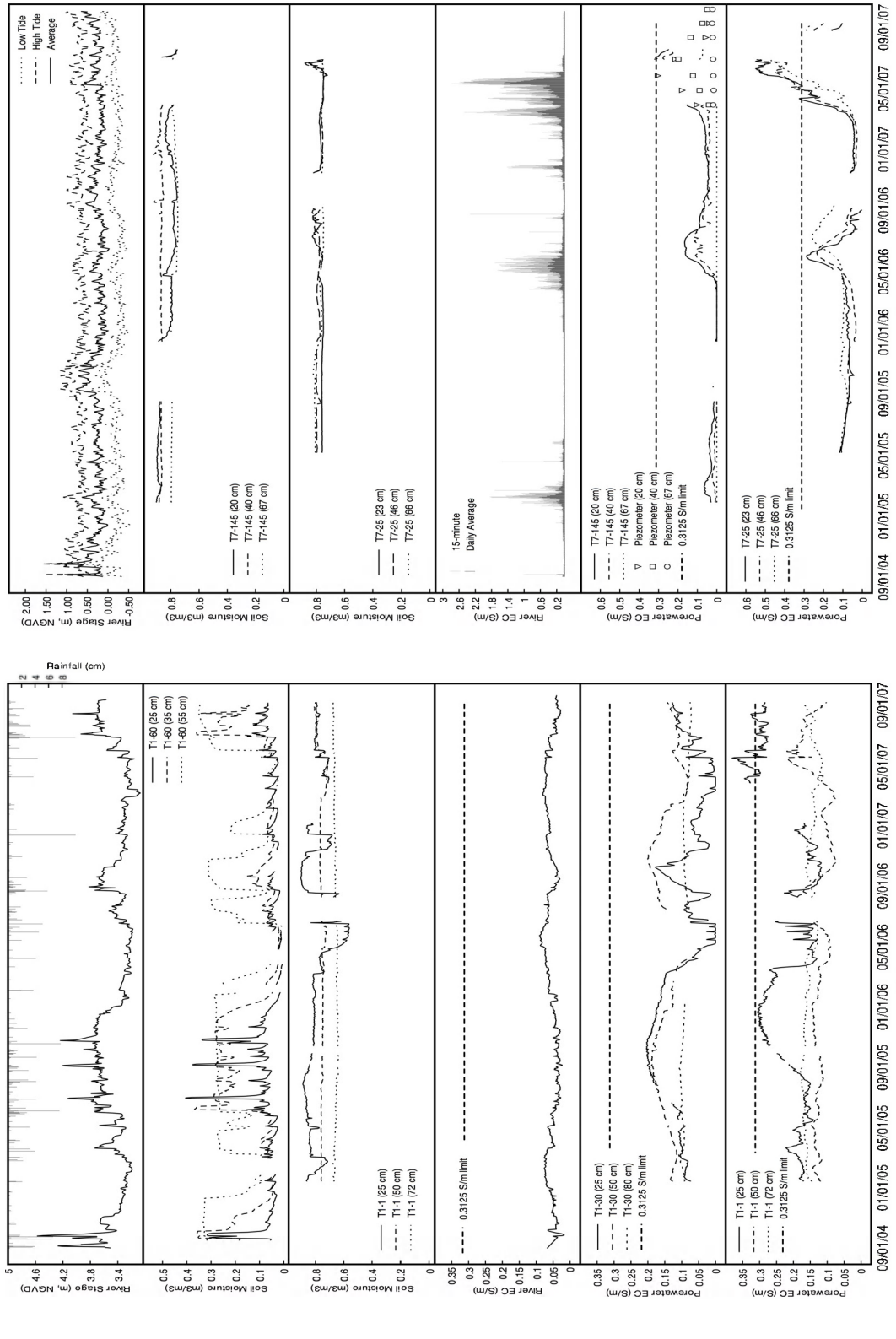

Figure 1. River stage, precipitation, soil moisture, river EC, and soil porewater EC measured at several stations on Transects 1 and 7 during the three-year study period. Station names indicate transect number (T1/T7), distance from river (m), and probe depth bgs (cm). EC at station T1-1 was negligible and is not shown. Piezometer data at station T7-145 are single monthly grab samples.

Soil porewater EC in the floodplain at Transect 1 (upriver) is slightly higher closer to the river and is relatively stable for most of the study period, with only the surface probes showing significant variation during the extended dry periods. Soil porewater is consistently higher than river EC (by a factor of 2-3), likely due to concentration of salts due to evapotranspiration. Dry season peaks in soil porewater EC were observed in all probes on Transect 7 (tidal transect), which mirrored peaks in river EC (Fig. 1). For the probes furthest from the river (T7-145), these peaks increased in magnitude in each of the study years, but reached the critical limit (2 ppt) only in 2007, and only in the most superficial soils (20 cm bgs). For the station 25 m from the river (T7-25), where floodplain vegetation begins to transition from bald cypress to mangroves, measured porewater EC was higher, exceeding the critical value for 83 days in surface soils (23 cm bgs), 85 days in middle soils (46 cm bgs), and 64 days in deeper soils (66 cm bgs).

DISCUSSION AND CONCLUSIONS

Analysis of data from Transect 1 (upriver) shows that soil moisture is dominated by distance from river and elevation, with precipitation, evapotranspiration, microtopography, and soil heterogeneity identified as additional factors. Since the health and reproductive success of bald cypress is dependent on freshwater conditions and varying flood levels and soil moisture throughout the year, the functional relationships developed here (sigmoidal curves) serve as a useful tool for the SFWMD to evaluate adopted MFL standards and proposed restoration scenarios. Soil porewater EC values in the lower floodplain of Transect 1 were often higher than EC values in the river, likely due to high rates of evapotranspiration by vegetation in the floodplain. At Transect 7 (tidal), it is apparent from the collected data that the soil porewater EC in the root zone of the floodplain vegetation reaches critical values (2 ppt) at times, but does not reach levels observed in the river. Higher peaks in soil porewater EC were observed in drier years, and maximum soil porewater EC values were also closer to peak river EC values during these years. Increases in soil porewater EC in floodplain during the dry season are related to the magnitude and duration of river salinity, however, there is a time lag between river and porewater EC peaks (22-64 days), which increases with depth and distance from river.

REFERENCES

Mortl, A. 2006. Monitoring Soil Moisture and Soil Water Salinity in the Loxahatchee Floodplain. Masters Thesis. University of Florida, Gainesville, FL. 101 pp.

SFWMD. 2005. Draft Evaluation of Restoration Alternatives for the Northwest Fork of the Loxahatchee River. Coastal Ecosystems Division, South Florida Water Management District, West Palm Beach, Florida, March 2005, draft.

Contact Information: David Kaplan, UF/IFAS, Ag. & Bio. Engineering Dept., P.O. Box 110570, Gainesville, FL 32611-0570, Phone: 352-392-1864, Fax: 352-392-4092, Email: dkaplan@ufl.edu

Dynamic Behaviors of Fresh-Saline Water Interactions in Coastal Zone

Kue-Young Kim[1], *Yun-Seok Park*[2], *Gi-Pyo Kim*[2] and *Ki-Hwa Park*[1]
[1]Korea Institute of Geoscience and Mineral Resources, Daejeon, Republic of Korea
[2]Water Resources Office of Jeju Special Self-Governing Province

ABSTRACT
This study is intended to evaluate fresh-saline water interactions in coastal region influenced by external forces including tidal fluctuations and seasonal rainfall variations. Five different coastal zones were considered on Jeju Island, Korea, and electrical conductivity (EC) profiles at these monitoring wells were examined to identify the configurations of fresh-saline water interface. In order to analyze the dynamic behaviors of fresh-saline water interactions, we utilized multi-depth EC and temperature probes and obtained a time-series data. The monitored data showed that EC and temperature vary with both tidal fluctuations and heavy rainfall. Spectral filter was used to remove the effects of tidal forces and provide the influence of heavy rainfall events on EC and temperature. Time-series data of EC and temperature in the subsurface at various depths enabled us in understanding the interaction processes between fresh and saline water.

INTRODUCTION
Understanding the mechanism of fresh-saline water interaction has become an important issue for studies on hydrology as well as water management aspect in coastal area. Many hydrogeologic studies on Jeju Island have been conducted. Kim et al. (2006) proposed a conceptual model of fresh-saline interactions for the eastern part of Jeju Island by combining the results of EC and temperature log and the 2-D flowmeter tests. On the extension of the study, Kim et al. (2008) analyzed the interaction of fresh-saline water influenced by tidal fluctuations with EC data and end-member mixing analysis. The objectives of this study are to identify the temporal variations of fresh-saline water interactions at coastal aquifers and to evaluate the influence of tidal fluctuations and seasonal rainfall.

METHODS
Jeju special self-governing province has established monitoring wells around the coast in order to understand the subsurface geology, to observe water-level fluctuations, and to investigate the EC variations. In this study, five monitoring wells which are HL-1, JC-1, JD-1, SS-1, and HC-1 were selected for installing multi-depth monitoring system (Figure 1a). All the monitoring wells have a screen over the entire interval. The location and configuration of the fresh-saline water interface were examined with EC log. The EC profiles were obtained at several points of time for each monitoring well in order to investigate the temporal variation. The geological log and EC profile from SS-1 borehole are illustrated for an example in Figure 1b. Although these profiles provide valuable information on fresh-saline water interactions, monthly logging data is unable to analyze a short term variations influenced by tidal oscillations and the effect of rainfall events on interactions between fresh and saline water. Thereafter, EC and temperature probe system which can monitor at multi depths were installed at each monitoring wells, and continuous measurements of EC and temperature were made at 30-min interval. Applying a spectral filter to the frequency domain data eliminates all identified periodicities. In this study, a low-pass fast Fourier transform (FFT) filter was applied to the EC and temperature data to remove the diurnal and semidiurnal fluctuations and the noise from the monitoring system.

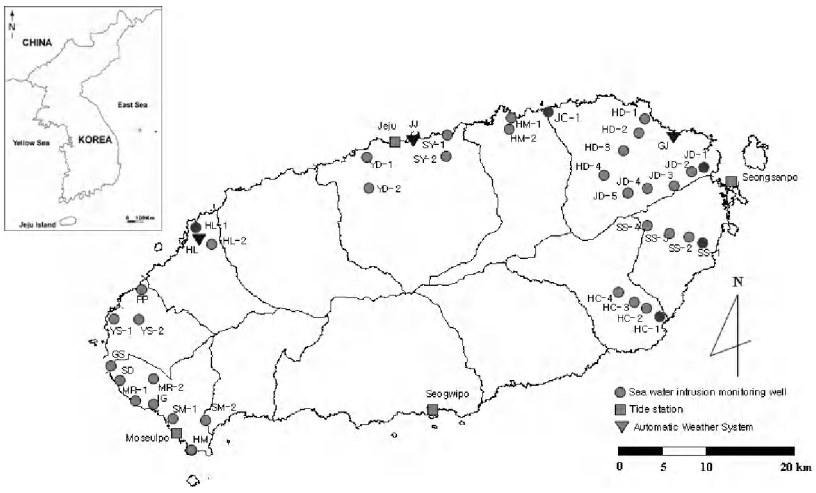

(a)

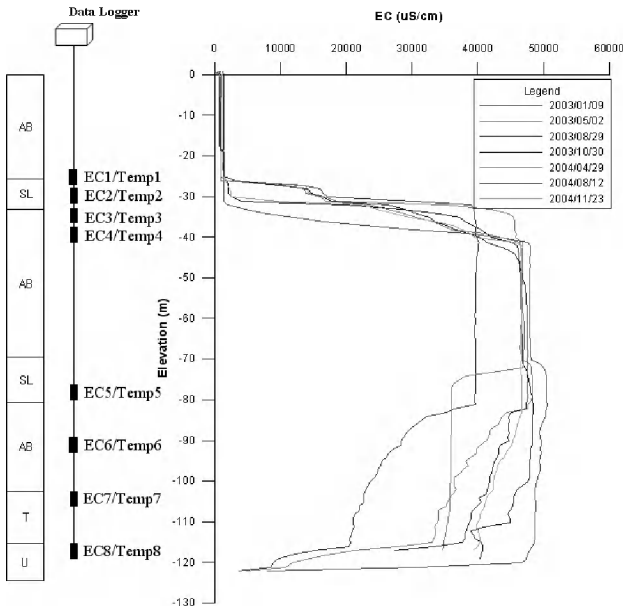

(b)

Figure 1. The location of the monitoring wells on Jeju Island (a) and the profiles of conductivity measurements at SS-1 monitoring well (b).

RESULTS AND DISCUSSION

Precipitation

For precipitation, we used the data obtained from automatic weather system (AWS). Three stations (Hanlim (HL), Jeju (JJ), Gu-Jwa (GJ) stations) were selected which are near to the monitoring wells. The monitoring was carried out from Jun 20 to Nov 20, 2007 and the study period includes both the wet and dry seasons. During the wet season, five heavy rainfall events were observed. The first event occurred between July 5 and July 7 with 93.5 mm (HL), 122.5 mm (JJ), and 144.0 mm (GJ). The largest rainfall was recorded during Sep 14 – 16 with 411.5 mm (HL), 590.0 mm (JJ), and 358.0 mm (GJ).

Fresh-saline water interface

Coastal groundwater tends to have a definable interface dividing the fresh and saline zones due to density difference. The geological log at SS-1 showed trachytic basalt, acicular basalt, hyaloclastite, U formation and sedimentary layers. EC profile showed two types of interface pattern for different points of time. One is interface lying at depth of -30 m, dividing fresh water and saline water zones. The other case shows another interface existing at lower part and relatively low TDS water flows at this zone.

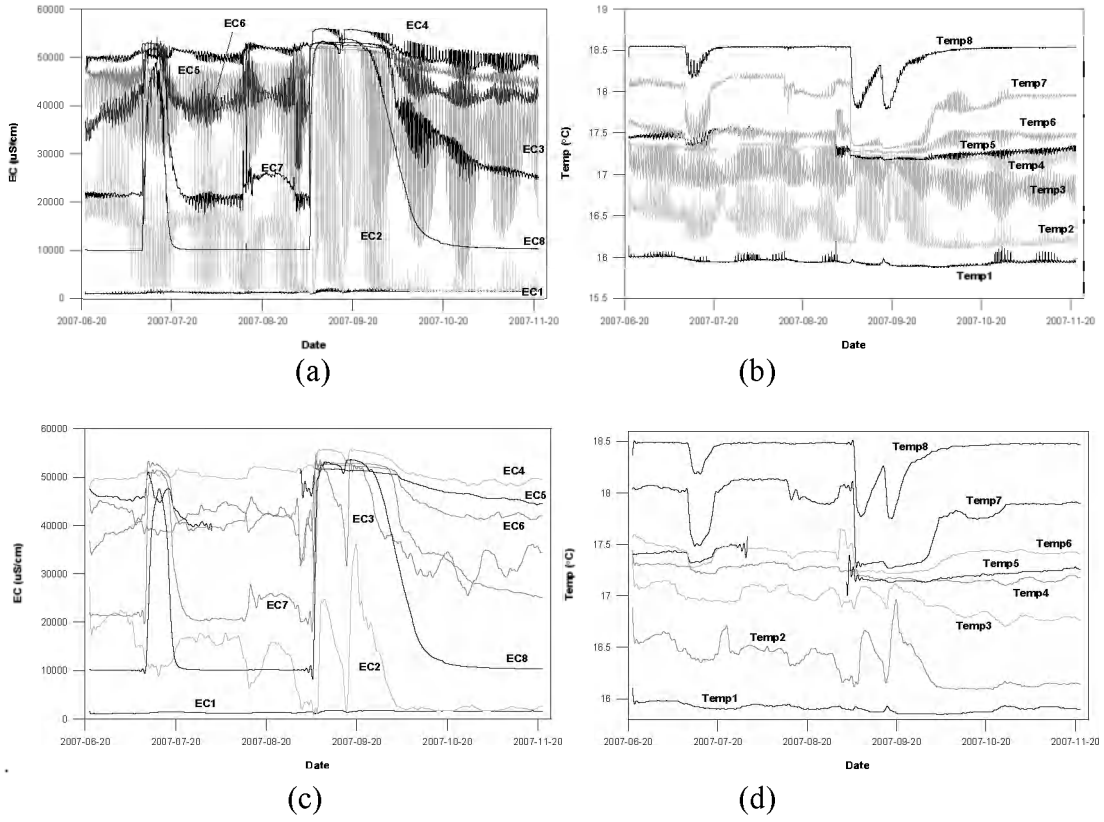

Figure 2. Time series data of EC (a) and temperature (b) at the SS-1 monitoring well and low-pass filtered signals from the EC (c) and temperature data (d).

EC and temperature data

The observed data from SS-1 monitoring well showed a dynamic variations of EC. EC at depth of -25 m showed ~1,000 μS cm^{-1} and did not responded to tide and rainfall while EC at depth of -30 m showed a wide range of EC variation fluctuating from 2,000 to 40,000 μS cm^{-1} due to tide. It is interesting to note that the range of EC variations increased at a range of 1,000 to 50,000 μS cm^{-1} after the 4^{th} heavy rainfall event. This implies that, in some cases, recharge strengthens the tidal effect on EC values. At SS-1 borehole, two distinctive interfaces appeared, one at around -30 m and the other at around -80 m. These interfaces relate well with the geology at this borehole; the location of interface matches good with the sedimentary layer. It is presumed that theses sedimentary layer takes a role as a confining layer and separates the hydraulic system into three zones in this coastal zone. These relationships between EC variations and geology show the importance of geology in fresh-saline water interactions in coastal zone.

CONCLUSIONS

This study elucidated some cases of dynamic variations of fresh-saline water interactions at coastal aquifers around Jeju Island. We set up multi-depth monitoring system at five boreholes to obtain time-series data of EC and temperature at various depths. The EC and temperature varied mainly by two external forces, tidal fluctuation and rainfall. The influence of heavy rainfall events on EC and temperature was analyzed by applying digital filter. Time series data of EC and temperature at various depths enabled us to quantify the interactions between freshwater and saline water in coastal aquifers and multi-depth monitoring system come out to be a powerful tool for examining fresh-saline water interaction process in coastal zone. As the monitoring wells were screened over the entire interval, there may be some effect of long screen that may cause mixing within the borehole. Considering the effect of long-screen is needed in the future study.

REFERENCES

Kim, K.-Y., C.-M. Chon, K.-H. Park, Y.-S. Park, and N.-C. Woo. 2008. Multi-depth monitoring of electrical conductivity and temperature of groundwater at a multilayered coastal aquifer: Jeju Island, Korea. Hydrological Processes, in print.

Kim, K.-Y., H. Seong, T. Kim, K.-H. Park, N.-C. Woo, Y.-S. Park, G.-W. Koh, and W.-B. Park. 2006. Tidal effects on variations of fresh-saltwater interface and groundwater flow in a multilayered coastal aquifer on a volcanic island (Jeju Island, Korea). Journal of Hydrology 330: 525-542.

Contact Information: Kue-Young Kim, Groundwater & Geothermal Resources Division, Korea Institute of Geoscience and Mineral Resources, Gajeong-dong 30, Yuseong-gu, Daejeon, Repbulic of Korea,
Phone: +82-42-868-3053, Fax: +82-42-868-3414, Email: kykim@kigam.re.kr

Analytical Benthic Flux Model Forced by Surface-Water Waves: Application to the South Atlantic Bight, USA

Jeffrey N. King
Florida Integrated Science Center, U.S. Geological Survey, Fort Lauderdale, FL, USA

ABSTRACT
Benthic flux is the flow rate per unit area of some physical, chemical, or biological property across the sediment-water interface (bed) of a water body. Riedl et al. (1972) used Reid and Kajiura's (1957) classic solution for the damping of a linear, surface-water wave by an infinitely deep, rigid, porous medium, to develop an analytical expression for benthic water flux forced by surface-water waves. The objectives of this work are to: (1) re-cast the Riedl et al. (1972) solution to observe Reid and Kajiura's (1957) use of a complex wave number; (2) detail an example calculation using Moore's (1996) South Atlantic Bight (SAB) study area; and (3) suggest that benthic discharge flux forced by surface-water waves explains Moore's (1996) observation of excess ^{226}Ra on the inner shelf of the SAB.

INTRODUCTION
Benthic flux (q_{bf}) is a vector quantity, oriented normal to a sediment-water interface. A benthic recharge flux (q_{br}) vector is oriented from a surface-water body toward the underlying porous medium; a benthic discharge flux (q_{bd}) vector is oriented from the porous medium toward the surface-water body. The units of q_{bf} depend on the flux property; for example, $[L^3T^{-1}L^{-2}=LT^{-1}]$ for a benthic volume flux or $[MT^{-1}L^{-2}]$ for a benthic mass flux, where L, M, and T are length, mass, and time dimensions, respectively. Various potential gradients across the sediment-water interface force q_{bf}. For example, a concentration gradient forces a Fickian diffusive benthic flux, and a pressure gradient forces an advective benthic flux. Benthic flux occurs in palustrine, lacustrine, riverine, estuarine, and marine environments. Related terms exist in the literature; for example, submarine ground-water discharge is a benthic discharge flux of water ($q_{bd,w}$) to an overlying marine water body, and the sub-tidal pump is a benthic flux of water ($q_{bf,w}$) forced by surface-water waves. Geographically constrained variations in porous-medium and surface-water characteristics govern q_{bf}. For example, Moore and Wilson (2005) explain that tidal pumping, episodic storm events, and leakage from underlying geologic units mix surface and pore water in the South Atlantic Bight (SAB). Precht et al. (2004) describe sediment oxygen dynamics forced by the interaction of wave-generated currents on a rippled flume bed.

FORMULATION
Reid and Kajiura (1957) solved a two-dimensional, x-z oriented, boundary value problem in which a linear surface-water wave of deep-water amplitude a_0 and period T, propagates through a domain described by Cartesian space dimensions x and z, where z is parallel to the gravity (g) vector. The surface-water wave generates pressure gradients in both the water column and the underlying rigid, porous, isotropic medium of permeability k. The water has density ρ, dynamic viscosity μ, and kinematic viscosity ν. The mean water surface is located at z=0; the sediment-water interface at z=-h; wave inception is in deep water, at x=0; the displacement η of the water surface in response to the wave is described by $\eta = a_0 e^{i(\lambda x - \sigma t)}$, where σ=$2\pi/T$ is the angular frequency of the wave, λ=λ_r+$i\lambda_i$ is a complex wave number with real λ_r and imaginary λ_i components, $i = \sqrt{-1}$, and t is time. The governing equations require that the Laplacian ∇^2 of the velocity potential $\phi(x,z,t)$ in the surface-water domain and pressure $p(x,z,t)$ in the ground-water domain equal zero ($\nabla^2\phi = 0$ and $\nabla^2 p = 0$). Reid and Kajiura (1957) employ four

boundary conditions: a dynamic free-surface boundary condition $g\eta = \partial\phi/\partial t$ at z=0; a kinematic free-surface boundary condition $w = \partial\phi/\partial t$ at z=0, where w is the vertical velocity component; a dynamic interface boundary condition p_s=p at z=-h, where subscript $_s$ denotes the value in the porous domain, and an absence of the subscript denotes the value in the surface domain; and a kinematic interface boundary condition w_s=w at z=-h. Reid and Kajiura (1957) assume solutions of the following form:

$$\phi = \left[A\cosh(\lambda h + \lambda z) + B\sinh(\lambda h + \lambda z)\right]e^{i(\lambda x - \sigma t)} \quad (1)$$

$$p_s = Ce^{\lambda h + \lambda z}e^{i(\lambda x - \sigma t)} \quad (2)$$

where A, B, and C are unknowns, and $w_s = 0$ at $z = -\infty$. Reid and Kajiura (1957) use the following relationships at $z = -h$: the Bernoulli Equation $p = \rho\,\partial\phi/\partial t$, the definition of velocity potential $w = -\partial\phi/\partial z$, and Darcy's Law $q_{bf.w} = w_s = -(k/\mu)\partial p_s/\partial z$, with the above-described boundary conditions to solve for A, B, C and λ. It can then be shown (King, 2007) that

$$\boxed{q_{bf.w} \approx -\hat{A}\left[\cos(\lambda_r x - \sigma t) - \beta\sin(\lambda_r x - \sigma t)\right]} \quad (3)$$

where $\hat{A}$ is the amplitude of $q_{bf.w}$, β is a $q_{bf.w}$ amplification parameter,

$$\hat{A} = kg\lambda_r a_0 e^{-\lambda_i x}/\left[\nu\cosh(\lambda_r h)\right] \quad (4)$$

$$\sigma^2 \approx g\lambda_r \tanh(\lambda_r h) \quad (5)$$

$$\lambda_i \approx 2R\lambda_r/\left[2\lambda_r h + \sinh(2\lambda_r h)\right] \quad (6)$$

$$R = \sigma k/\nu \quad (7)$$

$$\beta = \tanh(\lambda_r h)(R - \lambda_i h) + \lambda_i/\lambda_r \quad (8)$$

This formulation of Reid and Kajiura's (1957) solution includes wave damping. The Riedl et al. (1972) formulation does not include wave damping, but does include a bed slope term. Equation 4 is equivalent to the Riedl et al. (1972) amplitude, where the decayed, deep-water, wave amplitude $a_0 e^{-\lambda_i x}$ in the current formulation is replaced by a local wave amplitude a, such that $a = a_0 e^{-\lambda_i x}$. Benthic water flux in both formulations integrates to zero over one wave period, such that $\int_t^{t+T} q_{bf.w}\,dt = 0$. Gross $q_{bd.w}$ at any point, averaged over the wave period ($\overline{q}_{bd.w}$), is

$$\overline{q}_{bd.w} \approx (1/\sigma T)\int_{t+\sigma T/4}^{t+3\sigma T/4} q_{bf.w}\,dt = \hat{A}/\pi \quad (9)$$

where β is small (β<0.1) and $\eta/a = 1$ at $\lambda_r x - \sigma t = 0$. The current formulation utilizes the wave-generated pressure gradient across a planar bed to yield Equation 3. This pressure gradient is a function of the permeability of the porous medium that constitutes the planar bed, but not a function of bed roughness. Investigations—such as Precht et al. (2004)—of wave-generated currents interacting with a rippled bed address a related but different process, in which q_{bf} is a function of bed roughness.

APPLICATION

Riedl et al. (1972) detail parameters necessary to apply Equation 9 to Moore's (1996) study area (the inner shelf of the SAB, from shore to 20*km* offshore, over a 320-*km*-long section of coast, from the Savannah River to Cape Fear). Specifically, $0 < h < 18m$; $9.9\times10^{-12}m^2 < k < 2.0\times10^{-11}m^2$; and wave spectra, which show that $T < 6s$ more than 50% of the time. Assuming $k=10^{-11}m^2$, $\nu=1.17\times10^{-6}m^2/s$, $T=5.5s$, and $a_0=0.5m$ at $X=20km$ in Moore's (1996) study area, where X is a shore-normal distance ($X=0m$ at shore), then $\overline{q}_{bd.w}$ integrated over the study area ($\overline{Q}_{bd.w}$) is

$$\overline{Q}_{bd.w} = \iint \overline{q}_{bd.w}\,dydX = \int_{10m}^{20km}\int_{0}^{320km} \frac{\hat{A}}{\pi}\,dydX \approx 8{,}100\,m^3/s \qquad (10)$$

where y is shore parallel. Bathymetric contours are assumed to be locally straight and parallel to the coast, and the wave field oriented such that it does not refract. A well-known wave breaking condition is assumed, where $2a/h > 0.78$. The wave shoals as a function of a_0, deep-water wave speed, and wave-group velocity; the wave damps as a function of λ_i and x; and $\beta<10^{-5}$ is small. Maximum $\hat{A}=1.3\times10^{-5}m/s$ occurs at $X=37m$, where the shoaled, damped wave breaks. Shore-proximate $\hat{A}=7.9\times10^{-6}m/s$ at $X=10m$; deep-water $\hat{A}=1.0\times10^{-6}m/s$ at $X=20km$; 99% of $\overline{Q}_{bd.w}$ is generated offshore of the break point at $X=37m$. If $T=6.0s$ and $a_0=0.55m$, then $\overline{Q}_{bd.w} \approx 9{,}500\,m^3/s$; if $T=5.0s$ and $a_0=0.45m$, then $\overline{Q}_{bd.w} \approx 6{,}600\,m^3/s$.

DISCUSSION AND CONCLUSIONS

Moore (1996) observed $0.19dpm/\ell$ average ^{226}Ra activity for inner-shelf surface waters, and suggested maximum contributions of 0.01 and $0.08dpm/\ell$ to the inner shelf from estuaries and the ocean, respectively. He determined that $2.1\times10^{11}dpm/d$ excess ^{226}Ra must then be explained by some other source, by assuming an inner-shelf volume of $6.4\times10^{13}\ell$ and a 30-day residence time for the unexplained $0.10dpm/\ell$ [from $(0.19 - 0.01 - 0.08)(6.4\times10^{13}) / 30 = 2.1\times10^{11}$]. Moore (1996) then assumed an inner-shelf, pore-water ^{226}Ra activity equivalent to an observed $7dpm/\ell$ ^{226}Ra activity for brackish ground water at North Inlet, South Carolina, to suggest that $Q_{bd.w} = Q_{Moore} = 3\times10^{10}l/d = 350m^3/s$ reasonably generates the $2.1\times10^{11}dpm/d$ excess ^{226}Ra $\left(2.1\times10^{11}/7 = 3\times10^{10}\right)$. Younger (1996) invoked a mass balance argument to suggest that benthic freshwater discharge to Moore's (1996) study area is approximately $14m^3/s$ (4% of Q_{Moore}). Li et al. (1999) identified two additional near-shore, physical processes capable of forcing $\overline{Q}_{bd.w}$: near-shore tidal pumping generates $\overline{Q}_{bd.w} = 130\,m^3/s$ (37% of Q_{Moore}), and wave set-up generates $\overline{Q}_{bd.w} = 190\,m^3/s$ (54% of Q_{Moore}). Li et al. (1999) suggest that $\overline{Q}_{bd.w}$ forced by wave set-up, tidal oscillation, and Younger's (1996) benthic freshwater discharge can be summed linearly, such that a composite $\overline{Q}_{bd.w}$ explains 95% of Q_{Moore}.

Moore and Wilson (2005) measured 1.3, 2.0, 3.5, and $8.0dpm/\ell$ pore water ^{226}Ra activity at 0.50, 1.00, 1.25, and 1.75*m* depths below the bed, on the outer edge of Moore's (1996) study area. Surface-water ^{226}Ra activity was $0.2dpm/\ell$. Based on these observations, Moore's (1996) $7dpm/\ell$ ^{226}Ra activity assumption may be high for inner-shelf pore water just below the bed. Assume $0.5dpm/\ell$ ^{226}Ra activity for inner-shelf pore water just below the bed and recognize that $\overline{Q}_{bd.w} = \overline{Q}_{br.w}$. Moore's (1996) implicit assumption that inner-shelf ^{226}Ra lost to q_{br} is small

compared to inner-shelf ^{226}Ra gained by q_{bd} is not appropriate in the current formulation, where surface-water and pore-water ^{226}Ra activity are of the same order of magnitude. Then, $\overline{Q}_{bd.w} = 2.1\times10^{11} dpm/d \div (0.5 dpm/\ell - 0.2 dpm/\ell) = 7\times10^{11}\ \ell/\text{d} = 8{,}100 m^3/s$. The $0.5 dpm/\ell$ ^{226}Ra activity is reasonable in that it agrees with Moore and Wilson (2005), is greater than surface-water activity but less than the activity in deeper portions of the sediment column. The linearly summed trio of near-shore forcing mechanisms examined by Li et al. (1999) and Younger (1996) then explain 334/8100=4% of the updated excess ^{226}Ra activity. The higher-magnitude $\overline{Q}_{bd.w} = 8{,}100 m^3/s$ forced by surface-water waves over the entire study area, detailed in Equation 10, with an updated pore water ^{226}Ra activity assumption, explains Moore's (1996) excess ^{226}Ra observation.

REFERENCES

King, J.N. 2007. Selective mechanisms for benthic water flux generation in coastal waters. University of Florida Dissertation, 231p.

Li, L., D.A. Barry, F. Stagnitti, and J.-Y. Parlange. 1999. Submarine groundwater discharge and associated chemical input to a coastal sea. Water Resources Research 35: 3253-3259.

Moore, W.S. 1996. Large groundwater inputs to coastal waters revealed by Ra-226 enrichments, Nature 380: 612-614.

Moore, W.S., and A.M. Wilson. 2005. Advective flow through the upper continental shelf driven by storms, buoyancy, and submarine groundwater discharge, Earth and Planetary Science Letters 235: 564-576.

Precht, E., U. Franke, L. Polerechy, and M. Huettel. 2004. Oxygen dynamics in permeable sediments with wave-driven pore water exchange. Limnology and Oceanography 49: 693-705.

Reid, R.O., and K. Kajiura. 1957. On the damping of gravity waves over a permeable sea bed, Transactions, American Geophysical Union 38: 662-666.

Riedl, R.J., N. Huang, and R. Machan. 1972. The subtidal pump: a mechanism of interstitial water exchange by wave action. Marine Biology 13: 210-221.

Younger, P.L. 1996. Submarine groundwater discharge. Nature 382: 121-122.

Contact Information: Jeffrey N. King, Florida Integrated Science Center, U.S. Geological Survey, 3110 S.W. 9th Avenue, Fort Lauderdale, Florida, 33315. E-mail: jking@usgs.gov

Dynamic Groundwater Equilibrium during a Base Level Drop: The Dead Sea Case

Y. Kiro[1,2], *Y. Yechieli*[1], *V. Lyakhovsky*[1], *E. Shalev*[1] and *A. Starinsky*[2]
[1]Geological Survey of Israel, Jerusalem
[2]Institute of Earth Sciences, The Hebrew University of Jerusalem

The effect of sea level changes on groundwater and sea water intrusion is of great importance in relation to global sea level changes and water resources management. The Dead Sea's rapid level drop due to human influences makes it a suitable place for studying such effects in the phreatic aquifer in its vicinity. The absence of tides and waves isolates the effect of the base level drop and seasonal changes. Furthermore, the rapid drop (1 m/yr) allows detecting the effect of the level changes on the groundwater levels and the transition zone between the fresh and saline water in a relatively short period.

During the past few years the groundwater level and transition zone were monitored in the Dead Sea region. A groundwater level drop was detected in most boreholes in the region ranging from 20% to 100% of the Dead Sea level drop rate [*Yechieli, et al.*, 2007]. The groundwater level in the specific study area (Wadi Arugot) has been dropping at the same rate as the Dead Sea level [*Kiro*, 2006], keeping the hydraulic gradient constant (Figure 1).The transition zone's general trend is downward, but seasonal changes in the Dead Sea level cause an upward movement of the transition zone in the winter (Figure 2).

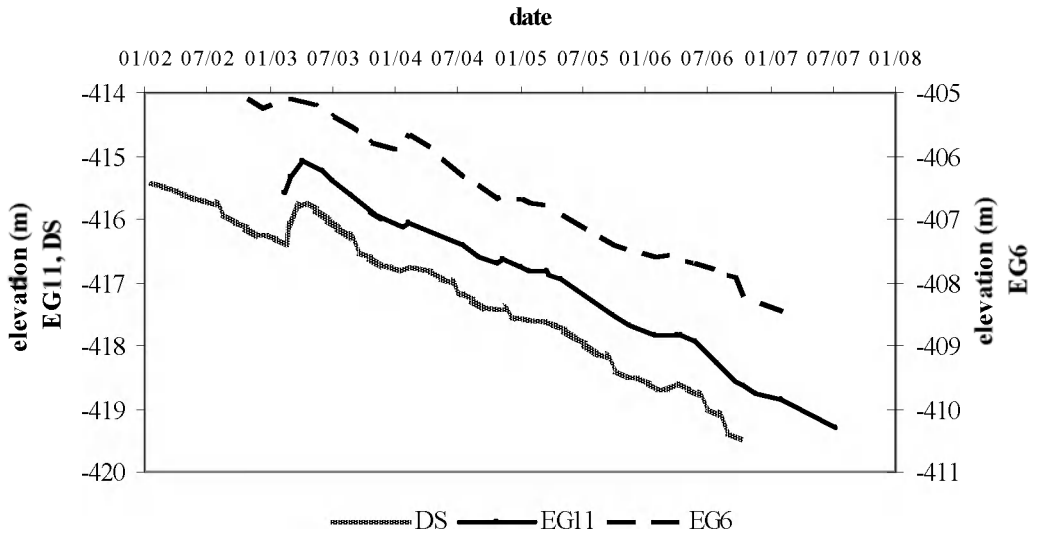

Figure 1. Groundwater levels measured in boreholes near the Dead Sea during recent years. EG11 is 100 meters from the shore and EG6 is 700 meters from the shore.

Theoretical analysis and simulations with the USGS SUTRA code [*Voss*, 1984] were done in order to understand the field data and define the parameters that effect the response rate of the groundwater system. The field data and the simulation show a difference between the groundwater level response and the transition zone response. Groundwater flow is defined by a diffusion equitation [*Bear*, 1979] and in general the time required to obtain equilibrium in a diffusion process is given by $t \propto L^2 / D$ [*Turcotte and Schubert*, 1982], where L[m] is a characteristic length and D[m^2/s] is the diffusion coefficient. The diffusion coefficient in a phreatic aquifer is n/T [*Bear*, 1979] where n is the porosity and T [m^2/s] is the transmissivity.

Therefore, the characteristic time of the groundwater level response should be proportional to the expression nL^2 / T.

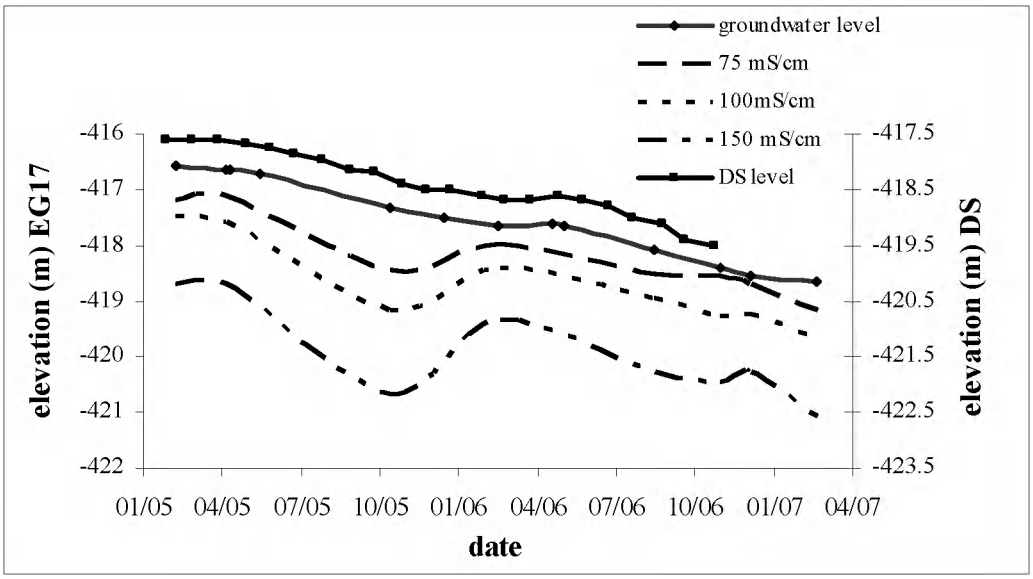

Figure 2. The transition zone between the fresh and saline water in a borehole located 200 ??? m from the Dead Sea shore (values are of electrical conductivity which represent salinity up to about half of that of the Dead Sea) . The transition zone moves downward during the Dead Sea level drop. Seasonal rises in the Dead Sea level cause an upward movement of the transition zone.

The transition zone response rate, however, is a function of the density gradient in a density-dependent flow [*Voss*, 1999]. Since the flow is almost lateral, there is a significant influence of the transition zone slope, which depends on the hydraulic gradient. Therefore, the transition zone response is a function of the groundwater level response and the hydraulic gradient.

According to these principles, we defined two characteristic times using simulations, analyzing the response of both the groundwater level and the transition zone to an instantaneous drop of a base level. These characteristic times are useful for understanding the equilibrium state of groundwater in the entire Dead Sea region and can be used with some modification in other system elsewhere.

The difference between the groundwater level characteristic time and the transition zone characteristic time creates different types of responses of the groundwater system:

- *Fast response of both the groundwater level and the transition zone* - both groundwater level and transition zone are close to equilibrium with the lake level.
- *Slow response of the groundwater and fast response of the transition zone*. The transition zone is always in equilibrium with the groundwater level. This response occurs in a relatively large hydraulic gradient.
- *Fast response of the groundwater level and slow response of the transition zone.* The transition zone becomes wider with time and is not in equilibrium with the groundwater level as occurs in the study area.

The second stage was to examine the response of the groundwater system to a continuous lake level drop represents the situation in the Dead Sea. Theoretically, a continuous lake level drop could be approximated as a sum of discrete instantaneous lake level drops. In this case, the

discharge increases gradually until it reaches a constant value, and a new dynamic equilibrium is attained (Figure 3). At this point, the groundwater level drops but the hydraulic gradient remains constant, as we see at some sites in the Dead Sea region. According to the simulations, the saline water initially flows toward the lake, but after a period of time the saline water circulation tends to return (as occurs in steady-state).

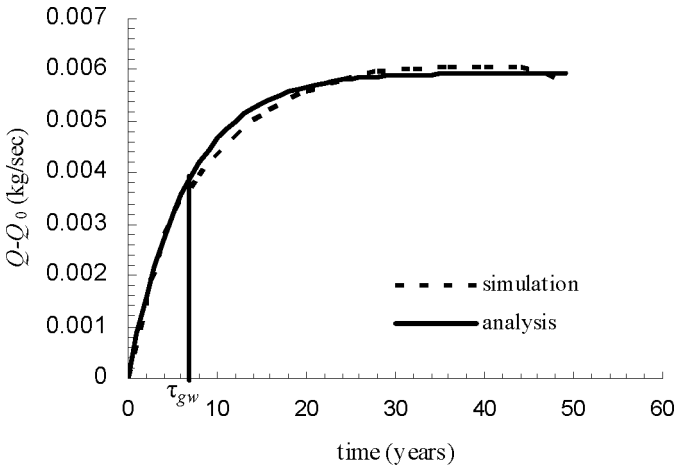

Figure 3. Discharge to the lake during a lake level drop. The discharge attains a constant value after a certain period of time.

The vertical movement of the transition zone that results from the lake level drop causes a widening of the transition zone due to the vertical effect of the longitudinal dispersivity. Hence, the bathymetry affects the thickness of the transition zone during the drop of the lake level. A high boundary slope will cause a thicker transition zone.

The response rate of the groundwater around the Dead Sea can be useful for parameter estimation, which can be achieved by calculating the characteristic times. On the other hand, calculating the characteristic times in a given location can give a good estimation of the equilibrium state in that location.

REFERENCES

Bear, J. (1979), *Hydraulics of Groundwater*, 569 pp., McGraw-Hill, New York.

Kiro, Y. (2006), The effect of the Dead Sea level drop in the past 50 years on the groundwater system in the alluvial aquifer in its vicinity, MSc thesis, 116 pp, The Hebrew University of Jerusalem.

Turcotte, D. L., and G. Schubert (1982), *Geodynamics: Applications of Continuum Physics to Geological Problems*, 450 pp., J. Wiley, New York.

Voss, C. I. (1984), SUTRA: Finite-element simulation model for saturated-unsaturated, fluid-density-dependent groundwater flow with energy transport or chemically-reactive single-species solute transport, Water Resources Investigations Report, 299 pp, U.S. Geological Survey.

Voss, C. I. (1999), *USGS SUTRA Code - History, Practical Use, and Application in Hawaii*, 625 pp., Kluwer Academic Publishers, Dordrecht.

Yechieli, Y., E. Shalev, and H. Hemo (2007), Groundwater levels in boreholes in the Dead Sea region - sinkholes project, TRI-GSI/09/2007, Geological Survey of Israel, Jerusalem.

Contact Information: Y. Kiro, Institute of Earth Sciences, Givat Ram Campus, The Hebrew University, Jerusalem, 91904, Israel, Phone: +972-2-6584053, Email: yael.kiro@mail.huji.ac.il

The Use of Mapping the Salinity Distribution Using Geophysics on the Island of Terschelling for Groundwater Model Calibration

Michel Groen[1], ***Arjen Kok***[2], *Kees Jan van der Made*[3] and *Vincent Post*[1]
[1]VU University Amsterdam, Faculty of Earth and Life Sciences, Amsterdam, The Netherlands
[2]Vitens, Water supply company, Leeuwarden, The Netherlands
[3]Wiertsema & Partners, Consultants, Tolbert, The Netherlands

GENERAL

The island of Terschelling is situated in the Wadden Sea in the northern part of The Netherlands. It measures 30 km by 3 km. An extensive belt of coastal dunes extends along the north and west sides of the island, which is vegetated mainly by dune shrubs and pine trees. South of the dunes is an agricultural area (indicated as "polder" area) where water levels are artificially maintained. These water levels are lower than the groundwater table in the dunes so there is a steady flow (ground- & surface water) towards the polder-area and the North Sea.

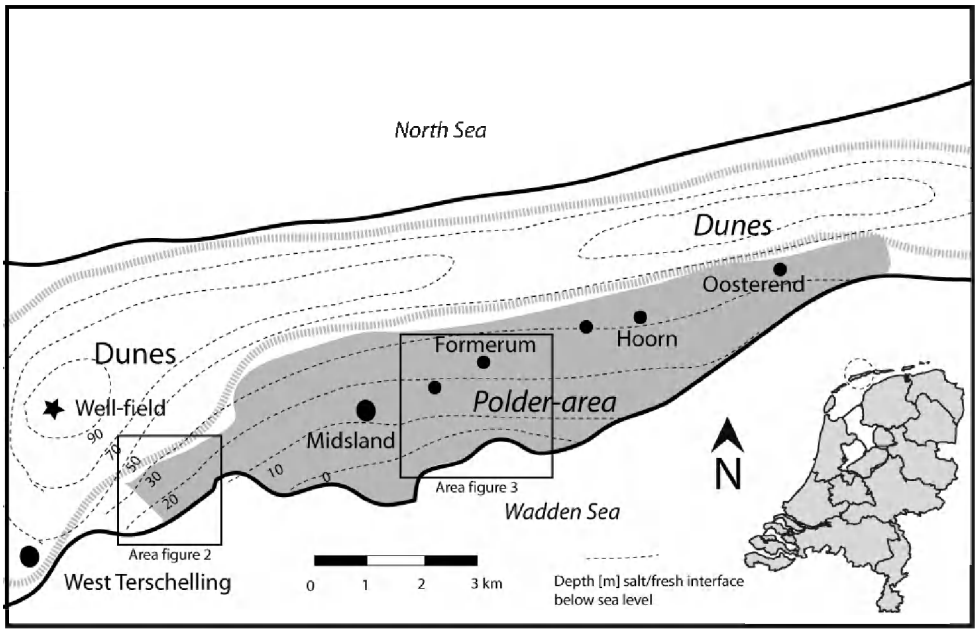

Figure 1. Overview island Terschelling

The island is a popular holiday destination and the demand for drinking water is strongly related to the number of tourists on the island, which peaks during summer time. The annual water consumption averages 550,000 m^3/year. Approximately 200,000 m^3 /year is produced annually by the well field that withdraws groundwater from the fresh water lens in the western part of the dune area (see Figure 1) and circa 350,000 m^3/year is delivered to the island by a pipeline from the main shore. In 2006 Vitens (water supply company) has started a pilot study to investigate if a self supporting and sustainable water supply on the island is possible. One of the options to be considered is to increase the abstraction of fresh groundwater in the dunes or polder area. A groundwater model is being developed to assess the feasibility of various design alternatives, the risk of salinization and the potential ecological consequences for dune slacks. In order to calibrate the groundwater model sufficient data are required regarding the distribution of fresh and saline groundwater on the island as well as the presence of confining strata. An intensive field campaign was launched to collect the required data. Geophysical methods (based on resistivity) combined with cone penetration tests (CPT's) were used to map both the groundwater

salinity and lithology. In the polder area the sediments in the upper 5 meters of the subsurface consist of tidal flat and salt marsh deposits composed of clay, silt and sand of Holocene age. These deposits partly extend below the present dune belt. The sediments below the Holocene strata predominantly consist of Pleistocene coarse sands of fluvial origin. Intercalations of silt, peat, loam and clay layers can occur at various depths in a very irregular fashion. Standard DC geo-electrical investigations during the 1960's have shown that a fresh water lens with a maximum thickness of 100 meters has developed in the dune area Hoogervoorst (1970). Also the location of a fresh and saltwater interface in the "polder area" was interpretated. The fresh water lens is recharged by rainwater infiltrating in the dune area.

METHODOLOGY

According the measurements, carried out in the 1960's, part of the fresh groundwater flows towards and underneath the polder area. Prior to the field campaign the existing geo-electrical measurements by Hoogervoorst were critically re-evaluated to obtain a general overview of the resistivity distribution of the subsurface below the island. The fresh and salt water interface seemed to be more complicated than the interpretation's in the sixties. Based on this information, a number of 400 m transects were selected for continuous 2 dimensional vertical electrical soundings. The soundings were carried out using an ABEM terrameter SAS-4000 with an array of 64 electrodes in a Wenner configuration was used, resulting in a depth of investigation of approximately 70 m. In order to get a good lateral resolution more than 500 electrode combination are measured in one profile. Due to terrain conditions, time-domain electromagnetic measurements were used in the dune area using a Zonge zerotem system with a square transmitter and receiver loop with a surface area of 1600 meters and 400 meters, respectively. To minimize equivalence problems during the interpretation of the CVES (Continuous Vertical Electrical Sounding) to overcome similarities in resistivity of different lithologies, 33 cone penetration tests with a conductivity probe were conducted in the polder area and at the beach. With the standard truck mounted 20 ton hydraulic system a maximum depth of 32 meters was reached. These CPT-measurements provided ground-truth measurements of the subsurface resistivity and information about the lithology.

RESULTS OF THE FIELDWORK

With the 33 CPT's and the 10 CVES-profiles it was established that rapid changes of water quality and lithology occur in the polder area. The depth of the salt / fresh interface in this area varies between zero tot 50 m. The CPT measurements provided valuable detailed information regarding lithology and conductivity and facilitated the interpretation of the CVES-profiles. The general pattern is that the depth of the interface between fresh and salt groundwater is deepest below the coastal dune and decreases towards the south in the polder area (Figure 2).
The survey revealed unexpected new insights in the groundwater system. At certain locations in the polder area, for example south of the village of Landerum, the interface is much shallower than expected (figure 3). This phenomenon is related to the presence of tidal channels up to 500 years ago, before the present polder was established.

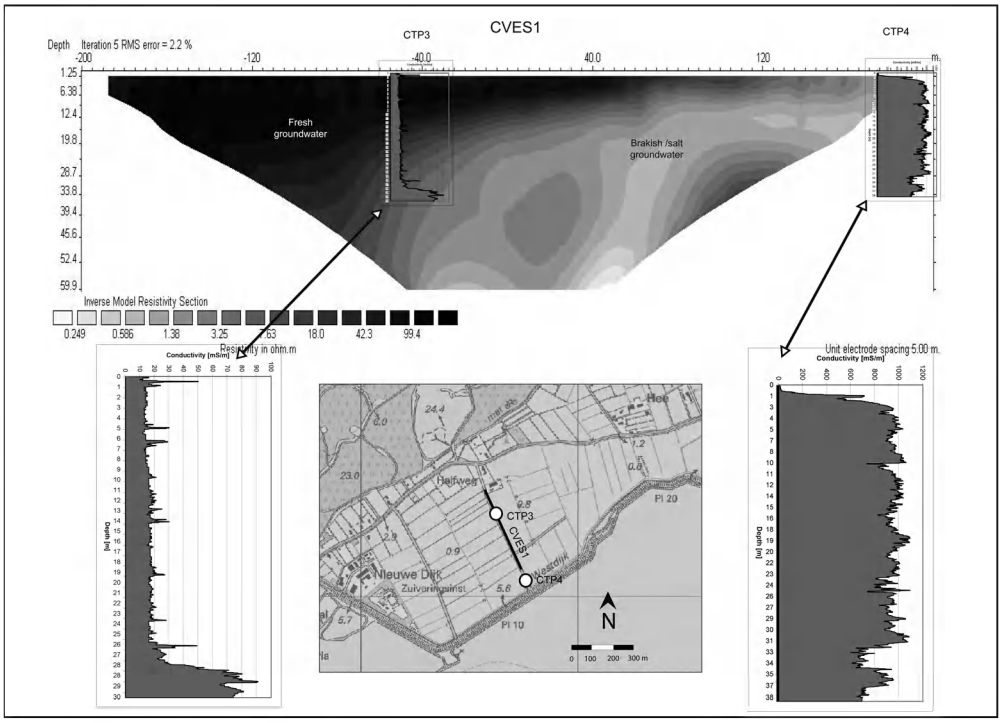

Figure 2. North-South transect in the polder area showing the resistivity distribution as measured with the CVES and the conductivity with depth at two locations along the CVES transect as measured with a conductivity probe.

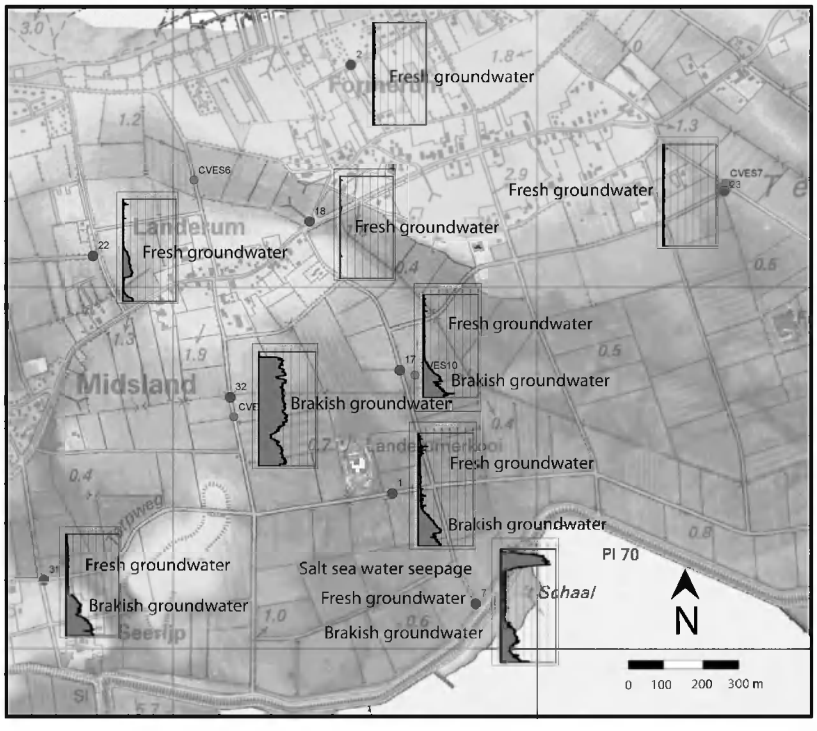

Figure 3. CPT-Resistivity graphs in the polder area.

The pattern of the depth of the interface is in these areas is much more complicated then was previously calculated with MODFLOW and the SWI- package. The newly obtained information about the lithology, and water quality was used to improve the calibration of the groundwater model. This resulted in a better fit with reality and therefore should also result in a more realistic prediction of the effects of possible activities.

In the dune area the fresh – saltwater interface lies too deep to measure with standard CPT's. The 5 TDEM measurements showed that the depth of the interface varies between 70 and 90 m below mean sea level. These values corroborated the existing information from geophysical borehole logs and water quality data. Because of the high resistivity contrasts less equivalence problems were expected and encountered in the interpretation of the TDEM measurements so that the depth of the interface could be established with a high degree of certainty.

The CVES and CPT measurements that were carried out on the beach at low tide revealed the occurrence of fresh groundwater below a 15 m thick layer of saline groundwater, up to 60 meters below sea level at the low water line. Similar results were found by De Panne and Wassenaar along the coast of Belgium and the western part of the Netherlands. Further investigations will be carried out to establish if this fresh water lens is part of the present hydrological system or a relic of the former fresh water lens that became submerged by the sea as the island migrated south in this highly active sedimentary environment.

CONCLUSION

In sandy areas with a shallow fresh/salt interface geo-electrical measurements combined with cone penetration tests with a conductivity probe, can provide detailed relevant information within a couple of days. The information obtained regarding lithology and groundwater quality is much more detailed than what can be obtained in a field campaign based on drilling with the same budget. The combination of CVES method and the CPT's proved to be an excellent method to map lateral changes. The problem of equivalence can be solved and therefore changes due to water quality can be distinguished from changes in lithologie. This detailed information can be used to improve the calibration of groudwatermodels used for predicting the effects of possible activities on the location of fresh and saltwater interfaces.

REFERENCES

Hoogervorst, G.H.T.C. 1970. Het geo-elektrisch onderzoek naar de diepte van het zoetwater voorkomen op het eiland Terschelling. Afdeling geofysica en hydrologie Rijksuniversiteit Leiden

Vandenbohede A. and L. Lebbe .2006. Occurrence of salt water above fresh water in dynamic equilibrium in a coastal groundwater flow system near De Panne, Belgium. Hydrogeology Journal 14, nr 4, 462-472

Post, V, Groen, M. Groen, J. Kooi. 2007. Using seaborne TDEM measurements to detect the offshore extension of fresh groundwater systems. XXXV IAH congress, Lisbon

Contact Information: Arjen Kok, Vitens, department Water technology, PO-box 1090, 8200 BB Lelystad, The Netherlands. Phone: ++31582945423, Email: arjen.kok@vitens.nl

Numerical Simulation of a Coastal Aquifer in Rhodes Island

Georgios Kopsiaftis and *Aristotelis Mantoglou*
Department of Rural and Surveying Engineering, National Technical University of Athens, Greece

ABSTRACT
Numerical models are developed and applied to a heterogeneous unconfined coastal aquifer located at the northern part of Rhodes Island in Greece. An initial single phase flow model is used to determine the aquifer hydraulic conductivities using PEST algorithm. Then a more complex three-dimensional variable density mass transport model is developed based on finite elements and FEFLOW. The estimated piezometric head distribution is identical for both single flow and mass transport model, except in a narrow region near the coast.

INTRODUCTION
Rhodes is a very touristy island of the South-Eastern Aegean Sea. The available water resources are limited, while water demands are very high, especially during summer months. Therefore, reliable aquifer models are needed in order to manage island water recourses and to determine their vulnerability on future water balance changes. The primary goal of this study is to develop such model for the most important aquifer of the island. Since no field data concerning the aquifer parameters are available, an initial calibration is performed. Parameter estimation using variable density models is a complex and data demanding procedure. Therefore, an attempt is made to calculate the basic parameters (hydraulic conductivities), using a single phase flow model.

COASTAL AQUIFER MODELS
Two single phase models are investigated and their results are compared to a complex variable density model. The first single phase flow model is a 3-D layered model which uses a depth dependent freshwater head along the sea boundary, (Iribar *et al*, 1997). The equivalent freshwater hydraulic head at elevation z above the datum is given by $h_f = (1+\alpha)h - \alpha z$ where $a = (\rho - \rho_f)/\rho_f$ and h is the head (Guo & Langevin, 2002), (ρ is saline groundwater density and ρ_f is freshwater density). This boundary condition allows reversing of flow direction from the sea towards the land at the lower parts of the aquifer.

The second flow model is based on the sharp interface model described in Mantoglou *et al* (2004), which is based on a 2D Strack solution.

The coupled fluid flow – mass transport model is governed by the following equations (Diersch & Kolditz, 1998), ($i, j = 1,2,3$, and Einstein summation convention is used):

$$S_h \frac{\partial h}{\partial t} + \frac{\partial q_i}{\partial x_i} = Q_\rho + Q_{EB}(C), \quad \text{(continuity equation)} \tag{1}$$

$$q_i = -K_{ij} f_\mu \left(\frac{\partial h}{\partial x_j} + \frac{\rho - \rho_0}{\rho_0} e_j \right), \quad \text{(Darcy equation)} \tag{2}$$

$$\frac{\partial}{\partial t}(nC) + \frac{\partial}{\partial x_i}\left(q_i C - D_{ij} \frac{\partial C}{\partial x_j} \right) - Q_C = 0, \text{(transport equation)} \tag{3}$$

$$\rho = \rho_0 \left\{ 1 + \frac{\bar{\alpha}}{(C_s - C_0)} (C - C_0) \right\}, \quad \text{(fluid density)} \qquad (4)$$

where h is the hydraulic head, q_i is the Darcy fluid velocity vector, C is concentration of salt, S_h is specific storage coefficient, Q_ρ is a fluid source/sink, Q_c is contaminant mass source/sink, Q_{EB} is a term related to Boussinesq approximation (see Diersch & Kolditz, 1998), K_{ij} is the aquifer hydraulic conductivity tensor, f_μ is a constitutive viscosity relation function, e_j is the gravitational unit vector, ρ, ρ_0 are the fluid and reference fluid density respectively, n is the aquifer porosity, D_{ij} is the hydrodynamic dispersion tensor, and C_0, C_s are reference and maximum concentration, respectively. For each time step, the coupled system of flow and transport equations is solved numerically and the resultant concentration is used to calculate the density and Darcy velocity. Changes of viscosity are not considered here and it is assumed that $f_\mu = 1$. A constant mass concentration $C(x_i, t) = C_s$ and a similar head distribution $h_f = (1+\alpha)h - \alpha z$ described above are used at the saltwater boundary. The differential equations are solved numerically using FEFLOW package based on finite elements.

RHODES ISLAND CASE STUDY

The aquifer is located at the northern part of Rhodes Island and is of considerable size (400km^2). The aquifer geology is characterized by a complex geological and hydrolithological structure. Figure 1 shows the aquifer location along with a piezometric map produced by the variable density model as discussed below. Since the aquifer is quite large, the area within the frame is magnified in the following figure, to provide a more detailed preview of the final results. The dominant tectonic unit of the studied area consist of gravely-sandy, marly-sandy and conglomerate facies, while some areas consist of psephitic, psammitic and pelitic clastic deposits, and of bioclastic limestone. A limestone formation appears at the central region of the aquifer with a general NE – SW direction, due to a rift zone action.

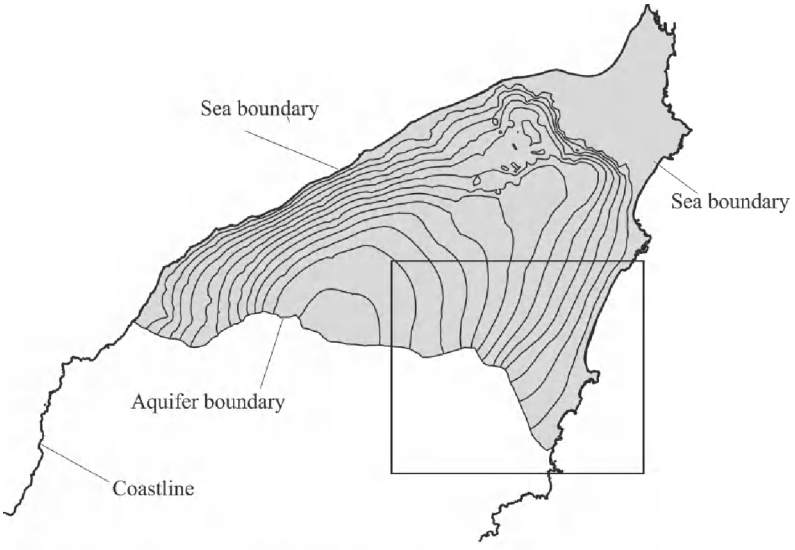

Figure 1. Rhodes Island aquifer with a piezometric map.

Due to lack of sufficient borehole data, the aquifer depth is not known exactly. For this reason a sensitivity analysis is performed for aquifer depths of 100m, 120m and 150m indicating a strong dependence of the results on the aquifer depth. For the current study the aquifer depth is assumed at 100m below sea level. Further field study would provide more data regarding the aquifer geometry.

The aquifer hydraulic conductivity is first calibrated against historic hydrological and piezometric data. The aquifer area is divided into several small hydrological basins and a uniform recharge is assigned in each basin, recommended by previous studies. The 3-D single phase model discussed above, based on vertically distributed freshwater head along the sea boundary, is selected for estimation of hydraulic conductivities. A zonation parameterization and the PEST algorithm are utilized to estimate the hydraulic conductivity values. Based on hydrolithologic data the aquifer is divided into six zones. Measured piezometric data are used to perform calibration. The calibrated model is able to follow the measured data very well.

Using calibrated hydraulic conductivities, a comparison between the 3-D single phase flow model, the 2-D sharp interface model of Mantoglou *et al* (2004) and the 3-D variable density model is performed next. The values of the remaining aquifer parameters required by the 3-D variable density model are obtained from previous studies and literature. The final simulation results are shown in Figure 2, and depict an almost identical piezometric head distribution for the three models.

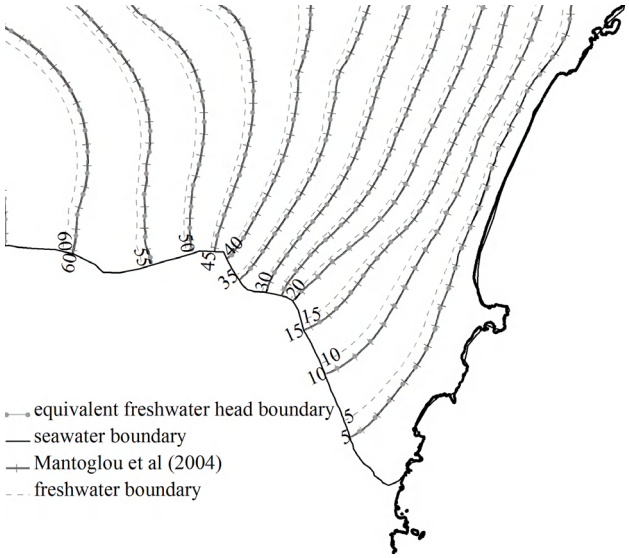

Figure 2. Comparison of piezometric heads produced by different models

Notice that some modellers use simple 2-D single phase flow models using a freshwater boundary condition at the sea. This results in considerable decrease of hydraulic heads, since a reduced resistance is imposed on freshwater discharge to the sea. In order to illustrate this, Figure 2 compares the results of the three modelling approaches described above, to the simplified 2-D single phase model. Notice that while the three modelling approaches presented here produce essentially similar hydraulic heads, the 2-D model based on freshwater boundary condition produces significant error.

DISCUSSION AND CONCLUSIONS

A 3D variable density model is developed for a Rhodes Island aquifer and compared to a 3-D single flow model and a sharp interface model. The results indicate that in this aquifer, which is of considerable size and the transition zone is expected to be relatively narrow, the piezometric head of the aquifer depends mainly on head boundary conditions, while transport processes can be simplified except for a narrow zone near the sea. A 2-D model on the other hand, based on freshwater boundary condition produces significant error. Undergoing field work will provide more data concerning the aquifer geometry and parameters, in order to improve these models.

REFERENCES

Diersch, H.-J. G., and O. Kolditz, 1998. Coupled groundwater flow and transport: 2 Thermohaline and 3D convection systems, Adv. Water Resour., 21, 401-425.

Guo, W., C. D Langevin., 2002. User's guide to SEWAT: A Computer Program for Simulation of Three – Dimentional Variable – Density Ground - Water Flow, BOOK 6, Chapter A7, Techniques of Water – Resources Investigations of the U. S. Geological Survey, 7-18.

Iribar V., J. Carrera, E. Custodio, 1997. A. Medina, Inverse modelling of seawater intrusion in the Llobregat delta deep aquifer, Journal of Hydrology, 198, 226-244.

Mantoglou A., M. Papantoniou, P. Giannoulopoulos, 2004. Management of coastal aquifers based on nonlinear optimization and evolutionary algorithms, Journal of Hydrology, 297, 209-228.

ACKNOWLEDGMENT

This work was supported by Research Grant No. 65/1628, National Technical University of Athens.

Contact Information: Georgios Kopsiaftis, Department of Rural and Surveying Engineering, National Technical University of Athens, Heroon Polytechniou 9,15780 Zografou, Greece, Tel. +30(210)7722649, Fax: +30(210)7722632, Email: gkopsiaf@survey.ntua.gr | Aristotelis Mantoglou, Email: mantog@central.ntua.gr

Tidal Effects on Transient Dispersion of Simulated Contaminant Concentrations in Coastal Aquifers

Ivana La Licata[1], *Christian D. Langevin*[2], *Alyssa M. Dausman*[2] and *Luca Alberti*[1]
[1]D.I.I.A.R., Politecnico di Milano, Milan, Italy
[2]U.S. Geological Survey, Florida Integrated Science Center, Fort Lauderdale, FL, USA

ABSTRACT
Variable-density flow and transport models require extensive computational resources often resulting in lengthy runtimes, particularly for simulations that represent saltwater intrusion and tidal fluctuations. The majority of saltwater intrusion models do not explicitly represent tidal variations; instead, an average tidal level is assigned to the ocean boundary. By neglecting tidal fluctuations, errors may be introduced if a contaminant included in the simulation reaches the seawater/freshwater interface, and then discharges into the ocean. This paper presents multiple variable-density flow and transport simulations of a coastal aquifer. Each model is conceptually similar; however, tides are either neglected or explicitly included in the ocean boundary. An analysis was performed to determine if the effects of tides could be approximated in simulations with a constant ocean boundary by using apparent dispersivities. The apparent dispersivity value was calculated for each model cell using the velocity variations from the tidal simulation. The transport and discharge patterns of a contaminant plume were used to examine the accuracy of this approach. Use of apparent dispersivity in models with a constant ocean boundary seems to provide a reasonable approach for approximating tidal effects in simulations where explicit representation of tidal fluctuations is not feasible.

INTRODUCTION
Simulating variable-density flow and contaminant transport in coastal aquifers is intrinsically complex and computationally expensive when the effect of tides is included. Tidal variations necessitate the use of a short time step, resulting in substantial computational effort (Volker et al. 1998). The purpose of this paper is to investigate the influence of transient dispersion on the concentration distribution in a variable-density flow and transport model. Simulations with steady-state conditions are compared with simulations of transient flow that include tidal fluctuations in the ocean boundary. The simulations are simple two-dimensional cross-sectional models that explicitly represent coastal groundwater flow within the freshwater and saltwater transition zone. The work in this paper follows previous work from La Licata et al. (2007).

SIMULATIONS AND RESULTS
To analyze the influence of tidal fluctuations on contaminant transport, simulations that neglected (*No Tide*) and included (*Tide*) a tidally fluctuating ocean boundary were compared. *Tide* represents a 2-year simulation period using 3-hour stress periods (8 stress periods per tidal cycle). Longitudinal and transverse dispersivities were constant over the entire section (longitudinal dispersivity [α_L] = 10 m, transverse dispersivity [α_T] = 0.1 m). A contamination source, releasing a hypothetical pollutant, was located 75 m from the western border of the model domain. The constant-concentration cell representing the contaminant source was assigned an arbitrary concentration value of 100 kg/m^3. The contaminant was simulated as being conservative. Contaminant concentrations were compared for *Tide* and *No Tide* simulations to analyze the influence of tidal variations on the contaminant and salinity distributions. Differences are evident in the contaminant and salinity concentrations between *No Tide* and *Tide* (Figure 1). The tidally driven hydraulic transients in *Tide* increase the overall mixing resulting in a relatively broader saltwater/freshwater transition zone. The increased mixing in *Tide* also

caused contaminant concentrations near the ocean to be lower than for the *No Tide* simulation (Figure 1). Differences in contaminant concentrations between the two simulations were as high as 15% within the freshwater/saltwater transition zone (Figure 2a).

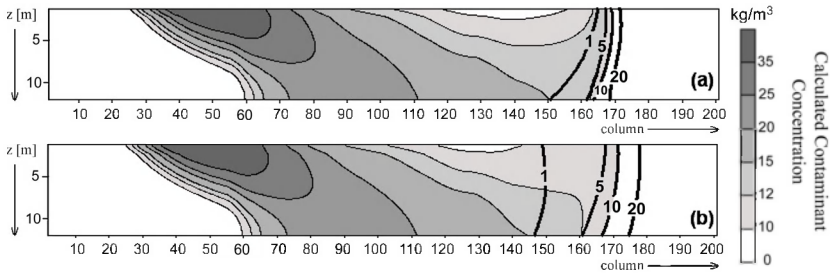

Figure 1. Overlap of calculated contaminant concentration on freshwater/saltwater interface in simulation: (a) without tides, *NO TIDE*, and (b) with tidal variations, *TIDE*. Dark black contours represent salinity isosurfaces in kg/m^3.

Simulations with spatially varying dispersivity values were performed with the *No Tide* model to determine if the mixing due to tidally driven hydraulic transients could be approximated with an increase in dispersivity. Additional details on this test are provided in La Licata et al. (2007). The dispersivity was increased in the area around the freshwater/saltwater transition zone where the hydraulic transients were greatest. With this change in the dispersivity value the difference in simulated contaminant concentration between cases with and without tides decreases to about 8% (Figure 2b). Results suggest that it may be possible to approximate tidal effects in a simulation without tides by spatially altering the dispersivity value. The error that occurs in the estimation of contaminant concentration near the ocean is a function of dispersivity corresponding to the location of the freshwater/saltwater transition zone.

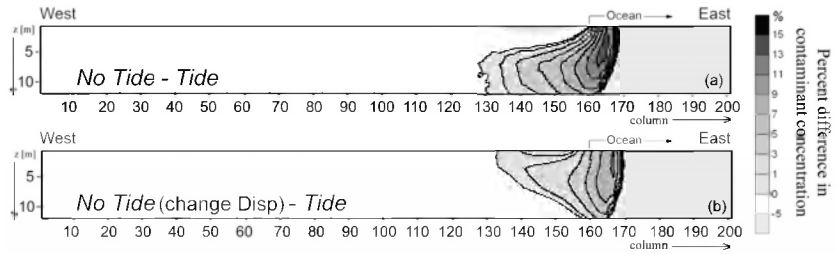

Figure 2. Percent difference in contaminant concentration (a) without and (b) with spatially varying dispersivity.

Goode and Konikow (1990) define apparent dispersivities as "those values that yield the best match or calibration of the solute transport model under steady state flow conditions to a plume that developed under transient flow conditions". The concept of transient dispersion is used here to test the hypothesis that the effects of tidal mixing can be included in a *No Tide* model by calculating and using apparent dispersivities. Apparent dispersivities for the longitudinal and transverse directions were calculated using the equations presented by Ackerer and Kinzelbach (1986). The distribution of apparent transverse dispersivity is shown in Figure 3; the distribution of apparent longitudinal dispersivity is not shown. The equations required the transient velocity variations at each model cell, which were taken from the *Tide* simulation. The following calculations were applied to each cell of the domain to calculate apparent longitudinal and transverse dispersivity values that characterize the velocity variation in that cell during one tidal cycle (8 stress periods). In the equations below, V is velocity, θ is the angle relative to the

horizontal, and α is dispersivity. With the exception of the large apparent dispersivities near the upper right corner of the model (which are due to boundary effects), the largest apparent dispersivities are located within the interface between freshwater and saltwater (Figure 3). This is an area where the velocity variations are the largest.

$$V_i = \left(V_{xi}^2 + V_{zi}^2\right)^{1/2}$$

$i = 1 \ldots 8$ *Stress Period*

$$\overline{V} = \frac{\Sigma V_i}{8}$$

$$\theta_i = \begin{cases} arctg(V_z/V_x) & Vx > 0 \\ arctg(V_z/V_x) + 180^\circ & Vx < 0 \end{cases}$$

$$\overline{\theta} = \frac{\Sigma \theta_i}{8}$$

$$\overline{\theta}_V = \theta_i - \overline{\theta}$$

$$V_{Li} = V_i \cos(\theta_V)$$

$$\overline{V_L} = \frac{\Sigma V_{Li}}{8}$$

$$\overline{V}_L^2 = \frac{\Sigma V_{Li}^2}{8}$$

$$V_{Ti} = V_i \, sin\left|\theta_{Vi}\right|$$

$$\overline{V}_T^2 = \frac{\Sigma V_{Ti}^2}{8}$$

$$\alpha_{La} = \frac{\alpha_L \overline{V}_L^2}{\overline{V}\,\overline{V_L}} + \frac{\alpha_T \overline{V}_T^2}{\overline{V}\,\overline{V_L}}$$

$$\alpha_{Ta} = \frac{\alpha_T \overline{V}_L^2}{\overline{V}\,\overline{V_L}} + \frac{\alpha_L \overline{V}_T^2}{\overline{V}\,\overline{V_L}}$$

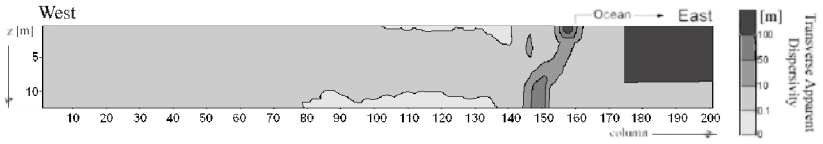

Figure 34. Calculated apparent dispersivity.

The contaminant concentration plume simulated under transient conditions is compared to the plume simulated with steady-state conditions using the apparent dispersivity distribution in Figure 3. The use of apparent dispersivities seems to provide a reasonable approximation of tidal effects. The maximum difference in simulated concentrations is still 15%, but for this simulation, the large differences are confined to areas where contaminant concentrations are relatively low (Figure 4).

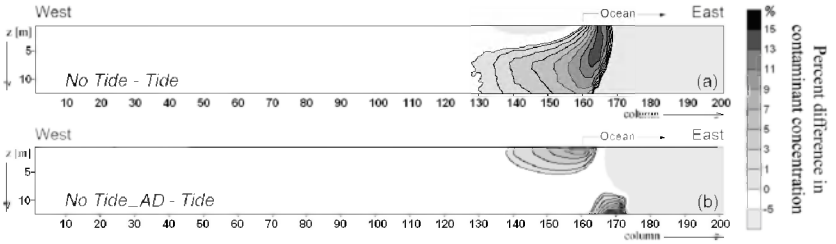

Figure 4. Percent difference in contaminant concentration with (a) constant dispersivity and (b) apparent dispersivity.

CONCLUSION

Simulations reveal that the mixing from tides results in a contaminant and salinity concentration distribution that is more mixed than the distribution for an equivalent steady-state model without tidal effects. These results could have critical implications for model calibration where erroneous adjustments to parameters may be required to match concentrations in a steady-state model because tides are not explicitly represented. Results also indicate that the mixing effects of tides can be represented in a steady-state model by arbitrarily increasing the dispersivity value in the area around the interface. A more rigorous approach based on the calculation and use of apparent dispersivity values provides a better method for including the effects of tidal mixing in a steady-state model. The apparent dispersivity distribution created and assigned to the steady-state model using the velocities from a transient model result in similar contaminant and salinity distributions between the two models. The calculated apparent dispersivity correction, therefore, appears to be

a practical way to replace tidal effects when calibrating a model. Using the concept of apparent dispersivity could save time and money in model development and calibration because the steady-state model does not require multiple stress periods; therefore, the model simulations require less time to run.

REFERENCES

Ackerer, P., and W. Kinzelbach. 1986. Modelisation du transport de contaminant par la méthode de marche au hasard - Influence des variations du champ d'écoulement au cours du temps sur la dispersion. In Proceeding of Stochastic Approach to Subsurface Flow Symposium at the International Association of Hydraulic Research, Montvillargenne, France. v. 1: 517-529.

Goode, D. J., and L. F. Konikow. 1990. Apparent Dispersion in Transient Groundwater Flow. Water Resources Research 26, no. 10: 2339-2351.

La Licata, I., C.D. Langevin, and A.M. Dausman. 2007. Effect of tidal fluctuations on contaminant transfer to the ocean. In Proceedings of A new focus on groundwater-seawater interactions, Perugia, Italy. 334-341.

Volker, R.E., B. Ataie-Ashtiani, and D.A. Lockington. 1998. Unconfined coastal aquifer response to sea boundary condition. In Proceedings of International Groundwater Conference, Melbourne, Australia. 771-777.

Contact Information: Ivana La Licata, Dipartimento di Ingegneria Idraulica Ambientale e del Rilevamento (D.I.I.A.R.), Politecnico di Milano, 20133 Milan, Italy, Phone: +39-02-23996654, Fax: +39-02-23996602, Email: ivana.lalicata@polimi.it

Assessment of Groundwater Resources in Rmel Coastal Aquifer (Morocco) by SEAWAT

A. Larabi[1], *M. Faouzi*[1] and *A. H. -D. Cheng*[2]
[1]LIMEN, Ecole Mohammadia d'Ingénieurs, Rabat
[2]Department of Civil Engineering, University of Mississippi, USA

ABSTRACT
The Rmel coastal aquifer is located in the north of Morocco, and is a part of the main sub-Atlantic coastal aquifers. The aquifer supplies good quality groundwater that is easily accessible. This favorable situation has increased pumping, and caused environmental problems, such as water table decline and salt water intrusion. For the purpose of planning and management, the SEAWAT, which is a variable density solute transport computer code, is used to study the groundwater quantity and quality. The simulation shows that in order to improve water quality, surface water recharge is needed.

INTRODUCTION
Groundwater quality in the Rmel aquifer is generally good. However, overexploitation due to agriculture activities has resulted in saltwater intrusion, which poses serious threat to future water supply. Hence, it is necessary to develop tools for predicting the response of coastal aquifers under different pumping scenarios. The objectives of this study is to develop a computer model that allows us to understand the conditions that govern the behavior of freshwater/saltwater transition zone in the coastal aquifer subject to the various input conditions, and to test management scenarios based on various economic assumptions. The best scenario will be presented to the regional water resources authorities for the recommended economic and water resources development.

DESCRIPTION OF THE RMEL AQUIFER
The Rmel is a part of the Moroccan coastal plain. It is located in the north of Morocco, to the south of the Larache city along the Atlantic coast, with an area of about 240 km^2, and length approximately 20 km. Climate in the region is semi-arid, but influenced by the Atlantic Ocean. The average mean temperature ranges from 24°C in summer to 12°C in winter. The average annual rainfall is around 700 mm, but most of the rainfall occurs in the period from October to April, and the rest of the year is almost completely dry. The annual mean of the evapotranspiration in the study area is estimated to be 500 mm/yr. The hydrogeology of the Rmel coastal aquifer consists of plio–quaternary sands and sandstone, but the bottom is composed of blue marls (Bentayeb, 1972).

Groundwater system characteristics
The regional groundwater flow is mainly SW-NE, discharging towards the Atlantic Ocean. However, due to groundwater pumping, the flow pattern is locally modified to the north, due to a cone of depression. The analysis of the piezometric records between 1980 and 2005 shows fluctuations due to surface water recharge from irrigation and pumping wells. The major source of renewable groundwater in the aquifer is rainfall and irrigation return flow. The total recharge to the aquifer is estimated to be 1,796 l/s, while the groundwater abstraction from the pumping wells was estimated to be 1,800 l/s, based on a field investigation in 2000. The outflow towards the Atlantic Ocean is estimated to be 459 l/s in 2000. The results of a hydrogeochemical analysis conducted between 1985 and 1992 show that the groundwater salinity values are different

between the water table level and the bottom for some coastal observation wells, varying between 1 to 6 g/l.

MODELING SEAWATER INTRUSION IN THE RMEL AQUIFER

Mesh discretization

The model developed, based on SEAWAT code (Langevin and Guo, 2002), simulates the transient variable density groundwater flow and solute transport for a period from 1972 to 2003, using a database developed by Larabi (2004). Regular spaced finite-difference cells of $500\text{m}\times500\text{m}$ size on the horizontal plane are used. The final grid consists of 42 rows and 31 columns in the horizontal, and 4 regular spaced layers in the vertical direction.

Boundary conditions and aquifer parameters

Based on test conducted in the area (DRPE 1995), the hydraulic conductivity ranges from 6.5×10^{-6} to 2.9×10^{-4} m/s. For storativity, only 13 values are available in the center and the northwest part of the aquifer, with measured values ranging from 0.17% to 3.6%. In the rest of the aquifer, parameters were estimated from Moroccan hydrogeological literature for similar type of soils. Constant head of 0 m and constant concentration of 35 kg/m^3 are specified to the cells along the Atlantic coast. In the rest of the aquifer, a no-flow boundary is specified except at the eastern boundary, where rivers are specified as drains. Internal hydrological stresses for the corresponding layers are included in the aquifer. The aquifer bottom is a no flux boundary, while on the top of the aquifer a recharge influx is assigned. The northern and southwestern boundaries are assumed to be no flow boundaries, due to the existence of impervious layers.

Calibration and model results

First, the numerical model is tested against steady state groundwater flow based on 1972 data. The results show good agreement between calculated and measured heads. Table 1 shows the resulting water balance of different components, including the discharge to the sea, which is estimated to be 356 l/s. It is observed from Table 1 that the main input component is the recharge from precipitation, and the main output component is the river drainage.

Table 1. Calculated water balance in steady state (year 1972)

	Water Balance Component	Volume in m^3/day	Volume in l/s
Input	Recharge by precipitation	119978	1389
	Return from irrigation	22853	264
	Total	146206	1692
Output	Agricultural withdrawals	31622	366
	Domestic water supply	8640	100
	Sea outflow	30746	356
	River drainage: Smid El Ma-El Kihel-Sakh Sokh	71878	832
	Total	142887	1654

Transient simulations are then conducted using the 1972 steady state condition as the initial head. The initial concentration in the aquifer is assumed to be 0 kg/m^3. Calculation is performed for the 1972-2003 target period (31 years). The results of the transient calculations show satisfactory agreement between measured and calculated heads in different observation wells for the considered simulation period. The simulation shows the beginning of the seawater intrusion and its evolution, the contamination concentration, the seawater intrusion volume, as well as

other components of the mass balance. Table 2 illustrates the water balance between 1972 and 2003, which shows that aquifer has more freshwater storage between 1972 and 1980, and a reduction takes place during 1980–1990. As a consequence, seawater advances inland in 1983 and 1992 (Fig. 1). It also shows that intensive groundwater pumping, especially since 1995, resulted in increasing seawater intrusion. The following invaded zones have been identified: (1) The first zone invaded by the seawater intrusion between 1995 and 2000 is located west of the ONEP pumping wells. Afterward, this invaded zone extended along the inshore line, to about 10 km of length and 1 km of width. (2) The aquifer is contaminated on the N-W coastal zone, in which the toe reaches about 1 km inland. Beyond these zones, the contamination of the aquifer is limited.

Table 2. Calculated water balance for the transient simulations 1973-2003.

	Water balance (Mm^3/year)	1972	1975	1980	1985	1990	1995	2000	2003
INPUT	Inflow storage variations	0	8.79	16.9	1.04	0.0054	13.4	6.95	3.89
	Returns from irrigation	0.577	0.577	0.577	16.5	16.5	16.5	16.5	16.5
	Seawater intrusion	0.0	0.0057	0.0125	0.0041	0.0002	0.736	2.12	2.66
	Recharge by precipitation	43.8	12.6	6.27	22.5	26.5	3.92	7.25	7.25
	Total	**44.4**	**22.0**	**23.7**	**40.0**	**43.0**	**34.5**	**32.8**	**30.2**
OUTPUT	Outflow storage variations	0	0	0	5.28	5.21	0	0.0005	0
	Net pumping	6.93	6.93	6.93	6.18	6.18	12.0	13.2	13.2
	Discharge to Atlantic Ocean	11.2	5.24	5.11	10.7	12.0	7.82	7.39	6.90
	Drainage by rivers: oueds Smid El Ma-El Kihel-Sakh Sokh	26.2	9.84	11.7	17.8	19.6	14.7	12.1	10.1
	Total	**44.4**	**22.0**	**23.7**	**40.0**	**43.0**	**34.5**	**32.8**	**30.2**

RATIONAL WATER MANAGEMENT

Three planning scenarios schemes were designed to simulate the future changes in drawdown and salinity concentrations in a period of 20 years. The first scenario assumes that the same conditions are maintained and the pumping from the aquifer of about 1.24 Mm^3/y will continues until 2020. The evolution of the groundwater quality of the aquifer is analyzed in order to define the affected area by seawater intrusion. The second scenario consists of increasing pumping rates to satisfy the increasing water demand of the Larache population until 2020. The third scenario increases even more groundwater abstractions until 2020 to satisfy the water demand of two urban centers, Larache and Ksar El Kebir cities.

Results of simulations

Table 3 shows the predicted saltwater volume intruded into the aquifer. It is clear that for scenario 1, the seawater intrusion volume decreases from 2003, but the equilibrium is not yet established in 2020. The groundwater quality in the northwestern sector becomes highly saline, and the contaminated area would extend more (Fig. 2). The results of scenarios 2 and 3 are also given in Table 3, which shows that the seawater intrusion volume increases progressively. The result of scenario 3 is presented in Fig. 3, which shows that the northwestern sector of the coastal part will be intruded with high salinity (15–25 g/l). The seawater would reach the first group of wells in 2010 with an expected salinity greater than 1.5 g/l.

CONCLUDING REMARKS

The coupled flow and transport code (SEAWAT) was applied to study seawater intrusion in the Rmel coastal aquifer in both qualitative and quantitative aspects. The results showed that seawater intrusion started in 1992 in the northwestern sector, due to intensive pumping from the wells and reduced recharge. The model is also applied to test the aquifer response to three planning scenarios for a period of 20 years. It is predicted that the first scenario will reduce the quantity of seawater intrusion, but without improvement of the groundwater quality. The other two scenarios predict a considerable quantity of seawater intrusion with deteriorating water quality. It should be cautioned, however, due to the missing aquifer data that need to be estimated, and the lack of field water quality data to validate the model result, more field measurements, such as vertical salinity profile and trace element studies for dispersivity need to be performed in order to increase the reliability of the model. Also, optimization model for rational management of the aquifer needs to be developed.

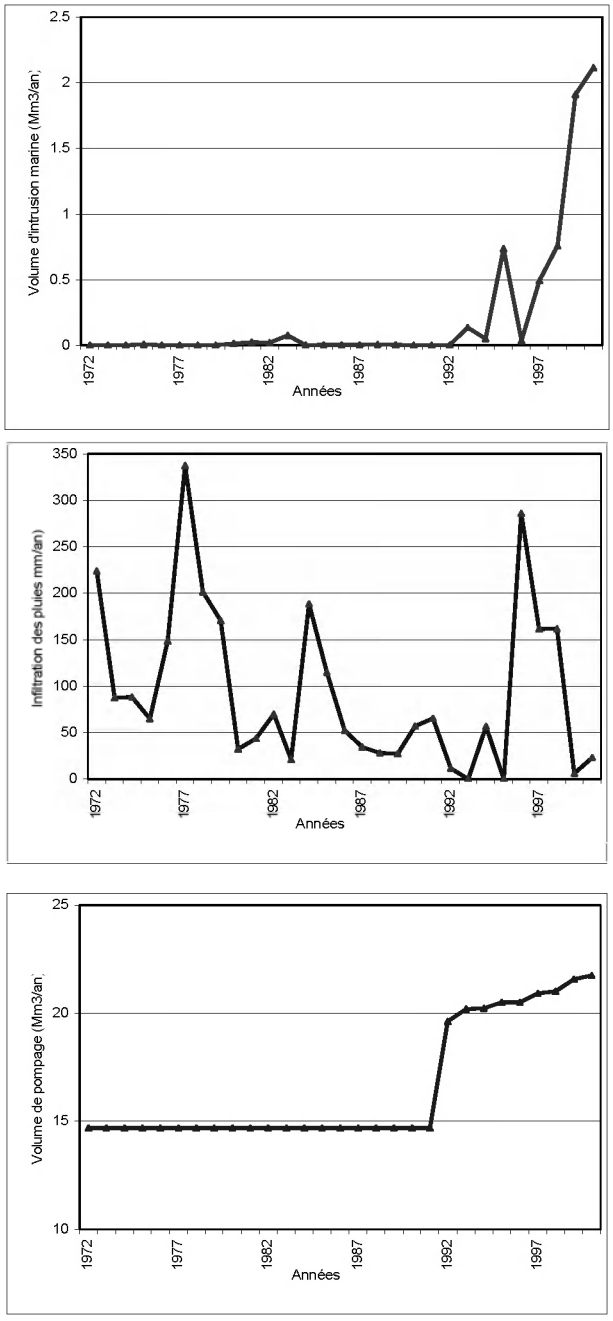

Figure 1. Evolution of seawater intrusion, natural recharge and withdrawals in the Rmel aquifer.

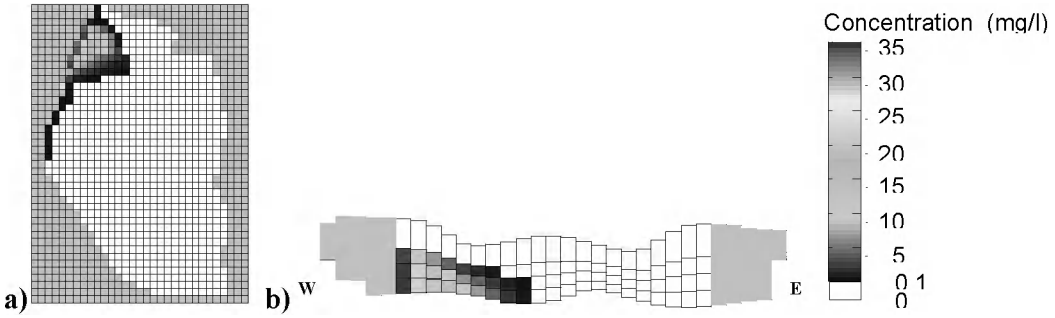

a) Calculated salinity for Scenario 1 in layer 2, **b)** Transversal section of salinity simulated in row 9.

Figure 2. Predicted salinity distribution for Scenario 1 in 2020.

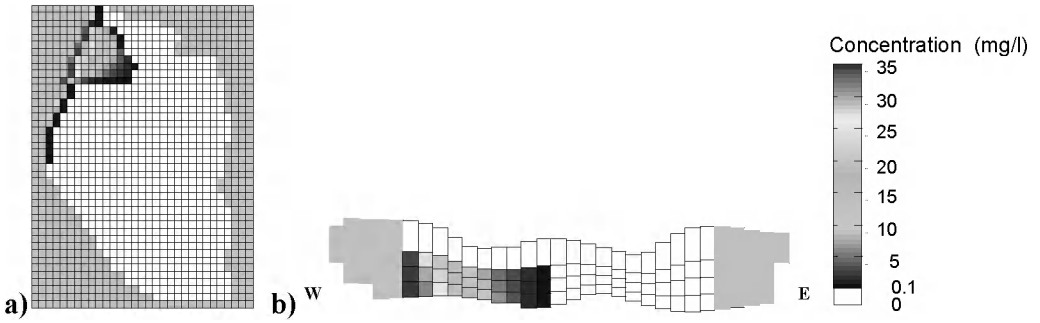

a) Calculated salinity for Scenario3 in layer 2, **b)** Transversal section of salinity simulated in row 9.

Figure 3. Salinity distribution of calculated salinity predicted by the model for Scenario 3 in 2010.

Table 3. Evolution of sea water intrusion volumes (2004 -2020)

	Volume in Mm^3/yr				
	2004	2005	2010	2015	2020
Scenario 1	1.5068	1.2480	0.7908	0.4492	0.3905
Scenario 2	2.9996	3.7544	4.5457	4.7273	4.9428
Scenario 3	3.0139	3.8145	4.7860	5.0961	5.7462

ACKNOWLEDGMENTS:

The authors are thankful to the Direction de la Recherche et de la Planification des Eaux for the fruitful collaborations between the University and the Administration. This study is also partially supported by the U.S. National Science Foundation grant OISE 0422868.

REFERENCES

Bentayeb, A, (1972). Etude hydrogéologique de la nappe côtière de Rmel avec essai de simulation mathématique en régime permanent. Thèse Univ. Scien. Tech. du Languedoc, Montpellier.

DRPE (1995). Etude hydrogéologique et modélisation mathématique de la nappe de Rmel côtière, Direction Générale de l'Hydraulique, Rabat (Internal report).

Langevin, C.D. and Guo W. (2002). User's Guide to SEAWAT, A computer program for simulation of three-dimensional variable density groundwater flow. U.S Geological Survey, Open-File Report 01-434, Tallahassee, Florida.

Larabi, A. (2004), Programme de gestion des ressources en eau : Modélisation de l'Intrusion Marine dans la Nappe de R'mel (région de Larache, Maroc), Rapport FAO (internal report).

Contact Information: Abdelkader Larabi, Ecole Mohammadia d'Ingenieurs, Laboratory LIMEN, B.P 765, Agdal, Rabat, Morocco, Phone: 21237772647, Email : larabi@emi.ac.ma

Modeling of Historical Evolution of Salt Water Distribution in the Phreatic Aquifer in and around the silted up Zwin Estuary Mouth (Flanders, Belgium)

Luc Lebbe, *Sarah Jonckheere* and *Alexander Vandenbohede*
Department of Geology and Soil Science, Ghent University, Ghent, Belgium

ABSTRACT
The evolution of the salt-water distribution around the Zwin estuary mouth is modeled for a period of about five centuries. The modeled area is situated in the Flemisch coastal plain near the border of The Netherlands and Belgium. The Zwin estuary is the former waterway to the medieval seaports of Bruges and Damme. During the considered period this alluvial estuary silted up and the modeled area changes from an area around a tidal channel, over a mud flat to a rather complex polder dune area. The evolution is simulated by the 3D density depended groundwater flow model MOCDENS3D (Lebbe & Oude Essink, 1999). The row direction of the applied finite-difference grid is parallel to the present coast line. The simulation is based on old paintings and a large number of maps which allow a relatively detailed reconstruction of the evolution of the landscape. The results show the historical evolution of a large number of different inverse density problems in this area.

INTRODUCTION
To simulate this five hundred years period ten stress periods are considered. Before the 20th Century the stresses which influence the groundwater flow and the salt water distribution were principally determined by the evolution of the landscape. The simulation starts with the first sound representation of the area in a painting of Pourbus (1571). At that time the waterway to the seaport Damme ran from the upper right to the lower left corner of the modeled area (Fig. 1). This tidal channel was bounded at both sides by relatively flat banks which were temporally inundated by sea water depending on the tides. At both sides of the estuary mouth there were peninsulas principally existing of dune areas. Behind the western dunes there was a tidal flat area with a central gully. During the high waters at spring tides this tidal flat area was completely inundated by sea water whereas the sea retreated completely from it at low water. The southern boundary of the tidal flat area was bounded by a dyke protecting the polders behind it from inundations.

The subsequent stresses on the phreatic aquifer are due to the lateral changes of the landscape elements. In the dune area fresh water recharges with a constant rate (280 mm/year). In the tidal flat area, the banks of the tidal channel and the shores, the average fresh water head in the uppermost layer is derived from the tidal fluctuations and the elevation of the ground surface at the treated point. When there is a recharge of groundwater in all the fore mentioned areas the water quality corresponds with that of sea water (100% salt water). In the polder areas the top of the aquifer is drained at a prescribed level and there is a smaller recharge of water than in the dune area. The salt content (2%) of the water infiltrating in the polder area is slighter higher than those of the recharging water in the dune area (1%). During the 20th and the beginning of the 21th century the landscape elements do not change any longer and the considered stress periods depend principally from the changing withdrawal rates in the dune area.

During the presentation of the simulated results the evolution of the groundwater flow and distribution are treated at different levels in the aquifer and in different cross-section through it. Because of the limited space of this abstract only a small number of selected results can here be shown. First, the applied finite difference grid is located and the initial conditions of the

simulation are described. Hereafter, a small number of results are selected so that the different inverse density problems can be demonstrated.

FINITE DIFFERENCE GRID, INITIAL CONDITIONS AND SOME RESULTS

The modeled area is 4.4 km on 3.5 km. The finite difference grid consists of 88 columns, 70 rows and 12 layers. All finite difference cells have the same size. These cells have a thickness of 2 m and a squared base plane with a side of 50 m. The evolution of the salt water distribution is calculated with the method of the characteristics. At the initial time one assumes that the phreatic aquifer was completely filled with salt water. So, eight particles per finite difference cell are places with a salt water percentage of 100%. The stresses on the aquifer during the first stress period depend of the different landscape elements derived from the painting of Pourbus (1571) as described in the introduction. The duration of this stress period was chosen so that a dynamic equilibrium is nearly reached in the salt water distribution (see Figure 1).

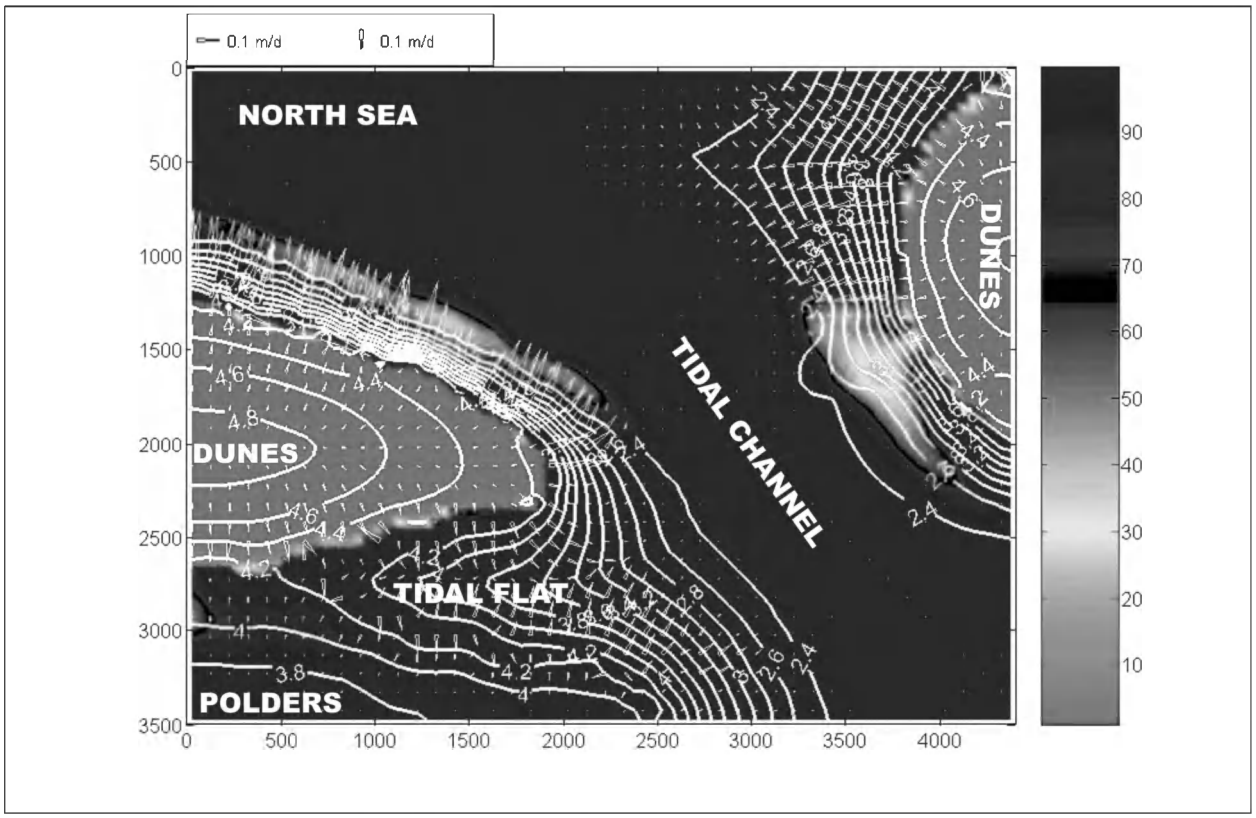

Figure 1. The modeled area with the principal landscape elements according to the painting of Pourbus (1571) along with the simulated fresh water head contour lines (in white), the groundwater flow (vectors) and the saltwater percentage (gray scale) of layer 2 (x and y coordinates in m)

In Figure 1 the simulated results are represented in a horizontal plane at level -2 m below mean sea level (bmsl) according to the landscape of 1571. Under the dunes the upper part of the phreatic aquifer was filled with fresh water. Before the western dunes there was an outflow of fresh and brackish water at the low water line of spring tides. The flow of fresh water from the eastern dune area to the eastern bank of the tidal channel was concentrated to the southern part of the bank which had a more permeable subsurface and a slightly steeper slow than its northern part.

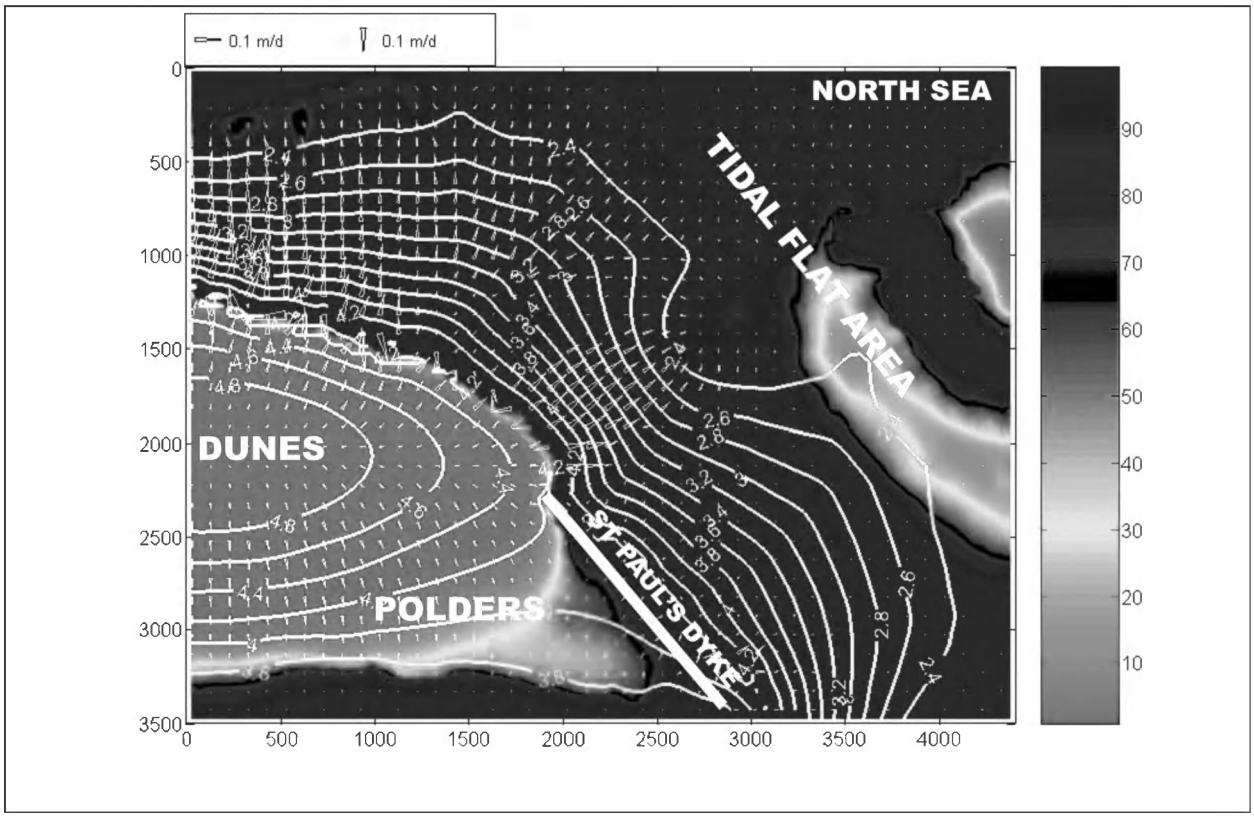

Figure 2. Principal landscape elements according to the map of Wilschut (1740) along with the simulated groundwater flow and the saltwater distribution in layer 2

During the 17th Century the tidal channel silted up. First, the eastern dunes grew towards the west resulting in a larger fresh water lens under these dunes. The deepest part of the channel moved towards the west and the channel became shallower. Due to this the slope of the western bank of the tidal channel decreased while the slope of the eastern bank increased. On the southern part of the eastern bank there was an important fresh water flow from the eastern dunes toward the low water line. Above this fresh water flow there was a large salt water lens. This density inversion developed in a similar way as the density inversion described by Vandebohede & Lebbe (2006). In the second half of the 17th Century there was an erosion of the feet of the eastern dunes and the high water line moved toward the east. Finally, this resulted in a tidal flat area in the upper right part of the modeled area (Fig.2) whereas the low water line of the North Sea retreated to the upper right corner of the modeled area. In this tidal flat area there were still remains of the fresh water lens of the former eastern dunes and also of the density inversion under the former eastern bank of the tidal channel. Because the hydraulic gradients under the tidal flat area are very limited, there was only a density dependent very slow flow due to the inversed distribution of salt and fresh water (Fig.3). In the beginning of the 18th Century the polders in the lower left part of the modeled area were enlarged by the construction of the Saint Paul's dyke. Due this reclaim of the former tidal flat a very slow freshening process started in the top of the phreatic aquifer.

DISCUSSION AND CONCLUSIONS

The historical evolution of the salt-water distribution around the Zwin estuary mouth results in a large number of different inverse density problems. The evolution of one of these inverse density problems is shown above. A detailed study of these inverse density problems along with present

day observation in area which show similar evolution as around the Zwin estuary mouth will be a future challenge in the salt water intrusion research.

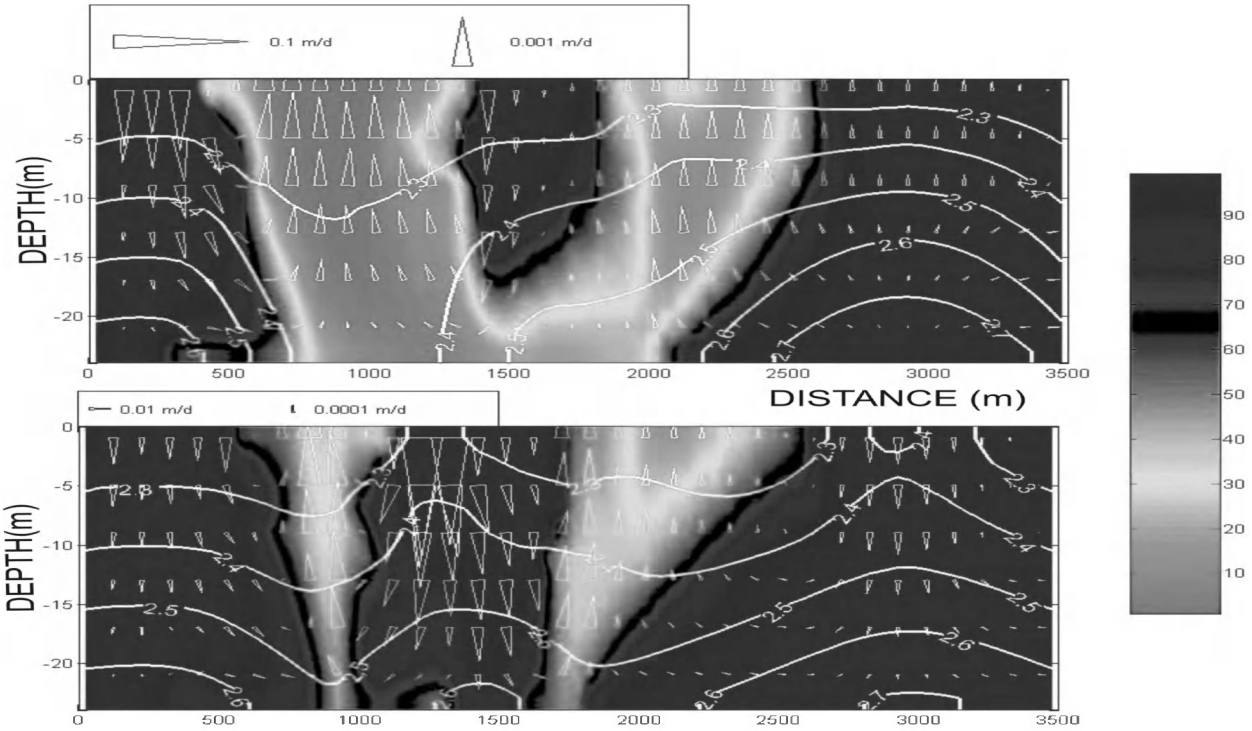

Figure 3. Simulated evolution of the remains of a fresh water lens of the eastern dunes and of the density inversion under the eastern bank of the tidal channel after the change of the area to a tidal flat area in the beginning (above) and at the end (below) of the 18th Century in a cross section along the row (x=4225 m)

REFERENCES

Lebbe, L. & Oude Essink, G., (1999) Section 12.11. MOC DENSITY / MOCDENS3D-code. p. 434-439, in Chapter 12. Survey of Computer codes and Case Histories, Eds. Sorek, S. & Pinder, G.F. in: *Seawater Intrusion in Coastal Aquifers, Concepts, Methods and Practices.* Eds. Bear, J., Cheng, H-D, Herrera, I., Sorek, S. and Ouazar D. Kluwers Academic Publishers

Vandenbohede, A. & Lebbe, L. (2006). Effects of tides on a sloping shore: groundwater dynamics and propagation of the tidal wave. *Hydrogeology Journal, 15 (4): 645 – 658*

Contact Information: Luc. C. Lebbe, Ghent University /Geology & Soil Science Department, Krijgslaan 281, B9000 Gent, Belgium, Phone & Fax: 32-92644635, Email: luc.lebbe@ugent.be

Proposal of a Methodology for the Optimal Design of Monitoring Networks Coastal Aquifers Management

Julia Maranganí
Department of Geophysics, University of Mexico, Mexico City, Mexico

ABSTRACT
In many coastal areas with a great density of population water supply depends, to a great extent, of groundwater, for this reason a monitoring network for coastal aquifers based in a reduced number of monitoring wells can represent an important alternative, because of the economical savings of this type of project. Therefore it is necessary to optimize number of sampling points when choosing suitable sampling times and positions.

A method for the design of an optimal network monitoring of a coastal aquifer is proposed here. The objective is to adecuate and use the methodology proposed for groundwater quality network monitoring design, that uses Kalman's filter in combination with stochastic simulation of the groundwater flow and the transport of solutes. This methodology is implemented using a computer program called GWQMonitor which uses ArgusOne as a graphical interface that controls only the first three parts, but it is also possible to use Ground Water Vistas as graphical interface.

In order to take into account variable water density, we are planning to use SEAWAT, developed by Guo and Bennett, (1998); Guo and Langevin, (2002) that is a combination of MODFLOW and MT3DMS (Zheng y Wang, 1999).
Keywords: coastal aquifers, monitoring network

INTRODUCTION
In many coastal zones with great density population, water supply depends to a great extent on groundwater, frequently coastal aquifers are over exploited and additionally present contamination problems, from industry and other sources (for example: diminution of charge as a result of the increase in urban establishments or marine intrusion because of its proximity to the sea).

Consequently, the planning, development, protection and handling of this aquifers is an important task. An alternative to solve this problem is based upon groundwater monitoring programs implementation (in number and quality), with the purpose of anticipating or controlling contamination sources and problems related with over exploitation or degradation of this resource. This task can be carried out through the use of tools such as the monitoring networks and mathematical simulation methods.

JUSTIFICATION
Groundwater monitoring network design, is indispensable to study and solve aquifer contamination problems, but at the same time represent a significant economic burden, because of the expenses associated with the monitoring wells operation, and those related with the sampling analyses obtained from observation wells. An alternative to diminish this economic impact consists on the reduction of the number of samples to collect. Such reduction can be obtained sampling fewer wells or sampling the same number of wells with less frequency, or by a combination of both strategies.

The main objective of this work, is to adapt and use a methodology proposed and developed for the efficient design of a water quality monitoring network, which considers an algorithm that helps to determine where and when to sample wells, in order to define groundwater polluting agents behaviour. This work is a contribution for the design of an optimal coastal aquifer monitoring network. Because there are few investigations related to this subject, we had to take into account information related to the design of the optimal monitoring groundwater quality, which can be carried out using a variety of approaches.

METHODOLOGY

In this work we try to adapt and use methodology of water quality monitoring network design, known as GWQMonitor, the methodology can be divided in four parts: in the first three parts, actual data are not required, just positions and times in which the underground water could be sampled. When we refer to the positions or times of sampling, these are the positions of possible monitoring wells and the possible monitoring times for each one of those wells. This methodology is implemented through a computer program GWQMonitor that works with a graphical interface called ArgusONE, which controls just the first three parts, but it is possible to adapt this program into Ground Water Vistas.

Part I: Calculation of an initial estimation for the concentration covariance Matrix of a transport stochastic model

An stochastic simulation is made using a transport stochastic model, in order to obtain a prior concentration estimation in space and time and its covariance matrix.

Part II: Covariance matrix calculation for the estimation of concentration error given positions and times

Initial estimated covariance matrix is combined with positions and monitoring times information through the Kalman's filter to obtain a new error estimation of the covariance concentration matrix. As far as the selection of the positions and times of sampling, the method uses an iterative algorithm in which chooses a position in space and time in a simultaneous form.

Part III: Construction of the sampling network

A sampling network is constructed by means of an optimization method that diminishes the estimation function of the estimation of the variance that is obtained in part II. To choose well positions and sampling times for the network and monitoring frequency, a function of estimation of the uncertainty is used. The function used, depends on the design objectives. In order to diminish the function, different optimization procedures can be used. The function used to measure the uncertainty associated with a given sampling plan, is the sum of the considered error of the variances in the positions and times of interest, this function is called total variance of the concentration error, and it is denoted by:

$$\sigma_T^2(n) = \sum_{i,p} \sigma_{ip}^2(n) \qquad (1)$$

where: $\sigma_T^2(n)$ is the variance of the error of estimation in the *i-th* position in Kalman's mesh and estimation time *p-th* when *n* samples are used. The $\sigma_{ip}^2(n)$ are obtained from Kalman's filter, the variances after taking *n* samples are the elements of the covariance diagonal matrix P^n.

$$P^n = E\left\{(C - \hat{C}^n)(C - \hat{C}^n)^T\right\} \qquad (2)$$

Part IV: Postprocessing

Postprocessing procedure allows a real time update of concentration estimate. It uses the mean contaminant concentration obtained by averaging the realizations from the stochastic simulation as an initial estimate of the contaminant concentration. The newly available concentration data are then used to update the prior estimate using Kalman's filter. As additional data become available Kalman's filter is used again to update the estimated concentrations.

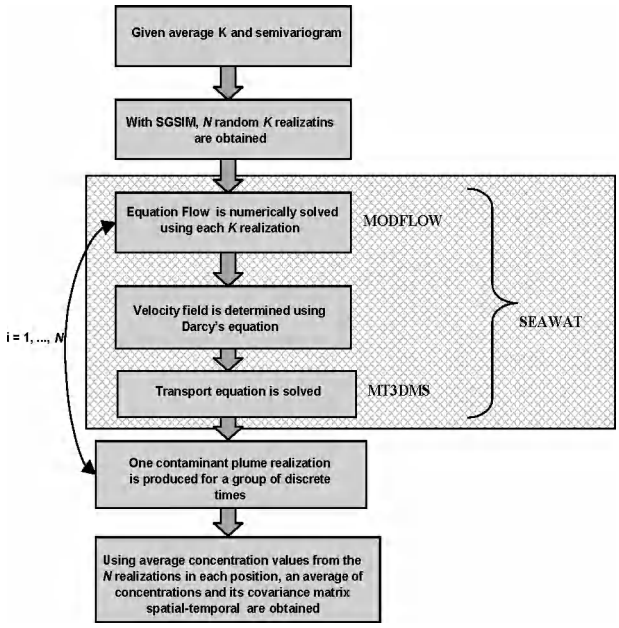

Figure 1. Flow chart of Variable density groundwater flow and transport solute simulation, used to obtain input files for GWQMonitor program.

In figure 1, the process of stochastic simulation is illustrated, using SEAWAT, in order to obtain the average concentrations and the space-time covariance matrix, that makes part of the Herrera-Pinder (1998) methodology. The procedure's results will be used as input data for GWQMonitor program, in order to obtain the optimal design of a coastal aquifers monitoring network.

CONCLUSION

Monitoring networks based on a reduced number of sampling wells can represent an important alternative in face of economic restrictions, therefore it is important to optimize the number of sampling points, choosing adequately times and sampling positions.

In this work a methodology for optimal coastal aquifers monitoring network design is proposed, constituting itself as an important contribution for the management of this type of groundwater resources.

REFERENCES

Alvarado Rivas, J. (1999), "Groundwater monitoring, over-explotation, vulnerability and groundwater protection in Cochabamba". National Geology and Mining Service. Cochabamba, Bolivia.

ASCE (American Society of Civil Engineers) (2003), "Long-Term Groundwater Monitoring: The state of the Art", Task Committee on the State of the Art in Long-Term Groundwater Monitoring Design, U.S.A., 2003.

Bear, J., Cheng, A.H., Sorek, S., Ouazar, D., Herrera, I. (1998), Seawater Intrusion in Coastal Aquifers Concepts, Methods and Practices.

Ciba (1999). Draft Feasibility Study Report for Operable Unit 2. Technical report, Ciba Speciality Chemicals Corporation, North America, Toms River, NJ.

Custodio, E. Coastal Aquifers as important Natural hydrogeological structures, Groundwater and human development. Bocanegra Martinez, Massone (Eds)2002 ISBN 987-544-063-9.

Deutsch, C. and André G. Journal (1998), GSLIB, Geostatistical Software Library and User's Guide, 2nd ed., New York, Oxford University Press.

Herrera, G. S., Pinder, G., (2005), Space-time optimization of groundwater quality sampling networks. Water Resources Research.

Herrera, G. (1998). "Diseño espacio temporal de redes de monitoreo de la calidad del agua subterránea". Instituto Mexicano de Tecnología del Agua. Jiutepec, Morelos.

Loaiciga, (1989). "An Optimization approach for groundwater quality monitoring network design" Water Resources Research, vol. XXV, 8, pp. 1771-1780.

Ponsati et al., (2003). "Diseño eficiente de redes de control de la intrusión salina en los acuíferos costeros a partir de información hidrogeoquímica y geofísica". Tecnología de la intrusión de agua de mar en acuíferos costeros: Países Mediterráneos. IGME, Madrid.

Virgos Soriano Luis Ignacio, López Bravo Juana. (1988). Los modelos matemáticos aplicables en problemas de intrusión marina desde el punto de vista del usuario hidrogeólogo. Tecnología de la Intrusión en acuíferos costeros Almuñecar (Granada España).

Contact Infromation: Julia Marangani, UNAM, Department of Geophysics, 45 Selva Street, colonia Insurgentes Cuicuilco, Mexico city, Mexico, Phone: 56066455, Email: posgrado_unam@hotmail.com

Mechanisms Driving Submarine Groundwater Discharge and Associated Radium Flux: Implications for Use of Radium as a Tracer

Holly A. Michael[1, 3], *Matthew A. Charette*[2] and *Charles F. Harvey*[1]

[1]Department of Civil and Environmental Engineering, Massachusetts Institute of Technology, Cambridge, MA, USA

[2]Department of Marine Chemistry and Geochemistry, Woods Hole Oceanographic Institution, Woods Hole, MA, USA

[3]Now at Department of Geological and Environmental Sciences, Stanford University, Stanford, CA and Department of Geological Sciences, University of Delaware, Newark, DE, USA

Groundwater is an important source of nutrients and contaminants to coastal waters (e.g., Valiela et al., 1990; Slomp and Van Cappellen, 2004; Kemp et al., 2005), and quantification of submarine groundwater discharge (SGD) is the first step toward understanding its potential impact on nearshore marine ecosystems. The diffuse and heterogeneous nature of SGD makes it difficult to quantify directly, so geochemical tracers with high concentrations in groundwater relative to surface water, such as radium and radon isotopes, barium, and methane, are often measured in coastal waters to estimate the fluid flux (e.g., Moore, 1996; Moore, 1997; Swarzenski et al., 2001; Burnett et al., 2006). These methods, while potentially extremely useful for making integrated large-scale discharge estimates, are dependent on knowledge of the tracer concentrations in groundwater. In the case of radium specifically, and likely other tracers, porewater concentrations are highly heterogeneous, particularly in coastal systems where salinity gradients are high. Concentrations may differ between locations because redox chemistry changes along flowpaths (e.g., Charette and Sholkovitz, 2002), subsurface residence times are variable (e.g., Robinson et al., 2007), and mixing between groundwater and surface water is significant. Consequently, the groundwater that contributes most to submarine groundwater discharge could have different tracer concentrations than the average concentration in groundwater for the region.

Detailed direct measurements of groundwater discharge and salinity were made with seepage meters in Waquoit Bay, MA over a period of five years (Michael et al., 2003; Michael et al., 2005). The mechanisms driving groundwater flow at the coast can explain, at least in part, the observed spatial discharge patterns. Discharge attributed to each of the primary driving mechanisms believed to be operating in Waquoit Bay were identified and quantified. Components of discharge likely driven by the upland freshwater hydraulic gradient, run-up of tides and waves onto the beachface, dispersion along the freshwater-saltwater interface, and seasonal hydraulic change were 0.004 m^3/s, 0.024 m^3/s, 0.023 m^3/s, and 0.026 m^3/s, respectively.

The activity of four radium isotopes, ^{226}Ra, ^{228}Ra, ^{223}Ra, and ^{224}Ra (with half-lives of 1600 years, 5.8 years, 11.4 days, and 3.7 days, respectively) was measured in 42 porewater samples (some of which are published in Abraham et al., 2003), and in water collected from 40 seepage meters combined into four zones over three time periods. The radium flux into Waquoit Bay associated with each zone of groundwater discharge (as opposed to each driving mechanism, the associated discharge of which overlap spatially in some areas) was calculated by integrating fluid discharge, salinity, and radium measurements. Results indicate that while discharge of groundwater in the brackish zone offshore of the freshest discharge comprises approximately 40% of the total SGD, 80% of the total ^{226}Ra discharge occurs in this zone. Offshore saline discharge, likely driven in part by seasonal motion of the interface, contributes 34% of total discharge, but only 6% of ^{226}Ra flux. Nearshore discharge of circulated saline water due to tides and waves contributes about 5% of fluid flux and 6% of ^{226}Ra flux, and discharge of groundwater from the freshest zone is 20%

of total fluid flux and only 8% of ^{226}Ra flux. The fluxes of other radium isotopes are similarly proportioned, though isotope ratios are somewhat spatially-variable.

This study indicates that radium activities vary in groundwater and are dependent to some extent on the forcing mechanism driving groundwater discharge. Detailed measurements of fluid flux and radium activities have allowed quantification of radium flux into Waquoit Bay, which displays significant spatial heterogeneity. This has implications for the use of radium as a tracer for total SGD, integrated over all components. Care should be taken that porewater radium activities are sufficiently sampled to understand heterogeneity within and among types of discharging groundwater. If radium activities are highly variable and the relative magnitude of fluid flux among different groundwater types is unknown, then bulk groundwater discharge is difficult to estimate by knowing only the radium flux to the surface water. Results suggest that brackish groundwater discharge offshore of freshwater outflow is the dominant contributor of radium to the Waquoit Bay estuary. Thus, radium could be most effective for estimating discharge of brackish groundwater driven by dispersion along the freshwater-saltwater interface, and perhaps for indicating motion of the interface. In addition to improving the use of geochemical tracers as indicators of groundwater discharge, understanding of the primary mechanisms driving flow and the concentrations of solutes associated with each type of groundwater could greatly improve our ability to predict the discharge of important nutrients and contaminants to coastal waters.

REFERENCES

Abraham DM, Charette MA, Allen MC, Rago A, Kroeger KD (2003) Radiochemical estimates of submarine groundwater discharge to Waquoit Bay, Massachusetts, Biological Bulletin, 205 246-247.

Burnett WC, Aggarwal PK, Aureli A, et al. (2006) Quantifying submarine groundwater discharge in the coastal zone via multiple methods, Science of the Total Environment, 367 498-543.

Charette MA, Sholkovitz ER (2002) Oxidative precipitation of groundwater-derived ferrous iron in the subterranean estuary of a coastal bay, Geophysical Research Letters, 29 10.

Kemp WM, Boynton WR, Adolf JE, et. al. (2005) Eutrophication of Chesapeake Bay: historical trends and ecological interactions, Marine Ecology Progress Series, 303 1-29.

Michael, HA, Mulligan AE, Harvey CF (2005) Seasonal oscillations in water exchange between aquifers and the coastal ocean, Nature, 436, 1145-1148.

Michael, HA, Lubetsky JS, and Harvey CF (2003) Characterizing submarine groundwater discharge: a seepage meter study in Waquoit Bay, Massachusetts, *Geophysical Research Letters*, 30 (6) 1297.

Moore WS (1996) Large groundwater inputs to coastal waters revealed by ^{226}Ra enrichments, Nature, 380 612-614.

Moore WS (1997) High fluxes of radium and barium from the mouth of the Ganges-Brahmaputra River during low river discharge suggest a large groundwater source, Earth and Planetary Science Letters, 150 141-150.

Robinson C, Li L, Barry DA (2007) Effect of tidal forcing on a subterranean estuary, Advances in Water Resources, 30 851-865.

Slomp CP, Van Cappellen P (2004) Nutrient inputs to the coastal ocean through submarine groundwater discharge: controls and potential impact, Journal of Hydrology, 295 64-86.

Swarzenski PW, Reich CD, Spechler RM, Kindinger JL, Moore WS (2001) Using multiple geochemical tracers to characterize the hydrogeology of the submarine spring off Crescent Beach, Florida, Chemical Geology, 179 187-202.

Valiela I, Costa J, Foreman K, Teal JM, Howes B, Aubrey D (1990) Transport of groundwater-borne nutrients from watersheds and their effects on coastal waters, Biogeochemistry, 10 177-197.

Contact Information: Holly Michael, Department of Geological and Environmental Sciences, Stanford University, 450 Serra Mall, Bldg 320 Braun Hall, Stanford, CA 94305, Telephone: 650-736-7179, Email: hmich@stanford.edu. Also, Department of Geological Sciences, University of Delaware, Newark, DE, USA, Email: hmichael@udel.edu

The Influence of Three-dimensional Dune Topography on Salt Water Intrusion in Marina Romea, Italy: A Numerical Modeling Study Using LIDAR Data

Pauline N. Mollema, *Marco Antonellini, Andrea Minchio* and *Giovanni Gabbianelli*
I.G.R.G. (Integrated Geoscience Research Group), University of Bologna, Ravenna, Italy.

ABSTRACT
This paper presents a 3-D variable density model of an area about 400m by 500 m including the beach, dunes and part of the Pine forest north east of the tourist town Marina Romea along the Adriatic Coast, Northern Italy. The 3D topography, derived from LIDAR data of the area is imported into this model, to test the hypothesis that the interruption of the dune belt for the construction of bathing establishments on the beach has enhanced saltwater intrusion into the unconfined aquifer underneath the Pine forest.

INTRODUCTION
Until the 1950's there was a continuous dune belt along the Adriatic coast of the southern Po-plain. The dune belt, then, was interrupted just north of our study area to create the mouth of the river Lamone and dunes were locally destroyed to create space for bathing establishments, a practice that has continued until now (Fig. 1). Monitoring of salinity in piezometers indicates that underneath the dunes directly adjacent to the beach, the shallow groundwater has a salt concentration of 1-5 g/l and further away from the coast and 150 m into the Pine forest, salinity values reach up to 15 g/l. The Pine forest, originally planted to protect farmland at the back from salt spray, is thought precious because of naturalistic value but the freshwater aquifer that quenches its thirst it is in danger of salinization. Previous work in this general area included the monitoring of the salinity to determine possible causes for salt water intrusion (Antonellini et al in press) and a 2D modeling study by Giambastiani et al (2007), simulating among others the subsidence history of the area.

TOPOGRAPHY
No detailed topographic maps were available and therefore we used Laser Imaging Detection and Ranging (LIDAR) data obtained by local authorities to define the topography. An elevation value was assigned to the nodes of a grid of 10 by 10 m, using the ESRI ArcGIS 9.0 Desktop extension HAWTH's tools, ARCGIS 3D Analyst Tools and the surface spot command. The resulting topographic map (Fig. 2) shows a discontinuous dune belt along the beach with tops up to 5 m high and a second dune belt 140 m from the coast. To the west of this narrow dune belt there is a 200 m wide low area with a drain running north - south along the lowest points at 0 m.s.l.

HYDROGEOLOGY
The coastal unconfined aquifer of our study area contains two main sandy units: a relatively thick (10 m) medium grained sand shallow unit and a lower fine-grained sand unit up to 5 m thick. These two sand layers connect more land inward but are in our study area separated by a clayey silt and sandy-silt unit, the so-called prodelta deposits (Fig. 2). The continental clay basement is at -30 m depth. See Giambastiani et al 2007 for a more detailed description of aquifer characterization and Fig. 2 for the hydraulic conductivity values assigned.

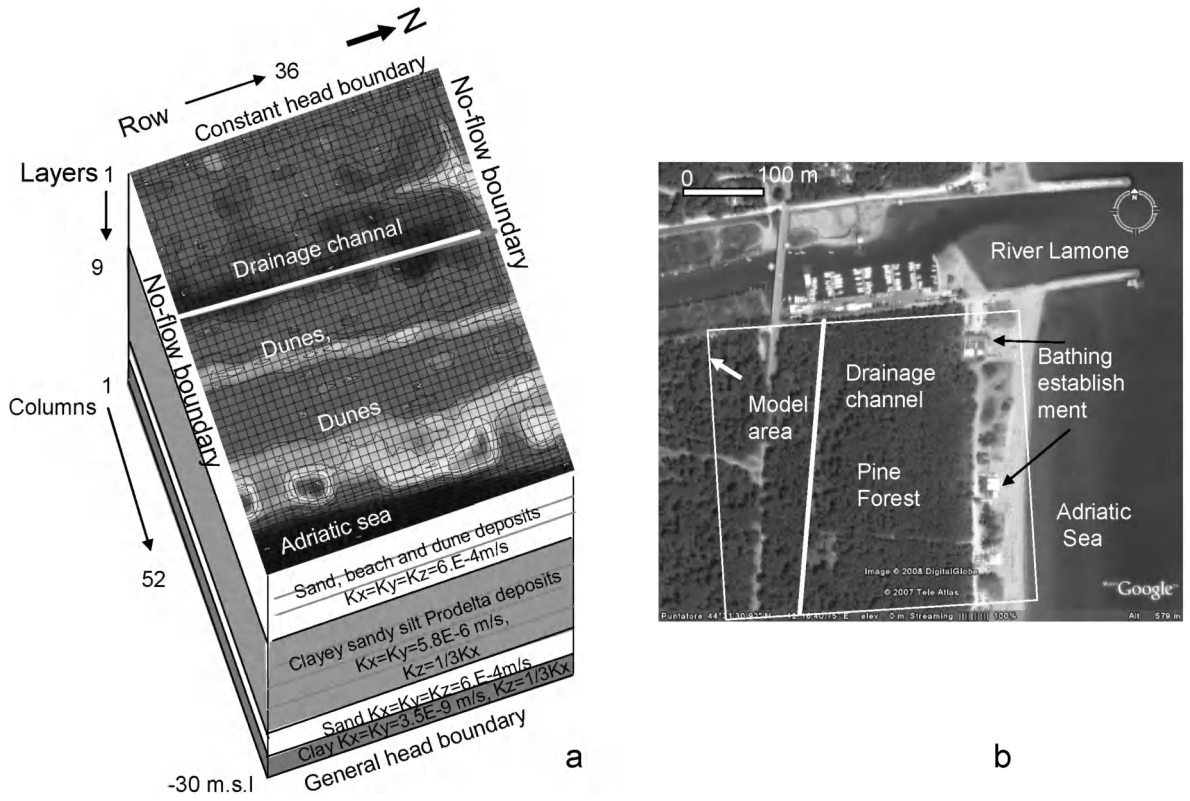

Figure 1.

a. Sketch of numerical model, including the topography, hydrogeological layering, mesh and boundary conditions. In general, dark colors are topographically low, lighter colors topographically high.

b. Aerial photo made with Google Earth showing bathing establishments and interruption of dunes along the coast

3D MODELLING

The numerical model used SEAWAT (Guo et al 2002), is a computer program for simulation of three-dimensional variable-density groundwater flow, based on two other programs MODFLOW and MT3D, in our study steered with the interface of Visual Modflow (Waterloo Hydrogeologic, 2006). Our numerical model of the study area consists of 9 layers, 52 columns and 36 rows. The mesh is refined vertically close to the sea (east) and in land (west) boundaries. A recharge boundary dependent on land use is imposed at the top: 15 mm/year for the area covered with forest based on water budget calculations (Antonellini et al. in press) and 200 mm /year on the dunes close to sea. See Fig. 1 for the other boundary conditions. In some models a north south drain boundary condition is added in the lowest area, conform to the existing drainage channel. The conductance of the drain assigned is 10 m^2/day. Two different initial salt concentrations were used for all models, one with a uniform *low initial concentration* of 1 g/l and one with a so-called *high initial concentration* where the upper 3 layers have a concentration of 1 g/l, layers 4, 5 6 and 7 have 15 g/l and 8 and 9 layers 30g/l. The initial salt concentration is thought to have a large influence on the final result (e.g. Oude Essink, 2004) in variable density models. Because our aquifer was actually covered by the sea not so very long ago (320 years,

Giambastiani et al 2007) there is the possibility that connate sea water is present at the bottom of the aquifer.

SUMMARY OF SIMULATION RESULTS

In the models *without a drain* and *low initial concentration*, salt invades mostly the high conductive sand layers in the first 13000 days of the simulation, advancing with a linear front. After about 18000 days, also the prodelta deposits between the more permeable sand layers are invaded and the fresh-salt water interface has the typical shape of a wedge leaving about 3 m of fresh water underneath the dunes and about 20 m of fresh water at the inland boundary. The total simulation time is 22000 days, about 60 years equal to the time that passed since the dune destruction and the drainage of the lower part started. The flowmodel has not yet reached equilibrium; the salt concentrations are still changing with time. The model *without a drain and high initial concentration* shows a similar pattern except that after only 5000 days the prodelta deposits fill up with saltwater.

In the models *with a drain and low initial concentration* of *the* intrusion of salt water into the upper sand layer is much faster and further. At 10000 days, the salt water in the upper sand formation has reached 200 m inland forming a horizontal saltwater tongue with the tip underneath the second row of dunes (Fig. 2), leaving a fresh water bubble in the prodelta deposits underneath. After 22000 days the fresh water bubble has almost disappeared and the front of the saltwater starts to approach wedge shape, although it is still changing at the end of the simulation. Results of the model *with a drain and high initial concentration* are very similar except that the low conductivity formation is invaded faster.

The models B *with high dispersivity and isotropic conductivity in all layers* result after a simulation time of 22000 days in a less distinct interface vertically between salt- and fresh water, leaving only small pockets of fresh water underneath the higher dunes. The horizontal advancing of the salt front is irregular with protrusions that correspond to gaps in the dunes along the coast.

DISCUSSION AND CONCLUSIONS

Both observed and modeled salinity values underneath the dunes closest to the coast fall between 1 and 5 g/l suggesting that the combination of positive topography and high recharge in this area is enough to sustain a freshwater lens. This holds also for the models with a drain. The second row of dunes inland seems to play an important role in halting the intrusion that is enhanced by the drain. Except Models B, all models do not show high salinity values in the low lying areas between the two dune belts or at the back of the dunes. Models B do show higher salinity value between the two dune belts but not around the drain. Therefore, perhaps the dispersivity and vertical conductivity are much higher than we thought realistic or other factors are contributing to saltwater intrusion such as the Lamone River to the north, the saltwater marshes to the West, or unknown water managing activities. Some conclusions from this study are: Lidar data has proven to be very useful in defining the topography. A high versus a low initial salt concentration only influences simulation results in early simulation times. The models with the drain do not seem to reflect a stable fresh-salt water interface after 22000 days or 60 years, suggesting that in reality also the salt –fresh water interface is still changing. Mitigation measures to protect the remaining fresh water must include strategies to preserve the dunes not only directly along the coast but also and perhaps foremost, the continuous row of dunes in the middle of the Pine Forest.

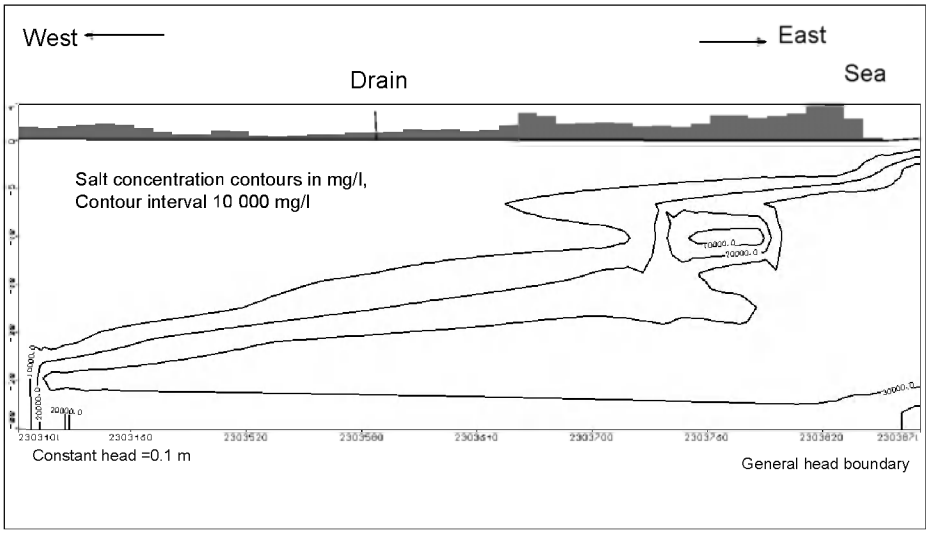

Figure 2. Contour plot of Simulation results for the case with a low initial concentration and a drain. Simulation time 22000 days.

REFERENCES

Antonellini M., Mollema P., Giambastiani B., Banzola E., Bishop K., Caruso L., Minchio A., Pellegrini L., Sabia M., Ulazzi E., and Gabbianelli G. Salt water intrusion in the coastal aquifer of the southern Po-plain, Italy. In press by the Hydrogeology Journal.

Giambastiani B. M. S. , Antonellini M., Oude Essink, G. H. P., Stuurman, R. J. 2007. Salt water intrusion in the unconfined coastal aquifer of Ravenna (Italy): a numerical model. Journal of Hydrology 340, p. 94-104.

Guo, W, and Langevin, C. D, 2002. User's Guide to SEAWAT: A computer program for simulation of three dimensional variable- density ground water flow: Techniques of Water-resources investigations Book6, Chapter A7, 77p.

Oude Essink, G. H. P. 2004. Modeling Three-Dimensional Density Dependant Groundwater flow at the Island of Texel, The Netherlands. In: Cheng, A H.-D and Ouazar, D. (Eds). Coastal Aquifer Management: monitoring, modeling and case studies. P. 77 -94.

Waterloo Hydrogeologic (2006). Now see Schlumberger Waterservices, www.swstechnology.com

Contact Information: Pauline N. Mollema, I.G.R.G. (Integrated Geoscience Research Group), University of Bologna, Via San Alberto 163, 48100 Ravenna, Italy. Email: pmollema@gmail.com

Verifying the Use of Specific Conductance as a Surrogate for Chloride in Seawater Matrices

Cristina Windsor and ***Rob Mooney***
In-Situ Inc., Fort Collins, CO, USA

ABSTRACT
Coastal ground water supplies, when overused, are particularly vulnerable to chloride contamination due to their close proximity to saltwater. Seawater has an average chloride concentration of 19,000 mg/L (Hem 1992). Elevated chloride concentration in ground water is the most commonly used indicator of saltwater intrusion in coastal aquifers. Rather well-defined relationships of specific conductance (SC) to chloride exist (Hem 1992). To validate the relationship between SC and chloride, SC measurements by electrochemical conductivity cells and chloride concentration measurements by ion-selective electrode (ISE) were determined for five concentrations of Standard Atlantic Seawater OSIL at six different temperatures (30 unique samples). A strong linear relationship was established thus demonstrating the validity of using SC as a surrogate for chloride estimation. This study also compared inherent measurement drift of a chloride ISE and a conductivity sensor under controlled laboratory conditions over an 11-day period. Minimal drift of the conductivity sensor coupled with a large drift of the chloride ISE demonstrates a significant advantage of the conductivity sensor for long-term field deployments.

INTRODUCTION
Chloride ISEs use a potentiometric design to measure the total chloride ion concentration in water. One downfall to using an ISE is the propensity for measurement drift and requirement for frequent recalibration to compensate for the drift. The most accurate sensor response is achieved by performing a bi-thermal, three-point calibration. This adds obvious complication when performing field calibrations and measurements. Manufacturers recommend performing calibrations on a weekly basis at a minimum, implying long-term instability of the ISE. In addition to chloride ISEs, titrimetric methods can be used. Titrimetric reagents for determining chloride in seawater are hazardous (e.g., mercuric nitrate, silver nitrate) and require appropriate disposal. Interferences may require neutralization or elimination. *Standard Methods* (Eaton, A.D., et al., 2005, pp. 4-3, 4-70) notes that ion chromatography is the preferred method for determining chloride because it eliminates the use of hazardous reagents, distinguishes among halides, and provides a single instrumental technique for rapid, sequential measurement. However, unlike conductivity sensors, ion chromatography is not suitable for field applications or real-time monitoring. Alternatively, the use of an electrode-based conductivity cell can be used to compute the chloride concentration of a solution—provided the conductivity-chloride relationship is known or developed for the matrix of interest. This method uses a much more stable measurement technology that minimizes calibration and maintenance issues. To estimate chloride concentrations, conductivity sensors can be used to spot-check various sites or installed to collect data continually. The following section describes the development of a linear relationship between SC and chloride in standard seawater.

METHODS
A Standard Atlantic Seawater OSIL sample (35.0 PSU) was diluted to five concentrations: 35, 26.25, 17.50, 9.25, and 4.63 PSU. These samples were divided into six subsamples of each concentration. A sample at each concentration level was brought to a temperature of 0, 10, 20, 30, 40, and 50° C, respectively, using a VWR Programmable Thermal Bath, for a total of 30 unique samples (five concentrations at six temperature set points). These samples were allowed

to stabilize for a minimum of one hour at the temperature set point. An Instrulab precision thermometer recorded true temperature values.

Chloride and temperature data was collected using an In-Situ® Inc. TROLL® 9500 water quality sonde with chloride ISE. Prior to sample analysis, the chloride ISE was calibrated using a three-point, bi-thermal calibration with NIST-traceable chloride standards. Five replicate readings were taken at each of the 30 chloride/temperature test points. The five readings were averaged to determine a final response value for each testing point. The testing procedure was repeated using two factory calibrated In-Situ Aqua TROLL® 200 sensors. SC and temperature data were collected. SC values were compared with the corresponding chloride values, and the relationship was evaluated for validity (see Figure 1).

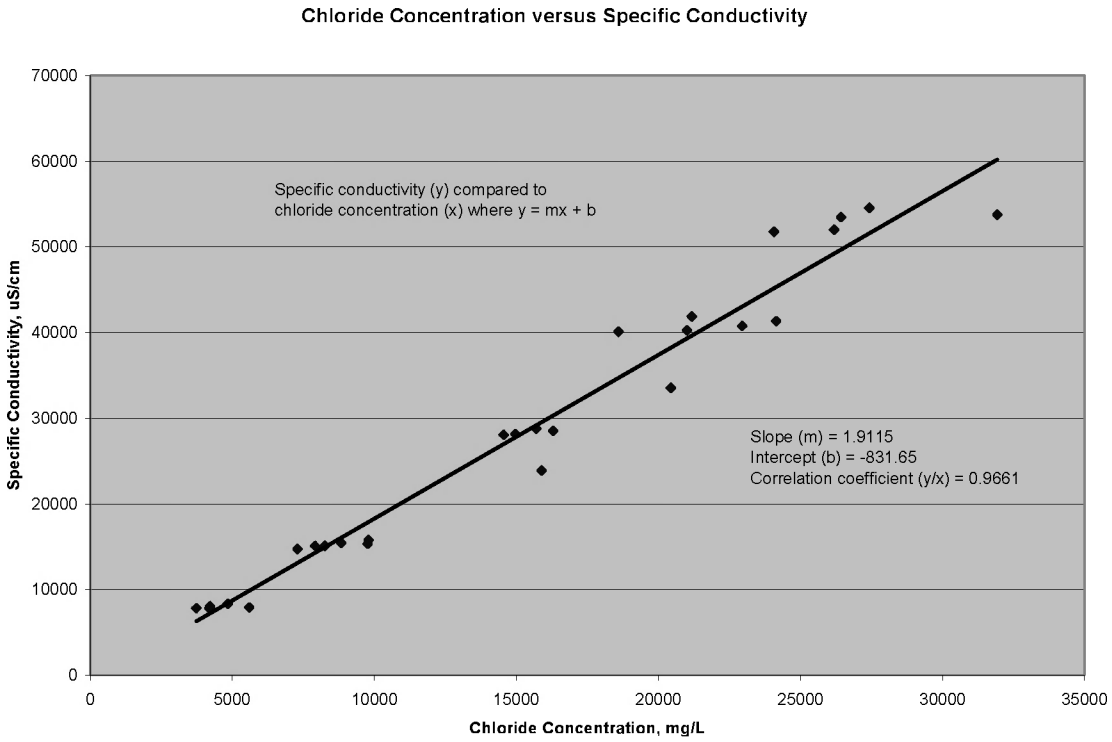

Figure 1. Relation of specific conductance to chloride concentration

To evaluate ISE and conductivity sensor drift, hourly readings were taken in a 17 PSU Standard Atlantic Seawater Standard over an 11-day period under controlled laboratory conditions. The sample was closed to the environment to prevent evaporation or any potential change to the solution. Two Aqua TROLL 200 sensors and a TROLL 9500 with chloride ISE were set to log data at hourly intervals. A third party, NIST-calibrated conductivity sensor was used to record daily values of the test solution. A freshly calibrated chloride ISE was used to measure final chloride concentration of the solution. Drift values were calculated based on the final test instrument reading minus the initial test instrument reading, and compared to the actual readings generated by the reference sensors to ensure that there was no solution drift.

RESULTS

Figure 1 shows the linear relationship between SC (µS/cm) and chloride concentration (mg/L). Statistical analysis on the ratio of SC values (y) and chloride concentration (x) showed a strong linearity ($R^2 = 0.9661$). Two outliers were removed from the data set due to a large offset in

these readings; the suspected cause for the erroneous data was a loss of electrical ground contact from the chloride sensor.

To determine sensor drift, the absolute variation for the conductivity and chloride sensors was calculated and compared with true reference meter results over an 11-day period (see Figure 2). The conductivity sensor drift was 54µS/cm or 0.2% of reading, which was within the manufacturer's stated accuracy specification of 0.5%. Secondary conductivity meter results indicated no drift of the solution throughout the 11-day test. The chloride sensor drift was 7,374 mg/L or 39% of reading. The secondary chloride ISE reading confirmed the significant drift of the chloride sensor.

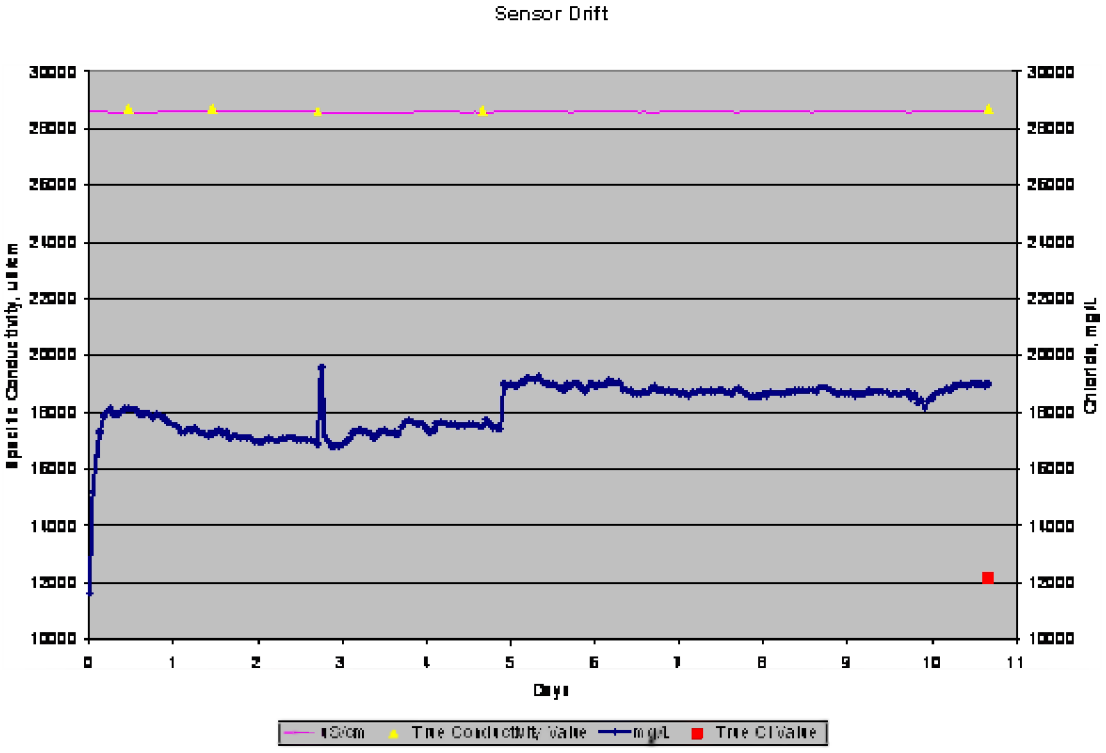

Figure 2: Comparison of chloride sensor drift and conductivity sensor drift

The stability of the conductivity sensor and the strong linear correlation of these two parameters indicate a clear advantage for use in chloride estimation over currently available methods. This is especially true for field deployment applications or long-term monitoring projects, in which sensor reliability is essential for accurate results.

DISCUSSION AND CONCLUSIONS

The conductivity sensor is a proven, stable method for measuring SC. Using this technology to estimate chloride concentrations offers several advantages over currently available chloride analysis methods, such as chloride ISEs, titrations, or ion chromatography. ISEs are accurate when recently calibrated, but are sensitive to drift, fouling, and are not ideal for field monitoring. Titrimetric methods are less precise than conductivity measurements (Farland 1975) and can generate hazardous wastes that require disposal. Ion chromatography is an accurate laboratory method, but cannot produce real-time data needed for rapid decisions in the field. To generate real-time field data that avoids using methods sensitive to drift, fouling, and other instabilities,

SC (surrogate) and chloride relationships can be developed. The study verifies the strong linear relationship between SC and chloride for seawater and demonstrates that SC is much less susceptible to drift and requires less maintenance than available ISEs. SC can provide more robust data sets for long-term projects such as saltwater intrusion studies of coastal aquifers, salt marsh studies, and coastal wetlands monitoring projects.

REFERENCES

Christensen, V.G., J. Xiaodong, and A.C. Ziegler. 1999. Regression analysis and real-time water-quality monitoring to estimate constituent concentrations, loads, and yields in the Little Arkansas River, South-Central Kansas, 1995-1999. U.S. Geological Survey, Water-Resources Investigations Report 00-4126.

Eaton, A.D., L.S. Clesceri, E.W. Rice, and A.E. Greenberg. 2005. Standard Methods for the Examination of Water and Wastewater. American Public Health Association. Washington, DC.

Farland, R.J. 1975. Salinity intercomparison report, the oceanographic subprogramme for the GARP Atlantic tropical experiment (GATE). Nat. Oceanogr. Instrum. Center, Washington, DC, November 1975.

Hem, J.D. 1992. Study and interpretation of the chemical characteristics of natural water (3rd edition). U.S. Geological Survey, Water-Supply Paper 2254.

Contact Information: Robert Mooney, In-Situ Inc., 221 E. Lincoln Avenue, Fort Collins, CO 80524 USA;
Phone: 970-498-1655; Fax: 970-498-1598; Email: rmooney@in-situ.com

Assessing the Extent of Saltwater Intrusion in the Aquifer System of Southern Baldwin County, Alabama

Dorina Murgulet and *Geoffrey R. Tick*
Department of Geological Sciences, The University of Alabama, Tuscaloosa, AL

ABSTRACT
Contamination of groundwater due to saltwater intrusion has become a major concern for coastal communities which rely on groundwater as their principal source of drinking water. The protection of groundwater resources from saltwater intrusion and groundwater overdraft is a critical concern in these areas as both groundwater resources and environmentally sensitive areas such as coastal wetlands and ecological coastal habitats may be at risk. A regional-scale study was conducted to assess the extent of saltwater intrusion for Baldwin County, Alabama. Groundwater wells were sampled and analyzed for salinity, chloride (Cl^-), total dissolved solids (TDS), and other geochemical parameters to determine the extent of saltwater intrusion, and the location of the freshwater/saltwater interface in the region. To meet the objectives of this study, spatial iso-concentration maps (i.e. salinity, Cl^-, and TDS) for the aquifer system were constructed using ArcGIS. Concentration data show relatively low salinity levels in the central and northern extent of the study area. Elevated levels of salinity, Cl^-, and TDS were observed in the local aquifers A1 and A2 along the coastal areas adjacent to the Gulf of Mexico with the highest concentration at Romar Beach and continuing towards the Intracoastal Waterway. The study provides an initial current data set of areas impacted or most vulnerable to saltwater intrusion and provides a scientific basis for effective management of the coastal aquifers in the study region.

INTRODUCTION
The coastal regions of Baldwin County are characterized by a continuously increasing economy and rate of development. Protection of groundwater resources from seawater encroachment is a real concern for coastal communities in this area due to impacts associated with increasing population, development, local industries, and tourism. In addition, predictions of increasing sea level and increased frequency and intensity of tropical storms and hurricanes in the region may exacerbate the problem over the long term.

The purpose of this study was to determine the extent and severity of saltwater intrusion in the aquifers underlying southern Baldwin County, Alabama using the most recently collected geochemical, geological, and hydrogeological information. To meet these objectives, well surveys and groundwater analyses were conducted over a two year period (2006 and 2007) and integrated with existing data attained primarily from the Alabama Department of Environmental Management (ADEM), the Geological Survey of Alabama (GSA) well records, and GSA Bulletin 126 (Chandler *et al.* 1985).

Background
The study area comprises approximately 1,625 square kilometers (628 square miles) of southern Baldwin County and is bounded by Interstate 10 to the north, by the Gulf of Mexico to the south, and by Mobile Bay, Perdido River, and Perdido Bay on the west, southeast and east, respectively. This region includes areas vulnerable to saltwater encroachment such as Fort Morgan Peninsula, Gulf Shores, Orange Beach, and Perdido Beach. The population of Baldwin County increased significantly from the year 2000 with the highest growth rates in Fort Morgan Peninsula, Gulf Shores, Orange Beach, and Ono Island. As a result of increasing population,

tourism, and development, groundwater pumping in the region increased from 2.7 x 10^7 L/day to 1.6 x 10^8 L/day between 1966 and 1995 (Reed and McCain 1971; Robinson et al., 1996a). Land use in Baldwin County varies considerably. The major types of land use include agriculture, recreation and tourism, seafood industries, and urbanization. Agriculture makes up approximately 40% of the land use/land cover of southern Baldwin County (Murgulet 2006, unpublished).

The stratigraphy of southern Baldwin County, as well as that of coastal and offshore Alabama, consists of a relatively thick Jurassic to Holocene sedimentary rocks (Chandler *et al.*, 1985). At relatively shallow depths, interbedded sands, silts, gravels and clays comprise the middle Miocene to Holocene sedimentary rocks which hosts the freshwater aquifer zones of Baldwin County area. The sediments are part of three widely recognized geologic units defined by Reed (1971) as 1) the Miocene Series undifferentiated; 2) the Citronelle Formation; and 3) alluvium, low terrace, and coastal deposits. The aquifer system beneath southern Baldwin County that serves as the source of freshwater is divided into three distinct units: a) Aquifer zone A1, the upper unit, known as the Beach Sand aquifer, an unconfined aquifer that is roughly 6 to 20 meters thick in the study area (Chandler *et al.*, 1985); b) Aquifer zone A2, the Miocene-shallow Pliocene aquifer varies from confined to semi-confined (southern part of the study area) to unconfined throughout the extent of the study area (north of the Intracoastal Waterway); c) Aquifer zone A3, the lower unit known as the Deep Miocene aquifer, extends from the upper confining unit that underlies aquifer zone A2 to the top of the Pensacola Clay (200 meters to more than 300 meters below sea level). Moreover, the aquifer system consists of two distinct units through the central and northern portion of the study area.

METHODS

To meet the objectives of this paper, a multitude of tools were used to link the hydrogeologic system and groundwater geochemical data of southern Baldwin County to spatial statistics and map modeling. Such integration allows, for example, meaningful identification of the seawater contaminated regions. For this purpose, geologic and hydrogeologic information, and groundwater quality parameters including salinity, Cl^- and TDS concentration data were collected and compiled to generate spatial distribution and contamination maps. For the purposes of this study and consistency with current definitions, "freshwater" is considered to be water comprising concentrations no more than 500 mg/L, 250 mg/L, and 500 mg/L for salinity, Cl^-, and TDS, respectively (MCLs "maximum contaminant levels" reported by USEPA, 1986). Once these limits are exceeded, the water is no longer potable for drinking water purposes and additional water treatment is needed or well abandonment or discontinued operation is required. The relationships between the three parameters were examined as a means of assuring consistency between samples and verification of the saltwater source (i.e. seawater).

Digital maps have been produced and used to construct a spatial database for the study area. Results obtained from this methodology have been incorporated with data collected for this project and used to create the final contamination digital maps. Concentration and hydraulic head contour maps were prepared to determine areas most vulnerable to saltwater intrusion and the extent of saltwater intrusion for each of the developed aquifer zones.

RESULTS

Integration of hydrogeologic and geochemical data (i.e. salinity, Cl^-, TDS, etc.) from approximately 200 wells throughout Baldwin County, to spatial relations and map modeling allowed for comprehensive identification of the seawater contaminated regions. Elevated

concentrations of salinity, Cl^-, TDS and high conductivities were observed for both aquifer zones A1 and A2. Groundwater samples from aquifer zone A1 exhibited salinity, Cl^-, and TDS concentrations above MCLs in close coastal proximity to Gulf Shores (including part of Fort Morgan Peninsula), Orange Beach, and Ono Island. Groundwater in aquifer A2, near the coastal margin, was determined to possess lower water quality with relatively high salinity (e.g. Figure 1), Cl^- and TDS concentrations. As part of this current study, groundwater samples obtained from wells completed in aquifer zone A3 exhibited low concentrations of salinity, Cl^-, and TDS. The results shown here include only the chloride concentration map for aquifer A1. Groundwater head contour maps constructed using the head values corrected for the density effects, provided the current state of regional and local groundwater flow for the study. Groundwater flow trended generally south, south-southeast and south-southwest with relatively steeper hydraulic gradients observed in those areas less impacted by saltwater intrusion.

Figure 1. Aquifer zone A2- salinity concentration map.
Concentrations are in mg/L; contour lines are labeled correspondingly.

DISCUSSIONS AND CONCLUSIONS

The hydrogeochemical data (e.g. salinity, Cl^-, and TDS concentrations and resistivity and specific conductance) and the location of the impacted areas revealed the Gulf of Mexico and the Intracoastal Waterway as the main sources of saltwater intrusion. The results of this study indicate that saltwater intrusion may have occurred in aquifer A1, especially in regions relatively close to the Gulf of Mexico. Thus, the presence of saltwater in aquifer A1 is likely the result of a combination of both saltwater intrusion from the Gulf of Mexico (e.g. Fort Morgan Peninsula) and surface contamination (i.e. from storm events due to seawater surface infiltration). Another source of contamination of aquifer A1 is due to the direct infiltration from the Intracoastal Waterway which crosses the southern part of the study area from east to west and from saltwater ponds located north of Intracoastal Waterway. The results of this study indicate that saltwater intrusion has occurred in aquifer A2, specifically in the close proximity to the Gulf of Mexico (e.g. Romar Beach). The results are confirmed by geochemical data collected over a two year period. Back in 1985, Chandler et.al. (1985) revealed the fact that aquifer A2 was contaminated with seawater at Romar Beach from the Gulf of Mexico and that the saltwater ponds are an additional source of saltwater contamination to the aquifer A2. Therefore, based on these previous results and the new geochemical data it is speculated that the saltwater contamination of

aquifer zone A2 may be the result of aquifer overdevelopment and saltwater infiltration from upper aquifer A1. In addition to these sources we identify the Intracoastal Waterway as an important source of saltwater contamination to both aquifer A1 and A2. Groundwater samples and iso-concentration maps revealed that aquifer zone A3 did not exhibit significant degradation of water quality due to saltwater intrusion. The groundwater concentration data suggest that aquifer zone A3 is less vulnerable to saltwater contamination. However, this does not mean that saltwater intrusion has not occurred or exists within this aquifer zone (A3) but may rather be due to the absence of groundwater wells (i.e. water quality data) developed in this aquifer in close proximity to the coastline or that the surveyed wells are either established in a relatively shallow portion of the aquifer zone A3 or that aquifer A3 in that region has not been infiltrated with saline water.

The combination of tools used for the purpose of this study provides an opportunity to assemble, standardize, and analyze scientific data that comes from a variety of sources, making it available to others who may be able to continue with further research studies and/or use the information for improved groundwater management strategies in the area.

REFERENCES

Chandler, R.V.; Moore, J.D.; and Gillett, B. **1985**, Ground-Water Chemistry and Salt-Water Encroachment, Baldwin County, Alabama: *Geological Survey of Alabama Bulletin 126*. pp. 16, 17, 53, 54, 78-80, 84-86.

Reed, P.C. and McCain, J.F. **1971**, Water Availability of Baldwin County, Alabama: *Geological Survey of Alabama, Division of Water Resources, Map 96.*

Reed, P.C. **1971**, Geologic Map of Baldwin County, Alabama: *Alabama Geological Survey Special Map 94*, p.55.

Contact Information: Dorina Murgulet, Department of Geological Sciences, University of Alabama, 201 7th Ave. Room 202, Bevill Building, Tuscaloosa, AL 35487, Phone: (205)348-5095; Fax: (205)348-0818, Email: murguletd@yahoo.com

Evaluating Safe Yield for Supply Wells in an Aquifer with Fresh Water/Salt Water Interface

Gregory Nelson, *Liliana Cecan, Charles McLane* and *Maura Metheny*
McLane Environmental, LLC, Princeton, NJ, USA

ABSTRACT
Coastal communities often rely on groundwater resources for water supply. Ensuring a safe and adequate supply requires a balance that meets community demands while preventing deleterious hydrologic and environmental impacts. In coastal aquifer settings where supply wells are in proximity to a salt water front (lateral encroachment of a salt water wedge or vertical upconing of an underlying salt water interface) a determination of safe yield must account for the potential for groundwater withdrawals to introduce saline water into the well field, resulting in unacceptable water quality in the short term and a fouling of the aquifer near the well field for a longer period of time.
In this paper we examine factors affecting the safe yield of a well pumping above the salt water transition zone in a fresh water lens aquifer similar to those found on Cape Cod, Massachusetts. We begin with a discussion of traditional methods for determining safe yield and compare these preliminary estimates with the more refined and restrictive estimates produced using a sophisticated density-dependent salt water flow model. A simple example demonstrates that proper consideration of potential salinity impacts for a typical supply well may decrease the feasible safe yield by 30 percent or more.

ACKNOWLEDGMENTS
The authors wish to thank Mark White of Environmental Partners Group and Andrew Miller of Head First for many hours of discussions that have helped to improve this paper.

INTRODUCTION
Communities for which groundwater is a major source of water supply must carefully manage the resource by striking a balance between meeting community water demands while avoiding deleterious hydrologic and environmental impacts. In certain coastal aquifers, water supply wells are located in proximity to a zone of laterally encroaching salt water or are screened a short distance above a fresh water / salt water interface. A determination of safe yield must account for the potential for groundwater withdrawals to introduce saline water into the well field, resulting in unacceptable water quality in the short term and a fouling of the aquifer in the vicinity of the well field for a much longer period of time.
Traditional methods of determining safe yield or sustainable yield for a water supply well can include estimates based on specific capacity; a long term (e.g. 5-day) aquifer test (as some states require); or the requirement not to exceed a certain drawdown limit near a protected wetland or not to decrease discharges to a sensitive surface water body by more than a certain amount (Kalf and Woolley, 2005). Such methods, which do not explicitly consider potential salinity impacts at the wellhead, may overestimate safe yield when compared with more refined estimates produced using an analytical salt water interface model (which can provide some information regarding the likelihood of salinity impacts) or a more sophisticated density-dependent salt water numerical flow and transport model capable of simulating the drinking water quality for the well field.

AQUIFER CHARACTERIZATION FOR SAFE YIELD ANALYSIS

A number of aquifer parameters in a coastal setting affect the movement of the saline transition zone toward an operating supply well. These parameters, which should be characterized as part of the pre-permitting aquifer test, include:

Proper Delineation of the Fresh Water/Salt Water Interface

The accurate, before pumping, spatial definition of the interface and transition zone will provide an initial location of the interface and transition zone for modeling and for comparison with changes caused by pumping. The monitoring of changes to the interface and transition zone will provide data useful in model calibration and ultimately in safe yield determination. A protective safe yield value depends on how the interface reacts to pumping stresses, thus the design of a pumping test and monitoring of the test should be planned to define the interface and transition zone before and during the pumping test.

Characterization of the Fresh Water and the Salt Water Density Distributions

Density differences will not only influence groundwater flow in a coastal aquifer but can affect measurements of hydraulic head collected from piezometers or monitoring wells. A correction must be applied to measured groundwater elevations to account for density effects at measuring points in the salt water transition zone. These corrections can be significant (on the order of several feet) in determining groundwater flow and in analyzing potentiometric surfaces. A proper modeling code, such as SEAWAT (Gou and Langevin, 2002) which accounts for variable density flow, should be selected so that density dependent groundwater flow can be accurately modeled.

Characterization of the Horizontal and Vertical Hydraulic Conductivity

Safe yield for a well in a coastal aquifer near a potentially encroaching salt water zone is sensitive to the horizontal and vertical hydraulic conductivity of the aquifer material. Low values of vertical conductivity (i.e. strong vertical anisotropy) in the area surrounding the well, or locally beneath the well screen, will dampen salt water upconing and increase estimated safe yield (Ma et al., 1997; van Dam, 1999). Therefore, the hydrogeology and inclusion of the hydrogeology in the model below the pumping well is important in determining safe yield. A concurrent study (Cecan et al., this conference), describes a method of characterizing the hydraulic conductivity and vertical anisotropy in a fresh water lens aquifer through modeling of a pumping test.

Through characterization of the interface, density contrasts and distributions, and hydrogeology of the study area, an understanding of the interface can be incorporated into a salt water flow and transport model to better estimate the safe yield.

SALINITY IMPACT SAFE YIELD ANALYSES

Effect of Considering Potential Salinity Impacts

Water supply for the outer portions of Cape Cod, Massachusetts is derived primarily from pumping of fresh water lenses that range up to approximately 250 feet thick near their centers. Over-pumping of a well has been observed to result in salt water fouling. To augment the current water supply, a new well is proposed. Traditional safe yield analysis testing (based on the state of Massachusetts well permitting requirements) results in a specific capacity of 35 gpm/ft of

drawdown and an available drawdown of 20 ft; yielding a safe yield estimate of approximately 1.0 million gallons per day (MGD). This estimate does not consider salt water upconing.

The USGS model of Cape Cod (Masterson, 2004) [23 layers; horizontal grid spacing of 400 ft] developed using SEAWAT (Gou and Langevin, 2002) was used to simulate pumping 1.0 MGD from a single well located near the center of a fresh water flow cell. The vertical anisotropy in the aquifer zone between the well screen and the saltwater transition zone included in the model is 5:1, which is near the lower end of the range for this aquifer. Simulated Total Dissolved Solids (TDS) in the well exceeded the current drinking water MCL of 500 mg/L in approximately 40 years (Figure 1). However, if pumping is reduced to 0.72 MGD (approximate 30 percent reduction) salinity remains below the MCL for greater than 100 years of pumping (Figure 1).

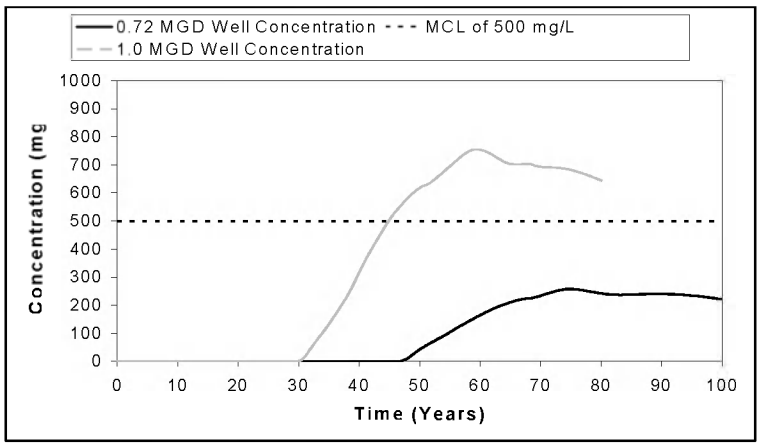

Figure 1 Simulated Total Dissolved Solids breakthrough in a well pumping at 1.0 and at 0.72 MGD from a fresh water lens.

A 30% reduction in pumping results in a well head concentration of 250 mg/L, which is approximately half of the TDS MCL. Depending on what is considered a safe or acceptable well head concentration, the safe yield rate could be adjusted accordingly. Through use of a model that incorporates the interface dynamics and salt water transport, a more protective safe yield estimate is obtained. Further reduction of the pumping rate may be required if water quality requirements are more stringent (e.g. that sodium concentration be less then a given value).

Effect of Vertical Anisotropy

To show the effects of anisotropy on the safe yield, two simulations with different anisotropies were run. In the stronger anisotropy scenario the vertical anisotropy in the area ranged from 6 to 1000, and in the weaker anisotropy scenario the anisotropy ranged from 3 to15. The pumping rate in both scenarios was chosen to be 0.6 MGD.

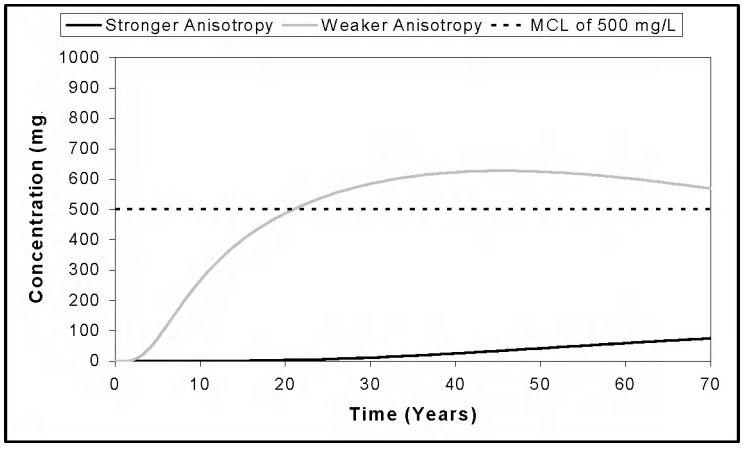

Figure 2 Simulated Total Dissolved Solids breakthrough in a well pumping at 0.6 MGD from a fresh water lens with different anisotropies.

The concentration-time plots in Figure 2 show clearly the influence of the stronger vertical anisotropy (dark line), which by decreasing the concentrations at the pumping well, allow for an increased safe yield.

DISCUSSION AND CONCLUSIONS

Safe yield estimates for water supply wells in coastal aquifer settings should consider the potential for withdrawals over long periods of time to cause saline water to be drawn toward and adversely impact the well or well field. Such an analysis can be accomplished using a computer model of groundwater flow that accounts for salt water density effects and the transport of salinity from the dilute portion (top) of the transition zone to the well. In this study the Cape Cod SEAWAT model developed by the USGS was used to perform a safe yield analysis based on salinity impacts to a water supply well in a freshwater lens aquifer. Comparison of model results with safe yield estimates derived using commonly applied and accepted methods, demonstrates consideration of potential salinity impacts may reduce estimates by 30 percent or more.

Since salt water intrusion impacts to a well field can render the well field unusable for decades, water managers responsible for the siting and operation of well fields in coastal aquifers should consider potential salinity impacts when establishing safe yield values as part of well field permitting or operational studies. Aquifer anisotropy and the location of, and density distribution surrounding, the transition zone can have a significant impact on the safe yield estimate and should be characterized as part of the well field testing program.

REFERENCES

Cecan, Liliana, Gregory Nelson, Charles McLane, Maura Metheny, *in prep.* Pumping Test Analyses in an Aquifer with Fresh water/Salt Water Interface, *This Meeting*.

Guo, Weixing and Christian D. Langevin. 2002. User's Guide to SEAWAT: A Computer Program for Simulation of Three-Dimensional Variable-Density Ground-Water Flow. U.S. Geol. Survey, Techniques of Water-Resources Investigations 6-A7. Tallahassee, Florida, 77 p.

Kalf, Frans R.P. and Woolley, Donald R. 2005. Applicability and methodology of determining sustainable yield in ground water systems. *Hydrogeology Journal* 13:295 – 312.

Ma, Tain Shing, Marios Sophocleous, Yun-Sheng Yu, and R. W. Buddemeier. 1997. Modeling saltwater upconing in a freshwater aquifer in south-central Kansas. *J. Hydrol.* v 201:120-137.

Masterson, John P. 2004. Simulated Interaction Between Freshwater and Saltwater and Effects of Ground-Water Pumping and Sea-Level Change, Lower Cape Cod Aquifer System, Massachusetts. U.S. Geological Survey, Scientific Investigations Report 2004-5014.

Missimer Thomas M., Maliva, Robert G. and Weixing Guo. 2007. Sustainability & the Management of Water Resources in Florida. Florida Water Resources Journal. 20 – 62.

van Dam, J.C. 1999. "Exploitation, Restoration and Management". In. Bear, Jacob, and others, Eds., Seawater Intrusion in Coastal Aquifers - Concepts, Methods and Practices, Dordrecht, The Netherlands, Kluwer Academic Publishers, pp. 73-125.

Contact Information: Gregory Nelson, McLane Environmental, LLC, 707 Alexander Road, Suite 206, Princeton, NJ 08540 USA, Phone: 609-987-1400, Fax: 609-987-8488, Email: gnelson@mclaneenv.com

Global Warming and Salt Water Intrusion: Bangladesh Perspective

Md. Abu Noman and *Chowdhury Mohammad Farouque*
Institute for Environment and Development Studies-IEDS, Dhaka-Bangladesh

ABSTRACT
Global Warming has already started to hit the Bangladesh coastal areas. The salty sea water intrusion and its disastrous effects in landscape, ecology and human health already created wide-scale agony amongst the inhabitants of Bangladesh coastal belts.

INTRODUCTION
The global climate change is one of the most significant environmental issues of the present world. The problem of this human-induced climate change first came to the attention of the global public and international policy makers when the Intergovernmental Panel on Climate Change (IPCC) published its first assessment report in 1990 (Huq and et.al).

The effects of global climate change are evident now, as we are experiencing through irregular weather conditions. These effects are multidimensional. Among the many effects, scientific evidence has proved that several low-lying countries of the world will be badly affected by climate change, and scientists are predicting that Bangladesh will be among the countries most affected by the change.

The sea level along the Bangladesh coast is rising at about 3 millimeters a year, and the sea surface temperature is also showing a rising trend.Bangladesh is facing the reality of climate change due to global warming like other parts of the planet.

The climate pattern is altering across the world due to global warming. This will have an impact on the composition of the atmosphere, hydrology, geomorphology, ecology, soil, land use, biological diversity, vegetation etc. The individual impacts on each environmental component also have interactive effects. Environmental components are interrelated, and the world's ecosystems are linked to these components. Therefore, many natural ecosystems will be changed as a result of climate change.

The tropical and subtropical countries will be more vulnerable to the potential impact of global warming through the effects on crops, soils, insects, weeds, and diseases (Bangladesh State of the Environment, 2001). Bangladesh is in the subtropical region. Therefore, the agriculture of this country will be affected. The effects of climate change are already evident in the agro-ecosystem of the country.

Salt Water Intrusion
Bhamia, a sea-shore village of Bangladesh situated adjacent to Patenge beach in Southern district of Chittagong. The Global warming has a taste in this village. It is the taste of salt.
Only a few years ago, water from the local pond was fresh and sweet on one habitant of the village Samit Biswas' tongue. It quenched his family's thirst and cleansed their bodies. But drinking a cupful now leaves a briny flavor in his mouth. Tiny white crystals sprout on Biswas' skin after he bathes and in his clothes after his wife washes them.

Gain, 65, once grew rice to support himself and his family, but his harvests started shrinking as saline levels in the water went up. To cope, he followed the example of many of his neighbors

and switched over to shrimp farming, a way to take advantage of the salty water washing over the fields.
For the first time, shrimp farming occupies more of the cultivable land than traditional crops in the area around Bhamia. While the shift has enabled some villagers to survive, it has also created other headaches. Less labor-intensive, shrimp farming has wound up boosting unemployment. Thousands of residents have migrated to other parts of Bangladesh or India in search of work.

Worse yet, deliberately trapping so much briny water to raise shrimp has increased the sodium concentration in the soil, which aggravates the salinity creeping into drinking-water supplies. "From ancient times, our people used [local] ponds for drinking water. Now they need to go four to five kilometers to collect sweet water," said Mohon Kumar Mondal, 31, a local environmental activist of IEDS. Residents report an increase in health problems such as diarrhea, skin diseases and dysentery. The salty water has also choked many of the palm and date trees that once lent a fecund beauty to the sun-baked landscape.

BACKGROUND
The change, international scientists say, is the result of intensified flooding caused by shifting climate patterns. Report on changing world weather by the United Nations said that global warming fueled by human activity could lift temperatures by 8 degrees and the ocean's surface by 23 inches by 2100. Here in southwest Bangladesh, the bleak future forecast by the report is already becoming a reality, bringing misery along with it.

Heavier-than-usual floods have wiped out homes and paddy fields. They have increased the salinity of the water, which is contaminating wells, killing trees and slowly poisoning the mighty mangrove jungle that forms a natural barrier against the Bay of Bengal.

Bangladesh, a densely crowded and painfully poor nation, contributes only a minuscule amount to the greenhouse gases slowly smothering the planet. But a combination of geography and demography puts it among the countries experts predict will be hardest hit as the Earth heats up.

RESULT
Nearly 150 million people, the equivalent of about half the U.S. population, live packed in an area the size of Iowa and about as flat. Home to where the mighty Brahmaputra, Ganges and Meghna rivers meet, most of Bangladesh is a vast delta of alluvial plains that are barely above sea level, making it prone to flooding from waterways swollen by rain, snowmelt from the Himalayas and increased infiltration by the ocean. Global warming trends have already exacerbated that, and the situation will probably only get worse, scientists say.

DISCUSSION AND CONCLUSIONS
Other low-lying countries are also at risk, such as the Netherlands and tiny islands in the South Pacific that could eventually be swallowed up by the expanding oceans. But the population of those countries is only a fraction of that of Bangladesh.

If the sea here rises by a foot, which some researchers say could happen by 2040, up to 12 percent of the population would be made homeless. A 3-foot rise by century's end — a possible scenario if polar ice caps melt at a more rapid pace — would wreak havoc in Bangladesh on an apocalyptic, Atlantis-like scale, according to scientific projections and models.

A quarter of the country would be submerged. Dhaka, now in the center of the nation, would sit within 60 miles of the coast, where boats would float over the drowned remnants of countless town squares, markets, houses and schools. As many as 30 million people would become refugees in their own land, many of them subsistence farmers with nothing to subsist on any longer.

"Lives in Bangladesh will be devastated through no fault of the people concerned," Sabihuddin Ahmed, the former ambassador to Britain and a former Environment Ministry official, wrote in the Guardian newspaper in September, 2006. For folks in the West, Ahmed said, the onslaught of global warming may seem decades away. In Bangladesh, "the future has arrived."

REFERENCES

IEDS Data Base, 5/12-15, Eastern View (5th floor), 50, D.I.T Ext. Rd. Dhaka-1000, Bangladesh

Daily Guardian, London, UK

Environment News, 5/12-15, Eastern View (5th floor), 50, D.I.T Ext. Rd. Dhaka-1000, Bangladesh

Contact Information: Md. Abu Noman, Institute for Environment and Development Studies, 5/12-15, Eastern View (5th floor), 50, D.I.T Extension Road, GPO Box-3691, Dhaka-1000, Bangladesh. Tel. + 880-2-935 4128, Fax + 880 2 831 5394, Email: iendesbk@accesstel.net

Causes of Borehole Flow and Effects on Vertical Salinity Profiles in Coastal Aquifers

Delwyn S. Oki and *Todd K. Presley*
U.S. Geological Survey, Pacific Islands Water Science Center, Honolulu, HI, USA

ABSTRACT
Freshwater thickness in a coastal freshwater-lens system commonly is evaluated from vertical salinity profiles (measured by fluid-electrical-conductivity logs or water-quality samples at various depths) in deep observation boreholes. Flow within an observation borehole caused by withdrawals from pumped wells and ocean tides can significantly affect measured salinity profiles. Borehole flow can be recognized from diagnostic step-changes in a salinity profile, comparisons between salinity profiles from deep and shallow boreholes, or flow measurements. Knowledge of borehole flow is important for proper interpretation of salinity profiles by water managers and ground-water modelers.

INTRODUCTION
In coastal aquifers, vertical salinity profiles commonly are collected from open or screened observation boreholes to evaluate the thickness of a freshwater body and underlying brackish-water transition zone (Meyer and Presley 2001; Gingerich and Voss 2005). By monitoring changes in the freshwater thickness over time, water managers can determine appropriate withdrawal rates from production wells in the aquifer. Vertical salinity profiles also represent valuable data for calibration of numerical ground-water models designed to simulate density-dependent ground-water flow and transport in coastal aquifers (Gingerich and Voss 2005).

The underlying assumption in using salinity profiles is that the measured vertical distribution of salinity in a borehole is representative of salinity in the adjacent aquifer. However, natural or human-induced vertical hydraulic gradients in the aquifer can produce flow in the borehole. Complex flow patterns may exist in observation boreholes in coastal areas (Paillet and Hess 1995). Flow within an observation borehole causes water that entered the borehole in one interval to be present in another interval and, thus, the salinity profile obtained from the borehole may differ from the profile in the adjacent aquifer.

INDICATORS OF BOREHOLE FLOW
One of the diagnostic indicators of borehole flow that is commonly seen in fluid-conductivity logs is a step-like change in conductivity. These step-like changes indicate where water may be either entering or exiting the borehole (Figure 1). Fluid-conductivity logs commonly have many step-like changes, which make it difficult to uniquely determine the direction of borehole flow and whether the measured conductivity overestimates or underestimates the value in the adjacent aquifer.

Differences in fluid-conductivity profiles measured in nearby boreholes that extend to different depths also provide valuable insight into the effects of borehole flow. Conductivity profiles measured in shallow and deep observation boreholes, located about 900 m apart on Oahu, show marked differences in water quality (Figure 2). The profile from the shallow borehole indicates freshwater throughout, whereas the profile from the deep borehole indicates brackish water of nearly uniform conductivity between depths of 20 and 220 m below sea level. Because production wells in the vicinity of the boreholes produce freshwater, it is unlikely that the measured profile from the deep borehole accurately reflects conditions in the aquifer. Rather,

upward flow within the deep borehole is affecting the measured profile and possibly the surrounding aquifer (brackish water flows up the well and out into the aquifer at shallow depths).

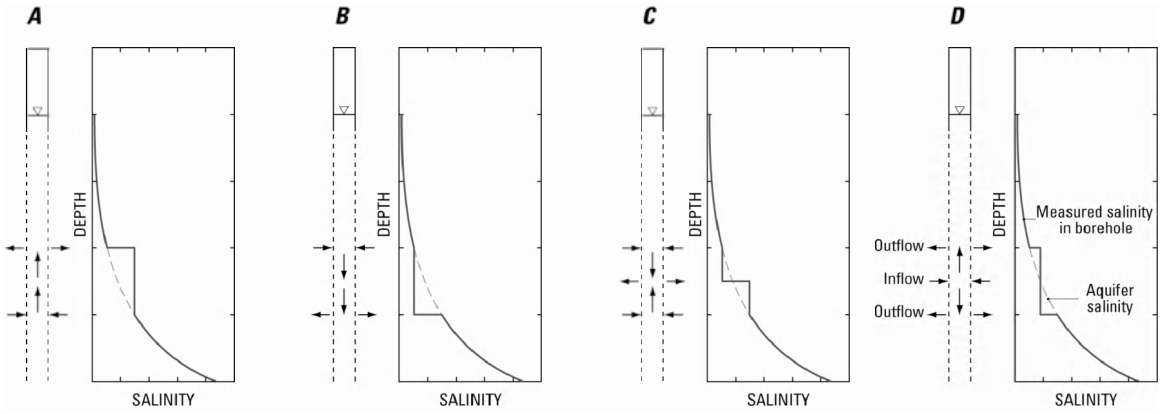

Figure 1. Schematic vertical salinity profiles in a borehole with (A) upward flow, (B) downward flow, (C) converging flow, and (D) diverging flow.

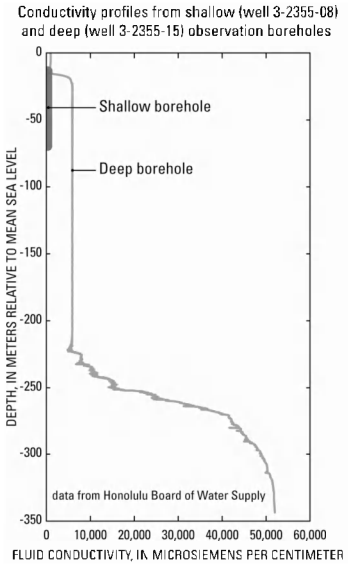

Figure 2. Comparison of fluid-conductivity profiles from shallow and deep observation boreholes, southern Oahu, Hawaii.

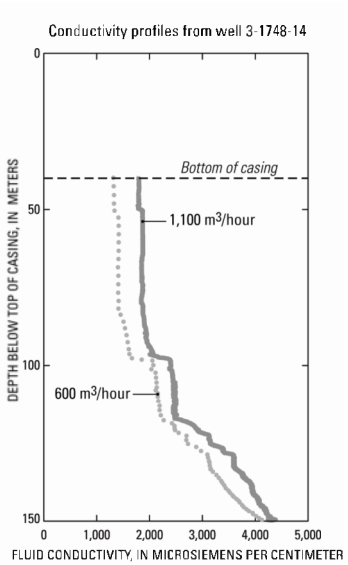

Figure 3. Fluid-conductivity profiles for nearby withdrawal of 600 m^3/hour and 1,100 m^3/hour, southern Oahu, Hawaii.

CAUSES AND EFFECTS OF BOREHOLE FLOW

Borehole flow is caused by vertical hydraulic gradients, which can be affected by both natural factors (ocean tides and variations in recharge) as well as anthropogenic factors (ground-water withdrawals). Fluid-conductivity profiles may be affected significantly by withdrawal rates at nearby pumped wells (Paillet et al. 2002). For example, measured profiles in an observation borehole on Oahu, Hawaii (Kaimuki deep monitor well 3-1748-14) indicate increased conductivity at comparable depths when nearby withdrawal wells are pumped at a higher rate (Figure 3). Electromagnetic-flow-meter measurements confirm that the increased fluid

conductivity at the higher withdrawal rate is caused by increased upward borehole flow and does not reflect an overall change in water quality in the adjacent aquifer.

Continuous monitoring of fluid conductivity at fixed depths in an observation borehole also can provide an indication of borehole flow. Data from an observation borehole on Guam show diurnal variations in fluid conductivity at a depth of 35 m below mean sea level. Variations in fluid conductivity are tidally influenced and are in phase with measured water-level variations. To investigate the possibility of borehole flow, an analysis was made to determine if the conductivity variations could be explained by simple vertical shifts (no rotation or expansion) of a depth-conductivity profile by amounts equal to the water-level variations. A conductivity time series was synthesized by shifting a depth-conductivity profile according to the water-level variations and determining the conductivity variations at the desired fixed depth (Figure 4). The synthetic time series indicates only a small fraction of the measured conductivity variations at the fixed depth, which probably do not accurately reflect conductivity variations in the adjacent aquifer. Rather, the measured conductivity variations likely reflect tidally driven borehole flow. This indicates that depth-conductivity profiles measured at extremes of the tidal cycle may differ significantly.

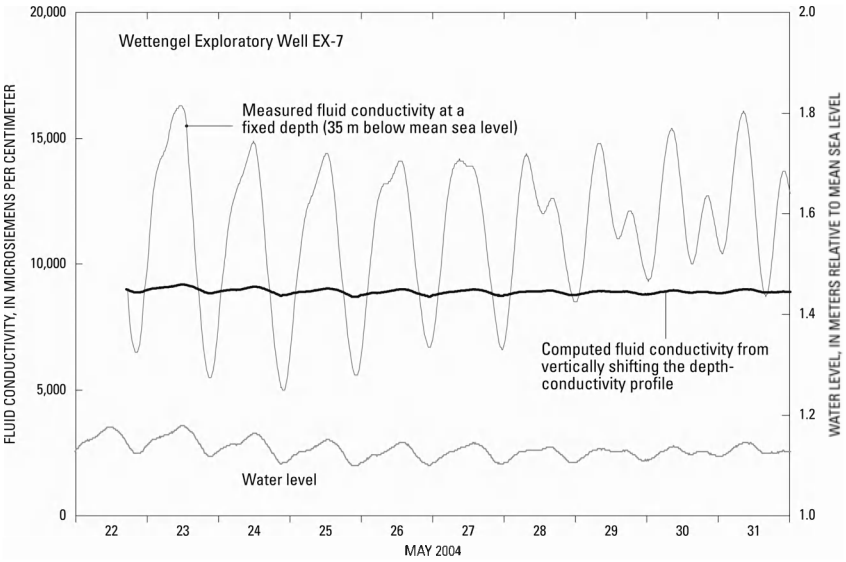

Figure 4. Time variation in measured fluid conductivity at a fixed depth and computed fluid conductivity from vertically shifting the depth-conductivity profile.

DISCUSSION AND CONCLUSIONS

For cases in which upward flow exists in an observation borehole, brackish water or saltwater from deeper zones can cause measured salinity in the borehole to overestimate salinity in the adjacent aquifer in shallower zones. In contrast, for cases in which downward flow exists, freshwater from shallow zones can cause measured salinity in the borehole to underestimate salinity in the adjacent aquifer in deeper zones. All other factors being equal, higher rates of borehole flow will have a greater effect on the measured salinity profile.

On the basis of borehole-flow measurements, Voss and Wood (1994) indicated that measured water-quality profiles from open boreholes in southern Oahu generally are representative of water quality in the aquifer, although local flow-related disturbances that affect 20 m sections of

the profile may exist. Paillet et al. (2002) indicated that the shapes of fluid-conductivity profiles from open boreholes in southern Oahu and profiles of pore-water electrical conductivity from induction-conductivity logs generally are the same. However, as indicated by Paillet et al. (2002) upward flow of saline water from deeper zones can be diluted by inflows of fresher water from shallower zones. Thus, measured fluid-conductivity logs may appear reasonable at the scale of the entire profile but may not accurately reflect conductivity at a particular depth in the aquifer. Water-quality sampling in conjunction with flow-meter measurements at discrete depths in an observation borehole can be used to estimate aquifer water quality using a simple mixing cell model (Izbicki et al. 2005). In addition, piezometers installed at different depths can be used to unequivocally determine aquifer water quality.

REFERENCES

Gingerich, S.B. and C.I. Voss. 2005. Three-dimensional variable-density flow simulation of a coastal aquifer in southern Oahu, Hawaii, USA. Hydrogeology Journal 13: 436-450.

Izbicki, J.A., A.H. Christensen, M.W. Newhouse, G.A. Smith, and R.T. Hanson. 2005. Temporal changes in the vertical distribution of flow and chloride in deep wells. Ground Water 43, no. 4: 531-544.

Meyer, W. and T.K. Presley. 2001. The response of the Iao aquifer to ground-water development, rainfall, and land-use practices between 1940 and 1988, Island of Maui, Hawaii. USGS Water-Resources Investigations Report 00-4223.

Paillet, F.L. and A.E. Hess. 1995. Geophysical log data from basalt aquifers near Waipahu on the Island of Oahu and Pahoa on the Island of Hawaii, Hawaii: USGS Open-File Report 95-383.

Paillet, F.L., J.H. Williams, D.S. Oki, and K.D. Knutson. 2002. Comparison of formation and fluid-column logs in a heterogeneous basalt aquifer. Ground Water 40, no. 6: 577-585.

Voss, C.I. and W.W. Wood. 1994. Synthesis of geochemical, isotopic and groundwater modeling analysis to explain regional flow in a coastal aquifer of southern Oahu, Hawaii. In Proceedings of Mathematical models and their applications to isotope studies in groundwater hydrology, a final Research Co-ordination Meeting held in Vienna, June 1-4, 1993, 147-178.

Contact Information: Delwyn S. Oki, U.S. Geological Survey, Pacific Islands Water Science Center, 677 Ala Moana Blvd., Suite 415, Honolulu, HI 96813 USA, Phone: 808-587-2433, Fax: 808-587-2401, Email: dsoki@usgs.gov

Brackish Groundwater as a New Resource for Drinking Water, Specific Consequences of Density Dependent Flow, and Positive Environmental Consequences

T. N. Olsthoorn[1,2]
[1]Delft University of Technology, Delft, the Netherlands
[2]Waternet, Amsterdam, the Netherlands

ABSTRACT
The Netherlands, like other deltaic areas have extended aquifers partly filled with brackish to saline groundwater most probably resulting from previous transgressions. Low-lying areas like previous lakes hat have been pumped dry in the past to allow development. In these so-called polders a dense network of surface canals and ditches maintain the surface water level and discharge the recharge surplus and the intense groundwater seepage. The network effectively creates a fixed-head top boundary condition. To a large extent this seepage, which is driven by the head difference with adjacent areas of mostly several meters, generates saltwater upconing. Much of the water management consists of flushing these polders to get rid of this brackish water, while this water itself poses environmental problems due to its salinity and high concentration of nutrients like phosphates, sulfates and ammonia.

INTRODUCTION
It is not easy to find and develop reliable sources for drinking water in this densely populated country with its intense agriculture and industrialization. But since reverse osmosis technology has developed so much, currently, drinking-water production from anaerobic, particle-free brackish to saline groundwater has become an economically attractive possibility especially due to its technical simplicity as compared to the complicated series of treatment steps necessary when using (polluted) surface water. A perceived major advantage of using brackish groundwater is that it is old and therefore anthropologically unpolluted. Another advantage is its short distance to consumers. A further advantage or opportunity is that extraction of brackish groundwater below deep polders will result in diminishing or even disappearing of saltwater seepage and thus reduction of pollution of fresh surface water. Hence, it would also solve currently persistent environmental problems.

In this presentation we discuss some hydrogeological effects of brackish water extraction. With the term brackish water we have to think of chloride concentrations in the order of 7000 mg/L, about 40% of sea water values. The density of this water is around 1010 kg/m^3 (as was used in the modeling) and cannot be ignored, as we will see. The extraction of this brackish water will take place below the interface with the overlying fresh water.

BRACKISH AND FRESH WATER FLOW
Currently, the brackish water seeps up over a wide area of the polder (fig. 1). Figure 1 shows the result of a 2D steady-state simulation with equilibrium interface. It shows the upconing and upward seeping groundwater. The steam lines are isolines of the stream function with a discharge of 0.25 m^2/d between any two adjacent lines. This works for the fresh as well as for the salt water. The streamline pattern shows that the intensity of the discharge is relatively low in the column of brackish water and high in the adjacent fresh water seepage as indicated by the curved arrows. Also, the zone of brackish seepage can be wide with moderate to low intensity seepage as compared to the intense fresh water seepage near adjacent to the brackish water cone. The

picture with density ignored is very different with a much more intense upward seepage in the center of the polder.

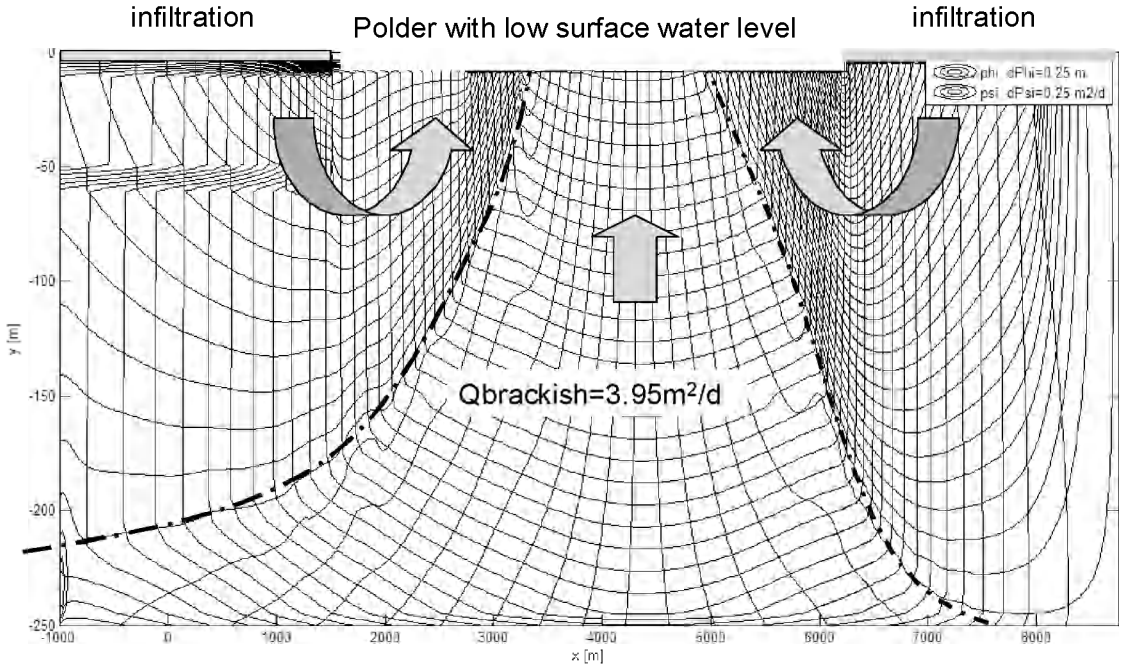

Figure 1. Cross section with brackish water upconing and seepage in the center. Streamlines at 0.25 m^2/d intervals and freshwater heads at 0.25 m intervals are shown. The interface between brackish and fresh water is indicated by the thick line. The brackish water had 1010 kg/m^3 density.

It turns out that even the moderate density of 1010 kg/m^3 that we have here has a large effect on the flow and the seepage. Hence we must include density in much of our modeling, at least more regularly than is customary today.

SEPARATION OF FRESH AND BRACKISH WATER BODIES

Fig.2 shows the situation with extraction of brackish water below the interface. The well screens have been placed between a depth of 150 and 200 m. The extraction is such that the interface does no longer reach the top of the aquifer. The extraction needed for this is about the same as the previous saltwater seepage into the polder. The shown situation is valid once the interface has reached equilibrium. There are several interesting points to be considered next.

In this situation the brackish and fresh groundwater remain separated by the interface as two distinct water bodies. Due to this, there can be no pollution of the brackish water from agriculture or any other uses of ground surface. This way it does not seem to be a problem to use brackish groundwater from urban areas as a resource.

A second point to be considered is that the brackish water extraction does not cause drawdowns in the fresh water system; the two water bodies are separated by their interface. This may be an advantage as this does not induce further subsidence of shallow Holocene peat layers. Such subsidence is a general problem in the Netherlands.

A last point to be considered is that the extraction of brackish water increases the overall seepage of fresh groundwater into the polder. This seemingly counter intuitive effect is due to the increase of the effective transmissivity of the layer of fresh water as a consequence of the lowering of the interface caused by the drawdown due to pumping in the brackish zone.

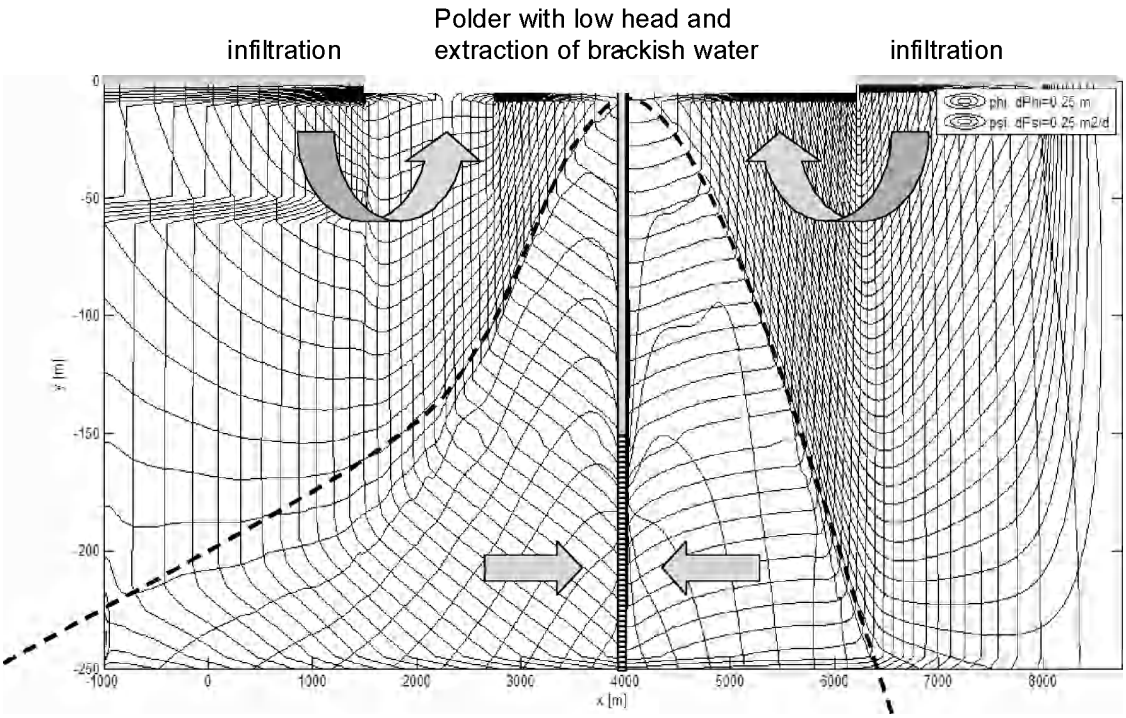

Figure 2. Cross section now including recovery of brackish water with a line of wells screened between 150 and 200 below ground surface. The equilibrium interface is indicated by the thick dashed lines. Interval between streamlines is 0.25 m^2/d, between fresh water head lines it is 0.25 m.

OTHER ASPECTS

Clearly, there are more effects to be dealt with. For instance, the desalination by reversed osmosis (membranes) generates a concentrate containing the removed salts. Effects of injection have to be carefully studied in the framework of an environmental assessment.
Another problem to be considered is the origin of the brackish water, which is still largely unresolved. Isotopic studies have revealed that the brackish water is of Holocene origin (Van der Linden & Appelo, 1988, Van der Molen, 1988, Post, 2004). This water likely results from downward percolation of one or more previous transgressions. It may well mean that the total amount of brackish water is limited, which would also limit the feasible life expectancy of its recovery. This life expectancy has to be investigated as well. One of the issues in such as study will be the distribution of salinities inside the brackish water zone and its consequences for variations of salt concentrations over time and the extent of the movement of the interface. Finally, transients in flow are of concern as well as the way in which such systems should be monitored and mentioned to guarantee protection from pollution.

CONCLUSION

Nevertheless, we have a number of such systems in the Netherlands which would provide opportunity for brackish water extraction for drinking water usage on a larger scale. This use would at the same time help solve various environmental problems due to upward seepage of nutrient-rich brackish groundwater that mixes with the surface water systems currently mainly concerned with flushing this water towards the sea along the shortest possible route.

A final conclusion is that analyzing such systems requires the use of density dependent modeling codes, even if we only deal with brackish water having moderate salinities such as the 40% of

seawater used here. Hitherto density-dependent flow has only scarcely been used in regional modeling (except by a few pioneers like Oude Essink (1996). Happily we have seen more and more use of Seawat and SWI in the last couple of years.

REFERENCES

Linden, F. van der and C.A.J. Appelo (1988) Hydrochemistry and origin of saline seepage water in the Horstermeer Polder. H_2O, Vol. 21, p 671-675. (In Dutch)

Molen, W.H. van der (1988) Saline groundwater in Western Netherlands: caused by density flows? (In Dutch). H2O Vol 22, No. 11, p 9-11. With reaction by Appelo, C.A.J. and F.J. van der Linden (1988). H_2O. Vol 22, No. 11, p331 and 346 (In Dutch)

Oude Essink, G. (1996) Impact of Sea Level Rise on Groundwater Flow Regimes. A Sensitivity Analysis for the Netherlands. PhD Thesis, TU Delft, ISBN 90-407-1322-7.

Post, V. (2004) Groundwater Saliniazation processes in the coastal area of the Netherlands due to transgressions during the Holocene. PhD. Free University of Amsterdam, ISBN 90-9017404-4

Contact Information: Theo N. Olsthoorn, prof.dr.ir., Delft University of Technology, Faculty of Civil Engineering and Geosciences, Water Resources Section, P.O. Box 5048; 2600 GA DELFT, The Netherlands. Phone:+31(0)6-20440256, Email: t.n.olsthoorn@tudelft.nl | Waternet. Vogelenzangseweg 21, 2114 BA Vogelenzang The Netherlands. Theo.Olsthoorn@waternet.nl

Impacts of Climate Change on the Coastal Groundwater Systems in The Netherlands

Gualbert H. P. Oude Essink
Deltares, Subsurface and Groundwater Systems, Utrecht, The Netherlands

ABSTRACT
Worldwide, deltaic areas are under stress due to climate and global change. Anthropogenic activities such as groundwater extractions for drinking, agricultural and industrial water supply as well as underground infrastructures increase the pressure on water management. In the densely populated Netherlands, climate and global change issues are even more pressing, taking into account that about 25% of our deltaic area is lying below mean sea level. In addition, three major rivers (Rhine, Meuse and Scheldt) flush to the North Sea, increasing the risk of (river) flooding and making our country vulnerable to sea level rise.

The awareness of climate change issues on the water system has been increased enormously. National research programs are being set up to investigate our changing system, to quantify the possible impacts and, already, to come up with adaptive and mitigative measures. In this presentation, we will focus on the physical impacts of sea level rise, land subsidence and the increasing river water levels on the vulnerable Dutch coastal groundwater system (fig. 1).

Numerical models, taking into account variable density groundwater flow and coupled solute transport, have been used to address and to quantify the above-mentioned phenomenae. These tools will eventually help us in developing feasible adaptation strategies. The attached figures will give an impression of the work done so far.

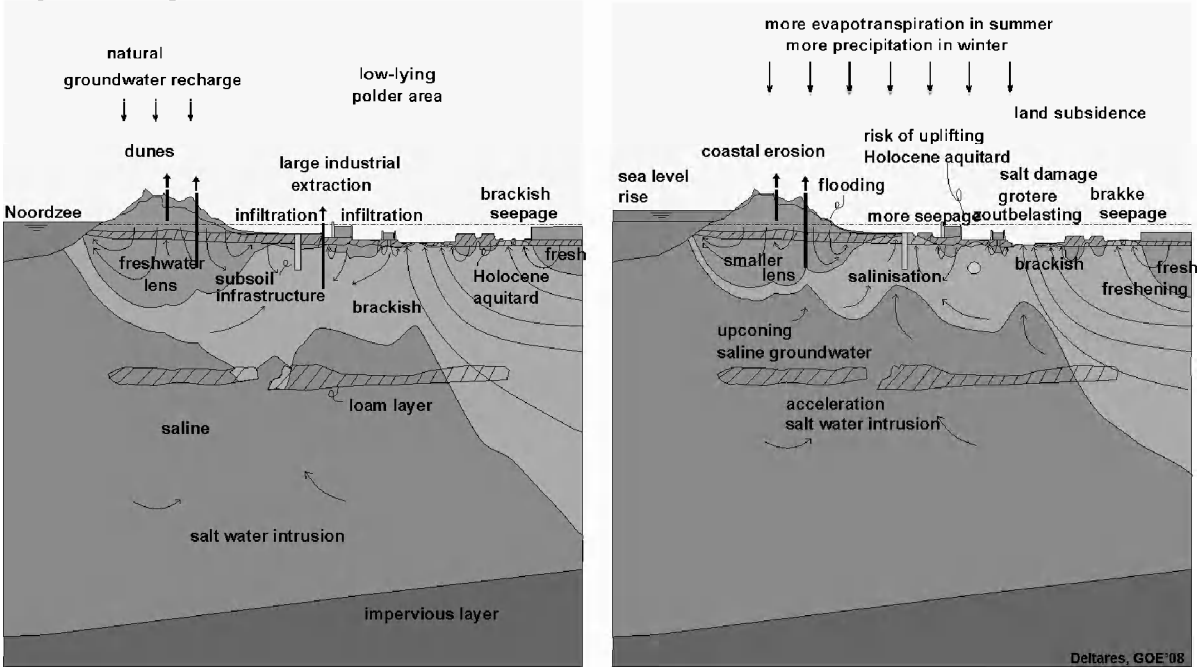

Figure 1. Schematization of the groundwater system in the Dutch coastal area; possible processes which occur in case of climate and global change.

We are investigating the increase in freshwater head in the coastal groundwater system (fig. 2 and 3 (detail)) and the change in seepage and salt load to the surface water system which affect the flow of salt and nutrients to the surface water system. These physical changes cause an

increase of the risk of uplifting and cracking of the covering Holocene top layer (fig 4). As a consequence, embankments may become unstable and may possibly fail to protect our country from flooding.

Water management in the Dutch delta will face difficulties due to the salinisation of the subsoil. Several geological and anthropogenic activities in the past have already created brackish to saline groundwater resources. The top of the coastal groundwater system will probably get even more salty as a result of sea level rise, land subsidence and a reduction in natural groundwater recharge due to climate change (fig. 5). In the low-lying areas, upconing brackish to saline groundwater may intrude agricultural parcels, which may cause salt damage to crops. In addition, the surface water system in low-lying areas will probably have to be flushed more frequently to dispose the excess of salt, which originates from the deeper groundwater system, affecting the capacity of the entire water management system.

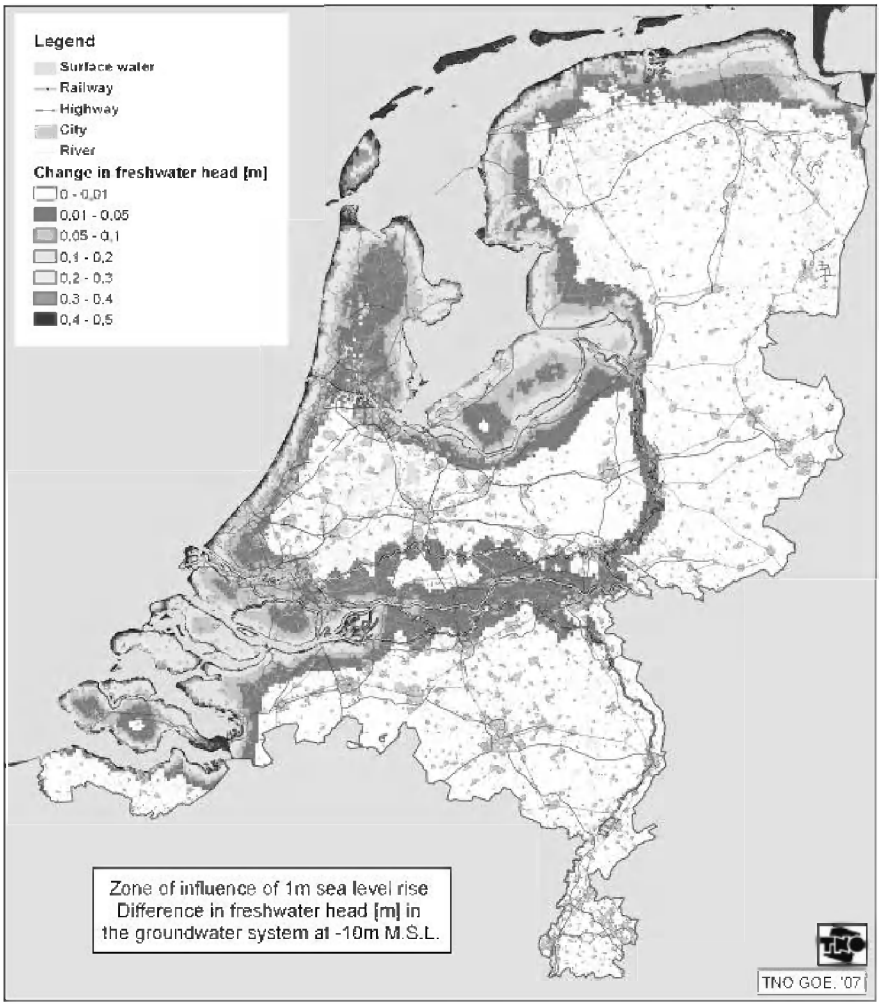

Figure 2. Zone of influence of a 1m sea level rise on the groundwater system; the coastal sand dune area of The Netherlands.

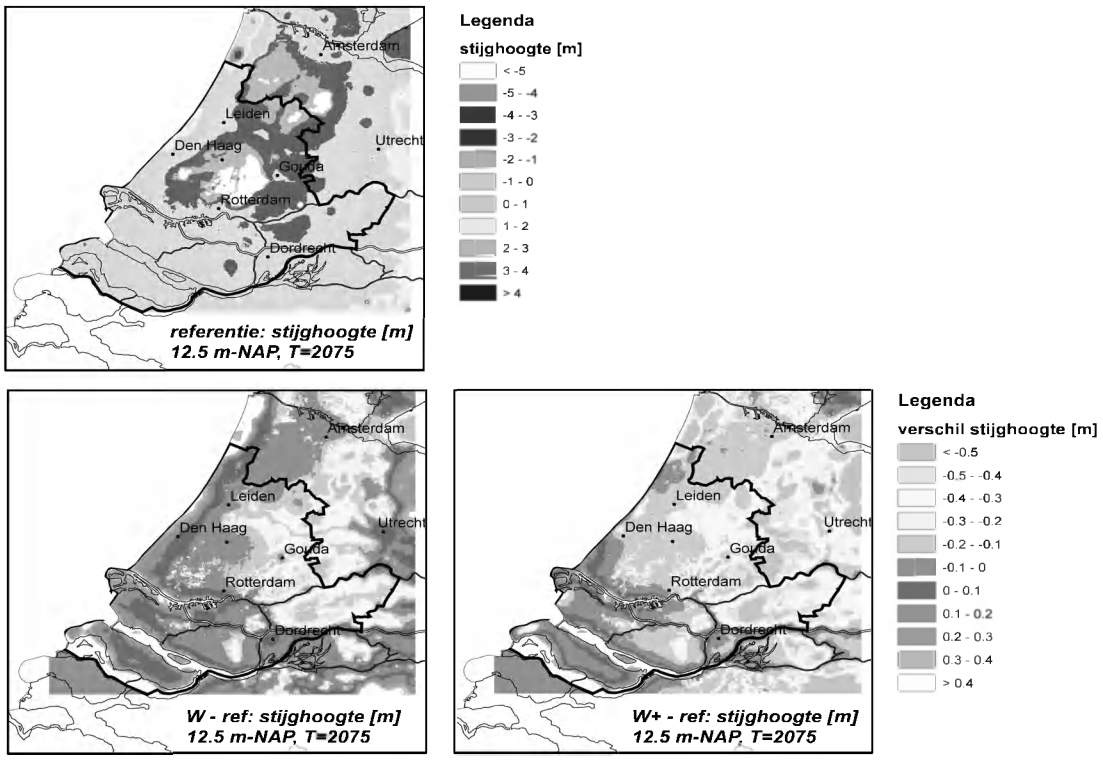

Figure 3. a. Freshwater head distribution (‘*stijghoogte*’) at -12.5m in the province of Zuid-Holland; b. Head difference (‘*verschil stijghoogte*’) [m] due to the KNMI06 ‘wet’ climate scenario, and c. Head difference [m] due to the KNMI06 ‘dry’ climate scenario.

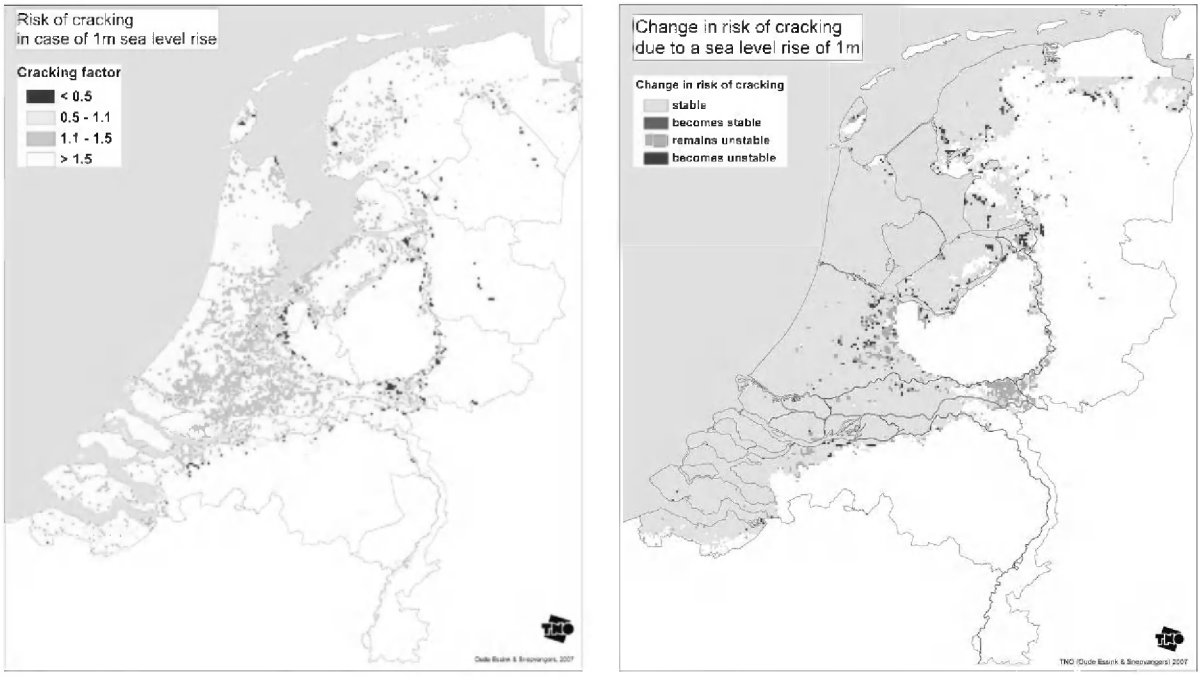

Figure 4. The cracking factor: values smaller than 1.1 represent areas where uplifting and cracking of the covering Holocene top layer are likely to occur, d. the change in cracking factor due to changes in climate change (precipitation and river discharges).

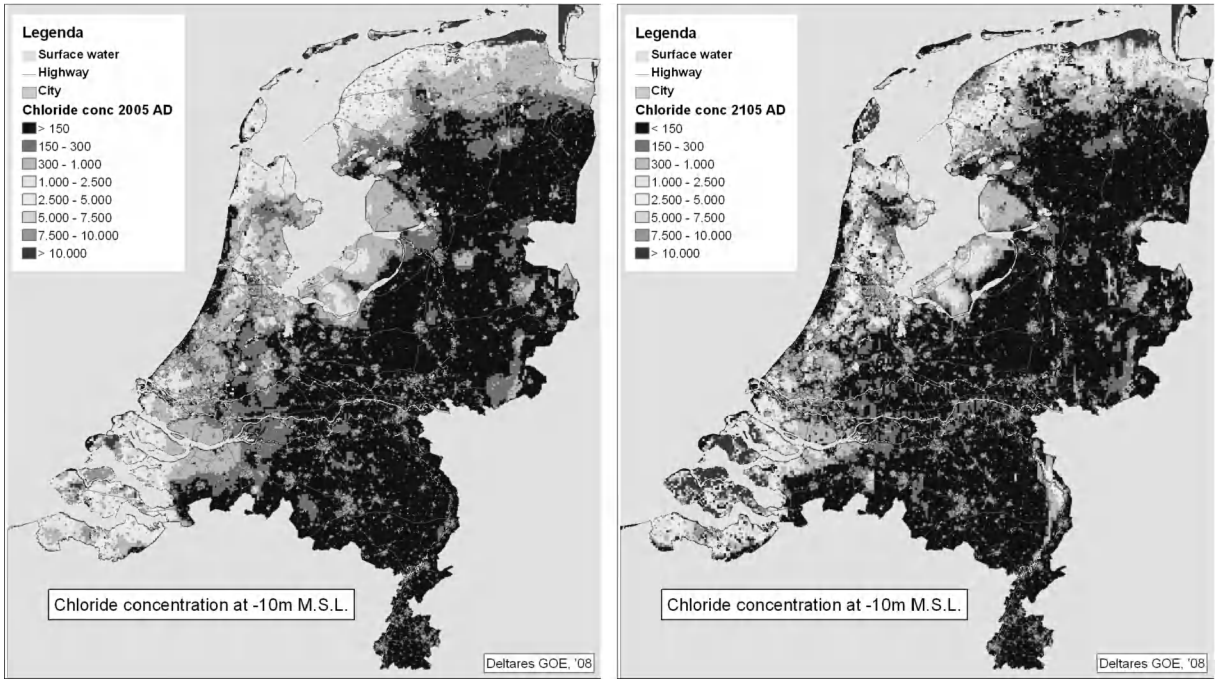

Figure 5. Chloride concentration in mg Cl-/l) at -10m M.S.L. for the years 2005AD and 2105 AD, including: sea level rise of 1 m, land subsidence according Water Policy 21nd century high scenario, and rise in river water level due to backwater effect.

Key words: coastal zone, salinisation, climate change, sea level rise, models, effects, The Netherlands

Contact Information: Gualbert H.P. Oude Essink, Deltares, Subsurface and Groundwater Systems, Princetonlaan 6, P.O.Box 85467, 3508 AL Utrecht, The Netherlands, Phone: +31-30-2564761, Fax: +31-30-2564855, Email: gualbert.oudeessink@deltares.nl

Analytical Method for Preliminary Management of Pumping and Injection in Coastal Areas

Namsik Park, *Lei Cui* and *Chanjong Lee*
Department of Civil Engineering, Dong-A University, Busan, Korea

ABSTRACT
In this work two algebraic equations are developed to estimate the maximum pumping rates and the minimum injection rates, respectively, subject to a pre-specified saltwater intrusion limit and a set of simplifying assumptions. Strack's single-potential solution is used to derive these equations. In general, the maximum pumping rate increases as more additional intrusion is allowed. However, critical points limit both the maximum pumping rate and the allowed saltwater intrusion limit. For injection rates there is no such limit. Design curves are developed from the equations.The equations can be presented as design curves for ease of use.

INTRODUCTION
Ground water development in coastal areas induces saltwater intrusion. If not developed carefully, saltwater may reach the pumping well. This type of problem is a typical optimization problem: maximizing the withdrawal while limiting the saltwater intrusion to a specified limit. Another type of optimization problem exists: In cases where aquifer is already saltwater contaminated, freshwater may be injected to push the saltwater toward the sea to reclaim the aquifer. In this case, minimization of freshwater injection while limiting the saltwater intrusion to a desired location is another typical optimization problem.

For general problems simulation and optimization techniques (Park and Hong, 2006) are needed to determine maximum pumping or minimum injection rates. However these techniques require detailed investigation and require intensive computing capabilities which may not be available for a preliminary assessment.

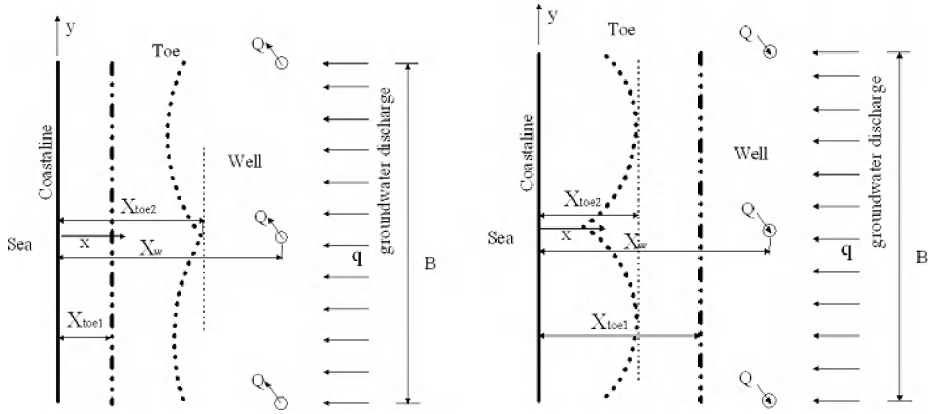

Figure 1. Plan views of coastal area for (a) pumping and (b) injecting freshwater

Prior to pumping or injection, the toe of a saltwater wedge, distance x_{toe1} away from the coastline, is aligned parallel to the coastline when the coastal groundwater discharge is uniform. When groundwater is pumped or freshwater is injected, the toe shall react. A preliminary management goal would be to estimate for groundwater development projects the maximum pumping rates or for aquifer restoration projects the minimum injection rates. Both types of projects are subject to a desired post-development maximum intrusion location (x_{toe2}, Figure 1).

When certain conditions are met, the maximum or injection rates can be determined directly without resorting to an optimization technique. In this work algebraic equations are developed and presented in the forms of design curves for quick assessment on groundwater development in planning stage with available hydrogeologic data.

ANALYTICAL METHOD

As metioned above, a new algebraic equaiton to estimate the maximum pumping rate and the minimum injection rate can be derived from Strack's single-potential solution for sharp interface moder. It is developed by Cheng and other researchers to determine the respose of the toe position to groundwater development via multiple wells. The solution shows the relationship between pumping or injection rate Q_i, the post-development toe coordinate (x , y), and well position coordinates (x_i , y_i)as follow:

$$\phi_{toe} = \frac{\lambda}{2} l^2 = \frac{q}{K} x + \sum_{i=1}^{N_w} \frac{Q_i}{4\pi K} \ln \left[\frac{(x - x_i)^2 + (y - y_i)^2}{(x + x_i)^2 + (y - y_i)^2} \right] \qquad (1)$$

where λ is set as $s(s-1)$and l is set as d for the unconfined aquifer, $\lambda = s - 1$ and $l = D$ for the confined aquifer. Herein D is the confined aquifer thickness, d is the elevation of mean sea level above the datum, s is the density ratio of the saltwater and freshwater(ρ_s / ρ_f). The groundwater discharge is expressed as q, and the N_w is the total number of wells. When there is no pumping or injection, i.e. Q_i=0, the pre-development toe position (x_{toe1}) can obtained from equation (1).

For the sake of applying the equation, the odd number of wells are assumed and distribution of the wells is symmetrical and parallel the coastaline, which is limited in a given length B. Such setting can guanarantee a well always placed along y=0 axis, thus the well coordinates can be express as $x_i = x_w$ and $y_i = -nb, \cdots, -b, 0, b, \cdots nb$, where $n = (N_w - 1)/2$.

Then assume that all the wells seperate from each other with the same distance, and the Q_i,has the same value, that is, each of the wells share the same pumping or injection rate. Additional assumptions can be employed for applying equation (1) for priliminary management. We limit our research into a B length homogeneous isotropic coastal area, distribute odd number wells symmetrically parallel the coastline, and assume all wells sharing same well space b, pumping rate or injection rate Q . In terms of the previous assumption with some defined dimensionless variables, like $\eta = x_{toe} / x_w; \quad \mu = y_{toe} / x_w; \quad \eta_1 = x_{toe1} / x_w; \quad \beta = b / x_w; \quad \xi = Q / \pi K l^2$, the equation can be simplified to

$$\xi = 2\lambda \left(\frac{\eta - \eta_1}{\eta_1} \right) \left\{ \sum_{i=-n}^{n} \ln \left[\frac{(\eta - 1)^2 + (\mu - n\beta)^2}{(\eta + 1)^2 + (\mu - n\beta)^2} \right] \right\}^{-1} \qquad (2)$$

The dimensionless equation of ξ is a function of dimensionless pre-development toe position η_1, dimensionless post development toe coordinates (η,μ) and well space β. From above equation, the variale ξ primarily vary with the post-development toe location under given aquifer with know well space. Due to the specified limit on saltwater intrusion (η_2, defined as x_{toe2}/x_w), there is maximum pumping rate or minimum injection rate, which will be obtained while maximum post-development toe (η) equal to η_2.

MAXIMUM PUMPING RATE

As shown in Figure 1(a), the post development toes move symmetrically because of the symmetrical distribution of the wells, hence the maximum saltwater intrusion will also happen along the y= 0 axis. Substitute dimensionless maximum intrusion coordinate (η_2, 0)into equation (2) will yield

$$\xi_{\max} = 2\lambda \frac{\eta_2 - \eta_1}{\eta_1} \left[\sum_{i=-n}^{n} \ln \frac{(1-\eta_2)^2 + (i\beta)^2}{(1+\eta_2)^2 + (i\beta)^2} \right]^{-1} \tag{3}$$

From above equation, it seems that the dimensionless pumping rate ξ_{max} is proportional to additional intrusion length, and by allowing more intrusion more ground water can be developed. However, as the intrusion approach a special toe called critical point x_c, an unstable situation will happen, at which the slightest increase of pumping rate will cause the saltwater intrusion into the well. It can be defined by requiring the stagnation point correspond to the toe position as

$$\eta_1 = \eta_c + \frac{1-\eta_c^{\,2}}{4} \sum_{i=-n}^{n} \ln \left[\frac{(\eta_c - 1)^2 + (i\beta)^2}{(\eta_c + 1)^2 + (i\beta)^2} \right] \tag{4}$$

where η_c is dimensionless value of x_c by x_w

MINIMUM INJECTION RATE

As shown in Figure 1(b), The effects of injection would be more pronounced along the symmetry line than near the edge of the well, thus the maximum intrusion would occur somewhere between the two marginal wells. The location of the maximum intrusion herein is pointed as the middle point and has been proved can be safely used to derive the minimum injection rate equation. Therefore, the dimensionless maximum intrusion coordinate becomes (η_2, (n-0.5)β) which yield

$$\xi_{\min} = 2\lambda \frac{\eta_2 - \eta_1}{\eta_1} \left(\sum_{i=-n}^{n} \ln \left[\frac{(1-\eta_2)^2 + [(n-0.5)\beta + i\beta]^2}{(1+\eta_2)^2 + [(n-0.5)\beta + i\beta]^2} \right] \right)^{-1} \tag{5}$$

DESIGN CURVES

The two equations can be combined into design curves for both pumping and injection cases with a given number of wells. Figure 2 depicts the design curves for 15- and 25-well cases. Values of the contour lines in Figure 2 represent the uniform pumping rate and injection rate from a single well for a combination of a predevelopment of toe position (η_1) and a desired limit of saltwater intrusion (η_2). The curve marked by '+' represents the critical points, and the blank areas at the right bottom is invalid for the sake of avoiding saltwater contaminated the well.

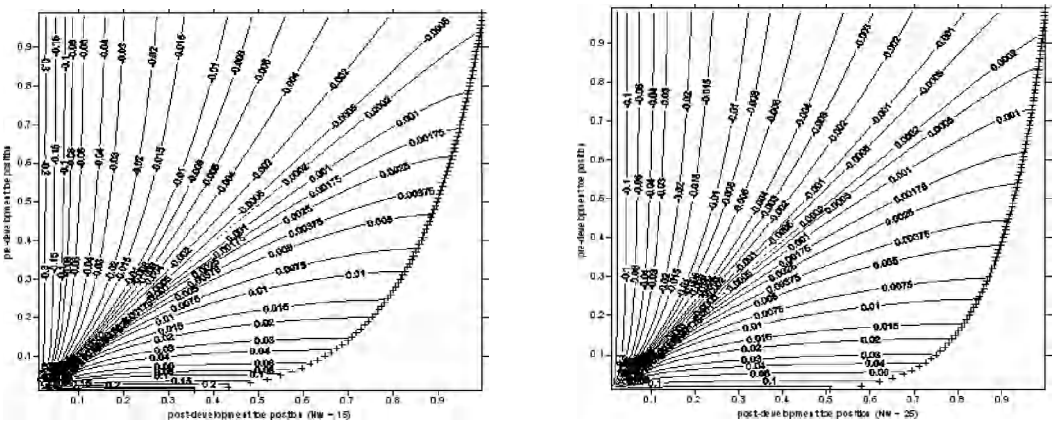

(a) (b)

Figure 2. Design curves for operation rates of individual well 15 (a) and 25 (b) wells.

ACKNOWLEDGEMENT

This research was supported by a grant (code # 3-3-3) from the Sustainable Water Resources Research Center of the 21st-Century Research Program.

REFERENCES

Cheng, A.H.D., Halhal, D., Naji, A., and Ouazar, D. 2000. Pumping optimization in saltwater intruded coastal aquifers. Water Resources Research 36, no. 8: 2155-2166.

Park, N.S. and Hong, S.H. 2006. Optimization Model for Groundwater Development in Coastal Aquifers. Advances in Geosciences, v. 4: 159-166.

Strack, O.D.L. 1976. A single-potential solution for regional interface problems in coastal aquifers. Water Resources Research, v. 12:1165-1174.

Contact Information: Lei Cui, Dong-A University, Civil Engineering Department, Hadan 2-Dong, Saha-gu, 840, Busan 604-714, Korea, Phone: +82-51-200-5743, Fax: +82-51-205-5187, Email: dazzle_linsong@msn.com

Field Validation of Simulation-Optimization Model for Protecting Excessive Pumping Wells

Namsik Park[1], *Sungyun Kim*[1], *Lei Shi*[1] and *Sungho Song*[2]
[1]School of Civil Engineering, Dong-A University, Busan, Korea
[2]Rural Environment Resources Research, Korea Rural Community & Agriculture Corporation, Kyonggi-do, Korea

ABSTRACT
In this work we investigated effects of saltwater pumping to protect an over-exploiting freshwater pumping well. The experiment was designed using a simulation-optimization numerical model taking into account various parameters. The model can identify the minimum saltwater pumping rate required to protect the over-exploiting pumping well. A field site with a freshwater-saltwater stratified aquifer is selected. The effect of saltwater pumping on freshwater pumping is shown with the electric conductivity (EC) values.

INTRODUCTION
One of the phenomena that limit fresh groundwater development in coastal area is saltwater intrusion. In this case when more groundwater than allowed is withdrawn, pumping wells may be contaminated by saltwater. Freshwater injection or saltwater pumping may be used to protect over-exploiting freshwater pumping wells from saltwater intrusion. In many cases freshwater injection is preferred to saltwater pumping because of two primary reasons. First saltwater pumping may waste freshwater because of down conning. Secondly disposal of salty water may pose difficulties. Waste of freshwater may be reduced by limiting saltwater pumping to the minimum rate. A rigorous simulation-optimization model can be used to identify the minimum saltwater pumping rate. In this work applicability of a simulation-optimization model for protecting over exploiting freshwater pumping wells is investigated at a small-scale experimental field.

SIMULATION-OPTIMIZATION MODEL
Park and Hong (2006) developed a simulation-optimization model for computing optimal schemes in managing coastal groundwater. A sharp-interface two-phase finite element model is used to simulate fresh and salt groundwater flows. A genetic algorithm is used as an optimization technique. The objective function is constructed to compute maximum freshwater pumping rates and minimum freshwater injection or saltwater pumping rates. Well locations can also be decision variables. A simple method is devised to compare sharp-interface model results with continuously-varying field-measured EC values. The model results are tested against an extensive series of laboratory sand-tank experiments.

FIELD EXPERIMENT
A field site with density-stratified unconfined aquifer is selected (Figure 1). An abandoned pumping well (two concentric circles in Figure 1.) due to increased salinity is chosen as a target well. The well is of about 60m deep (Figure 2(a)). The groundwater level is nearly constant at approximately 1m from the land surface. EC loggings conducted over 30 months indicate stable profiles (Figure 2(b)). The EC for the upper 15m-layer of the groundwater is about 11 mS/cm and it increases in steps to 35mS/cm roughly 25-27m below the ground surface. The thickness of the transition zone is shown to be about 10-12m.

Two pumps are installed at different depths: the freshwater pump at -10m and the saltwater pump at -40m. Three EC sensors were installed at -15m, -22m, and -30m to monitor the change in the transition zone. The EC value of the freshwater pump outlet is also monitored.

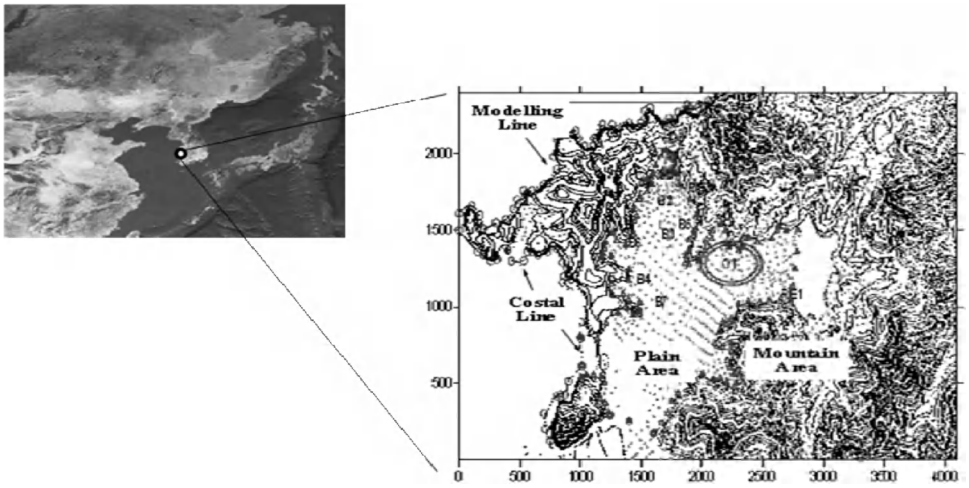

Figure 1. The Topographical Map of the Field Site

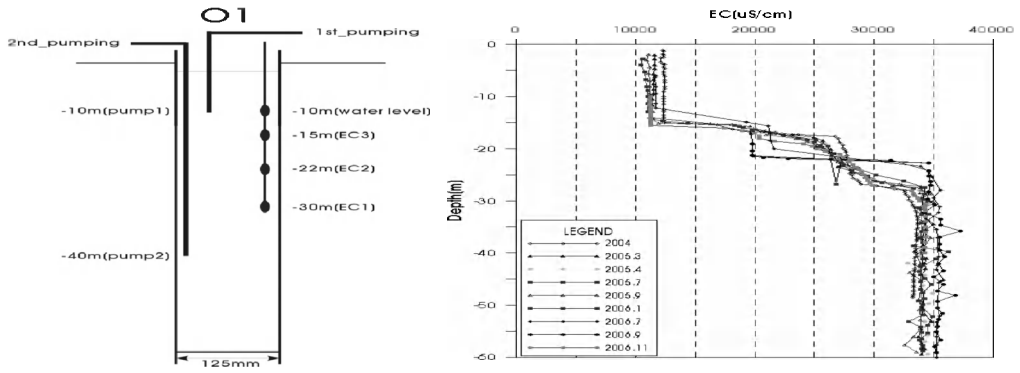

Figure 2. (a) Schematics of pumping well and (b) EC logging results.

EXPERIMENTAL SCENARIO

The objective of the experiment is to validate the design results of the simulation-optimization model for protecting excessive freshwater pumping via saltwater pumping. To identify the aquifer parameters a preliminary experiment is conducted. Model parameters are calibrated against the measurements.

The main experiment is designed in steps. In the first step, the optimal freshwater pumping rate from the upper well at -10m GL (Figure 2), that would not cause saltwater contamination due to up coning, is computed from the model. In the second step, the reaction of the groundwater flows to increased freshwater pumping rate is simulated. In the third step, the minimum saltwater pumping rate needed to suppress the up coning and restore the freshwater pumping well is computed.

The pumping pattern of various pumping stages is depicted in Figure 3. In the first step only the excessive freshwater pumping is applied to cause saltwater up coning. After 1200 minutes the minimum saltwater pumping is applied to the deeper pump to suppress the saltwater up coning while maintaining excessive freshwater withdrawal from the upper pump. In this manuscript water level and EC measurements are presented along with the computed values. The experimental scenario is designed such that the experiment is completed within two days.

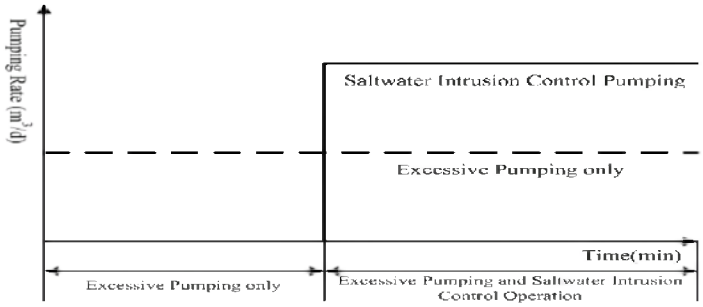

Figure 3. Freshwater and Saltwater Pumping Scenario.

EXPERIMENTAL RESULTS AND DISCUSSION

Figure 4(a) compares the computed and observed water levels measured during the experiment. Details in drawdown disagree but the general pattern is in good agreement. The water levels rise after both pumps were turned off at the completion of the experiment. Figure 4(b) compares the EC values at freshwater pump outlet. Again values are not in agreement, but the figure clearly shows that the trend is simulated accurately. Recall that the simulation model used is a sharp-interface model.

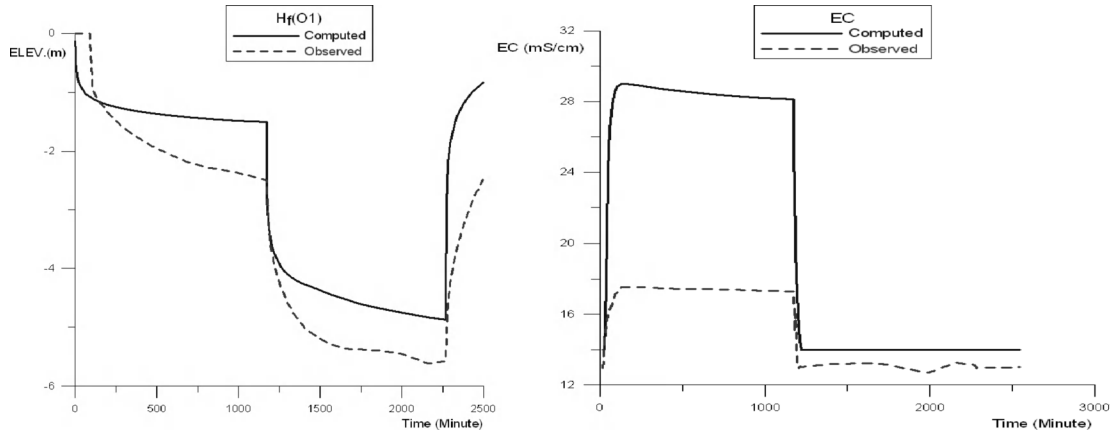

(a) (b)

Figure 4. Comparison of computed and observed (a) Water Levels and (b) EC values of pumped water

Figure 5 depicts the computed and observed EC values at different locations in the pumping well. The numerical results deviate from the measured values. But again, the numerical model is able to reproduce the general trend.

In this study we investigate the field applicability of the simulation-optimization model. Considering the limitations of the simplified sharp-interface simulation model two major

outcomes can be noted from this work. First, the sharp interface model can reasonably estimate EC values in both pumping and observation wells with a simple algorithm. Secondly, the simulation-optimization model can identify the minimum saltwater pumping rate to protect the excessive freshwater pumping well. Details of the model and experiments shall be presented at the Meeting.

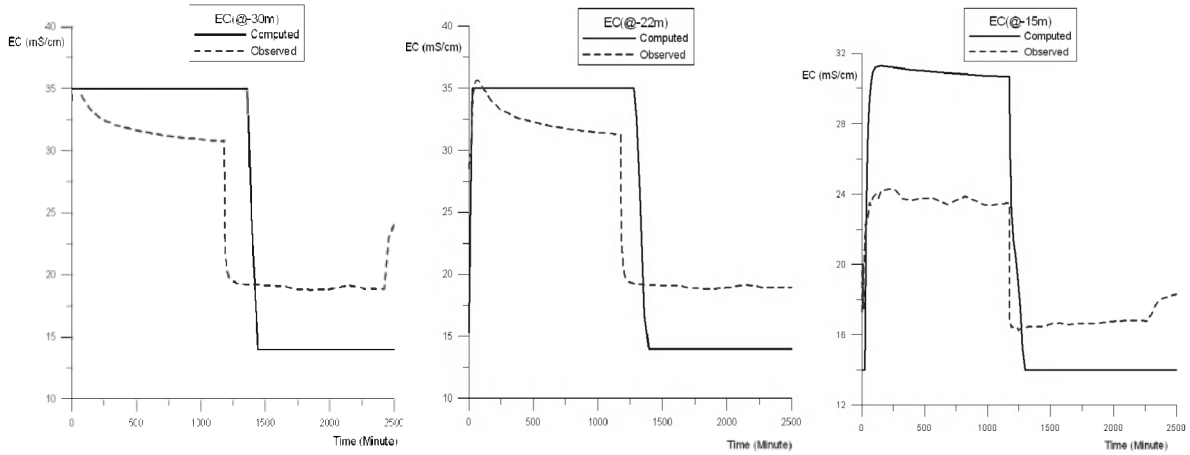

(a) (b) (c)

Figure 5. Comparison of EC values at Different Locations (a) -30m GL, (b) -22m, (c) -15m

REFERENCES

Park, N.S. and Hong, S.H. 2006. Optimization Model for Groundwater Development in Coastal Aquifers. Advances in Geosciences, v. 4: 159-166.

ACKNOWLEDGEMENT

This research was supported by a grant (code # 3-3-3) from the Sustainable Water Resources Research Center of the 21st-Century Research Program.

Contact Information: Namsik Park, Department of Civil Engineering, Dong-A University, Hadan 2-dong Saha-gu, 840, Busan 604-714, Korea, Phone: +82-51-500-5743, Fax: +82-51-205-5187, Email: nspark@dau.ac.kr

Virginia Ground Water Withdrawal Permitting Program – Modeling for Resource Management

Roberta W. Patton
Virginia Department of Environmental Quality, Richmond, VA, USA

ABSTRACT

The Virginia Department of Environmental Quality (VA-DEQ) strives to manage Coastal Plain ground-water resources through a dynamic and iterative process of framework and flow system investigations, predictive ground water model simulations, and regulation of withdrawals through a permitting process. This resource management program requires partnerships between the regulatory agency, the regulated community, local government, and the United States Geological Survey (USGS). The regulated community provides information about the geologic framework and aquifer hydraulics through field work and monitoring activities required to support withdrawal permits. The VA-DEQ evaluates withdrawal requests for sustainability using field data and regional flow models. Any proposed withdrawal that adversely affects the sustainability of the aquifer system (quality or quantity) must provide appropriate mitigation, when possible, or be denied. The VA-DEQ and local governments cooperate with the USGS to develop regional flow models that accurately reflect the latest information about the aquifer system. Field observation well nests and historic pumping records are used to calibrate and to evaluate the performance of these regional models.

INTRODUCTION

The Commonwealth of Virginia has actively managed ground water resources of the coastal plain regions since 1976. By Act of Virginia's General Assembly [Va. Code § 62.1-254 *et seq.*], the right to reasonable control of all ground water resources was recognized as a right of the public in order to ensure the public welfare, safety, and health. The duties associated with the management of the resource were delegated to the State Water Control Board (a citizen appointed board) and its regulatory Agency, the Virginia Department of Environmental Quality. Management of the resource seeks to protect the withdrawals of existing, lawful ground water users and to ensure the sustainability of the managed aquifers. A "Ground Water Management Area" can be initiated when any of the following conditions is found to exist:

1. Ground water levels in the area are declining or are expected to decline

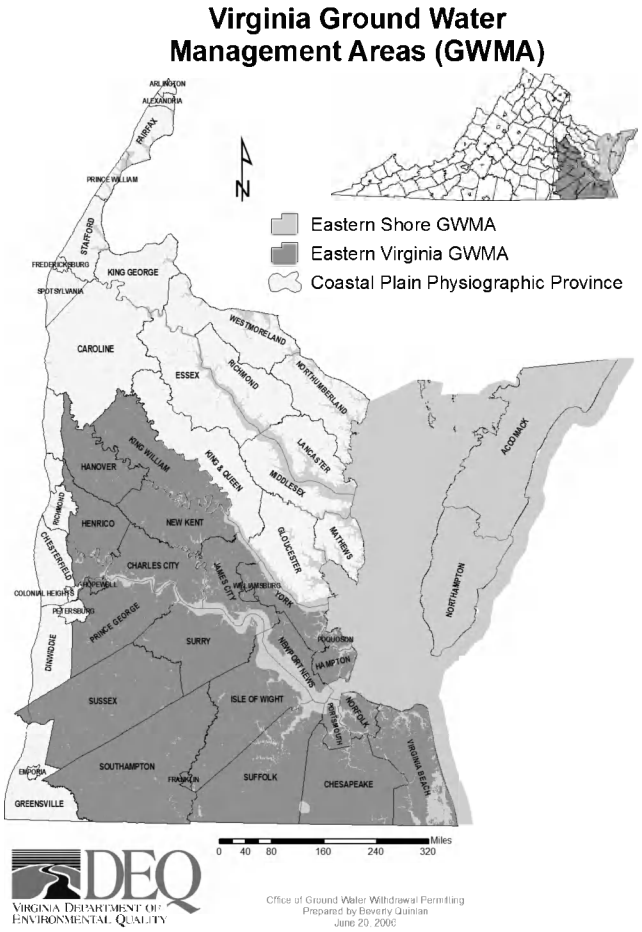

Figure 1 Ground-water withdrawals are regulated in Virginia Ground Water Management Areas.

excessively;

2. The wells of two or more ground water users within the area are interfering or may be reasonably expected to interfere substantially with one another;

3. The available ground water supply has been or may be overdrawn; or

4. The ground water in the area has been or may become polluted.

All four of the required conditions are considered applicable in the two Management Areas in Virginia's coastal plain.

The ground-water flow system in Virginia's Coastal Plain is an eastward thickening wedge of layered sands and clays. The wedge thins to a feather-edge on the western boundary at Virginia's Fall Zone and thickens to several thousand feet approaching the continental shelf. The transition to seawater occurs near Virginia's coast line, becomes more inland in position with depth, and is not well defined. The two counties of Virginia's Eastern Shore comprise the Eastern Shore Ground Water Management Area and the mainland region south of the Mattaponi River is designated the Eastern Virginia Ground Water Management Area. Reported ground water use within Virginia's Coastal Plain has remained relatively constant at 100 Mg/day (± 5%) for about 25 years although active permits authorize a total withdrawal rate that is approaching 200 Mg/day. Withdrawals that exceed 300,000 gallons in any month require a permit.

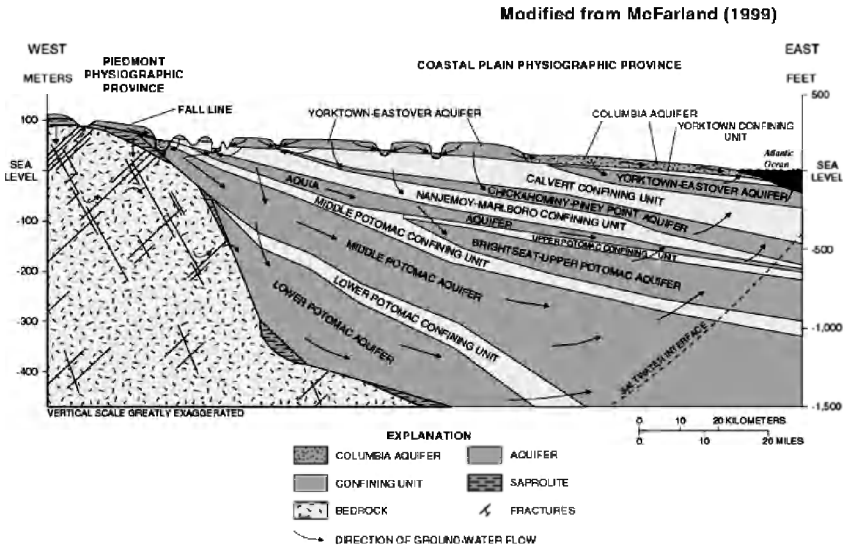

Figure 2 Generalized Coastal Plain Aquifer System (McFarland, 1999)

RESOURCE MANAGEMENT THROUGH PERMIT PROGRAM

Permits are issued for a maximum term of 10 years and specify withdrawal limits, source aquifer(s), withdrawal locations, and reporting requirements. Water Conservation & Management Plans are developed by the permittee specific to the permitted beneficial use and become an enforceable part of the final permit. The permittee is also required to mitigate any adverse impacts to existing, lawful withdrawals. These Mitigation Plans also become and enforceable part of the permit. Maps of the impact area(s) are developed by the DEQ's modeling staff and become part of the Mitigation Plan.

The DEQ staff geologists and modelers evaluate technical information provided by the applicant to evaluate the demand and to determine site-specific hydraulic parameters. Proposed uses must demonstrate that the requested withdrawal amount is the least (quantity and quality) required to support the beneficial use. Applicants are required to submit well construction information (including geophysical logs) and site-specific aquifer test data or reference an applicable nearby test. The modeling staff determines the area, in all affected aquifers, where one foot or more of

drawdown is predicted to occur as a result of the proposed withdrawal. Impact areas are an enforceable part of the permit document and identify areas where the permittee has mitigation responsibilities. The largest withdrawals require use of USGS regional models while small or water table well fields require two-dimensional analysis. Some sites require development of site-specific three-dimensional models in order to most accurately simulate impacts. The proposed withdrawal is then evaluated for cumulative effects with all existing lawful withdrawals simulated at their maximum permitted withdrawal limit (Total Permitted Simulation). This evaluation uses the regional model to test for compliance with regulatory limits on allowable stabilized drawdowns to ensure long-term aquifer sustainability.

The Virginia Ground Water Withdrawal Regulations [9 VAC 25-610-10 *et seq.*] prescribe a limit to allowable drawdown that is intended to prevent aquifer dewatering. Adverse changes to water quality are also prohibited and are considered by evaluating for potential upconing and reversal of flow. Regional and site-specific ground water flow models are used by the Virginia Department of Environmental Quality to evaluate the impacts from any new or expanded withdrawal for compliance with these requirements. The regional models developed by the USGS Water Science Center in Richmond, Virginia, are used to simulate total permitted conditions in the aquifer system.

REGIONAL FLOW MODELS USED FOR REGULATORY ASSESSMENT

The Virginia Coastal Plain Model was developed by the USGS in 80's and simulates nine confined aquifers and a constant head water table (Harsh et al. 1990) using MODFLOW (Harbaugh et al. 1996). The model considers confining units through vertical conductance between aquifers. Grid cells are 3.5 miles on each side and are a reminder of processing constraints from earlier desktop computers. The Eastern Shore Model (Richardson 1994) was developed in the 1990's to evaluate several pumping scenarios for Virginia's Eastern Shore and utilized the USGS SHARP model (Essaid 1990). The salt water boundary for this peninsula system is simulated as a sharp interface. It is also a pseudo 3-D model, simulating confining units through vertical conductance between aquifers.

With VA-DEQ and other stakeholders fully active in the modeling side of the management issue, we began to track critical areas and model performance. Each year reported withdrawals are simulated to check model performance with field conditions. These simulations of actual use began to show trending deviations from field conditions in several key areas. In addition, information gathered through the permitting process began to provide new details about previously undocumented portions of the aquifer system. Stakeholder research, also revealed conflicts between the conceptual framework of the models in use and the aquifer system, like identification of the Chesapeake Bay Impact Crater by USGS and VA-DEQ. As a result, stake holders cooperated to support the development of two new models by the USGS.

The new models have been developed for Virginia's Coastal Plain using the USGS SEAWAT code (Langevin et al. 2003). These new models allow for consideration of density dependent flow and explicitly simulate confining layers as well as aquifers. This change alone has challenged a foundation concept for the regulatory program and will likely result in a regulatory change. The vertical conductance paradigm in the first regional models did not consider storage in the confining layers and therefore approached steady-state conditions in approximately 10 years. The new models, with specific treatment of the confining layers, do not approach steady-state for over 100 years.

DISCUSSION AND CONCLUSIONS

As the limit of aquifer sustainability is approached, stakeholder cooperation and technical efficiencies will have to continue to improve in order to optimize use of the ground water resources. For the future, the permitting program plans to build on the successes of using predictive modeling to support management goals. It will be necessary for all stakeholders to operate in a dynamic and iterative process of data collection and model revision with the scientific community. Even though two new models are ready for application, projects are underway to utilize new techniques from Hill and Tiedeman (2007) to evaluate locations where new monitoring and/or framework data can provide additional model improvements. Operators of large municipal water systems are supportive of continuous monitoring of transient pumping in an effort to develop pumping strategies that minimize impacts to the resource and to other users. Perhaps the most important of the planned strategies is a schedule for regular evaluations of new data and model performance to identify the need for model revisions.

REFERENCES

Essaid, H.I. 1990. The computer model SHARP, a quasi-three-dimensional finite-difference model to simulate freshwater and saltwater flow in layered coastal aquifer systems. USGS Water-Resources Investigation Report, 90-4130.

Harbaugh, Arlen W., Banta, Edward R., Hill, Mary C., and McDonald, Michael G. 2000. MODFLOW-2000, The U.S. Geological Survey Modular Ground-Water Model - User Guide to Modularization Concepts and the Ground-Water Flow Process. USGS Open-File Report, 2000-92.

Harsh, John F. and Laczniak, Randell J. 1990. Conceptualization and analysis of ground-water flow system in the Coastal Plain of Virginia and adjacent parts of Maryland and North Carolina. USGS Professional Paper 1404-F.

Langevin, Christian D., Shoemaker, W. Barclay, and Guo, Weixing. 2003. MODFLOW-2000, the U.S. Geological Survey Modular Ground-Water Model--Documentation of the SEAWAT-2000 Version with the Variable-Density Flow Process (VDF) and the Integrated MT3DMS Transport Process (IMT). USGS Open-File Report, 2003-426.

McFarland, E.R., 1999, Hydrogeologic framework and ground-water flow in the Fall Zone of Virginia: U.S. Geological Survey Water-Resources Investigations Report 99-4093.

Richardson, Donna L., 1994. Hydrogeology and analysis of the ground-water-flow system of the Eastern Shore, Virginia. USGS Water Supply Paper, 2401.

Contact Information: Roberta W. Patton, Virginia Department of Environmental Quality, P.O. Box 1105, Richmond, VA 23218 USA, Phone: 804-698-4085, Fax: 804-698-4032, Email: rwpatton@deq.virginia.gov

Vulnerability Assessment of Groundwater Aquifer due to the Construction of the City Tunnel in Malmö, Sweden

Alina Meyn[1], ***Kenneth M Persson***[1,2] and *Bo Leander*[2]
[1]Dep of Water Resources Engineering, Lund University, Sweden
[2]SWECO, Malmö, Sweden

The main focus of this project is to make a vulnerability assessment of the groundwater aquifer during the construction of a new railway tunnel, the Citytunneln in Malmö, in south Sweden. The most important groundwater supply for the city of Malmö is a well area called Grevie, situated in the confined aquifer of Alnarpsströmmen east of the city of Malmö. The wells have been in operation for 108 years producing approximately 200 l/s drinking water mainly for the city of Malmö.

The aquifer is in contact with the Baltic Sea in the south and the Sound between Copenhagen and Malmö, Öresund jn the west. Although salinity of the salt water here is not high, about 9‰, salt water intrusion still can significantly impact fresh water quality and hence lead to soil salinisation. Some old buildings in the centre of Malmö city are built on wooden piles, which can be destroyed if groundwater levels sink. These can be attacked by fungus in aerobic conditions and decompose rapidly.

During construction work of the tunnel, about 1000m^3/hour of water from combined leaking groundwater and seepage of seawater from the harbour has been pumped. Also, groundwater abstraction for drainage of subsurface construction 300-3000 m from the shore has been performed. A vast part of the groundwater has been retrofitted in the aquifers, but some water has been replaced with municipal tap water in order to sustain the water heads of the aquifers.

In the paper, the extent of change of groundwater/seawater interface due to pumping and retrofitting during the construction face is presented and the net effect on water resources assessed. A number of observations will be presented, such as the effect on the piezometric level of fresh groundwater in the area, to what extent the lowering of groundwater level during construction work enhances salt water intrusion, how the freshwater/salt water balance is changed, to what extent changes in chemical composition of groundwater takes place due to ion exchange with the limestone bedrock, how the salt water/fresh water interfaces is affected by the tap water retrofitting, how redox is changed and if these effects are transient or permanent.

Evaluation and analysis of the obtained results according geological and hydraulic conditions can be used to predict probable response of the groundwater system to the underground construction work. Comparisons with the salt water/fresh water changes due to the recent construction of the underground Metro of Copenhagen will also be presented.

Contact Information: Kenneth M. Persson, Lund university, Water resources engineering, POBox 117, LUND, Sweden, Phone: 46734128167, Email: kenneth.persson@tvrl.lth.se

Saltwater Intrusion Monitoring in the Biscayne Aquifer near Florida City, Miami-Dade County, Florida: 1996-2007

Christopher J Peters[1] and *Jolynn Reynolds*[2]
[1]CH2M HILL, Deerfield Beach, FL, USA
[2]Florida Keys Aqueduct Authority, Key West, FL, USA

ABSTRACT
This paper documents changes in Biscayne Aquifer water quality monitored by the Florida Keys Aqueduct Authority's (FKAA's) saltwater intrusion monitoring (SWIM) program. Over 12 years of monthly data indicate that the 250 mg/L chloride concentration isochlor has remained stable in a relatively shallow interval (35 to 55 feet below land surface (ft bls)); however, inland migration has occurred at a greater depth (55 to 65 ft bls) in some areas. During this period, groundwater withdrawals for public supply have increased by approximately 10 million gallons per day and the area has experienced a severe drought. Continued monitoring is needed to ensure that groundwater withdrawals do not cause degradation of the portions of the Biscayne Aquifer used for groundwater supply.

INTRODUCTION
Saltwater intrusion has been a problem for South Florida water managers since the early 20th century. Parker et al. (1955) identified saltwater intrusion in the Miami area resulting from groundwater pumping and from the construction of uncontrolled canals, which lowered the water table in the Biscayne Aquifer and allowed saline water encroachment. The construction of the C-111 canal in southeastern Miami-Dade County in the early 1960's allowed saltwater to migrate inland during the 1970-1971 drought (Klein and Waller 1985). Meyer (1974) notes that storm surges from hurricanes have also contributed to saltwater intrusion in low-lying areas of southeastern Miami-Dade County. Sonenshein (1996) delineated the 1995 position of the fresh/salt water interface in Miami-Dade County using water quality and geophysical data.

The FKAA is the sole water supplier for residents of and visitors to the Florida Keys. At its wellfield and treatment plant near Florida City, the FKAA withdraws groundwater from the unconfined Biscayne Aquifer and pumps the treated water over 130 miles to Key West, serving customers throughout the Keys. The FKAA expects to meet future increases in demand through reverse-osmosis treatment of brackish water from the deeper Floridan aquifer; however the Biscayne Aquifer will remain an important resource for the FKAA and other utilities in the area (Miami-Dade Water and Sewer Department, Florida City, and the City of Homestead).

DATA COLLECTION METHODS AND ANALYSIS
The FKAA has monitored saltwater intrusion in the Biscayne Aquifer since 1991. Its SWIM network consists of 15 monitoring wells of different depths, some with multiple sampling depths. Chloride concentrations, conductivity, and water table elevations are monitored monthly in each well. The two intervals with the greatest number of sampling points are 35 to 45 ft bls (shallow) and 55 to 65 ft bls (deep). Water quality parameters are measured in the field (conductivity) and in the FKAA's water quality laboratory (chloride).

The multiquadratic radial basis function interpolation algorithm in SURFER (Golden Software 2007) was used to contour the annual average chloride concentration observed in the shallow and deep sampling intervals. The 250 mg/L chloride concentration isochlor was selected for this analysis because it is a secondary drinking water standard and its movement can serve as an indicator of saltwater intrusion occurring between the 250 mg/L isochlor and the saline source.

RESULTS

Figure 1 depicts the estimated location of the 250 mg/L chloride isochlor for each year from 1996 through 2007. The year-to-year configurations are fairly similar in the southern part of the monitoring network, indicating little to no water quality change in this interval of the Biscayne Aquifer.

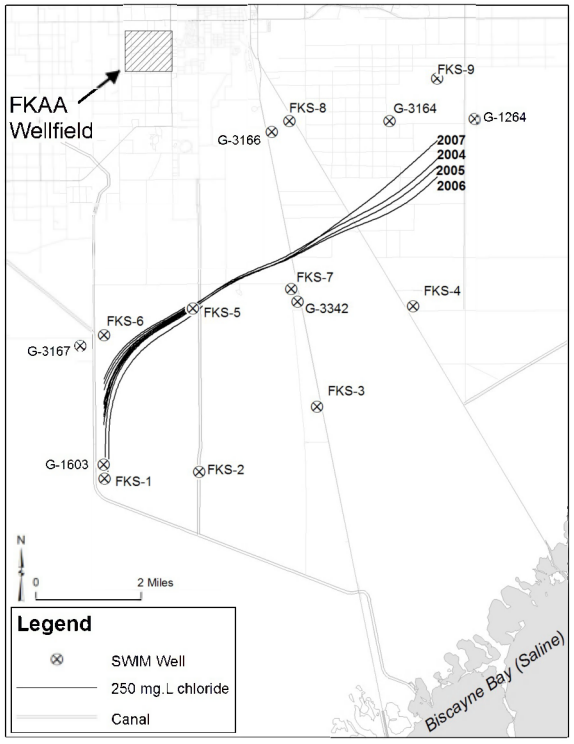

Note: Chloride isochlors for 1996-2004 not labeled due to overlap in the southern portion of the network.

Figure 1. Locations of Shallow Monitoring Wells and Interpolated 250 mg/L Chloride Isochlors, 35-45 ft below Land Surface, 1996-2007

Although the 250 mg/L chloride isochlor moves to the northwest near well G-3164 between 2006 and 2007, seaward movement is evident from 2004 through 2006, illustrating the dynamic nature of saline water intrusion in the area.

During the period from 1995 through 2005, total combined groundwater withdrawals by area utilities (FKAA, Miami-Dade Water and Sewer Department, Florida City, the City of Homestead, and Homestead Air Reserve Base) have increased from approximately 30 million gallons per day to approximately 40 million gallons per day (South Florida Water Management District (SFWMD), 2006). South Florida was affected by a severe drought during the 2000-2001 dry season, which resulted in lower groundwater elevations (Verdi, et al. 2006). As a result of the drought, water deliveries through the SFWMD's regional canal system were reduced, further lowering groundwater elevations in southern Miami-Dade County (SFWMD 2006).

Greater movement of the 250 mg/L isochlor is observed at the deeper interval of 55 to 65 ft bls (Figure 2). From 1996 through 2001, the 250 mg/L chloride isochlor moved inland and then retreated towards Biscayne Bay south of wells FKS-5, and FKS-6. In one year (2002) the 250 mg/L isochlor moved westward past well G-1264, which previously had chloride concentrations below 250 mg/L. Additional wells (FKS-7, -8, and -9) were installed in 2004 to provide additional information about Biscayne Aquifer water quality in this area.

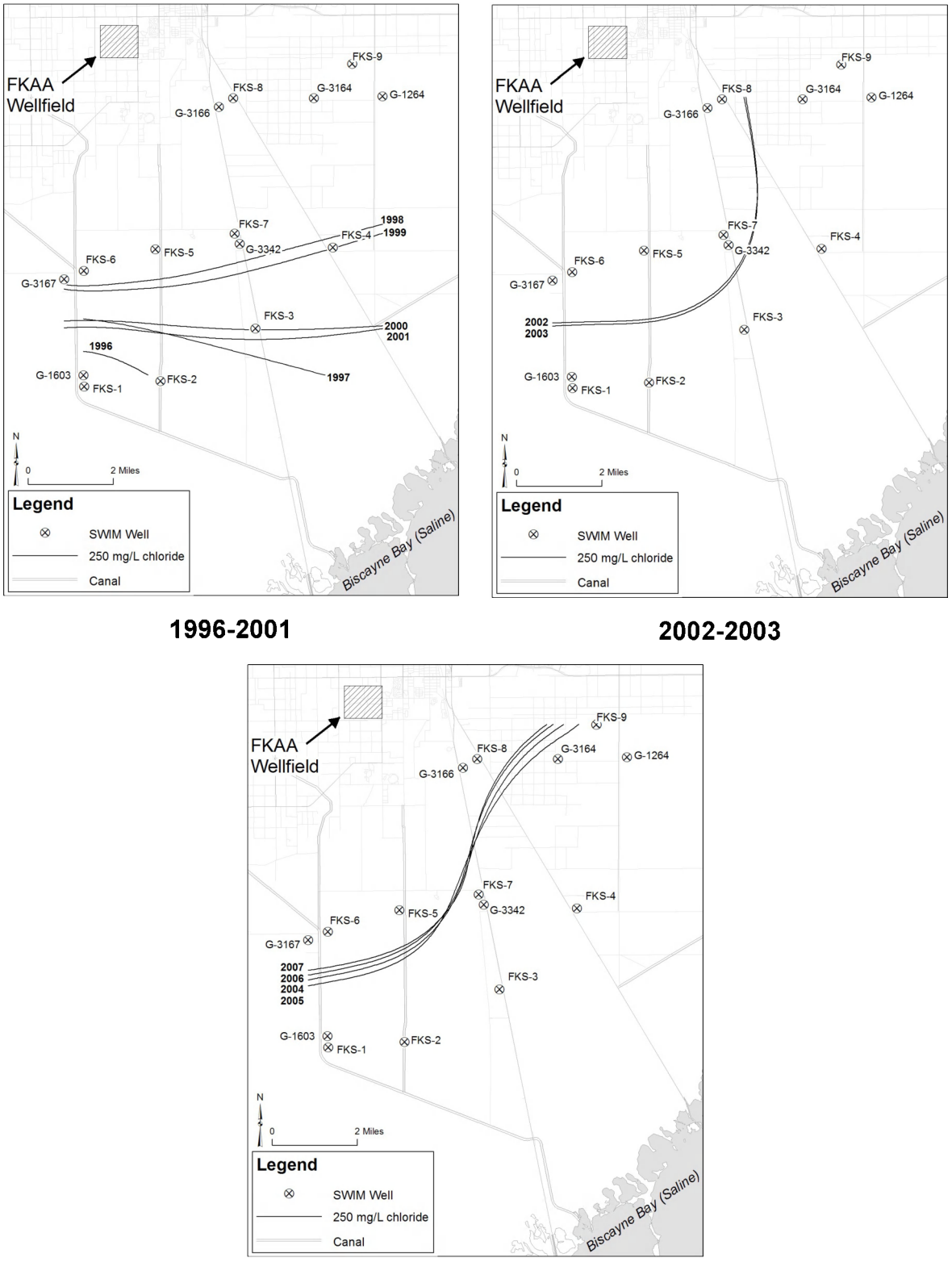

Figure 2. Locations of Deep Monitoring Wells and Interpolated 250 mg/L Chloride Isochlors, 55-65 ft below Land Surface, 1996-2007

DISCUSSION AND CONCLUSIONS

Over the past 10 years, groundwater withdrawals for public supply from the Biscayne Aquifer have increased by approximately 33 percent in southern Miami-Dade County. A severe drought in 2001 resulted in lower regional water levels in area canals and decreased fresh-water recharge to the Biscayne Aquifer. The effect of increased pumpage and reduced recharge can be seen in maps of the 250 mg/L chloride concentration isochlor in the area. At shallow depths (35-45 ft bls) there is little change; however some landward encroachment has occurred at greater depths in the vicinity of well G-1264. The concurrent stability of the shallow contour and the movement of the deeper contour are consistent with the typical wedge-shaped profile of the saltwater interface where encroachment is first observed at greater depths.

The FKAA is constructing a reverse-osmosis water treatment plant to treat brackish water from the Floridan Aquifer. Under its recently-authorized SFWMD water use permit, the FKAA's future Biscayne Aquifer average day withdrawals will be reduced from 19.93 to 17.8 mgd with a dry-season limitation of 17 mgd . This reduction in the FKAA's Biscayne Aquifer pumpage (along with expected future pumpage reductions by adjacent water suppliers) should increase the seaward fresh-water gradient and decrease the potential for further saltwater intrusion.

Continued monitoring to assess the position of the saline water interface is necessary to protect groundwater supplies in the Biscayne Aquifer in southern Miami-Dade County. The FKAA's SWIM network should be expanded to include additional wells to monitor the deeper intervals of the Biscayne Aquifer between the FKAA's wellfield and wells FKS-7, -8, and -9 where there are currently no monitoring wells between the saltwater interface and the FKAA's wellfield.

REFERENCES

Golden Software, 2007. SURFER. Computer Software.

Klein, Howard, and Waller, B.G. 1985. Synopsis of saltwater intrusion in Dade County, Florida, through 1984: U.S. Geological Survey (USGS) Water-Resources Investigations Report 85-4104.

Meyer, F.W. 1974. Availability of Ground Water for the U.S. Navy Well Field near Florida City, Dade County, Florida. USGS Open-File Report 74-014.

Parker, G.G., Ferguson, G.E., Love, S.K., et al. 1955. Water resources of southeastern Florida with special reference to the geology and ground water of the Miami area: U.S. Geological Survey Water-Supply Paper 1255, 965 p.

Sonenshein, R.S. 1996. Delineation of Saltwater Intrusion in the Biscayne Aquifer, Eastern Dade County, Florida, 1995. USGS Water Resources Investigation Report 96-4285.

SFWMD. 2006; Lower East Coast Regional Water Supply Plan 2005-2006 Update.

SFWMD, 2006. The 2000-2001 Drought in South Florida. SFWMD, West Palm Beach, FL.

Verdi, R.J., Tomlinson, S.A., and Marella, R.L. 2006, The Drought of 1998-2002: Impacts on Florida's Hydrology and Landscape: USGS Circular 1295.

Contact Information: Christopher Peters, CH2M HILL, 800 Fairway Drive, Suite 350, Deerfield Beach, FL 33441 USA, Phone: 954.426.4008, Fax: 954.698.6010, Email: chris.peters@ch2m.com

The Coastal Karstic Aquifer of Vlora (Albania)

Maurizio Polemio[1], *Arben Pambuku*[2] and *Olga Petrucci*[3]
[1]CNR-IRPI, Bari Department, Bari, Italy
[2]Albanian Geological Service, Hydrogeological Department, Tirana, Albania
[3]CNR-IRPI, Cosenza Department, Cosenza, Italy

ABSTRACT
The coastal karstic aquifer of Mt. Oyramanges (1864 m asl) is located in the Vlora Bay, along the Adriatic coast. The quality of the spring water there is so high that it is used to supply the drinking supply of the second largest Albanian town, Vlora. Starting from a geological and tectonic conceptualization of the area, a GIS approach based on long-term rainfall, temperature and river yield time series has been used to define hydrologic balance. The assessment of recharge and the measurement of sub-aerial spring discharge permit the rough assessment of submarine groundwater discharge. The definition of the flow domain and of groundwater chemical features is pursued with an on-going survey which includes chemical and isotopic analyses of rainfall, groundwater and sea water.

INTRODUCTION
Albania, has a surface of 28,748 km² and a perimeter of 720 km. The coasts, along the Adriatic and Ionian Seas extend for 362 km. 70% of the territory is mountainous with peaks higher than 2700 m asl. Along the coast, alluvial plains, 16 km in width as per the mean value, represent the unique flat areas. Despite the massive land reclamation for agricultural purposes, about 109 km^2 of coastal wetlands or lagoons still exist, especially along the Adriatic coast (Cullhaj et al. 2005).

The Albanian climate is subtropical Mediterranean. The mean annual temperature ranges from 7° to 15°, while the mean annual rainfall ranges from less than 600 mm to more than 3,000 mm (1,500 mm as mean). The mean national value is about 1,500 mm. Groundwater is the only source for drinking water in the whole country (Ministry of Environment 2002). A lack of detailed knowledge on groundwater availability and recharge and the non-systematic monitoring cause management problems where discharge is high and localized, as in some coastal areas in which seawater intrusion can also be observed.

The paper describes the study of the large karstic coastal aquifer of the Oyramanges Mt. (1864 m asl), located near Vlora (South-western Albania). Two main groups of springs are fed by the aquifer; one of which is of a coastal type. Spring groundwater fills the drinking supply of the town; the total spring discharge is roughly 4 m^3/s. A series of surveying campaigns has allowed for the characterization of hydrogeological balance and chemical-physical characterization. The study has been realised for the CISM project (www.cismalbania.it), an Italian-Albanian research project supported by INTERREG III.

GEOLOGICAL AND HYDROGEOLOGICAL FRAMEWORK
The analyzed aquifer is formed by carbonatic rocks of the large Tragjasi anticline, the periclinal of which is located in the S and SW parts of the study zone. The anticline is about 22 km in length and 6-10 km in width, with an asymmetric structure, inverted toward the West. Moving from the core, the anticline is composed of Upper Triassic (T_3) dolostone and limestone, Jurassic (J), Cretaceous (Cr) and Paleocene–Eocene (Pg_1–Pg_2^{1-2}) limestones, dolostones, and limestones with cherts. The carbonatic aquifer is bounded on the E, N and NW sides by Paleogene-Neogene flysch formations (claystones, siltstones and sandstones) (Meçaj et al. 2005); the area hosting aquifer outcrop is 147 km^2. The leakage from the aquifer is null, also due to a continuous outcrop

of quaternary clayey soils, locally including sands and gravels, which extend almost along the entire W side of the aquifer. The inland portion of the aquifer shows karstic features (Fig. 1).

On the western side, the carbonatic rocks and flysch come into transgressive contact with angle discordance placed in the Dukati valley. The relief of the left valley side constitutes the Acrocerauni belt which includes the carbonatic cretaceous relieves of the Karaburuni and Mali I Kanalit Mountains. The Karaburuni Mountain, where small bays and caves can be observed, creates a peninsula which closes the Vlora Bay. In the Dukati plain a shallow aquifer of Quaternary gravel, sand and poorly consolidated boulders can be distinguished. This aquifer, about ten meters thick, lies on hundreds of meters of impervious soils and rocks. The recharge is mainly due to the leakage of the Dukati River. On the left side of the coastal plain, the Orikumi Lagoon completes the environmentally precious bay. On the other side of the aquifer, we come across the hilly Shushica River valley, where Neogenic soils, mainly claystones siltstones and marlstones, which are hundreds of meters thick, outcrop. The discharge from the aquifer occurs as a result of the springs located near or immediately below the margin of outcropping limestone. There are no wells in the area where limestone outcrops but only in the valley of the Dukati River or where Quaternary soils outcrop.

HYDROLOGICAL BALANCE AND RECHARGE

Monthly data (covering a 20 to 32-year time-frame) concerning rainfall P, temperature T, (six gauges) and river flow yield R (1 gauge) were used to define the hydrological balance. Both rainfall and temperature show a statistically relevant straight-line correlation with altitude. On the basis of a DEM (cell size 40 m), the spatial variability of rainfall and temperature was assessed. The real or actual yearly evapotranspiration Er was calculated in each cell using Turc's

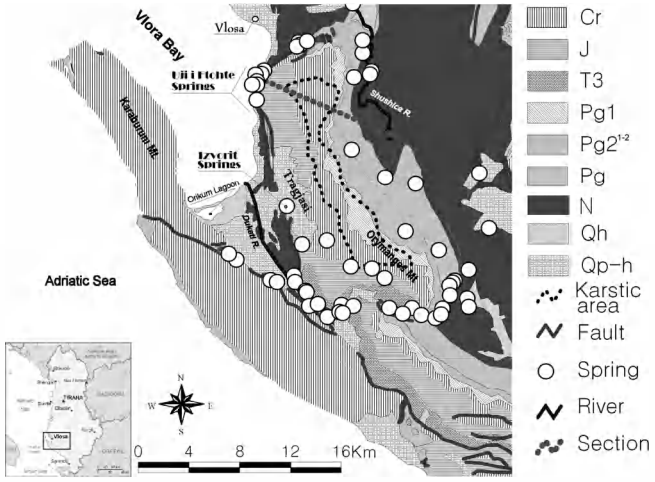

Figure 1. Geological and hydrogeological schematic map and section. Main aquifer: Cr, J, T_3, Pg_1 and Pg_2^{1-2} respectively are Cretaceous fissured and karstified limestones, dolomitic limestones and dolostones, Triassic fissured dolostones and Paleogene-Eocene limestones and limestones with cherts. Impervious formations: Pg and N respectively are Paleogenic and Neogenic soils and rocks, mainly claystones, silts and marlstones. Secondary aquifer: Qp-h and Qh respectively are Quaternary gravel, sand and poorly consolidated boulders, covered by shallow clay in the former case.

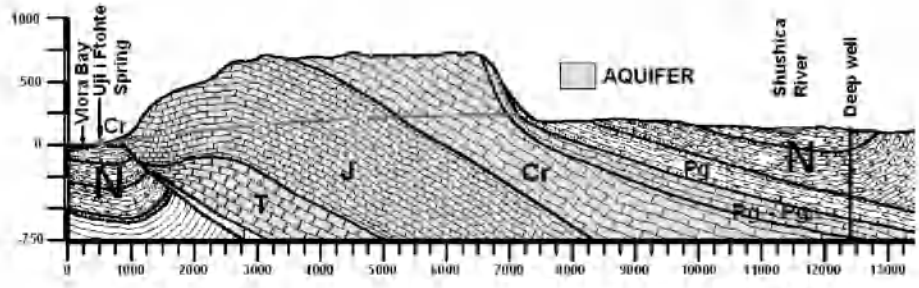

formula; the amount of net rainfall Pn was thus calculated as Pn=P-Er. On the basis of the map of hydrogeological complexes, which defines an infiltration coefficient Ci for each complex, the infiltration I is assessed in each cell as I=Pn Ci. The basin of the Shushica River was used to calibrate the hydrologic model. At the Drashovice gauge, the Shushica drainage basin is 587 km^2; while the mean river yield is 19.8 m^3/s, due to mean annual rainfall equal to 1840 mm. At the end of calibration, the mean river yield was assessed as being equal to 17.1 m^3/s. On this basis, the annual net recharge on the karstic aquifer outcrop is equal to 1,127 mm which corresponds to 5.2 m^3/s.

Two main flow paths go from the high karstic plateau of Mt. Oyramanges to two spring areas. These areas are placed at a distance of 10 km on the western side of the aquifer, where it outcrops at the lowest altitude. The former is the group of coastal springs of Uji i Ftohtë, located at sea level. The main coastal group of springs is called Uji i Ftohtë. The group includes three springs tapped by short tunnels and used for the Vlora aqueduct. The mean spring yield discharged in these tapping works is roughly equal to 2.0 m^3/s. The second group of springs is called Izvorit and it is located at about 40 m asl, in the Tragjasi Village. The springs are placed along a straight portion of the outcrop limit between carbonatic rocks ($J\text{-}T_3$) and clays of Neogene. The springs of both groups are roughly placed along a straight N-NW S-SE tectonic line. A low percentage of the Izvorit spring outflow rises up to some villages; the rest was measured with tracer tests. The whole mean outflow of the spring group is roughly equal to 1.8 m^3/s.

The difference between total spring outflow and recharge, roughly equal to 1.4 m^3/s, can be considered equal to groundwater submarine discharge, since the well discharge is almost null. The groundwater submarine discharge is concentrated near the Uji i Ftohtë spring area, where the carbonate aquifer is directly bordered by the sea. The hydrological relevance of groundwater submarine discharge was highlighted by a surveying cruise executed in the Vlora Bay, in which temperature, salinity, pH and dissolved oxygen of the sea water were measured (www.cismalbania.it).

Characteristics of the Uji i Ftohtë spring group

The tunnel of I Jonufrës Cape, 1,700 m in length, connects the outflow of 32 coastal springs, which taps in different sectors along the coastal line. Moving from North to South, the first sector includes tapping from the tunnel road which is 185 m in length. The mean annual discharge is roughly 0.40 m^3/s. Unexploited springs, some of them submarine, are placed from the end the of tunnel road to a maximum distance of about 300 m. From this point to the lighthouse, another tunnel is able to tap a mean discharge equal to 0.64 m^3/s. From the lighthouse to the Castle, about 400 m, four unexploited small springs can be observed. The last sector includes the old road tunnel where 11 tapped springs are placed, for a mean total discharge of 0.94 m^3/s. The chemical and physical characteristics of groundwater tapped springs are almost identical. On the basis of preliminary results (the first of two years of surveying has almost been completed), the spring groundwater is weakly alkaline (pH 7.6) and almost fresh (TDS roughly equal to 0.2 mg/l); the mean chloride concentration is 26 mg/l, but a relevant seasonal variation is observed (peak value equal to 50 mg/l). The hydrochemical type is HCO_3-Ca-Mg. There neither evidence of contamination nor relevant effects of seawater intrusion. The insignificant presence seawater intrusion effects can be tied to the high rate of groundwater flow, the favorable stratigraphical conditions and the Venturi effect (Fleury et al. 2007). The primary exception is due to small springs, mainly located near the first sector, where salinity rises up to 0.3-0.4 mg/l, the nitrate concentration (20-25 mg/l) becomes relevant and chloride is about

double the amount than the value observed in the main springs. This seem to be the result of contamination due to the recent diffuse house building, carried out upward the spring area yet where there are no sewage systems.

RESULTS

The study shows the peculiarities of this carbonate coastal aquifer and the importance of its groundwater which is the chief water resource for the second largest Albanian town. The amount of recharge and discharge was verified together with the conceptual model.Further investigations are necessary to assess groundwater degradation risks and to define management criteria for reducing these risks.

REFERENCES

Cullaja, A., Haskob, A., Mihoc, A., Schanzd, F., Brandle, H. and R. Bachofenf. 2005. The quality of Albanian natural waters and the human impact. Env. Int., 31: 133-146.

Fleury, P., Bakalowicz, M.and G. De Marsily. 2007. Submarine springs and coastal karst aquifers: a review. Journal of Hydrology, 339: 79-92.

Meçaj, S., Xhomo, A., Kodra, A., Shallo, M., Vranaj, A., Xhafa, Z., Nazaj, Sh., Nakuçi, V., Yzeiraj, D., Sadushi, P., Lula, F., Xhafa, F., Dimo, Ll. and F. Bakalli. 2005. Gjeologjia e Shqiperise.

Ministry of Environment. 2002. The First National Communication of Albania to the United Nations Framework Convention on Climate Change. Republic of Albania, Tirana.

Pano, N. and A., Flasheri. 2007. Principal aspects of the ecosystem Vlora bay - Narta lagoon - Vjosa river mouth. CISM Project, Tirana (Albania): www.cismalbania.it.

Contact Information: Maurizio Polemio, CNR-IRPI, Bari Department, Via Amendola 122/I, 70126 Bari, Italy, Phone: +39 080 5929584, Fax: +39 080 5929610, Email: m.polemio@ba.irpi.cnr.it

Dynamics of Negative Hydraulic Barriers to Prevent Seawater Intrusion

María Pool[1] , *Jesús Carrera*[2], *Emilia Bocanegra*[3] and *José L. Cionchi*[3]

[1]Department of Geotechnical Engineering and Geosciences, School of Civil Engineering, Technical University of Catalonia, Spain

[2]Institute of Earth Sciences "Jaume Almera", Spanish Research Council (CSIC), Barcelona, Spain

[3]Obras Sanitarias Company (OSSE), Water Resources Management, Mar del Plata, Argentina

ABSTRACT

Negative hydraulic barriers, which pump at the shore intercepting inflowing saltwater, are proposed as a corrective measure for seawater intrusion in aquifers where groundwater is the main water resources and restrictions on pumping are not feasible. Negative barriers prevent saltwater from moving inland and protect freshwater supply wells. While this barrier is pumping saltwater intrusion does not proceed further. The main drawback of negative hydraulic barriers is that wells end up pumping much more freshwater than saltwater, thus contaminating freshwater resources. To minimize the mixing process we propose a double-negative barrier system with two extraction wells. In this system one of the wells pumps freshwater and the other one saltwater, without mixing between them, controlling the saltwater intrusion and decreasing the piezometric head in the area. A careful analysis is required to bound the possible effects of this negative hydraulic barriers on the flow field. The approach suggested here uses three-dimensional variable density flow and transport simulations to study the sensitivity of the system by means of a set of dimensionless numbers which summarize the overall behavior of this system. Different sets of simulations have been carried out varying each of the dimensionless numbers each time to asses their effect. These dimensionless numbers depend on magnitudes such as the amount of water that should be extracted and the distance of the wells to the sea. We used the algorithm of *Furnival and Wilson Jr* (1974) to identify the parameters that best explain the dynamics of the system. An empirical expression is being developed by a regression model that describes how (combinations of) the defined dimensionless numbers control the salinity of pumping wells in the presence of hydraulic barriers.

Contact Information: Maria Pool, Department of Geotechnical Engineering and Geo-Sciences, Technical University of Catalonia (UPC), C/ Jordi Girona 1-3, Building D-2, 08034 Barcelona, Spain,
Phone: +34 934011858; Fax: +34 934017251, Email: merypool@yahoo.es

Vertical Integration for Modelling Seawater Intrusion

María Pool[2], *Jesús Carrera*[1], *Juan J. Hidalgo*[1], *Marco Dentz*[1] and *Elena Abarca*[3]
[1]Institute of Earth Sciences "Jaume Almera", Spanish Research Council (CSIC), Barcelona, Spain
[2]Department of Geotechnical Engineering and Geosciences, School of Civil Engineering, Technical University of Catalonia, Spain
[3]Civil Engineering Department, Auburn university, Auburn, Alabama, USA

ABSTRACT
In this paper we present a novel effective formulation for modelling seawater intrusion that relies on a dimensional reduction of the original flow and transport problem. Seawater intrusion in coastal aquifers is a three-dimensional process. Over the last decades the three-dimensional simulation of seawater intrusion has received increasing attention in the literature. However, three-dimensional regional aquifer models are limited by the availability of geological and hydrological data, and by numerical constraints. We probe simplified formulations for the coupled flow and transport problem which allow for a realistic yet efficient modelling of seawater intrusion into coastal aquifers. To this end, we develop a two-dimensional areal formulation for regional seawater intrusion that correctly reflects the effective dynamics in the three-dimensional system. We carry out a vertical integration of the three-dimensional coupled flow and transport problem and arrive at a coupled set of two-dimensional equations for the spatial mean flux and salt concentration. The impact of vertical fluxes on mixing and thus on flow and transport is integrated into this effective dimensionally reduced formulation in terms of an effective dispersion tensor and a sink/source term for the flow equation. The proposed methodology is verified by direct numerical simulations of the full threedimensional problem and numerical simulation of the projected two-dimensional flow and transport problem.

Contact Information: María Pool, Department of Geotechnical Engineering and Geo-Sciences, Technical University of Catalonia (UPC), C/ Jordi Girona 1-3, Building D-2, 08034 Barcelona, Spain,
Phone: +34 934011858; Fax: +34 934017251, Email: merypool@yahoo.es

Salinization by Free Convection in Heterogeneous Aquifers: Results from a Numerical Modeling Study

Vincent Post[1] and *Craig Simmons*[2]
[1]Department of Hydrology and Geo-Environmental Sciences, Vrije Universiteit, Amsterdam, The Netherlands
[2]School of Chemistry, Physics and Earth Sciences, Flinders University, Adelaide, South Australia, Australia

ABSTRACT
The effect of discrete low-permeability lenses on seawater intrusion by free convection was investigated using a numerical model. It was found that upward vertical flow components retard salinization of the lenses as these counteract the penetration of dissolved salts by diffusion and convection from above. Surprisingly, salinization of the low-permeability structures predominantly takes place from below as salt water is dragged upwards due to the upward flow field that is established within them.

INTRODUCTION
Numerous coastal areas throughout the world experience episodic flooding by seawater. Such events may be regular and anticipated (e.g. tidal flooding) or catastrophic (e.g. the 2004 tsunami in southeast Asia or the 2005 hurricane Katrina in New Orleans). Flooding potentially leads to deterioration of water resources when fresh groundwater becomes contaminated with seawater that infiltrates into the soil and enters the aquifers. Of particular importance in the case of seawater flooding is the unstable density stratification that develops when seawater is carried on top of fresh groundwater. This may give rise to the process of free convection during which the more saline water migrates vertically downward under the influence of its high density compared to the underlying fresh water. Typically, plumes of salt water form during this process which can sink down into the aquifer at considerable rates.

Natural porous media always contain at least some degree of permeability stratification. Previous studies of free convection have addressed this using a stochastic permeability field (e.g. Simmons et al. 2001). To date, no studies have been published that focus on the effect of discrete low-permeability structures on the free convection process at the (smaller) scale of the lense nor on the precise solute transport mechanisms that affect solute exchange between the layers of lower and higher permeability. It is expected that the presence of low-permeability lenses retards free convection and that salinization of the low-permeability zones occurs at a different rate than in the high-permeability zone.

The objective of the present study is to establish how structured permeability distributions affect the dynamics of convective-flow for characteristic natural geologic systems. We focus on small-scale systems (based on an accompanying laboratory experiment that is not shown here) where the length scale of permeability changes is in the order of decimeters. The intent is not to develop a universal theory but rather to demonstrate how salinization works in these systems.

METHODS
For the numerical experiments, the variable-density flow simulator SEAWAT-2000 was used (Langevin and Guo 2006). The model grid measured 110 by 60 cm (based on the dimensions of a laboratory tank experiment) and consisted of 180 columns in the horizontal and 164 rows in the vertical direction. The top model boundary was a fixed head, fixed concentration boundary, allowing water and solutes to enter and exit the model domain. The left, right and bottom boundaries are closed for both flow and solute transport. In nature, the left and right boundaries

are thought to represent flow lines and the bottom boundary a practically impermeable clay layer.

The initial solute concentrations of all the cells in the model domain were assigned a concentration of 0. A density contrast of 2.0 g/cm^3 between the saline and fresh water was used. This relatively low value was used to prevent very small plume dimensions that can not be resolved by the model grid. The fresh water hydraulic conductivity of the high-permeability zone of the model domain was 90 m/d; the conductivity of the low-permeability lenses was varied during the simulations. The total simulation time was 30 days with a transport numerical time step of approximately 3 seconds.

Three realizations of permeability fields where used that are thought to be representative for field conditions: horizontal lenses (discussed in this paper), vertical lenses and square blocks. For each of these configurations, simulations were performed with different permeability contrasts between the low and the high-permeability zones, i.e. 1:90, 1:900 and 1:9000. Due to the space constraint, only the results of the simulation with horizontal low-permeability lenses with the 1:90 permeability contrast are discussed in detail.

RESULTS

The panels in Figure 1 show the development of the solute concentration pattern and the flow vectors for the simulation (1:90 permeability contrast) . Initially, salt plumes emanate from the seafloor and move downward into the aquifer. After 0.8 days, the plumes in the central part of the domain reach the top of the uppermost low-permeability lens and further downward migration is hampered. Consequently, horizontal migration of the salt plumes starts to occur as well as diffusive salinization of the lens. On both sides of the uppermost lens salt plumes continue to sink down unhindered until they reach the top of the lower lenses where similar patterns develop.

The salt plumes reach the bottom of the model domain after 4 days. By that time, a fairly constant flow pattern has been established in which salt water essentially flows downward near the left- and, to a lesser extent, right-hand boundaries and fresh water moves upward in the central part of the model domain. Particularly strong vertical upward flow occurs in the high-permeability part of the model domain, immediately adjacent to the vertical sides of the fresh water lenses. Jets of fresh water can be seen to escape upwards on a regular basis.

The larger scale convection pattern also drives flow within the lenses as reflected by the development of upward flow components inside them. Initially, if the vertical flow component is still very small, diffusion of salt from above occurs. This saline water, however, is pushed back upwards as the magnitude of the upward flow component increases. At the same time, salt water that has flowed around and underneath the lenses starts to be dragged into the lenses from below.

After approximately 20 days, when concentration gradients in the high-permeability part of the model domain become increasingly smaller, the convective flow cell becomes weaker. Upward flow inside the lenses and the associated dragging up of salt water remains an important process, however, due to the buoyancy of the entrapped fresh water. Ultimately, as density gradients disappear, diffusion becomes the dominant transport mechanism. Flow becomes progressively weaker as diffusion begins to dominate transport behaviour and ceases altogether upon complete salinization of the system.

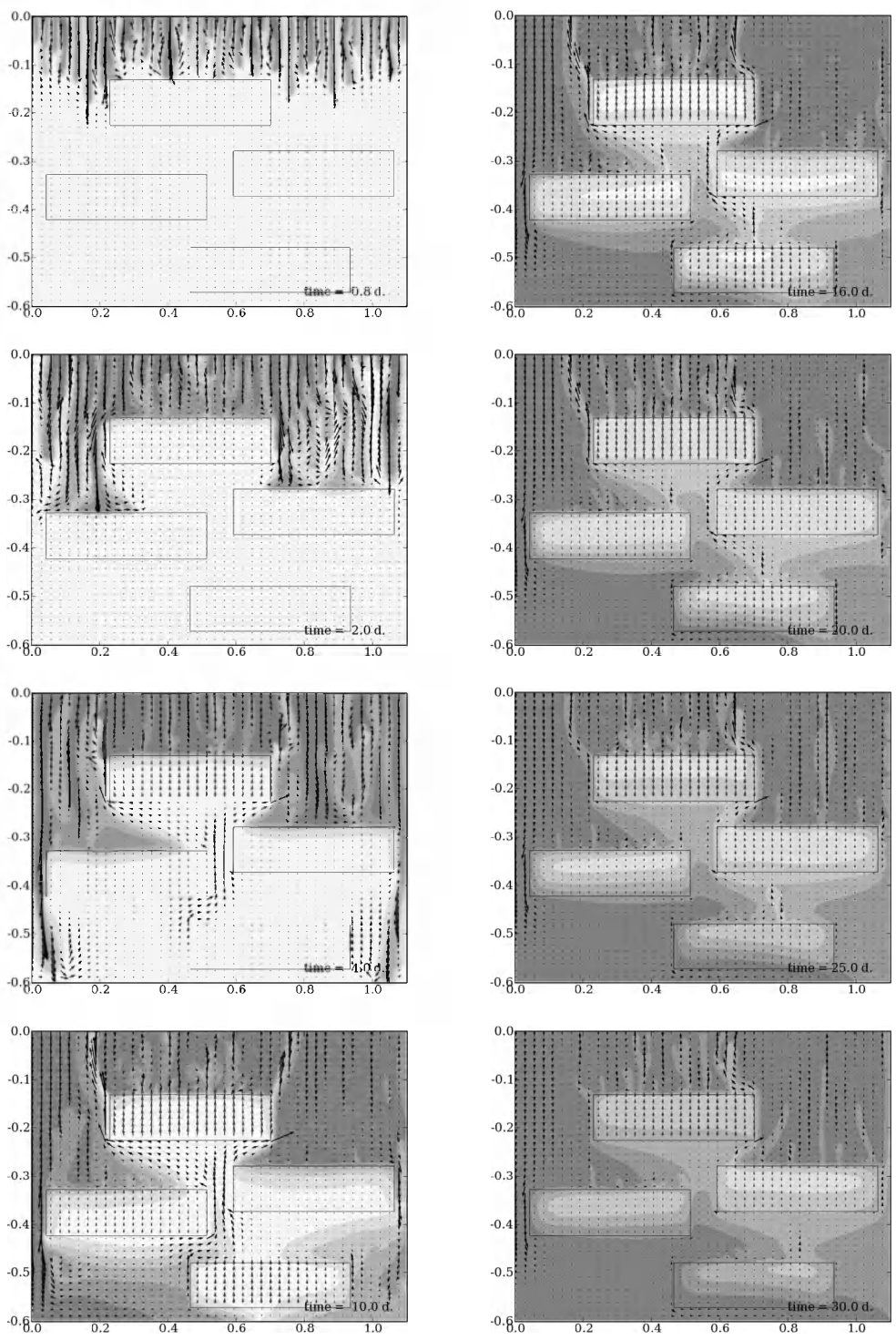

Figure 1. Concentration patterns and flow vectors after 0.8, 2.0, 4.0, 10.0, 16.0, 20.0, 25.0 and 30.0 days for the simulation with horizontal lenses. Darkest shading represents highest concentrations. Flow vector length within the low-permeability lenses has been increased by a factor of 10 compared to the surrounding area.

DISCUSSION AND CONCLUSIONS

The results discussed above demonstrate the importance of the presence of low-permeability structures for the convection cells and concentration patterns that develop during free convection. The large scale convective flow pattern that develops is mainly controlled by the permeability distribution. In response, vertically upward flow occurs within the low-permeability lenses, which causes them to become saline from below, even thought the intrusion of salt water is through the top of the model. This is mainly due to the dragging upward of salt water from below but partly also due to the counteracting action to diffusion through the top of the low-permeability structures.

Comparable behavior was observed for the simulations with different permeability distributions (not shown in this paper), although not as pronounced as in the simulation discussed above. These results indicate that salinization of the low-permeability structures in soils and aquifers may be significantly retarded due to the action of upward flow. It is expected therefore that for pulses of short duration (i.e. in the order of days) little salt water penetrates into the immobile parts of the sediment and hence the retarded delivery of salts during the freshening phase is abated.

REFERENCES

Simmons, C.T., T.R. Fenstemaker and J.M. Sharp Jr. 2001. Variable-density groundwater flow and solute transport in heterogeneous porous media: approaches, resolutions and future challenges. Journal of Contaminant Hydrology 52: 245-275.

Langevin, C.D. and W. Guo. 2006. MODFLOW/MT3DMS-based simulation of variable-density ground water flow and transport, Ground Water 44, no. 3: 339-351.

Contact Information: Vincent Post, Vrije Universiteit, Department of Hydrology and Geo-Environmental Sciences, De Boelelaan 1085, 1081 HV Amsterdam, The Netherlands, Phone: +31(0)20-5987402, Fax: +31(0)20-5989940, Email: vincent.post@falw.vu.nl

An Investigation of Groundwater Flow on a Coastal Barrier Using Multi Electrode Profiling

Søren E. Poulsen, *Steen Christensen, Keld R. Rasmussen, Jesper S. Mortensen* and *Andrea Viezzoli*
Department of Earth Sciences, University of Aarhus, Denmark.

ABSTRACT
Preliminary geophysical and hydrogeological investigations indicate that multi-electrode profiling (MEP) can be used to monitor groundwater salinity on a coastal barrier where a shallow thin aquifer discharges to the North Sea. A monitoring system including five groups of piezometers and five MEP probes, having closely spaced electrodes from above the groundwater table to a depth of 5 m below sea level, have been installed and tested. Using this system we will monitor resistivity and thus groundwater salinity variations in space and time. Analyzing the measurements using density dependent groundwater modeling we hope to be able to quantify how time varying recharge, tides, and storms hitting the barrier affect groundwater flow and discharge to the sea. At the conference we will present monitoring results from the winter and spring 2008.

INTRODUCTION
In the end of the 1950's and the beginning of the 1960's chemical waste including pesticides were deposited in a dune repository at the Harboøre Barrier, a coastal barrier on the North Sea coast of Jutland, Denmark. Most waste was removed in the 70's and 80's but residual contamination has been slowly leaking to the sea since then. The aim of our project is to investigate the significance of the physical processes that influence the groundwater flow with which the pollutants are transported from the repository to the sea.

Contaminants reaching the ground water of coastal aquifers are transported to the sea by Submarine Groundwater Discharge (*SGD*). Li et al. (1999) proposed a model for calculating the different contributions of *SGD* in order to evaluate their individual impact on chemical transfer rates. The contributions to total *SGD* (*TSGD*) considered by Li et al. (1999) are discharge due to groundwater recharge from precipitation D_r, discharge due to tidal forcing D_t, and discharge due to wave activity D_w. On the actual coastal barrier we add the discharge caused by flooding of the beach during storms, D_s, so

$$TSGD = D_r + D_t + D_w + D_s$$

The timescale of the four contributing terms is seconds for waves, hours for tides, hours to days for storms, and weeks or months for recharge. Neglecting the variation of the latter may lead to wrong estimates of *TSGD* (Charette et al., 1999). Michael et al. (2005) summarizes a study of *SGD* for a thick aquifer in Waquoit Bay, Massachusetts. They examined the effects of temporal variations in recharge by monitoring piezometers during a winter period and by measuring the saline seepage directly using seepage meters. Large saline discharges were observed but sufficient seawater inflow was not observed to balance this outflow. A lag between the precipitation cycle and the *SGD* was observed which implies that the larger precipitation in the winter recharges the aquifer during the summertime as it takes several months for the water to percolate to the water table.

For the coastal barrier we study, mainly D_r, D_t, and D_s are expected to contribute significantly to SGD. In order to quantify the terms we will monitor with an adequate temporal resolution the spatial and temporal variation of groundwater salinity along a profile perpendicular to the coast, set up and calibrate a model of density dependent groundwater flow on basis of time series of salinity, recharge, and water table, and subsequently use the model to analyze how recharge, tides, and storm flooding induce groundwater discharge. In this paper we present the monitoring system.

GEOLOGY, WATER TABLE, AND GROUNDWATER SALINITY

Figure 1 shows the geology on the barrier near the repository as it can be described on basis of lithological samples from borings. The deeper stratigraphic sequence consists of sandy coastal deposits overlain by a 40 m layer of fine grained clay which has its top surface approximately 9 m below mean sea level (MSL). The clay is superimposed by a 6 m silty sequence that in the eastern part of the profile is topped by less than 0.5 m clay. In the western part the clay is missing. The fine grained deposits are overlain by a sandy sequence that extends to the surface.

Groups of piezometers have been installed on each of the five locations named E1 to E5 in Figure 1. Measurements show that the water table is highest under the dune (in E2 and E3), where it is approximately 1 m above MSL, and that it falls towards the coast as well as towards the lagoon area behind the dune (to the east). The chloride concentrations measured in water samples from the piezometers vary from about 200 mg/l near the water table under the dune to about 8000 mg/l just above the thin clay layer at E1. Deeper piezometers have recently been installed in order to analyze the chloride content in the deeper silty sequence.

The lower part of Figure 1 shows the electrical resistivity along the profile as estimated from surface multi-electrode profiling (MEP). The measurements have been inverted without any constraints (for example not constrained by information about the actual depths of the water table in the piezometers), so the fairly deep unsaturated zone distorts the interpretation somewhat which makes the water table (where resistivity in Figure 1 transitions from very high values to a value less than 150 ohm-m) appear to be deeper than it really is. Anyhow, the important thing to notice is that there is a transition of resistivity with depth from about 100 ohm-m, in saturated sand deposits with low groundwater salinity, to resistivities of just a few ohm-m. The low resistivities in depth can be caused by the clayey deposits, or by high groundwater salinity, or most likely by both. The transition zone appears to be about 5 m thick below the dune whereas it is just a few meters thick outside the dune. This picture has been confirmed by several other MEP profiles made in the area as well as by electric logging at a number of positions using an geoelectrical auger.

MEP PROBE MONITORING OF RESISTIVITY CHANGES IN TIME AND SPACE

In the fall of 2007 a MEP probe was installed at each of the five positions E1 to E5 (Figure 1). Each probe has 32 electrodes (or 28 electrodes at E1 and E5) with a spacing of 0.25 m, and it was installed in an open bore hole that was left to collapse naturally. Installation of the probe was done so the top electrode is positioned about 1 m above the groundwater table while the bottom electrode is positioned approximately 5 m below MSL.

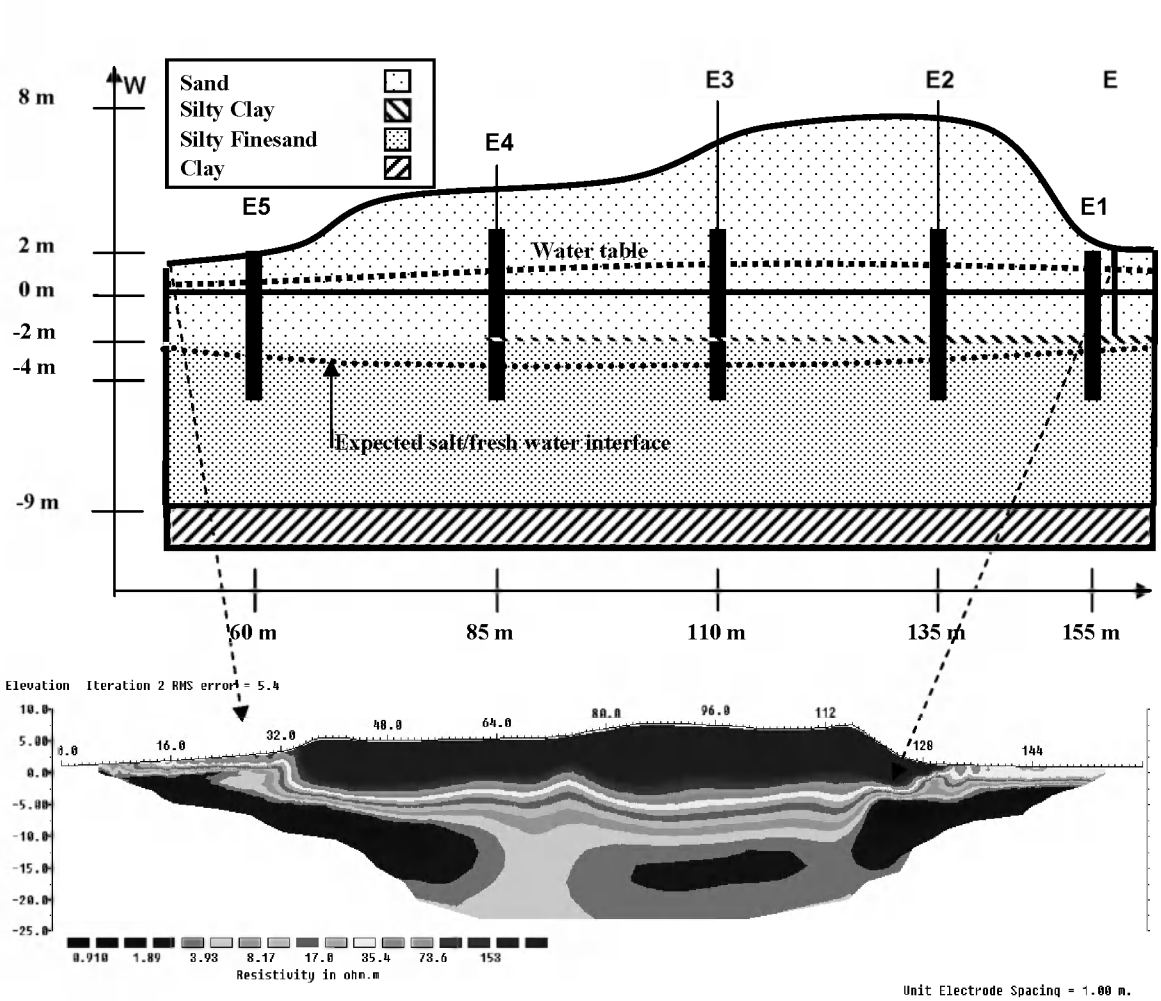

Figure 1: a) Schematic overview of the profile with MEP-probes E1-E5. X-axis: approximate distance the coastline [M]. Y-axis: Elevation DNN [m]. b) Interpretation of a horizontal MEP profile along the E1-E5. The North Sea is to the west, the lagoon area is to the east.

The purpose of installing the probes is to make it possible to make detailed vertical resistivity mapping at the five positions at any time we may wish to do so, and hopefully we can also obtain sufficiently accurate measurements of the induced polarization (IP) response using the time domain method. By interpreting the probe measurements together with water table measurements and salinity measurements in the nearby piezometers we expect to obtain good and detailed estimates of the variation in salinity with depth at the sampled times at the five positions. If the IP response can be measured by sufficient accuracy this will provide information about the clay content of the sediment surrounding the probes.

Two pilot series of measurement have been performed in order to check the probes, the geophysical equipment, and the measurement protocols (dipole-dipole as well as gradient protocols), and all seems to work properly. Rough preliminary inversions of the probe measurements give resistivity results that make sense when compared with the surface MEP results and with the salinity measurements made on groundwater samples.

CONCLUSIONS

The discharge of ground water to the sea is studied on a coastal barrier. Because the aquifer is shallow and thin it is expected that variations in recharge, tide, and beach flooding during storms have significant, time varying effects on the discharge and salinity of ground water. Geoelectric

augering, Surface MEP measurements, and chemical analysis of groundwater samples have shown that salinity can be mapped by using geoelectrical resistivity measurements. Multi-electrode probes have therefore been installed at five positions along a profile perpendicular to the coast from near the shore to behind the barrier. The probes, measurement protocols, and equipment have been tested and work. It is hereby possible to make detailed vertical resistivity mapping at the five positions. By interpreting these measurements together with water table and groundwater salinity data we expect to obtain detailed information about temporal and spatial salinity variations that can be used to quantify by modeling how recharge, tide, and flooding contributes to the time varying discharge of ground water to the sea.

At the time of submission of this paper the coastal barrier is hit by the first winter storm in 2008. MEP probe and MEP surface measurements are being made during and following the storm so soon the first interpreted measurements will show to what extent beach flooding affects groundwater flow and salinity under and behind the barrier. On basis of this experience we will decide on how and how frequent to monitor the probe system in the years to come.

REFERENCES

Charette, Matthew A., Herbold, Craig, Bollinger, Marsha S., Splivallo, Richard and

Moore, Willard S. *Salt marsh submarine groundwater discharge as traced by radium isotopes.* Marine Chemistry, 84:113-121, 2003.

Li, L., Barry, D. A., Stagnitti, F. and Parlange, J. Y. *Submarine groundwater discharge and associated chemical input to a coastal sea.* Water Resources Research, 35:3253-3259, 1999.

Michael, Holly A., Mulligan, Ann E. and Harvey, Charles F. *Seasonal oscillations in water exchange between aquifers and the coastal ocean.* Nature, 431:1145-1148, 2005.

Contact Information: Søren E. Poulsen, University of Aarhus, Department of Earth Sciences, Ny Munkegade, bld. 1520, DK-8000 Aarhus, Denmark, Phone: +45 89 42 55 24, Email: soeren.erbs@geo.au.dk

Geochemistry of Phosphorus in a Carbonate Aquifer Affected by Seawater Intrusion

René M. Price, *Jean L. Jolicoeur* and *Jeremy C. Stalker*
Florida International University, Dept. of Earth Sciences and SERC, Miami, FL, USA

ABSTRACT
The concentrations of total and dissolved phosphorus in groundwater were found to increase linearly with salinity within the seawater intrusion zone beneath southwestern Florida. Digestion of the limestone resulted in an average total phosphorus (TP) concentrations from 54 µg/g to over 850 µg/g. Adsorption experiments confirmed that the limestone aquifer had a high affinity to adsorb phosphate dissolved in fresh water. Phosphate adsorption decreased in the presence of seawater. Geochemical modeling determined that dissolution of calcite and aragonite was responsible for the release of phosphorus in brackish groundwater at low salinities. At higher salinities, desorption of phosphate as a result of bicarbonate sorption was the dominant reaction.

INTRODUCTION
Areas of seawater intrusion are geochemically active, particularly in carbonate aquifers, where carbonate mineral dissolution (Back et al., 1986) and ion exchange (Sivan et al., 2005) are important. These reactions maybe responsible for an observed linear increase of phosphorus with salinity in groundwater along the southwestern coast of Florida (Price et al., 2006). Dissolved phosphorous maybe transported to surface coastal waters via either submarine groundwater discharge (Moore, 1999) or coastal groundwater discharge (Price et al., 2006) where it can serve as an additional source of this important nutrient.

In carbonate aquifers with little iron, P exists either as phosphorus minerals such as apatite (Jensen et al., 1998) or adsorbed onto calcite and aragonite (DeKanel and Morse, 1978). TP in carbonate sediments throughout south Florida range from 56 – 678 µg/g soil (Chambers and Pederson, 2006; Zhou and Li, 2001). Adsorption and desorption of phosphate to calcium carbonate sediments from Florida Bay under both fresh water and seawater have been investigated with less P adsorption occurring with an increase in salinity (Millero et al., 2001). The capacity of P sorption by carbonate also depends strongly on its surface area with higher adsorption occurring on fine grain sediments (Zhou and Li, 2001). The objectives of this research were to 1) further document the occurrence of elevated total P concentrations in the brackish groundwater underlying south Florida; 2) quantify the amount of P available in the limestone of the Biscayne Aquifer, and 3) to identify which reactions were responsible for the release of P from the bedrock as a result of seawater intrusion.

METHODS
Groundwater sampling was conducted at 11 sites (Fig. 1) from Sept. 9-13, 2007. Groundwater temperature, pH, salinity, and dissolved oxygen were monitored until stable. Water samples were collected for TP and dissolved phosphate (soluble reactive phosphate; SRP) in vials that were first flushed with nitrogen and then evacuated to remove any exposure of the sample to oxygen.

Rock core was collected from five locations in the Biscayne Aquifer (Fig.1). Cores CP and RB were located near the coastline in a zone of known seawater intrusion. Core LMB was collected from Florida Bay. Cores (G3778 and G3784) were far inland in a region of fresh groundwater. A

sub-sample of 0.5 g of rock was taken from the interior of each half of the core at determined intervals. These rock samples were digested for TP determination.

A cube, 0.2m on a side, was extracted from a large block of Key Largo Limestone (Fig 1). The limestone cube was sealed in a Plexiglass permeameter. A constant discharge was maintained at 120 L d^{-1} using a 20 L carboy filled with a solution of phosphate (PO_4^{3-}) varying from 0 to 20µM in either Dionized water (DIW) or seawater. The final part of the experiment consisted of flushing the stone with DIW and then seawater to observe SRP desorption. Water discharging from the block was monitored for pH, salinity, and temperature. A subsample of 40 ml of water for every liter discharged was collected for determinations of SRP, alkalinity, potassium, calcium, sodium, magnesium, chloride and sulfate. The concentrations of the major ions, pH, temperature, and alkalinity were input to the geochemical model PHREEQC version 2.14.2 to determine the saturation states of the water with respect to calcite and aragonite.

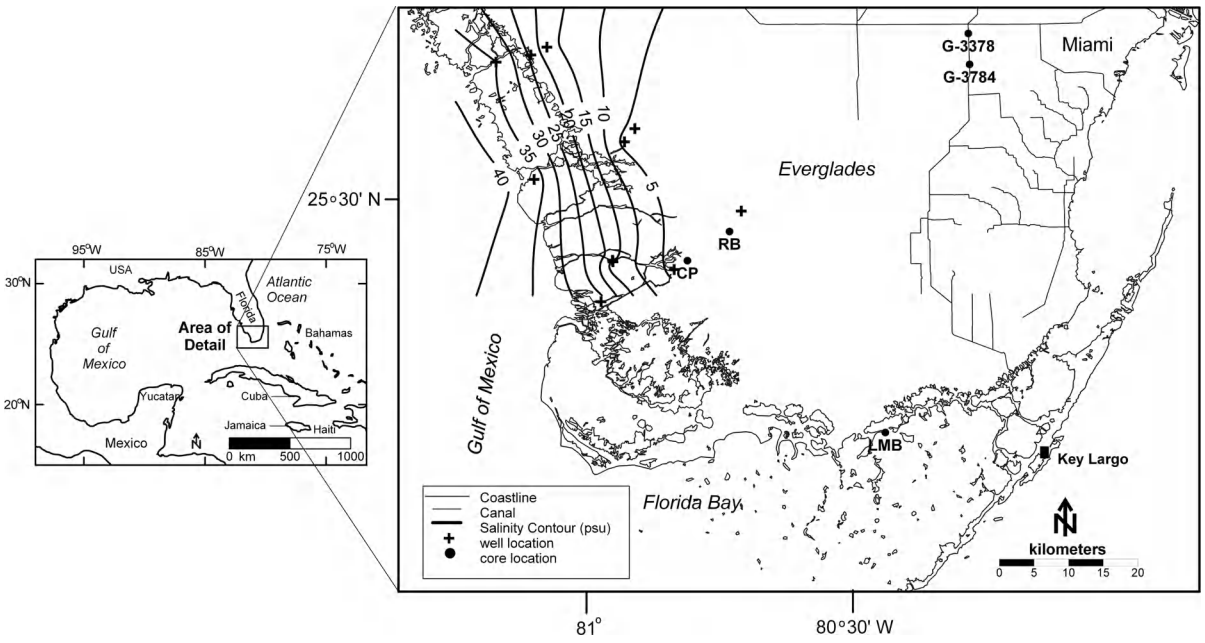

Figure 1. Site location map of groundwater wells (+), rock core (●), and Key Largo limestone (■) used in this study. Contour lines represent salinity of groundwater collected from wells that ranged in depth from 2 to 8 m.

RESULTS

TP in the brackish groundwaters ranged from 0.6 µM to 6.9 µM, and varied linearly with salinity (Fig. 2A). SRP also varied linearly with salinity and ranged from 0.06 to 6.9 µM (Fig. 2B). The concentrations of both TP and SRP in the groundwaters were consistently higher than in either fresh Everglades surface water, or in surface water from the Gulf of Mexico.

The TP concentrations of the limestone core collected from 0 to 10 m depth averaged 54 µg/g of rock (±17 µg/g of rock). Between 10 m and 20 m deep, the concentration of P increased from 200 to 850 µg/g of rock. There was no significant difference in the P concentrations of the limestone core collected from a region of fresh groundwater versus seawater intrusion.

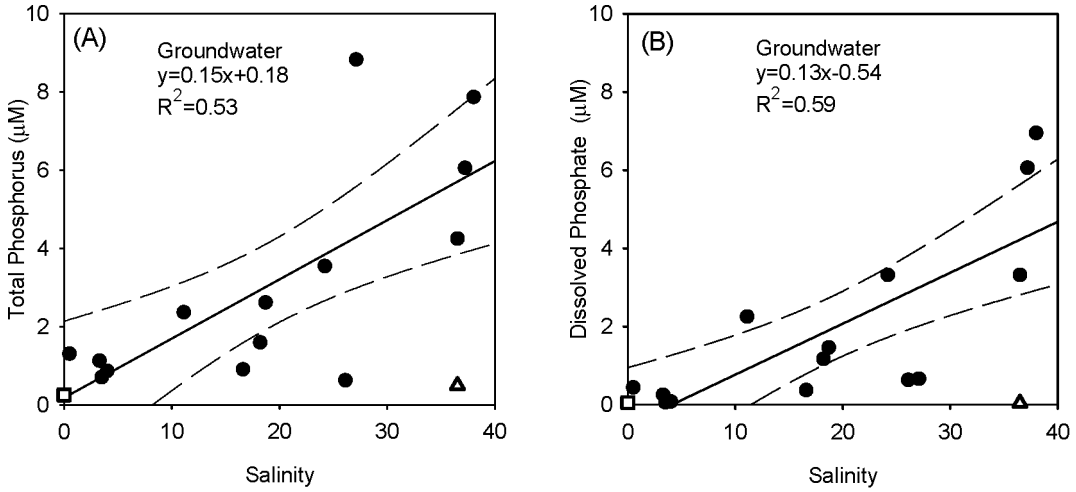

Figure 2. (A) total phosphorus and (B) dissolved phosphate with salinity of groundwater (●),surface water of the Everglades (□), and Gulf of Mexico (Δ). The linear regression through the groundwater data is the solid black line with a 95% confidence interval.

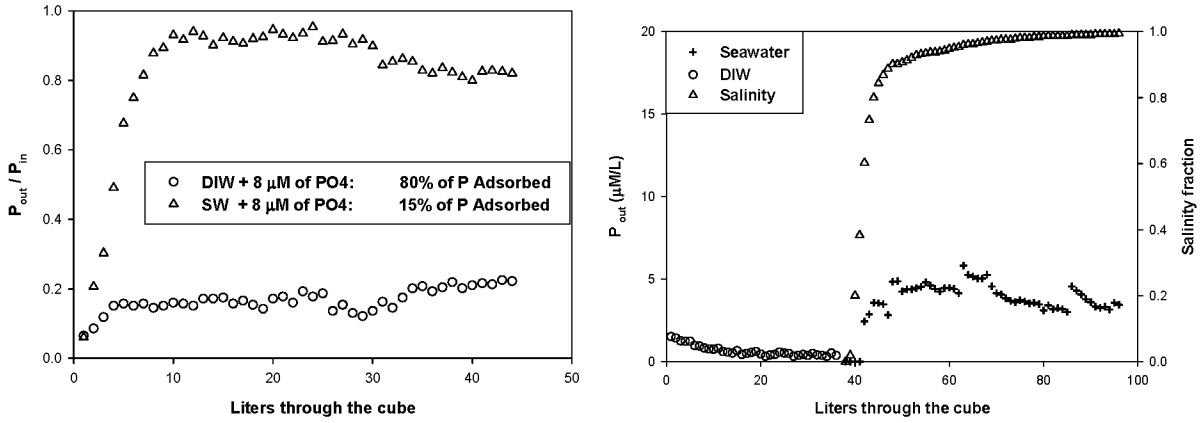

Figure 3. Results of (A) adsorption experiments and (B) desorption of phosphorus from Key Largo limestone in both DIW and seawater.

The adsorption experiments on the Key Largo limestone resulted in more than 80% of the initial phosphate retained on the limestone when the phosphate was dissolved in DIW. Conversely, only 15% of the phosphate was adsorbed in the seawater matrix (Figure 3A). In the desorption experiments, significantly higher concentrations of P were removed from the limestone with seawater than with DIW (Figure 3B). Calcium, magnesium and bicarbonate were found to be in excess in the DIW and in the seawater matrix when salinities were less than 90% seawater. The PHREEQC results predicted undersaturation with respect to both calcite and aragonite in these waters, supporting the geochemical results that these minerals are dissolving in the lower salinity groundwaters, thereby releasing any P either adsorbed or incorporated into the aquifer matrix. At salinities representative of 90% seawater and higher, the PHREEQC results predicted oversaturation with respect to calcite and aragonite. Geochemical analysis of the water at these higher salinities resulted in calcium and magnesium being described by conservative mixing of seawater with DIW, but bicarbonate concentrations were lower than expected for conservative

mixing. These results suggest that at the higher salinities the carbonate minerals are not being dissolved, but instead bicarbonate ions are adsorbed to the aquifer matrix.

SUMMARY AND CONCLUSIONS

Elevated concentrations of P are observed in groundwaters of southwest Florida affected by seawater intrusion. An increase in P with salinity suggests that reactions related to seawater intrusion are responsible for the P in the groundwater. However, conservative mixing of fresh Everglades waters with Gulf of Mexico seawater cannot produce the P, therefore an additional source of P is needed. Water-rock interactions such as carbonate mineral dissolution and adsorption-desorption are most responsible for the P in the brackish groundwaters. Digestion of limestone from the region indicates the present of available P. Adsorption experiments reveal that the limestone has a high affinity to adsorb P dissolved in fresh groundwater. As the groundwater salinity increases in the presence of seawater intrusion, dissolution of calcite and aragonite minerals in the limestone result in a release of P to the brackish groundwater. At higher salinities equivalent to 90% seawater and higher, bicarbonate ions adsorption forces P to desorb from the limestone to the surrounding groundwater.

REFERENCES

Back, W., Hanshaw, B.B., Herman, J.S. and Van Driel, J.N., 1986. Differential dissolution of a Pleistocene reef in the ground-water mixing zone of coastal Yucatan, Mexico. Geology, 14:137-140.

Chambers, R.M. and Pederson, K.A., 2006. Variation in soil phosphorus, sulfur, and iron pools among south Florida wetlands. Hydrobiologia, 569: 63-70.

DeKanel, J. and Morse, J.W., 1978. The chemistry of orthophosphateuptake from seawater on to calcite and aragonite. Geochim. et Cosmo. Acta, 42: 1335-1340.

Jensen, H.S., McGlathery, K.J., Marino, R. and Howarth, R.W., 1998. Forms and availability of sediment phosphorus in carbonate sand of Bermuda seagrass beds. Lim. and Ocean. 43: 799-810.

Millero, F., Huang, F., Zhu, X., Liu, X. and Zhang, J.-Z., 2001. Adsorption and Desorption of Phosphate on Calcite and Aragonite in Seawater. Aquatic Geochemistry, 7: 33-56.

Moore, W.S., 1999. The subterranean estuary: a reaction zone of ground water and sea water. Marine Chemistry, 65: 111-125.

Price, R.M., Swart, P.K. and Fourqurean, J.W., 2006. Terrestrial Brackish Groundwater Discharge - a significant source of phosphorus for the oligotrophic wetlands of the Everglades. Hydrobiologia, 569:

Sivan, O., Yechieli, Y., Herut, B. and Lazar, B., 2005. Geochemical evolution and timescale of seawater intrusion into the coastal aquifer of Isreal. Geochim. et Cosmo. Acta, 69(3): 579-592.

Zhou, M. and Li, Y., 2001. Phosphorus-Sorption characteristics of calcareous soils and limestone from the southern Everglades and Adjacent Farmlands. Soil Sci. Soc. of American Journal, 65: 1404-1412.

Contact Information: René M. Price, Florida International University, Dept. of Earth Sciences and the Southeast Environmental Research Center, 11200 SW 8th St., PC-344, Miami, FL 33199, 32611 USA,
Phone: 305-348-3119, 305-348-2877, Email: pricer@fiu.edu

Study of Saltwater Intrusion into the Coastal Aquifer of Tavabe-e Arsanjan, Iran

Mehrdad Bastani[1], ***G. Reza Rakhshandehroo***[2] and *Majid Kholghi*[3]
[1]Master's Student, Civil Engineering Department, Shiraz University, Shiraz, Iran
[2]Associate Professor, Civil Eng. Department, Shiraz University, Shiraz, Iran (Currently a visiting scholar at CE Dept, Michigan State University, East Lansing, MI, USA)
[3]Water & Soil Engineering Department, University of Tehran, Tehran, Iran

ABSTRACT
Tavabe-e Arsanjan is an agricultural plain located in southern Iran, northwest of Tashk Salt Lake, where the only source for irrigation water is groundwater. Tashk Lake is one of the most salty lakes in Iran with Electrical Conductivities (EC) of up to 61420 μmhos/cm. Increasing demand for freshwater and overexploitation of the aquifer has caused a drawdown in groundwater levels followed by a seawater intrusion into the coastal aquifer. A total of 22 observation and sampling wells existed in the area with periodic measurements which were used to study the situation of saltwater intrusion into Tavabe-e Arsanjan aquifer over time. Results show that saltwater intrusion into the aquifer may occur from two main directions; south and southeast of the region originating from Tashk salt lake, and from the northern adjacent aquifer.

INTRODUCTION
Seawater intrusion is a natural process that occurs in most coastal aquifers, but when it causes groundwater salinization, it becomes a concern. There exists no comprehensive review of the extent of saltwater intrusion cases around the world. Well documented cases, however, include for example the Hawaiian, Californian, Floridian, Atlantic and Gulf coastal plains in the United States (Konikow and Reilly 1999). The purpose of this paper is to study the past and recent conditions of salinization in Tavabe-e Arsanjan coastal aquifer in Iran.

SITE DESCRIPTION
Tavabe-e Arsanjan is situated near the Tashk Salt Lake in northeast of Fars province, southern Iran (Fig. 1). The study area is located between 29° 39' and 29° 48' north latitude and 53° 08' and 53° 24' east longitude. Despite the mountains surrounding the region, it has an almost flat topography with an approximate surface area of 248 km^2. The superficial study area elevation, ranges from 1562 *m* in the southern corner of the region along the shore of the Tashk Lake to 2270 *m* in the northern corner on the Siyah Mountain; the average elevation being ~1580 *m*. This region is one of the oldest agricultural areas in the world, where farmers extensively use groundwater for irrigation (Nadji 1997). With due attention to the quality of water resources and fertility potential of soil, the major crops in Tavabe-e Arsanjan are wheat, barley, alfalfa and corn. Except the salty land near Tashk Lake, these crops are grown in the whole of the plain.

Climate and surface hydrology
There is not any rain gauge or climatologic station in the study area. The closest rain gauge station in the region is located in Arsanjan, ~30 km outside Tavabe-e Arsanjan to the north. According to ~15 years of measured data at this station, the average annual rainfall and temperature are about 333.6 mm and 17°c, respectively. Monthly rainfalls fluctuations show that precipitation is increased in the area during winter months and decreased sharply in spring months. Total annual rainfall demonstrates a sharp increase in years 2004 and 2005. Considering these values, Tavabe-e Arsanjan is identified as a region with typical semi-arid climate. The plain is adjacent to a lake, has a small aerial extent with an almost flat topography, relatively

high infiltration rate, and not much precipitation to start with. Therefore, there are no rivers in Tavabe-e Arsanjan and the only source of freshwater supply is groundwater. The highly saline lake (Tashk Salt Lake) with EC of up to 61420 μmhos/cm and chloride concentration of up to 44756 mg/l situated in the southeast of the study area makes the groundwater susceptible to salinization.

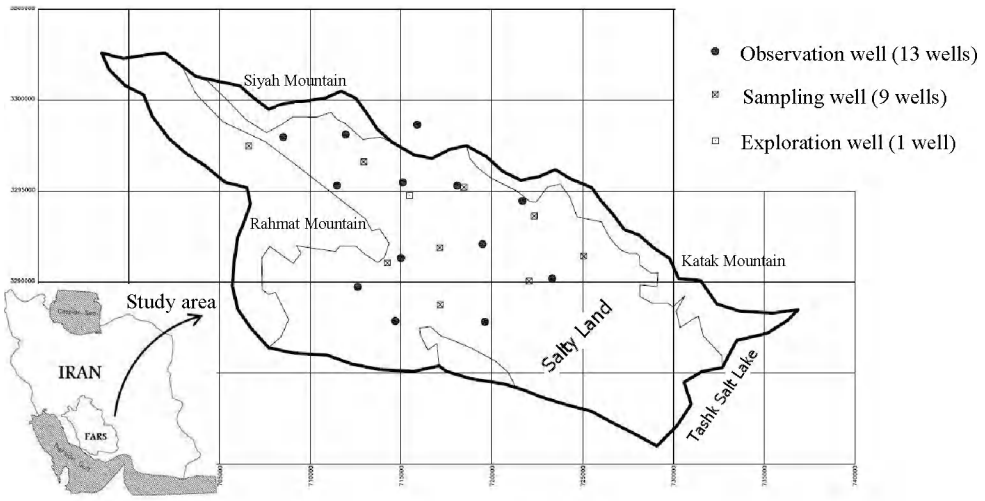

Figure 1: Location of the study area and the wells inside the plain

Geology

Tavabe-e Arsanjan consists of an unconfined aquifer which is filled with Quaternary sediments in its main plain. Thickness of the sediments varies from 30 to 50 *m* in the northwest, and gradually increases toward the southeast. A maximum thickness of ~400 *m* can be found near the lake. The alluvial deposits consist of rubble stone, gravel, sand (near the margins of the mountains) with low amount of clay and silt added close to the lake. Mountains formation in the northwest is composed of dense limestone of the middle-upper Cretaceous formation. However, the extent that the limestone is in hydraulic contact with alluvial deposits is not well known (Jooyab Consulting Engineers, 1976).

Hydrogeology

The main source of groundwater recharge in Tavabe-e Arsanjan aquifer is the natural infiltration of precipitation on the basin. 15 existing Qanats in the study area have all dried up over the past 10~15 years, due to the dropping water table (Rasoulzadeh 2007). Fars Regional Water Authority has installed 13 observation wells in the study area, where monthly water table elevation measurements are obtained (Fig. 1). In addition, a single exploration well was drilled to a depth of 115 *m* by Fars Regional Water Authority in 1974 to perform pump tests and determine hydraulic properties of the aquifer. According to results of the pump test, the average hydraulic conductivity, storativity, and transmissivity of the aquifer are 3.28 m/d, 3.42%, and 446.6 m^2/d, respectively (Acting Organization for Groundwater Management, 1999). In general, water table elevation and slope followed those of topography, with the regional groundwater flow from northwest of the plain to south and southeast. Average water table drawdown in Tavabe-e Arsanjan aquifer during the 13-year period of 1994 to 2007 was 8.6 m; ~0.66 m per year.

Hydrochemistry

EC measurements were conducted twice a year on sampling wells in the region (data not shown for brevity). Well depths are less than 80 *m* and EC measurements were performed at the upper levels of the wells. Recent EC data indicate that freshwater still exists in the northwestern parts of the aquifer while south and southeast of the area are intruded by saltwater. It basically reflects the fact that in the northwestern highlands, natural fresh groundwater has received no contamination from Tashk Lake. According to the Piper diagram analysis, groundwater of the study area, with the exception of northwest part, is Chloride/Sodium type (Rasoulzadeh, 2007).

RESULTS AND DISCUSSIONS

Water table elevation contours in the study area were drawn based on the monthly measurements in the observation wells. Figure 2 shows such contours for two different dates; Oct. 1994, and Aug. 2007. Regional groundwater flow from northwest to southeast is obvious at both dates. However, an overall drop in water table elevation (up to 12 m) at the later date, and a local cone of depression at the central parts of the aquifer (with its low elevation limb stretching towards the salty lake) is worrisome. The cone of depression would locally draw groundwater from southeast of the region (near Tashk lake) inward; a situation which could lead to salt water intrusion. It is postulated that the installment of (too) many discharge wells, with high rates of discharge, at the central parts of the aquifer has resulted in this worrisome condition.

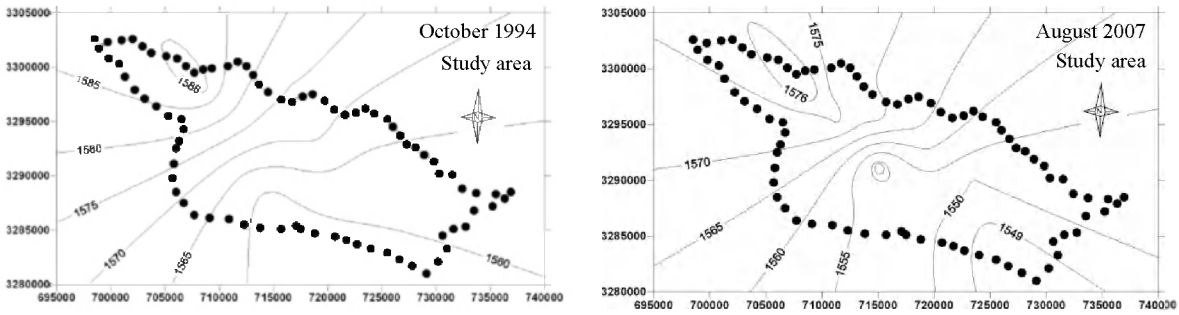

Figure 2. Water table elevation contours in the study area for two different dates (Axes are the U.T.M.: X- and Y-coordinates)

According to farmers in Tavabe-e Arsanjan, groundwater had little significance during 70's. However, in late 80's pumping rates increased drastically following a boost in the number of deep and shallow wells, and this was the start of groundwater quality deterioration in the area. In fact, during early 90's the water table had declined considerably and intrusion of saltwater from Tashk Lake had started. Moreover, the adjacent aquifers were (and still are) contributing some salty groundwater into Tavabe-e Arsanjan aquifer. Those aquifers are in east and northeast vicinity of the study area and are in direct hydraulic contact with Tashk Lake. The extent of saltwater intrusion into Tavabe-e Arsanjan aquifer is shown as contour maps of groundwater EC in Figure 3. Boundary of the study area is marked by white dots on the figure. As shown, during the 1994 there has been a seawater intrusion (fingering) into the aquifer mainly from the northern vicinity. This intrusion shifted to the east in the following years leading to 2000, leaving behind isolated pockets of less salty water in the central parts of the aquifer with ECs lower than 5000 μmhos/cm. Contour maps for 2006 reflects saltwater intrusion solely from Tashk Lake's saltwater on the east of the aquifer whilst pockets of EC concentrations in the center are smoothed out. It was concluded that saltwater intrusion in the aquifer may occur from two main directions; south and southeast of the region originating from Tashk salt lake, and from the northern adjacent aquifer.

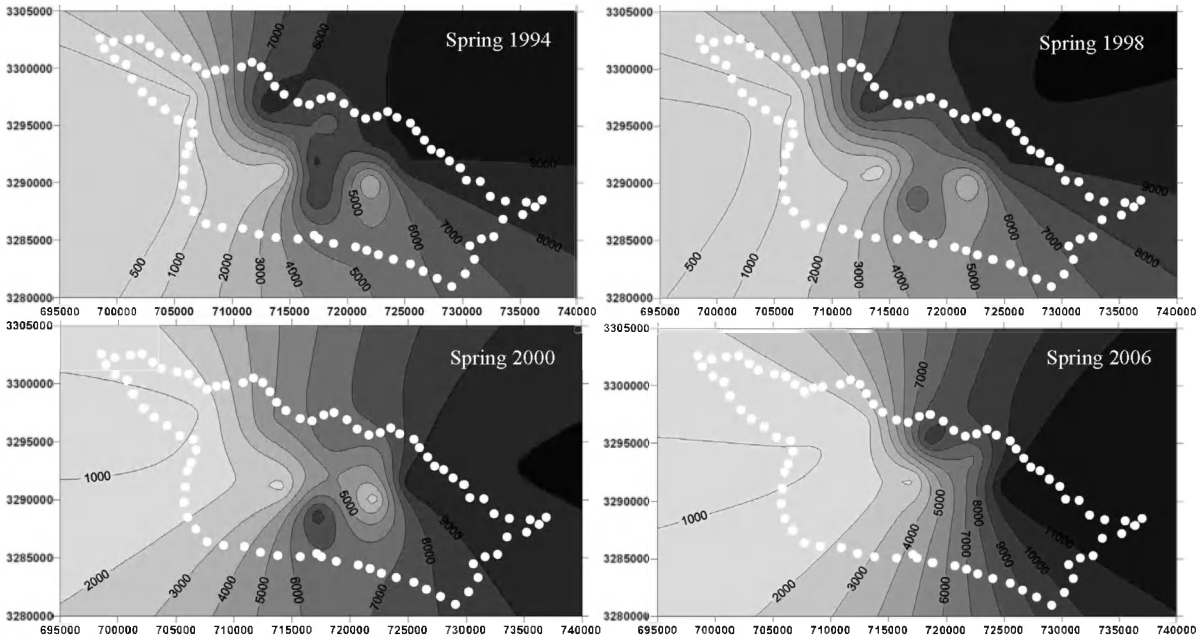

Figure 3. Contour map of EC concentration in groundwater of the study area (µmhos/cm) at different dates (Axes are the U.T.M.: X- and Y-coordinates)

REFERENCES

Acting Organization for Groundwater Management. 1999. Continued report of Tavabe-e-Arsanjan field study. Fars Regional Water Authority.

Jooyab Consulting Engineers. 1976. Arsanjan groundwater hydrology project. Fars Regional Water Authority.

Konikow, L.F., and Reilly, T.E. 1999. Seawater intrusion in the United States. In: Bear J, Cheng AHD, Sorek S, Ouazar D, Herrera I (eds) Seawater intrusion in coastal aquifers—concepts, methods and practices. Kluwer Academic Publishers, pp 463–506

Nadji, M. 1997. Rerouting Kor River from the Zagros region into the Persian Gulf a proposal solution to the problem of salinization in the Persepolis basin. Iran, Z. Angew. Geol., vol. 43: 171-178.

Rasoulzadeh, A., and Moosavi, S. A. A. 2007. Study of groundwater recharge in the vicinity of Tashk Lake area. Iranian J. Science & Technology, vol. 31, no. B5: 509-521.

Contact Information: G. Reza Rakhshandehroo, Shiraz University, Shiraz, Iran, Phone: 517-432-2689, Email: rakhshan@msu.edu

Management of Coastal Aquifers – The Case of a Peninsula – State of Qatar

Kamel M. Amer[1], *Abdul A. Aziz Al-Muraikhi*[1] and ***Nauman Rashid***[2]
[1]Dept. of Agricultural & Water Research, Ministry of Municipal Affairs & Agriculture, Doha, Qatar
[2]Schlumberger Water Services, Dubai, United Arab Emirates

ABSTRACT

The State of Qatar is a desert country characterized by its arid to hyper-arid climate. The setting is that of a peninsula, measuring an average of approximate ly 80 km across and 185 km long, covering an area of around 11493 km2. Much of the population resides in the urban, coastal setting of Doha city, with a number of farming areas scattered across the country, especially in the northern half. The tremendous fast paced development throughout the country is leading to increased population, improved standards of living and industrial growth. Obviously, this is putting immense pressure and demand on water sustainability.

The average annual rainfall for the period from 1972 to 2005 (figure 1) is 80.2 mm (Agro-hydro-meteorological Yearbook 2006). This has been the main source of recharge to the groundwater aquifers which are used mainly for agricultural applications. However, the rate of abstraction is becoming far greater than the rate of natural recharge, resulting in lowered aquifer water levels and sea water intrusion that has led to increases in groundwater salinity. Historical data has been collected and a number of steps put in place to address the issues of water quality and quantity in this coastal settings.

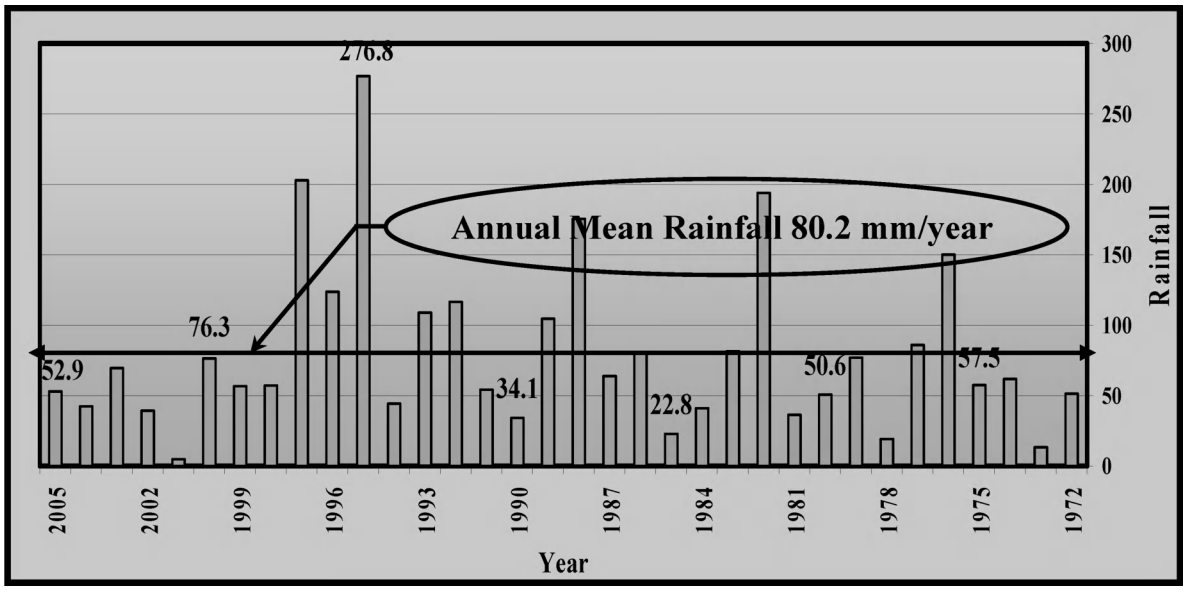

Figure 1. Annual Total Rainfall for the State of Qatar (1972 – 2005)

Steps taken in assessing and addressing saltwater intrusion have included groundwater monitoring, data management, aquifer characterization and modeling, artificial and enhanced recharge and other relevant remediation techniques. The plans and taken actions being carried out are expected to lead to a net positive groundwater balance.

INTRODUCTION

In the light of a sparse, often unreliable, winter rainfall, sustainable agricultural development remains the main goal of a groundwater resources management plan in the State of Qatar. Agriculture is the main user of the groundwater, and its unplanned extraction can lead to deterioration of its quality and quantity in this coastal environment.

Potable water supplies are met through a rapidly growing production of desalinated water, without putting any stress on the groundwater. In addition to that, an ambitious expansion and upgrading of existing wastewater treatment facilities is underway, providing a potential source of high quality, treated wastewater for irrigating fodder crops and landscape needs. In the urban setting of Doha city, the shallow water table is known to recharge through rainfall, (landscape) excess irrigation and leaking utilities. A rising water table, compounded with saltwater intrusion and storm water management in this area of high rise commercial and residential buildings, is making it necessary to provide an effective control system.

BACKGROUND

In the last couple of decades, groundwater in the State of Qatar has shown severe decline in actual water levels, seawater intrusion, upcoming and a rapid increase in water salinity. The depletion in groundwater resources is revealing itself in the abandonment of farms especially in coastal areas and in rapid soil degradation (Amer and Al-Mahmoud, 2003).

Qatar had realized early the need to put in place a program to address saltwater intrusion and support groundwater recharge through artificial and enhanced techniques. Some 341 recharge stations were identified, designed and established within over 850 identified depressions. These stations capture the flood events and other than having the primary objective of groundwater recharge, also helped mitigate runoff damage to surrounding agricultural land. Monitoring stations have assisted in evaluating the benefits of this significantly enhanced recharge scheme. This early success has led to plans through further enhancements to boost the annual recharge by a staggering 50%.

Although studies have shown the existence of relatively good quality groundwater in the central areas, saltwater intrusion has progressed indiscriminately over the years in the coastal areas (fig. 2). This progression is now threatening the long term sustainability of the groundwater aquifers in the country.

METHODS

As a result of the rapid expansion of farming areas in the northern part of Qatar, the fresh and slightly brackish groundwater resources are being over-exploited at an accelerating rate. This is leading to a fast rate of depletion of the aquifers, accompanied by a deterioration of water quality. The evaluation of the natural and artificial groundwater recharge in the country is becoming an essential requirement of any future groundwater development. A number of investigations and studies are in various stages of planning and implementation to improve the long term groundwater sustainability and address the issues of saltwater intrusion in the country. Departmental coordination is being practiced to facilitate the interaction of all stakeholders towards a common goal.

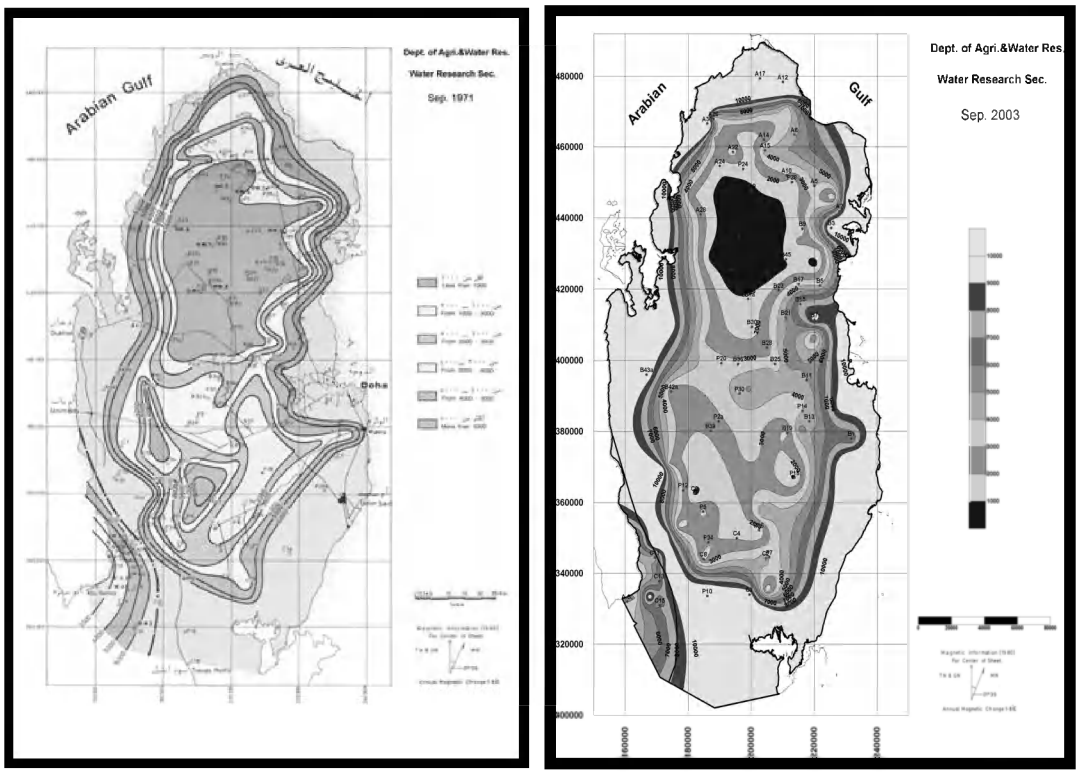

Figure 2. Comparison of the freshwater lens (TDS < 1000 ppm) for the years 1971 & 2003

The backbone of the field studies of groundwater program in the country is the wells survey and abstraction and recharge study. It calls for the determination of absolute water levels, water quality measurements, abstraction rates, recharge wells efficiency, water use, topography related surface flows, etc. It will lead to the creation of a master data repository that will be hosted on an online Geographic Information System (GIS) database. An example of such a system is illustrated in fig. 3. Data that is compiled as part of the projects and all related analysis, interpretation and visualization results will be made available for real time access through this application. This will greatly facilitate the analysis, implementation and evaluation of different techniques for saltwater intrusion control programs. The updating of the current groundwater monitoring system and its expansion will provide valuable insight into the state of the aquifers.

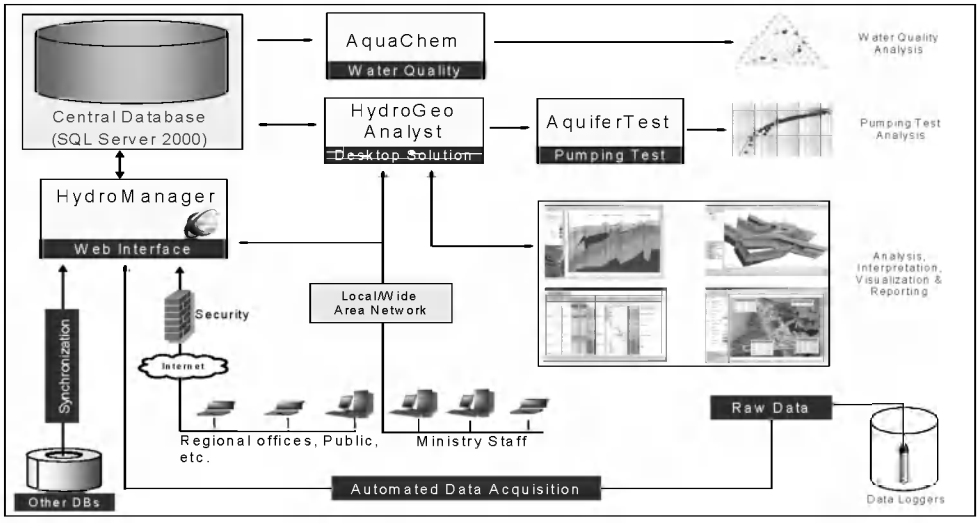

Figure 3. An Example of an Online GIS Data Management System

Capitalizing on the growing availability of alternate water sources such as desalinated water, artificial recharge has received much attention with a view to improve groundwater sustainability.

For the urban setting of Doha city, the evaluation of the groundwater conditions in the areas of interest and a selection of suitable groundwater monitoring sites to understand and address saltwater intrusion is required. On a few sites, the grouping together of shallow and deeper sites as monitoring nests will help improve the understanding of the vertical flows from the upper aquifer to any underlying aquifers and vice versa. Areas of potential groundwater issues within Doha city will be influenced if groundwater is moving through fractures to deeper units. Based on the preliminary work and the carrying out of land surveys, initial monitoring sites can be selected. Investigative drilling, geophysical logging and hydraulic pump testing can then be carried out at these sites. The advanced geophysical logging improves our understanding of the geology across the drilled wells. It provides vertical profile for the aquifer specific yield, hydraulic conductivity, water salinity, and the existence or absence of fractured layers.

DISCUSSION AND CONCLUSIONS

The country's saltwater intrusion control program lays the emphasis on predicting the impact of saltwater intrusion as a result of the severe over pumping of groundwater in the coastal regions of the country. In the urban coastal areas, it calls for the design and optimization of the pumping well locations for dewatering projects aimed at mitigating the impact of saltwater intrusion on the foundations of high rise buildings. Recommendations and actions will include the evaluation of the pertinent and effective groundwater remediation systems in this arid setting and an assessment of remaining risks. Learning from the past practices and recent and ongoing work, harnessing the full potential of available water sources through the means of artificial and enhanced recharge is starting to present a very promising future for groundwater sustainability and saltwater intrusion control in the State of Qatar. Through the past, ongoing and future studies, techniques and methods in hydrogeology and data management are expected to be combined in order to establish a comprehensive groundwater information system as a powerful planning tool for remediation techniques in order to ensure sustainable groundwater use.

REFERENCES

Amer, K. M. and Al-Mahmoud, A. M. (2003), "Water Resources Management and Development to Combat Water Scarcity in Qatar", Proceedings of Water Middle East, International Exhibition and Conference for Water Technology, Manama, Kingdom of Bahrain, 6-8 October, pp. 13-26

Agro-hydro-meteorological Yearbook 2006. Agro-hydro-meteorological sub-section, the Department of Agriculture and Water Research, Doha, State of Qatar.

Contact Information: Nauman Rashid, Schlumberger Water Services, PO Box 9261, Dubai, UNITED ARAB EMIRATES, Phone: +971-4-3067777, Fax: +971-4-3293196, Email: rashid@dubai.oilfield.slb.com

Utilizing Stable Isotopes (^{2}H, ^{18}O) to Better Identify Different Water Types of the Floridan Aquifer System in Southwest Florida

Edward Rectenwald[1] and *Michael Bennett*[2]
[1]MWH Americas, Cape Coral, Florida
[2]Boyle Engineering, Palm City, Florida

ABSTRACT
Stable isotopes (^{2}H, ^{18}O) were used to complement inorganic data to define different water masses within the Floridan aquifer system (FAS). In southwestern Florida, the FAS is separated into three hydrostratigraphic units, the upper Floridan aquifer, middle-confining unit, and the lower Floridan aquifer. This paper better defines the hydrogeologic framework, using stable isotopes to identify different groundwaters contained within the FAS and identifies recharge sources and interaction between the two aquifers.

INTRODUCTION
The stable isotope, and inorganic (major cation and anion) data were obtained from eight multi-zone FAS test wells owned by the South Florida Water Management District (SFWMD) and eight multi-zone FAS monitor wells operated by various Utilities for a total of 42 samples. The location of these FAS wells are shown on Figure 1. Samples were collected at various depth intervals within the FAS. They were collected during packer tests within the open borehole or from completed multi-zone monitor wells.

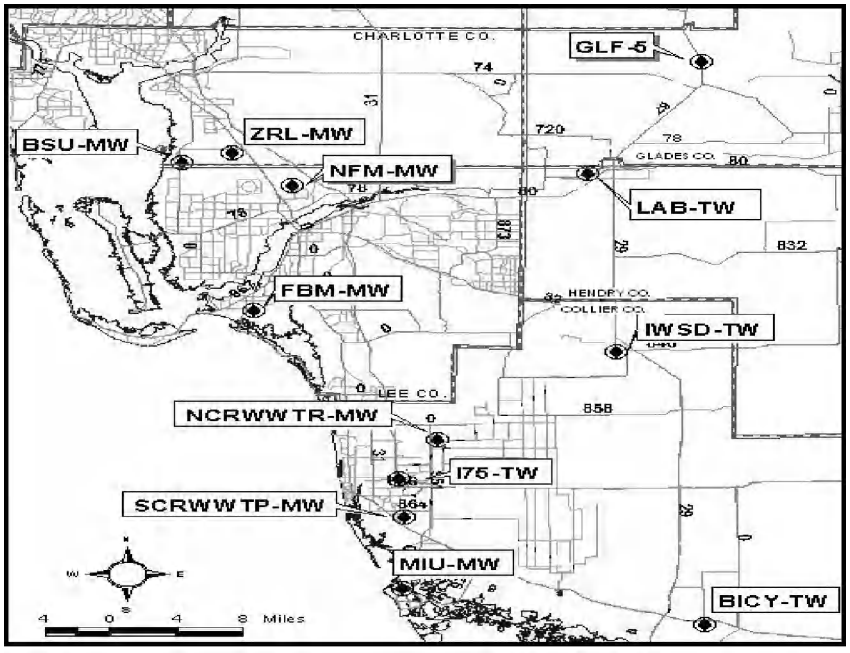

Figure 1. Site Map with Well Locations

HYDROGEOLOGY
Three major aquifer systems underlie Southwest Florida: the Surficial Aquifer System (SAS), the Intermediate Aquifer System (IAS), and the Floridan Aquifer System (FAS). These aquifer systems are composed of multiple, discrete aquifers separated by low permeability "confining" units that occur throughout this Tertiary/Quaternary age sequence. The aquifers occurring in the

FAS are the focus of this study. Figure 2 shows a generalized hydrologic cross-section from northwest to southeast across south Florida.

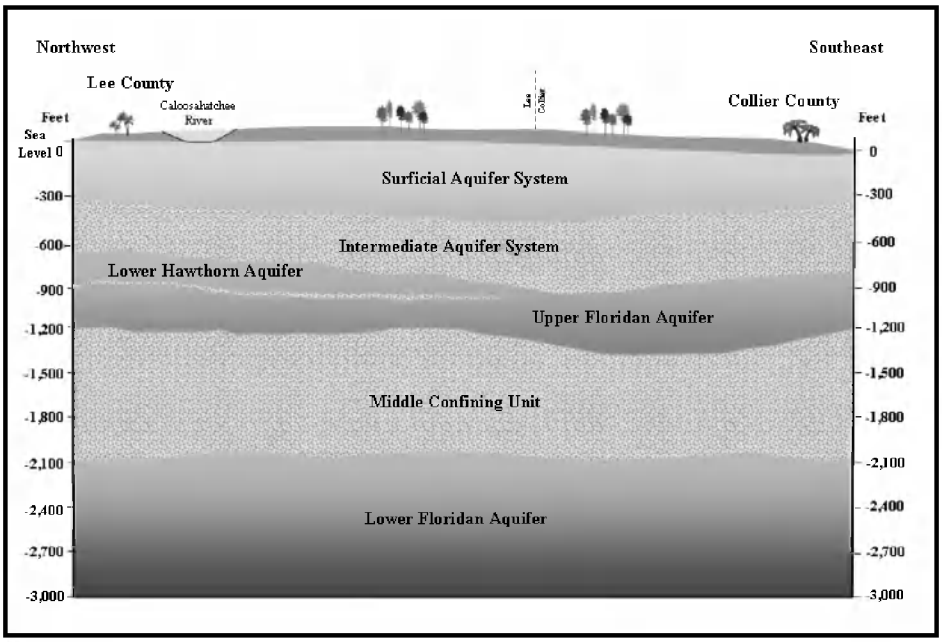

Figure 2. Generalized Hydrologic Cross-section of Southwest Florida

The FAS in the study area is separated into three hydrostratigraphic units, Upper Floridan aquifer (UFA), middle confining unit (MCU), and Lower Floridan aquifer (LFA). These units are composed predominately of limestone with dolomitic limestone and dolomite. The UFA chiefly consists of permeable zones in the lower Hawthorn Group and Suwannee Limestone (Reese, 1998). The middle-confining unit consists of low permeable dolomitic zones in the Ocala Limestone and upper part of the Avon Park Formation (Reese, 1998 and Bennett, 2001). The LFA consists of permeable dolostones in the lower part of the Avon Park Formation, Oldsmar Formation, and the upper part of the Cedar Keys Formation (Meyer, 1989 and Bennett, 2001).

INORGANIC CHEMISTRY AND STABLE ISOTOPES

More than 90% of the dissolved constituents in groundwater can be attributed to eight ions: sodium (NA^{+}), calcium (Ca^{2+}), potassium (K^{+}), magnesium (Mg^{2+}), sulfate (SO_4^{2-}), chlorine (CL^{-}), bicarbonate (HCO_3^{-}), and carbonate (CO_3^{2-}) (Fetter, 2001). The differences in inorganic composition of the ground water can be classified into hydrochemical facies which are a function of the lithology, solution kinetics, and flow patterns of the aquifer system (Fetter, 2001). Inorganic and stable isotopic data were used to identify different water masses and the dominant recharge source of the groundwater within the hydrologic units of the FAS.

Deuterium (^{2}H) and oxygen-18 (^{18}O) are two stable isotopes commonly used in hydrologic studies to complement and better define groundwater systems. These stable isotopes do not undergo radioactive decay, but because of the difference in mass between the more common isotopes of their respective elements, protium (^{1}H) and oxygen-16 (^{16}O), they react differently with other atoms and molecules as they move through the hydrologic system (Swancar and Hutchinson, 1992). The higher mass of ^{2}H and ^{18}O causes them to bond more tightly in molecules (including water), thus requiring more energy to break the bonds when these molecules participate in chemical reactions. Consequently, these two isotopes become enriched during the chemical reactions (Swancar and

Hutchinson, 1992). These data can therefore be particularly useful because they provide additional criteria linking water chemistry with mineral mass transfer, which can ultimately be used to better understand the geochemical processes and ground water interactions within the FAS.

RESULTS

The results from the inorganic analyses indicate that Na^+ and CL^- are the dominant ions and along with total dissolved solids (TDS) concentrations increase with depth. The inorganic data tend to group together near the right apex when plotted on a Piper Trilinear Diagram which suggests that seawater is the dominant recharge source for the FAS in costal portion of southwestern Florida using the method developed by Frazee (1985).

Scatter plots of ^2H and ^{18}O (Figure 3) indicate two different types of water within the FAS; this is consistent with findings from previous studies (Meyer, 1989; Swancar and Hutchinson, 1992, Bennett m, 2001). The ^2H and ^{18}O values from LFA waters plot close to 0.0 per mil concentration, which is similar to the standard mean ocean water standard of present day ocean water. The isotopically heavier waters within the LFA suggest inland migration of ocean water. The UFA values are isotopically lighter than ocean water (more negative valves). These values parallel the Global Meteoric Water Line (GMWL), which suggest the source of the water in the UFA is precipitation from recharge areas north of the study area. The stable isotope composition of the MCU is distributed more or less evenly among isotopically light and heavy values that fall along the GMWL. This suggests potential interactions between the upper and lower Floridan aquifers, within the middle-confining unit via the presence of vertical fractures, cracks or fissures.

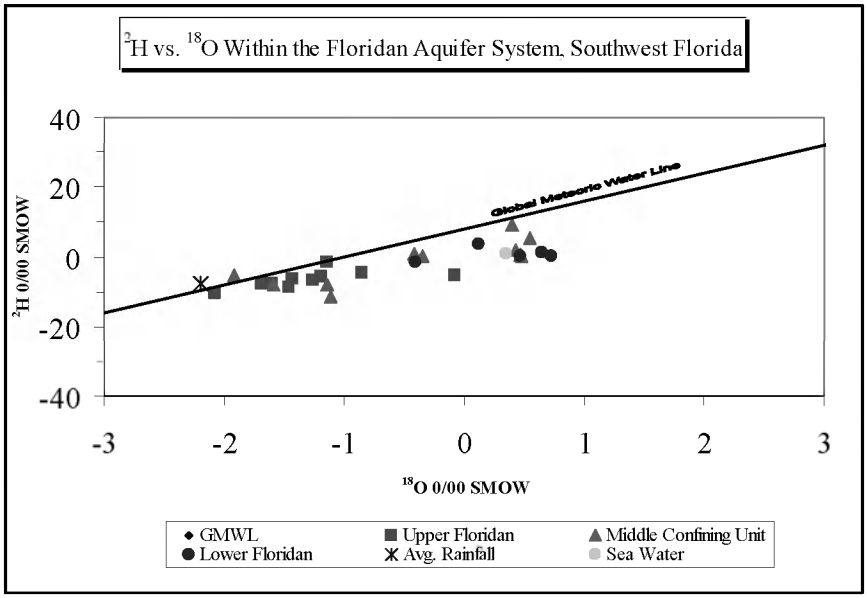

Figure 3. Floridan Aquifer System ^2H vs ^{18}O stable isotope compositions plotted with the GMWL.

CONCLUSIONS

Inorganic constituents and stable isotopes were used to identify different water masses in the FAS. The inorganic data identified sodium and chloride as the dominant ions and that the concentration of these ions including TDS increased with depth. The ^2H and ^{18}O plots suggests two distinct water masses within the FAS and suggest groundwater interaction in some parts of this region between the upper and lower Floridan aquifers. In time, we may have an even better

understanding of the complexity and interaction of the hydrologic unit of the FAS in southwest Florida as research continues by state and local agencies.

REFERENCES

Bennett, M. W., 2001, Hydrogeologic Investigation of the Floridan Aquifer System: I75 Canal Site, Collier County, Florida, Technical Publication WS-7, 48p.

Fetter, C. W., 2001, Applied Hydrogeology, Fourth Edition, Upper Saddle River, New Jersey, 598p.

Frazee, J. M., 1982, Geochemical Pattern Analysis: Method of Describing the Southeastern Limestone Regional Aquifer System, Studies of the Hydrogeology of the southeastern United States, Georgia Southwestern College, Special Publications: No. 1, p. 46-58.

Meyer, F. W., 1989, Hydrogeology, Ground-Water Movement, and Subsurface Storage in the Floridan Aquifer System in Southern Florida, U.S. Geological Survey, Professional Paper 1403-G, p. G3-G10, G19-G33.

Reese, R. S., 1998, Hydrogeology and the Distribution and Origin of Salinity in the Floridan Aquifer System, Southwestern Florida, Water Resource Investigations Report 99-4253, 86p.

Swancar, A., and Hutchinson, C. B., 1992, Chemical and Isotopic Composition and Potential for Contamination of Water in the Upper Floridan Aquifer, West-Central Florida, 1986-89, US Geological Survey, Open-File Report 92-47, p. 19-20.

Contact Information: Ed Rectenwald, MWH Americas, 2503 Del Prado Blvd., Suite 430, Cape Coral, Florida 33904 USA, Phone: 239.242.1323, Fax: 239.573.6007, Email: edward.rectenwald@mwhglobal.com

Calibration of a Density-Dependent Groundwater Flow Model of the Lower West Coast Floridan Aquifer System

Jorge I. Restrepo[1], *David Garces*[1], *Angela Montoya*[2] and *Laura Kuebler*[2]
[1]Department of Geosciences, Florida Atlantic University, Boca Raton, FL, USA
[2]South Florida Water Management District, West Palm Beach, FL. USA

ABSTRACT
A three dimensional density dependent groundwater model was developed as a predictive and interpretive tool for the Lower West Coast Floridan aquifer system using a modified version of SEAWAT-2000 (Langevin et al. 2003). This paper describes an automated calibration procedure for this model, the Lower West Coast Floridan Aquifer System Model (LWCFAS), using pilot points, regularization and the prior information option from PEST (Doherty 2004). A stepwise approach, starting with the least known parameter, was used to optimize three decision variables: vertical hydraulic conductivity of the confining units, storage and horizontal hydraulic conductivity of the aquifers. This approach allows for manageable computer run times while allowing the decision variables to improve in each step. A finer resolution model that meets calibration targets is achieved after calibrating a coarser model with PEST.

INTRODUCTION
The ever-increasing population of south Florida has put a strain on water supplies, which are mostly taken from the surficial and intermediate aquifer systems. Alternative water sources are being sought to curb the pressures exerted on present water supplies and to guarantee the long term survival of the Everglades. The South Florida Water Management District (SFWMD) initiated the development of the Lower West Coast Floridan Aquifer System (LWCFAS) Model in cooperation with Florida Atlantic University to investigate possible alternative water sources. The active zone is defined, when possible, as larger than the Lower West Coast (LWC) Planning Area, such that a buffer zone is created around the study area. Vertically, the model includes the three major aquifer systems that underlie southern Florida: the surficial aquifer system (SAS), the intermediate aquifer system (IAS), and the Floridan aquifer system (FAS); however, the model focuses on the IAS and FAS. The hydrostratigraphy follows that laid out by Reese and Richardson (2004). The only hydrologic stress is groundwater extraction and/orinjection.

This paper describes an automated calibration procedure that uses a series of steps, resulting in three versions of the LWCSFAS Model. The quasi-steady-state model was initiated to generate initial conditions and boundary conditions for the transient models. Two transient models were developed; the first model was created for semi-automatic calibration with a coarser resolution, and the second model was created with a finer resolution for predictions. These models are herein referred to as: Q3K-CP, T12K-UNCP and T3K-UNCP and correspond to a quasi-steady-state coupled model with a 3,000 ft by 3,000 ft resolution, a transient uncoupled model with a 12,000 ft by 12,000 ft resolution and a transient uncoupled model with a 3,000 ft by 3,000 ft resolution. The T3K-UNCP Model is the final product of the calibration approach.

MODEL DESIGN
A modified version of SEAWAT-2000 was selected for the LWCFAS Model. This version includes the UGEN (Restrepo et al., 2001) and HBXY (Restrepo et al., 2006) packages to handle data efficiently and interpolate boundary conditions. A combination of no-flow, constant head and general-head boundaries were used in this particular model. The western boundary coincides with the Gulf of Mexico. In the top and bottom model layers, constant head boundaries are

specified for all cells. In Layers 2 through 11, constant head boundaries are specified for the southern-most and western-most active cells in coastal regions along the Gulf and Florida Bay. The eastern (following a groundwater divide) and northern model boundaries contain general head boundaries for Layers 2 and 3 and no-flow boundaries for Layers 4 to 11.

CALIBRATION METHOD

PEST, a nonlinear, least-square, inverse modeling program developed by Doherty (2004) was used to auto-calibrate the LWCFAS Model, along with some manual calibration. This approach uses pilot points (PPs) and regularization parameterization scheme with SVD-Assist.

Q3K-CP Version of Model

The purpose of the Q3K-CP Model was to generate initial conditions and refine boundary conditions for the transient models. When the coupled model was initially executed, unreasonable values of concentration and hydraulic conductivities were needed to maintain the head in the model domain and keep the model stable. The Gulf boundary was refined during several manual, trial-and-error calibration runs until the surface around the boundary was smooth (e.g., avoiding significant gradients). The depiction of the Gulf boundary is hypothetical due to the unknown nature of the western boundary conditions; however, the Gulf boundary is located 60,000 feet off-shore, away from the main study area.

Predetermined ranges for initial input values were set by a combination of site-specific data or literature-cited values (Freeze and Cherry 1979). For this modeling effort, transient potentiometric heads were selected as calibration targets. Targets included daily and random samples from monitoring wells with time series consisting of frequent observations (i.e., 14,788 total weekly observations in 65 wells from Layers 2 through 10) over a maximum of five years.

T12K-UNCP Version of Model

For the LWCFAS Model transient calibration, in order to have reasonable running times, the original quasi-steady-state 3,000 feet by 3,000 feet model was aggregated into a coarser model with a resolution of 12,000 feet by 12,000 feet; this model was run uncoupled and has 12 layers, 72 rows, 37 columns and 260 weekly stress periods. In the decision process for the calibration, computer time for a simulation was also taken into consideration.

For the transient, uncoupled calibration, a stepwise calibration approach was used. The first step estimated the decision variables at PPs at a coarser resolution. The algorithm based upon sequential optimization steps increased the number of PPs to produce spatial disaggregation of the domain. This procedure was followed since a large model is being calibrated and PEST is a very calculation intensive program. In this approach, the same type of objective function was used. Transient calibration was undertaken to determine sequentially: vertical hydraulic conductivity in the confining layers (K_z), then the specific storage (S_s) of aquifer systems, and finally the horizontal hydraulic conductivity (K_x).

Step 1. Initial conditions created by the Q3K-CP Model were used to start the transient calibration. PPs were located every 8 cells for a total of 27 per layer. The total number of PPs in a model simulation depends on the decision variables. The range of values for horizontal hydraulic conductivity was purposefully constrained, since it was the best available data. The optimal solution for the three decision variables was found using PEST. Several rounds of Step 1 were carried out until the solution did not change substantially and arrived to a minimum.

Step 2. The second step used the estimated parameters from Step 1 and increased the number of PPs to every 7 cells for a total of 36 per layer. The parameter space for K_x was kept very tight as described in Step 1. The optimal solution for the three decision variables was found again. One round of Step 2 was carried out. The objective function improved only for S_s and K_z.

Step 3. An additional round of runs was made to allow for refinement of the lower-layer parameters starting with the solution from Step 2. The PPs are located every 6 cells for a total of 49 PPs per layer. The objective function improved only for K_z.

In Layer 1, the original K_z was used with an upper limit defined as one order of magnitude of the starting value and three orders of magnitude for a lower limit. The limits for the other confining layers were set from 1.0E-9 to 2.E+1 and the initial values were based on the few published leakance values available. Values for S_s were derived from literature (Freeze and Cherry 1979) and ranged from 5.0E-06 feet-1 to 1.0E-4 feet-1. The upper and lower bounds of the horizontal conductivity were set to 35 percent above and below the initial data. The final results for K_x are relatively close to the field-measured data. In the current optimization procedure, two weights for the observations were used in all steps. For Layers 1 to 4, weights are equal to 1. For Layers 5 to 11, weights are equal to 8. These criteria put more weight to the focus area – Layers 5 to 12.

T3K-UNCP Version of Model

After the T12K-UNCP Model is calibrated through PEST, the T3K-CP Model was generated based on the estimated parameters from the T12K-UNCP Model. The purpose of the T3K-CP Model is to produce predictions using a finer grid resolution; this model did not undergo further calibration, but rather relies on the calibration from the coarser model.

CALIBRATION RESULTS

Calibration targets, for groups of observations per aquifer, within the model domain, are displayed in Figure 1 (for T12K-UNCP and T3K-UNCP Models).

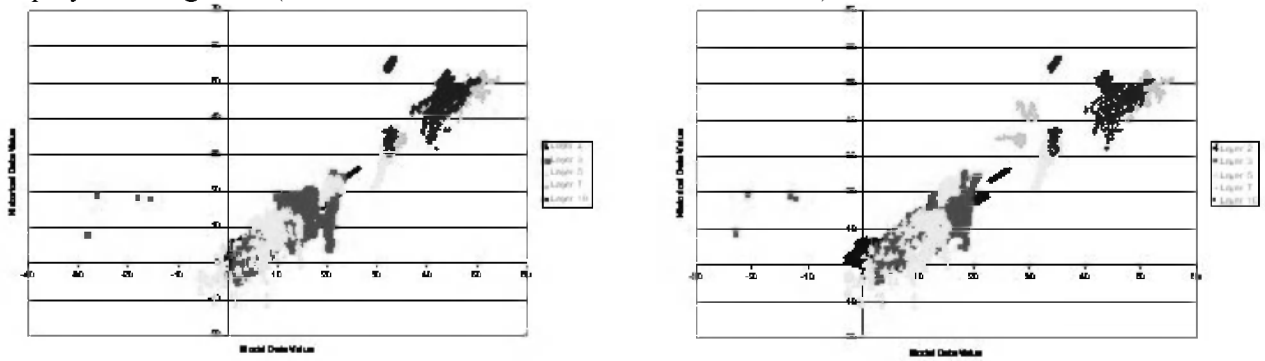

Figure 1.Calibration scatter plots for the T12K-UNCP and T3K-UNCP Models.

Table 1 provides the standard error and correlation coefficient (r-value) for each layer. The results indicate that there is a good linear relationship between the observed and simulated data for all layers for both models.

Table 1. Standard error and correlation coefficient for T12K-UNCP and T3K-UNCP Models.

Model Layer	Standard Error (ft)		Correlation Coefficient	
	T12K-UNCP	T3K-UNCP	T12K-UNCP	T3K-UNCP
3	4.12	3.99	0.75	0.76
5	3.50	4.97	0.95	0.91
7	1.68	5.34	0.97	0.91
10	6.99	7.40	0.40	0.32

CONCLUSIONS

This approach was applied to a regional model in a confined system. Model statistics indicate that the model does an acceptable job of matching the historical data. The combination of reasonable parameter distributions and a good fit between modeled values and field observations indicates that the model can be useful for evaluating regional groundwater issues where the concentration is not expected to change significantly over long periods of time. K_z is the most sensitive hydraulic parameter in the LWCFAS Model, followed by S_s and K_x. This is of utmost importance since the model has shown extensive spatial variability in the vertical conductance values. This approach allows for manageable computer run times while allowing the decision variables to improve in each step. A finer resolution model that meets calibration targets is achieved after calibrating a coarser model with PEST.

REFERENCES

Doherty, J., 2004, PEST Model-Independent Parameter Estimation, Watermark Numerical Computing, Australia.

Langevin, C.D., W.B. Shoemaker, and W. Guo. 2003. SEAWAT-2000, the United States Geological Survey Modular Ground-Water Model–Documentation of the SEAWAT-2000 Version with the Variable-Density Flow Process and the Integrated MT3DMS Transport Process. United States Geological Survey, Open File Report 03-426, 43p.

Reese, R.S. and E. Richardson. 2004. Preliminary Hydrogeologic Framework ASR Regional Study (Draft Version). United States Geological Survey, Tallahassee, FL.

Restrepo, J.I., A.M. Montoya, and D. Garces. 2001. The Utility Generation Package (UGEN) for the Groundwater Flow Model, MODFLOW. Submitted to the Conference MODFLOW 2001. Golden, CO.

Restrepo, J.I., A.M. Montoya, and D. Garces. 2006. HBXY for Interpolating Boundary Conditions. Boca Raton, FL.

Contact Information: Jorge I. Restrepo, Florida Atlantic University, Geoscience Department, 777 Glades Road, Boca Raton, FL 33431 USA, Phone: 561-297-2795, Fax: 561-297-2745, Email: restrepo@fau.edu

Time Scale of Water-Rock Interaction Processes in the Fresh-Saline Water Interface of Coastal Aquifers

Amos Russak[1,2], *Orit Sivan*[1], *Yoseph Yechieli*[2] and *Boaz Lazar*[3]
[1]Department of Geological and Environmental Sciences, Ben Gurion University, Beer Sheva, Israel
[2]Geological Survey of Israel, Jerusalem, Israel
[3]Institute of Earth Sciences, Hebrew University, Jerusalem, Israel

ABSTRACT
The goal of this work is to estimate the time scale of water-rock interaction processes in the fresh-saline water interface (FSI) in a coastal aquifer. For this purpose we conducted high resolution groundwater sampling of the FSI of the coastal aquifer of Israel. Seasonal and diurnal variations of the FSI were investigated in a research well located 70m (landwards) from the sea shore and perforated all along the length of the pipe.

Sampling of groundwater was conducted with a bailer in the FSI zone and below and above it as well. In addition, sampling with high vertical resolution (15 cm) was done with Multi Layer Sampler (MLS; Ronen et al., 1987). The groundwater was analyzed for major ions, alkalinity, dissolved inorganic carbon (DIC) and $\delta^{13}C$ of the DIC ($\delta^{13}C_{DIC}$).

The chemistry of the groundwater at the FSI zone indicates that the composition is not controlled only by simple mixing of freshwater with seawater but also by cation exchange. The calcium is up to 50% higher than in seawater (Figure 1**Figure 15**), while the potassium is significantly depleted. The mass balance shows that the cation exchange occurs in different magnitude during the year.

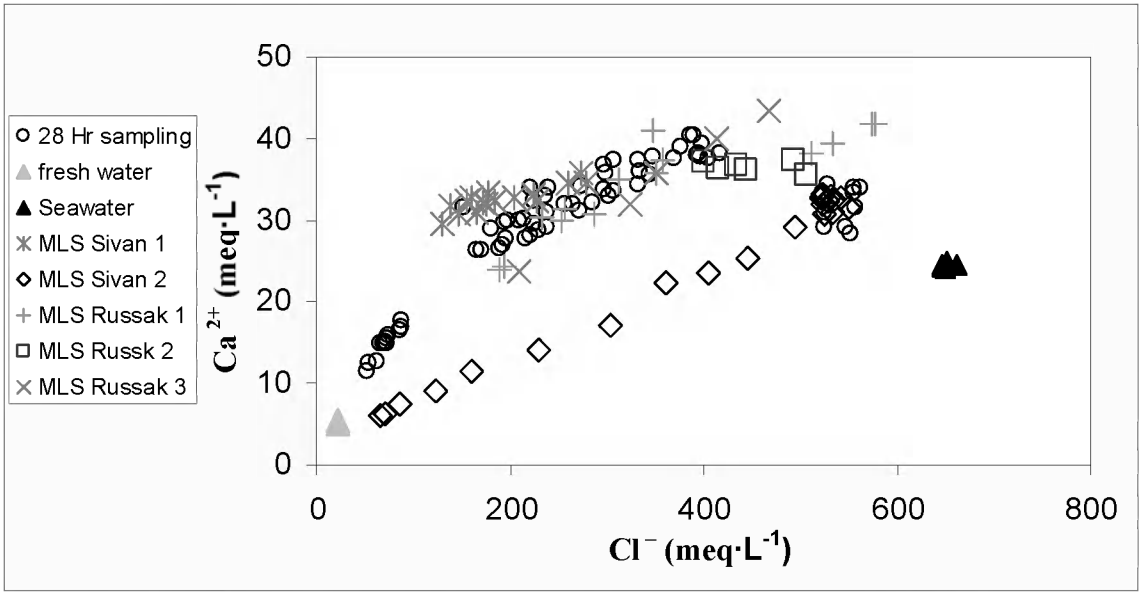

Figure 15. Calcium versus Chloride (field results)

The diurnal behavior of the FSI was examined by sampling water in six depths, every 2 hours for 28 hours. Water samples were taken above the FSI (depth of 20 m), below the FSI (depth of 27 m) and in four depths within the FSI. These depths were chosen following an electrical conductivity measurement by a submersible profiler. Thin pipes were fitted to the well, reaching each of the selected sampling depths, and the groundwater was sampled by a peristaltic pump.

The diurnal variations in the chemical composition were mainly tidal and, similarly to the case of seasonal behavior, did not follow a simple freshwater and seawater mixing behavior (Figure 1). The differences between low tide and high tide may imply that cation exchange processes are fast and occur already on a daily scale; however more measurements and calculations are needed to corroborate this conclusion. It should be mentioned that the diurnal changes could be, at least partly, caused by the well artifact and do not necessarily represent the actual aquifer.

Cation exchange estimates were conducted in the laboratory using experimental column filled with coastal aquifer sediments taken near the research well. The column was first saturated with freshwater from the research well; then seawater was pumped into the column by peristaltic pump and the water at the exit of the column was sampled regularly. The experiments show clear indication for cation exchange with the same trends as observed in the field but in larger magnitude. The conservative ions (e.g. Cl^-) showed a simple breakthrough curve between the two end members (freshwater and seawater). Calcium increased after salinization to a peak of much higher value than in seawater (45 and 52 meq·L^{-1} compare to 24 meq·L^{-1} in the Mediterranean Sea) and then decreased to seawater levels (Figure 2**Figure**). Potassium concentrations after salinization were lower than expected from simple mixing. Sodium show little depletion relatively to its concentration and magnesium seem conservative as chloride. It should be noted that the same cation exchange pattern was observed either in low or high flow velocities (200 and 1000 m·y^{-1}). Flow velocity of 1000 m·y^{-1} is ten times higher than was described in previous experiments (Appelo et al., 1990; Gomis-Yagües et al., 1997). The present research included also analysis of $\delta^{13}C_{DIC}$, and was not conducted in previous experiments. The $\delta^{13}C_{DIC}$ results indicate that slight oxidation of organic matter already occurs within the experimental column (Figure 2).

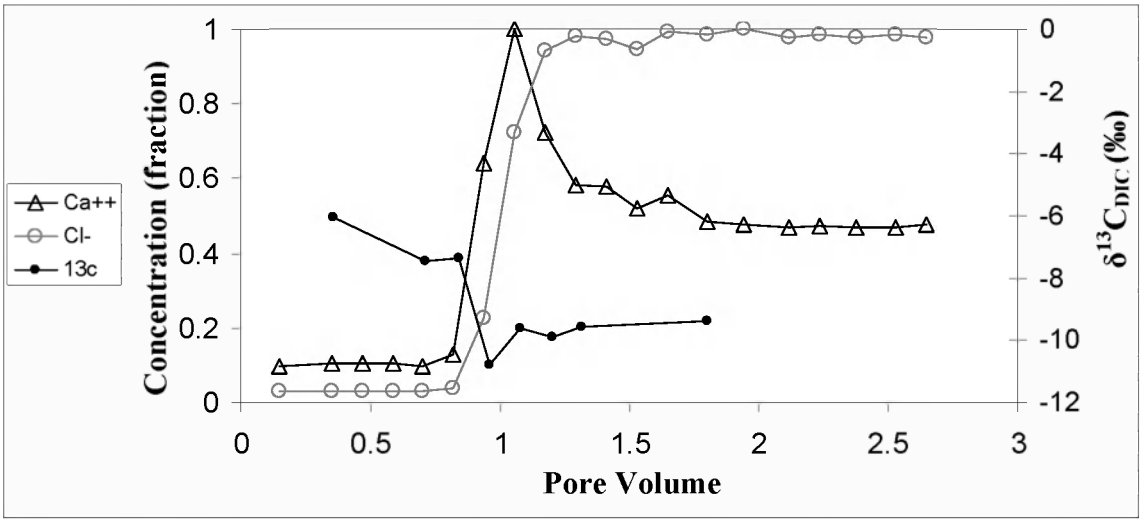

Figure 2. Seawater intrusion experiment results (200 m·y-1).

The diurnal field data was not conclusive for the role of tide in affecting the cation exchange processes within the aquifer. The cation exchange patterns observed in the well's vertical profiles however, were similar to those of the seawater intrusion column experiments. We conclude that cation exchange is an important process controlling the water chemistry of the FSI in the coastal aquifer of Israel on a seasonal time scale at least.

REFERENCES

Appelo, C. A. J., Willemsen, A., Beekmen, H. E. and Griffioen, J. (1990), Geochemical calculation and observation on saltwater intrusion II. Validation of geochemical model with laboratory experiment. *Journal of Hydrology* 120, 220-250.

Gomis-Yagües, V., Boluda-Botella, N. and Ruiz-Beviá, F. (1997), Column displacement experiments to validate hydrogeochemical models of seawater intrusions. *Journal of Contaminant Hydrology* 29, 81-91.

Ronen, D. Magaritz M., and Levy I. (1987), An in situ multilevel sampler for preventive monitoring and study of hydrochemical profiles in aquifers. *Ground water Monitoring Review* 7, 69-74.

Sivan, O., Yechieli, Y., Herut, B. and Lazar, B. (2005), Geochemical evolution and timescale of seawater intrusion to the coastal aquifer of Israel. *Geochimica et Cosmochimica Acta* 69(3), 579-592.

Contact Information: Amos Russak, Department of Geological and Environmental Sciences, Ben Gurion University, Beer Sheva 84105, Israel, Phone: +972-52-6968943, Fax: +972-8-6472997, Email: russak@bgu.ac.il

Modeling Brine Discharge into the Soil

Kais CHARFI[1] and ***M. J. Safi***[2]
[1]School Engineering of Tunis, B.P 37. 1002 Belvedere. TUNISIA
[2]School Engineering of Tunis, B.P 37. 1002 Belvedere. TUNISIA

ABSTRACT
To face the water shortage, many countries are recurring more and more to brackish water desalination. In the remote zones, R.O technique is usually used to desalt ground water at a salinity varying from 3 to 6 g/l. The desalt water is used to supply fresh water to the local population and to irrigate greenhouses, while the concentrated brine is released in the environment or injected into the ground without any "regulation". As a consequence the local agriculture will suffer and ground water quality will degrade. Therefore an efficient system is to find. As a first step towards the design of the system, a *numerical simulation* of brine discharge solutions are considered. The soil is simulated by *stratified porous layers* of different thickness and geological properties (porosity, permeability, etc…). The discharge is assumed to be at the surface in vertical direction (Fig.1). The transport phenomenon is described by *Navier-Stokes* and *concentration equations* including the *Darcy-Brinkman-Forcheimer* terms in the *streamline and vorticity* formulation (Ψ, Ω). The flow is considered two dimensional with an aspect ratio equal to 40. The set of coupling equations are solved using *Difference Finite Scheme* and A.D.I (*Alterning Direction Implicit*) technique. Numerical simulations were conducted for Reynolds number, Re = 5000, Sc = 770. The porosity and Darcy number values of the five porous layers are respectively (from top to bottom) equal to (ε_i; Da_i) = (0.8; 0.3210^{-7}), (0.7; 0.2810^{-7}), (0.6; 0.2410^{-7}), (0.5; 0.210^{-7}) and (0.4; 0.1610^{-7}) and (ε; Da) = (0.576; 0.230410^{-7}).

The results were presented in stream and iso-concentration lines. It was found that considering only one equivalent layer in steal of five ones allows good results.

INTRODUCTION
The mechanism of flow transport and concentration becomes strongly coupled and the prediction of its behavior can be obtained, often, only by numerical way. In this direction, Christophe Filder (2001) have been studied numerically the behaviour of a panache resulting from an injection located in a heterogeneous vertical porous medium made up of two superimposed layers of the same thickness and different permeabilities. This study shows that the propagation of the aqueous solution is characterized by the presence of two dissymetries convective cellular with a weak deformation of the panache in the direction of the initial ambient flow whatever the distribution of permeability and the type of injection. Our objective is to study flow and concentration transport through saturated soil including many stratified porous layers of different thickness and geological properties of various porosities and permeabilities by injection in concentration in top of the first porous layer and to assume that the bottom of the whole system is impermeable thus only vertical sides are permeable to the fluid.

PHYSICAL MODEL EQUATIONS
The system is represented by a stack of layers with different interface boundary layers. The flow in such a configuration is three dimensional and need parallel computers for real study.
As a first step, we make the following assumptions (which could in fact be realistic):
(1) The layers are homogenous but different each from the other (2) The soil is 20 times larger than the height (3) The bottom and the surface are non permeable (4) The brine at high

concentration is still considered as Newtonian fluid (5) Geological layers are represented by porous media that we assume isotropic. With these assumptions, the flow could be considered two dimensional and *Boussinesq approximation* is valid. Hence the transfer phenomenon is described by *Navier-Stokes* and concentration equations including the *Darcy-Brinkman-Forchheimer* formulation. To reduce the number of unknowns and overcome the resolution of the pressure equation, the streamline and vorticity formulation is used.
The consequent set of equations is:

$$\nabla^2 \Psi = \Omega \tag{1}$$

$$\frac{1}{\varepsilon}\frac{\partial \Omega}{\partial t} + \frac{1}{\varepsilon^2}\left(\frac{\partial u\Omega}{\partial x} + \frac{\partial v\Omega}{\partial y}\right) = \frac{\Omega}{\mathrm{Re}Da} + \frac{(1+2.5\varepsilon)\nabla^2\Omega}{\mathrm{Re}} + \frac{b}{Da^{1/2}}\left(\frac{\partial |u| v}{\partial x} - \frac{\partial |u| u}{\partial y}\right) - R_i \frac{\partial C}{\partial x} \tag{2}$$

Brinkman term; Darcy Term; Forchheimer term

$$\varepsilon \frac{\partial C}{\partial t} + \left(\frac{\partial uC}{\partial x} + \frac{\partial vC}{\partial y}\right) = \frac{\varepsilon \nabla^2 C}{\tau \,\mathrm{Re}\, Sc} \tag{3}$$

These equations have been non-dimensionnelized by defining:

$$(u,v) = \left(\frac{U^*}{V_0}, \frac{V^*}{V_0}\right), (x,y) = \left(\frac{X^*}{H}, \frac{Y^*}{H}\right), \quad C = \frac{C^* - C_2^*}{\Delta C_{ref}}, \quad t = \frac{t^*}{t_0}, \quad t_0 = \frac{H}{V_1^*} \text{ and } u = -\frac{\partial \Psi}{\partial y}, \quad v = \frac{\partial \Psi}{\partial x}, \quad \Omega = \frac{\partial v}{\partial x} - \frac{\partial u}{\partial y}$$

It results that the flow depends on the *dimensionless parameters*:

Reynolds number: $\mathrm{Re} = \frac{V_0 H}{\upsilon}$; Grashof number: $Gr = \frac{g\alpha \Delta C_{ref}^* H^3}{\upsilon^2}$;

Richardson number: $R_i = \frac{Gr}{\mathrm{Re}^2}$; Schmidt number: $Sc = \frac{\upsilon}{D}$;

Darcy number: $Da = \frac{K}{H^2}$; $Rv = \frac{\upsilon_e}{\upsilon}$.

Each porous layer is characterized by its porosity ε and tortuosity $\tau = 1$. b is the Forchheimer coefficient given by the following expression: $0.55\sqrt{Da}$ (Hwa-Chong 1999). The solving domain is reduced to a rectangular cavity as shown in Fig 1. The boundary conditions are defined in the following way: all the walls are considered rigid and impermeable except at entry and exit where flow is considered parallel.

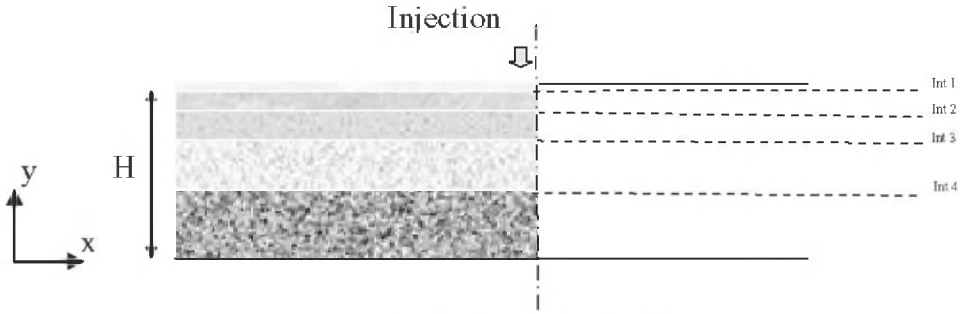

Fig.1 Physical Model

NUMERICAL METHOD

The set of coupling equations (1-3) are solved using a compact *Hermetian method* where the function and its first and second derivates are considered as unknowns. This method allows to reach a good accuracy: fourth order O (h^4) for Ψ and second order O (h^2) for, ω, T and C. The whole components of the system are represented by only one domain of resolution instead considering *multi-domain approach* but using *non regular discretization*. The A.D.I (*Alternate Direction Implicit*) technique is used to integrate the *parabolic equations* and is well described in the literature and has been widely used for *natural convection* and *recirculation zones* (M.J.SAFI 1994). This procedure has the advantage that the resulting *tridiagonal matrix* instead of a matrix with five occupied diagonals can easily be solved by *factorization algorithm*. The numerical study was carried out in a rectangular field with a grid of 1001x51 nodes. In order to achieve real time simulations to ensure *numerical stability* and good *convergence* and the set of equations was solved in *transient regime* using small time steps. The flow was simulated for 7 days, consequently time calculation using *Pentium 4 with 1 Go*, was very long. Two types of results are presented: quantitative information contour plots of concentration and steam function at different physical times.

RESULTS

Numerical simulations were investigated for a rectangular cavity with 5 m deep and 200 m large hence the aspect ratio is equal to 40. The five layers heights are respectively (from top to bottom): $h_1 = 0.6$ m, $h_2 = 0.8$ m, $h_3 = 1$ m, $h_4 = 1.2$ m, $h_5 = 1.4$ m. Due to the symmetry of the geometry only the mid-domain is considered so the injection brine is located at the top corner and the exit was set along the horizontal boundaries. A flow rate of brackish water equal to $1m^3/h$ and conversion rate of 40% was considered. The dimensionless parameters values are: Reynolds number Re = 5000, and Sc = 770.

Five Stratified layers

The characteristics of the five porous layers are respectively taken as follows (from top to bottom): Layer 1: 6 meshes, $\varepsilon_1 = 0.8$, $Da_1 = 0.3210^{-7}$, Layer 2: 8 meshes, $\varepsilon_2 = 0.7$, $Da_2 = 0.2810^{-7}$, Layer 3: 10 meshes, $\varepsilon_3 = 0.6$, $Da_3 = 0.2410^{-7}$, Layer 4: 12 meshes, $\varepsilon_3 = 0.5$, $Da_3 = 0.210^{-7}$, Layer 5: 16 meshes, $\varepsilon_3 = 0.4$, $Da_3 = 0.1610^{-7}$. The results of simulation (Fig.2) show that:

- At the beginning of calculation, a *vortex* appears at the entry. The *flow* seems to be *laminar* in the rest of the cavity. *Diffusion of the concentration* is also limited to the vicinity to the entry. At the first step, only the entry influences the flow.

- Later, only one cell occupies the whole medium, with a maximum at the exit. Consequently the concentration is realised in the whole cavity. *Iso-concentration lines* are vertical segments. This indicates that the *diffusion* is dominating with to respect the *convection*. During this second step, the flow is strongly influenced by the exit. In this study the *interfaces* have no influence on the containing of C.

Only one equivalent layer

Here, we consider only one layer whose thickness is the sum of 5 layers thicknesses and whose thermo-physical propertiesis defined as:

$$\Phi = \frac{1}{N}\sum_{l=1} \eta\Phi_l \qquad (4)$$

With η: number of nodes in layer *l*, *l*: A number of layers, N: Numbers of total nodes in the medium. Thus this equivalent layer will have as properties: $\varepsilon = 0.576$ and $Da = 0.230410^{-7}$. Figure 3, illustrates the results obtained with only one equivalent layer. The flow is characterized by a *recirculation zone* which evolves in the x direction. This is due to the fact the only exit region was fitted at the end of x direction (boundary condition). The comparison of the two results at the same time indicates: (a) At the beginning of the injection, the phenomena are similar but the equivalent layer presents a perceptible *dephasing time* in the *streamlines* and the *Iso-concentrations* which are still located near the injection. (b) After a sufficiently long time (7days) *the recirculation zones* are very comparable with a maximum close to the exit.

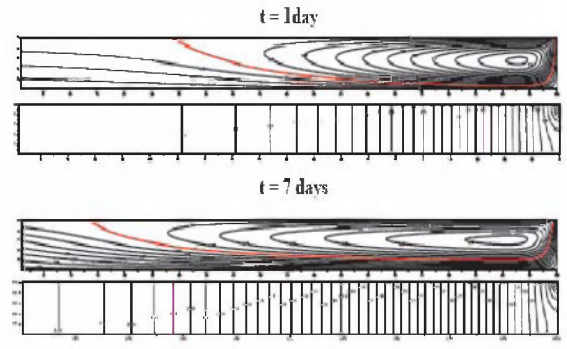

Fig.2 Temporal evolution of the Streamlines and the Iso-concentrations (Five stratified layers)

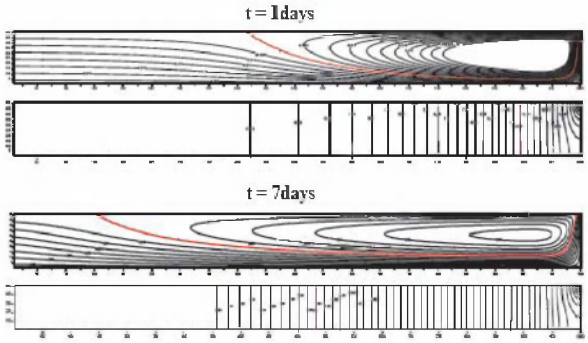

Fig. 3 Temporal evolution of the Streamlines and the Iso-concentrations (Only one equivalent layer)

The *numerical simulation* of the transport of concentration and momentum in five saturated porous layers has been investigated numerically with a new approach which consists of taking the whole components like only one field. This has the advantage to overcome the conditions at interfaces which are generally unknown. *The numerical simulation*, allowed us to calculate the temporal evolution of *concentration* and *streamlines fields*. In this study for Re up to 5000, the recirculation zone made only accelerate the *diffusion* without bringing the flow to be governed by *convection*. The simulation of five layers by only one equivalent layer proved to be acceptable from the *dynamic* point of view but an improvement of *thermal modelling* is desirable.

REFERENCES

Chritophe FELDER, Constantin Oltean. 2001. Michel Buès. Infiltration d'une solution saline dans un milieu poreux hétérogène en présence d'un gradient hydraulique, XV^{ème} Congrés Français de Mécanique.

Hwa-Chong Tien, Kwang- Sheng Chiang. 1999. Non Dary flow and heat transfer in a porous insulation with infiltration and natural convection, J. of Marine Science technology, v.2, 125-131.

M.J.SAFI and T.P. Loc. 1994. Development of thermal stratification in two-dimensional cavity: a numerical study, In.J. Heat Mass Transfer, v.14, 2017-2024.

Contact Information: M. J. Safi, School Engineering of Tunis, B.P 37. 1002 Belvedere. TUNISIA,
Phone: 21697661554 ; Fax: 216872729, Email: Mohamed.safi@enit.rnu.tn

The Delayed Effects of Variable Density Flow on Flow and Heads in Fresh Groundwater

Frans W. Schaars[1], *T.N Olsthoorn*[2,3] and *M. Bakker*[2,4]
[1]Artesia Water Research, Schoonhoven, The Netherlands
[2]Water Resources Section, Faculty of Civil Engineering and Geosciences, Delft University of Technology, Delft, The Netherlands
[3]Waternet, Vogelenzang, The Netherlands
[4]Kiwa WR, Nieuwegein, The Netherlands

ABSTRACT
Variable density flow may often be neglected in groundwater calculations, unless there is a special interest in the movement of brackish or salt water, for example when there is an environmental risk of salinization of wells or discharge areas. The presence of salt or brackish groundwater has a major impact on the flow and heads in the fresh part of the aquifer, and sometimes in a surprising fashion. We will show that extraction of brackish water below a discharge area may eventually result in an increase of total freshwater discharge. The underlying principles are demonstrated by conceptual models. Through the use of transient numerical calculations using MODFLOW-SWI (Bakker et al. 2005) we will show how the effects of short-term changes in the freshwater regime may be magnified or reduced by the long-term movement of an interface. Results for the island of Terschelling in The Netherlands are presented at the end of the paper.

CONCEPT
Suppose we have an aquifer with fresh groundwater, overlying stagnant salt or brackish groundwater. The interface is at rest and there is a steady state flowfield in the fresh groundwater zone. In this case the interface may be seen as an impermeable boundary, and the transmissivity is determined by the thickness and conductivity of the fresh groundwaterzone only. A change in the hydrology will cause the interface to move towards a new equilibrium position. While the interface is not at equilibrium, the heads and flows are dependent on the transmissivity of the entire aquifer.

In the new equilibrium position, the effective transmissivity has decreased again to the fresh groundwater zone only. This time-dependent transmissivity may lead to an unexpected transition between the two steady-state situations, as will be shown in the following two cases.

Case 1.
Figure 1 shows the developement of a phreatic freshwater zone in a cross-sectional model of an elongated island. The simulation starts with a completely salt aquifer. When the equilibrium is reached after 27 years the recharge is suddenly increased by 50 percent. As a result, the head jumps approximately 10 cm, as shown in Fig. 2. After this initial jump, the head rises an additional 5 cm. This secondary rise is caused by the slow movement of the interface towards a new equilibrium; the secondary effect may be responsible for a significant portion of the total increase in head.

Case 2.
Polders are areas where the water level is fixed by drains and ditches, and they are generally discharge areas of groundwater. In this case we have a crossection through an elongated polder with a drainage level that is one meter below the surrounding polders. In the equilibrium situation there is significant upconing in the center of the polder area (dashed line in figure 3).

Next, we will evaluate what happens when we pump salt groundwater, using a series of wells along the center line of the polder. We are especially interested in the evolution of the discharge. We know that the aquifer will freshen, and eventually the discharge to the polder will increase due to the increased fresh transmissivity. However, the salt water extraction initially results in a decrease of freshwater discharge into the polder. While the interface continues to move the freshwater discharge will increase to a level that is higher than the initial value (Fig. 3, lower right graph).

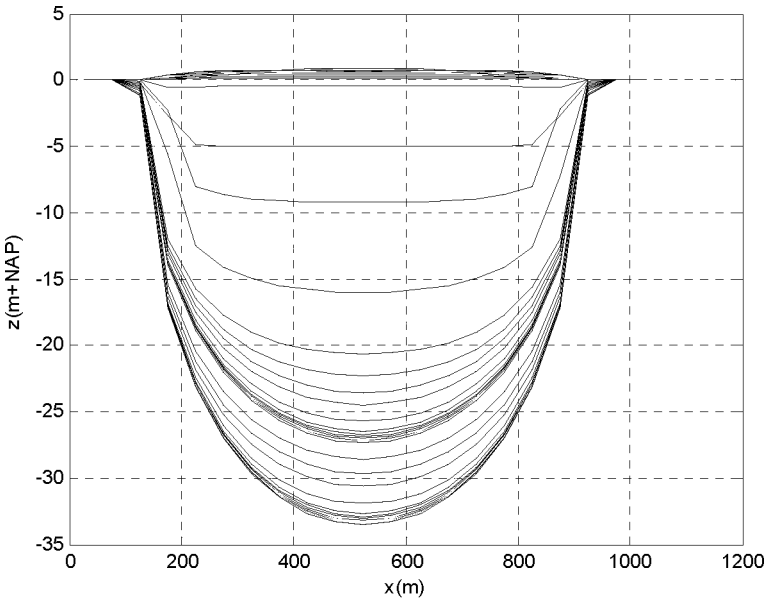

Figure 1. Phreatic groundwaterlevel and position of the interface.

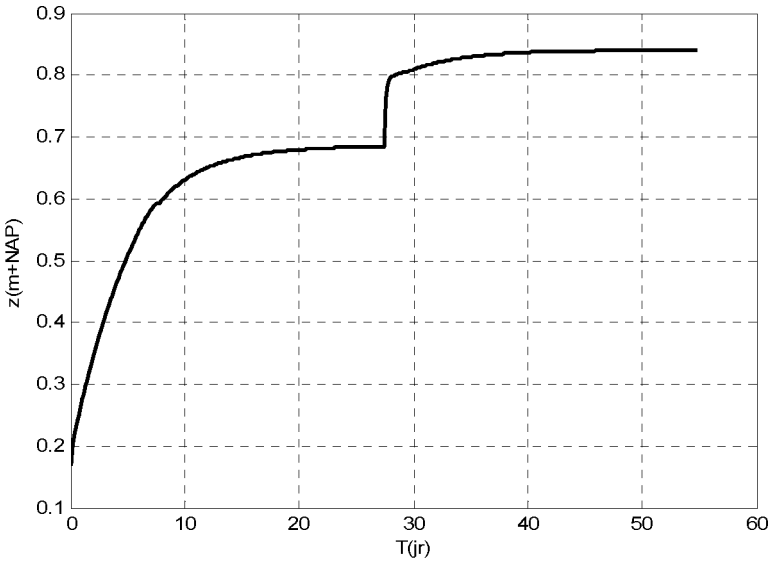

Figure 2. Development of the phreatic groundwaterlevel in the center of the cross-section.

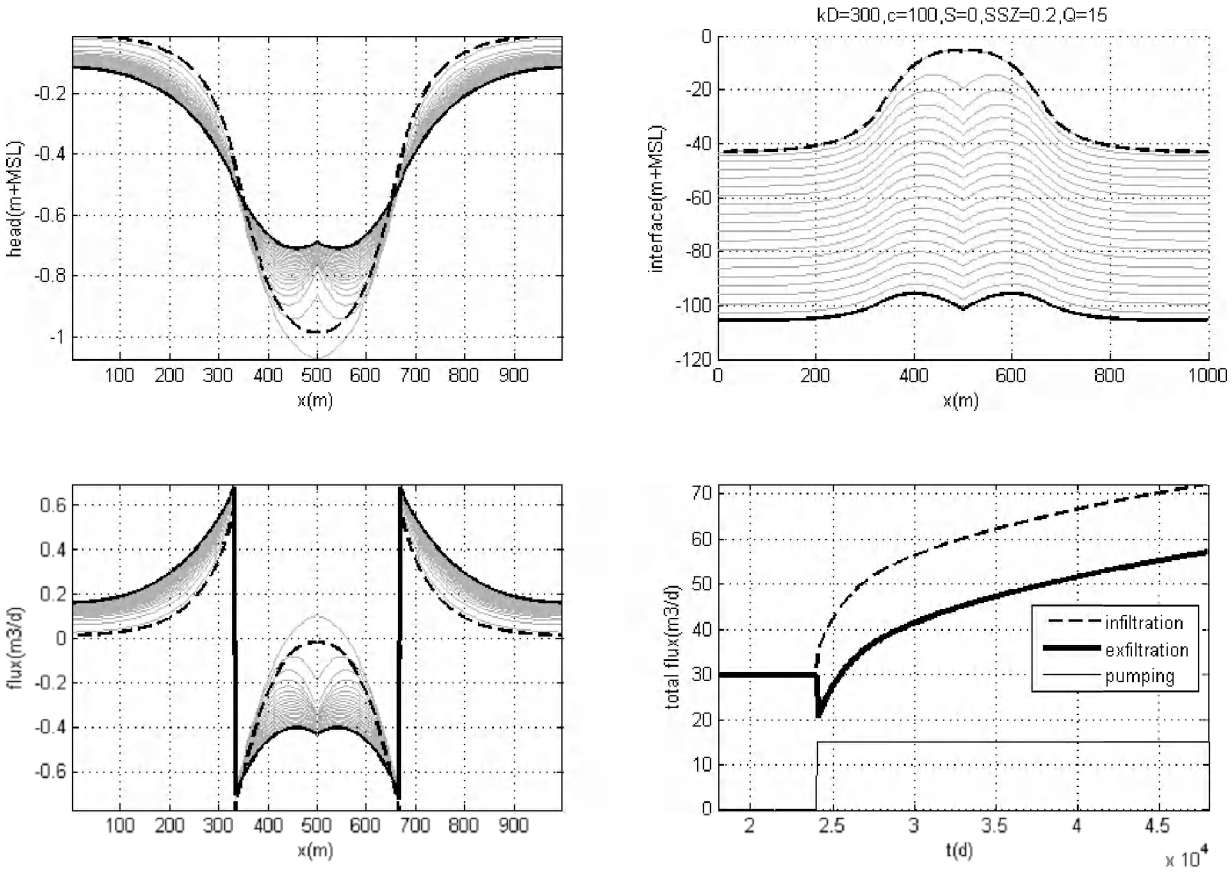

Figure 3. Effect of salt groundwater pumping under a discharge area. Cross-section for head (upper left), interface position (upper right), flux (lower left), and total flux vs. time (lower right).

CASE TERSCHELLING ISLAND

The island of Terschelling is situated in the northern part of The Netherlands. It is divided in a dune area in the North and an agricultural (polder) area in the South. In 2006 the Vitens water supply company started a pilot study to investigate if a self-supporting and sustainable water supply on the island is possible (Kok et al. 2008). One of the options is a salt groundwater extraction in the center of the polder area. In figure 4 the results are shown for three different extraction rates after twenty years. In the dunes the dashed contours represent the 5 centimeter drawdown area. As expected the drawdown area is larger for higher extraction rates. However, in the polder the extraction leads to an increase in head (5 cm head increase, solid contours) close to the pumping well. These increased heads are caused by the increased fresh transmissivity as a result of the lowering of the interface.

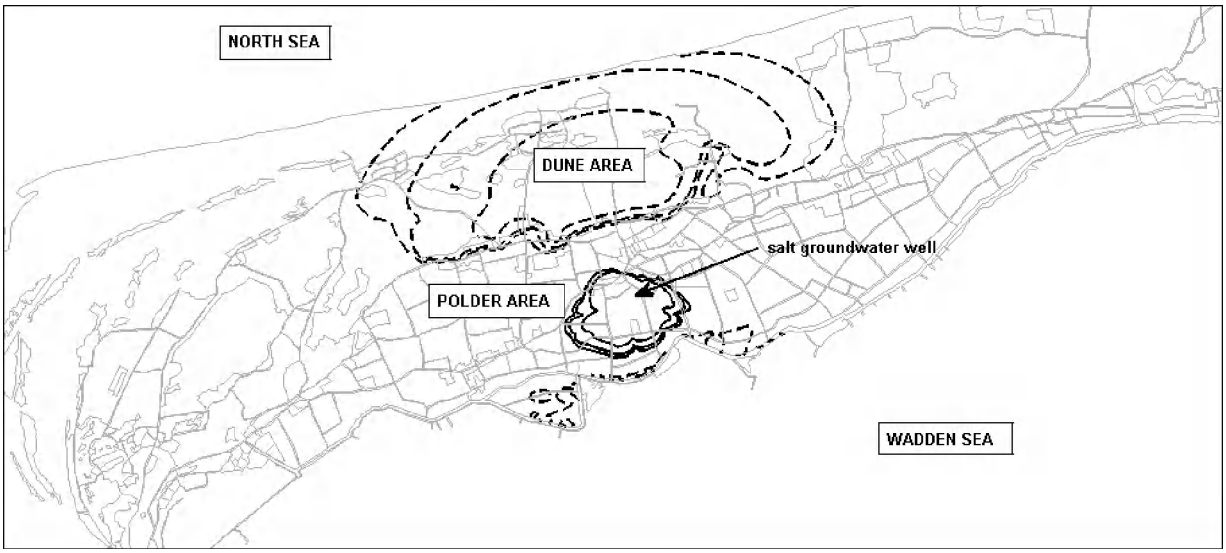

Figure 4. 5 cm contours for different extraction rates at the island of Terschelling.

CONCLUSIONS

The movement of brackish or salt water can have a considerable impact on the flow and heads in the fresh groundwater zone. The magnitude and direction of the effect is time-dependent. For predictions the transmissivity should be adapted to the considered timescale.

REFERENCES

Bakker, M., and F.W. Schaars. 2005. The Sea Water Intrusion (SWI) Package Manual Part I. User Manual and Examples. Version1.2., www.bakkerhydro.org

Kok, A., K.J. van der Made., and V. Post. 2008. The use of mapping the salinity distribution using geophysics on the island of Terschelling for groundwater model calibration., Proceedings of 20th SWIM.

Contact Information: F. Schaars, Artesia Water Research, Korte Weistraat 12, 2871 DG Schoonhoven, the Netherlands, Phone: +31 182387138, Fax: +31 182387140, Email: f.schaars@artesia-water.nl

Large-scale Geoelectrical Measurements to Investigate a Buried Valley and its Interaction to Deep Saltwater Intrusion

Andreas Junge[2], ***Joern Schuenemann***[1] and *Thomas Guenther*[1]
[1]Leibniz Institute for Applied Geosciences, Hannover, Germany
[2]Institute for Geosciences, University of Frankfurt, Germany

ABSTRACT
Resistivity measurements are important to investigate hydrogeophysical questions. But structures in depths of several hundred meters are difficult to explore. Hence, three-dimensional large-scale geoelectrical measurements were used to obtain additional information from a buried valley in the North Sea area in Germany. Resistances are determined as fraction of voltage and current. A combination of forward modeling and inversion is used to find an appropriate subsurface model. As result the valley is imaged very well and in greater depths the saltwater intrusions can be seen also.

INTRODUCTION
The actual aim of the study was a buried glacial valley from the Pleistocene, which is up to 400 m deep, 1-2 km wide and several km long. It is covered by a clay layer, the so-called Lauenburg Clay, which protects the valley from pollutions which may intrude from the surface. The second aim is the determination of the saltwater/freshwater interface. Many types of geophysical measurements such as seismics, airborne electromagnetics and gravimetry were already applied to that area, to investigate its structure and the generation process (BurVal Working Group, 2006 and Gabriel et al. 2003). So, the structural underground is well known from seismic and gravity measurements. But the electrical properties of the deeper regions of the valley mostly remain unknown, especially the regions below the clay, because the layer impedes the penetration of the electromagnetic field (EM) into the ground. And, because of the limited frequency range of the EM equipment information could only be obtained from depths up to 200 m. To investigate the deeper regions of the valley a three-dimensional large-scale direct current dipole-dipole experiment was done.

EXPERIMENT AND DATA EVALUATION
The area of investigation is located in Northern Germany, south of the city of Cuxhaven near the coast of the North Sea. An area of approx. 4x3 km was chosen and 20 receiver stations were installed. Every station consisted of four electrodes arranged in a star shape with a center electrode and the three remaining electrodes pointing at directions to North (0°), 120° and 240°. The dipole lengths were 75 m. A 3-channel GEOLORE transient recorder (Golden et al. 2004) registered voltages from the three dipoles with a frequency of 8 Hz. Similar arrays were used to inject currents up to 40 A supplied by a high current generator at 10 locations (figure 1). A total of 1800 independent data (20 receiver sites x 10 transmitters x 3 injections directions x 3 measuring directions) could be obtained.

The processing of the recorded time series included time corrections and re-sampling of the current signal due to different sampling frequencies. Various filters were applied for both voltage and current signal to remove anthropogenic and long-periodic telluric noise. Resistances are estimated as a correlation coefficient between current and voltage (Schünemann et al, 2007).

Figure 1. Measuring area. The borders of the valley are shown by north-south running lines. Current positions are marked by E1-E10, receiver sites are represented two-digit or as "F number".

RESULTS

For the inversion the DC3dInvRes code from Günther (2004) was used. To predict accurate voltages the continuity equation was solved with the finite difference method. Starting with a homogeneous model the inversion was done using smoothness constrains with decreased vertical weights. Errors obtained from the resistance determination are used for individual weighting of the data to account for the different quality of the resistances. A resulting model is presented in figure 2.

Eight different layers with increasing thicknesses are shown. The depth is denoted above the according picture. Additionally the electrode positions are marked in the first picture. Lower resistivity values are indicated by darker colors, higher values by lighter colors.

We can mark out different regions in the subfigures. In subfigures one to four between x=0 and x=1000 the buried valley is visible. The darker gray zones in comparison to the surrounding area stem from the clay layer, which can mostly be found in the valley. The resistivity values are between 30-60 Ωm. In subfigures two to four the gray band reaches over the whole area from South to North. In this depth the clay reaches its greatest extension.
The other interesting fact, the saltwater intrusion, begins in the 5th subfigure at a depth between 180-290 m. Its center is near the coordinates x=2000 and y=3500. With increasing depth it becomes clearer and in the last layer the included area reaches from the right margin of the figure to the center. That implies that the saltwater moves southwards from the North Sea (figure 1) and the freshwater/saltwater interface can be found at depth of about 200 m. From earlier measurements a saltwater intrusion was already known in lower depth, but far north of the actual measuring area (Siemon et al. 2001). Because of the limited penetration depth of the airborne

electromagnetic method the deeper regions could not be imaged and so the saltwater was not recognized. The same authors mentioned a second saltwater intrusion from the west. In the upper left corner of the last two subfigures there is also a low resistive area. This may be a branch of the second saltwater intrusion. In the last figure both appear close to each other and are expected to join in greater depth.

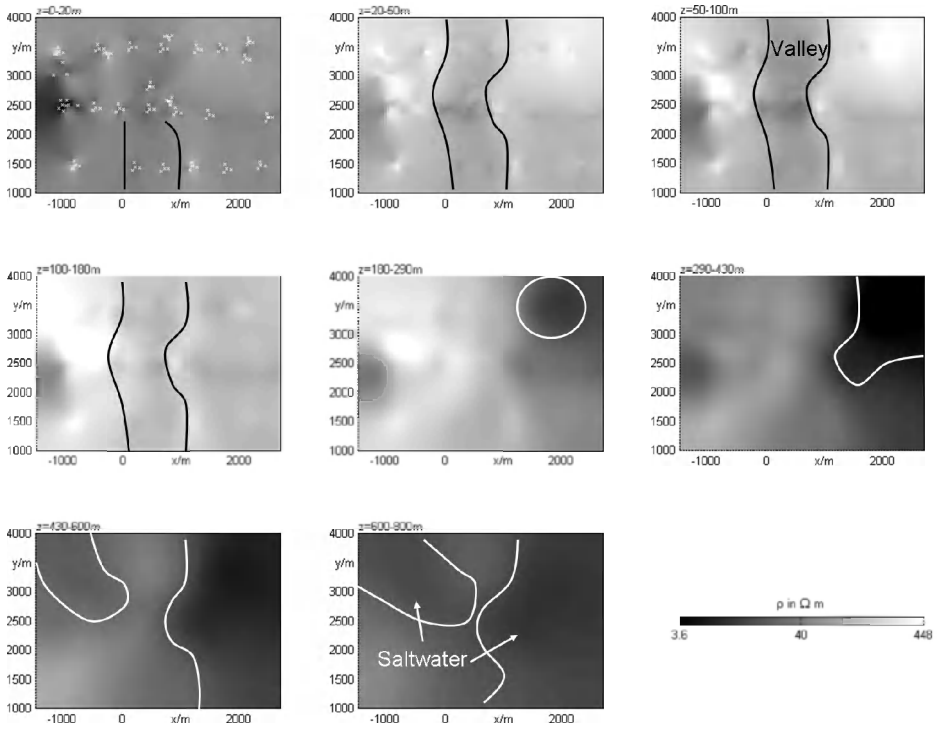

Figure 2. Model received from inversion. Depth slices from 0-20m to 600-800 m. Saltwater intrusions encircled with white lines, the valley is encircled with black.

DISCUSSION AND CONCLUSIONS

Large-scale dc measurements are a valuable tool for obtaining resistivity values from greater depth. It can close the gap between EM and seismics. The measurements yielded a lot of information regarding the buried valley and the saltwater intrusions. The valley could be identified clearly by the position of the clay layer (figure 2). Higher resistivity values from below the layer indicate sandy material. Two saltwater intrusions are found in the area. Both intrusions are far inland. Probably they have a wedge shaped form and move slowly inland under the freshwater. While the first intrusion has proceeded further and reaches depths that correspond to the valleys greatest depth, the second one has not moved that far. Another problem arises with the ascending saltwater. The valley is indeed protected against pollution from the surface through the clay layer, but it is not protected from beneath. So there is a danger of intruding saltwater into the reservoir. The valley and its surrounding areas are used by water works for freshwater supply. Hence it should be considered to monitor the progress of the saltwater/freshwater interface and to initialize counteractive measures if necessary. A new project comes up in the next months for further investigation on this subject.

REFERENCES

BurVal Working Group. 2006. Groundwater resources in buried valleys – a challenge for geosciences. Hannover: Leibniz Inst. For Appl. Geosciences

Gabriel, G., Kirsch, R., Siemon, B. and Wiederhold, H. 2003. Geophysical investigation of buried Pleistocene subglacial valleys in Northern Germany. Journal of Applied Geophysics 53, 159– 180

Golden, S., Rossberg, R. and Junge, A. 2004. The data logger geolore and its application in lake bottom magnetotellurics. In 17th workshop on electromagnetic induction in the earth, Hyderabad, India

Günther, T. 2004. Inversion Methods and Resolution Analysis for the 2D/3D Reconstruction of Resistivity Structures from DC Measurements, PhD Thesis, TU Bergakademie Freiberg

Siemon, B., Sengpiel, K.-P., Rehli, H.-J., Röttger, B. and Eberle, D. 2001. Identification of Saltwater Intrusions and Coastal Aquifers using the BGR Helicopter-borne Geophysical –System, First International Conference on Saltwater Intrusion and Coastal Aquifers-Monitoring, Modeling, and Management. Essaouira, Morocco, April 23–25, 2001

Schünemann, J., Günther, T. and Junge, A. 2007. 3-dimensional subsurface investigation by means of large-scale tensor-type dc resistivity measurements, Proceedings of the 4th International Symposium on Three-Dimensional Electromagnetics, Freiberg, Germany, September 27-30, 2007, 122-125, available at http://www.geophysik.tu-freiberg.de/3dem4

Contact Information: Joern Schuenemann, Leibniz Institute for Applied Geosciences, Stilleweg 2, 30655 Hannover, Germany, Email: joern.schuenemann@gga-hannover.de

Freshwater-Saltwater Mixing Zone in Coastal Aquifers: Biased vs. Reliable Monitoring

Eyal Shalev[1], *Ariel Lazar*[1,2], *Stuart Wollman*[1], *Shushanna Kington*[2,3], *Yoseph Yechieli*[1] and *Haim Gvirtzman*[2]

[1]Geological Survey of Israel, 30 Malkhe Israel, Jerusalem, 95501, Israel
[2]Institute of Earth Sciences, Hebrew University, Jerusalem 91904 Israel
[3]currently at Technion Israel Inst Technol, Dept Civil & Environm Engn, Haifa, 32000, Israel

ABSTRACT

The installation of monitoring boreholes may cause local vertical flow due to a natural vertical hydraulic gradient at the well location. This causes the borehole to act as a "short circuit" along the gradient, connecting the higher and lower hydraulic head zones. As a result, flow in the borehole (ambient flow) is often large enough to compromise the integrity of water samples and groundwater table measurements. Until the 1980's, it was still argued that long screen boreholes were more sensitive to the presence of different water bodies than short screen wells because of a better hydrologic connection with the aquifer and the ability to use discrete sampling based on electrical conductivity profiles. Since the late 1980's, the use of long-screen boreholes for groundwater sampling has been countered in the literature by many studies.

Most of the ~500 monitoring boreholes in the coastal aquifer of Israel are installed with 10-50 m long screens. Our knowledge of the freshwater-saltwater mixing zone is mainly supported by data from hundreds of these long-screened boreholes and from geophysical studies.

In this study we present measurements of groundwater levels and freshwater-saltwater mixing zone fluctuations from a long screened borehole in the coastal aquifer of Israel along with a three dimensional numerical model. The groundwater tidal effects are modeled using FeFlow, a 3D finite element simulator that solves the coupled variable density groundwater flow and solute transport. Although the undisturbed groundwater flow in a coastal aquifer can be simplified into a two dimensional flow on a vertical cross-section, the borehole introduces a radial flow with a component perpendicular to the cross-section; therefore, a 3D model is required for this problem (Figure 1). With this modeling, we are able to describe the biased monitoring of a fully screened observation-well, in which the fluctuation magnitude of the mixing zone is an order of magnitude larger than that in the porous media. The primary parameters that affect the magnitude of this bias in the observations are the anisotropy of the hydraulic conductivity and the differences between the aquifer and borehole hydraulic parameters (borehole hydraulic conductivity depends on its diameter). With no sea-tide, borehole interference is higher for the anisotropic case because the vertical hydraulic gradients are high. When tides are introduced, the amplitude of the mixing zone fluctuation is higher for the isotropic case because the overall effective hydraulic conductivity is greater than the conductivity in the anisotropic case. The large fluctuations of the freshwater-saltwater mixing zone occur only in the borehole and do not occur in the aquifer.

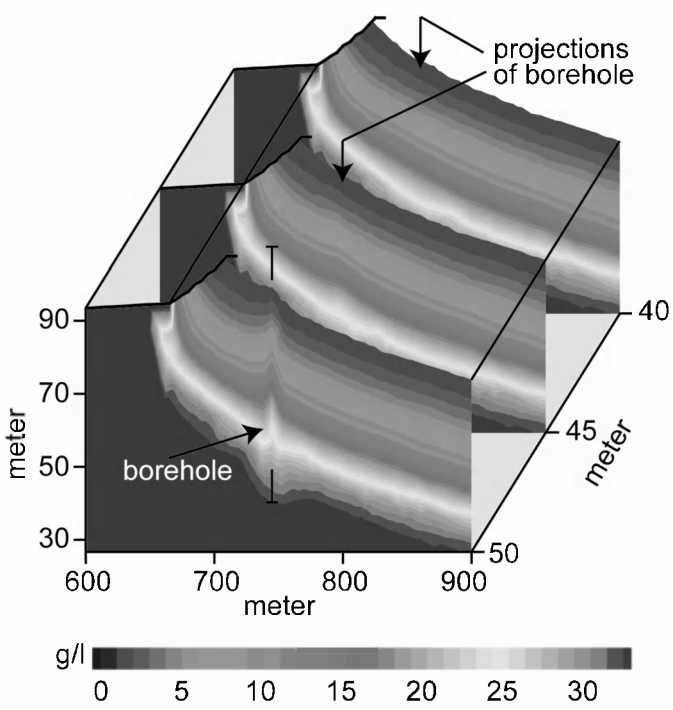

Figure 1. Simulation results showing salinity distribution around the borehole for the anisotropic case. The borehole affects the natural flow and elevates the freshwater-saltwater mixing zone. Away from the borehole the natural flow is undisturbed.

Contact Information: Eyal Shalev, Geological Survey of Israel, 30 Malkhe Israel st., Jerusalem, 95501 Israel, Phone: 972-2-531-4230, Fax: 972-2-538-0688, Email: eyal@gsi.gov.il

Influence of Sea Water Ingress: A Case Study from East Coast Aquifer in India

S. K. Sharma
Department of Environmental Education, Carman School, Dehradun, India

ABSTRACT

One of the sources of pollution, in addition to organic matter; pathogens and microbial contaminants; nutrients; acidification (precipitation and runoff); heavy metals; toxic organic compounds and micro-organic pollutants; thermal and silt and suspended particles, that impact water resources at local scale in parts of eastern coast of India, is SALINIZATION due to sea water ingress. The eastern coast of India is also hit by the cyclones every year. With the result drinkable water is becoming increasingly scarce. By the year 2025, it is predicted that water abstraction will increase by 50% in the region, as population growth and development drive up water demand. In recent years, the availability of water and its quality have emerged as the major constraints to economic development and quality of life.

In parts of Krishna - Godavari Basin of Andhra Pradesh, number of bore wells have been drilled for drinking water abstraction. Salinity hazards have occurred due to sea water intrusion as the aquifers are open to the sea, entraps sea water in the marine sediments and seawater intrusions through tidal cracks. Indiscriminate pumping has resulted in groundwater overexploitation and sea water ingress with salinization of aquifers and landward movement of saline water – freshwater interface for several kilometres in Krishna - Godavari Basin area. In parts of Krishna - Godavari Bsin bore wells yield saline / brakish water due to seawater ingress. The groundwater is of brakish type, having Na^+ : Cl^- facies. The soils of the area have the ability to pick up these ions during pre monsoon period and during post monsoon period the water becomes more saline thus, suggesting that the ions are leached from the soils by the infiltrating recharge waters and are added to groundwater bodies. The TDS (1912 / 1948 mg/l), TH (365/393 mg/l - Ca^{++} + Mg^{++}), Na^+ (721/ 739 mg/l), Cl^- (781/ 797 mg/l), SO_4^{++} (122/ 112 mg/l) and F(1.6/1.9 mg/l) concentrations are in excess of the safe limit in accordance with the domestic and industrial water quality standard of WHO. Excessive amounts of fluoride (more than 1.5 mg/l) in drinking water is toxic. Discoloration of teeth and crippling skeletal effects caused by long-term ingestion of large amounts are prominent in the region, where millions people suffer from chronic fluorosis disease. Thus, these ground waters are not safe to drink.

The basic problem of groundwater management of the region is its development without disturbing the saltwater / freshwater interface. This may be achieved by limiting the groundwater abstraction through enactment of groundwater legislation and recharging the aquifer artificially by rainwater.

Key words : Salinization, Aquifer, Brakish, Fluorosis, Leaching

INTRODUCTION

Needless to say that water is perhaps the scarcest commodity of the 21st century. On global scale it is assessed that over the next two decades, water use by human beings will increase by 40% and that 17% more water will be needed to grow more food for the increasing population. The World Water Vision Commission drew attention to the "gloomy arithmetic of water" as water

demand will out strip its availability. The scenario of water in India is equally gloomy. When India gained independence in 1947, the per capita availability of water was 6000 cubic meters and had only 1000 bore holes in the country but today with population crossing one billion, the per capita availability has fallen to 2300 cubic meters which is further expected to go down to 2000 cubic meters by the year 2015 though the number of bore holes have increased to more than 6 million. The evident reasons for this down fall are attributed to the rapid increase in population since independence and over withdrawal of *under ground water*. In another 15 to 20 years, the country will be in the grip of acute water shortage. The water supply of the eastern coast of India comprising the states of Andhra Pradesh, Orissa and Tamil Nadu is facing the problem of salinization of groundwater due to growing population's demand of water for various uses. The United Nation's recent report stating that about two-third of humanity would suffer from moderate to severe water shortage, is already proving true for India. The freshwater in shallower layers above *saltwater* is useful for agriculture and other industrial purposes until the slat content of the *groundwater* does not exceed certain limits. The *water table* is declining at an alarming rate and if the suitable measures to conserve water and recharge the aquifers are not initiated immediately, then some of the *reservoirs* may deplete permanently and the situation might worsen further.

Wide spread *marine incursions* has caused the water pollution and has resulted in increased water scarcity, poor public health, lower agricultural yields and a declining quality of *aquatic life* in coastal areas of India.

STUDY AREA

In Krishna - Godavari Basin of Andhra Pradesh, number of bore wells have been drilled for drinking water abstraction. *Semiconsolidated* sediments of *fluviomarine* origin of *Tertiary* to *Quaternary* age, comprising thick, coarse, well sorted sand layers ranging from a few meters to nearly 700 meters in thickness build up this eastern part of the Indian coast that serves as the repository of *groundwater* and from *prolific aquifers*. *Salinity* hazards have occurred due to sea *water intrusion* as the *aquifers* are open to the sea, entraps sea water in the *marine sediments* and *seawater intrusions* through tidal cracks. Indiscriminate pumping has resulted in *groundwater* overexploitation and sea water ingress with *salinization* of *aquifers* and landward movement of *saline water – freshwater interface* for several kilometres in Krishna - Godavari Basin area. In parts of Krishna - Godavari Bsin bore wells yield saline / brakish water due to seawater ingress The study area of Krishna - Godavari Basin in Andhra Pradesh experiences *tropical* and *humid* climate with mean monthly *temperature* raging between 25^0C to 38^0C and the mean rainfall of about 900 mm. *Physiographically*, the area has low relief with gentle slope from northwest to southeast making it prone to *flash floods*. *Quaternary alluvium* forms a multi-aquifer system, consisting of alternate layers of *clayey sands* and sandy clays of various thickness. The region is frequently hit by *cyclones* during monsoon period and the high *tides* traversing inland is very common. The average depth of water table in these wells during dry or non-monsoon period varies from 10.50 to 12.40 m and during monsoon period it is elevated between 8.74 to 9.84 m.

OBJECTIVE OF THE STUDY

With the increase in *saltwater* intrusion, the availability of *freshwater* is decreasing in the area particularly in the dry season. Therefore, the objective of the study is to analyze the *groundwater* samples from the existing bore holes situated in the coastal areas of east coast for assessing the

water quality which is the key to socio-economic development and quality of life of the habitants of the region.

METHODOLOGY

In order to assess the *groundwater quality* and the affects of *intrusive sea water*, 160 water samples from the bore holes representing shallow *groundwater* zone up to 50m were collected from the coastal areas of Andhra Pradesh from east coast. The *electrical conductivity* of the borehole samples were measured in the field and was found to be around 487 *uS/cm* at 25^0C at a *pH* of about 8.1 as compared to the surface water having more than 3090 *uS/cm* at 25^0C at a *pH* of around 7.2. This itself is an indicative of the higher *salinity* in *groundwater* due to *marine* incursions. The collected water samples were brought to the laboratory and as per standard procedure of APHA, 1985 they were analyzed for *TDS, TH* ($Ca^{++} + Mg^{++}$), HCO_3, CO_3^{--} Na^+ Cl^- SO_4^{++} and *F* and the *ionic ratios* calculated to see the influence of contaminated *marine* incursions in the area.

HYDROGEOCHEMISTRY

The following Table1 summarizes the chemical composition of *groundwater* in the pre and post monsoon periods (all concentrations are expressed in *mg/l*).

Bore Hole No.	*TDS*	*TH* ($Ca^{++} + Mg^{++}$)	HCO_3	CO_3^{--}	Na^+	Cl^-	SO_4^{++}	*F*
1.	3261 /3301	520/ 522	510/ 515	30/ 30	1011/ 1024	1244/ 1260	268/ 260	1.5/ 1.7
2.	1924 /1965	301/ 352	420/ 427	-------	760/ 785	870/ 895	102/ 90	1.3/ 1.5
3.	1530 /1590	411/ 430	310/ 324	25/ 24	880/ 910	270/ 289	75/ 68	1.6/ 1.8
4.	0758 /0801	256/ 303	212/ 227	20/ 20	180/ 202	160/ 163	23/ 18	1.2/ 1.6
5.	2081 /2022	330/ 355	456/ 467	-------	678/ 680	854/ 864	98/ 88	1.4/ 1.7
6.	1965 /2001	398/ 403	417/ 437	-------	588/ 512	880/ 889	105/ 89	2.1/ 2.5
7.	3940 /3990	512/ 553	556/ 571	30/ 28	1202/ 1245	1544/ 1566	302/ 289	1.4/ 1.7
8.	0748 /0799	219/ 265	217/ 230	-------	167/ 176	167/ 179	58/ 52	1.6/ 1.9
9.	1924 /1965	378/ 401	391/ 403	-------	755/ 790	830/ 855	99/ 88	1.6/ 2.0
10.	0988 /1052	327/ 347	272/ 282	20/ 20	988/ 1012	990/ 1012	89/ 82	2.2/ 2.5
Mean	1912/ 1948	365/393	376/ 388	12.5/ 12.2	721/ 739	781/ 797	122/ 112	1.6/ 1.9

Ionic ratios	*Na /Cl*	Cl/CO_3+HCO_3	*Na/Ca+Mg*	*F*
	0.91/ 0.92	2.0/ 1.9	1.9/ 1.8	1.6 – 1.9

DISCUSSION OF RESULTS

Though there has been tremendous progress in the water supply infrastructure after setting up of the Rajiv Gandhi National Drinking Water Mission in 1986, the goal to provide safe drinking water to all is still to be achieved. India's population has recently crossed one billion. Ever-increasing population and the increased need for agriculture and industries has resulted in water scarcity. The country thus faces a series of threats to the management of water resources. This leads the rural population and even urban also to depend upon water from local tanks and tube wells and the consumption of untreated water for all purposes. Groundwater classification based

on *Total Dissolved Solids* categorizes *Freshwater* ranging in *TDS* from 0 to 1,000 *mg/l* ; *Brackish water* from 1,000 to 10,000 *mg/l* ; *Saline water* 10,000 to 100,000 *mg/l* and *Brine* > 100,000 *mg/l.*

The major *ionic ratio Na/Cl* is equal to 0.9 in the samples which is quite comparable to the seawater *ionic ratio* of 0.85. Another important *Na/Ca+Mg ionic ratio* of 1.9 indicate the influence of *tidal* recharge into these waters. In addition, the *ionic ratio* $Cl/CO_3 + HCO_3$ with a value of around 2.0 clearly indicates the injuriously contaminated *marine* incursion. The average *seawater* has a ratio of about 2.3. It is clear from the electrical conductivity values and the ionic ratios obtained from the chemical analyses that the *groundwater* in the bore holes are contaminated and are influenced by the sea proximity. Such water can not be used for drinking purpose and up to some extent for irrigation also without treating it with the desalination plants.

The higher and varying concentration of F^- in *groundwater* in the area is due to varying degree of contamination with *tidal* recharge and also due to *ion exchange* phenomenon affecting intrusive waters prior to contamination with *groundwater*. The ill affects of high *fluoride* content in water are manifested in the form of *'Endemic fluorosis'* which is an acute public health problem in India. Medical advice recommends the drinking water should not contain more than 1.5 ppm of *fluoride*. Concentration of *fluoride* below 1.5 *ppm* are helpful in prevention of *tooth decay*, and such level of *fluoride* also assists in the development of perfect bone structure in human and animals. However, doses of *fluoride* above 1.5 ppm increases the severity of tooth *mottling* and induces the prevalence of *osteoporosis* and *collapsed vertebrae*. The disease resulting from excessive consumption of *fluoride* (found to be in the range of 1.6 to 1.9 *mg/l* in the area) is '*fluorosis*" which has no treatment available at present and is considered to be deadly disease. High *fluorine* consumption leads to the *fluorosis* of the bones which is generally found in Asian region but it is more acute in nine states of India including Andhra Pradesh. Hence, possibilities of reducing the high *fluorine* content of *groundwater* by *defluorination process / dilution* with the surface water is one very simple technique but addition of Ca^{++} ions to solution in contact with *fluorite* when experimented in *distilled water* caused appreciable decrease in *fluoride* concentration which appears to be more suitable solution to high *fluoride* problem in an otherwise water scarce India.

Contact Information: S. K. Sharma, Department of Environmental Education, Carman School, Premnager, Dehradun 248007, India, Phone: +91 135 2728076, Fax: +91 135 2773381, Email: sks105@rediffmail.com

Pumping of Brackish and Saline Water in Coastal Aquifers: An Effective Tool for Alleviation of Seawater Intrusion

Mohsen Sherif[1] and *Anvar Kacimov*[2]
[1]Department of Civil & Environmental Engineering, UAE University, Al-Ain, UAE
[2]Department of Soils, Water and Agriculture Engineering, College of Agriculture, SQU, Muscat, Sultan of Oman

ABSTRACT
The increase of water demands in coastal areas is often covered by extensive pumping of fresh groundwater, upsetting the dynamic balance between freshwater and saline water bodies. The classical result of such a development is the seawater intrusion problem. In this paper, it is proposed to pump the brackish water, encountered between the freshwater and saline water bodies, to reduce the extension of seawater intrusion. To that end, SUTRA is used to examine different pumping scenarios. The simulation is conducted in the vertical view and the equi-concentration lines and velocity vectors were identified for the different cases. Results of numerical simulations indicated the effectiveness of this methodology in controlling the seawater intrusion and enhancing the groundwater quality in coastal aquifers.

INTRODUCTION
Seawater intrusion phenomena are of main concern in almost all coastal aquifers around the globe. The problem is more severe in arid and semi-arid regions where the groundwater constitutes the main freshwater resource. The growth of population in coastal areas and the associate increase in human, agricultural, and industrial activities have imposed an increasing demand for freshwater in such areas. This increase in water demand is often covered by extensive pumping of fresh groundwater, causing subsequent lowering of the water table (or piezometric head) and upsetting the dynamic balance between freshwater and saline water bodies.

The shape and degree of the seawater intrusion in a coastal aquifer depend on several factors. Some of these factors are natural and cannot be controlled while others are manmade and could, thus, be managed. These factors, include among others, the type of the costal aquifer (confined, phreatic, leaky, or multi-layer) and its geology and geometry, water table and/or piezometric head, seawater concentration and density, natural rate of flow, capacity and duration of water withdrawal or recharge, rainfall intensities and frequencies, evaporation rates, physical and geometric characteristics of the porous media, geometric and hydraulic boundaries, tidal effects, variations in barometric pressure, earth tides, earthquakes and other vibrational effects, water wave actions, and chemical changes. The depth of the aquifer at the seaside through which the seawater intrudes inland as well as pumping and recharge rates and locations are the most critical factors to be considered, Sherif and Singh (1996) [1]. Under natural conditions, fully steady state conditions in groundwater systems may not be achieved as pumping activities, recharge from surface water bodies and rainfall events can not be controlled. However, steady state simulation of seawater intrusion phenomenon may be considered to identify the ultimate intrusion conditions and also for comparison among different pumping/recharge scenarios.

EFFECT OF PUMPING FRESH AND BRACKISH/SALINE GROUNDWATER
The main purpose of this numerical simulation is to examine the possibility of restoration of the groundwater quality in coastal aquifers by pumping saline (or brackish) groundwater from the area in the vicinity of the shoreline. SUTRA (Voss and Provost, 2003) [2] is a variable-density ground-water flow with solute or energy transport model. It is an upgrade of the 1984 SUTRA

computer code (Voss, 1984) [3]. The code employs a two- or three- dimensional finite-element and finite difference method to approximate the groundwater flow and solute transport equations.

In order to demonstrate the effect of pumping of the intruded seawater from the coastal regions, an idealized vertical study domain of 1000 m in length and 50 m in depth was considered. The porosity was set equal to 0.25. The system was considered homogeneous but anisotropy. The horizontal permeability, k_x, was set equal to 10^{-6} m^2, while the vertical permeability, k_y, was set as 10^{-7} m^2. The dispersivities in the horizontal and vertical directions, α_L and α_T, were both set equal to 5m. The other parameters were set as the default values of SutraGUI (Winston and Voss, 2004) [4].

The upper and lower boundaries were considered impermeable, i.e., no flux of water or salt ions is allowed to cross these two boundaries. A specified head boundary condition, H_1 was used at the land side and the head was set equal to 6.0m. At the seaside boundary, the seawater head was set equal to 4.0m. The head at this boundary was calculated as equivalent freshwater hydraulic head (Sherif et al., 1988) [5]. Therefore, the freshwater head, H_2, at the seaside was describe as

$$H_2 = 4.0 + k\,(50 - y), \quad (1)$$

where, k is a constant and can be expressed as

$$k = \frac{\rho_s - \rho_f}{\rho_f} \quad (2)$$

in which ρ_s and ρ_f are the densities of the seawater and freshwater, respectively. Also, y in equ. (1) is the elevation (m) of the nodal point above the aquifer bottom. Considering ρ_s and ρ_f to be 1000 kg/m^3 and 1025 kg/m^3, respectively, the constant a will be equal to 0.025. The maximum equivalent freshwater head at the seaside boundary is at y = 0 and is equal to 5.25m.

The study domain was discretized using the Fishnet (Winston and Voss, 2004) [4]. The length of the domain was divided into 200 equal intervals each with a length of 5.0 m, while the depth was divided into 20 equal intervals each with a length of 2.5 m. The domain is discritized into a total of 4000 rectangular elements (5.0 x 2.5 m) with 4221 nodal points. All simulations were conducted under the steady state conditions.

In run-1, the simulation was performed without any pumping to identify the seawater intrusion that would result due to the density difference between the freshwater and saline water bodies. The resulted equi-concentration lines are presented in Fig. 1a and the velocity vectors are presented in Fig. 1b. Equi-concentration lines 0.0 and 0.035, which represent the fresh and sea waters, migrated inland to a distance of 150 m and 104 m, respectively, measured along the bottom boundary. Meanwhile, a clear cyclic flow pattern is observed near the shoreline where the seawater intrudes the aquifer from the bottom and rotates back to the sea through the upper part of seaside boundary as brackish water.

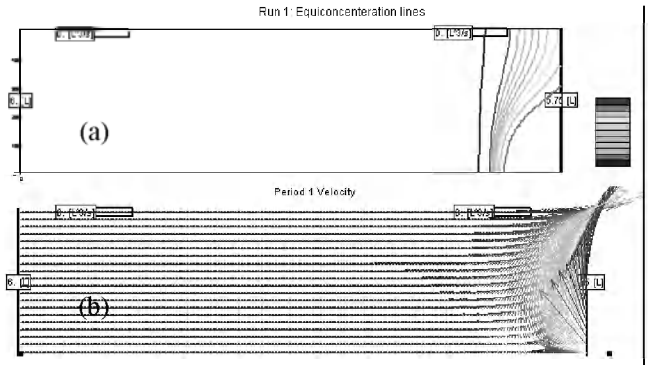

Figure 1. Equiconcentration lines and velocity vectors for run-1.

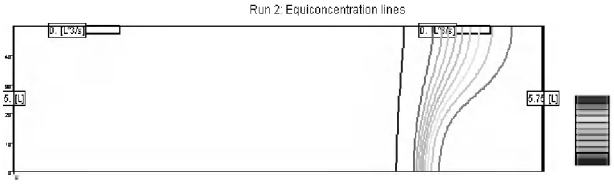

Figure 2. Equiconcentration lines for run-2.

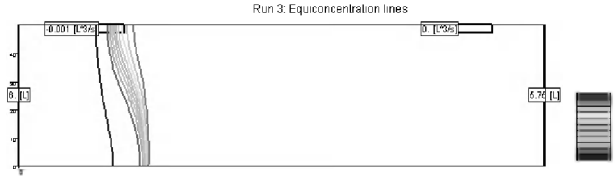

Figure 3. Equiconcentration lines for run-3.

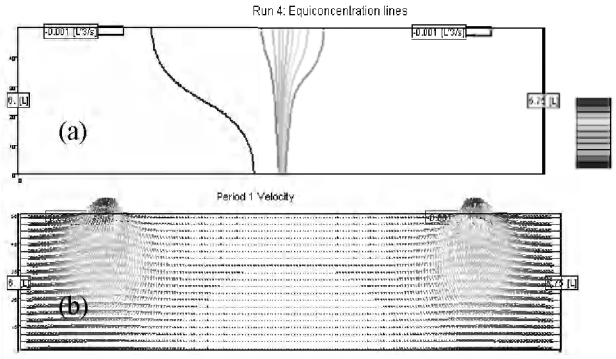

Figure 4. Equiconcentration lines and velocity vectors, run-4.

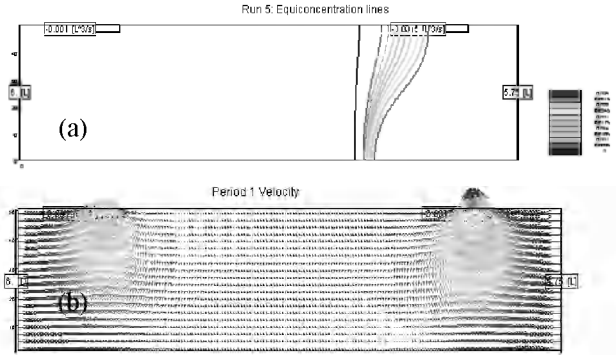

Figure 5. Equiconcentration lines and velocity vectors, run-5.

In run-2, the specified head was reduced to 5.0 m and all other parameters were kept the same. The resulted equi-concentration lines are presented in Fig. 2. The same equi-concentration lines 0.0 and 0.035 (defining the width of the dispersion zone) migrated inland to a distance of 277 m and 196 m, respectively, as measured along the bottom boundary from the seaside. As expected, reducing the hydraulic head at the land side increased the degree of intrusion and the width of the dispersion zone. In run-3, the hydraulic head at the land side was maintained at 6.0. In addition a uniform freshwater pumping of 86.0 m^3/d was introduced at distance 900 m < x < 800 m, from the sea boundary. All other parameters were unchanged. Equi-concentration lines 0.0 and 0.035 moved inland to a distance of 820 m and 754 m, respectively, measured along the bottom boundary from the seaside, Fig. 3.

In run-4, in addition to the freshwater pumping (included in run-3), saline groundwater was also pumped uniformly at a rate of 86.0 m^3/d from a distance 200 m < x < 100 m, measured from the sea boundary. Fig. 4a represents the resulted equi-concentration lines under the steady state conditions. Equi-concentration lines 0.0 and 0.035 retreated toward the seaside and intersected the bottom boundary at a distance of 553 m and 491m, respectively, measured along the bottom boundary. On the other hand, because of the velocity pattern, Fig. 4b, the width of the dispersion zone has increased near the upper boundary. In run-5, the pumping of saline groundwater was increased to 130 m^3/d and all other parameters remained unchanged. Figs. 5a and b present the resulted equi-concentration lines and velocity vectors in the study domain. Equi-concentration

lines 0.0 and 0.035 retreated more toward the seaside and the quality of the groundwater was enhanced considerably. The intrusion was mainly limited to the area between the sea boundary and saline groundwater pumping field. Despite the increase of total pumping of (fresh and saline) groundwater in runs 4 and 5, the overall quality of the groundwater in the aquifer has improved. This result is consistent with the findings of Sherif and Hamza (2001) [6]. Pumping of saline groundwater from coastal aquifers would mitigate the migration of seawater deep into the aquifer and would contribute to the enhancement of the groundwater quality.

CONCLUSION

A new methodology for controlling the seawater intrusion and enhancing the quality of the groundwater in the coastal aquifers is proposed. A two-dimensional finite element model, SUTRA, has been employed to verify the proposed methodology. The model is based on the variable density approach which accounts for the change in the fluid density with the change of its concentration. The effect of groundwater pumping from fresh/saline/brackish zone(s) on the equiconcentration lines and velocity fields in the vicinity of the shore line is investigated. It is concluded that seawater intrusion problems could be controlled through proper pumping of fresh/saline/brackish groundwater from the coastal zone.

ACKNOWLEDGEMENT

This research was funded equally by the research sectors of both UAE University and Sultan Qaboos University.

REFERENCES

[1] Sherif M.M. and Singh V. P., "Saltwater Intrusion", Chapter 10 in "Hydrology of Disasters", Book Series: Water Science and Technology Library, Vol. 18. pp.269-319. Kluwer Academic Publishers, The Netherlands, 1996.

[2] Voss, C.I., and Provost, A.M., SUTRA, A model for saturated-unsaturated, variable density ground-water flow with solute or energy transport, U.S. geological Survey Water-Resources Investigations Report 02-4231, 105p, 2002.

[3] Voss, C.I., A finite-element simulation model for saturated-unsaturated, fluid-density dependent ground-water flow with energy transport or chemically–reactive single-species solute transport: U.S. Geological Survey Water-Resources Investigation Report 81-4369, (rev. 1990), 409p, 1984.

[4] Winston, R.B. and Voss, C.I., SutraGUI, A Graphical User Interface for SUTRA, A Model for Ground-Water Flow with Solute or Energy Transport, U.S. Geological Survey, Open-File Report 03-285, 114p., 2004.

[5] Sherif M. M., Singh V.P. and Amer A.M., A Two Dimensional Finite Element Model for Dispersion (2D-FED) in Coastal Aquifers, Journal of Hydrology, Vol.103 (11-36), 1988.

[6] Sherif M.M. and Hamza K.I, Mitigation of Seawater Intrusion by Pumping Brackish Water, Transport in Porous Media, Vol. 43, pp. 29-44, 2001.

Contact Information: Mohsen M. Sherif, Civil and Environmental Engineering Department, College of Engineering, UAE University, P.O. Box: 17555, Al Ain, UAE, Phone: +971 50 7638044, Fax: +971 3 7623154, Email: msherif@uaeu.ac.ae

Solute Extraction in Variable Density Flow: Shock Wave Driven Transport Compared to Pumping

Yuval Ohana[1] and ***Shaul Sorek***[1,2]

[1]Environmental Hydrology & Microbiology, Zuckerberg Institute for Water Research, Blaustein Institutes for Desert Research,

[2]Mechanical Engineering, Pearlstone Center for Aeronautical Studies, Ben-Gurion University of the Negev, Israel

ABSTRACT

We present simulations of a one dimensional model addressing solute migration subsequent to an abrupt pressure change applied to a variable density Newtonian fluid saturating a deformable porous medium (Sorek 1996). Mass and momentum balance equations for the fluid and an elastic matrix together with the solute mass balance equation, are solved by the Total Variation Diminishing (TVD) scheme.

The efficiency of extracting solute mass is assessed on a ratio between pumping using an approximate analytical solution following Darcy's equation, and TVD numerical simulations addressing the emitting of an expansion wave. This ratio can be calibrated in reference to four groups of parameters associated with: expansion waves sequence, matrix geometrical properties, fluid characterization and pumping depth. It was found that solute mass extracted by shock wave can be an order of magnitude greater in comparison to that by pumping.

THE THEORETICAL MODEL

The conceptual model (Sorek 1996) may be summarized by the following set of assumptions: [A.1] The fluid is Newtonian. [A.2] The solid phase preserves its volume and the matrix is assumed to be elastic undergoing small vertical deformations. [A.3] Fluid dispersive and diffusive fluxes of the total mass and momentum are much smaller than the advective one and may, therefore, be neglected. [A.4] Isentropic conditions prevail. [A.5] Adsorption is governed by a linear equilibrium isotherm. [A.6] Porosity is mainly a function of pressure. [A.7] No fluid and solute sources are present. [A.8] Vertical pressure gradients are dominant and gravity body force is negligible. [A.9] Macroscopic stress-strain relationship for the solid matrix has the same form as that of the microscopic counterpart. [A.10] The solute component can be adsorbed on the matrix. Adsorption is governed by a linear isotherm. [A.11] The microscopic solid-fluid interfaces are material surfaces with respect to both phases mass. [A.12] Solid velocity is small in comparison to that of the fluid.

On the basis of assumptions [A.1] to [A.12] and in view of Bear et al. (1992), Krylov et al. (1996) and Sorek et al. (1996), following an abrupt pressure change (Sorek 1996), and accounting for Forchheimer tensor addressing the exchange of inertia at the microscopic solid-fluid interface ((Levy et al. 1995, 1999), during the wave propagation period we write the fluid $(\ )_f$ mass and momentum balance equations respectively

$$\frac{\partial}{\partial t}\left(\phi\rho_f\right)+\nabla\bullet\left(\phi\rho_f\boldsymbol{v}_f\right)=0, \tag{5}$$

$$\frac{\partial}{\partial t}\left(\phi\rho_f\boldsymbol{v}_f\right)+\nabla\bullet\left(\phi\rho_f\boldsymbol{v}_f\boldsymbol{v}_f\right)+\phi\nabla P\bullet\boldsymbol{T}_f^{*}+\phi\rho_f\left|\boldsymbol{v}_r\right|\boldsymbol{v}_r\bullet\tilde{\boldsymbol{F}}=0,\qquad \boldsymbol{v}_r\equiv\boldsymbol{v}_f-\boldsymbol{v}_s. \tag{6}$$

The solid $(\ )_S$ mass and momentum balance equations read respectively

$$\frac{\partial}{\partial t}\left[(1-\phi)\rho_s\right]+\nabla\bullet\left[(1-\phi)\rho_s\boldsymbol{v}_s\right]=0, \tag{7}$$

$$\begin{aligned}\frac{\partial}{\partial t}\left[(1-\phi)\rho_s\boldsymbol{v}_s\right]+\nabla\bullet\left[(1-\phi)\rho_s\boldsymbol{v}_s\boldsymbol{v}_s\right]+(1-\phi)\nabla P\bullet\boldsymbol{T}_s^{*}\\ -\nabla\bullet\boldsymbol{\sigma}_s^{'}-\phi\rho_f\left|\boldsymbol{v}_r\right|\boldsymbol{v}_r\bullet\tilde{\boldsymbol{F}}=0,\quad \boldsymbol{\sigma}_s'=(1-\phi)\left(\boldsymbol{\sigma}_s-\boldsymbol{\sigma}_f\right),\end{aligned} \tag{8}$$

where ρ denotes the phase density, $\boldsymbol{v}$ denotes its velocity vector, $\boldsymbol{\sigma}$ denotes its stress tensor with $\boldsymbol{\sigma}_s'$ as the matrix effective stress, $\boldsymbol{T}^{*}$ denotes its tortuosity tensor, P denotes pressure, ϕ denotes porosity and $\tilde{\boldsymbol{F}}$ denotes the Forchheimer tensor.

Following Sorek (1996), fluid density is pressure dominant at the period when its momentum balance equation conforms to a wave form. Neglecting the exchange of inertia at the microscopic solid-fluid interface and neglecting adsorption, solute mass balance equation reads (Sorek, 1996),

$$\frac{1}{C}\left(\frac{\partial C}{\partial t}+\boldsymbol{v}_f\bullet\nabla C\right)=-\frac{1-\phi}{\phi}\beta_\phi\rho_s k_d\boldsymbol{v}_f\bullet\nabla P-\frac{\phi\beta_p+\rho_s k_d S_0}{S_0}\nabla\bullet\boldsymbol{v}_f, \tag{9}$$

where C denotes solute concentration, β_ϕ denotes the constant matrix compressibility, k_d denotes the partitioning coefficient associated with the linear equilibrium isotherm, β_p denotes fluid compressibility and S_0 denotes specific storativity of the porous medium. Note that the right hand side of (9) represents source-like terms as (9) is decoupled from (5) and (6). These two latter equations can be combined into one for the case of a traveling wave (Landau and Lifshitz, 1987) when fluid's density, its pressure and velocity are mutually dependent (Sorek 1996). The state function when considering a liquid with constant compressibility β_P reads

$$P=P\big|_0+\beta_P^{-1}\ell n\left(\rho_f\big/\rho_f\big|_0\right), \tag{10}$$

where $(\ )\big|_0$ denotes a reference value. For a perfect, compressible, gas we consider,

$$P\big/\rho_f=Const.,\qquad \beta_p=(\gamma P)^{-1}, \tag{11}$$

where γ denotes the ratio of the fluid specific heat. Assuming a high Struhal number associated with porosity, small Mach number for the slightly deformable solid matrix, we follow Krylov et al. (1966) and account for

$$\phi=\phi\big|_0+\frac{\left(1-\phi\big|_0\right)^2}{\lambda_S^{''}}T_f^{*}\left(P-P\big|_0\right), \tag{12}$$

where $\lambda_S^{''}$ denotes the macroscopic Lamé constant for an elastic matrix, associated with vertical strain. When considering an elastic matrix undergoing small deformations, we refer to a constitutive relation for $\boldsymbol{\sigma}_S^{'}$ equivalent to the microscopic Hooks law and a strain tensor $\boldsymbol{e}_S$ that read,

$$\boldsymbol{\sigma}_S^{'}=\lambda_S^{''}\nabla\bullet\boldsymbol{w}_S\boldsymbol{I}+2\mu_S'\boldsymbol{e}_S,\qquad \boldsymbol{e}_S=\frac{1}{2}\left[\nabla\boldsymbol{w}_S+\left(\nabla\boldsymbol{w}_S\right)^T\right], \tag{13}$$

where μ'_S denotes the macroscopic Lamé constant associated with the shear strain, $\boldsymbol{I}$ denotes the unit tensor and $\boldsymbol{w}_S$ denotes the matrix displacement vector.

SIMULATIONS OF SOLUTE MASS EXTRACTION

Following Sorek (1996), we consider a one dimensional model for fluid pressure and velocity based on (5), (6) and solute migration (9), for an apparent new fluid (without Forchheimer term) concerning a traveling wave, a perfect gas, a slightly deformable matrix with (12) as its state function or for a deformable matrix accounting for (7) and (8). Emitting an expansion wave generates a pressure gradient governing the fluid flow that carries the solute towards the surface domain (Fig. 1).

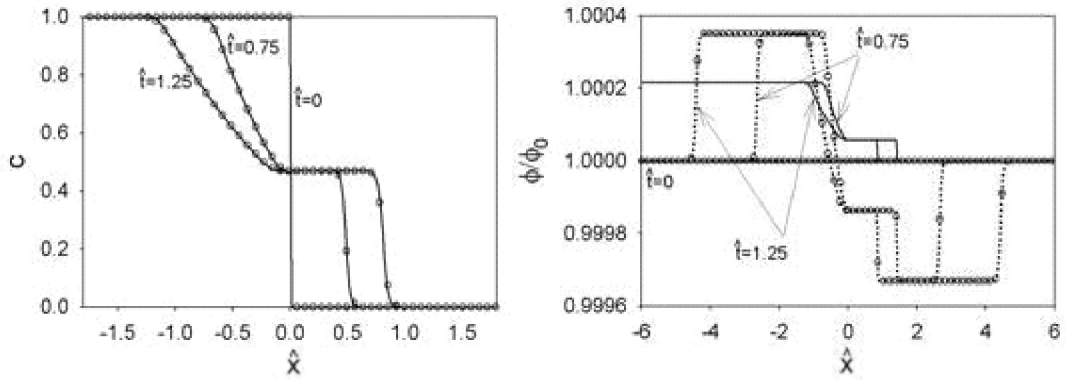

Figure 1. TVD numerical solution for Riemanns' problem considering gas, high matrix stiffness ($\lambda''_S \gg 1$) and neglecting inertia transfer expressed with Forchheimer term. The case of a deformable (○○○○○) and of a slightly deformable (——) matrix.

Solute extraction by shock waves is simulated by imposing pulses of abrupt pressure rise at the boundary ($x = 0$), each of which emits an expansion wave into the domain. During the time interval between pulses, pressure at the boundary reverts to its former value during which it has no affect on the solute and the fluid (assuming a large reservoir). Hence, during each wave time period t_{pulse} when a pressure pulse is implemented, solute transport is advection dominant (Sorek, 1996) and associated with a specific mass flux $Q_{solute} = \phi v_f C$. During the time span $[0, t_{final}]$ of several pressure pulses, $Q_{solute-W}$ $(\equiv \frac{1}{t_{final}} \int_0^{t_{final}} Q_{solute} dt \Rightarrow = Q_{solute-pulse} \frac{t_{pulse}}{t_{cycle}},\ iff\ t_{final} \gg t_{pulse})$ will be the average specific solute mass flux, t_{cycle} denotes the pulses time cycle and $Q_{solute-pulse}$ denotes the extraction of solute specific mass flux during the time of one pulse.

Simulation of solute extraction towards the domain surface by pumping will refer to Darcy's law neglecting gravitational body force, using (10) or (11) as the fluid's state functions. As for pumping simulation drag is assumed dominant at the solid-fluid interface, the matrix momentum balance equation (8) is assumed static and (13) accounts for its stress constitutive law. We considered a practically rigid matrix and an incompressible fluid so that the solution for solute extraction by pumping passes rapidly the transient period and reaches a steady state at which stage, for constant pumping intensity at the surface, a comparison is done with results of solute extraction by the expansion wave. Hence, we developed an approximate analytical solution for the specific solute extraction mass flux $Q_{solute-p}$ based on the aforementioned pumping conditions,

during the steady state period and for a compressible liquid following (10). The obtained expression reads.

$$\frac{Q_{solute-p}}{Q_{solute-w}} \cong \left(\frac{t_{cycle}}{t_{pulse}}\right) \frac{\kappa}{\mu_f} \frac{1}{\phi|_0 L} \sqrt{\frac{\rho_f|_0}{T_f^* \beta_p}}, \qquad (14)$$

where 1) Initial domain properties for extraction by an expansion wave are identical to the properties at $x = L$ (i.e. the undisturbed boundary considering the expansion wave) for the extraction by continuous pumping, namely, $(\ )_0 = (\ )_L$ and 2) The pressure impulse at the surface ($x = 0$) considering an expansion wave is identical to the pumping pressure for the continuous pumping. Table 1 is thus obtained in view of (14).

	Depth [m]	Pervious	Semi-Pervious	Impervious
		Sand & Gravel; Fractured Rocks	Silt; Loess; layered clay; Oil Reservoir Rocks	Unweathered Clay; Limestone; Dolomite
Water	30	0.06	5.0*E-05 to 5.0*E-07	5.0*E-09
Air	10	0.002	2.0*E-06 to 2.0*E-08	2.0*E-10

Table 1. Values of $Q_{solute-p}/Q_{solute-w}$ for typical matrix properties.

REFERENCES

Bear, J., Sorek, S., Ben-Dor, G. and Mazor, G., 1992, Displacement waves in saturated thermoelastic porous media. I. Basic equations, *Fluid dynamics research 9,* 155-164.

Krylov, A., Sorek, S., Levy, A., and Ben-Dor, G., 1996, Simple Waves in Saturated Porous Media (I. The Isothermal Case), JSME Int. J., Vol. 39, No. 2, 294-298.

Landau, L. D., and Lifshitz, E. M.: 1987, Fluid Mechanics, 2nd edition, Pergamon Press, London.

Levy, A., Sorek, S., Ben-Dor, G., and Bear, J., 1995, Evolution of the balance equations in saturated thermoelastic porous media following abrupt simultaneous changes in pressure and Temperature, Transport in Porous Media 21, 241-268.

Levy, A., Levi-Hevroni, D., Sorek, S. and Ben-Dor, G., 1999, Derivation of Forchheimer Terms and their Verification by Application to Waves Propagation in Porous Media, Intl. J. Multi-Phase Flow, 25, 683-704.

Sorek, S., 1996, A model for solute transport following an abrupt pressure impact in saturated porous media, Transport in Porous Media 22, 271-285.

Sorek, S., Krylov, A., Levy, A., and Ben-Dor, G., 1996, Simple Waves in Saturated Porous Media (II. The Non Isothermal Case), JSME Int. J., Vol. 39, No. 2, 299-304.

Contact Information: Shaul Sorek, Environmental Hydrology & Microbiology, Zuckerberg Institute for Water Research, Blaustein Institutes for Desert Research, Ben-Gurion University of the Negev, Midreshet Ben-Gurion, 84990 Israel. Phone: +972 4 6596901, Fax: +972 8 6596909, Email: sorek@bgu.ac.il

Base Exchange Indices as Indicators of Salinization or Freshening of (Coastal) Aquifers

Pieter J. Stuyfzand[1,2]
[1]Kiwa Water Research, Nieuwegein, Netherlands
[2]VU University Amsterdam, Dept. Hydrology & Geo-Environmental Sciences, Netherlands

ABSTRACT
Base exchange indices are frequently used in regional hydrochemical surveys, for indicating whether an aquifer is salinizing or freshening, or has been freshened or salinized in the past. Seven different base exchange indices are compared and evaluated. The best index, for aquifer systems without dolomite, is BEX = Na + K + Mg – 1.0716 Cl (meq/L), because it not only indicates the right direction (fresh or salt water intrusion), but also the magnitude of the exchange reaction and side reaction with $CaCO_3$. For dolomitic aquifers BEX_D = Na + K – 0.8768 Cl (meq/L) is to be preferred.

Great care must be taken in interpreting base exchange indices, because of various sources of bias, like errors in ionic balance, and disturbing water-rock and water-biomass interactions. Memory effects of ancient shifts in the position of the fresh/salt water interface may mask actual freshening or salinization processes.

INTRODUCTION
High quality data, good maps and intelligent interpretation tools are needed for on-time identification of spatial and temporal changes in the position of the fresh-salt groundwater interface(s) and the underlying causes, in order to protect the aquifer system or well field from unexpected, severe salinization. A proper cation exchange index with the right interpretation algorithm may constitute such a tool.

Base exchange indices are normally translated into a salinized or freshened facies, or into a state of equilibrium. It is assumed that intruding sea water (with high concentrations of Cl, Na, K and Mg) is displacing fresh water with high Ca and HCO_3 concentrations or vice versa, and that at least Na is adsorbed during salinization, and Ca during freshening of the aquifer system. The classical exchange reaction is therefore schematized as follows:

$$2Na^+ + Ca\text{-}EXCH \leftarrow \rightarrow Ca^{2+} + 2Na\text{-}EXCH \quad (1)$$

with: EXCH = the base exchanger, like clay and peat; forward (→) = salt water intrusion (salinization); backward (←) = fresh water intrusion (freshening).

THE BASE EXCHANGE INDICES
The first to recognize cation exchange in groundwater was not Renick (1924) as mentioned by several textbook writers, but Versluys (1916). Versluys (1916, 1931) used the ratio Na/(Na+Ca+Mg) as an index of base exchange. Schoeller followed in 1934 and 1956 with the 3 indices indicated in Table 1. Indices 1-4 in Table 1 are all expressed as a meq/L ratio, which makes them fit for the direction but unfit for quantifying the extent of the base exchange reaction. Delecourt (1941) was the first to introduce an index (see Table 1) that also quantifies the extent of the exchange reaction. Various problems with the above given indices are listed in Table 1. An index not suffering from most of the problems mentioned in Table 1, the Base

EXchange index (BEX) was proposed by Stuyfzand (1986), also as part of a chemical watertype classification.

Table 1. Overview of 5 base exchange indices from literature, with frequently encountered problems in their interpretation

No.	Author	Index [meq/L]
1	Versluys (1916, 1931)	Na / (Na + Ca + Mg)
2	Schoeller (1934)	[Cl - (Na + K)] / Cl
3	Schoeller (1956)	(Na + K) / Cl
4	Schoeller (1956)	(Ca + Mg) / (HCO3 + CO3 + SO4)
5	Delecourt (1941)	Na + K - Cl
6	Stuyfzand (1986) #	Na + K + Mg - 1.0716 Cl
7	This publication ##	Na + K - 0.8768 Cl

Problems:
1-7: other processes may influence values
1-5: bias due to analytical errors, no threshold
1-4: do not quantify amount of cation exchange

1: $CaCO_3$ dissolution influences ratio
2: ocean water already positive
5: ocean water already negative

#: for aquifers without dolomite

##: for aquifers containing dolomite

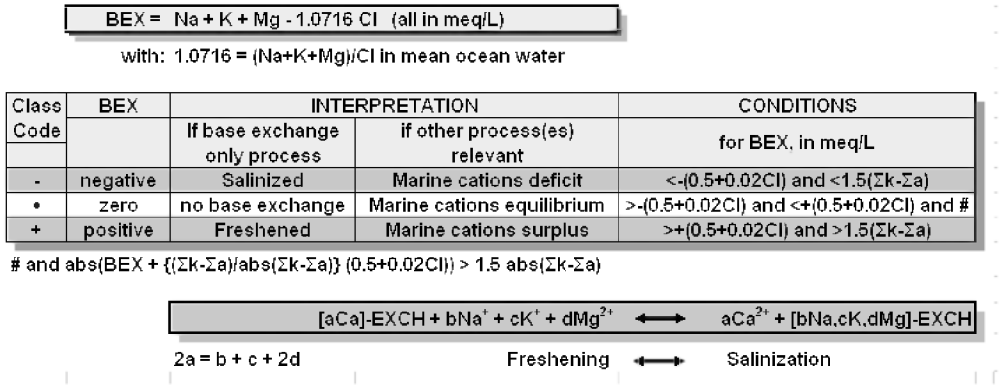

Figure 1. The Base Exchange index BEX as proposed by Stuyfzand (1986) with minor modifications according to Stuyfzand (1993).

The factor 1.0716 is equal to $\{[Na^+ + K^+ + Mg^{2+}]/Cl^-\}$ in meq/L for mean ocean water (Riley & Skirrow, 1975). The boundary limits at ± (0.5 + 0.02 Cl) indicated in Fig.1, were introduced as a threshold against (a) the expected errors in chemical analyses, and (b) waters without base exchange, that derive from silica terrains where some Na^+, K^+ and Mg^{2+} ions dissolve by chemical breakdown of silicates. 1.5(Σk - Σa) is used as a measure of ionic imbalance (see Fig.1).

BEX does not apply to dolomitic aquifer systems, because significant amounts of Mg derive from the dissolution of dolomite. Therefore BEX was slightly modified into BEX_D for application to dolomitic systems. Its definition is given in Table 1, and its further characteristics are equal to those of BEX (Fig.1).

PROBLEMS WITH THE INTERPRETATION OF BASE EXCHANGE INDICES

Any of the presented base exchange indices suffers from bias in the interpretation of its value, in addition to bias due to analytical errors. The most important ones are listed in Table 2, which more specifically holds for BEX and BEX_D.

Table 2. Algorithm for interpreting base exchange index BEX.

1	False positive BEX:	
		Dissolution of minerals like dolomite (+Mg), albite (+Na)
		Mineralization of fresh biomass (+K)
		Leaching of fertilizers or manure (+K)
2	False negative BEX:	
		Dissolution of halite (lack of K and Mg)
		Mineral transformations like dolomitization (-Mg)
		New formation of minerals (-K, -Na, -Mg)
		Synthesis of biomass (rapid growing forest; -K)
		Significant atmosferic deposition of Cl_2 gas (+Cl)
3	BEX (not false) indicates results of past shifts in fresh / salt interface	
		Positive BEX at specific point does not mean system is actually freshening
		Negative BEX at specific point does not mean system is actually salinizing
4	If chloride decreasing or constant and BEX trend:	
		from positive to 0, then Freshening
		from 0 to positive, then Salinization or False pos BEX
		more negative, then False negat BEX
5	If chloride increasing and BEX trend negative, then Salinization	
6	If chloride increasing and BEX trend positive, then Salinization by special source water#	

= for instance brackish surface water from a canal, with inputs from exfiltrating freshened groundwater or from agriculture

BEX: THE INDIVIDUAL CATIONS AND SIDE REACTIONS

Na^+, K^+ and Mg^{2+} do not always ad- or desorb simultaneously during salt or fresh water intrusion respectively. This means that their individual concentrations corrected for a contribution of sea salt (X*), do not always indicate the right direction of displacement while BEX does (Fig.2).

Deviations from the reaction in Fig.1 are quantitatively insufficient, however, to influence the sign of BEX. This pleads for its use as an indicator of salinization or freshening.

Changes in Ca concentration are related to BEX as follows (Fig.2), provided other reactions like methanogenesis do not significantly contribute:

$$Ca^* = Ca^*_0 - f\,BEX \qquad (3)$$

With: Ca^* = calcium concentration corrected for sea salt (= Ca – 0.0376 Cl) after base exchange [meq/L]; Ca^*_0 = ditto before base exchange [meql/L]; f = reaction coefficient [<1].

Factor f is 0.5 during freshening in the calcareous coastal dune aquifer systems, which indicates that the Ca losses are compensated for by dissolution of an amount of $CaCO_3$ equal to BEX/2. During salinization f is 1.0 (Stuyfzand, 1993).

Changes in TIC concentration are related to BEX, only during freshening, as follows (Fig.2):

$$TIC = TIC_0 + 2f\,BEX \qquad (4)$$

With: TIC, TIC_0 = Total Inorganic Carbon resp. after and before base exchange [mmol/L].

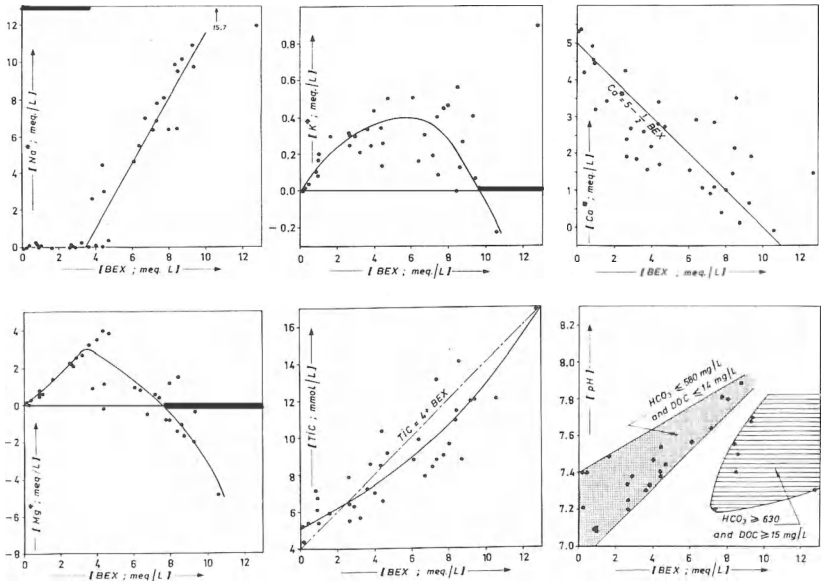

Figure 2. Plot of sea salt corrected, main cations (X*), total inorganic carbon (TIC) and pH in 36 deep anoxic groundwater samples, versus BEX for a sandy coastal dune aquifer system without dolomite in the Netherlands (slightly modified after Stuyfzand, 1993). Heavy bars indicate samples where BEX correctly indicates freshening, while Na*(= Na - 0.8581 Cl), K* (= K - 0.0187 Cl) and Mg*(= Mg - 0.1948 Cl) do not.

REFERENCES

Delecourt, J. 1941. Le Titre natronique (1re note). Bull. Soc. belge de Géol., Paléont. et Hydrol. 50, 152-166.

Riley, J.P. & G. Skirrow (Eds) 1975. Chemical oceanography. Acad. Press, London & NY.

Schoeller, H. 1934. Les échanges de bases dans les eaux souterraines; trois exemples en Tunisie. Bull. Soc. Géol. Fr. 4, 389-420.

Schoeller, H. 1956. Geochemie des eaux souterraines. Revue de l'Instit. Francaise du Petrole 10, 230-244.

Stuyfzand, P.J. 1986. A new hydrochemical classification of water types : principles and application to the coastal dunes aquifer system of the Netherlands. Proc. 9th Salt Water Intrusion Meeting, Delft 12-16 may, Delft Univ. Techn., 641-655.

Stuyfzand, P.J. 1993. Hydrochemistry and hydrology of the coastal dune area of the Western Netherlands. Ph.D Thesis Vrije Univ. Amsterdam, KIWA, ISBN 90-74741-01-0, 366 p.

Stuyfzand, P.J. 1999. Patterns in groundwater chemistry reflecting groundwater flow. Hydrogeology J. (7), 15-27.

Versluys, J. 1916. Chemische werkingen in den ondergrond der duinen. Verslag Gewone Vergad. Wis- & Nat. afd. Kon. Acad. Wetensch. Amsterdam, 25-3-1916, XXIV, 1671-1676.

Versluys, J. 1931. Subterranean water conditions in the coastal regions of The Netherlands. Econ. Geol. 26, 65-95.

Contact Information: Pieter J. Stuyfzand, Kiwa Water Research, PO Box 1072, 3430 BB Nieuwegein, Netherlands. Phone: +31-30-6069552; Email: pieter.stuyfzand@kiwa.nl

Alternative Approaches for Water Extraction in Areas Subject to Saltwater Upconing

David L. Tarbox and *William C. Hutchings*
HSA Engineers & Scientists, Tampa, FL, USA

ABSTRACT
Upconing of the saltwater interface beneath a pumping well can result when the hydrostatic balance between saltwater and the overlying freshwater is disturbed. The combination of the rate of pumping, the method of extraction, the distance from the intake of the well to the interface, the relative horizontal and vertical hydraulic conductivities of the aquifer, and the longitudinal and lateral dispersivities determine the degree of upconing. The numerical 3D, variable density model SEAWAT was used to simulate alternative methods of groundwater extraction and the resulting upconing. The model is an effective tool for predicting saltwater upconing and selecting appropriate pumping rates and the best method of groundwater development.

INTRODUCTION
Extraction of freshwater in coastal areas can lead to lateral saltwater intrusion and upconing. Lateral intrusion results from the decrease in the flux of freshwater moving seaward and impacts a relatively large area. It can be approximately modeled by simulating a decrease in the amount of recharge instead of modeling the quantity of water withdrawn (Mather, 1975). In contrast, the degree of upconing is significantly influenced by the local method of groundwater extraction. Experience has shown that pumping from a well is more likely to induce saltwater into the well than recovering the same quantity of water from a shallow extraction system (multiple shallow wells or a horizontal trench/drain) that distributes the stresses on the aquifer over a larger area. The purpose of this paper is to demonstrate a means of assessing the degree of potential upconing resulting from different groundwater extraction methods.

METHODOLOGY
The simulation of the impacts resulting from the different methods of groundwater extraction on an unconfined coastal aquifer assumes that the extraction site is located sufficiently far from the coast so the phreatic surface and the saltwater-freshwater interface are essentially parallel, and the geometry of the discharge zone does not affect the model. The less dense freshwater is in hydrostatic balance with the denser underlying saltwater in accordance with the Ghyben-Herzberg relationship. Governing equations for such a condition have been fully addressed by others (Bear, Zhou, and Bensbat, 2004; Bower, Motz, and Durden, 1999; Hamza, 2006; and Larabi, A., 2001) and will not be repeated here.

Qualitatively, the Ghyben-Herzberg hydrostatic relationship holds that one foot of drawdown in a well will result in 40 feet of rise at a sharp freshwater-saltwater interface beneath the well. Assuming adequate aquifer recharge, there is a critical pumping rate below which the upconing of saltwater will not intersect the bottom of the borehole. The total quantity of water that can be pumped from an aquifer is related to the pumping rate, the distance of the intake above the interface, and the horizontal and vertical hydraulic conductivities of the aquifer. The longitudinal and lateral dispersivities also have some impact, but are not as critical (Hamza, 2006). The thicker the transition zone, the less accurate the Ghyben-Hertzberg relationship becomes.

It seems logical that the greater the distance between the bottom of the well and the freshwater-saltwater interface, the less likely it is that the interface will rise to the bottom of the well. However, complications arise when it is considered that as the open portion of the well is shortened, the specific capacity of the well decreases. Therefore, the amount of drawdown per gallon pumped increases, thus increasing the potential for upconing of the interface.

The increase in drawdown at the individual well can be minimized by reducing the withdrawal rate at that well and simultaneously adding additional shallow wells to provide the same total quantity of water. Another alternative is to pump from a long, continuous, permeable subdrain that will skim water from the very top of the watertable with minimal drawdown.

In order to evaluate the optimum method of withdrawal, a numerical model was used to simulate a single deep well, a single shallow well, and a horizontal drain. The simulation considers stratigraphy typical of South Florida, with a moderately permeable sand overlying highly permeable oolitic limestone with an intervening layer of low permeability clayey sand.

MODELING SIMULATIONS

The three-dimensional, finite-difference, variable-density numerical model SEAWAT-2000 (Langevin, 2003) was used to simulate extraction of groundwater from the two wells and the horizontal trench. The general model consists of four layers with varying hydraulic conductivities. Additional layers were included to simulate the shallow well and the trench. The models for the deep and the shallow wells consist of 75 rows and 83 columns. In order to simulate the trench, the number of rows was increased to 119. The model domain is 6,600 meters by 3,800 meters. The row spacing ranges from 1.7 meters to 110 meters and the column spacing ranges from 1.7 meters to 200 meters. The trench model has row spacings that range from 2.2 meters to 110 meters.

Saltwater and freshwater specified head boundaries were set on the east side and west sides of the models, respectively. The saltwater boundary was assigned an elevation of sea level and the freshwater head was assigned a concentration of zero and an elevation of one meter NGVD. The top and bottom of the model were set at elevations of 3.5 meters and –55 meters NGVD, respectively. The hydraulic conductivities were varied as follows from top to bottom of the models: Kh=25 meters/day (m/d) and Kv=2.5 m/d from 3.5 to -15 meters NGVD; Kh=100 m/d and Kv=1 m/d from –15 to –27.5 meters NGVD; Kh and Kv=0.1 m/d from –27.5 to –40 meters NGVD; and Kh=100,000 m/d and Kv=10 m/d from –40 to –55 meters NGVD. The transition from 500 mg/L total dissolved solids (TDS) to > 30,000 mg/L TDS is approximately 35 meters thick, between -15 and -50 meters National Geodetic Vertical Datum (NGVD). The freshwater in the aquifer occurs in the layer extending from the water table and a depth of approximately –15 meters NGVD. The transition from 500 mg/L total dissolved solids (TDS) to > 30,000 mg/L TDS is approximately 35 meters thick, between -15 and -50 meters National Geodetic Vertical Datum (NGVD). The model was initially run without pumping for 10,000 days until steady state was reached to establish the initial conditions for the transient pumping simulations. A uniform recharge of 0.001 m/day was used. The discharge rate in every case is 384 m^3/day.

The first simulation was constructed with a well that fully-penetrates the aquifer from 3.5 to -15 meters. The second simulation was constructed with a partially-penetrating well extending only to a depth of only –5 meters NGVD. The third model considers a horizontal trench oriented perpendicular to groundwater flow. The bottom of the trench is at elevation –0.5 meters NGVD. The trench measures 183 meter-long by 4 meters wide by 1.7 meters deep and was simulated by

two methods. The first method includes 59 wells extracting at 6.51 m^3/day from the aquifer matrix. The second method uses one well extracting 384 m^3/day from a highly conductive series of cells. In the latter case, the trench was assigned a hydraulic conductivity of 10,000 m/day and a specific yield of 1. The transient simulations were subsequently run for 90 days and 900 days. The finite-difference scheme was used to solve the flow equations and the Preconditioned Conjugate-Gradient (PCG2) solver was used for the transport solution of each simulation.

FINDINGS AND CONCLUSIONS

It was found that the 90 day pumping scenario was of insufficient duration to show the impacts from the different extraction methods and demonstrates the need to consider the time required to reach a new equilibrium.

The results of the first simulation (**Figure 1a**) demonstrates that after pumping the deep fully penetrating well for 900 days, drawdown in the well will be approximately 0.9 meters (specific capacity = 427 m^3/day/m), and water containing in excess of 2,000 mg/L TDS will upcone into bottom of the well. The second simulation (**Figure 1b**) shows that after 900 days, the drawdown in the shallow well will be approximately 2.4 meters (specific capacity = 160 m^3/day/m) and water with a salinity of over 1,000 mg/L TDS will still reach the bottom of the well. The third simulation using the horizontal drain will result in less than 0.5 meters of drawdown at the middle of the trench, with less at the ends (**Figure 1c**), and has the least amount of upconing. The salinity of the water entering the trench ranges from less than 200 mg/L TDS at the ends of the trench to approximately 600 mg/L TDS at the center (**Figure 1d**). Assuming complete mixing, water with salinity on the order of 350 mg/L TDS could be withdrawn from the trench.

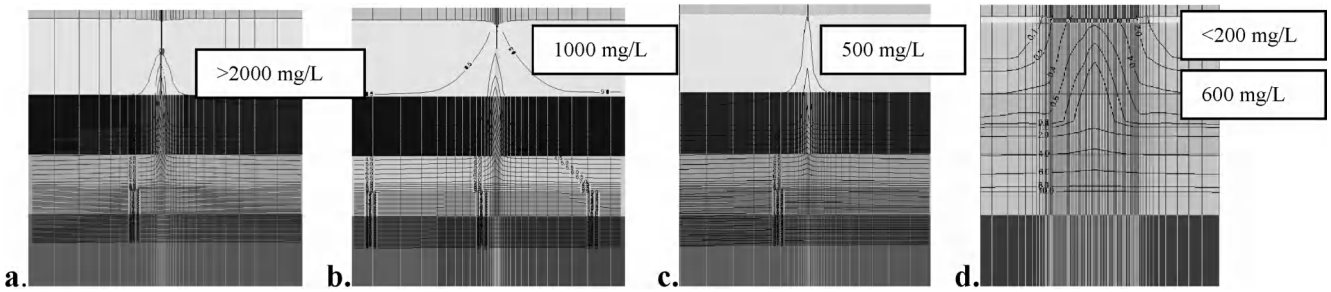

Figure 1.

The concept discussed above was used for an irrigation system expansion located less than 150 meters from a saltwater canal in Naples, Florida. The system had previously pumped irrigation water from an unlined pond that was replenished from a single, 18.3 meter deep well. An increase in the Water Use Permit allocation was requested, but the South Florida Water Management District was reluctant to issue the permit due to the risk of saltwater intrusion and upconing.

As an alternative, a 192-meter long shallow drain oriented perpendicular to the direction of shallow groundwater flow along the upgradient side of the property was proposed. The invert of the perforated pipe in the drain was set at one foot above sea level. Modeling **(Figure 2)** predicted, and experience has confirmed, that the drawdown along the length of the pipe is minimal compared the single well, and the watertable quickly recovers following cessation of pumping. In spite of recent drought conditions, the system has supplied adequate quantities of irrigation water with no indications of saltwater contamination or impacts to nearby wetlands. In

contrast, a nearby deep well continues to replenish a similar pond from which irrigation water is withdrawn. The salinity in that neighboring pond is more than double that in the pond with the horizontal drain, even though it is located farther from the sea.

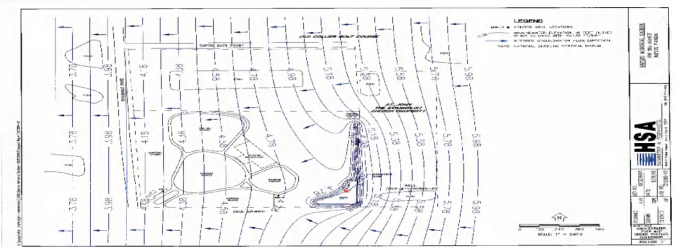

Figure 2.

Where conditions are suitable, large users of irrigation water (*esp.* golf courses, nurseries, subdivisions, cemeteries, etc.) should be encouraged to develop similar approaches to protecting groundwater resources from saltwater intrusion.

REFERENCES

Aharmouch, A., Larabi, A. 2001. Numerical Modeling of Saltwater Interface Upconing in Coastal Aquifers. Proceedings, First International conference on Saltwater Intrusion and Costal Aquifers – Monitoring, Modeling, and Management. Essaouira, Morocco,

Bower, J.W., Motz, L.H., and Durden D.W. 1999. Analytical solution for determining the critical condition of saltwater upconing in a leaking artesian aquifer, J. Hydrol., vol 221, 43-54

Hamza, K. I. 2006. Numerical Analysis of Saltwater Upconing Beneath a Pumping Well. Proceedings, 10th International Water Technology Conference, IWTC10 2006, Alexander, Egypt

Langevin, C.D., 2003. SEAWAT-2000, the U.S. Geological Survey Modular Ground-Water Model and the integrated MT3DMS Transport Process: U.S. Geological Survey Open-File Report 03-426, 43 p. Tallahassee, Florida.

Mather, J.D., 1975. Development of Groundwater Resources of Small Limestone Islands; Quarterly v.8, p. 140-150

Zhou, Q., Bear, J., and Bensbat, J. 2004. Saltwater Upconing and Decay Beneath a Well Pumping Above an Interface Zone

Contact Information: David Tarbox, HSA Engineers & Scientists, 6019 E. Fowler Ave., Tampa, FL, USA, Phone 813-971-3882, FAX 813-971-1862; Email dtarbox@hsa-env.com

An Assessment of the Impact of Geologic Heterogeneity on Predictions of Seawater Intrusion in Coastal Aquifers

Whitney J. Trainor[1], *R. Knight*[1] and *J. Caers*[2]
[1]Geophysics Department, Stanford University, Stanford, CA, USA
[2]Energy Resources Engineering, Stanford University, Stanford, CA, USA

INTRODUCTION

Coastal communities throughout the world are facing the threat of seawater intrusion due to extensive pumping of groundwater aquifers. A great need exists for water management strategies that can address these aquifer overdrafts. Effective groundwater management requires subsurface hydrogeologic models but also requires an assessment of the uncertainty of these models. How simple can the subsurface model be while still providing accurate predictions? The risks associated with poor predictions could justify the cost of collecting additional high quality data. The long-term goal of our research is to develop methodologies that quantify the value of information (VOI) derived from geophysical data for the benefit of water managers. The work presented in this paper represents an initial sensitivity analysis of the impact of geologic heterogeneity on predictions of the extent of seawater intrusion.

DECISION ANALYSIS METHOD

By developing a VOI methodology for geophysical data for water managers, we hope to build a tool that will address the question: 1) When are geophysical data worth the cost of acquiring? Modern decision theory has been developed to address questions of this nature. The general approach for this study is borrowed from a decision analysis procedure (Howard 1966). The reason for this approach is twofold. Firstly, decision analysis provides a probabilistic platform for engineers, scientists, managers and legal staff to communicate across expertise. And secondly, with decision analysis tools the "dollar value of uncertainty" can be assessed, thus providing a needed perspective on the cost of acquiring additional information.

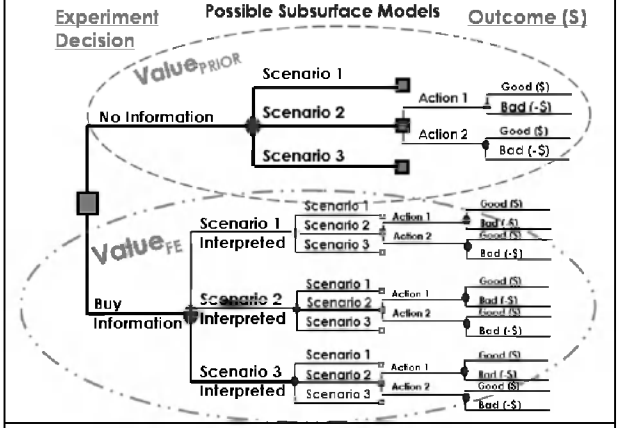

Figure 1. Decision Tree. Red: possibility nodes. Blue: decision node. Purple: Prior Value. Orange: Value with free experiment.

Decision analysis can be described in three phases: a sensitivity analysis, a probabilistic evaluation, and the postmortem analysis (Howard, 1966). In the sensitivity analysis, the decision, the profit function and the state variables all must be defined. The state variables are defined by testing which parameters affect the output (the profit function) the most. The uncertainty of each of these variables (that are deemed important in the sensitivity analysis) is evaluated in the stochastic phase. The postmortem phase evaluates whether the decision maker is comfortable with the level of uncertainty. Figure 1 demonstrates a decision tree, which is constructed using the information gathered in the first two phases. The blue square nodes of the tree represent the decisions to be made; red nodes represent the possibility nodes (some branches omitted due to space limitations). For our case, the key state variables are the possible scenarios of the subsurface. Therefore, in the stochastic phase, the probabilities gathered are assigned to

each of the different subsurface scenarios. The purple dashed line encircles the information that was used to calculate the expected value of this decision without additional information.

Suppose the decision makers do not feel comfortable with the level of uncertainty regarding the outcomes of a decision and consequently decide to gather more information prior to making a decision. The bottom branches of Figure 1 (contained in the orange circle) demonstrate how interpreted geophysical information is treated as the additional information. The concept of the "value of information" (VOI) offers guidance on how the change in uncertainty should influence a decision. VOI is the expected gain in value after conditioning on the relevant new information, or the difference between the value after a free experiment (V_{FE}) and the value prior (V_{PRIOR}).

$$VOI = V_{FE} - V_{PRIOR}$$

Note that VOI is independent of the cost of information gathering (Eidsvik et al, 2007). If the VOI is greater than the cost of the experiment, then it is a sound decision to perform (purchase) the experiment.

SENSITIVITY ANALYSIS FOR A HYDROGEOLOGICAL PROBLEM

The goal of the first stage, the sensitivity analysis, is to determine which state variables affect the profit function the most. Modeling in subsequent stages will then focus on these variables. State variables and profit functions are straightforward for typical business problems. To demonstrate how a hydrogeologic problem can be framed in these terms, this study uses a hypothetical example of a coastal basin. In this example, we consider a scenario where the coastal aquifers are over-drafted due to a $250 million agricultural industry, which takes 90% of its water from the groundwater. This has resulted in seawater intrusion. We model a situation where the water managers have used artificial recharge to remediate some of the seawater intrusion. However, water managers question whether the costs of recharge are justified given the uncertainty of the heterogeneity of subsurface flow properties.

The key state variables in this study are the parameters that control seawater intrusion and artificial recharge: heterogeneity parameters such as the type of geologic depositional system present, the clay (flow-barrier) percentage, and clay spatial distribution. The two interpreted geologic depositional settings are fluvial and estuarine. Figure 2 displays the two different training images (TI) that were used to represent these depositional patterns and were used in the multiple-point geostatistical algorithm SNESIM (Strebelle, 2002) to generate subsurface models of clay and sand distribution (Figure 3). Thirty-six different facies realizations were generated and populated with permeability values ($1x10^3$mD for clay and $1x10^5$mD for sand).

In this study, reservoir flow simulation is a function that transforms the state variables of clay location and proportion into profit. Under the same pumping conditions, flow simulation is performed on each permeability model with the seawater modeled as a pressure-dependent boundary condition.

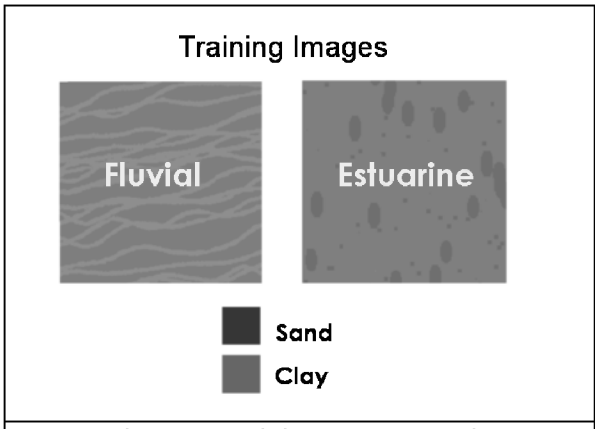

Figure 2. Training Images used in SNESIM algorithm

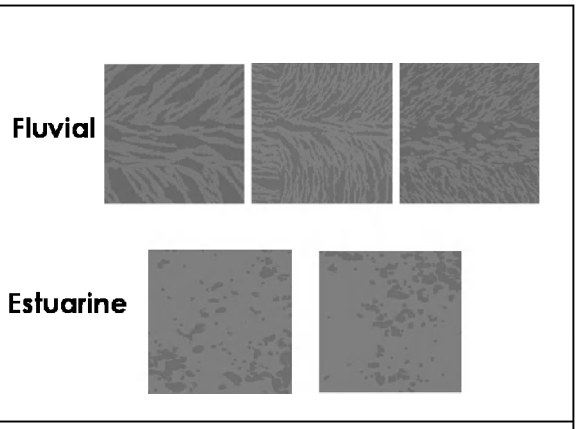

Figure 3. Example Realizations

SENSITIVITY ANALYSIS RESULTS

As described, the goal of the sensitivity analysis is to identify which state variables impact the profit function the most. The tornado charts, shown in Figures 4-6, display the input (either the TI or the channel connectivity) on the left and the output (the salt produced at the pumping wells) on the right. The salt produced at the well represents the revenue potential for each model. Figure 4 shows all models with 12% clay. The variance in the salt production for the models with 12% clay is almost 5 times greater for the fluvial models than the estuarine models. Variance is almost twice as great in models with 25% clay.

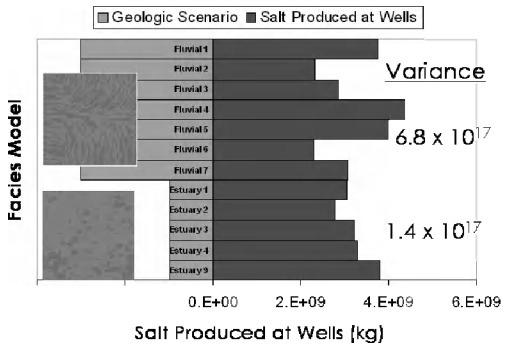

Figure 4. All models with 12% clay, top group from fluvial TI, bottom from Estuarine TI

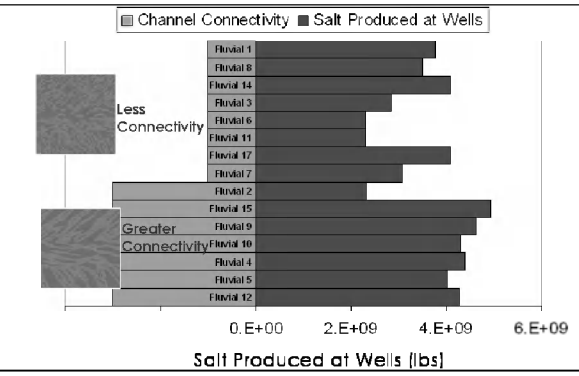

Figure 5. All Fluvial Models

Figure 5 shows the salt production results for all fluvial models, with the top group having less channel connectivity.

CONCLUSIONS AND FUTURE WORK

After performing the sensitivity analysis, it was found that the profit function was most sensitive to the fluvial training image, clay percentage and channel locations. Channel identification is critical in locating the preferential flow paths for seawater intrusion. Therefore, it will be these variables that will be included in the next stage, the stochastic phase, in the decision analysis framework.

Recall the expression for VOI: $VOI=V_{FE}-V_{prior}$. The prior value calculation reveals value without data. The posterior value is calculated using data. To initiate the stochastic phase, another set of multiple, equi-probable permeability realizations are used to represent the prior

value. This time we consider the maximum value of four actions on each realization. Three of the actions will perform artificial recharge at 3 different locations. The last flow simulation will be performed without artificial recharge. The value of one flow result will be evaluated at time = 40 years:

$$V_{FE} = R \times \sum_{i=1}^{N} \phi_i (s_{fresh_i}) - C$$

where R is the revenue for the area of crop that could be grown by groundwater in gridblock *i* (if below a salinity threshold), N is the total number of gridblocks, ϕ_i is the porosity, and s_{fresh_i} represents the saturation of fresh water at gridblock *i*.

Location of preferential flowpaths is the key subsurface uncertainty that will determine the value of the subsurface model after a 40 year simulation. We will consider the use of airborne EM data to obtain information on lithology (clay or sand). Figure 6 displays the workflow for calculating flow models conditioned to geophysical data.

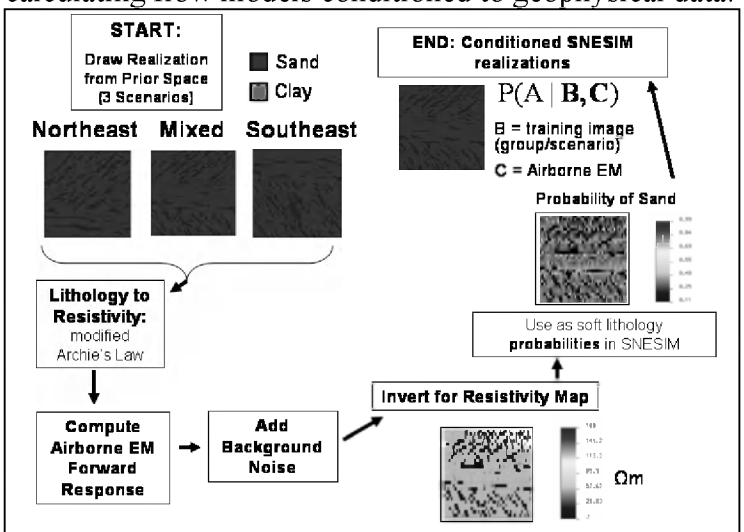

Figure 6. Workflow for conditioning lithology models to EM data

SNESIM realizations will use the inverted geophysical models as a soft probability for sand or clay locations. These SNESIM conditioned models are used to calculate V_{FE}. Flow simulations will be performed using these models to find the maximum value of all 4 actions (described above), allowing us to calculated the total value with the free experiment. In the final step, the value of information will be calculated: VOI = $V_{FE} - V_{prior}$.

ACKOWLEDGMENTS

The authors would like to acknowledge the support of Schlumberger Water Services and the affiliates of Stanford Center for Reservoir Forecasting. Discussions with Tapan Mukerji and Debarun Bhattacharjya contributed to this work.

REFERENCES

Eidsvik, J., Bhattacharjya, D., and Mukerji, T. [2007] Estimating the value of information in spatial decision making for reservoir development, *Society of Exploration Geophysics Annual Meeting*, Expanded Abstracts, 26, pp. 1367-1371.

Howard, R.A. [1966] Decision analysis: applied decision theory, *Proceedings of the Fourth International Conference on Operational Research*, Wiley-Interscience, pp. 55-71.

Strebelle, S. [2002] Conditional simulation of complex geological structures using multiple-point statistics. *Mathematical Geology*, V. 34, No. 1, 1-26.

Contact Information: Whitney J. Trainor, Geophysics Dept., Stanford University, 397 Panama Mall, Stanford, CA 94305 USA, Phone: 650-575-8661; Fax: 650-725-7344, Email: wtrainor@stanford.edu

Saltwater Intrusion and Hydraulic Conductivity Estimation in East Baton Rouge Parish, Louisiana

Frank T-C. Tsai and *Xiaobao Li*
Department of Civil and Environmental Engineering, Louisiana State University, Baton Rouge, LA, USA

ABSTRACT
This research developed a regional saltwater intrusion model to study the on-going saltwater intrusion problem in East Baton Rouge (EBR) Parish, Louisiana. The model was based on SEAWAT. We used multiple generalized parameterization (GP) methods and Bayesian model averaging (BMA) method to estimate spatially correlated hydraulic conductivity. The model was applied to saltwater intrusion simulation in the "1,500-foot" sand for 90 years. The simulation results indicated that major saltwater intrusion would bypass the current network of monitoring wells and reach the Lula Avenue pumping center within 75 years via the west side of the monitoring well, EB-807A. Additional observation wells would be needed to place at the west of EB-807A to monitor potential large saltwater intrusion.

INTRODUCTION
This research studied the saltwater intrusion problem in East Baton Rouge (EBR) Parish. In EBR, there are twelve freshwater aquifers. Ten of the aquifers were originally named according to their general depth in the Baton Rouge industrial district (Meyer and Turcan 1955). Most of the aquifers have been reported the saltwater intrusion problem for more than fifty years due to excessive groundwater withdrawal. In this study, we focused on the "1,500-foot" sand, which is one of the major sources of drinking water in EBR. Groundwater withdrawal from the "1,500-foot" sand began in 1927 (Torak and Whiteman 1982). From 1940 to 2001 water level has declined about 52.8 meters (160 ft) at the observation well EB-168. To better understand the on-going saltwater intrusion problem in the "1,500-foot" sand, this study adopted SEAWAT (Guo and Langevin 2002) to develop a saltwater intrusion model.

METHODS

Data collection and groundwater model calibration
The study area shown in Figure 1 extended about 300 km^2 and included major part of the Baton Rouge metropolitan area. Northern area of the Baton Rouge Fault was the "1,500-foot" sand and southern area of the fault was the "1,200-foot" sand. Through the USGS National Water Information System website, we collected 706 groundwater head data from 18 observation wells located at the "1,500-foot" sand (see Figure 1a). These head data were recorded between January 1990 and December 2004 and were used to calibrate the groundwater model. The groundwater data at well EB-780A at the "1,200-foot" sand determined the south boundary condition. The Louisiana Capital Area Ground Water Conservation Commission (CAGWCC) provided monthly pumping data of 16 production wells located in the study area (see Figure 1b). The specific storage was 0.0000221 $meter^{-1}$. We used the groundwater data at EB-917 and EB-780A to estimate hydraulic characteristic (HC) for the Baton Rouge fault. The identified HC value was 0.000155 day^{-1}. USGS Water Resources Division in Louisiana provided electrical resistivity data at 21 E-log sites (see Figure 1a). The resistivity data determined the thickness of the "1,500-foot" sand as well as the average formation resistivity. We used the Archie's law to interpret the formation factor into porosity and used the Kozeny-Carman equation to estimate hydraulic conductivity.

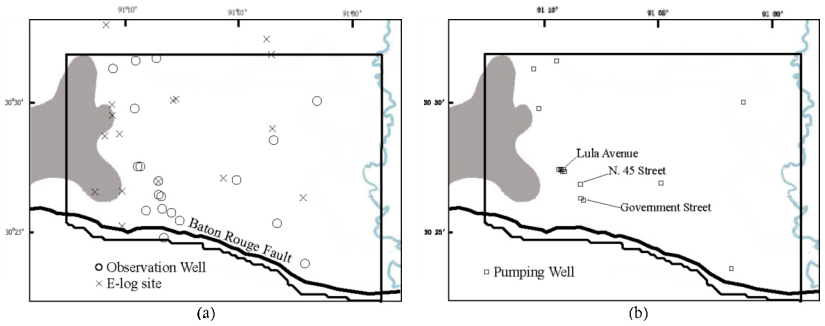

Figure 1. The study area.
(a) The location of groundwater head observation wells and E-log wells.
(b) The location of production wells.

We adopted the generalized parameterization (GP) method (Tsai 2006) and Bayesian model averaging (BMA) approach (Hoeting et al. 1999) to estimate the hydraulic conductivity distribution. Three GP methods were considered in the BMA including NN-VT (combination of natural neighbor interpolation and Voronoi tessellation methods), ID-VT (combination of inverse distance interpolation and Voronoi tessellation methods), and OK-VT (combination of ordinary kriging and Voronoi tessellation methods). The identified hydraulic conductivity distribution was shown in Figure 2a. Figure 2b showed the groundwater head distribution for April 2001.

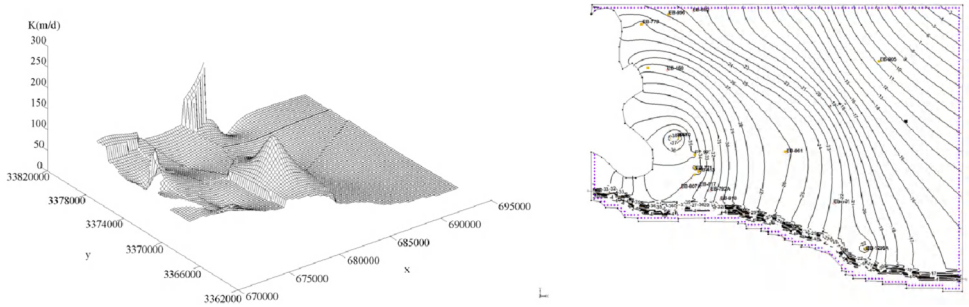

Figure 2. (a) The hydraulic conductivity distribution using BMA.
(b) The groundwater head distribution for April 2001.

The groundwater model also incorporated the connector well, EB-1293, which connects the "800-foot" and "1,500-foot" sands. The CAGWCC installed EB-1293 between the municipal supply wells on Government Street and the freshwater-saltwater interface in the "1,500-foot" sand. The connector well started to operate in 1998 as an initial test of a recharge barrier to mitigate saltwater encroachment in the "1,500-foot" sand. The recharge rate from the "800-foot" sand was estimated around 500 gallons per minute (gpm) (CAGWCC Newsletter, January 2002). The groundwater model considered the connector well as a recharge well with a rate of 500 gpm.

RESULTS

Using individual zonation and interpolation methods, the NN method gave better model goodness of fit to the groundwater head observations than the ID and OK methods. Nevertheless, three GP methods significantly reduced the fitting residuals and performed better than the zonation and interpolation methods. The fitting residual could not be reduced much because large model error came from model structure error. The identified hydraulic conductivity distribution using BMA with three GPs was obtained. Using BMA, we found that the within-GP

variances were much higher than the between-GP variances. This was because the GP methods resulted in similar hydraulic conductivity distributions.

The saltwater intrusion simulation results showed the following observations:

(1) Saltwater had strong lateral transport along the Baton Rouge Fault once it crossed the fault. The cause of saltwater intrusion is due to the huge cone of depression formed by the production wells at Lula Avenue. The salt dispersion width at the region east of EB-918 was around 850 meters from the fault and was almost unchanged after 30 years simulation.

(2) Saltwater accumulated at two spots. One spot was at 600 meters southeast of EB-807A. Higher salt concentrations migrated clockwise across EB-807A toward the Lula Avenue pumping center. The other spot was at 2200 meters southwest of EB-807A.

(3) The 100 ppm isochlor (the front line) migrated to the production well adjacent to the observation well, EB-1295A, before year 2035.

(4) The 100 ppm isochlor first touched down the observation well, EB-918, and few years later it touched EB-807A. Due to the clockwise movement of saltwater along the fault from the east, the salt concentrations in EB-807A and EB-918 were similar.

(5) The 100 ppm isochlor touched EB-917 and EB-792A almost at the same time. The simulation results showed similar salt concentrations in EB-917 and EB-792A due to the clockwise movement of saltwater along the fault.

(6) Before year 2080, the 100 ppm isochlor reached the Lula Avenue pumping center.

(7) Saltwater began to move eastward approaching the Government Street pumping center after year 2035.

(8) The connector well demonstrated halting the saltwater intrusion northward approaching the Government Street pumping center.

(9) Although the saltwater was close to the Government Street pumping center, the simulation results showed that saltwater would reach the Lula Avenue pumping center before it reached the Government Street pumping center.

CONCLUSIONS

Using multiple generalized parameterization (GP) methods with Bayesian model averaging (BMA) was able to consider non-uniqueness in parameterization methods for groundwater inverse modeling. According to the simulation results major saltwater intrusion would bypass the current network of monitoring wells and reach the Lula Avenue pumping center within 75 years via the west side of EB-807A. An array of additional monitoring wells is suggested at the west of EB-807A to monitor potential large saltwater intrusion.

ACKNOWLEDGMENTS

This research was supported in part by Louisiana Board of Regents under award LEQSF(2005-08)-RD-A-12 and Department of the Interior, U.S. Geological Survey under Grant No. 05HQGR0142 in collaboration between USGS and LSU A&M College. We acknowledge Don Dial at CAGWCC and Dan Tomaszewski at USGS for invaluable discussions.

REFERENCES

Hoeting, J.A., D. Madigan, A.E. Raftery, and C.T. Volinsky, 1999, Bayesian model averaging: A tutorial. Statistical Science 14(4), 382-401.

Guo, W., and C.D. Langevin, 2002, User's guide to SEAWAT: A computer program for the simulation of three-dimensional variable-density ground-water flow. U.S. Geological Survey Open-File Report 01-434.

Meyer, R.R., and A.N. Jr. Turcan, 1955, Geology and ground-water resources of the Baton Rouge area, Louisiana, U.S. Geological Survey Water-Supply Paper 1296, 138p.

Torak, L.J., and C.D. Whiteman, 1982, Applications of digital modeling for evaluating the ground-water resources of the "2,000-foot" sand of the Baton Rouge area, Louisiana, Louisiana Department of Transportation and Development, Office of Public Works Water Resources Technical Report no. 27, 87p.

Tsai, F.T-C., 2006, Enhancing random heterogeneity representation by mixing the kriging method with the zonation structure: Water Resources Research, 42, W08428, doi:10.1029/2005WR004111.

Contact Information: Frank T-C. Tsai, Department of Civil and Environmental Engineering, Louisiana State University, 3418G Patrick F. Taylor Hall, Baton Rouge, LA 70803-6405 USA; Phone (225) 578-4246; Fax (225) 578-4945; Email: ftsai@lsu.edu

Evolution of Seawater Intrusion in Coastal Aquifers of Pontina Plain (Italy)

Luigi Tulipano[1], *M. D. Fidelibus*[2], *G. Sappa*[1] and *M. T. Coviello*[1]
[1]Department of Hydraulics, Transportation and Roads, Sapienza University of Rome (Italy)
[2]Department of Civil and Environmental Engineering - Politecnico di Bari (Italy)

ABSTRACT
In the last ten years it has been carried on a research project on the evolution of seawater intrusion in coastal aquifers of Pontina Plain (Italy). As a matter of fact groundwater in the coastal plain between Sabaudia and Terracina, south of Latina, Latium shows a number of problems, including salinization deriving from sea water intrusion or from different processes and from the superimposition of theirselves. The test site is an area of about 80 km2, most part of which coastal and wetland since the beginning of the previous century. In the last fifty years, when the wetland became a plan, they have been stood up in it many different human activities like industrial firms, and agricultural plantations, which represent the most part of fruits and vegetables feeding people of Centre Italy. The effects of groundwater overexploitation on seawater intrusion and on groundwater resource availability start nowadays to be sensitive. In this paper are presented and discussed the results of the study, which involved the analysis of 4891 stratigraphical reports, 91 VES (Vertical Electrical Soundings) utilizing the Schlumberger electrode array, driven in 2004, starting from the results of two previous geophysical investigation campaigns achieved in 1952 first, and in later sixties later, 45 logs meter by meter (CTD data, TDS and PH measurements), 58 groundwater level measurements, driven in 2004, 15 isotopic analysis on ground water samples. As it could be well understood it has been adopted a multisystem approach based on the integrated application of different investigation methods to set up the actual framework of seawater intrusion and the evolution it has had in the last fifty years.

INTRODUCTION
Groundwaters in the coastal plain between Sabaudia and Terracina, at the south of Latina, in the Latium region (Italy) show a number of problems, including salinization deriving from sea water intrusion, and from different processes. The test site is an area of about 80 km2, most part of which coastal and wetland since the beginning of the previous century. In the last fifty years, when the wetland became a plan, they have been stood up in it many different human activities like industrial firms, and agricultural plantations, which represent the most part of fruits and vegetables feeding people of Centre Italy. The total territorial crop's water requirement is about 20*106 m3/a, mostly satisfied by groundwater withdrawals; but the area is nowadays crossed by two main nets of irrigation canals, because complementary irrigation is an highly efficient resource to increase such yields. In this umid region, the periodic occurrence of droughts of different intensity is one of the most important factors in the variability of crop yield.

The uncontrollable withdrawal and the release of contaminants is slowly but continuosly leading to the deterioration of the resource. A particular question of the Pontina plain which worry, because of its incidence on the resource, is a remarkable expansion of kiwi and mais growing in the last ten years. Thanks to a favourable clima and the water availability for the irrigation, they constitute a good profit, but on the other side, they increase much the total water abstraction per year and the effect of enriching soils of nitrates coming from crops fertilization.

GEOLOGICAL AND HYDROGEOLOGICAL FRAMEWORK

Geologically the area is included in an ancient tectonic hollow, over 800 meters deep, and covered by recent Quaternary deposits, made of sands, silts and clays. More ancient outcroppings are located along the south west coast and are represented by organogeous limestones or Pliocene and Pleistocene clay. (Figure 1)

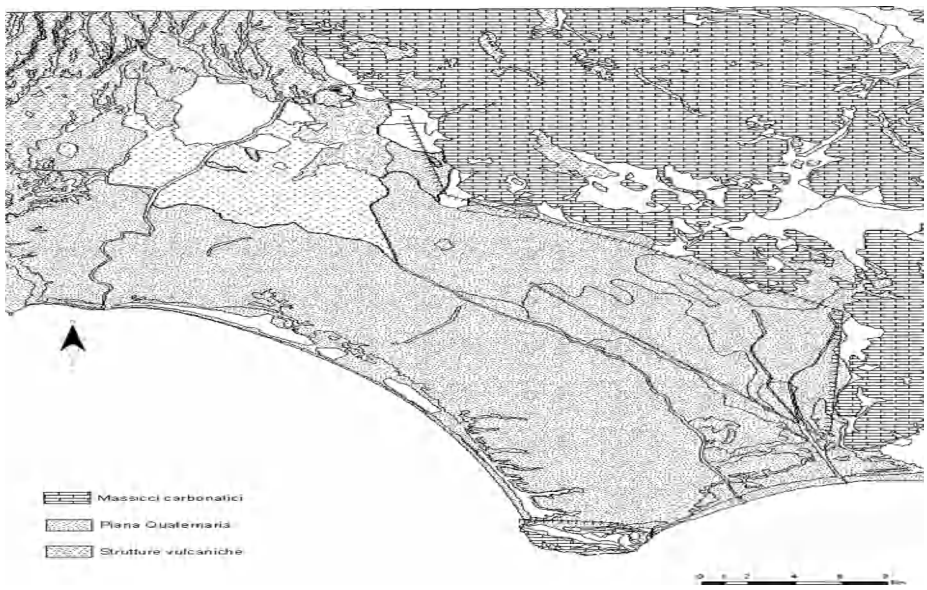

Figure 1. The geological sketch

Stratigraphic data collected by the interpretation of deep borehole and geophysical investigation show that above the Mesozoic–Cenozoic limestone deposit, characterized by normal faults sets, the following sequence is found (Accordi, 1967):

- Upper Pliocene clay passing to calcarenite in the sectors closer the Lepini ridge.
- Lower Pleistocene clay - Middle Pleistocene littoral deposits passing to saltier transitional deposits. These sediments contain large amounts of reworked pyroclastic deposits.
- Marine and transitional clays, sands and gravels deposited during the Upper Pleistocene. Northward of the Plain, volcanic activity of the Colli Albani complex was initiated.
- Large amounts of peat deposited in the continental fluvio-lacustrine basins during the Holocene.

The Pontina Plain sedimentary succession first developed from a marine depositional system to a transitional fluvial–coastal system, and then to a fluvial–continental depositional system (all of this within the Pliocene–Pleistocene). Therefore, the entire system is characterized by both vertical and lateral variability that is strongly reflected in its hydrodinamic trend.

Four different aquifers have been distinguished in. As a matter of fact there are two shallow aquifers made by sands the first, and by eluvial deposits the latter, which are separeted by the deeper carbonatic one by a clay layer. The Sisto stream represents a drainage axis for these two Quaternary formation aquifers. The first, the dune aquifer (at the western zone of Sisto), in fact, floats on the sea and it is drained by the lakes, the sea and partially by Sisto stream, that delimits

the Pontina depression at south - west. The second one, corresponding to the inner band of the coast (to the eastern bank of Sisto), is constituted by fluvial marsh outcrops, and is characterized by a lower permeability (10^{-6} m/s). The composition of these strata is really variable, and as a consequence of it, the different hydraulic conductivity of them makes the aquifer a multistrata one. Nevertheless the groundwater circulation can be considered unique, thanks to water exchange among the different strata, the thickness of which is not defined, because of its geological complexity which makes it very variable from point to point inside the area.

The fourth and minor aquifer is a suspended one, and it is localized between the sea and the litoral sandbank (dunal cordon), characterized by low storage coefficient. (Conforto B., Di Ricco G., Sappa M.,1962)

EXPLORATION APPROACH AND METHODS

The aim of the present work is the recognition, dating and genesis of groundwaters salinization. Its reliability results by testing the feasibility of different investigation methods to map spatial variation of it, in the last thirty years, and by comparing the results obtained by the interpretation of each detecting method afterwards described:

- Analysis of 4891 stratigraphical report on the local scale of the test site
- 91 Vertical Electrical Soundings

  Starting from the results of two previous geoelectrical investigation campaigns, a new SEV campaign has been important to locate the evolution of saltwater intrusion and a probable trend of it.
- 46 Temperature and conductibility logs

  The temperatures and conductivity profiles, building their trend along vertical and horizontal sections, have been very useful in the recognition of flow systems, preferential grounwater pathways and salinisation origin
- 15 Chemical and isotopic analyses on D and ^{18}O composition of groundwater

RESULTS

In the following figure 3 it is shown an example of overlaying the VES results on the geological section build up by the analysis of stratigraphical reports. On the other hand in the following figures 4 and 5 they are presented the results of different geoelectrical investigation campaign and the difference in electrical resistivity distribution between nowadays investigation and one carried on in 1967.

The other investigations carried on in this project was aimed to verify the results of geoelectrical investigation, and to be sure that electrical resistivity decrease is due actually to seawater intrusion.

DISCUSSION AND CONCLUSIONS

As it can be well point out there are areas where electrical resistivity has descreased of more than 80% as in the shallower layer investigated as in the deeper one.

The other investigations carried on in this project was aimed to verify the results of geoelectrical investigation, and to be sure that electrical resistivity decrease is due actually to seawater intrusion.

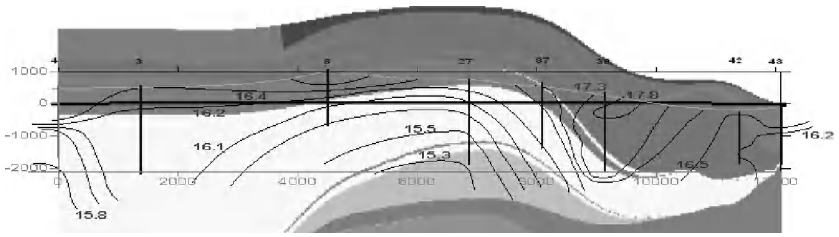

Figure 3 – Overlaying of geological section and geoelectrical interpretation

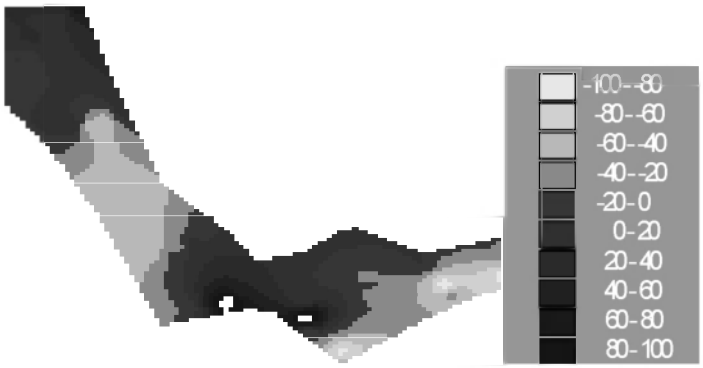

Figure 4 – Difference in percentage of electrical resistivity distribution between 2003 and 1967 investigation campaigns with Sclumberger array AB = 60 m

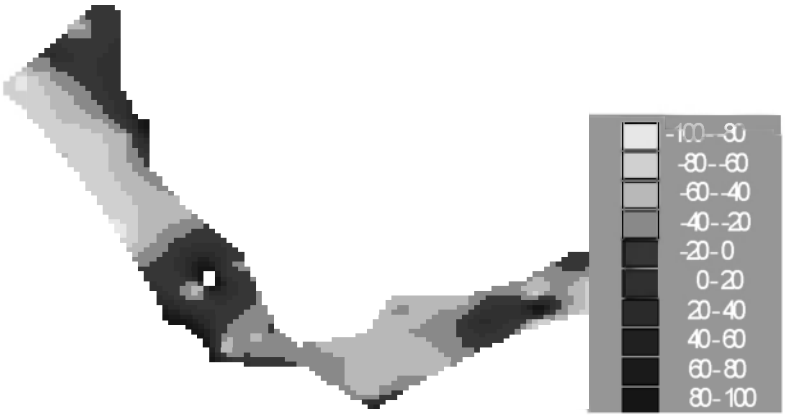

Figure 5 – Difference in percentage electrical resistivity distribution between 2003 and 1967 investigation campaigns with Sclumberger array AB = 1000 m

REFERENCES

Accordi B. (1966) - La componente traslativa ne/la tettonica dell'Appennino laziale - abruzzese. Geologica Rom., v. 5, 355-406.

Conforto B., Di Ricco G., Sappa M. (1962) – Indagine sulle acque sotterranee dell'Agro Romano e Pontino – parte seconda: Agro Pontino

Contact Information: Luigi Tulipano - Department of Hydraulics, Transportation and Roads, Sapienza University of Rome (Italy) – Via Eudossiana, 18 – 00186 Rime (ITALY) – Tel. +393396917983 Fax +390644585016 – Email: luigi.tulipano@uniroma1.it

Artificial Recharge of Fresh Water in the Belgian Coastal Dunes

Alexander Vandenbohede[1], *Luc Lebbe*[1] and *Emmanuel Van Houtte*[2]
[1]Geology and Soil Science, Ghent University, Gent, Belgium
[2]Intermunicipal Water Company of the Veurne region (IWVA), Koksijde, Belgium

ABSTRACT
Since July 2002, the Intermunicipal Water Company of the Veurne region (IWVA) artificially recharges fresh water in the dunes of the western Belgian coastal plain by means of two recharge ponds. This recharge water is produced from secondary treated waste water effluent by the combination of ultra filtration and reverse osmosis. The artificial recharge project loops the water cycle: extracted water goes to the users and their waste water is purified and re-used. In this paper, the results of simulations of the artificial recharge are discussed and descriptions of the hydrochemistry of dune water, recharge water and extraction water are given. This artificial recharge project is an example of sustainable water management in coastal aquifers.

INTRODUCTION
The dunes of the western Belgian coastal plain are of importance as source of fresh water. In the surrounding areas (sea, shore and polder) mainly brackish to salt water is found. Otherwise, fresh water lenses which are present in the polder contain very limited fresh water resources (Vandenbohede and Lebbe, 2002). Groundwater exploitation in the dune aquifer for the production of drinking water started in 1947 at the water extraction site St-André by the Intermunicipal Water Company of the Veurne region (IWVA). The IWVA is responsible for the distribution of drinking water in the western part of the Belgian coastal plain. The extraction rate rose steadily from about 0.5 million m³/y during the 1950s to 1.75 million m³/y during the 1960s. From then on extraction rate fluctuated around 2 million m³/y up to the second millennium. Initially the water extraction started with one well battery with 109 wells. In 1968, a second well battery was put in use with 54 wells. Extraction rates of both well batteries were more or less the same. Extraction wells have screens between 6 and 10 m below surface or between 12 to 16 m below surface. In 2002, 70 wells were active with the first well battery and 112 wells with the second well battery. To ensure a water extraction which meets the demands and preserve further the ecological values of the dunes, it was decided to artificially recharge the dune aquifer. This started in July 2002 and is an example of sustainable water management in coastal aquifers. The aim of this paper is to illustrate some characteristics and benefits of the artificial recharge project.

The system which is used consists of two ponds which are in the centre of the wells of well battery 2 (figure 1). The two ponds are connected to each other through a pipe. The recharge water is effluent from a nearby waste water treatment plant. Before recharge, this effluent is further treated using ultra filtration (UF) and reverse osmosis (RO) (Van Houtte and Verbauwhede, 2005). The recharge water is thereafter extracted via the wells of well battery 2. These wells are situated north and south of the ponds. The artificial recharge project loops the water cycle: extracted water goes to the users and their waste water is purified. After UF and RO treatment, this water is recharged in the dune aquifer and can be reused. Up to 2.5 million m³/year can be recharged and the same amount of water can be extracted. Additionally 1.7 million m³ natural dune water can be extracted (1 million by well battery 2 and 0.7 million by well battery 1). This means that the capacity of the water extraction has more than doubled (from 2 million to 4.2 million m³/year) whereas the net amount of water extracted from the dune

aquifer is reduced from 2 million to 1.7 million m³/year. This way of reusing limited fresh water resources in a sustainable way remains up to the present day a unique system in Europe.

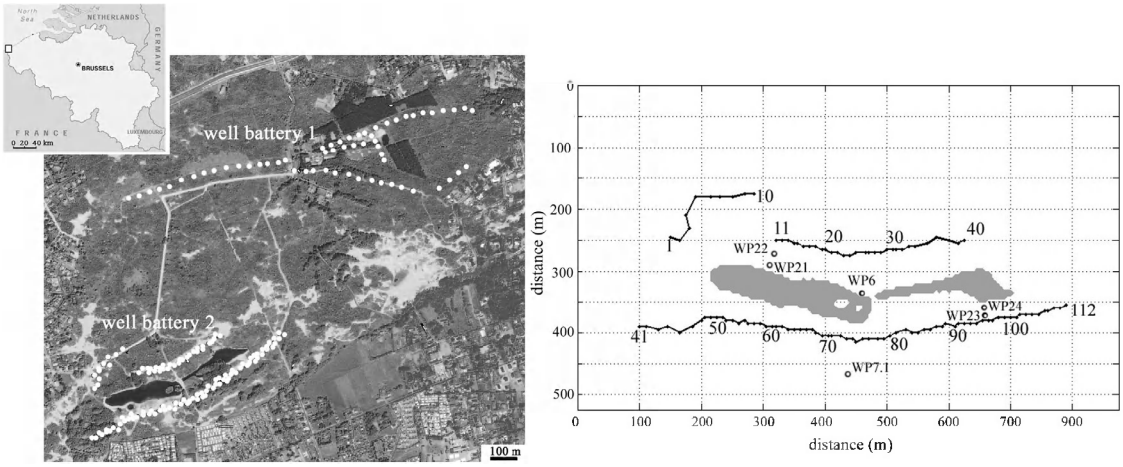

Figure 1. Location of the St-André water extraction in the dunes of the western Belgian coastal plain. Location of both well batteries and the artificial recharge pond between the wells of well battery 2 are indicated. Right figure gives a detailed overview of the location of wells of well battery two, the two ponds and some observation wells.

GROUNDWATER FLOW MODELLING

Since July 2002, a large number of data (hydraulic heads; water quality data of recharge water, extraction water and groundwater; borehole measurements, tracer tests) has been gathered. The combination of these different data sets give a unique insight in the hydraulics and hydrochemistry in the vicinity of recharge ponds and the water extraction. First step in the analyses of the data is the construction of a groundwater flow model. This was done in two steps. In first instance, a regional density dependent flow model of the dunes and neighbouring sea and polders was made (Vandenbohede et al., in review a), using MOCDENS3D (Oude Essink, 1998) and the Visual MOCDENS3D user interface (Vandenbohede, 2007). The model measures 4200 by 4500 m and includes the quaternary phreatic aquifer. The aquifer is subdivided in 12 layers, 60 columns and 56 rows (height 2.5 m, width and length 75 m) resulting in 40320 finite difference cells. The natural salt-fresh water distribution is calculated after which the extraction history up to the present day is included in the model. Artificial recharge results in a general increase in fresh water heads corresponding to the situation in 2002. In the vicinity of the infiltration ponds there is an important increase of the fresh water heads. Also of importance is the fact that the natural flow of fresh water from the dunes towards the sea and the polder is restored in large parts of the aquifer. This flow was importantly reduced before the artificial recharge project. In second instance, a more detailed model was made of the vicinity of the ponds (Vandenbohede et al., in review b). This model measures 975 by 525 m and consists of 105 rows and 195 columns. Dimension of every finite-difference cell is 5 by 5 m and 12 layers are considered each with a thickness of 2.5 m. The boundary conditions of this model are derived from the larger regional flow model. This model shows the increase of the amount of recharged water (about 50 mg/l) in the fresh ground water (about 550 mg/l). Modelling shows further that the depth of the lens of recharge water under the eastern pond is slightly less than 20 m whereas this is slightly more than 20 m for the western pond. This was confirmed by geophysical borehole measurements. Because of its larger surface, more recharge water is present under the western than under the eastern pond. Groundwater flow and flow paths show that the occurrence

of recharge water is not restricted to the zone between the ponds and the extraction wells, especially around the western pond. Water flows south of the southern wells of well battery 2 before flowing back to the extraction wells. This is due to a shallow semi-permeable layer which is present below the western pond. However, this does not mean that not all recharge water is not recovered since flow paths show that all recharge water flows towards the extraction wells. This was also confirmed by comparing chloride concentrations in dune water, recharge water and extraction water. Analysis of residence times have indicated that 50% of the water recharged at one instance reaches the extraction wells in less than 60 days. It takes up to almost 5 years for the last water which was recharged at one instance to reach the extraction wells. These calculations are confirmed by the results of a tracer test. The distribution of residence times indicate that the water which is extracted is a mix of water with a wide range of residence times, ranging from slightly less than 30 days up to almost 5 years. Large residence times are the result of water which flows in a longer and deeper flow cycle towards the extraction wells. The spread of the residence times, together with the fact that also native dune water is extracted (80% recharge and 20% native dune water) makes water quality of the total extraction water stable throughout the year.

HYDROCHEMISTRY

Four different water types were recognized in the aquifer (Vandenbohede et al., in review c). First water type is the dune water. The native fresh water is a F2CaHCO$_3$Ø water type, using the Stuyfzand classification (1993). Mean TDS of shallow natural dune water is 550 mg/l whereas this is 800 mg/l for deeper dune water. The second water type is the extraction water. This water is a mixture of dune water (20%) and recharged water (80%). This mixing is, however, highly dependent on the recharge and extraction rates. Water extracted before May 2004 is a F2CaHCO$_3$Ø water type, thus the same water type as mean shallow dune water. After May 2004, AR water became less mineralised and this is also reflected in the extracted water which becomes a g2CaHCO$_3$Ø water type. This difference is due to a change in the production process of the recharge water. Third water type is the artificial recharge water. The artificial recharge water before May 2004 was g0NaMixØ type before May 2004 and becomes a G0NaHCO$_3$Ø water type afterwards. TDS of the recharge water is very low in comparison with the dune water. Fourth water type is the artificial recharge water which is present between the recharge ponds and the extraction wells. During passage through the aquifer to the extraction wells, the recharged water is mineralised mainly by carbonate dissolution and is thus importantly enriched by calcium and bicarbonate and in a lesser extent by magnesium, potassium and fluoride. Although it can not be excluded that cation exchange also occurred, carbonate dissolution is the main process determining the remineralisation of the recharge water. Redox reactions are a second important process due to the artificial recharge of oxygenated water in a mainly anoxic aquifer. Oxygen in the recharge water is relatively quickly consumed. Also, nitrate is oxidized. Concentration of iron and sulphate is increased because of oxidation of iron sulphide minerals. Oxidation of manganese minerals results in an increase of the latter concentration.

CONCLUSIONS

The experience gained with the artificial recharge of tertiary treated waste water in the dunes led us to conclude that this is a very interesting method to assure a sustainable drinking water production. It resulted in an increase of the capacity of the extraction although a decrease of the extraction of natural dune water is achieved. Consequently, hydraulic heads and groundwater flow in the dunes are partly restored. The extracted water is a mix of recharged and native dune water and concerning the recharge water a mix of water with different residence times. This results in a stable quality of the extracted water.

REFERENCES

Oude Essink GP (1998). MOC3D adapted to simulate 3D density-dependent groundwater flow. In: Proc. of MODFLOW '98 Conference, October, 4-8, 1998, Golden, Colorado, USA, Volume I, 291-303.

Stuyfzand, P.J. (1993). Hydrochemistry and Hydrology of the Coastal Dune area of the Western Netherlands. Ph.D. Thesis, Nieuwegein, KIWA, Afd. Onderzoek & Advies.

Vandenbohede A and Lebbe L (2002). Numerical modelling and hydrochemical characterisation of a fresh water lens in the Belgian coastal plain. Hydrogeology Journal, 10(5), 576-586.

Vandenbohede, A. (2007). Visual MOCDENS3D: visualisation and processing software for MOCDENS3D, a 3D density dependent groundwater flow and solute transport model. User Manual. Research Unit Groundwater Modelling, Ghent University.

Vandenbohede, A., Van Houtte, E. and Lebbe, L. (in review, a). Sustainable groundwater extraction in coastal areas: a Belgian example. Environmental Geology.

Vandenbohede, A., Van Houtte, E. and Lebbe, L. (in review, b). Groundwater flow in the vicinity of two artificial recharge ponds in the Belgian coastal dunes. Hydrogeology Journal.

Vandenbohede, A., Van Houtte, E. and Lebbe, L. (in review, c). Water quality changes in the dunes of the western Belgian coastal plain due to artificial recharge of tertiary treated wastewater. Applied Geochemistry.

Van Houtte E and Verbauwhede J (2005). Artificial recharge of treated wastewater effluent enables sustainable groundwater management of a dune aquifer in Flanders, Belgium. Proceeding Ismar 5, 5th International Symposium on Management of Aquifer Recharge Systems for protecting and Enhancing Groundwater Resources, 10-16 June 2005, Berlin.

Contact Information: Alexander Vandenbohede, Research Unit Groundwater Modelling, dept. Geology and Soil Science, Ghent University, Krijgslaan 281 (S8), B-9000 Gent, Belgium, Phone: 32-9-2644652, Fax: 32-9-2644653, Email: avdenboh@yahoo.co.uk

Salt Water Intrusion Modeling in the Flemish Coastal Plain Based on a Hydrogeological Database

Luc Lebbe[2], *J. Lermytte*[1], ***Dieter Vandevelde***[1], *A. Vandenbohede*[2], *D. D'hont*[1] and *P. Thomas*[1]
[1]Flemish Environment Agency - division Operational Water Management, Brussels, Belgium
[2]Department of Geology and Soil Science, Ghent University, Ghent, Belgium

ABSTRACT

The Flemish Environment Agency (VMM) is responsible for providing recommendations related to the withdrawal of groundwater in the phreatic aquifer of the Flemish Coastal Plain. To assess the impact of this withdrawal on the freshwater heads and on the distribution of fresh and salt water in the aquifer, the agency uses a 3D density dependent groundwater flow model MOCDENS3D (Lebbe & Oude Essink 1999). Although a large number of hydrogeological data were already collected and stored in a database of the agency, the draw up of the input file for this model was very time consuming. Therefore, an interface was needed between the model and the hydrogeological database to reduce the time for the set up of the needed input files.

This model program interface (SWIFLEC3D) was developed so that it requires only one simple input file. This file should contain the X and Y Lambert coordinates of the lower left and the upper right corner of the modeling window together with the azimuth of the row direction, the horizontal cell size of the finite-difference grid, the level of the base plane of the uppermost layer of the finite-difference grid, the number of layers, the unique thickness of all layers, the code of the hydrogeological unit which will be considered as the impervious substratum of the model and finally data describing the evolution of the withdrawals in the different stress periods.

The boundaries of the selected model area must be chosen so they can be treated either as impervious boundaries or as constant head boundaries. Flow lines which can be considered as impervious boundaries, can be derived from the map representing the fresh-salt water interface in the phreatic aquifer (De Breuck et al. 1974). This map also allows the location of groundwater divides in the phreatic aquifer which can be considered as impervious boundaries. The constant head boundaries are in most cases chosen a few hundred of meters below the low water line at spring tide of the North Sea or of the Scheldt estuary. At these boundaries the constant fresh water heads in the uppermost layer correspond with the mean sea level whereas the fresh water heads in the underlying cells are set so that there is no vertical flow of the water which is initially present at this boundary. The initial distribution of salt water at these boundaries and in the complete model area is derived from the above mentioned map of the fresh-salt water interface.

The base levels of the different hydrogeological units are used to derive the lateral and transversal variation of the hydraulic conductivities of the deposits composing the complex phreatic aquifer in the Flemish coastal plain. These data are however not sufficient, due to the complexity of the quaternary deposits which constitute the major part of the phreatic aquifer. Therefore, the base level data are completed by a profile type map of the quaternary deposits. This profile type map was drawn and digitized in the framework of the development of the interface (SWIFLEC3D).

The lateral variation of the recharge rate in the coastal plain is derived from the soil map. The file describing the drainage is generated using the soil map and the digital terrain model. In the Flemish coastal plain there is a dense network of rather narrow draining canals filled with fresh water and a small number of broad (sometimes infiltrating) navigable channels and rivers

containing salt water which are related or connected to the harbors of Nieuwpoort, Oostende or Zeebrugge. The file including the information of the interaction between the phreatic aquifer and these surface waters is made by means of two files already present in the database. The first file contains the location and the characteristic level, width, conductance of the riverbed of the narrow drainage canals. The second file contains the location and the characteristic of the navigable waterways and data of their water quality.

The application of the model interface (SWIFLEC3D) will be demonstrated by means of a groundwater withdrawal problem of which the VMM had to assess the impact on the freshwater heads and on the distribution of the salt content in the groundwater. In the Flemish coastal plain large amounts of fresh water are withdrawn in a relatively short time at very large discharge rates during the construction of large apartment buildings. This is one of the typical problems regarding the management of the limited amount of fresh water in the coastal plain.

The studied problem is situated near the IJzer Estuary. In the time span of two years three buildings have been constructed. During the construction of the underground car parks, large amounts of fresh water were withdrawn. The three construction places were located close to the entrance of the harbor of Nieuwpoort. The distance between estuary and the construction sites was about 200 meter. The first withdrawal started at construction site 1 at May 13, 2005. This withdrawal lasted one year at an average discharge rate of 960 m^3/d. The second withdrawal started at October 28, 2005 and ended at December 31, 2005; it had an average discharge rate of 1430 m^3/d and it was located at 600 m north of site 1. The third withdrawal started at December 5, 2005 and ended July 10, 2007; it had an average discharge rate of 900 m^3/d and was located between the first two withdrawals at about 200 m north of site 1. During the studied period (788 d) $0.97x10^6$ m^3 water was pumped from the phreatic aquifer.

The applied finite-difference grid consists of 12 layers, 54 columns, 83 rows and 6 different stress periods are considered. The horizontal cell size is 50 m. All layers have the same thickness of 1.5 m. The northern constant head boundary is situated 400 m north of the low water line at spring tide. The western and eastern boundaries are situated perpendicular to the coast line. Both are considered impervious because they coincide mainly with ground water flow lines. The northern half of the eastern boundary is located under the harbor of Nieuwpoort. The estuary and harbor are filled with salt water. The western half of the southern boundary is located in the artificially drained polder area with salt water in the lower part of the phreatic aquifer. The eastern half runs through an old dune ridge where the phreatic aquifer is mainly filled with fresh water (De Breuck et al, 1974). As described above the model interface (SWIFLEC3D) generates all input files for the MOCDENS3D model automatically, based on the information present in the hydrogeological database. The parameters determining the solute transport are held constant for all layers. The water conducting porosity is 0.38; the longitudinal dispersivity is 0.3 m; the horizontal transversal dispersivity is 0.05 m and the vertical transversal dispersivity is 0.03 m.

A limited number of results are depicted in the Figure 1 and 2 and are drawn by the graphical interface Visual MOCDENS3D (Vandenbohede 2007). These figures are used to describe the treated problem and to assess the impact of the withdrawal on the freshwater heads and on the distribution of the salt water percentages. In Figure 1 the contour lines of fresh water heads (in white) and of saltwater percentages (shades) are plotted for the level -12 m bmsl (below mean sea level) before (left part) and after (right) the water withdrawals. On this level the major part of the phreatic aquifer is filled with salt water under the sea (northern boundary), under the harbor and river estuary (bottle shaped area) and in the polder area (the western half of the southern

boundary). The three withdrawal sites are located around the north western corner of the harbor. At the end of the withdrawal there is still a depression cone around the last and most important withdrawal. This withdrawal attracts the salt water from under the harbor to the depression cone. This salt water intrusion is also depicted in a west-east cross section through the last withdrawal site (Figure 2). From this figure it becomes clear that the salt water advances laterally to the pumping area in the lower part of the aquifer and that there is an upward flow of salt and brackish water just underneath the lowest level of the well screen where the transition zone between the fresh and the salt water becomes larger.

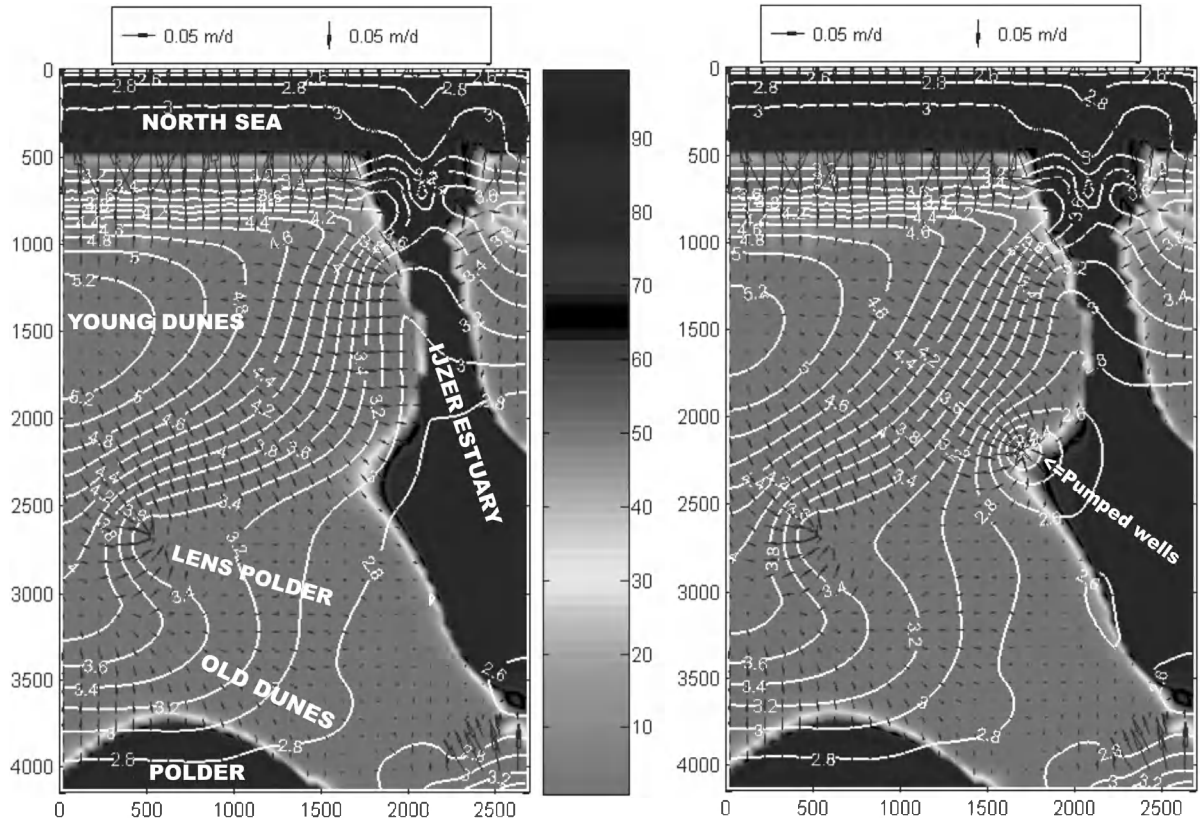

Figure 1. Contour lines of fresh water heads (in white) and saltwater percentages (shades) in layer 8 of finite-difference model (12 m below mean sea level) just before the start (left) and at the end (right) of the groundwater withdrawal of which its evolution is given in the text (x- and y-axis in meter).

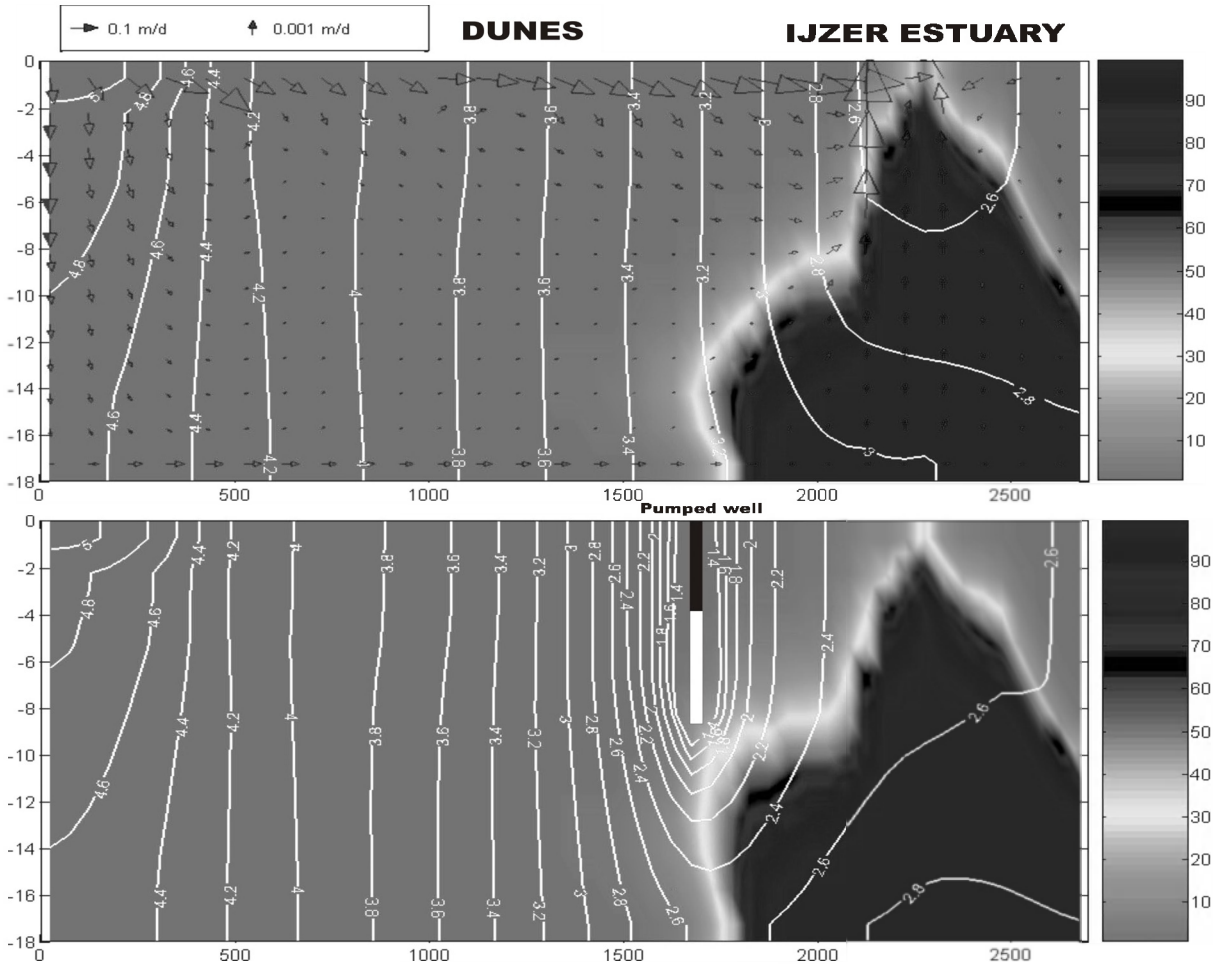

Figure 2. Vertical cross-section parallel to the x-axis (at y = 2175m in Figure 1): just before the start (above) and at the end (below) of the water withdrawal (vertical axis level in m below mean sea level, horizontal distance to the western boundary in meter). Remark the depression cone around the withdrawal (screen is white bar) in the lower half of the figure.

REFERENCES

De Breuck, W., G. De Moor, R. Maréchal, and R. Tavernier. 1974. Depth of the fresh-salt water interface in the unconfined aquifer of the Belgian coastal area (1963-1973). Appendix of Proceedings of 4th Salt Water Intrusion Meeting, Ghent, University of Ghent.

Lebbe, L. and G. Oude Essink. 1999. Section 12.11. MOC DENSITY / MOCDENS3D-code. p. 434-439, in Chapter 12. Survey of Computer codes and Case Histories, Eds. Sorek, S. & Pinder, G.F. in: *Seawater Intrusion in Coastal Aquifers, Concepts, Methods and Practices.* Eds. Bear, J., Cheng, H-D, Herrera, I., Sorek, S. and Ouazar D. Kluwer Academic Publishers

Vandenbohede, A. 2007. Visual MOCDENS3D: visualizations and processing software for MOCDENS3D, a 3D density dependent groundwater flow and solute transport model. User Manual. Research Unit Groundwater Modeling, Ghent University.

Contact Information: Dieter Vandevelde, VMM – div. Operational Water Management, Koning Albert II-laan 20, 1000 Brussels, Belgium, Phone: 32-50454257, Email: di.vandevelde@vmm.be

Variable Density Flow and Transport in Tsunami Impacted Coastal Aquifers: Laboratory Investigations in Homogeneous Saturated Porous Media

Meththika Vithanage[1,2], *Tissa Illangesekera*[3], *Karsten H Jensen*[1], *Jayantha Obeysekera*[4], *Peter Engesgaard*[1] and *Karen Villholth*[5]

[1]Department of Geography and Geology, University of Copenhagen, Denmark
[2]International Water Management Institute, Pelawatta, Battaramulla, Sri Lanka
[3]Center for Experimental Study of Subsurface Environmental Processes, Colorado School of Mines, Golden, CO, USA
[4]South Florida Water Management District, West Palm Beach, FL, USA
[5]Geological Survey of Denmark and Greenland, Copenhagen, Denmark

ABSTRACT

The objective of this work was to improve the understanding of a tsunami related process of the behaviour of an unstable saltwater plume overlying fresh groundwater in the saturated zone of an aquifer using an intermediate-scale experimental set up in a laboratory. Dense saltwater plume behaviour was investigated mainly as a function of rate of application, duration of the application, and fresh water flux after the salt water flux (tsunami), imitating rainfall after the tsunami. Free convection, micro-scale heterogeneity and local density differences resulted in the onset of gravitational instabilities. They are manifested by lobe-shaped fingers that first grow along the bottom of the plume and later within the plume. The freshwater flux immediately following the saltwater input does not appear to affect the timing of migration of the saltwater plume significantly. As in previous studies, the bottom of the saltwater plume exhibited significant fingering. However no such instabilities were observed in the interface between saltwater and freshwater.

INTRODUCTION

The Tsunami which occurred on December 26th, 2004, caused extensive contamination of coastal aquifers in Sri Lanka by salt water infiltration. This situation could result in an unstable density-dependent contamination problem with a denser fluid (sea water) on top of a less dense fluid (fresh groundwater). This resulted in hydraulically driven forced convection and buoyancy driven free convection in the aquifer. Both of these phenomena contributed to mixing and migration of saltwater. In addition, free convection results in gravitational instabilities within the saturated zone of the aquifer system. Since the system is attempting to return to stable condition through mixing, there is a potential to contaminate larger regions (Oostrom et al. 1992). Consequently, it is important to study the variable density flow and transport processes associated with groundwater contamination by the tsunami.

Extensive experimental work has been carried out by Schincariol and Schwartz (1990), Oostrom et al. (1992), Hayworth (1993) and Simmons et al. (2002). Schincariol and Schwartz (1990) showed that a density difference as low as 0.0008 g/cm^3 produce gravitational instabilities. Oostrom et al., (1992) and Hayworth (1993) stated that the relative density difference, the horizontal Darcy flux, the leachate leakage rate, and the hydraulic conductivity of the medium have an influence on plume stability. However, they did not test the effect of dispersion on plume stability. Simmons et al. (2002) carried out experiments to observe the variable-density free convective flow processes under static water table conditions without any ambient flow. They found that instabilities do not grow in the unsaturated zone and that density plays a critical role in determining the place of origin of the instabilities. Hogan (2006) performed different types of experiments which reflect various kinds of saltwater contamination events by the tsunami. The objective of our work was to improve the understanding of the behaviour of the salt

water plume associated with the tsunami using visual observations from a physical experimental set up.

EXPERIMENTAL PROCEDURE

Five different salt water application configurations were investigated in the flow tank with homogeneous packing, by changing the rate of application, duration of the application zone on the ground surface, and fresh water flux after the salt water flux, imitating rainfall after the tsunami. Saltwater used for the experiment had an Electrical Conductivity value of 56 mS/cm and a density of ~1025g/cm^3. The experiments were performed using pre-sieved sand which can be identified by the effective sieve sizes (# 30 and # 70) from Unimin Corp., Emmett, Idaho, USA. Details of the experimental set ups are shown in Table 1 and Figure 1. The flow container, with dimensions of 480x5x120 cm, was constructed with Plexiglas for visualization of the dyed contaminant plume. The hydraulic conductivity of the sand type 30 was obtained using two separate techniques; 1) Ex-situ measurement using constant head set up and 2) in-situ measurement of flow though the flow container using a known head difference. A non-intrusive photographic measurement technique and ECH$_2$O-TE conductivity sensors were used to understand the plume behaviour and migration.

Table 1. Homogeneous experimental setup

Exp. #	Flux rate (RPM)	Flux length (m)	Volumetric Flux (m/min)	Flux time (hrs)	Hydraulic head (m)	Fresh water flux	Time (hrs)
1	300	2.80	2.4 x 10^{-3}	2.0	0.057		
2	300	2.80	2.4 x 10^{-3}	2.0	0.085		
3	300	2.80	2.4 x 10^{-3}	1.0	0.085		
4	400	2.80	3.2 x 10^{-3}	1.0	0.085		
5	300	2.80	2.4 x 10^{-3}	1.0	0.085	√	1.0

Note: The difference between Experiment 3 and 5 was the application of freshwater after saltwater representing rainfall after the tsunami in experiment 5

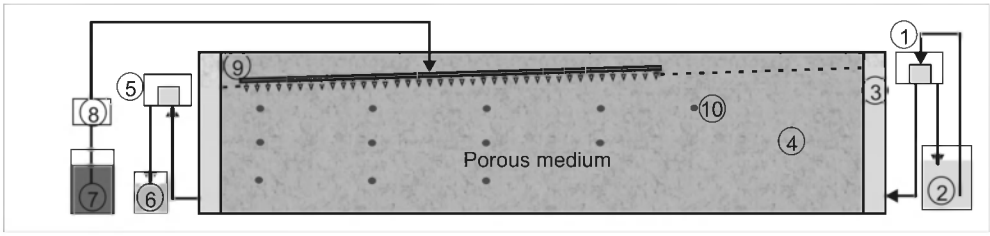

Figure 1. Physical experimental set up for homogeneous experiments. (1) Inflow head chamber, (2) Water storage tank, (3) Gravel pack, (4) Homogeneous porous media, (5) Outflow head chamber, (6) Waste water storage, (7) Salt water container, (8) Peristaltic pump, (9) Salt water injection system and (10) Conductivity sensors.

RESULTS AND DISCUSSION

Only three experiments (exp. 3, 4 and 5) will be discussed in this paper. As expected, the tendency for the plume to move faster increases as the hydraulic gradient increases (exp 1 and 2). In all the experiments, immediately after the dense salt water entered the saturated zone, large lobes of saltwater started to form (Figure 2) but they were observed to be quite stable. However, right after the salt water application stopped, small gravitational instabilities (fingering) took place in the aquifer system. The digitized pictures showed (Figure 2) that the rapid and relatively steep penetration of the dense water plumes into the porous media.

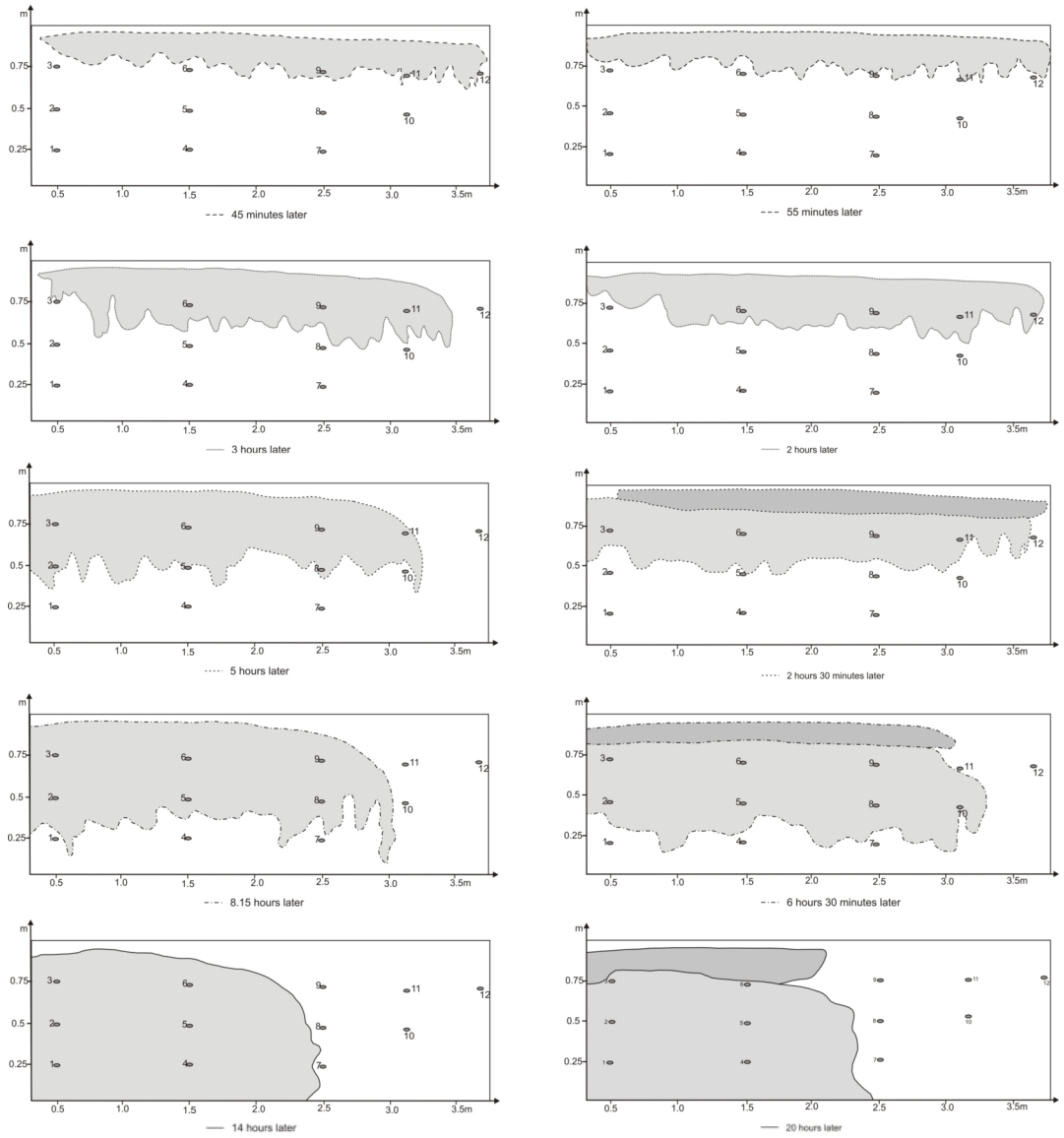

Figure 2. Digitized pictures of plume outline for homogeneous experiment 3 (left) and 5 (right) showing the behavioural difference due to displacement of saltwater plume (light color) by neutral plume (dark color)

The breakthrough curves (not shown) further illustrate the random and oscillatory nature of the unstable plume. This is consistent with visualization results. As observed by Wooding (1969), the development of gravitational instabilities is characterised by rapid and intense fingering to begin with, which gradually results in the coalescence and vertical development of fewer larger fingers with time. Increase of salt water flux (Q_L) by 25% is tested in the exp. 3 and 4 which showed a flushing time difference of about 5 hours. Exp. 5 was set up to observe the dense salt water plume movement when it is displaced by a neutral plume. Figure 2 shows the sequence of plume movement. The dense salt water plume was with interfacial instabilities while the neutral plume showed very stable interfaces in that the interface between the two plumes was sharp. Although the application of freshwater pushed the saltwater plume down faster than in the exp. 3, the total duration of plume movement did not show much of a difference. However, introduction of freshwater into the system reduced the time of the presence of gravitational instabilities in the system.

With the development of the plume, lobe shaped 'packets' appeared to form along the bottom boundary of the plume, gradually becoming more pronounced with time and sometimes detaching from the main body of the plume. This plume behaviour appeared to be completely random, highly unstable and varying with time. Although the lobes were observed on the other side of the flow container, the position, shape and time of appearance of the instabilities of plume were found to be different. This indicates the plume was three dimensional as also observed by Oostrom et al., (1992). As the experiment continued, the plume reaching the bottom of the tank and moved towards the flow tank boundary in the form of a mixed, well shaped plume without any gravitational instabilities or lobe shaped features.

CONCLUSION

Under fully saturated conditions in a homogeneous porous media a dense saltwater plume created by a phenomenon such as a tsunami lead to gravitational instabilities. However, the neutral plume exhibited a stable behaviour. Based on these findings it can be concluded that pore scale heterogeneities, local density differences between contaminated and ambient water and dominancy of free convection serve as perturbations to generate gravitational instabilities. A more quantitative analysis of the stability criteria, numerical modeling and the effect of heterogeneity required for further elucidation of the behaviour of density driven unstable plume resulting from tsunami like flooding event are in progress.

ACKNOWLEDGEMENT

The experimental component of this research was conducted at the Center for Experimental Study of Subsurface Environmental Processes (www.CESEP.mines.edu) at Colorado School of Mines. The assistance of the team at CESEP and Rohit Goswamy are gratefully acknowledged.

REFERENCES

Hayworth, J.S., (1993), A physical and numerical model study of three dimensional behaviour of dense aqueous phase contaminant plumes in porous media, Doctoral Thesis, Department of Civil Enginnering. Auburn University, Alabama.

Hogan, M., (2006), Understanding the flow and mixing dynamics of saline water discharged into coastal freshwater aquifers. Masters Thesis, Department of Civil Enginnering. Auburn University, Alabama.

Oostrom, M., Dane, J. H., Guven, O. and Hayworth, J. S.: (1992), Experimental investigation of dense solute plumes in an unconfined aquifer model, *Water Resour. Res.* **28**(9), 2315–2326.

Schincariol, R. A., and F. W. Schwartz, 1990. An experimental investigation of variable density flow and mixing in homogeneous and heterogeneous media, *Water Resour. Res.*, *26*(10), 2317–2329,

Simmons, C.T., M. L. Pierini and J.L. Huston (2002), Laboratory investigation of variable density flow and solute transport in unsaturated-saturated porous media, Transport in Porous Media. 47, 215-244.

Wooding, R.A., (1969), Growth of fingers at an unstable diffusing interface in a porous medium or Hele-Shaw cell. J. Fluid Mech. 39, 477–495.

Contact Information: Meththika Vithanage, University of Copenhagen, Dept. of Geography and Geology, Østervoldgade 10 Copemhagen K, Denmark, Phone: 4535322433, Email: meth@geol.ku.dk

Benchmarks for Two- And Three-Dimensional Variable-Density Ground-Water Flow Simulators: Analytical Expressions for Unstable Convection

Clifford I. Voss[1], *Craig T. Simmons*[2], *Douglas Weatherill*[2] and *Neville I. Robinson*[2]
[1]U.S. Geological Survey, Reston, Virginia, USA
[2]Flinders University, Adelaide, Australia

EXTENDED ABSTRACT

Approximate stability criteria for unstable steady-state density configurations, determined analytically, may be used as benchmarks for both two-dimensional (2D) and three-dimensional (3D) numerical simulators of variable-density ground-water flow. One of the more difficult tasks of variable-density simulators is to correctly represent the physics of unstable density configurations; thus, these benchmarks may be among the more stringent tests of such computer codes.

In 2D, the benchmarks consist of approximate analytical stability criteria for steady unstable convection in a finite 2D box with top and bottom boundary conditions that maintain an unstable density configuration (dense fluid above less-dense fluid). These are closely related to the classic parallel plate analyses of Horton and Rogers (1945) and Lapwood (1948).

2D models may be tested by:

1- matching numerical results with analytical results for convective wavelength and critical Rayleigh number (Ra_c) for very wide horizontal boxes (wavelength results are sensitive to initial seeding, as described below),

2- matching Ra_c as a function of horizontal box geometrical aspect ratio with an analytical expression, and,

3- matching Ra_c as a function of box inclination with an analytical expression.

These 2D benchmarks were proposed by Weatherill et al. (2004).

In 3D, proposed benchmarks consist of approximate analytical stability criteria for steady unstable convection in a finite 3D box. These benchmarks are analogous to those for 2D, but refer to the regimes of convection that occur in 3D: polyhedral cells (occur for low angles when $Ra > Ra_c$), unicellular convection (occurs for all angles greater than zero when $Ra < Ra_c$), and longitudinal coils (occur for high angles when $Ra > Ra_c$). The 3D stability criteria are corrected from classic analyses of 3D convection in porous media that were reviewed by Caltagirone (1982).

3D models may be tested by:

1- matching numerical results with analytical results for convective wavelength of polyhedral cells and critical Rayleigh number (Ra_c) for horizontal boxes (wavelength results are sensitive to initial seeding, as described below),

2- matching the transition between unicellular and the other convective regimes as a function of box geometrical aspect ratio and box inclination, given by an analytical expression for Ra_c, and,

3- matching simulated transverse wavelength for the longitudinal coil regime.

At low angles of inclination, steady-state solutions are highly sensitive to the initial condition. This imposes two constraints on initial conditions, if simulation results are to be matched with analytical expressions. First, the initial condition must be a low Rayleigh number solution ($Ra < Ra_c$) that provides a quiescent initial state. For unstable energy transport, initial temperature is a vertically-decreasing linear function. For unstable solute transport, the initial concentration, expressed as a mass fraction of solute, is a non-linear function with increasing value along the vertical coordinate. This is a result of the mathematical expression of the diffusion process that dominates for such low Ra solutions. Second, the organization of steady-state convective flow as cells, particularly the convective wavelength, is sensitive to seeding of the initial quiescent state because a family of possible stable solutions exists. Without seeding superimposed on the above-described initial conditions, the simulated steady-state organization may be sensitive to otherwise innocuous numerical irregularities in the solution method used, which provide an unintentional seeding. This was demonstrated for the 2D box by Ataie-Ashtiani and Aghayi (2006).

If benchmarks that rely on seeding (specifically, comparison of simulated and analytical convective wavelength for low-angle boxes) are judged to be overly constrained and thus weak tests, the other proposed benchmarks remain as seeding-independent tests. These include: for 2D, matching the critical Rayleigh number (Ra_c) for any inclination and box aspect ratio, and for 3D, matching the theoretical transition between unicellular and longitudinal coil regimes for any inclination and box aspect ratio, and matching the wavelength of longitudinal coils, which occur irrespective of initial seeding.

REFERENCES

Ataie-Ashtiani, B. and Aghayi, M.M. A note on benchmarking of numerical models for density dependent flow in porous media. Advances in Water Resources, 29:12 2006, 1918-1923.

Caltagirone, J.P., Convection in a porous medium, in: Convective Transport and Instability Phenomena, J. Zierup and H. Oertel, eds., G. Braun, Karlsruhe, Germany, 1982, 199-232.

Horton CW, Rogers Jr. FT. Convection currents in a porous medium. J Appl Phys 1945, 16: 367-370.

Lapwood ER. Convection of a fluid in a porous medium. Proc Cambridge Phil Soc 1948, 44: 508-521.

Weatherill, D., Simmons, C.T., Voss, C.I., Robinson, N.I., Testing density-dependent groundwater models: two-dimensional steady state unstable convection in infinite, finite and inclined porous layers. Advances in Water Resources 2004; 27:5, 547-562.

Contact Information: Clifford I. Voss, U.S. Geological Survey, 431 National Center, Reston VA, 20192, USA, Phone: 703-648-5885, Fax: 703-648-5274, Email: cvoss@usgs.gov

General Guidance Concerning Inverse Modeling Techniques and Value of Field Data Types for Seawater Intrusion Simulation

Esteban Sanz[1] and ***Clifford I. Voss***[2]
[1]ExxonMobil Exploration Company, Houston, Texas, USA
[2]US Geological Survey, Reston, Virginia, USA

EXTENDED ABSTRACT
In coastal aquifers subject to seawater intrusion, measurements of fluid pressure and concentration may be used to determine the parameters of a ground-water model of the aquifer system, which may then be used to manage the water supply. Due to the complexity of aquifer systems and the nonlinear nature of seawater intrusion physics, manual calibration is often not feasible. This necessitates having a capability to calibrate a numerical model with an automatic inverse algorithm. Automatic inverse modeling, also called parameter estimation, has become a standard tool for ground-water flow models, though there have been fewer applications to modeling of heat or solute transport, and even fewer for inverse modeling of variable-density fluid flow and solute transport, the basis of seawater intrusion into aquifers. This paper presents insight into practical difficulties and general guidance concerning inverse modeling techniques for seawater intrusion gained from analyses of basic 2D-inverse problems: the classic Henry variable-density ground-water model benchmark (Sanz and Voss, 2005) and the Aquiferia problem, a hypothetical coastal multi-aquifer system.

For inverse modeling, simultaneous use of different types of field observation data can improve ground-water model structure, features, and parameter values. With regard to coupled flow and transport modeling, there can be some advantages to concurrent use of both hydraulic head (or pressure) and concentration (or temperature) data for model refinement and parameter estimation. Transport always depends on flow, thus, for both constant- and variable-density flow, measurements of concentration can be used to help estimate classical flow-model parameters such as hydraulic conductivity. When flow processes depend on transport processes, such as in variable-density flow, measurements of pressure can provide information to help estimate transport parameters such as dispersivity that are normally assumed to be estimatable only from measurements of concentration.

Study of spatial distributions of sensitivities in an aquifer system (change of observed pressure and concentration as a function of parameter values) allows some important aspects of the value of various types of data to be explained. Sensitivities of pressures and concentrations are mapped for both the Henry problem and for a more-realistic coastal aquifer system, showing where the most information can be measured for each parameter. Except for permeability, which is most strongly estimated from measurements at greater distance from the sea, all other parameters are most strongly estimated when based on data collected in the freshwater-seawater transition zone. Sensitivity maps can also indicate which parameters can be independently estimated.

Estimation is usually a process that requires the modeler to work through a series of inverse modeling attempts to estimate different sets of parameters for the system, possibly using different subsets of observations, when early attempts are not successful or are somehow unsatisfactory. Early attempts often involve estimation of too many parameters (some of which are co-dependent), leading to non-convergence of the inverse iteration process or to weak estimates. Co-dependence is demonstrated for parameters of the simple Henry problem, for which these relations are known a-priori from its semi-analytical solution. For more complex

inverse problems with initially unknown parameter co-dependence, a procedure that is demonstrated successively eliminates co-dependent estimated parameters in the series of attempts, providing a way forward.

Inverse modeling is carried out using software that combines the US Geological Survey SUTRA code (Voss and Provost, 2002) for variable-density ground-water flow, UCODE (Poeter and Hill, 1998; Poeter and others, 2005) for managing the inverse calculations, and SutraGUI (Winston and Voss, 2004), which provides a convenient graphical interface for setting up inverse simulations.

REFERENCES

Poeter, E.P. and Hill, M.C., 1998: Documentation of UCODE, a computer code for universal inverse modeling. U.S. Geological Survey, Water-Resources Investigations Report 98-4080.

Poeter, E.P., Hill, M.C., Banta, E.R., Mehl, Steffen, and Christensen, Steen, 2005, UCODE_2005 and Six Other Computer Codes for Universal Sensitivity Analysis, Calibration, and Uncertainty Evaluation: U.S. Geological Survey Techniques and Methods 6-A11, 283p.

Sanz, E. and Voss, C.I., 2005, Inverse modeling for seawater intrusion in coastal aquifers: Insights about parameter sensitivities, variances, correlations and estimation procedures derived from the Henry problem, Advances in Water Resources v. 29, no. 3, p. 439-457.

Voss, C. I., and Provost, A. M., 2002, SUTRA - A model for saturated-unsaturated variable- density ground-water flow with solute or energy transport, U.S. Geological Survey Water-Resources Investigations Report 02-4231, 250 p.

Winston, R.B. and Voss, C.I., 2004, SutraGUI – A graphical interface for SUTRA, a model for ground-water flow with solute or energy transport, U.S. Geological Survey Open-File Report 03-285, 114 p.

Contact Information: Clifford I. Voss, U.S. Geological Survey, 431 National Center, Reston VA, 20192, USA, Phone: 703-648-5885, Fax: 703-648-5274, Email: cvoss@usgs.gov

Tracing Vertical and Horizontal Migration of Injected Fresh Wastewater into a Deep Saline Aquifer using Natural Chemical Tracers

Virginia M. Walsh,[1,2] and *René M. Price*[2]
[1]Miami-Dade Water and Sewer Department, Miami, FL, USA
[2]Department of Earth Sciences, Florida International University, Miami, FL, USA

ABSTRACT
The Miami-Dade Water and Sewer Department (MDWASD), Miami-Dade County, Florida, operates two deep-well injection facilities which inject an average of 430 million liters per day of fresh treated wastewater into a deep saline aquifer approximately 900 meters below land surface. Although this deep aquifer is separated from overlying brackish aquifers by a confining unit 150 meters thick, evidence of migration of injected wastewater has been detected in the overlying aquifers. This injected fresh water is a source of freshwater recharge chemically distinct from the native brackish aquifer water. Ammonium contained in the injected wastewater is higher than native aquifer water background levels, and exhibits a high seasonal variability in response to the wet and dry climatic conditions in south Florida. Geochemical data indicate that the injected ammonium behaves conservatively when mixed with native water, and thus can be used as a tracer of injected wastewater. Ammonium data, in conjunction with major ion chemistry and stable isotope data, were used to identify source and pathways of the recharge. Data indicate multiple pathways that are chemically distinct depending on their pathway to the aquifer, and suggest vertical migration a result of either natural or anthropogenically-induced fractures. Once introduced into the overlying aquifer, horizontal migration appears to be the result of natural advection/diffusion through a highly heterogeneous carbonate aquifer with little mixing of native waters.

INTRODUCTION
South Florida has experienced rapid urban growth in the past several decades, which has placed extraordinary demands on the management of ground-water resources in southern Florida. Potable water has been produced from the Biscayne aquifer, a pristine karst surficial aquifer that has supplied an average of 1300 million liters per day (MLD). Due to restrictions on increased allocations from the Biscayne aquifer, the underlying Floridan aquifer in south Florida is becoming an alternate water supply source. Historically, the Floridan aquifer in south Florida has been used for aquifer storage and recovery (ASR) in the Upper Floridan aquifer, and for industrial and treated domestic wastewater disposal in a highly permeable zone in the Lower Floridan aquifer. Increasingly the Upper Floridan aquifer is used as becoming a source of brackish water to blend with Biscayne aquifer water.

The Floridan aquifer system in south Florida lies approximately 300 meters below land surface (BLS), and consists of heterogeneous permeability carbonate layers of Oligocene to Paleocene in age. The Upper Floridan aquifer (UFA) is an artesian aquifer and is used for ASR and a source of water for blending. Water quality is brackish, with total dissolve solids (TDS) averaging less than 10,000 milligrams per liter (mg l^{-1}), (Reese, 1994). The UFA is underlain by the middle confining unit 1 (MCU1) and the Middle Floridan aquifer (MFA) at approximately 420 m below land surface (BLS), with water quality becoming increasing saline (Reese et al, 2008). Beneath the MCU1 and the MFA is the Lower Floridan aquifer (LFA), which consists of water quality close to seawater, with TDS concentrations over 33,000 mg l^{-1}. The LFA outcrops along the Florida Straits, with water levels in the LFA near sea level.

MDWASD began injecting treated domestic wastewater in the early 1980's, and currently is injecting an average of 430 MLD into the highly permeable boulder zone 900 m BLS in the LFA. Domestic wastewater is treated to secondary drinking water standards, with TDS levels of 375 mg l^{-1}, and ammonia concentrations ranging from 15 to 35 mg l^{-1}, in response to the wet and dry seasons in south Florida. Evidence of upward migration of ammonia was observed at 440 m BLS in the UFA, as concentrations of 7 mg l^{-1} were detected above reported background levels of 0.05 mg l^{-1} (BC&E, 1977), with the implication that the MCU1 is actually not confining. The authors of this paper and others (Maliva et al, 2007) have suggested that the vertical migration pathway may most likely be along fractures. The purpose of this research is to determine the transport mechanisms and migration pathways of freshwater injectate into a highly saline aquifer.

METHODS

Historical water quality data for the FAS were collected and analyzed from utility, state and federal sources. Water quality samples were collected from following standard protocols from on-site dual-zone monitoring wells, representing the 300 m zone, 440 m zone, and the 550 m zones. The 300 m and 440 m zones are located in the UFA; the 550 m zone lies in the MCU1 and MFA. Samples were analyzed for major ions, pH, temperature, stable isotopes, and chemical parameters including ammonium, nitrate and nitrite. Ammonium was evaluated for use as a conservative tracer. As part of the nitrogen cycle, ammonium is oxidized to NO_3^- (nitrification) in the presence of O_2, and therefore ammonium reacts non-conservatively. Water quality data at the project site suggests otherwise, as dissolved O_2 values are < 1 mg l^{-1}, and nitrate values for all zones monitored on site in the Floridan aquifer, including wells with high ammonium concentrations, are typically less than 0.05 mg l^{-1}. Ammonia levels have remained constant over time in several wells, further suggesting a conservative nature. Therefore, mixing and ratio models of ammonium to major ions were developed to determine chemical evolution of the injected freshwater.

RESULTS

Time series historical ammonium and chloride water quality data were analyzed to determine if any patterns could be distinguished. Ambient levels of ammonium at the 300 m, 440 m, and 550 m zones typically are > 0.2 mg l^{-1}. Ammonium concentrations as high as 15 mg l^{-1} have been observed in wells in the 440 m zone on the west side of the site, and as high as 20 mg l^{-1} in the 550 m zone on the south side of the site. Two patterns were observed in the time-series analysis. Ammonium concentrations above ambient levels were observed in MWs in the UFA, however, they were at ambient levels in the monitoring zones beneath. Ammonium concentrations increased sharply, and exhibited apparent seasonal variation, very similar to the seasonal variations observed in the injected freshwater (Figure 1). Once ammonium was detected above ambient levels, data show relatively stable concentrations, with very slight increases. Levels in wells exhibiting this trend average 2 – 5 mg l^{-1}. Ammonium levels were compared to chloride levels for each monitoring zone. Ambient chloride levels were 750 mg l^{-1} for the 300 m, 3700 mg l^{-1} for the 440 m, and 19,000 mg l^{-1} for the 550 m zones. It was assumed that chloride and ammonium are conservative tracers, and ammonium/chloride mixing models were developed for each well, compared to ammonium concentration trends over time. End members of the mixing model were the ambient concentrations of chlorides and ammonium of each monitored zone. Several distinct mixing models were observed (Figure 1). Mixing models that showed strong increasing trend of ammonium concentrations comparative to freshwater injectate concentrations plot with time indicated relatively rapid mixing with the freshwater end member (well IDs 6U and 12L). This mixing model at the 440 m zone (well ID 6U) also showed no mixing with the

550 m zone. The models that showed ammonium concentrations to have slowly increased with time, or that have remained relatively static with time (well ID 10L) indicated slow progression of water chemistry evolution towards the freshwater end member.

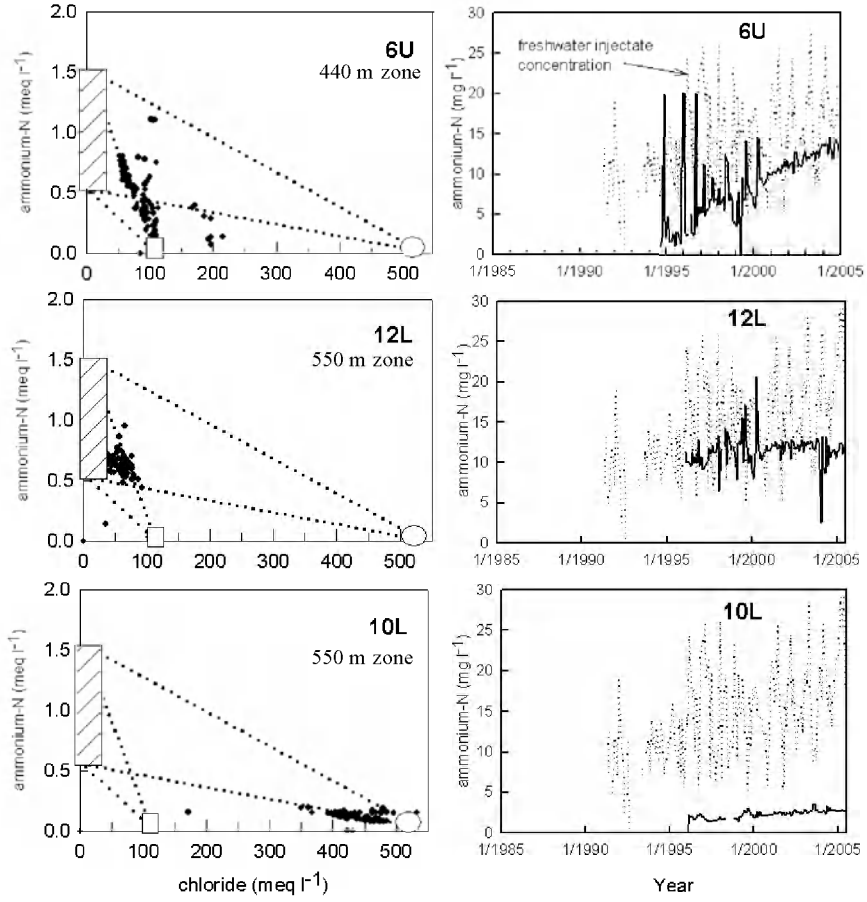

Figure 6. Graphs on the left are ammonium/chloride mixing end member models for the 440 m and 550 m zones. 6U, 12L and 10L are wells IDs. Hatched rectangle is injected freshwater end member, indicating the seasonal range in concentrations. Square is 440 m zone (brackish water) ambient water end member; circle is 550 m zone (saline water). Graphs on the right are ammonium concentrations over time. Solid black lines are concentrations from each well site; dotted line is injected freshwater concentration.

Calcium/chloride ion ratios analysis show a similar effect (Figure 2). The freshwater injectate calcium ion concentrations average 59 mg l^{-1}; calcium concentrations in the 440 m zone 176 mg l^{-1}, and at the 550 m zone 436 mg l^{-1}. When plotted against ambient ratios, chloride/calcium ratios for the 440 m and the 550 m impacted zones showed groundwater evolution towards the freshwater injectate (Figure 2). As with the ammonium/chloride end member model, the 440 m zone does not show any mixing with the underlying 550 m zone.

DISCUSSION AND CONCLUSIONS

Possible migration pathways of freshwater injectate were determined using chlorides, major ions, and ammonium. Analysis of time-series ammonium data shows two distinct ammonium patterns. The first pattern indicates a sharp increase of ammonium above ambient levels, with a strong seasonality component that closely matches the seasonality component of the freshwater injectate. The second pattern shows once ammonium appears in the water above ambient levels, concentrations remain static, or exhibit very small increasing concentration trends. This suggests that there are multiple pathways of

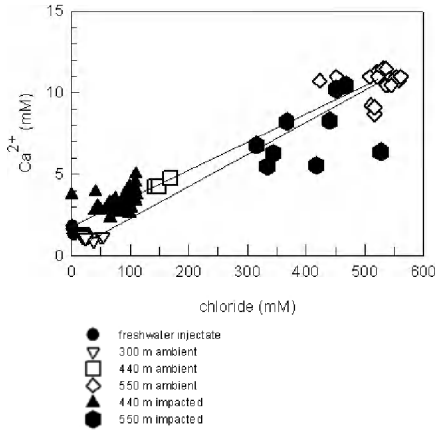

Figure 7. Chloride/calcium ion ratios.

migration of ammonium in the aquifers. Mixing models developed using ammonium/chloride end members and ion ratios as conservative tracers also suggest different migration pathways of freshwater injectate. In the 440 m zone where ammonium concentrations in the aquifer water closely follow the same concentration trends as the injectate, mixing models show no mixing with 550 m zone. This suggests that freshwater injectate is migrating directly to the 440 m zone, with little to no mixing of underlying highly saline water. If freshwater injectate were migrating up through the MCU1 it would be expected to exhibit a mixing line from the 550m to the 440 m zone. Both the end member and ion ratio models do not show such a mixing line. It appears that the freshwater injectate is traveling up through the MCU1 via natural or anthropogenically-induced fracturing, (possibly as a result injection well construction); and is probably vertically migrating due to the buoyancy effect of injecting freshwater into the highly saline LFA. Where ammonium concentrations are slowly increasing in time or remaining static, mixing and ratio models suggest that once the freshwater is introduced into the aquifer, it slowly advects/diffuses through the aquifer, with a slow groundwater evolution over time from brackish to gradual freshening, and remaining geochemically distinct. On-going research on this project includes helium/tritium dating and ^{15}Nitrogen isotope analysis to further differentiate freshwater injectate migration pathway.

REFERENCES

BC&E/CH2MHill. 1977. Drilling and testing of the test-injection well for the Miami-Dade Water and Sewer Authority. Contract S-153, BC&E/CH2M Hill, Gainesville, Florida.

Maliva, R.G., Guo, W., and Missimer, T. 2007. Vertical migration of municipal wastewater in deep injection well systems, South Florida, USA. Hydrogeology Journal.

Reese, R. S. 1994. Hydrogeology and the Distribution and Origin of Salinity in the Floridan Aquifer System, Southeastern Florida. U.S. Geological Survey WRIR 94-4010.

Reese, R.S. and Richardson, E. 2008 (in press). Synthesis of the hydrogeologic framework of the Floridan Aquifer System and delineation of a major Avon Park permeable zone in central and southern Florida. U.S. Geological Survey SIR 2007-5207.

Contact Information: Virginia Walsh, Miami-Dade Water and Sewer Department, 3071 SW 38 Ave, Miami, FL 33146 USA, Phone: 786-552-8266, Fax: 786-552-8640, Email: walshv@miamidade.gov

Significant Water Quality Trends Observed in the Lower Hawthorn Aquifer of Southwestern Florida, Occurrences and Solutions

Gordon Kennedy, P.G.[1], ***Michael L. Weatherby, P.G.***[2] and *Ed Rectenwald, P.G.*[1]
[1]MWH Americas, Cape Coral, Florida, USA
[2]MWH Americas, Tampa, Florida, USA

ABSTRACT
A majority of water utilities in Southwestern Florida use a brackish raw water supply treated by reverse osmosis water treatment to potable standards. The aquifer most commonly used for this brackish raw water supply is the Lower Hawthorn aquifer of the Upper Floridan aquifer system (FAS). This aquifer has typical chloride concentrations in the range of 500 mg/L to 2,000 mg/L. Anomalous high chloride concentrations have been observed in several wellfields during construction or operation of raw water production wells. These occurrences can be attributed to lateral saltwater intrusion, vertical upconing of poor quality water, or vertical conduits (fissures, cracks and fractures) which connect deeper saline water sources to the Lower Hawthorn aquifer. Manmade vertical conduits may result from old improperly abandoned agricultural or oil prospecting wells which may promote upward movement of groundwater from deeper more saline aquifers. The identification of possible sources for the degrading water quality in individual wells is needed prior to well modifications, or recommending operational changes to the wellfield to minimize salinity impacts.

INTRODUCTION
This paper describes the hydrogeologic framework and factors affecting increased chloride concentrations observed in separate wellfields throughout southwestern Florida. Water quality trends are affecting the quality and quantity of the Lower Hawthorn aquifer, a carbonate aquifer used for raw water supply for treatment to potable water to meet demands in southwestern Florida. Overall, certain wellfields have become more brackish over time as demands have increased. Also, there have been occurrences of localized saline water upconing or vertical migration. These trends are hard to predict because carbonate aquifers in general tend to have high degrees of heterogeneity due to their relatively high variability in depositional porosity, permeability and their susceptibility to diagenetic alteration, which can profoundly change the hydraulic properties of carbonate rock (Maliva et al. 2002).

Background
Historical water quality data was analyzed from several wellfields in southwest Florida. With permission, historical water quality data from two Lower Hawthorn aquifer brackish wellfields are presented here; the City of Cape Coral and City of Fort Myers Wellfields. The water quality was collected at varying times between 1988 and 2007 which is dependent on when the wellfield started operation.

HYDROGEOLOGY
Three major aquifer systems underlie the study area of Cape Coral, Florida: the Surficial Aquifer System (SAS), the Intermediate Aquifer System (IAS), and the Floridan Aquifer System (FAS), with the upper portion of the FAS being the focus of this study. These aquifer systems are composed of multiple, discrete aquifers separated by low permeability "confining" units that occur throughout this sequence. Salinity substantially increases with depth.

WELLFIELD WATER QUALITY TRENDS

Water quality trends can occur in two fashions; slow trends over time within the wellfield, and fast changes in individual wells. Certain mechanisms can be responsible for these trends or quick changes, however, many times the exact answer is not known without intense and potentially expensive investigations. There are ways to minimize the effects of water quality changes within a wellfield.

City of Cape Coral – Southwest RO Wellfield

Water quality declines were noted during the first 15 years of operation. During the 1984 wellfield expansion, chloride concentrations in the wellfield averaged approximately 550 mg/L. Changes in chloride concentration over time is presented in Figure 1, showing combined chloride levels in all wells increasing from 550 mg/L in 1988 to 850 mg/L in 2006. While average salinity levels for all wells combined have steadily increased between years 1988 and 2006, differences were observed in individual wells, as presented in Figure 5. It is evident that salinity in certain production wells exhibited dramatic TDS changes, such as evident in Well 214 that exhibited a TDS increase from 1,810 to 3,940 mg/L. The overall effect of the wellfield improvement strategies was to minimize stresses on individual wells and the wellfield alignments, and minimizing the potential for saltwater intrusion and upconing. Water quality of the raw water to the ROWTP has increased from about 1,400 mg/L TDS from 1988 to 1,900 mg/L in 2000. Water quality has remained stable since that time. The data suggest that readily implementable wellfield operational protocols can minimize water quality changes to manageable levels, thereby prolonging the life of the resource and treatment plant operational requirements.

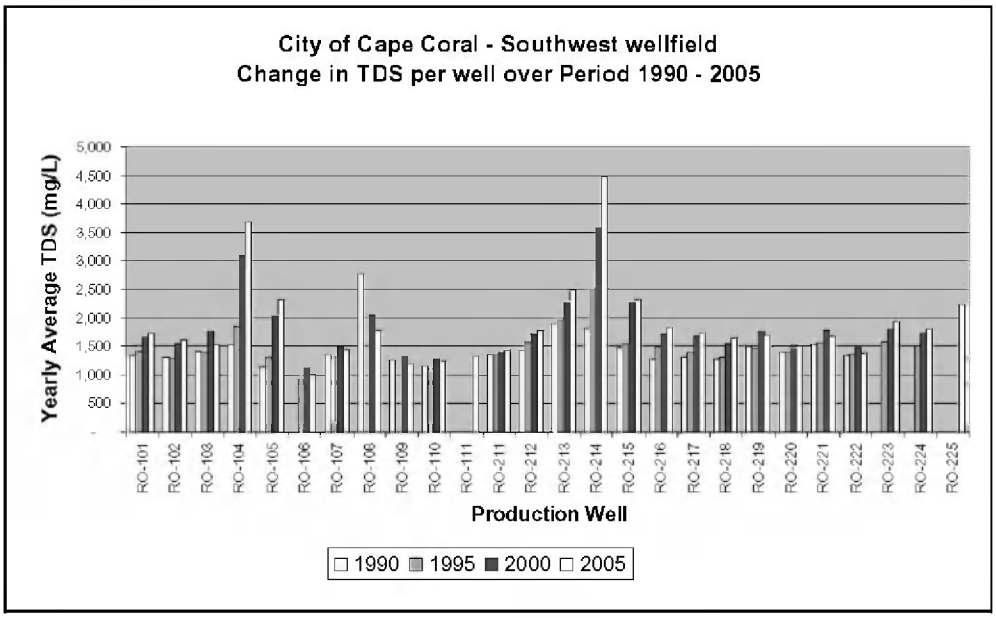

Figure 1. Total Dissolved Solids Trend in Southwest Production Wells Combined

City of Fort Myers Brackish Wellfield

The City of Fort Myers completed construction of the Phase I wellfield in 2000 (7 wells) and Phase II wellfield (5 wells) was initiated in 2003. During the development of the first production well in Phase II, the water quality quickly deteriorated from conductivity of approximately 7,000 microsiemens per centimeter (µS/cm) to 40,000 µS/cm (approximately 20,000 mg/L TDS or approximately 10,000 mg/L chloride). Because of the poor water quality and in concern for the

other wells, this well was partially back plugged and converted to a monitoring well. Due to the extreme need for water, construction carefully proceeded with the other wells in the area. The testing during construction did not reveal any water quality issues with the other four wells. By mid October 2004, it was apparent that the high salinity in the first well had begun migrating to the next closest new production wells. The City considered information concerning the possibility that the high salinity could be caused by some naturally occurring feature (fractures or other geologic anomalies) within the northern section of the wellfield. To date, the lateral migration of salt water has impacted three of the five Phase II brackish production wells.

POTENTIAL SOURCES OF POOR QUALITY WATER

In Florida, vertical or lateral saltwater intrusion can affect water quality over time. Lateral saltwater intrusion occurs when seawater migrates inland from a natural reduction of freshwater heads (drought) or pumping of wells. Fractures which are also evident in carbonate aquifers of southwestern Florida may also increase lateral movement of saltwater into these coastal wellfields. Vertical saltwater intrusion occurs when saline water moves upward through fractures from underlying more brackish aquifers. Production wells are occasionally drilled into fractures that are oriented vertically or at high angles. These fractures may act as intersecting conduits for high salinity water to move upward rapidly degrading the water quality of some wells soon after they go into production, while not directly impacting others. In general, the rapid water quality changes experienced at these utilities seem to be connected to a vertical conduit (vertical fractures or old borehole) that is allowing upward movement of saline water from a deeper aquifer. The changes observed in one or two wells appear to be isolated.

Improperly Abandoned Historical Exploratory Wells

After finding uncharacteristically poor water quality following the development of the first well at the City of Fort Myers, it was suspected that an improperly abandoned exploratory oil or gas "strat" well may be responsible. It is known that Lee County (and surrounding counties) has many of these types of wells which originated back in the 1940s and 1950s with the advent of oil and gas exploration of the area. Many of these wells or exploratory holes were not publicly well documented. For very saline water to enter into an aquifer, the changing of potentiometric heads can cause open vertical conduits to actively water to be exchanged between aquifers which did not occur when potentiometric heads were undisturbed.

SOLUTIONS TO MINIMIZE MIGRATION

There are some solutions that can be imposed on wells that are experiencing impacts from poor quality water. At times, multiple solutions need to be used simultaneously to achieve the desired effect. Abandonment of a well shall always be considered the last option available. Reducing the impacts of upward or lateral migration of poor quality water shall always be considered the first option as it is prudent to try to save the high capital investment in production wells of today.

Back Plugging with Cement

It is possible that wells may be usable in the future if they are back plugged thus reducing stresses which will cause less water to be pulled from the bottom of the borehole. Typically, the deep flow zones are responsible for the connection to poor quality water. It is possible that production can be increased by acidizing a less dominant flow zone higher in the borehole.

Hydraulic Control and Water Quality Blending

Since a well may be connected or in close proximity to (not intersecting) a vertical conduit, it is quite possible that back plugging or abandonment will not be completely successful. Further

operational analysis may show that the impacted well can be used at lower flow rate and the water produced can be diluted into the raw water stream to the ROWTP. This action has a higher chance of success when the additional wells exist or are planned in the immediate future. It is also possible that affected wells can continue being pumped and discharged to the ROWTP deep injection well for disposal, or used for a raw supply for a high pressure RO system. There are permitting and pipeline considerations to be made with this option, however, it can be a viable option if the current wellfield cannot be expanded to increase the blending capacity. Maintaining hydraulic control of the movement of the highly saline water may be the only option for a utility. An abandoned well provides no options for hydraulic control methods.

DISCUSSION AND CONCLUSIONS

Significant increases in salinity, which appear to be localized, may be caused by natural geologic features such as karst collapse features or localized vertical fractures, or man-made conduits of past activities, namely oil and gas exploration. Several existing wellfields in Lee County have exhibited significant water quality changes over time. These changes can affect single wells, multiple wells, or the entire wellfield. Efforts can be made to minimize effects of significant poor quality water migration. In some instances, sacrifices need to be made to protect the rest of the wellfield. These sacrifices can be loss of production from back plugging, reduction in production from a well with significant water quality changes, disposal the raw water from an impacted well to the concentrate deep injection well to maintain hydraulic control, endure lower ROWTP recovery efficiencies due to continued use of an affected well, endure higher ROWTP operational costs from higher feed pressures, costs for construction of a high pressure RO system, or abandonment of an affected well. The concept of hydraulic control is new in the municipal wellfield toolbox; however, it can prove to be a valuable way to protect water supplies from significant water quality changes that can impact an entire wellfield by migration.

REFERENCES

Maliva, R. G., Kennedy, G. P., Martin, K. W., Missimer, T. M., Owosina, E. S., and Dickson, J. A., 2002, *Dolomitization-Induced Aquifer Heterogeneity: Evidence From the Upper Floridan Aquifer, Southwest Florida*, GSA Bulletin, Vol 114, No. 4; p. 419-427.

Contact Information: Michael L. Weatherby, P.G., MWH Americas, Inc., 1000 N. Ashley Drive, Suite 1000, Tampa, FL 33602 USA, Phone: 813-204-3306, Fax: 813-226-2406, Email: michael.weatherby@mwhglobal.com

Freshwater Lens Development on Padre Island, Texas

Egon T. Weber II, *Robert Schulz* and *James R. Garrison Jr.*
Center for Water Supply Studies, Texas A&M – Corpus Christi, Corpus Christi, TX, USA

ABSTRACT
Padre Island is one of the most extensive barrier islands in the world. With a length of ~100km and a width of ~3km the island morphology is the acme of a wave dominated barrier island in the microtidal Gulf of Mexico. This study presents preliminary results of a hydrogeophysical and sedimentological study being conducted in a 3km transect of the island to elucidate sedimentary processes and controls on the development of the freshwater lens. The freshwater lens was characterized by water table elevation measurements and resistivity soundings acquired with a magnetotelluric technique. The FW/SW interface is significantly shallower than the Ghyben-Herzberg-Dupuit equation would predict from the water table elevations. We suggest that this difference exists because of lithological variability within the sedimentary package on the island and because of the submarine discharge of water along the island margins.

INTRODUCTION
Padre Island, Texas is one of the most extensive barrier island systems in the world, which borders the microtidal Gulf of Mexico in south Texas. This barrier island is approximately 3km wide in most areas, and, as presently configured, constitutes approximately 100 km of length without any active tidal passes (Garrison and McCoy, 2007).

In addition, Padre Island is primarily encompassed within the Padre Island National Seashore unit of the National Park Service, and is thus essentially undeveloped. On the shoreward side of Padre Island is the Laguna Madre, which can occasionally experience hypersaline conditions. The uninterrupted length of Padre Island and the fact that this island is located in a relatively dry, sub-humid climate zone makes this island distinct from many islands on the U.S. East Coast where barrier islands are more intensively studied for stratigraphic and hydrogeologic models.

The purpose of this study is to develop an understanding of the stratigraphic and hydrogeologic dynamics within such a barrier island setting. We present here preliminary results from Padre Island where a cross-section of the island is being examined using shallow wells and geophysical techniques.

METHODS
The investigation of Padre Island is being conducted using a variety of methods to characterize the surface and subsurface. To begin, a differential GPS survey was conducted along a transect perpendicular to the Gulf Coast which encompassed approximately 3,100 meters (Figure 1). Reference points were marked at regular/semi-regular intervals to accommodate the collection of ground penetrating radar (GPR) surveys. In addition, 12 points were marked where coring to the water table could be accomplished. Vertical accuracy is in the range of 2-3 cm. The GPR data is being processed and will be discussed in later works.

The first data evaluated in this study is the elevation profile of the topography and the water table. At each water table measurement site, an 8 cm auger was used to penetrate up to a meter below the water table and then a drive point screen was inserted to refusal. The dominantly fine-

sand subsurface allowed equilibration of the water level within several minutes. Then the water level was measured with respect to the surveyed point. The water table elevations are likely within 3-4 cm. The elevation of the ground surface was also measured. Elevations of the survey were reference to NAVD88. Data from a nearby Texas Coastal Ocean Observation Network observing station was used to correct the vertical datum to Mean Sea Level. The offset used here was derived from the Bob Hall Pier station which indicates a MSL 0.15m below NAVD88. All depth measurements here are referenced to this MSL estimate.

The geophysical data used in this study was acquired using a Stratagem™ EH4 magnetotelluric (MT) survey system. The data was acquired using a controlled source audio magnetotelluric mode (CSAMT) with 13 frequencies in the range of 0.8 kHz to 66 kHz. In brief, the impedance response of the subsurface represents deeper integrated depths for observations at lower frequencies.

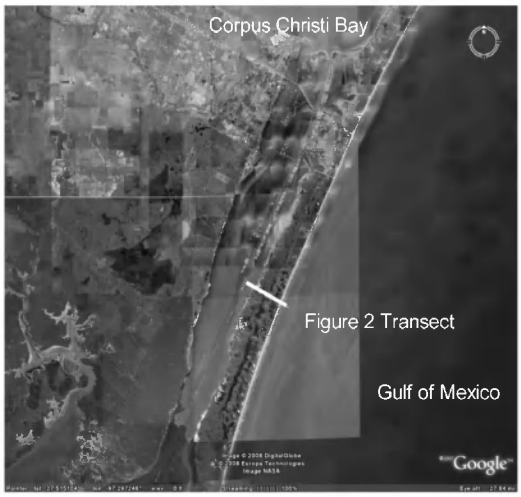

Figure 1. The Padre Island transect site on a Google Earth™ Image.

The data was then reduced to the impedance tensor measurements. In general, the data complies well with the geometric expectations of impedance isotropy, and 1-D behavior. However, the transverse electric data (Z_{xy}) appears to be somewhat noisy on some sites so the transverse magnetic (Z_{yx}) data is used for the presentation here. The Z_{yx} data was then used to generate curves of apparent resistivity (ρ_{app}) and phase (φ) versus frequency at each site (Simpson and Bahr, 2005).

All MT survey sites were then interpreted using a 1-D resistivity sounding model. This was accomplished by using a multiple-layer resistivity model based upon a Schmucker-Weidelt transfer function. This 1-D forward modeling approach uses a recursive algorithm to integrate the electromagnetic response of the subsurface from the deep subsurface to the surface response which is what the MT system actually measures (Simpson and Bahr, 2005). The profile of the resistivity curve was described as a polynomial which was optimized to minimize the predicted (ρ_{app}) and phase (φ) curves when compared with the MT data.

In addition to the above observations, the GPR survey is being complimented with coring along the transect. These data and results are not yet ready to present.

RESULTS

The preliminary results are presented in Figure 2 where the cross section of the island is shown along with the data and interpretations. The x-axis is the distance along the island with Laguna Madre on the Left and the Gulf of Mexico on the right, depth is displayed in meters from mean sea level. The surface of the island and the water table elevations at the 12 sites are shown on the top of the figure; both are extrapolated into the surrounding water body.

Figure 2 also shows an interpretation of the 18 MT resistivity soundings. All such soundings show a decrease in the resistivity with depth from values of over 100 Ωm at the top to values below 1 Ω−m at the bottom. The depth of investigation varies from less than 5 meters at the Laguna Madre side to up to 50 meters in the center of the island. The location of the FW/SW interface in the MT soundings was selected using either the 1 Ω−m layer or the inflection in the 1-5 Ω−m range depending on the structure of the data. The FW/SW interface is plotted as the thick blue line in Figure 2.

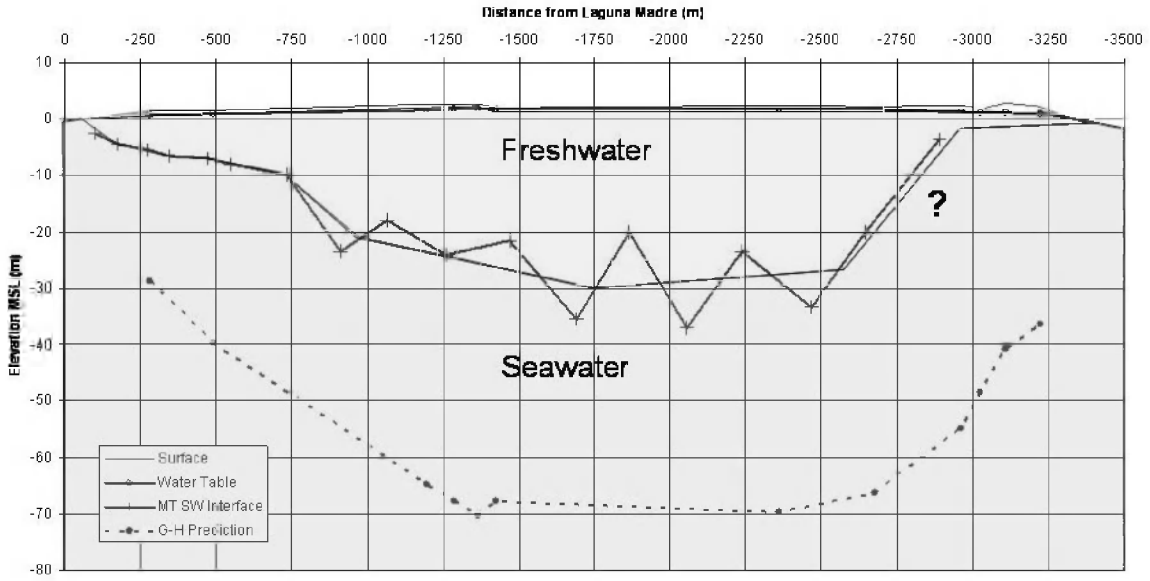

Figure 2. Padre Island Cross Section.

DISCUSSION AND CONCLUSIONS

Two pertinent observations can be made from the cross section presented in Figure 2. First, the depth of the FW/SW interface is much shallower than the Ghyben-Herzberg-Dupuit equation would suggest based upon the water table elevations; certainly, this static model of freshwater lens development is oversimplified (Urish and Ozbilgin, 1989). The freshwater lens system is most likely discharging along the shore face on both sides of the island (Fetter, 1972). In addition, the sandy material of the island is underlain by the somewhat clayey and heterolithic Beaumont formation at approximately 10 meters. This, and buried wetland soils likely effect the vertical hydraulic conductivity and may result in anomalous water table elevations (e.g., Anderson et al., 2000)

The second observation is that the depth of the FW/SW transition is variable in the center of the island where it is typically below 10 meters of depth. Although the interpretation in Figure 2 simplifies this variation, the variation may indeed be real. This variation in depth of the interface may indeed be real and related to variations in hydraulic conductivity in the Beaumont formation.

REFERENCES

Anderson, W.P. Jr., D.G. Evans, and S.W. Snyder. 2000. The effects of Holocene barrier –island evolution on water-table elevations, Hatteras Island, North Carolina, USA. Hydrogeology Journal. 8: 390-404.

Fetter C.W. 1972. Position of the saline water interface beneath oceanic islands. Water Resources Research. 8: 1307-1315.

Garrison, J.R., Jr., and B. McCoy. 2007. The Nueces Incised Valley revisited: A reinterpretation of the sedimentology and depositional sequence stratigraphy of preserved Pleistocene and Holocene valley-fill sediments: Gulf Coast Association of Geological Societies Transactions, 57, pp.

Simpson, F, and K. Bahr. 2005. Practical magnetotellurics: Cambridge University Press, Cambridge, U.K., 254 p.

Urish D.W., and Ozbilgin M.M. 1989. The coastal ground-water boundary. Ground Water. 27: 310-315.

Contact Information: Egon T. Weber II, Texas A&M University – Corpus Christi, Center for Water Supply Studies, 6300 Ocean Drive, Corpus Christi, TX, 78412-5864 USA, Phone: 361-825-2309; Fax: 361-825-2309, Email: egon.weber@tamucc.edu

The Role of Fresh and Saline Submarine Groundwater Discharge in Nutrient Contribution to Coastal Seawater, Dor Bay (Israel)

Yishai Weinstein[1], *Barak Herut*[2], *Y. Shalem*[1], *B. Burnett*[3] and *P. Swarzenski*[4], *Y. Yechieli*[5]
[1]Department of Geography and Environment, Bar-Ilan University, Ramat-Gan, Israel
[2]Israel Oceanogrphic and Limnological Research, Haifa, Israel
[3]Department of Oceanography, Florida State University, Tallahassee, FL, USA
[4]Coastal Marine Geology Program, U.S. Geological Survey, Santa Cruz, CA, USA
[5]Department of Water and Natural Resources, Geological Survey of Israel, Jerusalem, Israel

ABSTRACT
Submarine Groundwater Discharge (SGD) is widely accepted as a major factor in coastal water quality. More specifically, it was suggested by several authors (e.g. Moore 1996, 1999) that the circulation of seawater in the sediment and the resultant saline SGD is a dominant factor in the transport of nutrients and other solutes to the sea. A recent SGD study at Dor bay (southern Carmel coast, northern Israel) reveals that unlike fresh SGD, recirculated seawater in this site is nutrient poor. SGD at Dor is on the order of 8 cm/d. Two different geological units are discharging to the bay, a Pleistocene calcareous sandstone (locally called 'Kurkar') and an overlying Holocene loose sand. Based on salinity and radon, it was established that fresh water discharge is mainly from the Kurkar unit, while the saline SGD is mainly via circulation in the loose sand. Nutrient concentrations in the bay are very low (e.g. 2 μM NO_3), while high in onshore groundwater (e.g. 200-400 μM NO_3). Nutrient concentrations in water discharging from seepage meters deployed in the bay were relatively low (2-80 μM NO_3), and on a diagram of nitrate versus salinity, they plot below the mixing line between nutrient-rich groundwater and nutrient-poor seawater. This implies (1) that the saline SGD fraction (recirculated seawater) in the discharging water is nutrient-poor and (2) that even the nitrate in the fresh SGD is undergoing partial denitrification in the subterranean estuary. In a similar way, silica concentration is either on or below the mixing line between silica-rich groundwater and silica-poor seawater. Phosphate patterns are different, since phosphate is very low in the Kurkar groundwater and is similar to seawater concentrations (0.1-0.2 and 0.1 μM PO_4, respectively). On the other hand, phosphate concentrations in seepage meter water are mostly somewhat above the groundwater-seawater mixing line, probably due to the contribution from the subterranean estuary. In summary, the observations from Dor bay reveal that at least in this case recirculated seawater does not carry nutrients to the sea, thus raise questions about the significance of saline SGD to the quality of coastal seawater.

Contact Information: Y. Weinstein, Department of Geography and Environment, Bar-Ilan University, Ramat-Gan 52900, Israel, Phone: 972-3-531-8340, Fax: 972-3-534-4430, Email: weinsty@mail.biu.ac.il

Seawater Intrusion in Australia – A National Perspective of Future Challenges

Adrian D. Werner[1], *E. Nation*[2] and *M. A. (Rien) Habermehl*[2]
[1]School of Chemistry, Physics and Earth Sciences, Flinders University, Adelaide, SA, Australia
[2]Bureau of Rural Sciences, Dept of Agriculture, Fisheries & Forestry, Canberra, ACT, Australia

ABSTRACT
Extended periods of below-average rainfall combined with a rising population density in the Australian coastal margin has led to higher stresses on coastal water resources, and the risk of seawater intrusion has increased. Despite reports of seawater intrusion in the majority of states, comprehensive seawater intrusion investigations have only been completed for coastal systems in Queensland and to a lesser degree in Western Australia and South Australia. The most comprehensive studies include those of the Pioneer Valley and Burnett basins in Queensland, for which detailed conceptual and mathematical models have been developed at the regional scale. These studies have been used to underpin water resources management plans, which aim to control groundwater abstraction to protect the sustainability and supply reliability of the coastal groundwater resources of these areas. Seawater intrusion monitoring is widespread. In response to historical changes in seawater intrusion extent, artificial recharge and recycled-water schemes have been introduced or are planned in several areas (e.g. aquifers in the Bribie Island, Pioneer Valley and Lower Burdekin areas in Queensland) to alleviate the threat of seawater intrusion. A national-scale review of groundwater conditions in irrigation areas situated within Australia's coastal margins highlights high-risk areas. The level of seawater intrusion investigation of these high-risk areas was identified, and recommendations for prioritised (from a national perspective) further assessment are given.

INTRODUCTION
In Australia, groundwater contained in coastal aquifers represents a vital component of the freshwater resources available for urban, agricultural and industrial activities. Population increase and protracted periods of below-average rainfall have led to an enhanced dependency on coastal groundwater resources, and there is evidence of over-use in many major Australian aquifers (Ball et al., 2001). As a result of this, there is now evidence of the adverse impacts of seawater intrusion in several of Australia's coastal aquifers.

The deleterious impacts of bore salinisation resulting from seawater intrusion have caused significant losses in potable water supplies and in agricultural production globally (FAO, 1997). In some areas, the scale of seawater intrusion issues is expected to be exacerbated by sea-level rise and climate change. Despite evidence of widespread impacts of seawater intrusion, there is a lack of studies documenting the magnitude of the problem on a global, continental or national scale, and no studies have previously summarised the situation in Australia. While seawater intrusion is being assessed and managed in some areas, there is not a consistent approach to seawater intrusion investigation, monitoring, and management across the country. The aims of this study are to review the susceptibility of Australian coastal aquifers to seawater intrusion, to highlight important case studies, and to make recommendations relating to the investigation and management of seawater intrusion in Australia. This study is based on an overview of previous coastal groundwater investigations, combined with a nationwide analysis of available groundwater data.

A NATIONAL PERSPECTIVE OF SEWATER INTRUSION SUSCEPTIBILITY

Voice et al. (2006), in their gap-analysis of the vulnerability of Australia's coastal zones to the adverse impacts of climate change, identified increased seawater intrusion as a significant threat. However, no attempt to highlight areas of likely impact was undertaken. In the current study, available nationwide data relating to topography, groundwater condition and areas of irrigation were combined in a first-order assessment of the most likely regions requiring further investigation of their susceptibility to increased seawater intrusion. A somewhat simple analysis of potential sea-level rise impacts was also undertaken, but is not presented here for brevity.

A GIS-based approach was adopted in combining and analysing existing datasets. The analysis involved identifying overlaps between irrigation areas within the coastal fringe, regions of low topography, areas of intensive groundwater use, and indicators of groundwater system condition. Areas of low relief (<10 m AHD – i.e. 10 m above mean sea level) were identified using NASA SRTM (Shuttle Radar Topographic Mission) 90 m digital elevation model topographical information (see http://srtm.csi.cgiar.org). Groundwater information was obtained from the NAMS (National Agricultural Monitoring System) database (see www.nams.gov.au). Irrigation land-use types were defined according to Bureau of Rural Sciences data as at January 2007 (see http://adl.brs.gov.au/mapserv/landuse/land_use_data.html). Table 1 lists areas of irrigation in low-lying coastal zones on a state-by-state basis to provide an indication of the relative susceptibility (based on coastal proximity and topography) of the irrigation industry. The results indicate that 1.4% and 4.4% of the country's irrigation areas are situated near the coast and at elevations 0-5 m AHD and 0-10 m AHD respectively. Queensland (7.8%) and South Australia (6.2%) have the highest proportions of near-coastal, low lying (0-10 m AHD) irrigation areas.

Table 1. Summary of a GIS-based analysis of irrigation areas and coastal proximity

State	Total Irrigation Area	Major Land-use	Area at 0-5 m AHD	Area at 0-10 m AHD
NSW	867,516 ha	Cropping	7,663 ha	10,198 ha
NT	29,899 ha	Tree fruits	136 ha	402 ha
QLD	1,080,787 ha	Sugar	15,706 ha	84,749 ha
SA	271,319 ha	Sown grasses	9,481 ha	16,839 ha
TAS	128,795 ha	Cropping	2,922 ha	6,837 ha
VIC	837,886 ha	Modified pasture	9,624 ha	23,018 ha
WA	55,789 ha	Vine fruits	528 ha	2,814 ha
Total	3,271,991 ha	Cropping	46,060 ha	144,858 ha

The simple assumption was made that near-coastal groundwater conditions of high-salinity and/or low water levels are indicative of a higher likelihood of seawater intrusion susceptibility. It proved difficult to quantitatively assess seawater intrusion trends because the location and density of monitoring sites varies. Only a qualitative first-impression of "hot spots" was obtained. Decadal-minimum groundwater levels were obtained to illustrate temporal trends in groundwater conditions. The results for 2000-2008 are given in Figure 1. Maximum groundwater salt concentrations were also obtained, and these are illustrated in Figure 2.

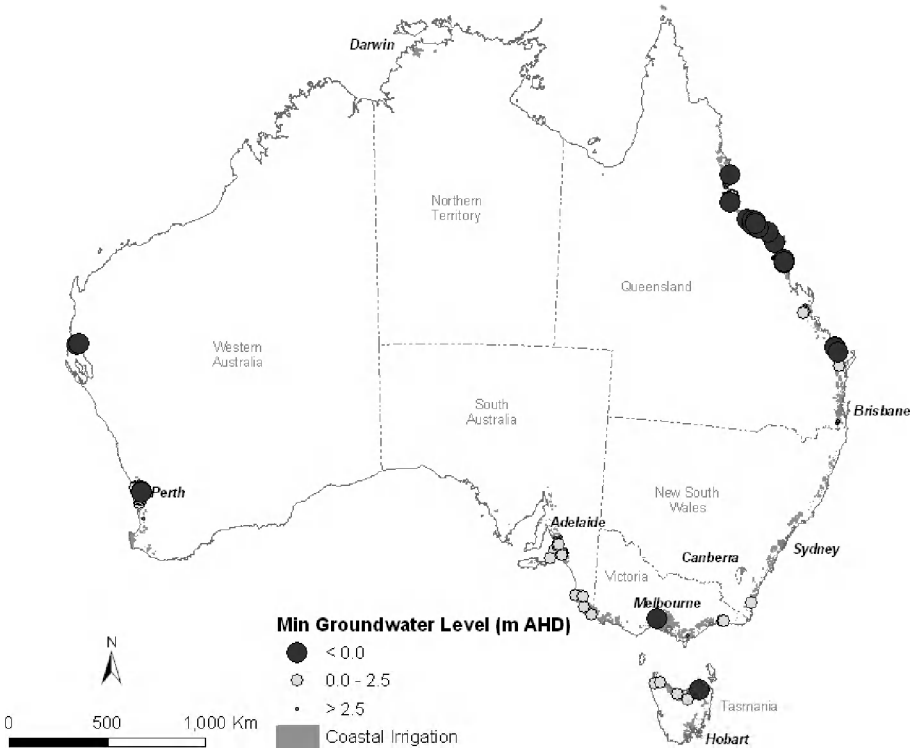

Figure 8. Minimum (lowest) groundwater levels during the period 2000-2008

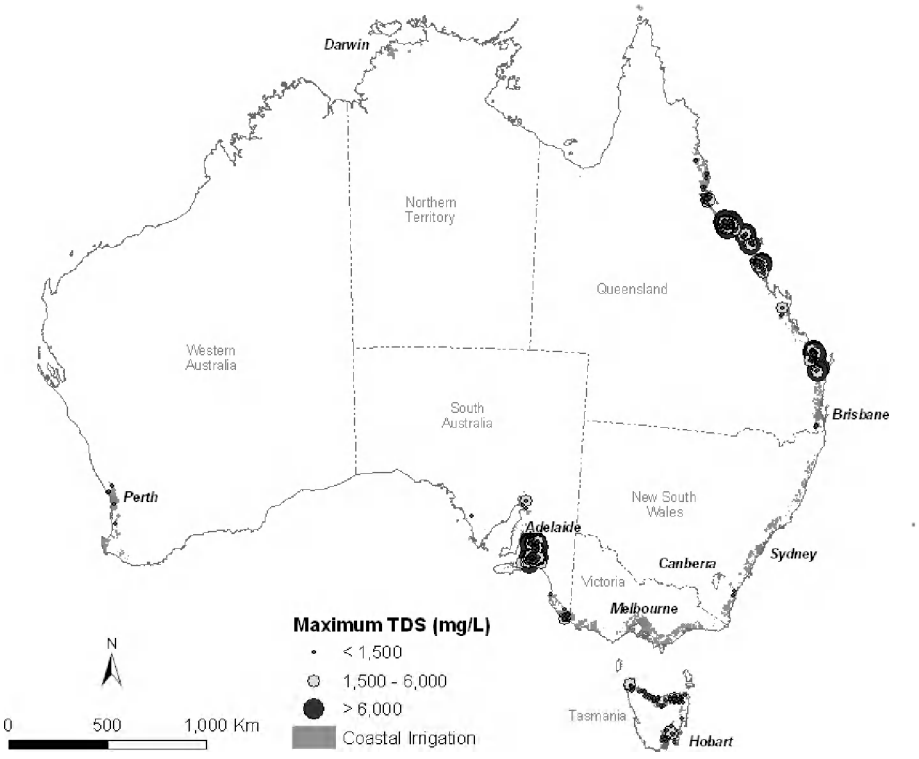

Figure 2. Maximum groundwater total dissolved solids (TDS)

PREVIOUS INVESTIGATIONS

Typically, an investigation of seawater intrusion for the purposes of water resources management requires activities related to: 1. data collection, 2. conceptualisation, and 3. computer modelling. Only a few investigations of Australian seawater intrusion include all three phases, despite many reports acknowledging significant threats of seawater intrusion degradation. The review indicated that the most advanced seawater intrusion investigations have been undertaken in Queensland, including investigations of the Pioneer Valley, Burnett and Lower Burdekin aquifers (Werner and Gallagher 2006; Bajracharya et al. 2006; Narayan et al. 2007). Seawater intrusion management studies of Western Australian systems have also been completed, although these typically do not progress to the development of computer models. There are several examples of management responses to seawater intrusion susceptibility, including targeted monitoring programs, groundwater pumping controls and artificial recharge schemes (e.g. Narayan et al. 2007).

CONCLUSIONS AND RECOMMENDATIONS

There is evidence of extensive seawater intrusion problems in Australia, most noticeably in Queensland and South Australia (SA), but also in regions of Western Australia (WA), Victoria and Tasmania. The extensiveness of near-coastal irrigation areas in Queensland has led to more detailed and comprehensive seawater intrusion studies being undertaken on Queensland aquifers. It is strongly recommended that a national framework for best-practice seawater intrusion monitoring, investigation, management and remediation be developed, based on experiences in Queensland. The dissemination of "lessons learnt" from Queensland studies would benefit other water resource management authorities, who are likely to soon require solutions to similar issues.

REFERENCES

Bajracharya, K., A. Moser, K. Heidke, A.D. Werner. 2006. Regional scale instructional seawater intrusion model for the Coastal Burnett Region in Queensland. In Proceedings of 30th Hydrology and Water Resources Symposium, 4-7 December 2006, Launceston, Tasmania.

Ball, J., L. Donnelley, P. Erlanger, R. Evans, A. Kollmorgen, B. Neal and M. Shirley. 2001, Inland waters, Australia State of the Environment Report 2001, CSIRO Publishing, Canberra.

FAO. 1997, Seawater intrusion in coastal aquifers: Guidelines for study, monitoring and control, Food and Agriculture Organization Water Reports, Rome, 163 pp.

Narayan, K.A., C. Schleeberger and K.L. Bristow. 2007. Modelling seawater intrusion in the Burdekin Delta Area, North Queensland, Australia. Agricultural Water Management 89: 217-228.

Voice, M., N. Harvey and K. Walsh (eds). 2006. Vulnerability to Climate Change of Australia's Coastal Zone. Report to the Australian Greenhouse Office, Canberra, Australia, 120 pp.

Werner, A.D., M.R. Gallagher. 2006. Characterisation of seawater intrusion in the Pioneer Valley, Australia using hydrochemistry and three-dimensional numerical modelling. Hydrogeology Journal 14: 1452-1469.

Contact Information: Adrian Werner, Flinders University of South Australia, School of Chemistry, Physics and Earth Sciences, Sturt Road, Bedford Park, Adelaide, Australia, Phone: 6-188-201-2710,
Email: adrian.werner@flinders.edu.au

Airborne Geophysical Investigation of the German North Sea Coastal Area

Helga Wiederhold[1], *Franz Binot*[1], *Klaus Kühne*[1], *Uwe Meyer*[2] and *Bernhard Siemon*[2]
[1]Leibniz Institute for Applied Geosciences (GGA-Institut), Hannover, Germany
[2]Federal Institute for Geosciences and Natural Resources (BGR), Hannover, Germany

ABSTRACT

In recent years airborne geophysical methods have turned out to have great potential in delineating subsurface information down to, e.g., 200 m depth. This information is essential for planning purposes for manifold geoscientific, economic or environmental questions, like, e.g., utilization and protection of fresh groundwater resources, land utilization or industrial planning. These data integrated into a three-dimensional geographical information system provide a perfect tool for spatial planning. Beside the geologic or geophysical basic information also changes of surface and subsurface data in time and space may be documented by repeated surveys. Especially electromagnetic induction is the most versatile of the airborne geophysical methods and widely applied in hydrogeological investigations because the measurements respond to both lithologic and water-chemistry variations. The applications include geologic mapping and aquifer structure, delineation of soil and groundwater salinization, salt-water intrusion into coastal aquifers etc.

In Germany, until today only small areas are covered by airborne geophysical surveys. Recently airborne geophysical data were gathered and interpreted for the mapping of buried valley aquifers (BURVAL Working Group 2006). Building on previous results and knowledge (e.g. Siemon et al. 2004 and 2007; Steuer et al. 2008; Siemon 2006) a general airborne survey of the German North Sea coastal area is projected and started in 2008. Emphasis is placed on the mapping of freshwater-saltwater interfaces, saltwater intrusions and the evaluation of the coastal aquifers as well as on the mapping of freshwater discharge to the sea. With the mapping a basis for monitoring should be set up.

The data will be archived in the Geophysics Information System (FIS GP) of GGA-Institute (Kühne 2005) where a database subsystem for aerogeophysical data (electromagnetic, magnetic and radiometric data) will be designed. The interpretation and visualization tools of FIS Geophysik enable a common processing with ground based surveys and data from other methods. A powerful web-interface: (https://www.gga-hannover.de/app/fis_gp/startseite/start.htm) provides the data for the scientific community. Further access to all contents of FIS GP will be able by end of this year by the European portal for geophysical data developed in the EU project GEOMIND = Geophysical Multilingual Internet-Driven Information Service (Vértesy et al. 2007).

First results of freshwater-saltwater interaction of the German North Sea coastal area will be discussed in the poster.

REFERENCES

BURVAL Working Group. 2006. Groundwater resources in buried valleys-a challenge for geosciences, ed R. Kirsch, H.M. Rumpel, W. Scheer, and H. Wiederhold. Hannover, Germany: Leibniz Institute for Applied Geosciences.

Kühne, K. 2005. Geophysik online - das Fachinformationssystem Geophysik. Mitteilungen Deutsche Geophysikalische Gesellschaft 3/2005: 23-29; Hannover.

Siemon, B. 2006. Airborne techniques. In Groundwater Geophysics - A tool for Hydrogeology, ed R. Kirsch, 348-362. Heidelberg: Springer.

Siemon, B., Steuer, A., Meyer, U. and Rehli, H.-J. 2007. HELP ACEH - a post-tsunami helicopter-borne groundwater project along the coasts of Aceh, northern Sumatra. Near surface geophysics 5, 4: 231 - 240.

Siemon, B., Eberle, D. and Binot, F. 2004. Helicopter-borne electromagnetic investigation of coastal aquifers in North-West Germany. Zeitschrift für geologische Wissenschaften 32, 5/6: 385 - 395.

Steuer, A., Siemon, B and Auken, E. 2007. A comparison of helicopter-borne electromagnetics in frequency- and time-domain at the Cuxhaven valley in Northern Germany. Journal of Applied Geophysics, doi:10.1016/j.jappgeo.2007.07.001.

Vértesy, L., Gulyás, Á., Detzky, G. and the GEOMIND CONSORTIUM. 2007. GEOMIND - A Project to Set up a Geophysical Multilingual Internet-Driven Information Service. 69th EAGE Conference & Exhibition Incorporating SPE EUROPEC 2007, 11-14 June 2007, London, Extended Abstracts. EAGE, Houten, The Netherlands.

Contact Information: Helga Wiederhold, Leibniz Institute for Applied Geosciences (GGA-Institut), Stilleweg 2, 30655 Hannover, Germany, Phone: +49-(0)511-6433520, Fax: +49-(0)511-6433665,
Email: helga.wiederhold@gga-hannover.de

Combined Groundwater Quality and Groundwater Model Approach as Main Tool of an Aquifer Management for Sustainable Water Supply in the Santo Domingo Valley, Baja California Sur, Mexico

Jobst Wurl, *Miguel Imaz Lamadrid, Juan Eduardo Martínez Meza, Cynthia Nayeli Martínez García* and *Genaro Martínez Gutiérrez*
Universidad Autónoma de Baja California Sur, CA Geohidrología y Geoinformatica

ABSTRACT
The extraction of groundwater and especially the over-exploitation of the Santo Domingo aquifer since 1957 has caused modifications in the natural flow system and induced lateral flow of seawater from the coastline. As a result the groundwater quality in the Santo Domingo Irrigation District is deteriorating. Seawater intrusion and irrigation-return combined with the mobilization of deeper groundwater have been identified as important sources of salinization.

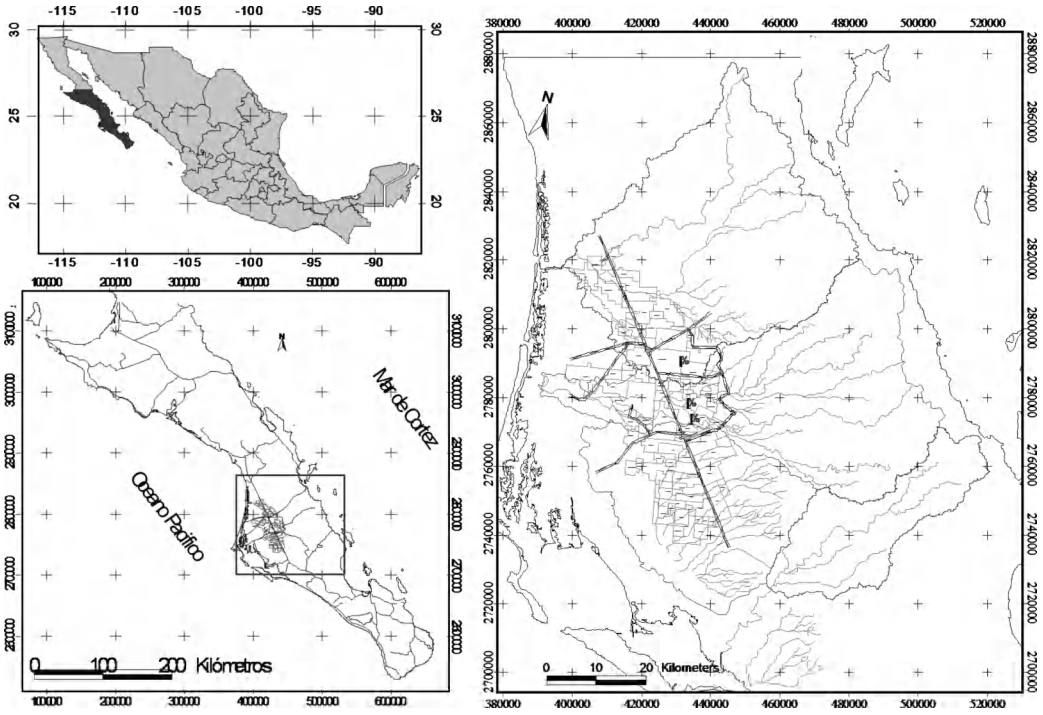

Figure 1. Location of the study area in Mexico, in the southern part of the Baja California Peninsula and detailed map of the Santo Domingo Irrigation District with the most important catchments and drainage systems

INTRODUCTION
Since its colonization in the 1950s the Santo Domingo Valley has become the most important agricultural district of Baja California Sur. As typical for semiarid regions the main source of freshwater is groundwater. Important factors in the water balance of the region are the very intensive rainfalls caused by storms and hurricanes. The runoff from the mountains infiltrates in the subsequent alluvial fans where it recharges the aquifers. The extraction of groundwater and especially the over-exploitation of the aquifer since 1957 has caused modifications in the natural

flow system and induced lateral flow of seawater from the coastline. As a result the groundwater quality in the Santo Domingo Irrigation District is deteriorating.

METHODS

The concentrations of the macro-constituents in 4375 ground water analyses, taken from 710 agriculture wells between 1986 and 2005, were interpreted in respect to changes in the groundwater composition. Another 100 groundwater samples, taken at selected wells in various sample campaigns since 2006 included a wide spectrum of analyzed elements, using an ICP OES Spectrometer.

In order to understand the groundwater flow regime in the past, we used the USGS MODFLOW model, which is widely used for groundwater studies. It was utilized to represent the lower part of the catchments model, and included 40000 cells in each of the two layers. To calibrate the regional groundwater flow, the hydraulic head data of more than 500 wells were included. Additionally runoff data were introduced to the MODFLOW model to represent the effects of catchments in the mountain area. The calculated runoff from these adjoining catchments was combined to the MODFLOW model using the STREAMFLOW package.

RESULTS

There is a strong annual variation in groundwater mineralization with lower values in autumn and winter and higher values in spring and summer (Figure 2 and 3), due to intensive rainfalls caused by tropical storms during the hurricane season (May to November). Although former studies indicated only minor influence of direct seawater intrusion on groundwater quality (Cardona et al. 2004), we found evidence that it is the main source of high mineralization in the three parts of the aquifer (see Figure 4).

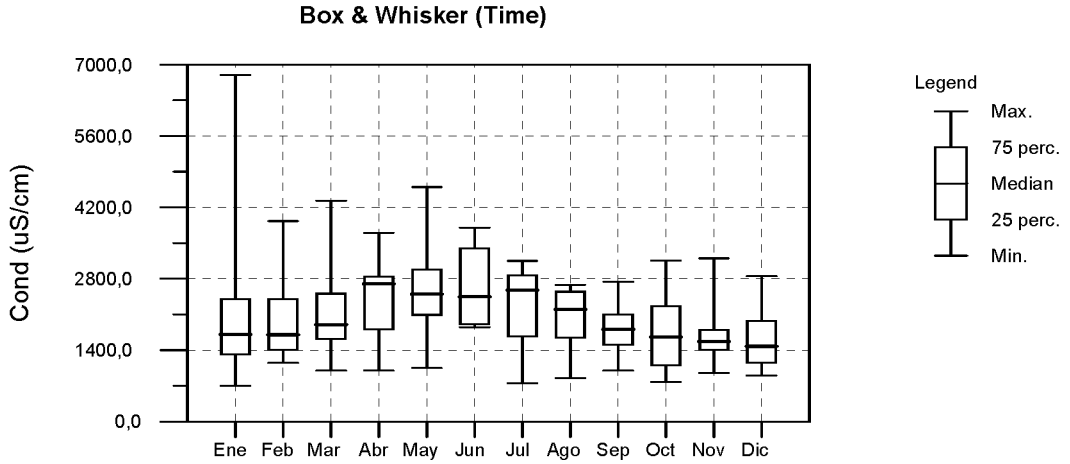

Figure 2. Monthly variation of the electric conductivity in 4375 ground water analyses from 710 agriculture wells between 1986 and 2005

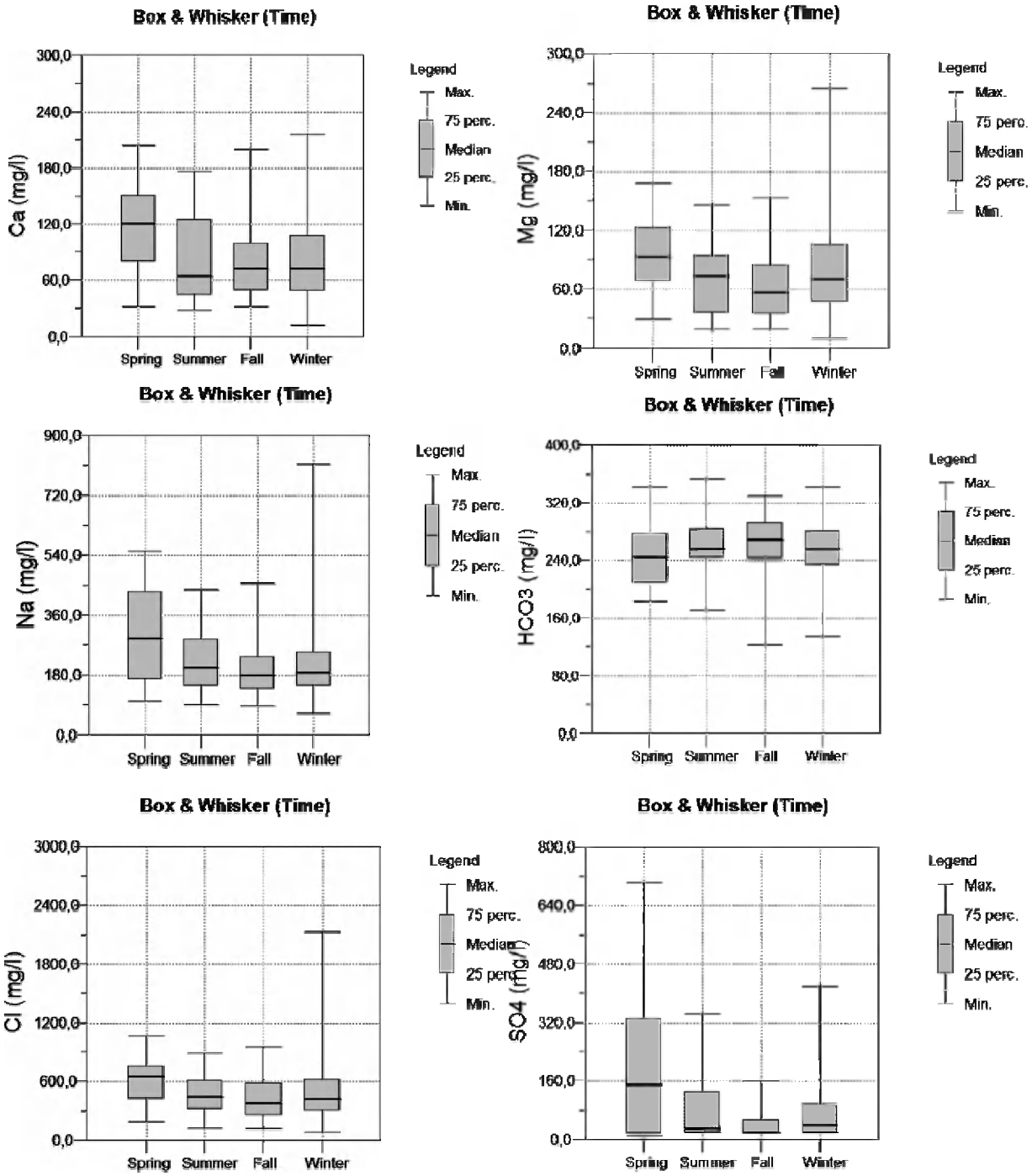

Figure 3. Seasonal variation of Ca, Mg, Na, HCO_3, Cl and SO_4 concentrations in 4375 ground water analyses

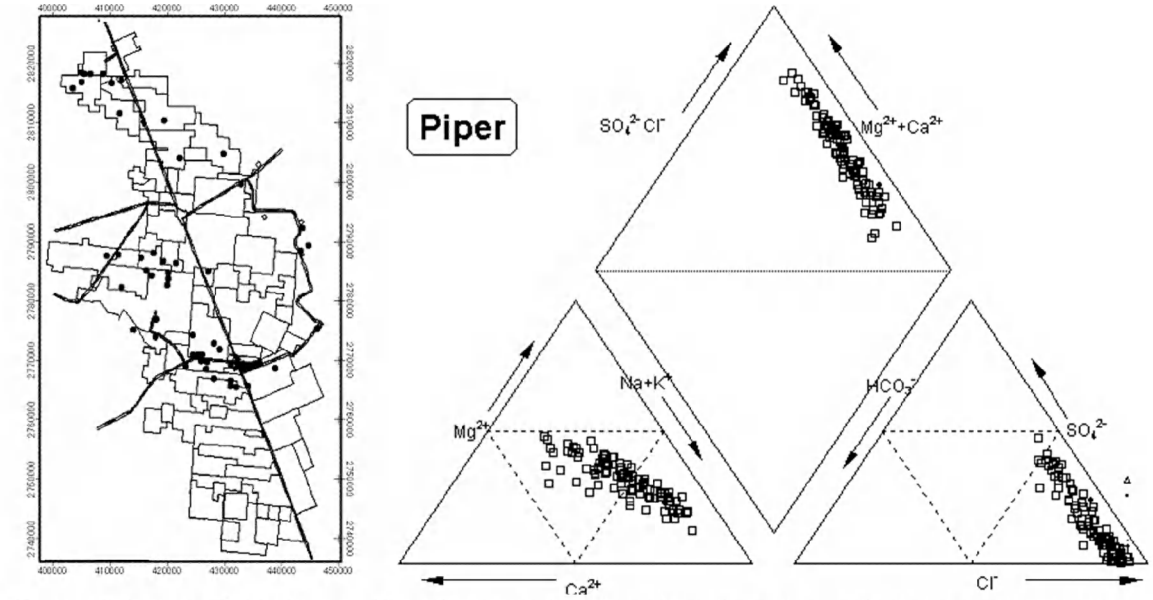

Figure 4. Map of the Santo Domingo Irrigation District. Points indicate wells with salt water intrusion represented by high Cl/SO_4 ratios (>50) and Piper diagram of water samples with electric conductivity of more than 4000 µS /cm

The combined watershed and groundwater model was able to represent the observed groundwater levels including the interaction between runoff and recharge in the lower part of the watershed. In years without runoff infiltration the recharge rate is about 20 % below permitted extraction rate. The recharge caused by base flow is a significant component of the total recharge in the watershed.

OUTLOOK

After the calibration of the coupled watershed groundwater model the next step will be the implantation of scenarios based on the analysis of projected water demands (including the population projections and the future split up of the demand between various generic users). The model will help to plan the water supply and management in the region and to promote sustainable water supply strategies.

REFERENCES

Cardona A; JJ, Carrillo-Rivera; R, Huizar-Alvarez y E, Graniel-Castro, 2004. Salinization in coastal aquifers of arid zones: an example from Santo Domingo, Baja California Sur, Mexico. Environmental Geology, Vol 45 No 3, 350-366.

Contact Information: Jobst Wurl; Universidad Autónoma de Baja California Sur, CA Geohidrología, Carretera al Sur Km 5.5, 23080 La Paz, B.C.S., México, Telephone: 52-612-1238800 Ext. 4230, Email: JWURL@UABCS.mx

Simulation of Processes Controlling Migration of Saline Water and Brine above a Flooded Salt Mine in Western New York, USA

Richard M. Yager[1] and *Paul E. Misut*[2]
[1]U.S. Geological Survey, Ithaca, New York, NY, USA
[2]U.S. Geological Survey, Coram, New York, NY, USA

ABSTRACT
Variable-density/vicosity simulations were conducted to investigate processes controlling the migration of brine and saline water in the aftermath of a salt mine collapse, which threatens to contaminate an overlying glacial-drift aquifer. The simulations represent 10.7 years of water-level recovery after mine flooding, followed by a one year of brine pumping. Model results indicate that movement of brine and saline water is controlled by displacement of brine from the mine and mixing of waters from bedrock fracture zones.

INTRODUCTION
The Retsof mine in western New York State, one of the world's largest salt mines, was abandoned after roof collapses in 1994 triggered flooding by water from a confined glacial-drift aquifer. The roof collapses propagated upward through overlying bedrock and formed two rubble zones or chimneys that connected the mine to the aquifer. Inflow rates averaged about 74 m^3 per minute until the mine was completely flooded in January 1996. Flooding of the mine caused dissolution of unmined halite and lowered water levels in the aquifer near the collapse area by as much as 120 m by January 1996 (Yager et al., 2001). By 2005 water levels in the aquifer had nearly recovered to pre-collapse conditions and the mine cavity contained about 60 million m^3 of saturated halite brine.

As the mine cavity closes through continued salt creep, about 80 percent of the brine could be displaced and migrate upward through the rubble chimneys toward the aquifer (L.L. Van Sambeek, RE/SPEC Inc., written commun., July 2007). Saline water flowing through carbonate rocks between the mine and the aquifer could also migrate upward through the rubble chimneys toward the aquifer. A brine mitigation project that includes pumping and desalination of saline water and brine from the rubble chimneys was begun in September 2006 to limit contamination of the glacial-drift aquifer. This study used variable-density simulations to examine the factors that control movement and mixing of waters in the collapse area in support of this project.

HYDROGEOLOGIC SETTING
The flooded Retsof salt mine underlies a bedrock valley that was deepened and widened by ice during the Pleistocene Epoch. The bedrock valley is partly filled with glacial drift deposited during the last deglaciation. The 8-m-thick lower confined aquifer (LCA) is 154 m below land surface in the collapse area and was the principal source of water that flooded the salt mine. About 180 m of nearly flat-lying Devonian and Silurian bedrock separates the aquifer from the mined salt bed in the Salina Group shale. Drilling conducted in 2004 indicated that the rubble chimneys are surrounded by a deformation zone, bedrock that contains numerous bedding fractures created as rock layers sagged toward the mine cavity (Alpha Geoscience, 2005). Borehole geophysical surveys conducted by USGS in 1994 and 2004 detected water-bearing fracture zones at the top and bottom of the Bertie Limestone, 20 m and 50 m below the bedrock surface, respectively. The upper fracture zone is regionally extensive and discharged 4.1 L/s of water in 1986 to a vertical shaft in the salt mine 2 km northwest of the collapse area (Richard F. Langill and Associates, 1990).

VARIABLE-DENSITY/VISCOSITY MODELS

Variable-density/vicosity, transient ground-water-flow models were constructed using SEAWAT-2000 (Langevin and others, 2003) to simulate water-level recovery during the 10.7-yr period following flooding (January 1996 to September 2006), and the subsequent movement of brine, saline and fresh water within the rubble chimneys and surrounding deformation zone. Transport simulations used a migrating tracer to represent halite saturation because the relations between saturation and density, and saturation and viscosity in saline water and brine are relatively linear. The advection-dispersion equation was solved using the total-variation-diminishing (TVD) method with a Courant number of one to minimize numerical dispersion. The flow and transport equations were explicitly coupled and solved alternately; the flow solution was updated whenever the maximum change in density was greater than $5x10^{-3}$ g/cm^3.

The simulation models represented the area within 1 km of the rubble chimneys, coinciding with the location of wells north and south of the collapse area (Fig. 1A). The model grid defined 283,558 active cells with dimensions ranging from 10 m to 300 m; the layer spacing ranged from 0.6 m in the upper half of the domain to 4 m in the lower half. The models simulated flow through the LCA, the two rubble chimneys and surrounding deformation zone, and a portion of the flooded Retsof salt mine (Fig. 1B).

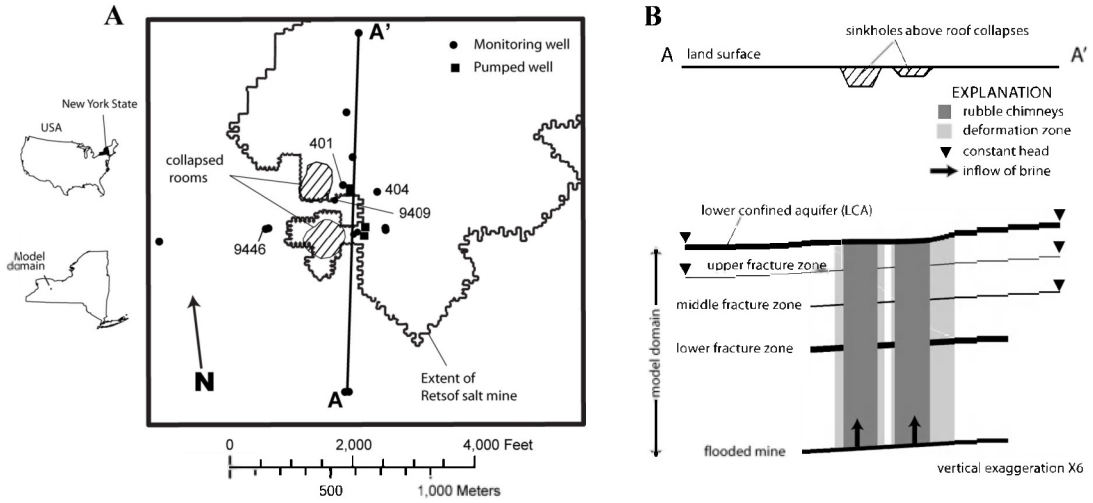

Figure 9. Model domain showing (A) collapse area, mine and well locations, and (B) section with water-bearing units and boundary conditions represented in model.

Three fracture zones in the bedrock were also represented in some models (Fig. 1B). Simulated saturations were compared with a salinity profile constructed from nine discrete-depth samples collected in borehole 9409 in September 2006. Although model parameters were adjusted by trial-and-error to reproduce the measured salinity profile, the resulting models were intended to illustrate the important processes controlling transport, rather than as calibrated representations of the flow system.

Solute at 100 percent saturation was introduced in the bottom model layer to represent brine displaced from the mine at declining rates ranging from 8 to 1.6 L/s, as estimated from subsidence monitoring (RE/SPEC Consulting & Services, 2003). Annually-varying constant heads were specified at the northern and southern boundaries in the top model layer (LCA) based on measured water level recovery in well 9446. Boundaries also represent inflow of saline water through the upper fracture zone and outflow of saline water through the middle fracture zone.

Constant heads computed for the upper and middle fracture zones were based on the measured heads in well 9446 and the assumption that the vertical-pressure gradient was negligible during the 10.7-yr period. The lower fracture zone was assumed to be a cavity developed within the collapse area. Separate 11-month simulations were conducted to represent pumping of brine from the collapse area.

SIMULATION RESULTS

In model A the bedrock fracture zones were omitted and brine migration through the rubble chimneys and deformation zone was controlled only by advection and dispersion. The simulated saturations closely match those observed in the lower 80 percent of the profile, but measured saturations exceed those simulated at the top of the profile (Fig. 2A). Geochemical models constructed previously in this study suggest that saline water at the top of the profile is a mixture of fresh and saline water discharged from the upper fracture zone, and not brine discharged from the mine cavity (D.L. Parkhurst, U.S.G.S., written commun., May 2007), indicating that inflow of saline water has entered the rubble chimney from fracture zones and migrated upward in front of the brine.

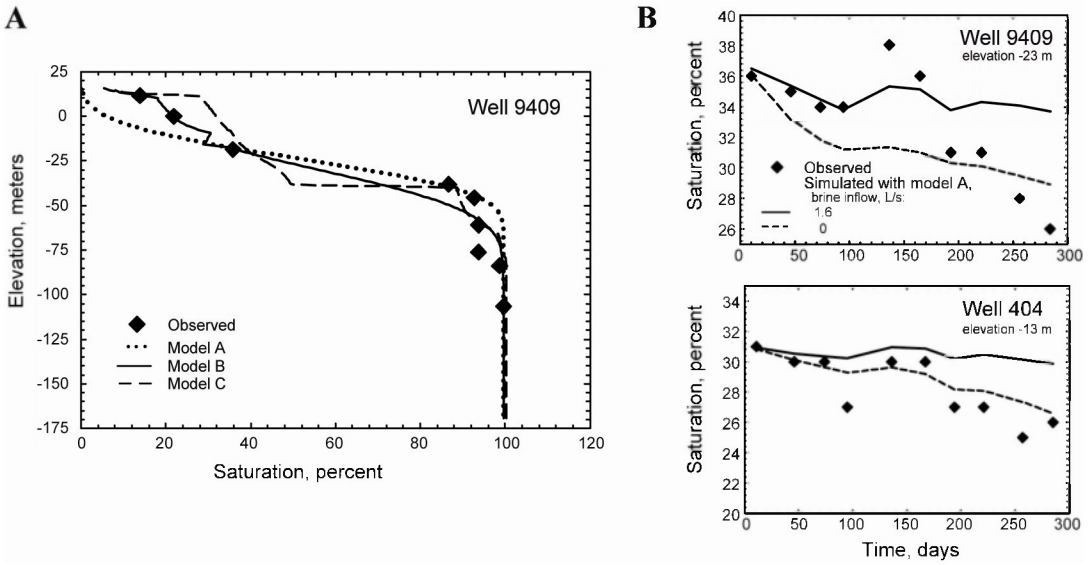

Figure 2. Observed and simulated halite saturations (A) after 10.7-yr water level recovery in borehole 9409, (B) during pumping in wells 9409 and 404.

Mixing of saline and fresh water was simulated in model B, in which saline water was allowed to enter through the upper fracture zone during water level recovery, and the lower and middle fracture zones were not represented. Simulated saturations with this model more closely match the upper part of the profile than results with model A (Fig. 2A). All three fracture zones were represented in model C, in which some of the displaced brine (0.3 L/s) was diverted laterally to the middle fracture zone (elevation -40 m). The resulting salinity profile is affected by mixing where the fracture zones intersect the rubble chimneys (Fig. 2A, elevations -10, -40 and -80 m). Simulation of pumping with model A indicates that the current rate of brine displacement is between 0 and 1.6 L/s (Fig. 2B), and that the salinity is gradually decreasing within the rubble chimneys at elevations above -25 m.

CONCLUSIONS

Pumping of saline water and brine appears to have prevented further contamination of the glacial-drift aquifer. Model simulations indicate that migration of brine and saline water above the flooded salt mine is controlled by advection, dispersion, and mixing of waters where fracture zones intersect the rubble chimneys. Simulations also suggest that some of the displaced brine could be diverted laterally into the middle fracture zone. The constructed models are not unique, however, because the exact geometry and the values of several parameters that affect simulated saturations cannot be estimated from the available data. Continued monitoring of the salinity profile together with borehole flowmeter surveys during pumping could provide additional data for model calibration. Additional boreholes are required to determine whether the displaced brine is migrating through the middle fracture zone.

REFERENCES

Alpha Geoscience. 2005. Comprehensive summary report, Retsof brine mitigation project: Clifton Park, N.Y.

Langevin, C.D., Shoemaker, W.B. and Guo, Weixing. 2003. MODFLOW-2000, the U.S. Geological Survey modular ground-water model—Documentation of the SEAWAT-2000 version with the variable-density flow process (VDF) and the integrated MT3DMS transport process (IMT): U.S. Geological Survey Open-File Report 03-426.

Langill, R.F. 1990. Subsidence and ground water inflow at the Sterling Mine: Germantown, MD., Richard F. Langill & Associates.

RE/SPEC Consulting & Services. 2003. Calculation of brine squeeze rate from Restof NY mine: Rapid City, SD. RESPEC Consulting & Services.

Yager, R.M., Miller, T.S., and Kappel, W.M. 2001. Simulated effects of 1994 salt-mine collapse on ground-water flow and land subsidence in a glacial aquifer system, Livingston County, New York. U.S. Geological Survey Professional Paper 1611.

Contact Information: Richard M. Yager, U.S. Geological Survey, 30 Brown Road, Ithaca, NY 14850 USA, Phone: 607-266-0217, Fax: 607-266-0521, Email: ryager@usgs.gov

A Case Study of Finite-Element Numerical Modeling on Salt Water Intrusion for the Ping-Tung Plain

Jing-Yea Yang
Stanley Consultants Inc., West Palm Beach, Florida

INTRODUCTION

Ping-Tung Plain is a center of agriculture and fisheries in Taiwan. Continuing population growth resulted in the increase of water use in the region. The total annual groundwater withdrawals had reached 2,181 million cubic meters. The Water Resources Planning Commission was facing challenges in water resources management and proposed several alternatives, such as construction of the Meinung Reservoir, Machia Reservoir, Nanhua Reservoir, and low dam/weirs along the Kaoping River. A conjunctive surface water and groundwater model was needed to assess the impacts associated with these alternatives to increase the efficiency of the water resources development in the Ping-Tung Plain. Over-pumping for fisheries along the coastal areas resulted in seawater intrusion, which was a major issue.

SIMULATION MODEL

Groundwater is the major source of water supply across the Ping Tung Plain. Groundwater withdrawals have been previously estimated as approximately twice the annual effective precipitation recharge to water-supply aquifers. Aquifers generally range in thickness from 60 to more than 110 meters. These aquifers contain very coarse, high-permeability sands and gravels in the northeast (alluvial fans), and multiple, thinner and less permeable confined aquifers in the southern part of the Ping-Tung Plain. Four soil types were simulated: gravel, sand, clay, and rock using available information on hydraulic properties for these soil types.

A three-dimensional (3D) finite-element model capable of predictive simulation of the effects of reservoirs on the groundwater system for the Ping Tung Plain in southwestern Taiwan was developed. The conjunctive surface water and groundwater simulation model also serves as a long-term management tool for evaluation of the effects from many water management alternatives, including the sea water intrusion of chloride front movement for 50 years simulation. The Ping Tung Plain was visualized in 3D using the Groundwater Modeling System (GMS) system. This system allowed the synthesis of a large number of available data sources, especially the large number of boreholes for which stratigraphic data were available. Importance for model calibration was the integration of complex, wet-season and dry-season river stage elevation with groundwater recharge rates. The finite-element numerical model FEMWATER, was selected as an appropriate model for simulating features at the Plain.

The discretization of the conceptual model contained a total of 9,070 elements and 5,291 nodes distributed in a 3D mesh representing 10 thin layers of elements capable of evaluating many thin and discontinuous confining layers. The 3D visualization was "discretized" into thin triangular prismatic elements that became the 3D finite element mesh used for numerical model simulation of the Ping-Tung Plain. The mesh was extended offshore to include the shelf area for effective simulation of shoreline conditions and seawater intrusion simulation. Bedrock is included on the West, North, and East sides of the model because seepage of water from bedrock to the aquifers is an important source of recharge to the Ping Tung Plain.

and data gaps. Bedrock was explicitly simulated as part of the model. Rainfall-seepage boundaries were used to simulate the recharge of groundwater to bedrock surrounding the Ping Tung Plain. Little or no information regarding the rate of seepage from bedrock into the aquifer system exists, so that sensitivity analyses were used to develop a reasonable constant value for bedrock hydraulic conductivity. Sensitivity analyses showed that bedrock seepage is an important and sensitive term in the numerical model simulation. Important features such as the Chao Chou Fault in the east part of the model were simulated as vertical bedrock interfaces with alluvial material.

Rainfall recharge was simulated as a seepage-type of boundary condition on the upper surface of the model. Pumping was simulated as a constant flux (Cauchy type) boundary condition on the bottom surface of model. The use of separate rainfall and pumping terms increased the complexity of the model and the uncertainties associated with precise estimates of either rainfall recharge or pumping. Extensive re-calibration of groundwater flow was therefore necessary prior to simulating seawater intrusion. Part of this re-calibration process included the use of a new material type " cobbles" in parts of the upper alluvial fans associated with the northwestern Lao Nung Creek and Ailiao Creek.

Initial conditions for chloride proved to be the most important and sensitive part of the modeling process. For this reason, the current chloride concentrations in groundwater were thoroughly evaluated. At several locations, variations in concentrations of compounds related to seawater intrusion varied substantially with depth. In areas immediately adjacent to the coastline, the shallowest aquifer is often highly contaminated by seawater. In several areas, however, chloride concentrations related to seawater intrusion increased with depth. This effect is widely known, and is related to the lateral migration of seawater from offshore areas rather than from downward seepage of seawater. This understanding is important because deeper wells are often viewed as a solution to seawater intrusion when, in fact, they may increase the problem of seawater intrusion.

Numerical modeling requires an initial condition dataset that accurately reflects actual chloride concentrations. To provide this dataset, a three-dimensional calculation of chloride concentrations was made using a numerical gridding algorithm to interpolate the chloride concentration at every model mesh node. The input data for this process was the chloride concentration in groundwater samples collected at monitoring wells. From these data the best approximation of current values of chloride concentration and each location were selected.

MODELING RESULTS

The results of numerical modeling indicate that the advancing chloride front (defined at a concentration averaging 250 ppm) will move north in the more permeable sand and gravel near the mouth of the Kaoping River. North of the Lin Yuan area, near the mouth of the Kaoping River, chloride concentrations will increase substantially over the next 50 years. The chloride front was calculated to be moving north at an average rate of 80 meters per year.

The concentration of chloride will generally increase along the entire Ping Tung County coastline. Deeper aquifers in the areas near the mouths of the Kaoping and Tung Kang creeks will experience continuing increases in chloride concentration. The shallow coastal aquifers already have significant damage. Near the mouths of the Kaoping and Tung Kang Creeks, shallow aquifers have already experienced seawater intrusion damage. The areas where the potential for chloride concentration changes due to the increase in groundwater pumping were identified and evaluated.

Chloride concentrations will increase with well depth, making deeper well drilling along the coast-line problematic. The areas around the southern Kaoping River and southern Tung Kang River will continue to experience increases in chloride content in groundwater. Preventing the expected increases in chloride concentration in coastal areas will require substantial reductions in groundwater pumping by fish farms in coastal areas, especially near the mouths of the Kaoping and Tung Kang Rivers.

The fisheries industry is a likely cause of some of the major groundwater withdrawals in the coastal areas, as are industrial, agricultural and domestic users of groundwater. Because the over-all mass balance for groundwater in the Plain is positive and stable, additional groundwater pumping in the central and northern parts of the plain could be used to provide additional water supplies if coastal pumping were reduced.

Contact Information: Jing-Yea Yang, Stanley Consultants, Inc., 1601Belvedere Road Suite 400 East, West Palm Beach, Florida 33406 USA, Phone: 561-712-2257, Fax: 561-689-3003, Email: yangjing-yea@stanleygroup.com

Chemical and Isotopic Evidence for Seawater Intrusion – Examples from the Coastal Aquifers of the Mediterranean and the Dead Sea

Yoseph Yechieli[1] and *Orit Sivan*[2]
[1]Geological Survey of Israel, Jerusalem, Israel
[2]Ben Gurion University, Beer-Sheva, Israel

Increase in salinity of groundwater is a major problem in coastal aquifers, impairing the use of groundwater for various purposes. It is essential to determine first the origin of salinity in order to be able to cope with this problem. In general, high salinity could result from several sources other than seawater intrusion. These include pollution from various origins, such as industrial and agriculture and also from brines which are not connected to the present sea. In such cases, one can not assume hydraulic connection between the saline and fresh water bodies as simple fresh-saline water interface. Therefore, the chemical characteristics should serve as constrains for the hydrological simulation in order to understand the present situation and forecast future trends.

Chemical and isotopic analyses are the best tools for identifying the specific sources of salinity and their geochemical evolution (e.g. Jones et al., 1999). Therefore, these tools have been used in studies of coastal aquifers in many parts of the world. This review discusses the cases of both the Mediterranean Sea and the Dead Sea. The chemical composition of the major ions in saline groundwater (Na, K, Ca, Mg, Cl, SO_4 and Br), as well as the isotope composition, were measured and compared to that of seawater in order to track its sources.

Most samples in the Mediterranean coastal aquifer were found to be quite similar to seawater, implying that the main process here is mixing of seawater with fresh groundwater. Simple mixing is also inferred from the stable isotope composition of both oxygen and hydrogen. The results, therefore, indicate that in most cases the source of the salinity in the Mediterranean coastal aquifer is seawater. The geochemical evolution of the seawater, along its penetration inland from the sea, was examined from the slight deviations from the simple mixing lines. The deviations are due to water rock interaction, mainly by cation exchange process (Appelo et al., 1990; Sivan et al., 2005). This process is expressed by the significant increase of the concentration of Ca and the decreasing of Na and K in the solution as compared to simple mixing. The various components of the carbonate system (including alkalinity, dissolved inorganic carbon (DIC), $\delta^{13}C_{DIC}$ and $^{14}C_{DIC}$) indicate that when seawater interacts with aquifer rocks the main process beside cation exchange is oxidation of organic matter, as reflected in relatively low $\delta^{13}C$ and ^{14}C values (Sivan et al., 2005, Russak et al., this proceeding). In some parts of the Israeli Coastal Aquifer, different water composition was found (e.g. high nitrate or other pollutants) implying that the salinity source is industrial or agricultural.

The hydrological situation in the Dead Sea Coastal Aquifer is more complicated since it hosts brines which probably originated from old lakes that existed in this area. The chemical composition of these brines is indeed different from that of the present Dead Sea (Figure 1), implying that they are not in a direct hydraulic connection with the sea and therefore can not be regarded as part of the regular fresh-saline water interface system. The brines near the sea are similar to the Dead Sea indicating on closer hydraulic connection.

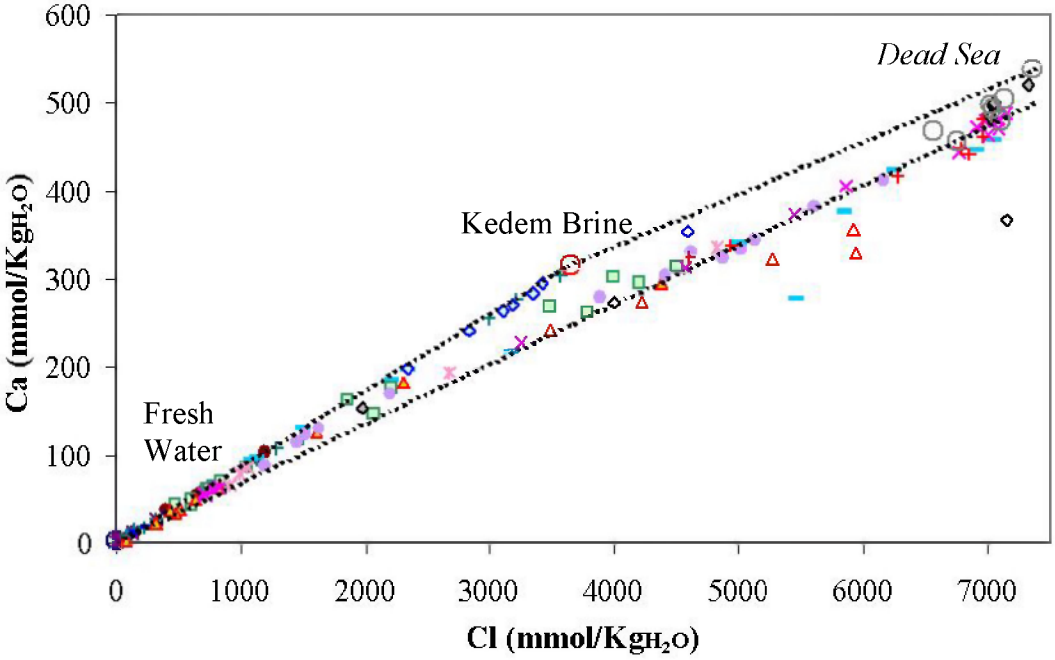

Figure 1. Chemical composition of groundwater in the Dead Sea area indicating that simple mixing between Dead Sea brine and fresh groundwater can not explain the chemistry of all water bodies (Levenberg, 2005).

The other importance of geochemical and isotopic analysis (mainly radioactive isotopes) is to determine the rate of seawater intrusion and the connection between the sea and the aquifer. The radioactive dating of groundwater (tritium and ^{14}C) yields mostly young seawater in the Mediterranean Aquifer, indicating relatively fast rate of seawater intrusion. In several locations, older seawater (>10000 years, Yechieli et al., 2008; Figure 2) was found implying either poor connection to the sea and/or existence of seawater from the time of sea level rise in Late Pleistocene.

Similarly, Dead Sea type brines were found at different distance from the sea exhibiting different preliminary ages, depending on the rate of intrusion. Age calculation with the ^{14}C method could be problematic in this area since groundwater may contain dissolved organic carbon (e.g Methane) which probably contributes very negative $\delta^{13}C$ and low ^{14}C values (Avrahamov et al., 2008). In some cases, relatively high radiocarbon and tritium values imply that, although the Dead Sea water level decline at extreme rate of 1 m/yr, its brines still penetrate into the coastal aquifer. The rate of brine penetration will be compared to that obtained by hydrological simulations.

Future tools can include other isotopic and chemical tracers, some of which were never used before. These can include tritium-helium, CFC and more for age determination and other stable isotopes (e.g. B, Sr and S isotopes).

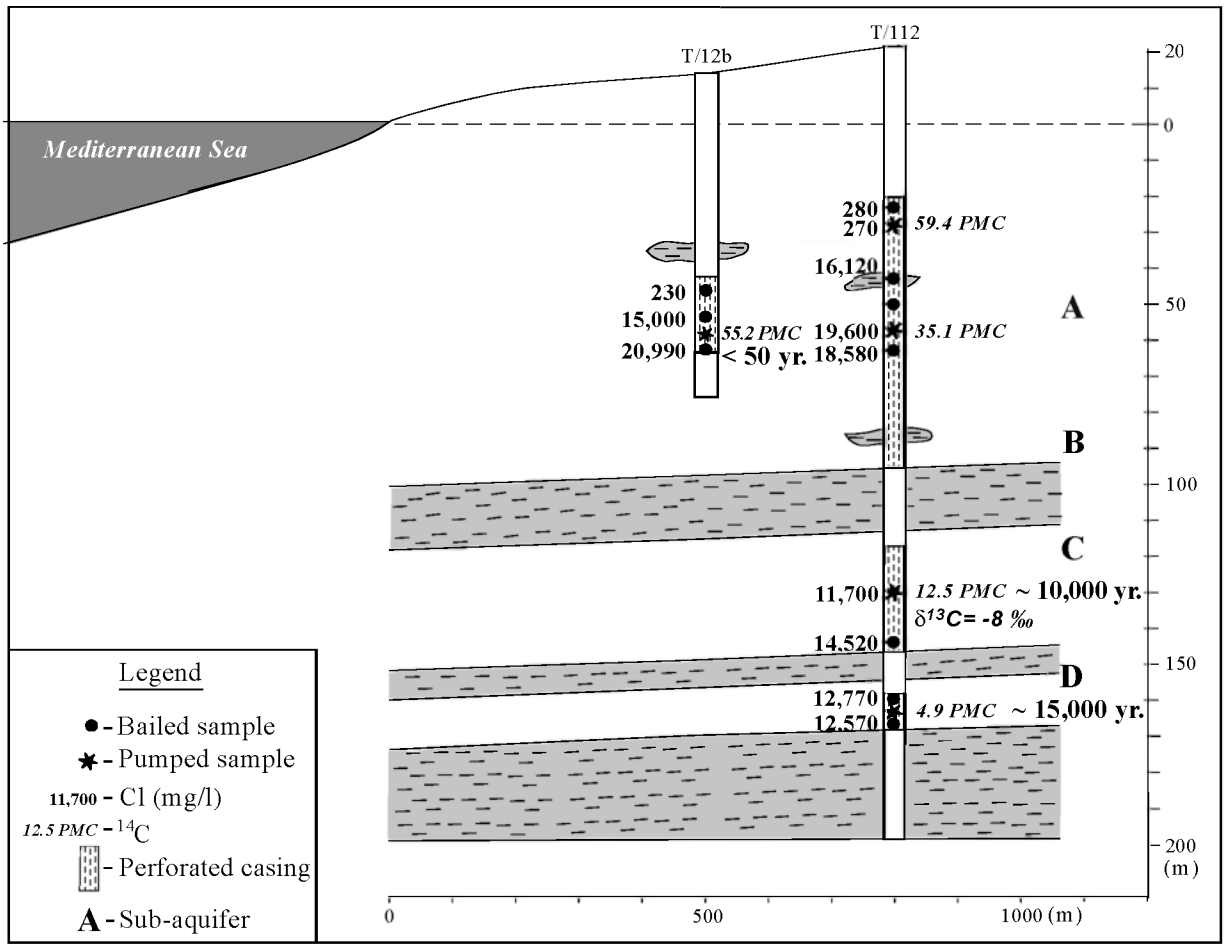

Figure 2. Preliminary ages of saline groundwater in the Mediterranean coastal aquifer in Israel (Yechieli et al., 2008).

REFERENCE

Appelo, C. A. J., Willemsen, A., Beekmen, H. E. and Griffioen, J. (1990), Geochemical calculation and observation on saltwater intrusion II. Validation of geochemical model with laboratory experiment. *Journal of Hydrology* 120, 220-250.

Avrahamov, N., Sivan, O., Lazar, B., Levenberg, O. and Yechieli, Y. (2008), The carbon system in the saline groundwater in the Dead Sea area. Isr. Geol. Soc. Meet. Abstract, p. 5.

Jones, B.F., Vengosh, A., Rosenthal, E. and Yechieli, Y. (1999) Geochemical investigations. In: Bear et al. (eds) Seawater Intrusion in Coastal Aquifers –Concepts, Methods and Practices, pp 51-72.

Levenberg, O. (2005), The hydrogeology and geochemistry of groundwater in the alluvial fan of Wadi Arugot, En Gedi Reservation. Report GSI/21/05.

Russak, A., Sivan, O., Yechieli, Y. and Lazar B. (2008), Time Scale of Water-Rock Interaction Processes in the Fresh-Saline Water Interface of Coastal Aquifers (this proceeding).

Sivan, O., Yechieli, Y., Herut, B. and Lazar, B. (2005), Geochemical evolution and timescale of seawater intrusion to the coastal aquifer of Israel. *Geochimica et Cosmochimica Acta* 69(3), 579-592.

Yechieli, Y., Kafri, U. and Sivan, O. (2008), The inter-relationship between coastal sub-aquifers and the Mediterranean Sea, deduced from radioactive isotopes analysis. *Hydrogeology Journal* (in press).

Contact Information: Yoseph Yechieli, Geological Survey of Israel, Jerusalem 95501, Israel,
Phone: 972-2-5314236; Fax: 972-2-5380688, Email: yechieli@gsi.gov.il

Quantifying Effects of Natural and Anthropogenic Stresses on Long-Term Saltwater Intrusion in a Coastal Aquifer

Michael R. Zygnerski and *Christian D. Langevin*
U.S. Geological Survey, Florida Integrated Science Center, Ft. Lauderdale, FL, USA

ABSTRACT
A variable-density groundwater flow and solute transport model representing the Pompano Beach area in southeastern Florida was developed to simulate the historical pattern of saltwater intrusion in response to drainage and wetland reclamation, groundwater withdrawals, rainfall, and water-management practices. Simulations of the past century (1900-2005) produce water-quality trends that closely correspond to historical chloride concentrations measured at observation wells. Sensitivity analyses indicate that the position of the saltwater intrusion line is most sensitive to changes in groundwater withdrawals and to decreases in rainfall.

INTRODUCTION
Saltwater intrusion has occurred near the Pompano well field, which is located in northern Broward County, Florida. Identifying the cause of saltwater intrusion in this area is not straightforward due to the complex interaction between various hydrologic stresses. During the past century, for example, sea level has risen and extreme variations in rainfall have occurred. In addition, a century of agricultural and urban development has changed the hydrologic landscape from a system dominated by the freshwater wetlands of the Everglades to one controlled by a highly managed network of canals used primarily for drainage. This development has resulted in inland water levels that are several meters lower than predevelopment elevations. Moreover, current municipal withdrawal rates in Broward County from the shallow surficial aquifer system (SAS) represent a 90-fold increase since the mid-1940s when saltwater intrusion was first recognized as a critical water-resource issue (Renken and others, 2005). Because many of these events overlapped in time, it is difficult to identify which anthropogenic and natural factors have had the greatest influence on saltwater intrusion.

To address these issues, a variable-density groundwater flow and solute transport model was developed to investigate the causes of saltwater intrusion over the past 105 years in northeastern Broward County, Florida (Figure 1). Parameter estimation was used to calibrate the numerical model to water levels and salinities observed in monitoring wells. This paper presents preliminary findings from numerical simulations, including sensitivity analyses designed to quantify the relative importance of natural stresses induced by rainfall and sea-level change, and anthropogenic stresses induced by groundwater withdrawals and canal management.

MODEL DEVELOPMENT AND RESULTS
A variable-density numerical model was developed using the SEAWAT computer code (Langevin and others, 2003). The model is based on many of the assumptions used in other numerical models of Broward County (Dausman and Langevin 2004; CDM/DHI, 2005) and on local hydrologic and geologic data. The simulation period extends from 1900 to 2005; the first 41 years were divided into three stress periods, whereas the remainder of the simulation used monthly stress periods.

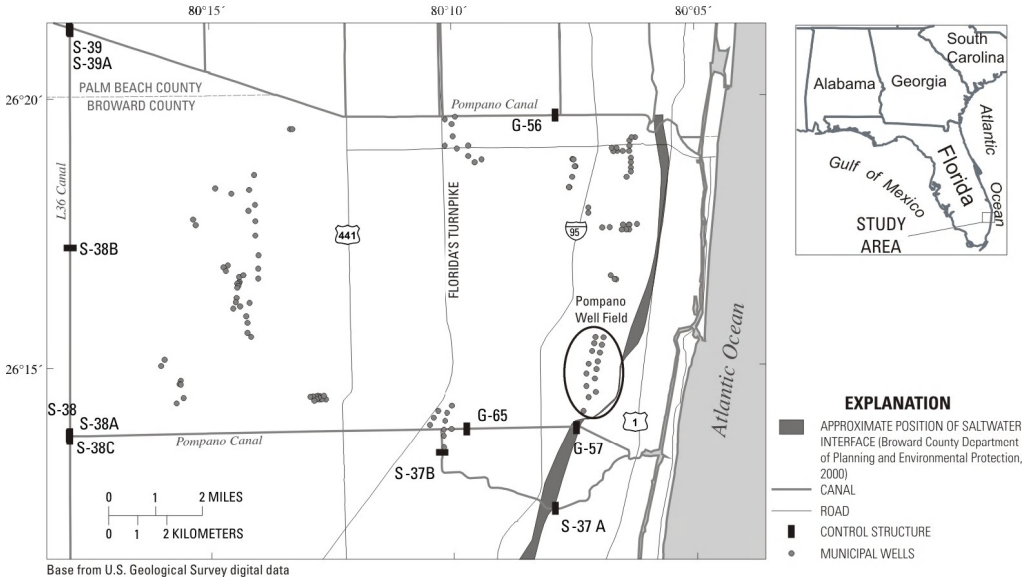

Figure 1. Northeastern Broward County, Florida, showing important hydrologic features and the approximate position of the saltwater intrusion line based on 1994 data.

A uniform finite-difference grid containing 115 rows and 160 columns (150 x 150 m cell size) was used to discretize the study area. The model consists of nine layers of varying thickness that extend from land surface to the base of the SAS. Canal heads were specified using historical field data. Heads used for the Atlantic Ocean were based on historical Atlantic Ocean stage data, which show a gradual increase of 24 cm over the past century. The salinity of the ocean boundary was held constant at 35,000 mg/L. Detailed pumping records were obtained for each municipal well field, and where possible, a time-varying pumping rate was used for individual pumping wells.

The PEST parameter estimation program (Doherty, 2007) was used to calibrate the model to observed heads and salinities. The estimated parameters included horizontal and vertical hydraulic conductivity, effective porosity, specific storage, specific yield, and net recharge. Calibration of the 105-year simulation (described herein as the base historical simulation) produced a reasonable representation of the measured trends in hydraulic head and chloride concentrations. The saltwater intrusion line, defined here as the inland extent of groundwater with salinity greater than or equal to 1,000 mg/L, for the base historical simulation is shown in Figure 2. Model results are generally consistent with historical observations in that the greatest encroachment occurred in the mid-1980s, which coincides with peak rates of coastal pumping and an extended period of drought. The model also captures the seaward movement of the saltwater intrusion line during the early 1990s. The seaward movement of the saltwater intrusion line is due to several factors. Withdrawals at the Pompano well field decreased and were reassigned to a well field located further inland. In addition, canal management strategies were refined to move water into coastal areas and raise the water table. The temporal and spatial extents of saltwater intrusion and subsequent flushing appear to be represented by the calibrated model.

Seven scenarios were performed to quantify the relative effects of sea-level rise, groundwater withdrawal rates, rainfall, and boundary canal levels on the position of the saltwater intrusion line. The scenarios were formulated as follows: no sea-level rise, no groundwater withdrawals, 100% increase in groundwater withdrawals, 16% increase and decrease in rainfall, and 0.5-m

increase and decrease in boundary canal levels. Figure 2 presents the results for the scenarios that showed a substantial difference from the base historical simulation. Although results from the other scenarios are not presented here, Zygnerski and Langevin (2007) showed that the combined effects of multiple hydrologic stresses can have a large effect on the position of the saltwater intrusion line. A qualitative comparison suggests that groundwater withdrawals and drought conditions had the largest effect on the position of the saltwater intrusion line over time (Figure 2). For the base historical simulation, the saltwater intrusion line moved inland a maximum distance of about 500 m. For the scenarios with a 100% withdrawal increase and a 16% decrease in rainfall, the saltwater intrusion line moved inland a maximum distance of 2110 m and 710 m, respectively. Conversely, the saltwater intrusion line advanced only 160 m when withdrawals where eliminated altogether.

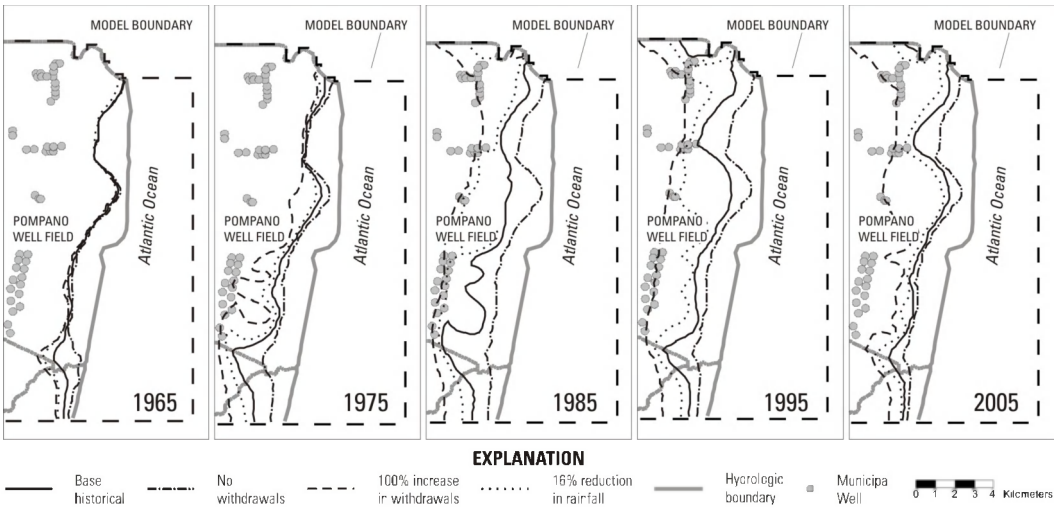

Figure 2. Lines depicting the landward limit of groundwater having salinity of 1,000 mg/L or greater. Lines are for model layer 3, which corresponds to the top of the primary production zone.

CONCLUSIONS

The Pompano well field, located in northern Broward County, withdraws groundwater from the shallow SAS. Chloride data collected at monitoring wells located between the well field and the Atlantic Ocean indicate that the saltwater intrusion line moved inland during the 1970s and 1980s toward the well field and retreated during the 1990s. A numerical model was developed for the northern part of Broward County, Florida, to quantify the effects of natural and anthropogenic stresses on the movement of the saltwater intrusion line in the SAS. Simulations were performed using the SEAWAT computer program, which represents variable-density groundwater flow and dispersive solute transport. The approach used involved calibrating the model to conditions observed over the past century and then using the calibrated model to evaluate the relative importance of selected hydrologic stresses.

When compared with the calibrated model, the hypothetical scenarios provide insight into the relative importance of several hydrologic stresses. Well-field withdrawals and periods with prolonged decreases in rainfall were identified as the factors that resulted in the most noticeable shift in the saltwater intrusion line. Although the decreased rainfall simulation proved to substantially affect the position of the saltwater intrusion line, the increased rainfall simulation did not show a large effect. This difference is probably due to the canal system, which prevents the water table from rising more than it could drop during the decreased rainfall simulation. Another important result is that the 100% withdrawal increase scenario shows the saltwater

intrusion line within the well field in 1985 and 1995; however, due to the reassignment of pumping to an inland well field, results suggest that a 100% increase in withdrawal would not cause the saltwater intrusion line to move into the well field under 2005 conditions.

This paper presents an important step in quantifying the causes of saltwater intrusion in northern Broward County. A quantitative understanding of the various causes of saltwater intrusion, their individual effects, and their combined effects is expected to provide a foundation for future management practices of coastal aquifers.

REFERENCES

CDM/DHI. 2005. Modeling Water Management Practices in North Broward County, Florida. 1-1 to 6-2.

Dausman, A.M., and Langevin, C.D. 2004. Movement of the Saltwater Interface in the Surficial Aquifer System in Response to Hydrologic Stresses and Water-Management Practices, Broward County, Florida: U.S. Geological Survey Scientific Investigations Report 2004-5256.

Doherty, J. 2007. PEST Model-Independent Parameter Estimation User Manual: 5th Edition: Watermark Numerical Computing. 1-1 to 13-15.

Langevin, C.D., Shoemaker, W.B., and Guo, W. 2003. MODFLOW-2000, the U.S. Geological Survey Modular Ground-Water Model- Documentation of the SEAWAT-2000 version with the variable density flow process (VDF) and the integrated MT3DMS Transport Process (IMT): USGS Open-File Report 03-426. 43.

Renken, R., Dixon, J., Koehmstedt, J., Ishman, S., Lietz, A.C., Marella, R., Telis, P., Rodgers, J., and Memberg, S. 2005. Impact of Anthropogenic Development on Coastal Ground-Water Hydrology in Southeastern Florida, 1900-2000: U.S. Geological Survey Circular 1275. 77.

Zygnerski, M.R., and Langevin, C.D. 2007. Long-Term Saltwater Intrusion in a Coastal Aquifer: Quantifying Effects of Natural and Anthropogenic Stresses: in Coastal Aquifers: Challenges and Solutions, Almeria, Spain, 2007, Proceedings: Almeria, Spain, TIAC 2007. 509-516.

Contact Information: Michael R. Zygnerski, U.S. Geological Survey, 3110 SW 9th Ave., Ft. Lauderdale, FL, USA 33315 USA, Phone: 954-377-5918, Fax: 954-377-5901, Email: mzygners@usgs.gov

Author Index

Bold numbers indicate presenting authors.

NOTES

NOTES

NOTES